Theorie der Quantensysteme im Nichtgleichgewicht (Vertiefung)

Theory of quantum systems in nonequilibrium

Vorlesung
Sommersemester 2017
Technische Universität Berlin

Dr. Gernot Schaller

April 19, 2019

Contents

Die Veranstaltung mit Vorlesung und Übung gilt als Vertiefungsfach (10 LP). Die Vorlesung wird Dienstags und Donnerstags von 8:15-9:45 im EW 203 stattfinden, die dazugehörige Übung wird von Dr. Javier Cerrillo angeboten und wird Mittwochs von 12:15-13:45 im EW 229 stattfinden. Die Veranstaltung ist erweiterbar zu einem vollen Wahlpflichtfach (12 LP), indem zusätzlich an einem Seminar oder einer Spezialvorlesung aus der Theoretischen Physik teilgenommen wird (in Absprache mit dem Dozenten).

Voraussetzungen für die Teilnahme: Quantenmechanik, Quantenmechanik II, Konzept der Dichtematrix und von bosonischen wie fermionischen Erzeugern und Vernichtern

Ein Vorlesungsskript wird online verfügbar sein unter

http://www1.itp.tu-berlin.de/schaller/lectures.html.

Korrekturen und Vorschläge sollten an folgende email-Adresse gesendet werden:

gernot.schaller@tu-berlin.de.

Ich bedanke mich bei vielen Mitarbeitern der früheren AG Brandes (insbesondere auch Dr. Javier Cerrillo und Dr. Georg Engelhardt), welche mir wertvolle Rückmeldungen gegeben haben. Tobias Brandes nat natürlich grundlegend zu diesem Skript beigetragen, seine Anregungen haben mich in meiner Arbeit immer bestärkt und haben dabei eine Vielzahl neuer Aspekte mit eingebracht.

Zuletzt noch ein Hinweis: Dieses Skript wird während der Vorlesung ausgebaut und verbessert werden. Es wird nach jeder Vorlesung in aktualisierter Fassung online gestellt, es empfiehlt sich daher, nicht gleich zu Anfang alles auszudrucken.

Literatur:

- H.-P. Breuer and F. Petruccione, *The Theory of Open Quantum Systems*, Oxford University Press, Oxford (2002). [1]
- G. Schaller, *Open Quantum Systems Far from Equilibrium* Springer Lecture Notes in Physics **881**, Springer (2014). [2]
- H. M. Wiseman and G. J. Milburn, *Quantum Measurement and Control*, Cambridge University Press, Cambridge (2010). [3]

Wir werden folgende Inhalte behandeln

- mikroskopische Ableitungen von Mastergleichungen
- Entropie-Produktion in Lindblad-Mastergleichungen
- Thermodynamik von Nichtgleichgewichtsreservoiren
- Fluktuationstheoreme und zweiter Hauptsatz
- getriebene Systeme (externes Treiben und RÃ$\frac{1}{4}$ckkopplung)
- stark gekoppelte Systeme

Chapter 1

Master equations

1.1 Definitions

Many processes in nature appear to us as random.

In classical physics, this randomness may result from our incomplete knowledge about the system. For example, the collisions of gas molecules in a box with the domain walls may appear random since we do not know the momenta and positions of each individual molecule.

On the other hand, in quantum mechanics already the equations of motion at the lowest level involve amplitudes rather than observables. Although the Schrödinger equation appears formally deterministic, its interpretation has a stochastic element, as probabilities for certain measurement outcomes can be derived from the squared amplitudes.

Such random processes can be described by probabilities, which may become time-dependent. The evolution of these probabilities may be governed by equations of different type, and we will discuss some of these.

First, we briefly recall the density matrix formalism from quantum mechanics. Whereas the Schrödinger equation

$$\left|\dot{\Psi}\right\rangle = -\mathrm{i}H\left|\Psi\right\rangle \tag{1.1}$$

is well suitable for describing closed systems and pure states, the density matrix formalism allows to describe more general quantum systems. Formally, a density matrix has to fulfill

$$\mathrm{Tr}\left\{\rho\right\} = 1\,, \qquad \rho = \rho^\dagger\,, \qquad \left\langle\Psi\right|\rho\left|\Psi\right\rangle \geq 0 \qquad \forall\left|\Psi\right\rangle\,. \tag{1.2}$$

The first property essentially demands that the sum of all probabilities has to be conserved, the second is necessary for the stochastic interpretation in terms of probabilities, and the last property encodes that the probabilities for measurement outcomes must be positive.

For closed quantum systems, the dynamics follows the *Liouville-von-Neumann equation*

$$\dot{\rho} = -\mathrm{i}[H,\rho] = \mathcal{L}_0\rho\,. \tag{1.3}$$

Such equations, where on the left hand side the first derivative of the density matrix with respect to time are connected with the action of a linear super-operator on the density matrix, are called *master equations*. There are different types of master equations, and in its most simple manifestation they are also well-known in classical physics, which will be discussed below.

Exercise 1 (Preservation of density matrix properties by unitary evolution)**.** *Show that the von-Neumann (1.3) equation preserves self-adjointness, trace, and positivity of the density matrix.*

Also the Measurement process can be generalized similarly. For a quantum state $|\Psi\rangle$, measurements are described by a set of measurement operators $\{M_m\}$, each corresponding to a certain measurement outcome, and with the completeness relation $\sum_m M_m^\dagger M_m = \mathbf{1}$. The probability of obtaining result m is given by

$$p_m = \langle\Psi| M_m^\dagger M_m |\Psi\rangle \tag{1.4}$$

and after the measurement with outcome m, the quantum state is collapsed

$$|\Psi\rangle \xrightarrow{m} \frac{M_m |\Psi\rangle}{\sqrt{\langle\Psi| M_m^\dagger M_m |\Psi\rangle}}\,. \tag{1.5}$$

The projective measurement is just a special case of that with $M_m = |m\rangle\langle m|$.

Def. 1 (Measurements with density matrix)**.** *For a set of measurement operators $\{M_m\}$ corresponding to different outcomes m and obeying the completeness relation $\sum_m M_m^\dagger M_m = \mathbf{1}$, the probability to obtain result m is given by*

$$p_m = \mathrm{Tr}\left\{M_m^\dagger M_m \rho\right\} \tag{1.6}$$

and action of measurement on the density matrix – provided that result m was obtained – can be summarized as

$$\rho \xrightarrow{m} \rho' = \frac{M_m \rho M_m^\dagger}{\mathrm{Tr}\left\{M_m^\dagger M_m \rho\right\}} = \frac{M_m \rho M_m^\dagger}{p_m} \tag{1.7}$$

It is therefore straightforward to see that description by Schrödinger equation or von-Neumann equation with the respective measurement postulates are equivalent. The density matrix formalism conveniently includes statistical mixtures in the description but at the cost of quadratically increasing the number of state variables.

Exercise 2 (Preservation of density matrix properties by measurement)**.** *Show that the measurement postulate preserves self-adjointness, trace, and positivity of the density matrix.*

1.2 Rate equations

When the master equation in a particular basis couples the diagonal elements of the density matrix only to other diagonal elements, it is also called *rate equation*. Such a rate equation can be represented by a linear rate matrix, which is acting on a vector of probabilities (composed by the diagonal elements of the density matrix) $\dot{\boldsymbol{P}} = T\boldsymbol{P}$.

Def. 2 (rate equation)**.** *A rate equation is a master equation describing only the evolution of the diagonal elements $P_k = \rho_{kk}$ of the density matrix For discrete states k it assumes the form*

$$\frac{dP_k}{dt} = \sum_\ell \left[T_{k\ell}P_\ell - T_{\ell k}P_k\right] , \qquad \dot{\boldsymbol{P}} = T\boldsymbol{P} , \tag{1.8}$$

where the $T_{k\ell} > 0$ are transition rates from state ℓ to state k. In matrix representation one has

$$T = \begin{pmatrix} -\sum\limits_{i\neq 1} T_{i1} & T_{12} & \dots & T_{1N} \\ T_{21} & -\sum\limits_{i\neq 2} T_{i2} & & T_{2N} \\ \vdots & & \ddots & \vdots \\ T_{N1} & \dots & \dots & -\sum\limits_{i\neq N} T_{iN} \end{pmatrix} . \tag{1.9}$$

The rate equation is said to fulfill *detailed balance*, when at steady state $T\bar{\boldsymbol{P}} = 0$ the equation $T_{k\ell}\bar{P}_\ell = T_{\ell k}\bar{P}_k$ is fulfilled separately for all pairs (k, ℓ). Furthermore, when the rate matrix is symmetric $T_{k\ell} = T_{\ell k}$, all processes are reversible in a thermodynamic sense.

It is simple to show that a rate equation must conserve the sum of all probabilities

$$\sum_k \frac{dP_k}{dt} = \sum_{k\ell} \left(T_{k\ell}P_\ell - T_{\ell k}P_k\right) = \sum_{k\ell} \left(T_{\ell k}P_k - T_{\ell k}P_k\right) = 0 . \tag{1.10}$$

Furthermore, all probabilities must remain real, since the transition rates are also real. This fulfills the second condition for a density matrix.

Last we show that rate equations preserve the positivity of probabilities. Let us assume that we start with a valid probability distribution, i.e., with non-negative probabilities $0 \leq P_i(0) \leq 1$. Let now P_k denote the probability that first vanishes at some time t, i.e., where all other probabilities are still non-negative. Then, we can conclude for the time-derivative of P_k, that

$$\left.\frac{dP_k}{dt}\right|_{P_k=0} = +\sum_\ell T_{k\ell}P_\ell \geq 0 , \tag{1.11}$$

which means that the boundary $P_k = 0$ is repulsive and cannot be crossed. This prohibits negative probabilities. In addition, all individual probabilities must remain smaller than one. This however immediately follows by contradiction from the conservation of their sum and their individual positivity.

Altogether one can say that a rate equation of the form (1.8) automatically preserves the probability interpretation, which of course only holds for a valid initialization.

1.2.1 Example 1: Fluctuating two-level system

Let us consider a system of two possible events, to which we associate the time-dependent probabilities $P_0(t)$ and $P_1(t)$. These events could for example be the two conformations of a molecule, the configurations of a spin, the two states of an excitable atom, etc. To introduce some dynamics,

let the transition rate from $0 \to 1$ be denoted by $T_{10} > 0$ and the inverse transition rate $1 \to 0$ be denoted by $T_{01} > 0$. The associated master equation is then given by

$$\frac{d}{dt}\begin{pmatrix} P_0 \\ P_1 \end{pmatrix} = \begin{pmatrix} -T_{10} & +T_{01} \\ +T_{10} & -T_{01} \end{pmatrix}\begin{pmatrix} P_0 \\ P_1 \end{pmatrix} \tag{1.12}$$

Exercise 3 (Temporal Dynamics of a two-level system)**.** *Calculate the solution of Eq. (1.12). What is the stationary state?*

The occupation of a dot tunnel-coupled to a junction with bare tunneling rate Γ will fluctuate depending on the Fermi level of the junction, see Fig. 1.1.

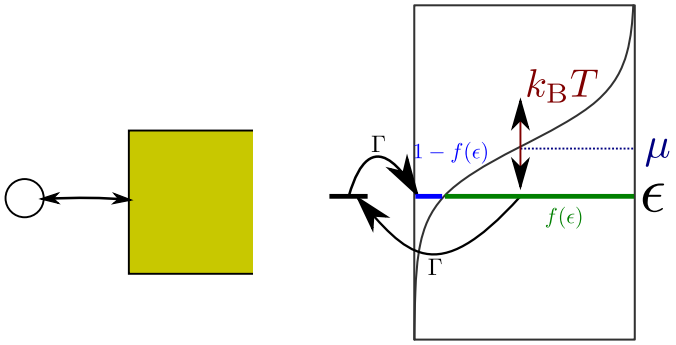

Figure 1.1: **Left:** Sketch of a single quantum dot hosting at most one electron, which is tunnel-coupled to a single junction. **Right:** Sketch of the dot transition frequency in relation with the Fermi occupation of the lead levels.

In particular, if at time t the dot was empty, the probability to find an electron in the dot at time $t + \Delta t$ is roughly given by $\Gamma \Delta t f(\epsilon)$ with the Fermi function defined as

$$f(\omega) = \frac{1}{e^{\beta(\omega-\mu)} + 1}\,, \tag{1.13}$$

where β denotes the inverse temperature and μ the chemical potential of the junction. The transition rate is thus given by the tunneling rate Γ multiplied by the probability to have an electron in the junction at the required energy ϵ ready to jump into the system. The inverse probability to find an initially filled dot empty reads $\Gamma \Delta t\,[1 - f(\epsilon)]$, i.e., here one has to multiply the bare tunneling rate with the probability to have a free slot at energy ϵ in the junction.

1.2.2 Example 2: Interacting quantum dots

Imagine a double quantum dot, where the Coulomb interaction energy is so large that the doubly occupied state can be omitted from the considerations. In essence, only three states remain. Let $|0\rangle$ denote the empty, $|L\rangle$ the left-occupied, and $|R\rangle$ the right-occupied states, respectively. Now assume the two quantum dots to be tunnel-coupled to two adjacent reservoirs but not among themselves, such that particle transport between the dots is prohibited.

Applying this recipe to every dot separately we obtain for the total rate matrix

$$T = \Gamma_L \begin{pmatrix} -f_L & 1 - f_L & 0 \\ +f_L & -(1 - f_L) & 0 \\ 0 & 0 & 0 \end{pmatrix} + \Gamma_R \begin{pmatrix} -f_R & 0 & 1 - f_R \\ 0 & 0 & 0 \\ +f_R & 0 & -(1 - f_R) \end{pmatrix}. \tag{1.14}$$

In fact, a microscopic derivation can be used to confirm the above-mentioned assumptions, and the parameters f_ν become the Fermi functions

$$f_\nu = \frac{1}{e^{\beta_\nu(\epsilon_\nu - \mu_\nu)} + 1} \tag{1.15}$$

with inverse temperature β_ν, chemical potentials μ_ν, and dot level energies ϵ_ν.

1.2.3 Example 3: Diffusion Equation

Consider an infinite chain of coupled compartments as displayed in Fig. 1.2. Now suppose that

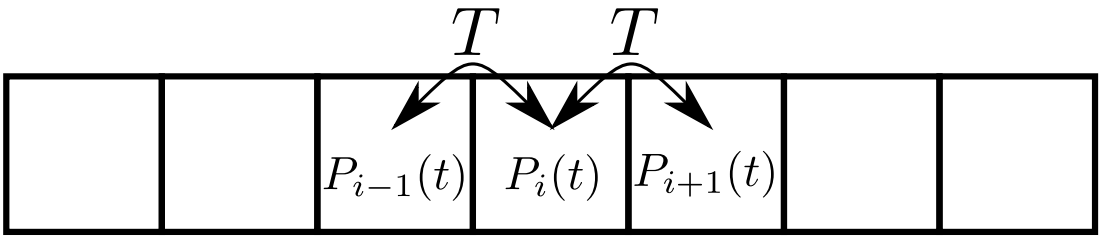

Figure 1.2: Linear chain of compartments coupled with a transition rate T, where only next neighbors are coupled to each other symmetrically.

along the chain, a molecule may move from one compartment to another with a transition rate T that is unbiased, i.e., symmetric in all directions. The evolution of probabilities obeys the infinite-size master equation

$$\begin{aligned} \dot{P}_i(t) &= TP_{i-1}(t) + TP_{i+1}(t) - 2TP_i(t) \\ &= T\Delta x^2 \frac{P_{i-1}(t) + P_{i+1}(t) - 2P_i(t)}{\Delta x^2} \,. \end{aligned} \tag{1.16}$$

We can introduce the probability density $\rho(x_i, t) = P_i(t)/\Delta x$, such that as $\Delta x \to 0$ and $T \to \infty$ in a way that $D = T\Delta x^2$ remains constant, we obtain the partial differential equation

$$\frac{\partial \rho(x,t)}{\partial t} = D\frac{\partial^2 \rho(x,t)}{\partial x^2} \qquad \text{with} \qquad D = T\Delta x^2 \,. \tag{1.17}$$

We note here that while the $P_i(t)$ describe (dimensionless) probabilities, $\rho(x,t)$ describes a time-dependent probability density (with dimension of inverse length).

Such diffusion equations are used to describe the distribution of chemicals in a soluble in the highly diluted limit, the kinetic dynamics of bacteria and further undirected transport processes. From our analysis of master equations, we can immediately conclude that the diffusion equation preserves positivity and total norm, i.e., $\rho(x,t) \geq 0$ and $\int_{-\infty}^{+\infty} \rho(x,t)dx = 1$. Note that it is straightforward to generalize the mapping between master equations and the diffusion equation to the higher-dimensional case.

One can now think of microscopic models where the hopping rates in different directions are not equal (drift) and may also depend on the position (spatially-dependent diffusion coefficient). A corresponding model (in next-neighbor approximation) would be given by

$$\dot{P}_i = T_{i,i-1}P_{i-1}(t) + T_{i,i+1}P_{i+1}(t) - (T_{i-1,i} + T_{i+1,i})P_i(t) \,, \tag{1.18}$$

where $T_{a,b}$ denotes the rate of jumping from b to a. An educated guess is given by the ansatz

$$\begin{aligned}\frac{\partial P}{\partial t} &= \frac{\partial^2}{\partial x^2}\left[A(x)P(x,t)\right] + \frac{\partial}{\partial x}\left[B(x)P(x,t)\right] \\ &\equiv \frac{A_{i-1}P_{i-1} - 2A_iP_i + A_{i+1}P_{i+1}}{\Delta x^2} + \frac{B_{i+1}P_{i+1} - B_{i-1}P_{i-1}}{2\Delta x} \\ &= \left[\frac{A_{i-1}}{\Delta x^2} - \frac{B_{i-1}}{2\Delta x}\right]P_{i-1} - \frac{2A_i}{\Delta x^2}P_i + \left[\frac{A_{i+1}}{\Delta x^2} + \frac{B_{i+1}}{2\Delta x}\right]P_{i+1}\,, \end{aligned} \tag{1.19}$$

which is equivalent to our master equation when

$$A_i = \frac{\Delta x^2}{2}\left[T_{i-1,i} + T_{i+1,i}\right]\,, \qquad B_i = \Delta x\left[T_{i-1,i} - T_{i+1,i}\right]\,. \tag{1.20}$$

We conclude that the Fokker-Planck equation

$$\frac{\partial \rho}{\partial t} = \frac{\partial^2}{\partial x^2}\left[A(x)\rho(x,t)\right] + \frac{\partial}{\partial x}\left[B(x)\rho(x,t)\right] \tag{1.21}$$

with $A(x) \geq 0$ preserves norm and positivity of the probability distribution $\rho(x,t)$.

Exercise 4 (Reaction-Diffusion Equation)**.** *Along a linear chain of compartments consider the master equation for two species*

$$\begin{aligned}\dot{P}_i &= T\left[P_{i-1}(t) + P_{i+1}(t) - 2P_i(t)\right] - \gamma P_i(t)\,, \\ \dot{p}_i &= \tau\left[p_{i-1}(t) + p_{i+1}(t) - 2p_i(t)\right] + \gamma P_i(t),\end{aligned}$$

where $P_i(t)$ may denote the concentration of a molecule that irreversibly reacts with chemicals in the soluble to an inert form characterized by $p_i(t)$. To which partial differential equation does the master equation map?

1.3 Lindblad master equation

Any dynamical evolution equation for the density matrix should (at least in some approximate sense) preserve its interpretation as density matrix, i.e., trace, Hermiticity, and positivity must be preserved. By construction, the measurement postulate and unitary evolution preserve these properties. However, more general evolutions are conceivable. If we constrain ourselves to master equations that are local in time and have constant coefficients, the most general evolution that preserves trace, self-adjointness, and positivity of the density matrix is given by a Lindblad form.

Def. 3 (Lindblad form)**.** *In an N-dimensional system Hilbert space, a master equation of Lindblad form [4, 5] has the structure*

$$\dot{\rho} = \mathcal{L}\rho = -\mathrm{i}\left[H,\rho\right] + \sum_{\alpha,\beta=1}^{N^2-1}\gamma_{\alpha\beta}\left(A_\alpha\rho A_\beta^\dagger - \frac{1}{2}\left\{A_\beta^\dagger A_\alpha,\rho\right\}\right)\,, \tag{1.20}$$

where the Hermitian operator $H = H^\dagger$ can be interpreted as an effective Hamiltonian and $\gamma_{\alpha\beta} = \gamma^*_{\beta\alpha}$ is a positive semidefinite matrix, i.e., it fulfills $\sum_{\alpha\beta} x^*_\alpha \gamma_{\alpha\beta} x_\beta \geq 0$ for all vectors x (or, equivalently that all eigenvalues of $(\gamma_{\alpha\beta})$ are non-negative $\gamma_i \geq 0$).

Exercise 5 (Trace and Hermiticity preservation by Lindblad forms)**.** *Show that the Lindblad form master equation preserves trace and Hermiticity of the density matrix.*

The Lindblad type master equation can be written in simpler form: As the dampening matrix γ is Hermitian, it can be diagonalized by a suitable unitary transformation U, such that $\sum_{\alpha\beta} U_{\alpha'\alpha}\gamma_{\alpha\beta}(U^\dagger)_{\beta\beta'} = \delta_{\alpha'\beta'}\gamma_{\alpha'}$ with $\gamma_\alpha \geq 0$ representing its non-negative eigenvalues. Using this unitary operation, a new set of operators can be defined via $A_\alpha = \sum_{\alpha'} U_{\alpha'\alpha} L_{\alpha'}$. Inserting this decomposition in the master equation, we obtain

$$\begin{aligned}
\dot\rho &= -\mathrm{i}\,[H,\rho] + \sum_{\alpha,\beta=1}^{N^2-1} \gamma_{\alpha\beta}\left(A_\alpha \rho A^\dagger_\beta - \frac{1}{2}\left\{A^\dagger_\beta A_\alpha, \rho\right\}\right) \\
&= -\mathrm{i}\,[H,\rho] + \sum_{\alpha',\beta'}\left[\sum_{\alpha\beta}\gamma_{\alpha\beta}U_{\alpha'\alpha}U^*_{\beta'\beta}\right]\left(L_{\alpha'}\rho L^\dagger_{\beta'} - \frac{1}{2}\left\{L^\dagger_{\beta'}L_{\alpha'},\rho\right\}\right) \\
&= -\mathrm{i}\,[H,\rho] + \sum_\alpha \gamma_\alpha\left(L_\alpha \rho L^\dagger_\alpha - \frac{1}{2}\left\{L^\dagger_\alpha L_\alpha,\rho\right\}\right), \qquad (1.21)
\end{aligned}$$

where γ_α denote the N^2-1 non-negative eigenvalues of the dampening matrix. Furthermore, we can in principle absorb the γ_α in the Lindblad operators $\bar L_\alpha = \sqrt{\gamma_\alpha} L_\alpha$, such that another form of a Lindblad master equation would be

$$\dot\rho = -\mathrm{i}\,[H,\rho] + \sum_\alpha\left(\bar L_\alpha \rho \bar L^\dagger_\alpha - \frac{1}{2}\left\{\bar L^\dagger_\alpha \bar L_\alpha,\rho\right\}\right). \qquad (1.22)$$

Evidently, the representation of a master equation is not unique.

Any other unitary operation would lead to a different non-diagonal form of $\gamma_{\alpha\beta}$ which however describes the same master equation. In addition, we note here that the master equation is not only invariant to unitary transformations of the operators A_α, but in the diagonal representation also to inhomogeneous transformations of the form

$$\begin{aligned}
L_\alpha &\to L'_\alpha = L_\alpha + a_\alpha \\
H &\to H' = H + \frac{1}{2\mathrm{i}}\sum_\alpha \gamma_\alpha\left(a^*_\alpha L_\alpha - a_\alpha L^\dagger_\alpha\right) + b\,, \qquad (1.23)
\end{aligned}$$

with complex numbers a_α and a real number b. The numbers a_α can be chosen such that the Lindblad operators are traceless $\mathrm{Tr}\,\{L_\alpha\} = 0$, which is a popular convention. Choosing b simply corresponds to gauging the energy of the system.

Exercise 6 (Shift invariance)**.** *Show the invariance of the diagonal representation of a Lindblad form master equation (1.21) with respect to the transformation (1.23).*

We would like to demonstrate the preservation of positivity here. Since preservation of Hermiticity follows directly from the Lindblad form, we can – since at any time we know that $\rho = \rho^\dagger$ – formally write the density matrix in its spectral representation

$$\rho(t) = \sum_j P_j(t) \left|\Psi_j(t)\right\rangle \left\langle\Psi_j(t)\right| \tag{1.24}$$

with eigenvalues $P_j(t) \in \mathbb{R}$ (we still have to show that these remain positive) and time-dependent orthonormal eigenstates. The eigenvectors themselves are normalized at all times $\langle\Psi_i(t)|\Psi_j(t)\rangle = \delta_{ij}$, and by acting on this expression with a time derivative we see that $\left\langle\dot{\Psi}_i|\Psi_i\right\rangle + \left\langle\Psi_i|\dot{\Psi}_i\right\rangle = 0$.

Therefore, the time-derivative of the density matrix becomes

$$\dot{\rho} = \sum_j \left[\dot{P}_j \left|\Psi_j\right\rangle \left\langle\Psi_j\right| + P_j \left|\dot{\Psi}_j\right\rangle \left\langle\Psi_j\right| + P_j \left|\Psi_j\right\rangle \left\langle\dot{\Psi}_j\right|\right] , \tag{1.25}$$

and sandwiching the time-derivative above with the eigenvector $|\Psi_i\rangle$ leads to the cancellation of two terms, such that $\langle\Psi_i(t)|\,\dot{\rho}\,|\Psi_i(t)\rangle = \dot{P}_i(t)$. On the other hand, we can also sandwich the right-hand side of the Lindblad equation to obtain

$$\begin{aligned}
\dot{P}_i &= -\mathrm{i}\left\langle\Psi_i\right| H \left|\Psi_i\right\rangle P_i + \mathrm{i} P_i \left\langle\Psi_i\right| H \left|\Psi_i\right\rangle \\
&\quad + \sum_\alpha \gamma_\alpha \left[\left\langle\Psi_i\right| L_\alpha \left(\sum_j P_j \left|\Psi_j\right\rangle \left\langle\Psi_j\right|\right) L_\alpha^\dagger \left|\Psi_i\right\rangle - \left\langle\Psi_i\right| L_\alpha^\dagger L_\alpha \left|\Psi_i\right\rangle P_i\right] \\
&= \sum_j \left(\sum_\alpha \gamma_\alpha |\left\langle\Psi_i\right| L_\alpha \left|\Psi_j\right\rangle|^2\right) P_k - \sum_j \left(\sum_\alpha \gamma_\alpha |\left\langle\Psi_j\right| L_\alpha \left|\Psi_i\right\rangle|^2\right) P_i \,.
\end{aligned} \tag{1.26}$$

This is nothing but a rate equation with positive but time-dependent transition rates

$$R_{j\to i}(t) = \sum_\alpha \gamma_\alpha |\left\langle\Psi_i(t)\right| L_\alpha \left|\Psi_j(t)\right\rangle|^2 \geq 0 \,, \tag{1.27}$$

and with our arguments from Sec. 1.1 it follows that the positivity of the eigenvalues $P_j(t)$ is granted, a valid initialization provided. Unfortunately, the basis within which this simple rate equation holds is time-dependent and also only known after solving the master equation and diagonalizing the solution. It is therefore not very practical in most occasions.

1.3.1 Example: Master Equation for a cavity in a thermal bath

Consider the Lindblad form master equation

$$\begin{aligned}
\dot{\rho} &= -\mathrm{i}\left[\Omega a^\dagger a, \rho\right] + \Gamma(1+n_B)\left[a\rho a^\dagger - \frac{1}{2}a^\dagger a\rho - \frac{1}{2}\rho a^\dagger a\right] \\
&\quad + \Gamma n_B \left[a^\dagger \rho a - \frac{1}{2}aa^\dagger\rho - \frac{1}{2}\rho aa^\dagger\right] ,
\end{aligned} \tag{1.28}$$

with bosonic operators $\left[a, a^\dagger\right] = \mathbf{1}$ and Bose-Einstein bath occupation $n_B = \left[e^{\beta\Omega} - 1\right]^{-1}$ and cavity frequency Ω. In Fock-space representation, these operators act as $a^\dagger |n\rangle = \sqrt{n+1}\,|n+1\rangle$ (where $0 \leq n < \infty$), such that the above master equation couples only the diagonals of the density matrix $\rho_n = \langle n|\,\rho\,|n\rangle$ to each other. This is directly visible by sandwiching the master equation with $\langle n|\ldots|n\rangle$

$$\begin{aligned}\dot{\rho_n} &= \Gamma(1+n_B)\left[(n+1)\rho_{n+1} - n\rho_n\right] + \Gamma n_B\left[n\rho_{n-1} - (n+1)\rho_n\right] \\ &= \Gamma n_B n\rho_{n-1} - \Gamma\left[n + (2n+1)n_B\right]\rho_n + \Gamma(1+n_B)(n+1)\rho_{n+1}\,, \end{aligned} \tag{1.29}$$

which shows that the rate equation arising for the diagonals even has a simple tri-diagonal form. That makes it particularly easy to calculate its stationary state recursively, since the boundary solution $n_B\bar{\rho}_0 = (1+n_B)\bar{\rho}_1$ implies for all n the relation

$$\frac{\bar{\rho}_{n+1}}{\bar{\rho}_n} = \frac{n_B}{1+n_B} = e^{-\beta\Omega}\,, \tag{1.30}$$

i.e., the stationary state is a thermalized Gibbs state with the same temperature as the reservoir.

Exercise 7 (Moments)**.** *Calculate the expectation value of the number operator $\hat{n} = a^\dagger a$ and its square $\hat{n}^2 = a^\dagger a a^\dagger a$ in the stationary state of the master equation (1.28).*

In general, the matrix elements of the density matrix $\rho_{nm} = \langle n|\,\rho\,|m\rangle$ will obey

$$\begin{aligned}\dot{\rho}_{nm} &= -\mathrm{i}\Omega(n-m)\rho_{nm} + \Gamma(1+n_B)\left[\sqrt{(n+1)(m+1)}\rho_{n+1,m+1} - \frac{n+m}{2}\rho_{nm}\right] \\ &\quad +\Gamma n_B\left[\sqrt{nm}\rho_{n-1,m-1} - \frac{n+1+m+1}{2}\rho_{nm}\right] \\ &= \left[-\mathrm{i}\Omega(n-m) - \Gamma\frac{(1+n_B)(n+m) + n_B(n+1+m+1)}{2}\right]\rho_{nm} \\ &\quad +\Gamma(1+n_B)\sqrt{(n+1)(m+1)}\rho_{n+1,m+1} + \Gamma n_B\sqrt{nm}\rho_{n-1,m-1}\,, \end{aligned} \tag{1.31}$$

and it is straightforward to see that vanishing coherences (off-diagonal matrix elements) $\bar{\rho}_{n\neq m} = 0$ are a valid steady-state solution. Not being aware of the Lindblad form we may nevertheless ask whether there are other solutions. The above equation shows that among the coherences, only few couple, and by arranging them in a favorable form we can write these equations in matrix form with infinite-dimensional tri-diagonal matrices (for brevity we use $\gamma = \Gamma n_B$ and $\bar{\gamma} = \Gamma(1+n_B)$)

$$W = \begin{pmatrix} & \vdots & & \\ \ddots & +\bar{\gamma}\sqrt{nm} & 0 & \\ \ldots\ +\gamma\sqrt{nm} & \left[-\mathrm{i}\Omega(n-m) - \bar{\gamma}\frac{n+m}{2} - \gamma\frac{n+1+m+1}{2}\right] & +\bar{\gamma}\sqrt{(n+1)(m+1)} & \ldots \\ 0 & +\gamma\sqrt{(n+1)(m+1)} & \ddots & \\ & \vdots & & \end{pmatrix}. \tag{1.32}$$

By examining every column in detail, we see that the real part of the diagonal entries has always larger magnitude than the sum of the off-diagonal entries, since

$$\bar{\gamma}\frac{n+m}{2} + \gamma\frac{n+1+m+1}{2} \geq +\bar{\gamma}\sqrt{nm} + \gamma\sqrt{(n+1)(m+1)}\,. \tag{1.33}$$

The above equation naturally follows from $(x-y)^2 = x^2 + y^2 - 2xy \geq 0$, with $x^2 \to \bar{\gamma} n$ and $y^2 \to \bar{\gamma} m$ or $x^2 \to \gamma(n+1)$ and $y^2 \to \gamma(m+1)$, respectively. Furthermore, we see that equality actually only holds for the diagonal elements ($n = m$). From Gershgorins circle theorem, we can therefore conclude that all the eigenvalues of the matrix W have for $n \neq m$ a negative real part. Consequently, the coherences must decay and the stationary state only contains populations in the Fock space representation.

A simpler way to solve the particular master equation at hand is by using it to calculate the expectation value $\langle n \rangle = \mathrm{Tr}\left\{a^\dagger a \rho\right\}$ of the particle number operator

$$\begin{aligned} \frac{d}{dt}\langle n \rangle &= \left\langle a^\dagger a \dot{\rho} \right\rangle \\ &= +\Gamma(1+n_B)\mathrm{Tr}\left\{\left[a^\dagger a^\dagger a a - \left(a^\dagger a\right)^2\right]\rho\right\} \\ &\quad +\Gamma n_B \mathrm{Tr}\left\{\left[a a^\dagger a a^\dagger - \frac{1}{2}a^\dagger a a a^\dagger - \frac{1}{2}a a^\dagger a^\dagger a\right]\rho\right\}, \end{aligned} \tag{1.34}$$

where we have used the invariance of the trace under cyclic permutations to move the density matrix to the right. Further using the bosonic commutation relations we get the very simple equation

$$\frac{d}{dt}\langle n \rangle = -\Gamma\left(1+n_B\right)\langle n \rangle + \Gamma n_B\left(1+\langle n \rangle\right), \tag{1.35}$$

which yields the same steady state solution

$$\frac{\bar{n}}{1+\bar{n}} = \frac{n_B}{1+n_B} = e^{-\beta\Omega}, \tag{1.36}$$

which we had before in Eq. (1.30). Mostly, one is not as lucky as in this case, that the resulting evolution equations close with just a single variable (see below), but deriving and solving equations of motion for observables from master equations is a popular tool for solving them.

1.3.2 Master Equation for a driven cavity

When the cavity is driven with a laser and simultaneously coupled to a vacuum bath $n_B = 0$, one often uses the time-dependent master equation

$$\dot{\rho_\mathrm{S}} = -\mathrm{i}\left[\Omega a^\dagger a + \frac{P}{2}e^{+\mathrm{i}\omega t}a + \frac{P^*}{2}e^{-\mathrm{i}\omega t}a^\dagger, \rho_\mathrm{S}\right] + \gamma\left[a\rho_\mathrm{S}a^\dagger - \frac{1}{2}a^\dagger a\rho_\mathrm{S} - \frac{1}{2}\rho_\mathrm{S}a^\dagger a\right] \tag{1.37}$$

with the Laser frequency ω and amplitude P. With using that $e^{+\mathrm{i}\omega a^\dagger a t} a e^{-\mathrm{i}\omega a^\dagger a t} = a e^{-\mathrm{i}\omega t}$ we see that the transformation $\rho = e^{+\mathrm{i}\omega a^\dagger a t}\rho_\mathrm{S} e^{-\mathrm{i}\omega a^\dagger a t}$ maps to a time-independent master equation

$$\dot{\rho} = -\mathrm{i}\left[(\Omega-\omega)a^\dagger a + \frac{P}{2}a + \frac{P^*}{2}a^\dagger, \rho\right] + \gamma\left[a\rho a^\dagger - \frac{1}{2}a^\dagger a\rho - \frac{1}{2}\rho a^\dagger a\right]. \tag{1.38}$$

Exercise 8 (Transformation to a time-independent frame)**.** *Show that this is true.*

This equation couples coherences and populations in the Fock space representation, and in the long-term limit we will also observe non-vanishing coherences. Nevertheless, it is possible to solve for the evolution of expectation values by just making use of the bosonic commutation relations. Here, the basic idea is to obtain a closed set of differential equations for observables

$$\left\langle \dot{O}_\alpha \right\rangle = \mathrm{Tr}\left\{O_\alpha \dot{\rho}\right\} = \mathrm{Tr}\left\{O_\alpha \mathcal{L}\rho\right\} = \sum_{\alpha\beta} \Gamma_{\alpha\beta} \left\langle O_\beta \right\rangle \,, \tag{1.39}$$

where the coefficients $\Gamma_{\alpha\beta}$ have to be obtained from inspection of the particular model, in a similar way as we did in the previous section.

Exercise 9 (Coherent state)**.** *Using the driven cavity master equation, show that the stationary expectation value of the cavity occupation fulfills*

$$\lim_{t\to\infty} \left\langle a^\dagger a \right\rangle = \frac{|P|^2}{\gamma^2 + 4(\Omega-\omega)^2}$$

One may wonder how many coefficients $\Gamma_{\alpha\beta}$ will arise, and in general, for a system Hilbert space dimension of N we can have N^2-1 independent Hermitian operators. For systems with an infinite Hilbert space one is in general not guaranteed to end up with a finite number of observables.

Alternatively, we can employ *coherent states* for the solution. These are defined as eigenstates of the annihilation operator

$$a\left|\alpha\right\rangle = \alpha\left|\alpha\right\rangle \tag{1.39}$$

and can also be represented as Fock states. It is indeed possible to show that the density matrix

$$\bar{\rho} = \left|\alpha\right\rangle\left\langle\alpha\right| \,, \qquad \alpha = \frac{-\mathrm{i}P^*}{\gamma + 2\mathrm{i}(\Omega-\omega)} \,, \tag{1.40}$$

is indeed a stationary solution of the above master equation. By inserting this ansatz we get terms either proportional to $\left|\alpha\right\rangle\left\langle\alpha\right|$, $a^\dagger\left|\alpha\right\rangle\left\langle\alpha\right|$, and $\left|\alpha\right\rangle\left\langle\alpha\right| a$, which we can group as

$$\begin{aligned} 0 \;=\; & \left|\alpha\right\rangle\left\langle\alpha\right| \left[-\mathrm{i}\frac{P}{2}\alpha + \mathrm{i}\frac{P^*}{2}\alpha^* + \gamma|\alpha|^2\right] \\ & + a^\dagger\left|\alpha\right\rangle\left\langle\alpha\right| \left[-\mathrm{i}\frac{P^*}{2} - \frac{\gamma}{2}\alpha - \mathrm{i}(\Omega-\omega)\alpha\right] \\ & + \left|\alpha\right\rangle\left\langle\alpha\right| a \left[+\mathrm{i}\frac{P}{2} - \frac{\gamma}{2}\alpha^* + \mathrm{i}(\Omega-\omega)\alpha^*\right] \,. \end{aligned} \tag{1.41}$$

By inserting the correct value of α, we see that all terms in brackets vanish, and in the rotating frame, we have a stationary state. The state back in the original frame is non-stationary and reads asymptotically

$$\rho(t) \to e^{-\mathrm{i}\omega a^\dagger a t}\left|\alpha\right\rangle\left\langle\alpha\right| e^{+\mathrm{i}\omega a^\dagger a t} \,. \tag{1.42}$$

1.4 Most general evolution

Finally, we mention here that the most general evolution preserving all the nice properties of a density matrix is the so-called Kraus map. A density matrix ρ (Hermitian, positive definite, and with trace one) can be mapped to another density matrix ρ' via

$$\rho' = \sum_{\alpha\beta} \gamma_{\alpha\beta} A_\alpha \rho A_\beta^\dagger \,, \qquad \text{with} \qquad \sum_{\alpha\beta} \gamma_{\alpha\beta} A_\beta^\dagger A_\alpha = \mathbf{1} \,, \tag{1.43}$$

where the prefactors $\gamma_{\alpha\beta}$ form a Hermitian ($\gamma_{\alpha\beta} = \gamma^*_{\beta\alpha}$) and positive definite ($\sum_{\alpha\beta} x^*_\alpha \gamma_{\alpha\beta} x_\beta \geq 0$ or equivalently all eigenvalues of $(\gamma_{\alpha\beta})$ are non-negative) matrix. It is straightforward to see that the above map preserves trace and Hermiticity of the density matrix. In addition, ρ' also inherits the positivity from $\rho = \sum_n P_n \left|n\right\rangle \left\langle n\right|$

$$\begin{aligned} \left\langle \Psi\right| \rho' \left|\Psi\right\rangle &= \sum_{\alpha\beta} \gamma_{\alpha\beta} \left\langle \Psi\right| A_\alpha \rho A_\beta^\dagger \left|\Psi\right\rangle = \sum_n P_n \sum_{\alpha\beta} \gamma_{\alpha\beta} \left\langle \Psi\right| A_\alpha \left|n\right\rangle \left\langle n\right| A_\beta^\dagger \left|\Psi\right\rangle \\ &= \sum_n \underbrace{P_n}_{\geq 0} \underbrace{\sum_{\alpha\beta} \left(\left\langle n\right| A_\alpha^\dagger \left|\Psi\right\rangle\right)^* \gamma_{\alpha\beta} \left\langle n\right| A_\beta^\dagger \left|\Psi\right\rangle}_{\geq 0} \geq 0 \,. \end{aligned} \tag{1.44}$$

Since the matrix $\gamma_{\alpha\beta}$ is Hermitian, it can be diagonalized by a suitable unitary transformation, and we introduce the new operators $A_\alpha = \sum_{\alpha'} U_{\alpha\alpha'} \bar{K}_{\alpha'}$

$$\begin{aligned} \rho' &= \sum_{\alpha\beta} \sum_{\alpha'\beta'} \gamma_{\alpha\beta} U_{\alpha\alpha'} \bar{K}_{\alpha'} \rho U^*_{\beta\beta'} K^\dagger_{\beta'} = \sum_{\alpha'\beta'} \bar{K}_{\alpha'} \rho \bar{K}^\dagger_{\beta'} \underbrace{\sum_{\alpha\beta} U_{\alpha\alpha'} \gamma_{\alpha\beta} U^*_{\beta\beta'}}_{\gamma_{\alpha'} \delta_{\alpha'\beta'}} \\ &= \sum_\alpha \gamma_\alpha \bar{K}_\alpha \rho \bar{K}^\dagger_\alpha \,, \end{aligned} \tag{1.45}$$

where $\gamma_\alpha \geq 0$ represent the eigenvalues of the matrix $(\gamma_{\alpha\beta})$. Since these are by construction positive, we introduce further new operators $K_\alpha = \sqrt{\gamma_\alpha} \bar{K}_\alpha$ to obtain the simplest representation of a Kraus map.

Def. 4 (Kraus map)**.** *The map*

$$\rho(t + \Delta t) = \sum_\alpha K_\alpha(t, \Delta t) \rho(t) K^\dagger_\alpha(t, \Delta t) \tag{1.46}$$

with Kraus operators $K_\alpha(t, \Delta t)$ obeying the relation $\sum_\alpha K^\dagger_\alpha(t, \Delta t) K_\alpha(t, \Delta t) = \mathbf{1}$ preserves Hermiticity, trace, and positivity of the density matrix.

Obviously, both unitary evolution and evolution under measurement are just special cases of a Kraus map. Though Kraus maps are heavily used in quantum information, they are not often very easy to interpret. For example, it is not straightforward to identify the unitary and the non-unitary part induced the Kraus map.

Chapter 2

Obtaining a Master Equation

2.1 Mathematical Prerequisites

Master equations are often used to describe the dynamics of systems interacting with one or many large reservoirs (baths). To derive them from microscopic models – including the Hamiltonian of the full system – requires to review some basic mathematical concepts.

2.1.1 Tensor Product

The greatest advantage of the density matrix formalism is visible when quantum systems composed of several subsystems are considered. Roughly speaking, the tensor product represents a way to construct a larger vector space from two (or more) smaller vector spaces.

Def. 5 (Tensor Product)**.** *Let V and W be Hilbert spaces (vector spaces with scalar product) of dimension m and n with basis vectors $\{|v\rangle\}$ and $\{|w\rangle\}$, respectively. Then $V \otimes W$ is a Hilbert space of dimension $m \cdot n$, and a basis is spanned by $\{|v\rangle \otimes |w\rangle\}$, which is a set combining every basis vector of V with every basis vector of W.*

Mathematical properties

- *Bilinearity* $(z_1 |v_1\rangle + z_2 |v_2\rangle) \otimes |w\rangle = z_1 |v_1\rangle \otimes |w\rangle + z_2 |v_2\rangle \otimes |w\rangle$
- *operators acting on the combined Hilbert space $A \otimes B$ act on the basis states as* $(A \otimes B)(|v\rangle \otimes |w\rangle) = (A |v\rangle) \otimes (B |w\rangle)$
- *any linear operator on $V \otimes W$ can be decomposed as* $C = \sum_i c_i A_i \otimes B_i$
- *the scalar product is inherited in the natural way, i.e., one has for* $|a\rangle = \sum_{ij} a_{ij} |v_i\rangle \otimes |w_j\rangle$ *and* $|b\rangle = \sum_{k\ell} b_{k\ell} |v_k\rangle \otimes |w_\ell\rangle$ *the scalar product* $\langle a|b\rangle = \sum_{ijk\ell} a^*_{ij} b_{k\ell} \langle v_i|v_k\rangle \langle w_j|w_\ell\rangle = \sum_{ij} a^*_{ij} b_{ij}$

If more than just two vector spaces are combined to form a larger vector space, the dimension of the joint vector space grows rapidly, as e.g. exemplified by the case of a qubit: Its Hilbert space is just spanned by two vectors $|0\rangle$ and $|1\rangle$. The joint Hilbert space of two qubits is four-dimensional, of three qubits 8-dimensional, and of n qubits 2^n-dimensional. Eventually, this exponential growth of the Hilbert space dimension for composite quantum systems is at the heart of quantum computing.

Exercise 10 (Tensor Products of Operators)**.** *Let* $\boldsymbol{\sigma}$ *denote the Pauli matrices, i.e.,*

$$\sigma^1 = \begin{pmatrix} 0 & +1 \\ +1 & 0 \end{pmatrix} \qquad \sigma^2 = \begin{pmatrix} 0 & -\mathrm{i} \\ +\mathrm{i} & 0 \end{pmatrix} \qquad \sigma^3 = \begin{pmatrix} +1 & 0 \\ 0 & -1 \end{pmatrix}$$

Compute the trace of the operator

$$\Sigma = a\mathbf{1} \otimes \mathbf{1} + \sum_{i=1}^{3} \alpha_i \sigma^i \otimes \mathbf{1} + \sum_{j=1}^{3} \beta_j \mathbf{1} \otimes \sigma^j + \sum_{i,j=1}^{3} a_{ij} \sigma^i \otimes \sigma^j \,.$$

Since the scalar product is inherited, this typically enables a convenient calculation of the trace in case of a few operator decomposition, e.g., for just two operators

$$\begin{aligned} \mathrm{Tr}\left\{A \otimes B\right\} &= \sum_{n_A, n_B} \langle n_A, n_B | \, A \otimes B \, | n_A, n_B \rangle \\ &= \left[\sum_{n_A} \langle n_A | \, A \, | n_A \rangle\right] \left[\sum_{n_B} \langle n_B | \, B \, | n_B \rangle\right] \\ &= \mathrm{Tr}_A\{A\}\mathrm{Tr}_B\{B\} \,, \end{aligned} \tag{2.-1}$$

where $\mathrm{Tr}_{A/B}$ denote the trace in the Hilbert space of A and B, respectively.

2.1.2 The partial trace

For composite systems, it is usually not necessary to keep all information of the complete system in the density matrix. Rather, one would like to have a density matrix that encodes all the information on a particular subsystem only. Obviously, the map $\rho \to \mathrm{Tr_B}\left\{\rho\right\}$ to such a reduced density matrix should leave all expectation values of observables A acting only on the considered subsystem invariant, i.e.,

$$\mathrm{Tr}\left\{A \otimes \mathbf{1}\rho\right\} = \mathrm{Tr}\left\{A \mathrm{Tr_B}\left\{\rho\right\}\right\} \,. \tag{2.0}$$

If this basic condition was not fulfilled, there would be no point in defining such a thing as a reduced density matrix: Measurement would yield different results depending on the Hilbert space of the experimenters feeling.

Def. 6 (Partial Trace)**.** *Let* $|a_1\rangle$ *and* $|a_2\rangle$ *be vectors of state space* A *and* $|b_1\rangle$ *and* $|b_2\rangle$ *vectors of state space* B*. Then, the partial trace over state space* B *is defined via*

$$\mathrm{Tr_B}\left\{|a_1\rangle\langle a_2| \otimes |b_1\rangle\langle b_2|\right\} = |a_1\rangle\langle a_2| \, \mathrm{Tr}\left\{|b_1\rangle\langle b_2|\right\} \,. \tag{2.1}$$

The partial trace is linear, such that the partial trace of arbitrary operators is calculated similarly. By choosing the $|a_\alpha\rangle$ and $|b_\gamma\rangle$ as an orthonormal basis in the respective Hilbert space,

one may therefore calculate the most general partial trace via

$$\begin{aligned}
\mathrm{Tr_B}\{C\} &= \mathrm{Tr_B}\left\{\sum_{\alpha\beta\gamma\delta} c_{\alpha\beta\gamma\delta}\,|a_\alpha\rangle\langle a_\beta|\otimes|b_\gamma\rangle\langle b_\delta|\right\} \\
&= \sum_{\alpha\beta\gamma\delta} c_{\alpha\beta\gamma\delta}\mathrm{Tr_B}\{|a_\alpha\rangle\langle a_\beta|\otimes|b_\gamma\rangle\langle b_\delta|\} \\
&= \sum_{\alpha\beta\gamma\delta} c_{\alpha\beta\gamma\delta}\,|a_\alpha\rangle\langle a_\beta|\,\mathrm{Tr}\{|b_\gamma\rangle\langle b_\delta|\} \\
&= \sum_{\alpha\beta\gamma\delta} c_{\alpha\beta\gamma\delta}\,|a_\alpha\rangle\langle a_\beta|\sum_\epsilon \langle b_\epsilon|b_\gamma\rangle\langle b_\delta|b_\epsilon\rangle \\
&= \sum_{\alpha\beta}\left[\sum_\gamma c_{\alpha\beta\gamma\gamma}\right]|a_\alpha\rangle\langle a_\beta|\,. \qquad (2.2)
\end{aligned}$$

The definition 6 is the only linear map that respects the invariance of expectation values.

Exercise 11 (Partial Trace)**.** *Compute the partial trace of a pure density matrix* $\rho = |\Psi\rangle\langle\Psi|$ *in the bipartite state*

$$|\Psi\rangle = \frac{1}{\sqrt{2}}(|01\rangle + |10\rangle) \equiv \frac{1}{\sqrt{2}}(|0\rangle\otimes|1\rangle + |1\rangle\otimes|0\rangle)$$

2.2 Derivations for Open Quantum Systems

In some cases, it is possible to derive a master equation rigorously based only on a few assumptions. Open quantum systems for example are mostly treated as part of a much larger closed quantum system (the union of system and bath), where the partial trace is used to eliminate the unwanted (typically many) degrees of freedom of the bath, see Fig. 2.1. Technically speaking, we will consider

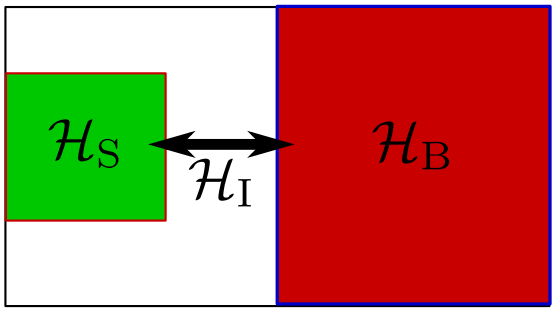

Figure 2.1: An open quantum system can be conceived as being part of a larger closed quantum system, where the system part ($\mathcal{H}_\mathrm{S}$) is coupled to the bath ($\mathcal{H}_\mathrm{B}$) via the interaction Hamiltonian $\mathcal{H}_\mathrm{I}$.

Hamiltonians of the form

$$H = \mathcal{H}_\mathrm{S}\otimes\mathbf{1} + \mathbf{1}\otimes\mathcal{H}_\mathrm{B} + \mathcal{H}_\mathrm{I}\,, \qquad (2.2)$$

where the system and bath Hamiltonians act only on the system and bath Hilbert space, respectively. Since the index clearly defines on which space the respective Hamiltonian is acting, we often also write

$$H = \mathcal{H}_\mathrm{S} + \mathcal{H}_\mathrm{B} + \mathcal{H}_\mathrm{I} \,. \tag{2.3}$$

It is important to note that the interaction Hamiltonian acts on both Hilbert spaces

$$\mathcal{H}_\mathrm{I} = \sum_\alpha A_\alpha \otimes B_\alpha \,, \tag{2.4}$$

where the summation boundaries are in the worst case limited by the dimension of the system Hilbert space $\alpha < N^2 - 1$. As we consider physical observables here, it is required that all Hamiltonians of system, bath, and interaction are self-adjoint.

Exercise 12 (Hermiticity of Couplings)**.** *Show that it is always possible to choose Hermitian coupling operators $A_\alpha = A_\alpha^\dagger$ and $B_\alpha = B_\alpha^\dagger$ using that $\mathcal{H}_\mathrm{I} = \mathcal{H}_\mathrm{I}^\dagger$.*

2.2.1 Standard Quantum-Optical Derivation

Here, we will derive the master equation generally, for an arbitrary system coupled to a thermal environment. This will at first appear a bit technical but may prove useful later-on, since it also allows us to show general properties for later reference.

In this section, we will use the example

$$H = \Omega a^\dagger a + (a + a^\dagger) \sum_k \left(h_k b_k + h_k^* b_k^\dagger \right) + \sum_k \omega_k b_k^\dagger b_k \,, \tag{2.5}$$

which describes a harmonic oscillator coupled to many other oscillator modes via their x-coordinates, and which may therefore serve to illustrate the general derivation.

Interaction Picture

When the interaction $\mathcal{H}_\mathrm{I}$ is small, it is justified to apply perturbation theory. The von-Neumann equation in the joint total quantum system

$$\dot{\rho} = -\mathrm{i} \left[\mathcal{H}_\mathrm{S} + \mathcal{H}_\mathrm{B} + \mathcal{H}_\mathrm{I}, \rho \right] \tag{2.6}$$

describes the full evolution of the combined density matrix. This equation can be formally solved by the unitary evolution $\rho(t) = e^{-\mathrm{i}Ht} \rho_0 e^{+\mathrm{i}Ht}$, which however is impractical to compute as H involves too many degrees of freedom.

Transforming to the interaction picture

$$\boldsymbol{\rho}(t) = e^{+\mathrm{i}(\mathcal{H}_\mathrm{S} + \mathcal{H}_\mathrm{B})t} \rho(t) e^{-\mathrm{i}(\mathcal{H}_\mathrm{S} + \mathcal{H}_\mathrm{B})t} \,, \tag{2.7}$$

which will be denoted by bold symbols throughout, the von-Neumann equation transforms into

$$\dot{\boldsymbol{\rho}} = -\mathrm{i} \left[\boldsymbol{\mathcal{H}}_\mathbf{I}(t), \boldsymbol{\rho} \right] \,, \tag{2.8}$$

where the in general time-dependent interaction Hamiltonian

$$\begin{aligned}\boldsymbol{\mathcal{H}_{\mathrm{I}}}(t) &= e^{+\mathrm{i}(\mathcal{H}_{\mathrm{S}}+\mathcal{H}_{\mathrm{B}})t}\mathcal{H}_{\mathrm{I}}e^{-\mathrm{i}(\mathcal{H}_{\mathrm{S}}+\mathcal{H}_{\mathrm{B}})t} = \sum_{\alpha} e^{+i\mathcal{H}_{\mathrm{S}}t}A_{\alpha}e^{-\mathrm{i}\mathcal{H}_{\mathrm{S}}t}\otimes e^{+i\mathcal{H}_{\mathrm{B}}t}B_{\alpha}e^{-\mathrm{i}\mathcal{H}_{\mathrm{B}}t} \\ &= \sum_{\alpha} \boldsymbol{A_{\alpha}}(t)\otimes \boldsymbol{B_{\alpha}}(t) \end{aligned} \tag{2.9}$$

allows to perform perturbation theory.

Without loss of generality we will for simplicity assume here the case of Hermitian coupling operators $A_\alpha = A_\alpha^\dagger$ and $B_\alpha = B_\alpha^\dagger$. One heuristic way to perform perturbation theory is to formally integrate Eq. (2.8) and to re-insert the result in the r.h.s. of Eq. (2.8). The time-derivative of the system density matrix is obtained by performing the partial trace

$$\dot{\boldsymbol{\rho}}_{\mathbf{S}} = -\mathrm{i}\mathrm{Tr}_{\mathrm{B}}\left\{[\boldsymbol{\mathcal{H}_{\mathrm{I}}}(\boldsymbol{t}),\rho_0]\right\} - \int_0^t \mathrm{Tr}_{\mathrm{B}}\left\{[\boldsymbol{\mathcal{H}_{\mathrm{I}}}(t),[\boldsymbol{\mathcal{H}_{\mathrm{I}}}(t'),\boldsymbol{\rho}(t')]]\,dt'\right\}\,. \tag{2.10}$$

This integro-differential equation is still exact but unfortunately not closed as the r.h.s. does not depend on ρ_{S} but the full density matrix at all previous times.

For our particular example, we can show that the master equation in the interaction picture reads

$$\dot{\boldsymbol{\rho}} = -\mathrm{i}\left[\left(ae^{-\mathrm{i}\Omega t}+a^\dagger e^{+\mathrm{i}\Omega t}\right)\sum_k\left(h_k b_k e^{-\mathrm{i}\omega_k t}+h_k^* b_k^\dagger e^{+\mathrm{i}\omega_k t}\right),\boldsymbol{\rho}\right]\,. \tag{2.11}$$

We see that there is just one system and bath coupling operator, respectively, and that therefore these operators are already Hermitian by construction. We see that the time-dependent interaction Hamiltonian has many oscillatory terms, and evaluating all these terms seems challenging at first.

Born approximation

To close the above equation, we employ factorization of the initial density matrix

$$\rho_0 = \rho_{\mathrm{S}}^0\otimes\bar{\rho}_{\mathrm{B}} \tag{2.12}$$

together with perturbative considerations: Assuming that $\boldsymbol{\mathcal{H}_{\mathrm{I}}}(t) = \mathcal{O}\{\lambda\}$ with λ beeing a small dimensionless perturbation parameter (solely used for bookkeeping purposes here) and that the environment is so large such that it is hardly affected by the presence of the system, we may formally expand the full density matrix

$$\boldsymbol{\rho}(t) = \boldsymbol{\rho_{\mathbf{S}}}(t)\otimes\bar{\rho}_{\mathrm{B}} + \mathcal{O}\{\lambda\}\,, \tag{2.13}$$

where the neglect of all higher orders is known as **Born approximation**. Eq. (2.10) demonstrates that the Born approximation is equivalent to a perturbation theory in the interaction Hamiltonian

$$\dot{\boldsymbol{\rho}}_{\mathbf{S}} = -\mathrm{i}\mathrm{Tr}_{\mathrm{B}}\left\{[\boldsymbol{\mathcal{H}_{\mathrm{I}}}(\boldsymbol{t}),\rho_0]\right\} - \int_0^t \mathrm{Tr}_{\mathrm{B}}\left\{[\boldsymbol{\mathcal{H}_{\mathrm{I}}}(t),[\boldsymbol{\mathcal{H}_{\mathrm{I}}}(t'),\boldsymbol{\rho_{\mathbf{S}}}(t')\otimes\bar{\rho}_{\mathrm{B}}]]\,dt'\right\} + \mathcal{O}\{\lambda^3\}\,. \tag{2.14}$$

Using the decomposition of the interaction Hamiltonian (2.4), this obviously yields a closed equation for the system density matrix

$$\begin{aligned}\dot{\boldsymbol{\rho}}_{\mathbf{S}} &= -\mathrm{i}\sum_{\alpha}\left[\boldsymbol{A}_{\boldsymbol{\alpha}}(t)\rho_{\mathrm{S}}^{0}\mathrm{Tr}\left\{\boldsymbol{B}_{\boldsymbol{\alpha}}(t)\bar{\rho}_{\mathrm{B}}\right\}-\rho_{\mathrm{S}}^{0}\boldsymbol{A}_{\boldsymbol{\alpha}}(t)\mathrm{Tr}\left\{\bar{\rho}_{\mathrm{B}}\boldsymbol{B}_{\boldsymbol{\alpha}}(t)\right\}\right]-\sum_{\alpha\beta}\int_{0}^{t}\Big[\\ &\quad+\boldsymbol{A}_{\boldsymbol{\alpha}}(t)\boldsymbol{A}_{\boldsymbol{\beta}}(t')\boldsymbol{\rho}_{\mathbf{S}}(t')\mathrm{Tr}\left\{\boldsymbol{B}_{\boldsymbol{\alpha}}(t)\boldsymbol{B}_{\boldsymbol{\beta}}(t')\bar{\rho}_{\mathrm{B}}\right\}\\ &\quad-\boldsymbol{A}_{\boldsymbol{\alpha}}(t)\boldsymbol{\rho}_{\mathbf{S}}(t')\boldsymbol{A}_{\boldsymbol{\beta}}(t')\mathrm{Tr}\left\{\boldsymbol{B}_{\boldsymbol{\alpha}}(t)\bar{\rho}_{\mathrm{B}}\boldsymbol{B}_{\boldsymbol{\beta}}(t')\right\}\\ &\quad-\boldsymbol{A}_{\boldsymbol{\beta}}(t')\boldsymbol{\rho}_{\mathbf{S}}(t')\boldsymbol{A}_{\boldsymbol{\alpha}}(t)\mathrm{Tr}\left\{\boldsymbol{B}_{\boldsymbol{\beta}}(t')\bar{\rho}_{\mathrm{B}}\boldsymbol{B}_{\boldsymbol{\alpha}}(t)\right\}\\ &\quad+\boldsymbol{\rho}_{\mathbf{S}}(t')\boldsymbol{A}_{\boldsymbol{\beta}}(t')\boldsymbol{A}_{\boldsymbol{\alpha}}(t)\mathrm{Tr}\left\{\bar{\rho}_{\mathrm{B}}\boldsymbol{B}_{\boldsymbol{\beta}}(t')\boldsymbol{B}_{\boldsymbol{\alpha}}(t)\right\}\Big]dt'\,. \end{aligned} \tag{2.15}$$

Without loss of generality, we proceed by assuming that the single coupling operator expectation value vanishes

$$\mathrm{Tr}\left\{\boldsymbol{B}_{\boldsymbol{\alpha}}(t)\bar{\rho}_{\mathrm{B}}\right\}=0\,. \tag{2.16}$$

This situation can always be constructed by simultaneously modifying system Hamiltonian $\mathcal{H}_{\mathrm{S}}$ and coupling operators A_α, see exercise 13.

For our example we see that for a thermal reservoir this is fulfilled by construction, since

$$\mathrm{Tr}\left\{b_k e^{-\beta\omega_k b_k^\dagger b_k}\right\}=0\,. \tag{2.17}$$

Exercise 13 (Vanishing single-operator expectation values)**.** *Show that by modifying system and interaction Hamiltonian*

$$\mathcal{H}_{\mathrm{S}}\to\mathcal{H}_{\mathrm{S}}+\sum_{\alpha}g_\alpha A_\alpha\,,\qquad B_\alpha\to B_\alpha-g_\alpha\mathbf{1} \tag{2.18}$$

one can construct a situation where $\mathrm{Tr}\left\{\boldsymbol{B}_{\boldsymbol{\alpha}}(t)\bar{\rho}_{\mathrm{B}}\right\}=0$*. Determine* g_α*.*

Using the cyclic property of the trace, we obtain

$$\begin{aligned}\dot{\boldsymbol{\rho}}_{\mathbf{S}} &= -\sum_{\alpha\beta}\int_{0}^{t}dt'\Big[C_{\alpha\beta}(t,t')\left[\boldsymbol{A}_{\boldsymbol{\alpha}}(t),\boldsymbol{A}_{\boldsymbol{\beta}}(t')\boldsymbol{\rho}_{\mathbf{S}}(t')\right]\\ &\quad+C_{\beta\alpha}(t',t)\left[\boldsymbol{\rho}_{\mathbf{S}}(t')\boldsymbol{A}_{\boldsymbol{\beta}}(t'),\boldsymbol{A}_{\boldsymbol{\alpha}}(t)\right]\Big]\end{aligned} \tag{2.19}$$

with the bath correlation function

$$C_{\alpha\beta}(t_1,t_2)=\mathrm{Tr}\left\{\boldsymbol{B}_{\boldsymbol{\alpha}}(t_1)\boldsymbol{B}_{\boldsymbol{\beta}}(t_2)\bar{\rho}_{\mathrm{B}}\right\}\,. \tag{2.20}$$

The integro-differential equation (2.19) is a **non-Markovian master equation**, as the r.h.s. depends on the value of the dynamical variable (the density matrix) at all previous times – weighted by the bath correlation functions. We will see later that non-Markovianity can also be defined

more rigorously based on violation of contractivity. It does preserve trace and Hermiticity of the system density matrix, but not necessarily its positivity. Such integro-differential equations can only be solved in very specific cases, e.g., when the correlation functions have a very simple decay law. Therefore, we motivate further approximations, for which we need to discuss the analytic properties of the bath correlation functions.

In our example, we have only a single system coupling operator $A(t) = \left(ae^{-\mathrm{i}\Omega t} + a^\dagger e^{+\mathrm{i}\Omega t}\right)$, and consequently also only a single correlation function

$$C(t_1,t_2) \;=\; \sum_{kk'} \mathrm{Tr}\left\{\left(h_k b_k e^{-\mathrm{i}\omega_k t_1} + h_k^* b_k^\dagger e^{+\mathrm{i}\omega_k t_1}\right)\left(h_{k'} b_{k'} e^{-\mathrm{i}\omega_{k'} t_2} + h_{k'}^* b_{k'}^\dagger e^{+\mathrm{i}\omega_{k'} t_2}\right)\bar{\rho}_B\right\} . \quad (2.21)$$

Without making further assumptions on the bath density matrix $\bar{\rho}_B$, we cannot further simplify this expression.

Markov approximation

It is quite straightforward to see that when the bath Hamiltonian commutes with the bath density matrix $[\mathcal{H}_\mathrm{B}, \bar{\rho}_\mathrm{B}] = 0$, the bath correlation functions actually only depend on the difference of their time arguments

$$C_{\alpha\beta}(t_1,t_2) = C_{\alpha\beta}(t_1-t_2) = \mathrm{Tr}\left\{e^{+i\mathcal{H}_\mathrm{B}(t_1-t_2)} B_\alpha e^{-i\mathcal{H}_\mathrm{B}(t_1-t_2)} B_\beta \bar{\rho}_\mathrm{B}\right\} . \quad (2.22)$$

Since we chose our coupling operators Hermitian, we have the additional symmetry that

$$C_{\alpha\beta}(\tau) = C^*_{\beta\alpha}(-\tau) . \quad (2.23)$$

One can now evaluate several system-bath models and when the bath has a dense spectrum, the bath correlation functions are typically found to be strongly peaked around zero, see exercise 14.

Exercise 14 (Bath Correlation Function)**.** *Evaluate the Fourier transform* $\gamma_{\alpha\beta}(\omega) = \int C_{\alpha\beta}(\tau) e^{+\mathrm{i}\omega\tau} d\tau$ *of the bath correlation functions for the coupling operators* $B_1 = \sum_k h_k b_k$ *and* $B_2 = \sum_k h_k^* b_k^\dagger$ *for a bosonic bath* $\mathcal{H}_\mathrm{B} = \sum_k \omega_k b_k^\dagger b_k$ *in the thermal equilibrium state* $\bar{\rho}_\mathrm{B}^0 = \frac{e^{-\beta\mathcal{H}_\mathrm{B}}}{\mathrm{Tr}\left\{e^{-\beta\mathcal{H}_\mathrm{B}}\right\}}$. *You may use the continous representation* $\Gamma(\omega) = 2\pi \sum_k |h_k|^2 \delta(\omega - \omega_k)$ *for the tunneling rates.*

The correlation function of our example can for a thermal reservoir $\bar{\rho}_B = e^{-\beta\sum_k \omega_k b_k^\dagger b_k}/Z_B$ be further evaluated

$$\begin{aligned} C(t_1-t_2) \;&=\; \sum_k |h_k|^2 \left[e^{-\mathrm{i}\omega_k(t_1-t_2)} \left\langle b_k b_k^\dagger \right\rangle + e^{+\mathrm{i}\omega_k(t_1-t_2)} \left\langle b_k^\dagger b_k \right\rangle\right] \\ &=\; \sum_k |h_k|^2 \left[e^{-\mathrm{i}\omega_k(t_1-t_2)}(1+n_B(\omega_k)) + e^{+\mathrm{i}\omega_k(t_1-t_2)} n_B(\omega_k)\right] \\ &=\; \frac{1}{2\pi}\int_0^\infty \Gamma(\omega)\left[e^{-\mathrm{i}\omega(t_1-t_2)}(1+n_B(\omega)) + e^{+\mathrm{i}\omega(t_1-t_2)} n_B(\omega)\right] d\omega , \end{aligned} \quad (2.24)$$

where we have introduced the *spectral coupling density*

$$\Gamma(\omega) = 2\pi \sum_k |t_k|^2 \delta(\omega - \omega_k) \quad (2.25)$$

and the Bose distribution $n_B(\omega) = [e^{\beta\omega} - 1]^{-1}$. For bosons, the frequencies of the reservoir oscillators must be positive $\omega_k > 0$, which explains the boundaries of the integrals. However, by analytically continuuing the spectral density as an odd function $\Gamma(-\omega) = -\Gamma(+\omega)$ and using the identity $n_B(-\omega) = -[1 + n_B(+\omega)]$, we can write this as a single term

$$C(t_1 - t_2) = \frac{1}{2\pi}\int_{-\infty}^{+\infty} \Gamma(\omega)[1 + n_B(\omega)]e^{-\mathrm{i}\omega(t_1-t_2)}d\omega\,, \tag{2.26}$$

from which we can – without calculation – identify the Fourier transform of the correlation function $\gamma(\omega) = \int C(\tau)e^{+\mathrm{i}\omega\tau}d\tau = \Gamma(\omega)[1 + n_B(\omega)]$. Importantly, we note that it is positive.

In superoperator notation, one can also write the integro-differential equation (2.19) as

$$\dot{\rho}_{\mathrm{S}} = \int_0^t \mathcal{W}(t - t')\rho_{\mathrm{S}}(t')dt'\,, \tag{2.27}$$

where the kernel $\mathcal{W}(\tau)$ assigns a much smaller weight to density matrices far in the past than to the density matrix just an instant ago. In the most extreme case, we would approximate $C_{\alpha\beta}(t_1, t_2) \approx \Gamma_{\alpha\beta}\delta(t_1 - t_2)$, but we will be cautious here and assume that only the density matrix varies slower than the decay time of the bath correlation functions. Therefore, we replace in the r.h.s. $\boldsymbol{\rho}_{\mathbf{S}}(t') \to \boldsymbol{\rho}_{\mathbf{S}}(t)$ (**first Markov approximation**), which yields in Eq. (2.14)

$$\dot{\boldsymbol{\rho}}_{\mathbf{S}} = -\int_0^t \mathrm{Tr}_{\mathrm{B}}\left\{[\boldsymbol{\mathcal{H}}_{\mathbf{I}}(t), [\boldsymbol{\mathcal{H}}_{\mathbf{I}}(t'), \boldsymbol{\rho}_{\mathbf{S}}(t) \otimes \bar{\rho}_{\mathrm{B}}]]\right\} dt' \tag{2.28}$$

This equation is often called **Born-Redfield** equation. It is time-local and preserves trace and Hermiticity, but still has time-dependent coefficients (also when transforming back from the interaction picture). We substitute $\tau = t - t'$

$$\begin{aligned}\dot{\boldsymbol{\rho}}_{\mathbf{S}} &= -\int_0^t \mathrm{Tr}_{\mathrm{B}}\left\{[\boldsymbol{\mathcal{H}}_{\mathbf{I}}(t), [\boldsymbol{\mathcal{H}}_{\mathbf{I}}(t-\tau), \boldsymbol{\rho}_{\mathbf{S}}(t) \otimes \bar{\rho}_{\mathrm{B}}]]\right\} d\tau \qquad (2.29)\\ &= -\sum_{\alpha\beta}\int_0^t \left\{C_{\alpha\beta}(\tau)\left[\boldsymbol{A}_{\boldsymbol{\alpha}}(t), \boldsymbol{A}_{\boldsymbol{\beta}}(t-\tau)\boldsymbol{\rho}_{\mathbf{S}}(t)\right] + C_{\beta\alpha}(-\tau)\left[\boldsymbol{\rho}_{\mathbf{S}}(t)\boldsymbol{A}_{\boldsymbol{\beta}}(t-\tau), \boldsymbol{A}_{\boldsymbol{\alpha}}(t)\right]\right\} d\tau\end{aligned}$$

The problem that the r.h.s. still depends on time is removed by extending the integration bounds to infinity (**second Markov approximation**) – by the same reasoning that the bath correlation functions decay rapidly

$$\dot{\boldsymbol{\rho}}_{\mathbf{S}} = -\int_0^\infty \mathrm{Tr}_{\mathrm{B}}\left\{[\boldsymbol{\mathcal{H}}_{\mathbf{I}}(t), [\boldsymbol{\mathcal{H}}_{\mathbf{I}}(t-\tau), \boldsymbol{\rho}_{\mathbf{S}}(t) \otimes \bar{\rho}_{\mathrm{B}}]]\right\} d\tau\,. \tag{2.30}$$

This equation is called the **Markovian master equation**, which in the original Schrödinger picture

$$\begin{aligned}\dot{\rho}_{\mathrm{S}} &= -\mathrm{i}\left[\mathcal{H}_{\mathrm{S}}, \rho_{\mathrm{S}}(t)\right] - \sum_{\alpha\beta}\int_0^\infty C_{\alpha\beta}(\tau)\left[A_\alpha, e^{-\mathrm{i}\mathcal{H}_{\mathrm{S}}\tau}A_\beta e^{+\mathrm{i}\mathcal{H}_{\mathrm{S}}\tau}\rho_{\mathrm{S}}(t)\right] d\tau\\ &\quad -\sum_{\alpha\beta}\int_0^\infty C_{\beta\alpha}(-\tau)\left[\rho_{\mathrm{S}}(t)e^{-\mathrm{i}\mathcal{H}_{\mathrm{S}}\tau}A_\beta e^{+\mathrm{i}\mathcal{H}_{\mathrm{S}}\tau}, A_\alpha\right] d\tau \qquad (2.31)\end{aligned}$$

is time-local, preserves trace and Hermiticity, and has constant coefficients – best prerequisites for treatment with established solution methods.

Exercise 15 (Properties of the Markovian Master Equation)**.** *Show that the Markovian Master equation (2.31) preserves trace and Hermiticity of the density matrix.*

In addition, it can be obtained easily from the coupling Hamiltonian: We have so far not used that the coupling operators should be Hermitian, and the above form is therefore also valid for non-Hermitian coupling operators.

There is just one problem left: In the general case, it is not of Lindblad form. Note that there are specific cases where the Markovian master equation is of Lindblad form, but these rather include simple limits. Though this is sometimes considered a rather cosmetic drawback, it may lead to unphysical results such as negative probabilities.

Coming back to our example, we would get

$$\begin{aligned}
\dot\rho &= -\mathrm{i}[\Omega a^\dagger a,\rho] - \int_0^\infty C(+\tau)[(a+a^\dagger), e^{-\mathrm{i}\Omega a^\dagger a\tau}(a+a^\dagger)e^{+\mathrm{i}\Omega a^\dagger a\tau}\rho]d\tau \\
&\quad - \int_0^\infty C^*(+\tau)\left[\rho e^{-\mathrm{i}\Omega a^\dagger a\tau}(a+a^\dagger)e^{+\mathrm{i}\Omega a^\dagger a\tau}, (a+a^\dagger)\right] \\
&= -\mathrm{i}[\Omega a^\dagger a,\rho] - \left\{\int_0^\infty C(+\tau)[(a+a^\dagger), \left(ae^{+\mathrm{i}\Omega\tau} + a^\dagger e^{-\mathrm{i}\Omega\tau}\right)\rho]d\tau + \mathrm{h.c.}\right\} \\
&= -\mathrm{i}[\Omega a^\dagger a,\rho] - \left\{\bar\Gamma(+\Omega)[(a+a^\dagger), a\rho] + \bar\Gamma(-\Omega)[(a+a^\dagger), a^\dagger\rho] + \mathrm{h.c.}\right\}, \qquad (2.32)
\end{aligned}$$

where we have used the conjugation property (2.23) valid for Hermitian coupling operators and defined the half-sided FT $\bar\Gamma(\omega) = \int_0^\infty C(\tau)e^{+\mathrm{i}\omega\tau}d\tau$ (not to be confused with the spectral coupling density).

Secular Approximation

To generally obtain a Lindblad type master equation, a further approximation is required. The **secular approximation** involves an averaging in the interaction picture over fast oscillating terms in time t. In order to identify the oscillating terms, it is necessary to at least formally calculate the interaction picture dynamics of the system coupling operators.

We first make this explicit for our example. In the interaction picture, we have

$$\begin{aligned}
\dot{\boldsymbol\rho} &= -\int_0^\infty C(\tau)\left[\left(ae^{-\mathrm{i}\Omega t} + a^\dagger e^{+\mathrm{i}\Omega t}\right), \left(ae^{-\mathrm{i}\Omega(t-\tau)} + a^\dagger e^{+\mathrm{i}\Omega(t-\tau)}\right)\boldsymbol\rho\right] + \mathrm{h.c.} \\
&\approx -\int_0^\infty C(\tau)e^{-\mathrm{i}\Omega\tau}d\tau[a, a^\dagger\boldsymbol\rho] - \int_0^\infty C(\tau)e^{+\mathrm{i}\Omega\tau}d\tau[a^\dagger, a\boldsymbol\rho] + \mathrm{h.c.} \\
&= -\bar\Gamma(-\Omega)\left(aa^\dagger\boldsymbol\rho - a^\dagger\boldsymbol\rho a\right) - \bar\Gamma(+\Omega)\left(a^\dagger a\boldsymbol\rho - a\boldsymbol\rho a^\dagger\right) \\
&\quad -\bar\Gamma^*(-\Omega)\left(\boldsymbol\rho aa^\dagger - a^\dagger\boldsymbol\rho a\right) - \bar\Gamma^*(+\Omega)\left(\boldsymbol\rho a^\dagger a - a\boldsymbol\rho a^\dagger\right). \qquad (2.33)
\end{aligned}$$

Here, we have neglected all terms that oscillate with $e^{\pm 2\mathrm{i}\Omega t}$. Furthermore, we can split $\bar\Gamma(+\Omega) = \frac{1}{2}\gamma + \frac{\mathrm{i}}{2}\sigma$ and $\bar\Gamma(-\Omega) = \frac{1}{2}\bar\gamma + \frac{\mathrm{i}}{2}\bar\sigma$ into real and imaginary parts, which eventually yields

$$\begin{aligned}
\dot{\boldsymbol\rho} &= \gamma\left[a\boldsymbol\rho a^\dagger - \frac{1}{2}\left\{a^\dagger a, \boldsymbol\rho\right\}\right] + \bar\gamma\left[a^\dagger\boldsymbol\rho a - \frac{1}{2}\left\{aa^\dagger, \boldsymbol\rho\right\}\right] \\
&\quad -\mathrm{i}\left[\frac{\sigma}{2}a^\dagger a + \frac{\bar\sigma}{2}aa^\dagger, \boldsymbol\rho\right]. \qquad (2.34)
\end{aligned}$$

This is a Lindblad form master equation when $\gamma > 0$ and $\bar{\gamma} > 0$. Indeed, we have already computed the Fourier transform of the full correlation function, which we showed to be non-negative. The real part of the half-sided Fourier transforms of the correlation function

$$\begin{aligned}\bar{\Gamma}(\omega) + \bar{\Gamma}^*(\omega) &= \int_0^\infty C(\tau)e^{+\mathrm{i}\omega\tau}d\tau + \int_0^\infty C^*(\tau)e^{-\mathrm{i}\omega\tau}d\tau \\ &= \int_0^\infty C(\tau)e^{+\mathrm{i}\omega\tau}d\tau + \int_0^\infty C(-\tau)e^{-\mathrm{i}\omega\tau}d\tau = \int_0^\infty C(\tau)e^{+\mathrm{i}\omega\tau}d\tau + \int_{-\infty}^0 C(\tau)e^{+\mathrm{i}\omega\tau}d\tau \\ &= \int_{-\infty}^{+\infty} C(\tau)e^{+\mathrm{i}\omega\tau}d\tau \end{aligned} \tag{2.35}$$

is given by the full Fourier transform of the correlation function, which we have shown to be positive.

Apart from our example, we may also formulate this generally. We begin by writing Eq. (2.30) in the interaction picture again explicitly – now using the Hermiticity of the coupling operators

$$\begin{aligned}\dot{\boldsymbol{\rho}}_{\mathbf{S}} &= -\int_0^\infty \sum_{\alpha\beta} \left\{C_{\alpha\beta}(\tau)\left[\boldsymbol{A}_{\boldsymbol{\alpha}}(t), \boldsymbol{A}_{\boldsymbol{\beta}}(t-\tau)\boldsymbol{\rho}_{\mathbf{S}}(t)\right] + \text{h.c.}\right\} d\tau \\ &= +\int_0^\infty \sum_{\alpha\beta} C_{\alpha\beta}(\tau) \sum_{a,b,c,d} \Big\{ |a\rangle\langle a|\boldsymbol{A}_{\boldsymbol{\beta}}(t-\tau)|b\rangle\langle b|\boldsymbol{\rho}_{\mathbf{S}}(t)|d\rangle\langle d|\boldsymbol{A}_{\boldsymbol{\alpha}}(t)|c\rangle\langle c| \\ &\quad - |d\rangle\langle d|\boldsymbol{A}_{\boldsymbol{\alpha}}(t)|c\rangle\langle c|a\rangle\langle a|\boldsymbol{A}_{\boldsymbol{\beta}}(t-\tau)|b\rangle\langle b|\boldsymbol{\rho}_{\mathbf{S}}(t)\Big\} d\tau + \text{h.c.}\,, \end{aligned} \tag{2.36}$$

where we have introduced the system energy eigenbasis

$$\mathcal{H}_{\mathrm{S}}|a\rangle = E_a|a\rangle\ . \tag{2.37}$$

We can use this eigenbasis to make the time-dependence of the coupling operators in the interaction picture explicit. To reduce the notational effort, we abbreviate $A^{ab}_\alpha = \langle a|A_\alpha|b\rangle$ and $L_{ab} = |a\rangle\langle b|$. Then, the density matrix becomes

$$\begin{aligned}\dot{\boldsymbol{\rho}}_{\mathbf{S}} &= +\int_0^\infty \sum_{\alpha\beta} C_{\alpha\beta}(\tau) \sum_{a,b,c,d} \Big\{ e^{+\mathrm{i}(E_a-E_b)(t-\tau)}e^{+\mathrm{i}(E_d-E_c)t}A^{ab}_\beta A^{dc}_\alpha L_{ab}\boldsymbol{\rho}_{\mathbf{S}}(t)L^\dagger_{cd} \\ &\quad - e^{+\mathrm{i}(E_a-E_b)(t-\tau)}e^{+\mathrm{i}(E_d-E_c)t}A^{ab}_\beta A^{dc}_\alpha L^\dagger_{cd}L_{ab}\boldsymbol{\rho}_{\mathbf{S}}(t)\Big\} d\tau + \text{h.c.}\,, \\ &= \sum_{\alpha\beta}\sum_{a,b,c,d}\int_0^\infty C_{\alpha\beta}(\tau)e^{+\mathrm{i}(E_b-E_a)\tau}d\tau e^{-\mathrm{i}(E_b-E_a-(E_d-E_c))t}A^{ab}_\beta (A^{cd}_\alpha)^*\Big\{L_{ab}\boldsymbol{\rho}_{\mathbf{S}}(t)L^\dagger_{cd} - L^\dagger_{cd}L_{ab}\boldsymbol{\rho}_{\mathbf{S}}(t)\Big\} \\ &\quad +\text{h.c.} \end{aligned} \tag{2.38}$$

The **secular approximation** now involves neglecting all terms that are oscillatory in time t (long-time average), i.e., we have

$$\begin{aligned}\dot{\boldsymbol{\rho}}_{\mathbf{S}} &= \sum_{\alpha\beta}\sum_{a,b,c,d}\Gamma_{\alpha\beta}(E_b-E_a)\delta_{E_b-E_a,E_d-E_c}A^{ab}_\beta(A^{cd}_\alpha)^*\Big\{+L_{ab}\boldsymbol{\rho}_{\mathbf{S}}(t)L^\dagger_{cd} - L^\dagger_{cd}L_{ab}\boldsymbol{\rho}_{\mathbf{S}}(t)\Big\} \\ &\quad +\sum_{\alpha\beta}\sum_{a,b,c,d}\Gamma^*_{\alpha\beta}(E_b-E_a)\delta_{E_b-E_a,E_d-E_c}(A^{ab}_\beta)^*A^{cd}_\alpha\Big\{+L_{cd}\boldsymbol{\rho}_{\mathbf{S}}(t)L^\dagger_{ab} - \boldsymbol{\rho}_{\mathbf{S}}(t)L^\dagger_{ab}L_{cd}\Big\} \end{aligned} \tag{2.39}$$

where we have introduced the half-sided Fourier transform of the bath correlation functions

$$\Gamma_{\alpha\beta}(\omega) = \int_0^\infty C_{\alpha\beta}(\tau) e^{+i\omega\tau} d\tau \,. \tag{2.40}$$

This equation preserves trace, Hermiticity, and positivity of the density matrix and hence all desired properties, since it is of Lindblad form (which will be shown later). Unfortunately, it is typically not so easy to obtain as it requires diagonalization of the system Hamiltonian first. By using the transformations $\alpha \leftrightarrow \beta$, $a \leftrightarrow c$, and $b \leftrightarrow d$ in the second line and also using that the δ-function is symmetric, we may rewrite the master equation as

$$\begin{aligned}
\dot{\boldsymbol{\rho}}_{\mathbf{S}} &= \sum_{\alpha\beta} \sum_{a,b,c,d} \left[\Gamma_{\alpha\beta}(E_b - E_a) + \Gamma^*_{\beta\alpha}(E_b - E_a)\right] \delta_{E_b - E_a, E_d - E_c} A^{ab}_\beta (A^{cd}_\alpha)^* L_{ab} \boldsymbol{\rho}_{\mathbf{S}}(t) L^\dagger_{cd} \\
&\quad - \sum_{\alpha\beta} \sum_{a,b,c,d} \Gamma_{\alpha\beta}(E_b - E_a) \delta_{E_b - E_a, E_d - E_c} A^{ab}_\beta (A^{cd}_\alpha)^* L^\dagger_{cd} L_{ab} \boldsymbol{\rho}_{\mathbf{S}}(t) \\
&\quad - \sum_{\alpha\beta} \sum_{a,b,c,d} \Gamma^*_{\beta\alpha}(E_b - E_a) \delta_{E_b - E_a, E_d - E_c} A^{ab}_\beta (A^{cd}_\alpha)^* \boldsymbol{\rho}_{\mathbf{S}}(t) L^\dagger_{cd} L_{ab} \,.
\end{aligned} \tag{2.41}$$

We split the matrix-valued function $\Gamma_{\alpha\beta}(\omega)$ into Hermitian and anti-Hermitian parts

$$\begin{aligned}
\Gamma_{\alpha\beta}(\omega) &= \frac{1}{2}\gamma_{\alpha\beta}(\omega) + \frac{1}{2}\sigma_{\alpha\beta}(\omega) \,, \\
\Gamma^*_{\beta\alpha}(\omega) &= \frac{1}{2}\gamma_{\alpha\beta}(\omega) - \frac{1}{2}\sigma_{\alpha\beta}(\omega) \,,
\end{aligned} \tag{2.42}$$

with Hermitian $\gamma_{\alpha\beta}(\omega) = \gamma^*_{\beta\alpha}(\omega)$ and anti-Hermitian $\sigma_{\alpha\beta}(\omega) = -\sigma^*_{\beta\alpha}(\omega)$. These new functions can be interpreted as full even and odd Fourier transforms of the bath correlation functions

$$\begin{aligned}
\gamma_{\alpha\beta}(\omega) &= \Gamma_{\alpha\beta}(\omega) + \Gamma^*_{\beta\alpha}(\omega) = \int_{-\infty}^{+\infty} C_{\alpha\beta}(\tau) e^{+\mathrm{i}\omega\tau} d\tau \,, \\
\sigma_{\alpha\beta}(\omega) &= \Gamma_{\alpha\beta}(\omega) - \Gamma^*_{\beta\alpha}(\omega) = \int_{-\infty}^{+\infty} C_{\alpha\beta}(\tau) \mathrm{sgn}(\tau) \mathrm{e}^{+\mathrm{i}\omega\tau} \mathrm{d}\tau \,.
\end{aligned} \tag{2.43}$$

Exercise 16 (Odd Fourier Transform)**.** *Show that the odd Fourier transform $\sigma_{\alpha\beta}(\omega)$ may be obtained from the even Fourier transform $\gamma_{\alpha\beta}(\omega)$ by a Cauchy principal value integral*

$$\sigma_{\alpha\beta}(\omega) = \frac{\mathrm{i}}{\pi} \mathcal{P} \int_{-\infty}^{+\infty} \frac{\gamma_{\alpha\beta}(\Omega)}{\omega - \Omega} d\Omega \,.$$

In the master equation, these replacements lead to

$$\begin{aligned}\dot{\boldsymbol{\rho}}_{\mathbf{S}} &= \sum_{\alpha\beta}\sum_{a,b,c,d}\gamma_{\alpha\beta}(E_b-E_a)\delta_{E_b-E_a,E_d-E_c}A^{ab}_{\beta}(A^{cd}_{\alpha})^*\left[L_{ab}\boldsymbol{\rho}_{\mathbf{S}}(t)L^{\dagger}_{cd}-\frac{1}{2}\left\{L^{\dagger}_{cd}L_{ab},\boldsymbol{\rho}_{\mathbf{S}}(t)\right\}\right]\\ &\quad -\mathrm{i}\sum_{\alpha\beta}\sum_{a,b,c,d}\frac{1}{2\mathrm{i}}\sigma_{\alpha\beta}(E_b-E_a)\delta_{E_b-E_a,E_d-E_c}A^{ab}_{\beta}(A^{cd}_{\alpha})^*\left[L^{\dagger}_{cd}L_{ab},\boldsymbol{\rho}_{\mathbf{S}}(t)\right]\\ &= \sum_{\alpha\beta}\sum_{a,b,c,d}\gamma_{\alpha\beta}(E_b-E_a)\delta_{E_b-E_a,E_d-E_c}A^{ab}_{\beta}(A^{cd}_{\alpha})^*\left[L_{ab}\boldsymbol{\rho}_{\mathbf{S}}(t)L^{\dagger}_{cd}-\frac{1}{2}\left\{L^{\dagger}_{cd}L_{ab},\boldsymbol{\rho}_{\mathbf{S}}(t)\right\}\right] \qquad (2.43)\\ &\quad -\mathrm{i}\left[\sum_{\alpha\beta}\sum_{a,b,c}\frac{1}{2\mathrm{i}}\sigma_{\alpha\beta}(E_b-E_c)\delta_{E_b,E_a}A^{cb}_{\beta}(A^{ca}_{\alpha})^*L_{ab},\boldsymbol{\rho}_{\mathbf{S}}(t)\right].\end{aligned}$$

To prove that we have a Lindblad form, it is easy to see first that the term in the commutator

$$H_{\mathrm{LS}} = \sum_{\alpha\beta}\sum_{a,b,c}\frac{1}{2\mathrm{i}}\sigma_{\alpha\beta}(E_b-E_c)\delta_{E_b,E_a}A^{cb}_{\beta}(A^{ca}_{\alpha})^*\left|a\right\rangle\left\langle b\right| \qquad (2.44)$$

is an effective Hamiltonian. This Hamiltonian is often called Lamb-shift Hamiltonian, since it renormalizes the system Hamiltonian due to the interaction with the reservoir. Note that we have $[\mathcal{H}_{\mathrm{S}},H_{\mathrm{LS}}]=0$.

Exercise 17 (Lamb-shift)**.** *Show that* $H_{\mathrm{LS}}=H^{\dagger}_{\mathrm{LS}}$ *and* $[H_{\mathrm{LS}},\mathcal{H}_{\mathrm{S}}]=0$.

To show the Lindblad-form of the non-unitary evolution, we identify the Lindblad jump operator $L_{\alpha}=\left|a\right\rangle\left\langle b\right|=L_{(a,b)}$. For an N-dimensional system Hilbert space with N eigenvectors of $\mathcal{H}_{\mathrm{S}}$ we would have N^2 such jump operators, but the identity matrix $\mathbf{1}=\sum_a\left|a\right\rangle\left\langle a\right|$ has trivial action, which can be used to eliminate one jump operator. It remains to be shown that the matrix

$$\gamma_{(ab),(cd)}=\sum_{\alpha\beta}\gamma_{\alpha\beta}(E_b-E_a)\delta_{E_b-E_a,E_d-E_c}A^{ab}_{\beta}(A^{cd}_{\alpha})^* \qquad (2.45)$$

is non-negative, i.e., $\sum_{a,b,c,d}x^*_{ab}\gamma_{(ab),(cd)}x_{cd}\geq 0$ for all x_{ab}. We first note that for Hermitian coupling operators the Fourier transform matrix at fixed ω is positive (recall that $B_{\alpha}=B^{\dagger}_{\alpha}$ and $[\bar{\rho}_{\mathrm{B}},\mathcal{H}_{\mathrm{B}}]=0$)

$$\begin{aligned}\Gamma &= \sum_{\alpha\beta}x^*_{\alpha}\gamma_{\alpha\beta}(\omega)x_{\beta}\\ &= \int_{-\infty}^{+\infty}d\tau e^{+\mathrm{i}\omega\tau}\mathrm{Tr}\left\{e^{\mathrm{i}\mathcal{H}_{\mathrm{S}}\tau}\left[\sum_{\alpha}x^*_{\alpha}B_{\alpha}\right]e^{-\mathrm{i}\mathcal{H}_{\mathrm{S}}\tau}\left[\sum_{\beta}x_{\beta}B_{\beta}\right]\bar{\rho}_{\mathrm{B}}\right\}\\ &= \int_{-\infty}^{+\infty}d\tau e^{+\mathrm{i}\omega\tau}\sum_{nm}e^{+\mathrm{i}(E_n-E_m)\tau}\left\langle n\right|B^{\dagger}\left|m\right\rangle\left\langle m\right|B\bar{\rho}_{\mathrm{B}}\left|n\right\rangle\\ &= \sum_{nm}2\pi\delta(\omega+E_n-E_m)|\left\langle m\right|B\left|n\right\rangle|^2\rho_n\\ &\geq 0\,. \qquad (2.46)\end{aligned}$$

Now, we replace the Kronecker symbol in the dampening coefficients by two via the introduction of an auxiliary summation

$$\begin{aligned}
\tilde{\Gamma} &= \sum_{abcd} x^*_{ab}\gamma_{(ab),(cd)}x_{cd} \\
&= \sum_{\omega}\sum_{\alpha\beta}\sum_{abcd}\gamma_{\alpha\beta}(\omega)\delta_{E_b-E_a,\omega}\delta_{E_d-E_c,\omega}x^*_{ab}\left\langle a\right|A_\beta\left|b\right\rangle x_{cd}\left\langle c\right|A_\alpha\left|d\right\rangle^* \\
&= \sum_{\omega}\sum_{\alpha\beta}\left[\sum_{cd}x_{cd}\left\langle c\right|A_\alpha\left|d\right\rangle^*\delta_{E_d-E_c,\omega}\right]\gamma_{\alpha\beta}(\omega)\left[\sum_{ab}x^*_{ab}\left\langle a\right|A_\beta\left|b\right\rangle\delta_{E_b-E_a,\omega}\right] \\
&= \sum_{\omega}\sum_{\alpha\beta}y^*_\alpha(\omega)\gamma_{\alpha\beta}(\omega)y_\beta(\omega)\geq 0\,. \qquad (2.47)
\end{aligned}$$

Transforming Eq. (2.43) back to the Schrödinger picture (note that the δ-functions prohibit the occurrence of oscillatory factors), we finally obtain the Born-Markov-secular master equation.

Def. 7 (BMS master equation)**.** *In the weak coupling limit, an interaction Hamiltonian of the form* $\mathcal{H}_{\rm I}=\sum_\alpha A_\alpha\otimes B_\alpha$ *with Hermitian coupling operators* ($A_\alpha=A^\dagger_\alpha$ *and* $B_\alpha=B^\dagger_\alpha$) *and* $[\mathcal{H}_{\rm B},\bar{\rho}_{\rm B}]=0$ *and* $\mathrm{Tr}\left\{B_\alpha\bar{\rho}_{\rm B}\right\}=0$ *leads in the system energy eigenbasis* $\mathcal{H}_{\rm S}\left|a\right\rangle=E_a\left|a\right\rangle$ *to the Lindblad-form master equation*

$$\begin{aligned}
\dot{\rho}_{\rm S} &= -\mathrm{i}\left[\mathcal{H}_{\rm S}+\sum_{ab}\sigma_{ab}\left|a\right\rangle\left\langle b\right|,\rho_{\rm S}(t)\right] \\
&\quad+\sum_{a,b,c,d}\gamma_{ab,cd}\left[\left|a\right\rangle\left\langle b\right|\boldsymbol{\rho}_{\mathbf{S}}(t)\left(\left|c\right\rangle\left\langle d\right|\right)^\dagger-\frac{1}{2}\left\{\left(\left|c\right\rangle\left\langle d\right|\right)^\dagger\left|a\right\rangle\left\langle b\right|,\boldsymbol{\rho}_{\mathbf{S}}(t)\right\}\right], \\
\gamma_{ab,cd} &= \sum_{\alpha\beta}\gamma_{\alpha\beta}(E_b-E_a)\delta_{E_b-E_a,E_d-E_c}\left\langle a\right|A_\beta\left|b\right\rangle\left\langle c\right|A_\alpha\left|d\right\rangle^*, \qquad (2.48)
\end{aligned}$$

where the Lamb-shift Hamiltonian $H_{\rm LS}=\sum_{ab}\sigma_{ab}\left|a\right\rangle\left\langle b\right|$ *matrix elements read*

$$\sigma_{ab}=\sum_{\alpha\beta}\sum_c\frac{1}{2\mathrm{i}}\sigma_{\alpha\beta}(E_b-E_c)\delta_{E_b,E_a}\left\langle c\right|A_\beta\left|b\right\rangle\left\langle c\right|A_\alpha\left|a\right\rangle^* \qquad (2.49)$$

and the constants are given by even and odd Fourier transforms

$$\begin{aligned}
\gamma_{\alpha\beta}(\omega) &= \int_{-\infty}^{+\infty}C_{\alpha\beta}(\tau)e^{+\mathrm{i}\omega\tau}d\tau\,, \\
\sigma_{\alpha\beta}(\omega) &= \int_{-\infty}^{+\infty}C_{\alpha\beta}(\tau)\mathrm{sgn}(\tau)\mathrm{e}^{+\mathrm{i}\omega\tau}\mathrm{d}\tau=\frac{\mathrm{i}}{\pi}\mathcal{P}\int_{-\infty}^{+\infty}\frac{\gamma_{\alpha\beta}(\omega')}{\omega-\omega'}\mathrm{d}\omega' \qquad (2.50)
\end{aligned}$$

of the bath correlation functions

$$C_{\alpha\beta}(\tau) = \mathrm{Tr}\left\{e^{+\mathrm{i}\mathcal{H}_{\rm B}\tau}B_\alpha e^{-\mathrm{i}\mathcal{H}_{\rm B}\tau}B_\beta\bar{\rho}_{\rm B}\right\}. \qquad (2.51)$$

The above definition may serve as a recipe to derive a Lindblad type master equation in the weak-coupling limit. It is expected to yield good results in the weak coupling and Markovian limit (continuous and nearly flat bath spectral density) and when $[\bar{\rho}_{\mathrm{B}}, \mathcal{H}_{\mathrm{B}}] = 0$. It requires to rewrite the coupling operators in Hermitian form, the calculation of the bath correlation function Fourier transforms, and the diagonalization of the system Hamiltonian.

In the case that the spectrum of the system Hamiltonian is non-degenerate, we have a further simplification, since the δ-functions simplify further, e.g. $\delta_{E_b,E_a} \to \delta_{ab}$. By taking matrix elements of Eq. (2.48) in the energy eigenbasis $\rho_{aa} = \langle a| \rho_{\mathrm{S}} |a\rangle$, we obtain an effective rate equation for the populations only

$$\dot{\rho}_{aa} = +\sum_b \gamma_{ab,ab}\rho_{bb} - \left[\sum_b \gamma_{ba,ba}\right] \rho_{aa}\,, \tag{2.52}$$

i.e., the coherences decouple from the evolution of the populations. The transition rates from state b to state a reduce in this case to

$$\gamma_{ab,ab} = \sum_{\alpha\beta} \gamma_{\alpha\beta}(E_b - E_a) \langle a| A_\beta |b\rangle \langle a| A_\alpha |b\rangle^* \geq 0\,, \tag{2.53}$$

which – after inserting all definitions – condenses basically to Fermis Golden Rule. Therefore, with such a rate equation description, open quantum systems can be described with the same complexity as closed quantum systems, since only N dynamical variables have to be evolved.

The BMS master equation is problematic for near-degenerate systems: For exact degeneracies, couplings to coherences between energetically degenerate states have to be kept, but for lifted degeneracies, they are neglected. This discontinuous behaviour may map to observables and poses the question which of the two resulting equations is correct, in particular for near degeneracies. Despite such problems, the BMS master equation is heavily used since it has many favorable properties. For example, we will see later that if coupled to a single thermal bath, the quantum system generally relaxes to the Gibbs equilibrium, i.e., we obtain simply equilibration of the system temperature with the temperature of the bath.

2.2.2 Equilibrium Thermodynamics

The BMS limit has beyond its relatively compact Lindblad form further appealing properties in the case of a bath that is in thermal equilibrium

$$\bar{\rho}_{\mathrm{B}} = \frac{e^{-\beta\mathcal{H}_{\mathrm{B}}}}{\mathrm{Tr}\left\{e^{-\beta\mathcal{H}_{\mathrm{B}}}\right\}} \tag{2.54}$$

with inverse temperature β. These root in further analytic properties of the bath correlation functions such as the Kubo-Martin-Schwinger (KMS) condition

$$C_{\alpha\beta}(\tau) = C_{\beta\alpha}(-\tau - \mathrm{i}\beta)\,. \tag{2.55}$$

Exercise 18 (KMS condition)**.** *Show the validity of the KMS condition for a thermal bath with* $\bar{\rho}_{\mathrm{B}} = \frac{e^{-\beta\mathcal{H}_{\mathrm{B}}}}{\mathrm{Tr}\left\{e^{-\beta\mathcal{H}_{\mathrm{B}}}\right\}}$.

For the Fourier transform, this shift property implies

$$\begin{aligned}\gamma_{\alpha\beta}(-\omega) &= \int_{-\infty}^{+\infty} C_{\alpha\beta}(\tau)e^{-\mathrm{i}\omega\tau}d\tau = \int_{-\infty}^{+\infty} C_{\beta\alpha}(-\tau-\mathrm{i}\beta)e^{-\mathrm{i}\omega\tau}d\tau \\ &= \int_{+\infty-\mathrm{i}\beta}^{-\infty-\mathrm{i}\beta} C_{\beta\alpha}(\tau')e^{+\mathrm{i}\omega(\tau'+\mathrm{i}\beta)}(-d\tau)' = \int_{-\infty-\mathrm{i}\beta}^{+\infty-\mathrm{i}\beta} C_{\beta\alpha}(\tau')e^{+\mathrm{i}\omega\tau'}d\tau' e^{-\beta\omega} \\ &= \int_{-\infty}^{+\infty} C_{\beta\alpha}(\tau')e^{+\mathrm{i}\omega\tau'}d\tau' e^{-\beta\omega} = \gamma_{\beta\alpha}(+\omega)e^{-\beta\omega}\,, \end{aligned} \tag{2.56}$$

where in the last line we have used that the bath correlation functions are analytic in τ in the complex plane and vanish at infinity, such that we may safely deform the integration contour. Finally, the KMS condition can thereby be used to prove that for a reservoir with inverse temperature β, the density matrix

$$\bar{\rho_{\mathrm{S}}} = \frac{e^{-\beta\mathcal{H}_{\mathrm{S}}}}{\mathrm{Tr}\left\{e^{-\beta\mathcal{H}_{\mathrm{S}}}\right\}} \tag{2.57}$$

is one stationary state of the BMS master equation (and the $\tau \to \infty$ limit of the CG appraoch).

Exercise 19 (Thermalization). *Show that* $\bar{\rho_{\mathrm{S}}} = \frac{e^{-\beta\mathcal{H}_{\mathrm{S}}}}{\mathrm{Tr}\left\{e^{-\beta\mathcal{H}_{\mathrm{S}}}\right\}}$ *is a stationary state of the BMS master equation, when* $\gamma_{\alpha\beta}(-\omega) = \gamma_{\beta\alpha}(+\omega)e^{-\beta\omega}$.

Things become a bit more complicated when the reservoir is in the grand-canonical equilibrium state

$$\bar{\rho}_{\mathrm{B}} = \frac{e^{-\beta(\mathcal{H}_{\mathrm{B}}-\mu N_{\mathrm{B}})}}{\mathrm{Tr}\left\{e^{-\beta(\mathcal{H}_{\mathrm{B}}-\mu N_{\mathrm{B}})}\right\}}\,, \tag{2.58}$$

with the chemical potential μ and the particle number operator N_B of the bath. Then, the normal KMS condition is not fulfilled anymore by the correlation function. Chemical potentials become relevant for models discussing particle transport. To talk about transport, it is natural to assume that the total particle number $N = N_{\mathrm{S}} + N_{\mathrm{B}}$ is a conserved quantity $[\mathcal{H}_{\mathrm{S}}, N_S] = [\mathcal{H}_{\mathrm{B}}, N_B] = [\mathcal{H}_{\mathrm{I}}, N_S + N_B] = 0$. In this case one can show that [6] the KMS relation is generalized according to

$$\sum_{\bar{\alpha}} A_{\bar{\alpha}} C_{\alpha\bar{\alpha}}(\tau) = \sum_{\bar{\alpha}} e^{+\beta\mu N_S} A_{\bar{\alpha}} e^{-\beta\mu N_S} C_{\bar{\alpha}\alpha}(-\tau-\mathrm{i}\beta)\,. \tag{2.59}$$

This modifies the detailed-balance relation of the master equation coefficients to

$$\frac{\gamma_{ab,cd}}{\gamma_{dc,ba}} = e^{\beta[(E_b-E_a)-\mu(N_b-N_a)]}\,. \tag{2.60}$$

In the end, these modified relations can be used to show that a stationary state of the BMS master equation is given by

$$\bar{\rho_{\mathrm{S}}} = \frac{e^{-\beta(\mathcal{H}_{\mathrm{S}}-\mu N_{\mathrm{S}})}}{\mathrm{Tr}\left\{e^{-\beta(\mathcal{H}_{\mathrm{S}}-\mu N_{\mathrm{S}})}\right\}}\,, \tag{2.61}$$

i.e., both temperature β and chemical potential μ must equilibrate with the reservoir.

Exercise 20 (Equilibration). *Show that Eqns. (2.59) and (2.60) hold. It will be useful to use conservation of the total particle number and Eq. (2.50).*

Finally, we consider the evolution of the system entropy. We first recall an early result by Lindblad [7] stating that completely-positive trace-preserving maps (Kraus maps) are contractive. To this end, we first start with some definitions. First, we define the von-Neumann entropy of the system

Def. 8 (von-Neumann entropy). *The von-Neumann entropy of a system described by density matrix ρ is defined as*

$$S(\rho) = -\mathrm{Tr}\left\{\rho \ln \rho\right\} . \tag{2.62}$$

We have $0 \leq S(\rho) \leq \ln N$ and for an $N \times N$ density matrix ρ.

The von-Neumann entropy can serve as an entanglement measure for states that are globally pure. It is sometimes used synonymously with the Shannon entropy $S_{\mathrm{Sh}} = -\sum_i P_i \ln P_i$ but is strictly speaking not the same. They only coincide in the basis where the density matrix is diagonal. The Shannon entropy is formally basis-dependent whereas the von-Neumann entropy is not.

Exercise 21 (von-Neumann entropy). *Compute the von-Neumann entropy of the reduced density matrix ρ_1 of $\rho_{12}^{a/b} = \left|\Psi^{a/b}\right\rangle \left\langle\Psi^{a/b}\right|$ for*

$$|\Psi^a\rangle = \frac{1}{\sqrt{2}}\left[|01\rangle + |10\rangle\right] , \qquad \left|\Psi^b\right\rangle = \frac{1}{2}\left[|01\rangle + |00\rangle + |10\rangle + |11\rangle\right] . \tag{2.63}$$

Furthermore, we introduce a pseudo-distance between density matrices

Def. 9 (Quantum Relative Entropy). *The quantum relative entropy between two density matrices ρ and σ is defined as*

$$D(\rho||\sigma) = \mathrm{Tr}\left\{\rho\left(\ln \rho - \ln \sigma\right)\right\} . \tag{2.64}$$

Obviously, the relative entropy vanishes when the two density matrices are equal $D(\rho||\rho) = 0$. Furthermore, the relative entropy can be shown to be non-negative $D(\rho||\sigma) \geq 0$. It is also not a real distance, since it is not symmetric. Lindblads result states that Kraus maps $\mathcal{K}\rho = \rho'$ are contractive, i.e., that

$$D(\mathcal{K}\rho||\mathcal{K}\sigma) \leq D(\rho||\sigma) . \tag{2.65}$$

This can be exploited for Lindblad generators in the following way: Taking the Kraus map $\mathcal{K} = e^{\mathcal{L}\Delta t}$ and choosing the distance to the steady state $\sigma = \bar{\rho}$, which fulfils $\mathcal{L}\bar{\rho} = 0$, we can expand the inequality

$$D\left(\rho||\bar{\rho}\right) - D\left(e^{\mathcal{L}\Delta t}\rho||\bar{\rho}\right) \geq 0 \tag{2.66}$$

for small Δt to obtain Spohn's inequality.

Def. 10 (Spohn's inequality [8]). *Let $\mathcal{L}$ be a Lindblad-type generator and $\bar{\rho}$ its stationary state fulfilling $\mathcal{L}\bar{\rho} = 0$. Then the physical evolution obeys at all times the inequality*

$$-\mathrm{Tr}\left\{[\mathcal{L}\rho][\ln\rho - \ln\bar{\rho}]\right\} \geq 0\,. \tag{2.67}$$

What is the meaning of this inequality, apart from its formal meaning as some contraction rate? Clearly, the first term is just the time derivative of the von-Neumann entropy

$$\dot{S}(\rho) \;=\; -\mathrm{Tr}\left\{\dot{\rho}\ln\rho\right\} - \mathrm{Tr}\left\{\rho\frac{d}{dt}\ln\rho\right\} = -\mathrm{Tr}\left\{(\mathcal{L}\rho)\ln\rho\right\}\,. \tag{2.68}$$

Here, we have used that the density matrix is always diagonalizable $\rho = U\rho_D U^\dagger$, leading to

$$\begin{aligned}
\mathrm{Tr}\left\{\rho\frac{d}{dt}\ln\rho\right\} &= \mathrm{Tr}\left\{U\rho_D U^\dagger\dot{U}(\ln\rho_D)U^\dagger + U\rho_D U^\dagger U(\ln\rho_D)\dot{U}^\dagger + U\rho_D U^\dagger U\rho_D^{-1}\dot{\rho}_D U^\dagger\right\} \\
&= \mathrm{Tr}\left\{\rho_D U^\dagger\dot{U}(\ln\rho_D) + \rho_D(\ln\rho_D)\dot{U}^\dagger U + \dot{\rho}_D\right\} \\
&= \mathrm{Tr}\left\{\rho_D(\ln\rho_D)\left(\dot{U}^\dagger U + U^\dagger\dot{U}\right) + \dot{\rho}_D\right\} = 0\,,
\end{aligned} \tag{2.69}$$

where we have used that $U^\dagger U = \mathbf{1}$, correspondingly $\dot{U}^\dagger U + U^\dagger\dot{U} = \mathbf{0}$, and $\mathrm{Tr}\left\{\dot{\rho}_D\right\} = 0$ (conservation of probabilities). The interpretation of the second term is different. When the stationary state of the system is a thermal Gibbs state $\bar{\rho} = e^{-\beta(H_S - \mu N_S)}/Z_S$ with inverse temperature β, chemical potential μ, system Hamiltonian H_S, and system particle number operator N_S, we would get

$$\mathrm{Tr}\left\{\rho(\ln\bar{\rho})\right\} = -\beta\mathrm{Tr}\left\{(\mathcal{L}\rho)(H_S - \mu N_S)\right\} - \ln Z_S\mathrm{Tr}\left\{\mathcal{L}\rho\right\} = -\beta\mathrm{Tr}\left\{(H_S - \mu N_S)\mathcal{L}\rho\right\} = -\beta\dot{Q} \tag{2.70}$$

where $\dot{Q}$ denotes the heat current entering the system from the reservoir. This terminology also implies that it counts positive when entering the system. Therefore, Spohn's inequality can be written as

$$\dot{S} - \beta\dot{Q} \geq 0\,, \tag{2.71}$$

which bounds the rate at which heat enters the system by the change of its entropy. The arguments we used for the system entropy also hold for the reservoir, such that

$$\dot{S}_{\mathrm{res}} = -\mathrm{Tr}\left\{\dot{\rho}\ln\rho\right\}\,. \tag{2.72}$$

Our simple master equation approach does not allow us to track the reservoir density matrix, such that of course the change of it is formally zero. However, if it were allowed to change, we would get by inserting at a specific time a thermal state $\rho = e^{-\beta(H_B - \mu N_B)}/Z_B$,

$$\dot{S}_{\mathrm{res}} = \beta\mathrm{Tr}\left\{\dot{\rho}(H_B - \mu N_B)\right\} + \ln Z_B\mathrm{Tr}\left\{\dot{\rho}\right\} = \beta\mathrm{Tr}\left\{\dot{\rho}(H_B - \mu N_B)\right\} = \beta\dot{Q}_{\mathrm{res}}\,, \tag{2.73}$$

where in the last equality we have simply inserted the definition of the heat entering the reservoir. Identifying the change of the reservoir energy and particle number with the corresponding negative changes in the system (this neglects effects of the interaction) we would get $-\beta\dot{Q} = \dot{S}_{\rm res}$, and eventually Spohn's inequality can be read as

$$\dot{S}_{\rm sys} + \dot{S}_{\rm res} \geq 0. \tag{2.74}$$

This is the second law of thermodynamics formulated for both system and reservoir (neglecting higher-order interaction effects)! Clearly, the system entropy may decrease (e.g. when a system relaxes down to its ground state), but at the same time, entropy is generated in the reservoirs. Since our master equation treatment is so far incomplete, we can up to now not track this contribution.

2.2.3 Coarse-Graining

Perturbation Theory in the Interaction Picture

Although the BMS approximation respects of course the exact initial condition, we have in the derivation made several long-term approximations. For example, the Markov approximation implied that we consider timescales much larger than the decay time of the bath correlation functions. Similarly, the secular approximation implied timescales larger than the inverse minimal splitting of the system energy eigenvalues. Therefore, we can only expect the solution originating from the BMS master equation to be an asymptotically valid long-term approximation.

Coarse-graining in contrast provides a possibility to obtain valid short-time approximations of the density matrix with a generator that is of Lindblad form. We start with the von-Neumann equation in the interaction picture (2.8). For factorizing initial density matrices, it is formally solved by $\boldsymbol{U}(t)\rho_{\rm S}^0 \otimes \bar{\rho}_{\rm B}\boldsymbol{U}^\dagger(t)$, where the time evolution operator

$$\boldsymbol{U}(t) = \hat{\tau}\exp\left\{-\mathrm{i}\int_0^t \boldsymbol{\mathcal{H}}_{\mathbf{I}}(t')dt'\right\} \tag{2.75}$$

obeys the evolution equation

$$\dot{\boldsymbol{U}} = -\mathrm{i}\boldsymbol{\mathcal{H}}_{\mathbf{I}}(t)\boldsymbol{U}(t)\,, \tag{2.76}$$

which defines the time-ordering operator $\hat{\tau}$. Formally integrating this equation with the evident initial condition $\boldsymbol{U}(0) = \mathbf{1}$ yields

$$\begin{aligned}
\boldsymbol{U}(t) &= \mathbf{1} - \mathrm{i}\int_0^t \boldsymbol{\mathcal{H}}_{\mathbf{I}}(t')\boldsymbol{U}(t')dt' \\
&= \mathbf{1} - \mathrm{i}\int_0^t \boldsymbol{\mathcal{H}}_{\mathbf{I}}(t')dt' - \int_0^t dt'\boldsymbol{\mathcal{H}}_{\mathbf{I}}(t')\left[\int_0^{t'} dt''\boldsymbol{\mathcal{H}}_{\mathbf{I}}(\boldsymbol{t''})\boldsymbol{U}(t'')\right] \\
&= \sum_{n=0}^{\infty}(-\mathrm{i})^n\int_0^t dt_1\int_0^{t_1} dt_2\ldots\int_0^{t_{n-1}} dt_n\boldsymbol{\mathcal{H}}_{\mathbf{I}}(t_1)\ldots\boldsymbol{\mathcal{H}}_{\mathbf{I}}(t_n)\,.
\end{aligned} \tag{2.77}$$

In particular, we can define the truncated operator to second order

$$\boldsymbol{U}_2(t) \;=\; \mathbf{1} - \mathrm{i}\int_0^t \boldsymbol{\mathcal{H}}_{\mathbf{I}}(t_1)dt_1 - \int_0^t dt_1 dt_2 \boldsymbol{\mathcal{H}}_{\mathbf{I}}(t_1)\boldsymbol{\mathcal{H}}_{\mathbf{I}}(t_2)\Theta(t_1-t_2)\,, \tag{2.78}$$

where we have introduced the Heaviside function to account for the ordering of the integral bounds. For the Hermitian conjugate operator we obtain

$$\boldsymbol{U}_2^\dagger(t) = \mathbf{1} + \mathrm{i}\int_0^t \boldsymbol{\mathcal{H}}_{\mathbf{I}}(t_1)dt_1 - \int_0^t dt_1 dt_2 \boldsymbol{\mathcal{H}}_{\mathbf{I}}(t_1)\boldsymbol{\mathcal{H}}_{\mathbf{I}}(t_2)\Theta(t_2-t_1)\,. \tag{2.79}$$

To keep the discussion at a moderate level, we assume $\mathrm{Tr}\left\{\boldsymbol{\mathcal{H}}_{\mathbf{I}}\bar{\rho}_{\mathrm{B}}\right\} = 0$ from the beginning. The exact solution $\boldsymbol{\rho_{\mathrm{S}}(t)} = \mathrm{Tr}_{\mathrm{B}}\left\{\boldsymbol{U}(t)\rho_{\mathrm{S}}^0\otimes\bar{\rho}_{\mathrm{B}}\boldsymbol{U}^\dagger(t)\right\}$ is then approximated by

$$\begin{aligned}\boldsymbol{\rho}_{\mathbf{S}}^{(\mathbf{2})}(t) \;\approx\; & \rho_{\mathrm{S}}^0 + \mathrm{Tr}_{\mathrm{B}}\left\{\int_0^t dt_1\int_0^t dt_2 \boldsymbol{\mathcal{H}}_{\mathbf{I}}(t_1)\rho_{\mathrm{S}}^0\otimes\bar{\rho}_{\mathrm{B}}\boldsymbol{\mathcal{H}}_{\mathbf{I}}(t_2)\right\} \\ & - \int_0^t dt_1 dt_2 \mathrm{Tr}_{\mathrm{B}}\left\{\Theta(t_1-t_2)\boldsymbol{\mathcal{H}}_{\mathbf{I}}(t_1)\boldsymbol{\mathcal{H}}_{\mathbf{I}}(t_2)\rho_{\mathrm{S}}^0\otimes\bar{\rho}_{\mathrm{B}} + \Theta(t_2-t_1)\rho_{\mathrm{S}}^0\otimes\bar{\rho}_{\mathrm{B}}\boldsymbol{\mathcal{H}}_{\mathbf{I}}(t_1)\boldsymbol{\mathcal{H}}_{\mathbf{I}}(t_2)\right\}\,.\end{aligned} \tag{2.80}$$

Again, we introduce the bath correlation functions with two time arguments as in Eq. (2.20)

$$C_{\alpha\beta}(t_1,t_2) \;=\; \mathrm{Tr}\left\{\boldsymbol{B}_{\boldsymbol{\alpha}}(t_1)\boldsymbol{B}_{\boldsymbol{\beta}}(t_2)\bar{\rho}_{\mathrm{B}}\right\}\,, \tag{2.81}$$

such that we have

$$\begin{aligned}\boldsymbol{\rho}_{\mathbf{S}}^{(\mathbf{2})}(t) \;=\; & \rho_{\mathrm{S}}^0 + \sum_{\alpha\beta}\int_0^t dt_1\int_0^t dt_2 C_{\alpha\beta}(t_1,t_2)\Big[\boldsymbol{A}_{\boldsymbol{\beta}}(t_2)\rho_{\mathrm{S}}^0\boldsymbol{A}_{\boldsymbol{\alpha}}(t_1) \\ & -\Theta(t_1-t_2)\boldsymbol{A}_{\boldsymbol{\alpha}}(t_1)\boldsymbol{A}_{\boldsymbol{\beta}}(t_2)\rho_{\mathrm{S}}^0 - \Theta(t_2-t_1)\rho_{\mathrm{S}}^0\boldsymbol{A}_{\boldsymbol{\alpha}}(t_1)\boldsymbol{A}_{\boldsymbol{\beta}}(t_2)\Big]\,.\end{aligned} \tag{2.82}$$

Typically, in the interaction picture, the system coupling operators $\boldsymbol{A}_{\boldsymbol{\alpha}}(t)$ will simply carry some oscillatory time dependence. In the worst case, they may remain time-independent. Therefore, the decay of the correlation function is essential for the convergence of the above integrals. In this way, Markovian approximation and weak-coupling assumptions are related. In particular, we note that the truncated density matrix may remain finite even when $t\to\infty$, rendering the expansion convergent also in the long-term limit.

Coarse-Graining

The basic idea of **coarse-graining** is to match this approximate expression for the system density matrix at time $t=\tau$ with one resulting from a Markovian generator

$$\boldsymbol{\rho_{\mathrm{S}}}^{\mathrm{CG}}(\tau) \;=\; e^{\mathcal{L}_\tau^{\mathrm{CG}}\cdot\tau}\rho_{\mathrm{S}}^0 \approx \rho_{\mathrm{S}}^0 + \tau\mathcal{L}_\tau^{\mathrm{CG}}\rho_{\mathrm{S}}^0\,, \tag{2.83}$$

such that we can infer the action of the generator on an arbitrary density matrix

$$\begin{aligned}\mathcal{L}_\tau^{\mathrm{CG}}\boldsymbol{\rho_{\mathrm{S}}} &= \frac{1}{\tau}\sum_{\alpha\beta}\int_0^\tau dt_1\int_0^\tau dt_2 C_{\alpha\beta}(t_1,t_2)\Big[\boldsymbol{A_\beta}(t_2)\boldsymbol{\rho_{\mathrm{S}}}\boldsymbol{A_\alpha}(t_1)\\ &\quad -\Theta(t_1-t_2)\boldsymbol{A_\alpha}(t_1)\boldsymbol{A_\beta}(t_2)\boldsymbol{\rho_{\mathrm{S}}}-\Theta(t_2-t_1)\boldsymbol{\rho_{\mathrm{S}}}\boldsymbol{A_\alpha}(t_1)\boldsymbol{A_\beta}(t_2)\Big]\\ &= -\mathrm{i}\left[\frac{1}{2\mathrm{i}\tau}\int_0^\tau dt_1\int_0^\tau dt_2\sum_{\alpha\beta}C_{\alpha\beta}(t_1,t_2)\mathrm{sgn}(\mathrm{t}_1-\mathrm{t}_2)\boldsymbol{A_\alpha}(\mathrm{t}_1)\boldsymbol{A_\beta}(\mathrm{t}_2),\boldsymbol{\rho_{\mathrm{S}}}\right]\\ &\quad +\frac{1}{\tau}\int_0^\tau dt_1\int_0^\tau dt_2\sum_{\alpha\beta}C_{\alpha\beta}(t_1,t_2)\left[\boldsymbol{A_\beta}(t_2)\boldsymbol{\rho_{\mathrm{S}}}\boldsymbol{A_\alpha}(t_1)-\frac{1}{2}\left\{\boldsymbol{A_\alpha}(t_1)\boldsymbol{A_\beta}(t_2),\boldsymbol{\rho_{\mathrm{S}}}\right\}\right] \quad (2.84)\end{aligned}$$

where we have inserted $\Theta(x)=\frac{1}{2}\left[1+\mathrm{sgn(x)}\right]$ – in order to separate unitary and dissipative effects of the system-reservoir interaction.

Def. 11 (CG Master Equation)**.** *In the weak coupling limit, an interaction Hamiltonian of the form $\mathcal{H}_{\mathrm{I}}=\sum_\alpha A_\alpha\otimes B_\alpha$ leads to the Lindblad-form master equation in the interaction picture*

$$\begin{aligned}\dot{\boldsymbol{\rho}}_{\mathbf{S}} &= -\mathrm{i}\left[\frac{1}{2\mathrm{i}\tau}\int_0^\tau dt_1\int_0^\tau dt_2\sum_{\alpha\beta}C_{\alpha\beta}(t_1,t_2)\mathrm{sgn}(\mathrm{t}_1-\mathrm{t}_2)\boldsymbol{A_\alpha}(\mathrm{t}_1)\boldsymbol{A_\beta}(\mathrm{t}_2),\boldsymbol{\rho_{\mathrm{S}}}\right]\\ &\quad +\frac{1}{\tau}\int_0^\tau dt_1\int_0^\tau dt_2\sum_{\alpha\beta}C_{\alpha\beta}(t_1,t_2)\left[\boldsymbol{A_\beta}(t_2)\boldsymbol{\rho_{\mathrm{S}}}\boldsymbol{A_\alpha}(t_1)-\frac{1}{2}\left\{\boldsymbol{A_\alpha}(t_1)\boldsymbol{A_\beta}(t_2),\boldsymbol{\rho_{\mathrm{S}}}\right\}\right],\end{aligned}$$

where the bath correlation functions are given by

$$C_{\alpha\beta}(t_t,t_2) = \mathrm{Tr}\left\{e^{+\mathrm{i}\mathcal{H}_{\mathrm{B}}t_1}B_\alpha e^{-\mathrm{i}\mathcal{H}_{\mathrm{B}}t_1}e^{+\mathrm{i}\mathcal{H}_{\mathrm{B}}t_2}B_\beta e^{-\mathrm{i}\mathcal{H}_{\mathrm{B}}t_2}\bar{\rho}_{\mathrm{B}}\right\}. \quad (2.85)$$

We have not used Hermiticity of the coupling operators nor that the bath correlation functions do typically only depend on a single argument. However, if the coupling operators were chosen Hermitian, it is easy to show the Lindblad form. For completeness, we also note there that a Lindblad form is also obtained for non-Hermitian couplings. Obtaining the master equation requires the calculation of bath correlation functions and the evolution of the coupling operators in the interaction picture.

Exercise 22 (Lindblad form)**.** *By assuming Hermitian coupling operators $A_\alpha=A_\alpha^\dagger$, show that the CG master equation is of Lindblad form for all coarse-graining times τ.*

Thus, we have found that the best approximation to the exact solution can be written as $\rho(t)=e^{\mathcal{L}_t^{\mathrm{CG}}t}\rho_0$. Unfortunately, this is not the solution to a (single) master equation only. By acting with a time-derivative, we can see that $\dot{\rho}\neq\mathcal{L}_t^{\mathrm{CG}}\rho(t)$. Rather, if interested in the solution at a specific time t, we would have to derive the Liouville superoperator and then exponentiate it.

Correspondence to the quantum-optical master equation

Let us make once more the time-dependence of the coupling operators explicit, which is most conveniently done in the system energy eigenbasis. Now, we also assume that the bath correlation functions only depend on the difference of their time arguments $C_{\alpha\beta}(t_1,t_2)=C_{\alpha\beta}(t_1-t_2)$, such that we may use the Fourier transform definitions in Eq. (2.43) to obtain

$$\begin{aligned}
\dot{\boldsymbol{\rho}}_{\mathbf{S}} &= -\mathrm{i}\left[\frac{1}{2\mathrm{i}\tau}\sum_{abc}\int_0^\tau dt_1\int_0^\tau dt_2\sum_{\alpha\beta}C_{\alpha\beta}(t_1-t_2)\mathrm{sgn}(\mathrm{t_1-t_2})\left|\mathrm{a}\right\rangle\left\langle\mathrm{a}\right|\boldsymbol{A_\alpha}(\mathrm{t_1})\left|\mathrm{c}\right\rangle\left\langle\mathrm{c}\right|\boldsymbol{A_\beta}(\mathrm{t_2})\left|\mathrm{b}\right\rangle\left\langle\mathrm{b}\right|,\boldsymbol{\rho}_{\mathbf{S}}\right]\\
&\quad+\frac{1}{\tau}\int_0^\tau dt_1\int_0^\tau dt_2\sum_{\alpha\beta}\sum_{abcd}C_{\alpha\beta}(t_1-t_2)\Big[\left|a\right\rangle\left\langle a\right|\boldsymbol{A_\beta}(t_2)\left|b\right\rangle\left\langle b\right|\boldsymbol{\rho}_{\mathbf{S}}\left|d\right\rangle\left\langle d\right|\boldsymbol{A_\alpha}(t_1)\left|c\right\rangle\left\langle c\right|\\
&\quad-\frac{1}{2}\left\{\left|d\right\rangle\left\langle d\right|\boldsymbol{A_\alpha}(t_1)\left|c\right\rangle\left\langle c\right|\cdot\left|a\right\rangle\left\langle a\right|\boldsymbol{A_\beta}(t_2)\left|b\right\rangle\left\langle b\right|,\boldsymbol{\rho}_{\mathbf{S}}\right\}\Big]\\
&= -\mathrm{i}\frac{1}{4\mathrm{i}\pi\tau}\int d\omega\sum_{abc}\int_0^\tau dt_1\int_0^\tau dt_2\sum_{\alpha\beta}\sigma_{\alpha\beta}(\omega)e^{-\mathrm{i}\omega(t_1-t_2)}e^{+\mathrm{i}(E_a-E_c)t_1}e^{+\mathrm{i}(E_c-E_b)t_2}A_\beta^{cb}A_\alpha^{ac}\left[L_{ab},\boldsymbol{\rho}_{\mathbf{S}}\right]\\
&\quad+\frac{1}{2\pi\tau}\int d\omega\int_0^\tau dt_1\int_0^\tau dt_2\sum_{\alpha\beta}\sum_{abcd}\gamma_{\alpha\beta}(\omega)e^{-\mathrm{i}\omega(t_1-t_2)}e^{+\mathrm{i}(E_a-E_b)t_2}e^{+\mathrm{i}(E_d-E_c)t_1}A_\beta^{ab}A_\alpha^{dc}\times\\
&\quad\times\left[L_{ab}\boldsymbol{\rho}_{\mathbf{S}}L_{cd}^\dagger-\frac{1}{2}\left\{L_{cd}^\dagger L_{ab},\boldsymbol{\rho}_{\mathbf{S}}\right\}\right].
\end{aligned}\tag{2.86}$$

We perform the temporal integrations by invoking

$$\int_0^\tau e^{\mathrm{i}\alpha_k t_k}dt_k=\tau e^{\mathrm{i}\alpha_k\tau/2}\mathrm{sinc}\left[\frac{\alpha_\mathrm{k}\tau}{2}\right]\tag{2.87}$$

with $\mathrm{sinc(x)}=\mathrm{sin(x)/x}$ to obtain

$$\begin{aligned}
\dot{\boldsymbol{\rho}}_{\mathbf{S}} &= -\mathrm{i}\frac{\tau}{4\mathrm{i}\pi}\int d\omega\sum_{abc}\sum_{\alpha\beta}\sigma_{\alpha\beta}(\omega)e^{\mathrm{i}\tau(E_a-E_b)/2}\mathrm{sinc}\left[\frac{\tau}{2}(\mathrm{E_a-E_c}-\omega)\right]\mathrm{sinc}\left[\frac{\tau}{2}(\mathrm{E_c-E_b}+\omega)\right]\times\\
&\quad\times\left\langle c\right|A_\beta\left|b\right\rangle\left\langle c\right|A_\alpha^\dagger\left|a\right\rangle^*\left[\left|a\right\rangle\left\langle b\right|,\boldsymbol{\rho}_{\mathbf{S}}\right]\\
&\quad+\frac{\tau}{2\pi}\int d\omega\sum_{\alpha\beta}\sum_{abcd}\gamma_{\alpha\beta}(\omega)e^{\mathrm{i}\tau(E_a-E_b+E_d-E_c)/2}\mathrm{sinc}\left[\frac{\tau}{2}(\mathrm{E_d-E_c}-\omega)\right]\mathrm{sinc}\left[\frac{\tau}{2}(\omega+\mathrm{E_a-E_b})\right]\times\\
&\quad\times\left\langle a\right|A_\beta\left|b\right\rangle\left\langle c\right|A_\alpha^\dagger\left|d\right\rangle^*\left[\left|a\right\rangle\left\langle b\right|\boldsymbol{\rho}_{\mathbf{S}}\left(\left|c\right\rangle\left\langle d\right|\right)^\dagger-\frac{1}{2}\left\{\left(\left|c\right\rangle\left\langle d\right|\right)^\dagger\left|a\right\rangle\left\langle b\right|,\boldsymbol{\rho}_{\mathbf{S}}\right\}\right].
\end{aligned}\tag{2.88}$$

Therefore, we have the same structure as before, but now with coarse-graining time dependent dampening coefficients

$$\begin{aligned}
\dot{\boldsymbol{\rho}}_{\mathbf{S}} &= -\mathrm{i}\left[\sum_{ab}\sigma_{ab}^\tau\left|a\right\rangle\left\langle b\right|,\boldsymbol{\rho}_{\mathbf{S}}\right]\\
&\quad+\sum_{abcd}\gamma_{ab,cd}^\tau\left[\left|a\right\rangle\left\langle b\right|\boldsymbol{\rho}_{\mathbf{S}}\left(\left|c\right\rangle\left\langle d\right|\right)^\dagger-\frac{1}{2}\left\{\left(\left|c\right\rangle\left\langle d\right|\right)^\dagger\left|a\right\rangle\left\langle b\right|,\boldsymbol{\rho}_{\mathbf{S}}\right\}\right]
\end{aligned}\tag{2.89}$$

with the coefficients

$$\begin{aligned}\sigma^{\tau}_{ab} &= \frac{1}{2\mathrm{i}}\int d\omega \sum_c e^{\mathrm{i}\tau(E_a-E_b)/2}\frac{\tau}{2\pi}\mathrm{sinc}\left[\frac{\tau}{2}(\mathrm{E_a}-\mathrm{E_c}-\omega)\right]\mathrm{sinc}\left[\frac{\tau}{2}(\mathrm{E_b}-\mathrm{E_c}-\omega)\right]\times \\ &\quad\times\left[\sum_{\alpha\beta}\sigma_{\alpha\beta}(\omega)\left\langle c\right|A_\beta\left|b\right\rangle\left\langle c\right|A^\dagger_\alpha\left|a\right\rangle^*\right], \\ \gamma^{\tau}_{ab,cd} &= \int d\omega e^{\mathrm{i}\tau(E_a-E_b+E_d-E_c)/2}\frac{\tau}{2\pi}\mathrm{sinc}\left[\frac{\tau}{2}(\mathrm{E_d}-\mathrm{E_c}-\omega)\right]\mathrm{sinc}\left[\frac{\tau}{2}(\mathrm{E_b}-\mathrm{E_a}-\omega)\right]\times \\ &\quad\times\left[\sum_{\alpha\beta}\gamma_{\alpha\beta}(\omega)\left\langle a\right|A_\beta\left|b\right\rangle\left\langle c\right|A^\dagger_\alpha\left|d\right\rangle^*\right]. \end{aligned} \tag{2.90}$$

Finally, we note that in the limit of large coarse-graining times $\tau\to\infty$ and assuming Hermitian coupling operators $A_\alpha = A^\dagger_\alpha$, these dampening coefficients converge to the ones in definition 7, i.e., formally

$$\begin{aligned}\lim_{\tau\to\infty}\sigma^{\tau}_{ab} &= \sigma_{ab}\,, \\ \lim_{\tau\to\infty}\gamma^{\tau}_{ab,cd} &= \gamma_{ab,cd}\,. \end{aligned} \tag{2.91}$$

Exercise 23 (CG-BMS correspondence)**.** *Show for Hermitian coupling operators that when $\tau\to\infty$, CG and BMS approximation are equivalent. You may use the identity*

$$\lim_{\tau\to\infty}\tau\mathrm{sinc}\left[\frac{\tau}{2}(\Omega_\mathrm{a}-\omega)\right]\mathrm{sinc}\left[\frac{\tau}{2}(\Omega_\mathrm{b}-\omega)\right] = 2\pi\delta_{\Omega_\mathrm{a},\Omega_\mathrm{b}}\delta(\Omega_\mathrm{a}-\omega)\,.$$

This shows that coarse-graining provides an alternative derivation of the quantum-optical master equation, replacing three subsequent approximations (Born-, Markov- and secular) by just one (perturbative expansion in the interaction).

2.2.4 Example: Spin-Boson Model

The spin-boson model describes the interaction of a spin with a bosonic environment

$$\begin{aligned}\mathcal{H}_\mathrm{S} &= \Omega\sigma^z + T\sigma^x\,, \qquad \mathcal{H}_\mathrm{B} = \sum_k \omega_k b^\dagger_k b_k\,, \\ \mathcal{H}_\mathrm{I} &= \sigma^z\otimes\sum_k\left[h_k b_k + h^*_k b^\dagger_k\right], \end{aligned} \tag{2.91}$$

where Ω and T denote parameters of the system Hamiltonian, σ^α the Pauli matrices, and $b^\dagger$ creates a boson with frequency ω_k in the reservoir. The model can be motivated by a variety of setups, e.g. a charge qubit (singly-charged double quantum dot) that is coupled to vibrations. We note the a priori Hermitian coupling operators

$$A_1 = \sigma^z\,, \qquad B_1 = \sum_k\left[h_k b_k + h^*_k b^\dagger_k\right]. \tag{2.92}$$

For completeness, we state these operators in the interaction picture

$$\begin{aligned} A_1(t) &= \frac{2\Omega T}{T^2+\Omega^2}\sin^2\left[2t\sqrt{T^2+\Omega^2}\right]\sigma^x + \frac{T}{\sqrt{T^2+\Omega^2}}\sin\left[2t\sqrt{T^2+\Omega^2}\right]\sigma^y \\ &\quad + \left(\frac{\Omega^2}{T^2+\Omega^2}+\frac{T^2}{T^2+\Omega^2}\right)\cos\left[2t\sqrt{T^2+\Omega^2}\right]\sigma^z \\ B_1(t) &= \sum_k \left[h_k b_k e^{-\mathrm{i}\omega_k t} + h_k^* b_k^\dagger e^{+\mathrm{i}\omega_k t}\right]. \end{aligned} \tag{2.93}$$

Exact solution of the pure-dephasing limit

The limit when $T = 0$ can be solved exactly. Then, we can apply the so-called *polaron* or Lang-Firsov transformation to the whole Hamiltonian

$$U = \exp\left\{-\sigma^z \sum_k \left(\frac{h_k}{\omega_k} b_k - \frac{h_k^*}{\omega_k} b_k^\dagger\right)\right\}. \tag{2.94}$$

We note the following relations

$$\begin{aligned} U\sigma^z U^\dagger &= \sigma^z, \\ U\sigma^\pm U^\dagger &= e^{\pm 2\sum_k \left(\frac{h_k^*}{\omega_k} b_k^\dagger - \frac{h_k}{\omega_k} b_k\right)}\sigma^\pm, \\ U b_k U^\dagger &= b_k - \frac{h_k^*}{\omega_k}\sigma^z. \end{aligned} \tag{2.95}$$

Exercise 24 (Polaron transform)**.** *Find a way to derive these relations.*

From this we conclude that in the Schrödinger picture (recall that $T = 0$)

$$\begin{aligned} UHU^\dagger &= \Omega\sigma^z + \sigma^z \sum_k \left(h_k b_k + h_k^* b_k^\dagger - 2\frac{|h_k|^2}{\omega_k}\sigma^z\right) + \sum_k \omega_k \left(b_k^\dagger - \frac{h_k}{\omega_k}\sigma^z\right)\left(b_k - \frac{h_k^*}{\omega_k}\sigma^z\right) \\ &= \Omega\sigma^z - \sum_k \frac{|h_k|^2}{\omega_k} + \sum_k \omega_k b_k^\dagger b_k. \end{aligned} \tag{2.96}$$

This means that in this frame, the evolution of spin and boson are completely decoupled. Consequently, we can e.g. compute the expectation value of σ^α via

$$\begin{aligned} \langle\sigma^\alpha\rangle &= \mathrm{Tr}\left\{e^{+\mathrm{i}Ht}\sigma^\alpha e^{-\mathrm{i}Ht}\rho_0\right\} = \mathrm{Tr}\left\{U^\dagger U e^{+\mathrm{i}Ht} U^\dagger U \sigma^\alpha U^\dagger U e^{-\mathrm{i}Ht} U^\dagger U \rho_0\right\} \\ &= \mathrm{Tr}\left\{U^\dagger e^{+\mathrm{i}UHU^\dagger t} U\sigma^\alpha U^\dagger e^{-\mathrm{i}UHU^\dagger t} U\rho_0\right\} \\ &= \mathrm{Tr}\left\{U^\dagger e^{+\mathrm{i}\Omega t\sigma^z} e^{+\mathrm{i}\sum_k \omega_k t b_k^\dagger b_k} U\sigma^\alpha U^\dagger e^{-\mathrm{i}\sum_k \omega_k t b_k^\dagger b_k} e^{-\mathrm{i}\Omega t\sigma^z} U\rho_0\right\}. \end{aligned} \tag{2.97}$$

For $\alpha = +$ we further calculate

$$\begin{aligned}
\langle \sigma^+ \rangle &= \mathrm{Tr}\left\{ U^\dagger e^{+\mathrm{i}\sum_k \omega_k t b_k^\dagger b_k} e^{2\sum_k \left(\frac{h_k^*}{\omega_k} b_k^\dagger - \frac{h_k}{\omega_k} b_k\right)} e^{-\mathrm{i}\sum_k \omega_k t b_k^\dagger b_k} e^{+\mathrm{i}\Omega t \sigma^z} \sigma^+ e^{-\mathrm{i}\Omega t \sigma^z} U \rho_0 \right\} \\
&= e^{+2\mathrm{i}\Omega t} \mathrm{Tr}\left\{ U^\dagger e^{2\sum_k \left(\frac{h_k^*}{\omega_k} b_k^\dagger e^{+\mathrm{i}\omega_k t} - \frac{h_k}{\omega_k} b_k e^{-\mathrm{i}\omega_k t}\right)} U U^\dagger \sigma^+ U \rho_0 \right\} \\
&= e^{+2\mathrm{i}\Omega t} \mathrm{Tr}\left\{ e^{2\sum_k \left(\frac{h_k^*}{\omega_k}(b_k^\dagger + \frac{h_k}{\omega_k}\sigma^z) e^{+\mathrm{i}\omega_k t} - \frac{h_k}{\omega_k}(b_k + \frac{h_k^*}{\omega_k}\sigma^z) e^{-\mathrm{i}\omega_k t}\right)} e^{-2\sum_k \left(\frac{h_k^*}{\omega_k} b_k^\dagger - \frac{h_k}{\omega_k} b_k\right)} \sigma^+ \rho_0 \right\} \\
&= e^{+2\mathrm{i}\Omega t} \mathrm{Tr}\left\{ e^{4\mathrm{i}\sum_k \frac{|h_k|^2}{\omega_k^2} \sin(\omega_k t)\sigma^z} \sigma^+ \rho_S^0 \right\} \mathrm{Tr}\left\{ e^{2\sum_k \left(\frac{h_k^*}{\omega_k} b_k^\dagger e^{+\mathrm{i}\omega_k t} - \frac{h_k}{\omega_k} b_k e^{-\mathrm{i}\omega_k t}\right)} e^{-2\sum_k \left(\frac{h_k^*}{\omega_k} b_k^\dagger - \frac{h_k}{\omega_k} b_k\right)} \bar{\rho}_B \right\} \\
&= e^{+2\mathrm{i}\Omega t} \mathrm{Tr}\left\{ e^{4\mathrm{i}\sum_k \frac{|h_k|^2}{\omega_k^2} \sin(\omega_k t)\sigma^z} \sigma^+ \rho_S^0 \right\} B(t)\,, \qquad (2.98)
\end{aligned}$$

where we have used initial factorization $\rho_0 = \rho_S^0 \otimes \bar{\rho}_B$. Using that $e^X e^Y = e^{X+Y+[X,Y]/2}$ when $[X,[X,Y]] = [Y,[X,Y]] = 0$, we can further evaluate the decoherence factor resulting from the reservoir

$$\begin{aligned}
B(t) &= \mathrm{Tr}\left\{ \exp\left\{ 2\sum_k \left[\frac{h_k^*}{\omega_k} b_k^\dagger \left(e^{+\mathrm{i}\omega_k t} - 1\right) - \frac{h_k}{\omega_k} b_k \left(e^{-\mathrm{i}\omega_k t} - 1\right) \right] \right\} \bar{\rho}_B \right\} e^{-4\mathrm{i}\sum_k \frac{|h_k|^2}{\omega_k^2} \sin(\omega_k t)} \\
&= \mathrm{Tr}\left\{ \exp\left\{ +2\sum_k \frac{h_k^*}{\omega_k} b_k^\dagger \left(e^{+\mathrm{i}\omega_k t} - 1\right) \right\} \exp\left\{ -2\sum_k \frac{h_k}{\omega_k} b_k \left(e^{-\mathrm{i}\omega_k t} - 1\right) \right\} \bar{\rho}_B \right\} \times \\
&\quad \times e^{-4\sum_k \frac{|h_k|^2}{\omega_k^2}[1 - \cos(\omega_k t) + \mathrm{i}\sin(\omega_k t)]}\,. \qquad (2.99)
\end{aligned}$$

Now, we can use that

$$\begin{aligned}
\mathrm{Tr}\left\{ e^{+\alpha_k b_k^\dagger} e^{-\alpha_k^* b_k} \frac{e^{-\beta\omega_k b_k^\dagger b_k}}{Z_k} \right\} &= \sum_{n,m=0}^{\infty} \frac{(+\alpha_k)^n (-\alpha_k^*)^m}{n!m!} \mathrm{Tr}\left\{ (b_k^\dagger)^n b_k^m \frac{e^{-\beta\omega_k b_k^\dagger b_k}}{Z_k} \right\} \\
&= \sum_{q=0}^{\infty} \sum_{n=0}^{q} \frac{(-|\alpha_k|^2)^n}{(n!)^2} (1 - e^{-\beta\omega_k}) e^{-\beta\omega_k q} \frac{q!}{(q-n)!} \\
&= e^{-|\alpha_k|^2 n_B(\omega_k)} \qquad (2.100)
\end{aligned}$$

with $|\alpha_k|^2 = 8|h_k|^2/\omega_k^2[1 - \cos(\omega_k t)]$. This then implies for the decoherence factor

$$B(t) = \exp\left\{ -\frac{2}{\pi} \int_0^\infty \frac{\Gamma(\omega)}{\omega^2} [1 - \cos(\omega t)][1 + 2n_B(\omega)] d\omega \right\} \exp\left\{ -\frac{2\mathrm{i}}{\pi} \int_0^\infty \frac{\Gamma(\omega)}{\omega^2} \sin(\omega t) d\omega \right\} \qquad (2.101)$$

Eventually, it follows that the populations remain unaffected and that in the interaction picture the coherences decay according to [2]

$$\begin{aligned}
\boldsymbol{\rho_{01}}(t) &= \exp\left\{ -8\sum_k |h_k|^2 \frac{\sin^2(\omega_k t/2)}{\omega_k^2} \coth\left(\frac{\beta\omega_k}{2}\right) \right\} \rho_{01}^0 \\
&= \exp\left\{ -\frac{4}{\pi} \int_0^\infty \Gamma(\omega) \frac{\sin^2(\omega t/2)}{\omega^2} \coth\left(\frac{\beta\omega}{2}\right) \right\} \rho_{01}^0\,. \qquad (2.102)
\end{aligned}$$

BMS master equation

We first diagonalize the system part of the Hamiltonian to obtain the eigenbasis $\mathcal{H}_{\rm S}\left|n\right\rangle = E_n\left|n\right\rangle$, where

$$E_\pm = \pm\sqrt{\Omega^2+T^2}\,, \qquad \left|\pm\right\rangle = \frac{1}{\sqrt{T^2+\left(\Omega\pm\sqrt{\Omega^2+T^2}\right)^2}}\left[\left(\Omega\pm\sqrt{\Omega^2+T^2}\right)\left|0\right\rangle + T\left|1\right\rangle\right], \tag{2.103}$$

where $\left|0/1\right\rangle$ denote the eigenvectors of the σ^z Pauli matrix with $\sigma^z\left|i\right\rangle = (-1)^i\left|i\right\rangle$.

Exercise 25 (Eigenbasis)**.** *Confirm the validity of Eq. (2.103).*

Second, we calculate the correlation function (in this case, there is just one). Transforming everything in the interaction picture we see that the annihilation operators just pick up time-dependent phases

$$\begin{aligned} C(\tau) &= \mathrm{Tr}\left\{\sum_k\left[h_k b_k e^{-\mathrm{i}\omega_k\tau} + h_k^* b_k^\dagger e^{+\mathrm{i}\omega_k\tau}\right]\sum_q\left[h_q b_q + h_q^* b_q^\dagger\right]\bar{\rho}_{\rm B}\right\} \\ &= \sum_k |h_k|^2\left[e^{-\mathrm{i}\omega_k\tau}\left(1+n_B(\omega_k)\right) + e^{+\mathrm{i}\omega_k\tau} n_B(\omega_k)\right] \\ &= \frac{1}{2\pi}\int d\omega\Gamma(\omega)\left[e^{-\mathrm{i}\omega\tau}\left(1+n_B(\omega)\right) + e^{+\mathrm{i}\omega\tau} n_B(\omega)\right], \end{aligned} \tag{2.104}$$

where we have introduced the spectral coupling density $\Gamma(\omega) = 2\pi\sum_k |h_k|^2\delta(\omega-\omega_k)$ and the Bose distribution

$$n_B(\omega) = \frac{1}{e^{\beta(\omega-\mu)}-1}\,. \tag{2.105}$$

Exercise 26 (Bose distribution)**.** *Confirm the validity of Eq. (2.105), i.e., show that*

$$\delta_{kq} n_B(\omega_k) = \mathrm{Tr}\left\{b_k^\dagger b_q \frac{e^{-\beta(\mathcal{H}_{\rm B}-\mu N_{\rm B})}}{Z}\right\}, \tag{2.106}$$

where $\mathcal{H}_{\rm B} = \sum_k \omega_k b_k^\dagger b_k$, $N_{\rm B} = \sum_k b_k^\dagger b_k$, *and* $Z = \mathrm{Tr}\left\{e^{-\beta(\mathcal{H}_{\rm B}-\mu N_{\rm B})}\right\}$.

We can directly read off the even Fourier transform of the correlation function

$$\gamma(\omega) = \Gamma(+\omega)\Theta(+\omega)[1+n_B(+\omega)] + \Gamma(-\omega)\Theta(-\omega)n_B(-\omega)\,. \tag{2.107}$$

We note that for bosons we necessarily have $\Gamma(\omega<0)=0$, since all oscillator frequencies in the reservoir must be positive. We compute some relevant dampening coefficients from Def. 7

$$\begin{aligned} \gamma_{-+,-+} &= \Gamma(+2\sqrt{\Omega^2+T^2})[1+n_B(+2\sqrt{\Omega^2+T^2})]|\langle-|\,\sigma^z\,|+\rangle|^2\,, \\ \gamma_{+-,+-} &= \Gamma(+2\sqrt{\Omega^2+T^2})n_B(+2\sqrt{\Omega^2+T^2})|\langle-|\,\sigma^z\,|+\rangle|^2\,, \\ \gamma_{--,++} &= \gamma(0)\,\langle-|\,\sigma^z\,|-\rangle\,\langle+|\,\sigma^z\,|+\rangle = \gamma_{++,--}\,. \end{aligned} \tag{2.108}$$

We have to say that finite $\gamma(0) = \lim_{\omega\to 0}\Gamma(\omega)[1+n_B(\omega)]$ requires that for small frequencies the spectral coupling density should grow only mildly.

The explicit calculation of the non-vanishing Lamb-shift terms σ_{--} and σ_{++} is possible but more involved. Fortunately, it can be omitted for many applications. Since the system Hamiltonian is non-degenerate, the populations evolve according to

$$\dot\rho_{--} = +\gamma_{-+,-+}\rho_{++} - \gamma_{+-,+-}\rho_{--}\,, \qquad \dot\rho_{++} = +\gamma_{+-,+-}\rho_{--} - \gamma_{-+,-+}\rho_{++}\,, \tag{2.109}$$

which is independent from the coherences

$$\dot\rho_{-+} = -\mathrm{i}\left(E_- - E_+ + \sigma_{--} - \sigma_{++}\right)\rho_{-+} + \left[\gamma_{--,++} - \frac{\gamma_{-+,-+}+\gamma_{+-,+-}}{2}\right]\rho_{-+} \equiv \eta\rho_{-+}\,. \tag{2.110}$$

Altogether, we can write this as a superoperator

$$\mathcal{L}\begin{pmatrix}\rho_{--}\\ \rho_{++}\\ \rho_{-+}\\ \rho_{+-}\end{pmatrix} = \begin{pmatrix}-\gamma_{+-,+-} & +\gamma_{-+,-+} & 0 & 0\\ +\gamma_{+-,+-} & -\gamma_{-+,-+} & 0 & 0\\ 0 & 0 & \eta & 0\\ 0 & 0 & 0 & \eta^*\end{pmatrix}\begin{pmatrix}\rho_{--}\\ \rho_{++}\\ \rho_{-+}\\ \rho_{+-}\end{pmatrix}\,, \tag{2.111}$$

which has the block structure in the system energy eigenbasis. Since the Lamb-shift terms σ_{ii} are purely imaginary, the quantities at hand already allow us to deduce that the coherences will decay since $\Re\eta \leq 0$. More precisely, we have $|\rho_{-+}|^2 = e^{-(-2\gamma_{--,++}+\gamma_{-+,-+}+\gamma_{+-,+-})t}\left|\rho^0_{-+}\right|^2$, which shows that the decoherence rate increases with temperature (finite n_B) but can also at zero temperature not be suppressed below a minimum value. A special (exactly solvable) case arises when the system parameter T vanishes: Then, the interaction commutes with the system Hamiltonian leaving the energy of the system invariant. Consistently, the eigenbasis is in this case that of σ^z and the coefficients $\gamma_{-+,-+}$ and $\gamma_{+-,+-}$ do vanish. In contrast, the coefficient $\gamma_{--,++} \to -\gamma(0)$ may remain finite. Such models are called pure dephasing models (since only their coherences decay). However, for finite T the steady state of the master equation is given by (we assume here $\mu = 0$)

$$\frac{\bar\rho_{++}}{\bar\rho_{--}} = \frac{\gamma_{+-,+-}}{\gamma_{-+,-+}} = \frac{n_B(+2\sqrt{\Omega^2+T^2})}{1+n_B(+2\sqrt{\Omega^2+T^2})} = e^{-2\beta\sqrt{\Omega^2+T^2}}\,, \tag{2.112}$$

i.e., the stationary state is given by the thermalized one.

Coarse-Graining master equation

In a completely analogous way, we can set up the coarse-graining master equation. However, we also see that computation of the involved integrals becomes a bit tedious. Therefore, we constrain ourselves here only to the trivial pure-dephasing limit $T = 0$. Then, the system coupling operator becomes time-independent $e^{+\mathrm{i}H_S t}\sigma^z e^{-\mathrm{i}H_S t} = \sigma^z$, and with using that $\sigma^z\sigma^z = \mathbf{1}$, such that the Lamb-shift vanishes, the coarse-graining master equation in the interaction picture from Def. 11 reads

$$\begin{aligned}\dot{\boldsymbol\rho} &= \frac{1}{\tau}\int_0^\tau dt_1\int_0^\tau dt_2 C(t_1-t_2)\left[\sigma^z\boldsymbol\rho\sigma^z - \boldsymbol\rho\right]\\ &= \frac{1}{2\pi\tau}\int_0^\tau dt_1\int_0^\tau dt_2\int d\omega\Gamma(\omega)[1+n_B(\omega)]e^{-\mathrm{i}\omega(t_1-t_2)}\left[\sigma^z\boldsymbol\rho\sigma^z - \boldsymbol\rho\right]\\ &= \frac{1}{2\pi}\int d\omega\Gamma(\omega)[1+n_B(\omega)]\tau\mathrm{sinc}^2\left(\frac{\omega\tau}{2}\right)\left[\sigma^z\boldsymbol\rho\sigma^z - \boldsymbol\rho\right]\\ &\equiv \Gamma(\tau)\left[\sigma^z\boldsymbol\rho\sigma^z - \boldsymbol\rho\right]\,,\end{aligned} \tag{2.113}$$

where we have used that

$$\int_0^\tau dt_1 \int_0^\tau dt_2 e^{-\mathrm{i}\omega(t_1-t_2)} = 4\frac{\sin^2(\omega\tau/2)}{\omega^2} = \tau^2 \mathrm{sinc}^2\left(\frac{\omega\tau}{2}\right) \tag{2.114}$$

with the band-filter function $\mathrm{sinc}(x) = \sin(x)/x$. We note that this dynamics can be solved exactly, and that coarse-graining readily provides the exact solution. In the limit of infinite coarse-graining times $\tau \to \infty$, this would yield

$$\dot{\boldsymbol{\rho}} \;=\; \gamma(0)\left[\sigma^z \boldsymbol{\rho} \sigma^z - \boldsymbol{\rho}\right] , \tag{2.115}$$

where we have used that $\gamma(0) = \lim_{\omega\to 0}\Gamma(\omega)[1+n_B(\omega)]$. Generally, the evolution equation $\dot{\rho} = \Gamma(\tau)[\sigma^z\rho\sigma^z - \rho]$ leads to the expectation values

$$\frac{d}{dt}\left\langle\sigma^\pm\right\rangle = -2\Gamma(\tau)\left\langle\sigma^\pm\right\rangle , \qquad \left\langle\sigma^\pm\right\rangle_t = e^{-2\Gamma(\tau)t}\left\langle\sigma^\pm\right\rangle_0 . \tag{2.116}$$

Therefore for time-dependent coarse-graining time $\Gamma(\tau) = \Gamma(t)$ we obtain a time-dependent coherence decay rate exponent, which can also be written as

$$\rho_{01}(t) = e^{-2\Gamma(t)t}\rho_{01}^0 . \tag{2.117}$$

With

$$\begin{aligned} 2\Gamma(t)t &= \frac{1}{\pi}\int d\omega\Gamma(\omega)[1+n_B(\omega)]\frac{4\sin^2(\omega t/2)}{\omega^2} \\ &= \frac{4}{\pi}\int_0^\infty d\omega\Gamma(\omega)[1+2n_B(\omega)]\frac{4\sin^2(\omega t/2)}{\omega^2} \\ &= \frac{4}{\pi}\int_0^\infty d\omega\Gamma(\omega)\coth\left(\frac{\beta\omega}{2}\right)\frac{\sin^2(\omega t/2)}{\omega^2} . \end{aligned} \tag{2.118}$$

This is precisely the same as the decay predicted in Eq. (2.102)

Chapter 3

Nonequilibrium Case I: Multiple Reservoirs

The most obvious way to achieve non-equilibrium dynamics is to use reservoir states that are non-thermalized, i.e., states that cannot simply be characterized by just temperature and chemical potential. Since the derivation of the master equation only requires $[\bar{\rho}_{\mathrm{B}}, \mathcal{H}_{\mathrm{B}}] = 0$, this would still allow for many nontrivial models, $\langle n| \bar{\rho}_{\mathrm{B}} |n\rangle$ could e.g. follow multi-modal distributions. Alternatively, a non-equilibrium situation may be established when a system is coupled to different thermal equilibrium baths or of course when the system itself is externally driven – either unconditionally (open-loop feedback) or conditioned on the actual state of the system (closed-loop feedback).

First, we will consider the case of multiple reservoirs at different thermal equilibria that are only indirectly coupled via the system: Without the system, they would be completely independent. Since these are chosen at different equilibria, they drag the system towards different thermal states, and the resulting stationary state is in general a non-thermal one. Since the different compartments interact only indirectly via the system, we have the case of a multi-terminal system, where one can most easily derive the corresponding master equation, since each contact may be treated separately. Therefore, we do now consider multiple (K) reservoirs

$$\mathcal{H}_{\mathrm{B}} = \sum_{\ell=1}^{K} \mathcal{H}_{\mathrm{B}}^{(\ell)} \tag{3.1}$$

with commuting individual parts $\left[\mathcal{H}_{\mathrm{B}}^{(\ell)}, \mathcal{H}_{\mathrm{B}}^{(k)}\right] = 0$. These are held at different chemical potentials and different temperatures

$$\bar{\rho}_{\mathrm{B}} = \frac{e^{-\beta(\mathcal{H}_{\mathrm{B}}^{(1)} - \mu N_{\mathrm{B}}^{(1)})}}{\mathrm{Tr}\left\{e^{-\beta(\mathcal{H}_{\mathrm{B}}^{(1)} - \mu N_{\mathrm{B}}^{(1)})}\right\}} \otimes \ldots \otimes \frac{e^{-\beta(\mathcal{H}_{\mathrm{B}}^{(K)} - \mu N_{\mathrm{B}}^{(K)})}}{\mathrm{Tr}\left\{e^{-\beta(\mathcal{H}_{\mathrm{B}}^{(K)} - \mu N_{\mathrm{B}}^{(K)})}\right\}} \,. \tag{3.2}$$

To each of the reservoirs, the system is coupled via different coupling operators

$$\mathcal{H}_{\mathrm{I}} = \sum_{\alpha} A_{\alpha} \otimes \sum_{\ell=1}^{k} B_{\alpha}^{(\ell)} \,. \tag{3.3}$$

Since we assume that the first order bath correlation functions vanish $\left\langle B_{\alpha}^{\ell} \bar{\rho}_{\mathrm{B}} \right\rangle = 0$, the second-order bath correlation functions may be computed additively

$$C_{\alpha\beta}(\tau) = \sum_{\ell=1}^{K} C_{\alpha\beta}^{(\ell)}(\tau) \,. \tag{3.4}$$

Exercise 27 (Additive Reservoirs)**.** *Show with using Eqns. (3.1) and (3.2) that expectation values of coupling operators belonging to different reservoirs vanish, i.e.,*

$$C_{(\alpha,\ell),(\beta,k)}(\tau) = \mathrm{Tr}\left\{\boldsymbol{B}^{(\ell)}_{\boldsymbol{\alpha}}(\tau)B^{(k)}_{\beta}\bar{\rho}_{\mathrm{B}}\right\} = \delta_{k\ell}C_{(\alpha,\ell),(\beta,\ell)}\,.$$

This obviously transfers to their Fourier transforms and thus, also to the final Liouvillian (to second order in the coupling)

$$\mathcal{L} = \mathcal{L}^{(0)} + \sum_{\ell=1}^{K}\mathcal{L}^{(\ell)}\,. \tag{3.4}$$

Here, $\mathcal{L}^{(0)}\rho \hat{=} -\mathrm{i}\,[\mathcal{H}_{\mathrm{S}},\rho]$ describes the action of the system Hamiltonian and $\mathcal{L}^{(\ell)}$ denotes the Liouvillian resulting only from the ℓ-th reservoir. The resulting stationary state is in general a non-equilibrium one.

3.1 Example: Effective equilibrium dynamics

Let us however first identify a special case where even in a non-equilibrium setup we can determine the non-equilibrium steady state analytically. For some simple models, one obtains that the coupling structure of all Liouvillians is identical for different reservoirs

$$\mathcal{L}^{(\ell)} = \Gamma^{(\ell)}\left[\mathcal{L}_A + n^{(\ell)}\mathcal{L}_B\right]\,, \tag{3.5}$$

i.e., the reservoirs trigger exactly the same transitions within the system. Here, $n^{(\ell)}$ is a parameter encoding the thermal properties of the respective bath (e.g. a Fermi-Dirac or a Bose-Einstein distribution evaluated at one of the systems transition frequencies), and $\mathcal{L}_{A/B}$ simply label parts of the Liouvillian that are proportional to thermal characteristics (B) or not (A). Finally, $\Gamma^{(\ell)}$ represent coupling constants to the different reservoirs. For coupling to a single reservoir, the stationary state is defined via the equation

$$\mathcal{L}^{(\ell)}\bar{\rho}^{(\ell)} = \Gamma^{(\ell)}\left[\mathcal{L}_A + n^{(\ell)}\mathcal{L}_B\right]\bar{\rho}^{(\ell)} = 0 \tag{3.6}$$

and thus implicitly depends on the thermal parameter $\bar{\rho}^{(\ell)} = \bar{\rho}(n^{(\ell)})$. Obviously, the steady state will be independent of the coupling strength $\Gamma^{(\ell)}$. For the total Liouvillian, it follows that the dependence of the full stationary state on all thermal parameters simply given by the same dependence on an average thermal parameter

$$\begin{aligned}\mathcal{L}\bar{\rho} &= \sum_{\ell}\mathcal{L}^{(\ell)}\bar{\rho} = \sum_{\ell}\Gamma^{(\ell)}\left[\mathcal{L}_A + n^{(\ell)}\mathcal{L}_B\right]\bar{\rho} = \left[\sum_{\ell}\Gamma^{(\ell)}\right]\left[\mathcal{L}_A + \frac{\sum_{\ell}\Gamma^{(\ell)}n^{(\ell)}}{\sum_{\ell'}\Gamma^{(\ell')}}\mathcal{L}_B\right]\bar{\rho}\,,\\ &= \left[\sum_{\ell}\Gamma^{(\ell)}\right]\left[\mathcal{L}_A + \bar{n}\mathcal{L}_B\right]\bar{\rho}\,,\end{aligned} \tag{3.7}$$

where

$$\bar{n} = \frac{\sum_{\ell}\Gamma^{(\ell)}n^{(\ell)}}{\sum_{\ell}\Gamma^{(\ell)}} \tag{3.8}$$

represents an average thermal parameter (e.g. the average occupation). Formally, this is the same equation that determines the steady state for a single reservoir, which may now however be non-thermal.

This can be illustrated by upgrading the Liouvillian for a single resonant level coupled to a single junction

$$\mathcal{L} = \begin{pmatrix} -\Gamma f & +\Gamma(1-f) \\ +\Gamma f & -\Gamma(1-f) \end{pmatrix}, \tag{3.9}$$

where the Fermi function $f = \left[e^{\beta(\epsilon-\mu)}+1\right]^{-1}$ of the contact is evaluated at the dot level ϵ, to the Liouvillian for a single-electron transistor (SET) coupled to two (left and right) junctions

$$\mathcal{L} = \begin{pmatrix} -\Gamma_L f_L - \Gamma_R f_R & +\Gamma_L(1-f_L) + \Gamma_R(1-f_R) \\ +\Gamma_L f_L + \Gamma_R f_R & -\Gamma_L(1-f_L) - \Gamma_R(1-f_R) \end{pmatrix}. \tag{3.10}$$

Now, the system is coupled to two fermionic reservoirs, and in order to support a current, the dot level ϵ must be within the transport window, see Fig. 3.1. This also explains the name single-

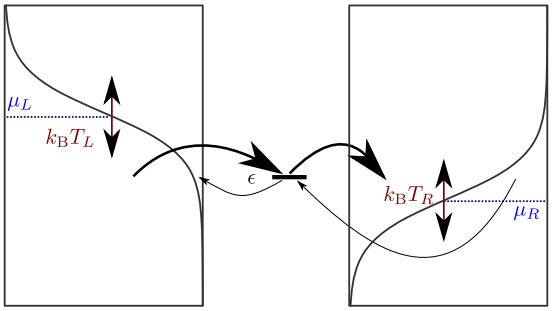

Figure 3.1: Sketch of a single resonant level (QD at energy level ϵ) coupled to two junctions with different Fermi distributions (e.g. with different chemical potentials or different temperatures. If the dot level ϵ is changed with a third gate, the device functions as a transistor, since the current through the system is exponentially suppressed when the the dot level ϵ is not within the transport window.

electron transistor, since the dot level ϵ may be tuned by a third gate, which thereby controls the current.

Exercise 28 (Pseudo-Nonequilibrium)**.** *Show that the stationary state of Eq.(3.10) is a thermal one, i.e., that*

$$\frac{\bar{\rho}_{11}}{\bar{\rho}_{00}} = \frac{\bar{f}}{1-\bar{f}}.$$

Determine $\bar{f}$ in dependence of Γ_α and f_α.

3.2 Phenomenologic definition of currents

Strictly speaking, a conventional master equation only tells us about the state of the system and not about the changes in the reservoir. For a system that is coupled to a single reservoir, we might from

total conservation laws and the dynamics of the system conclude how much energy or how many particles have passed into the reservoir. This is different however for multiple reservoirs, which at non-equilibrium may give rise to steady-state currents. However, the additive decomposition of the Liouville superoperators allows us to phenomenologically identify contributions to the currents from individual reservoirs.

From Eq. (3.4) we can conclude for the energy of the system

$$\frac{d}{dt}\langle E\rangle = \mathrm{Tr}\left\{H_S\dot{\rho}\right\} = -\mathrm{iTr}\left\{H_S[H_S,\rho]\right\} + \sum_\nu \mathrm{Tr}\left\{H_S(\mathcal{L}^{(\nu)}\rho)\right\} . \tag{3.10}$$

We immediately see that the first term vanishes, and that the contributions of the individual reservoirs is additive. This gives rise to the definition of the energy current entering the system from reservoir ν

$$I_E^{(\nu)} = \mathrm{Tr}\left\{H_S(\mathcal{L}^{(\nu)}\rho)\right\} = \mathrm{Tr}\left\{\mathcal{H}_S\mathcal{L}^{(\nu)}\rho\right\} . \tag{3.11}$$

Similarly, we can define a particle current. This only makes sense if the system Hamiltonian conserves the total particle number $[N_S, H_S] = 0$, which leads to

$$\frac{d}{dt}\langle N\rangle = \mathrm{Tr}\left\{N_S\dot{\rho}\right\} = -\mathrm{iTr}\left\{N_S[H_S,\rho]\right\} + \sum_\nu \mathrm{Tr}\left\{N_S(\mathcal{L}^{(\nu)}\rho)\right\} . \tag{3.12}$$

Again, the commutator term vanishes and the particle (or matter) current entering the system from reservoir ν becomes

$$I_M^{(\nu)} = \mathrm{Tr}\left\{N_S(\mathcal{L}^{(\nu)}\rho)\right\} = \mathrm{Tr}\left\{\mathcal{N}_S\mathcal{L}^{(\nu)}\rho\right\} . \tag{3.13}$$

We note that in these definitions we have mixed superoperator (calligraphic) and operator notations, which explains why we have put some brackets in the expressions. Let us first consider the simple case where each Liouvillian $\mathcal{L}^{(\nu)}$ has block structure in the system energy eigenbasis separating populations and diagonals, with the evolution of the diagonals being given by the usual rate equation

$$\dot{\rho}_{aa} = \sum_\nu \sum_b \gamma^{(\nu)}_{ab,ab}\rho_{bb} - \sum_\nu \sum_b \gamma^{(\nu)}_{ba,ba}\rho_{aa} . \tag{3.14}$$

Representing the density matrix, particle number operator, and Hamiltonian in the time-independent energy eigenbasis as

$$\rho = \sum_a \rho_{aa}\left|a\right\rangle\left\langle a\right| + \sum_{a\neq b}\rho_{ab}\left|a\right\rangle\left\langle b\right| , \qquad N_S = \sum_a N_a\left|a\right\rangle\left\langle a\right| , \qquad H_S = \sum_a H_a\left|a\right\rangle\left\langle a\right| , \tag{3.15}$$

we see that

$$I_M^{(\nu)} = \sum_a N_a\left[\sum_b \gamma^{(\nu)}_{ab,ab}\rho_{bb} - \sum_b \gamma^{(\nu)}_{ba,ba}\rho_{aa}\right] = \sum_{ab}(N_a - N_b)\gamma^{(\nu)}_{ab,ab}\rho_{bb} . \tag{3.16}$$

At steady state $\rho_{bb} \to \bar{\rho}_{bb}$, this corresponds to the traditional definition of the matter current, given by the steady state occupation multiplied by the transition rate $\gamma^{(\nu)}_{ab,ab}$ and the particle

number difference between the new state a and the old state b. In a completely analogous fashion, we obtain for the energy current entering the system from reservoir ν

$$I_E^{(\nu)} = \sum_a E_a \left[\sum_b \gamma^{(\nu)}_{ab,ab} \rho_{bb} - \sum_b \gamma^{(\nu)}_{ba,ba} \rho_{aa} \right] = \sum_{ab} (E_a - E_b) \gamma^{(\nu)}_{ab,ab} \rho_{bb} \,. \tag{3.17}$$

We have defined these currents from the perspective of the system. These definitions just require an additive decomposition of the Liouville superoperator, it does actually not need to be of Lindblad form. But can they really be associated with the corresponding change of energy and particle number in the reservoir? Where does e.g. in case of energy balances the energy contained in the interaction Hamiltonian enter? This requires a more careful analysis to be provided later. Below, we will discuss the phenomenologic thermodynamics arising from these definitions.

3.3 Nonequilibrium thermodynamics

We first phrase the necessary prerequisites. Let us assume that we have a system coupled to many reservoirs and subject to slow driving $H_S \to H_S(t)$. This assumption is necessary to ensure that all previous approximations are applicable, such that only the parameters in the dissipators become time-dependent, eventually leading to a master equation of the form

$$\dot\rho = -\mathrm{i}[H_S(t), \rho] + \sum_\nu \mathcal{L}^{(\nu)}(t) \rho \,. \tag{3.18}$$

Looking at the energy balance of the system, we can directly state the first law of thermodynamics

$$\begin{aligned} \dot E &= \frac{d}{dt} \mathrm{Tr} \left\{ H_S(t) \rho_S(t) \right\} \\ &= \mathrm{Tr} \left\{ \dot H_S \rho_S \right\} + \sum_\nu \mu_\nu \mathrm{Tr} \left\{ N_S (\mathcal{L}^{(\nu)} \rho) \right\} + \sum_\nu \mathrm{Tr} \left\{ (H_S - \mu_\nu N_S) (\mathcal{L}^{(\nu)} \rho) \right\} \,. \end{aligned} \tag{3.19}$$

Here, the first term can be identified as mechanical work rate

$$\dot W = \mathrm{Tr} \left\{ \dot H_S \rho_S \right\} \,, \tag{3.20}$$

the second as chemical work rate injected by reservoir ν

$$\dot W^{(\nu)} = \mu_\nu \mathrm{Tr} \left\{ N_S (\mathcal{L}^{(\nu)} \rho) \right\} \,, \tag{3.21}$$

and the third as a heat current entering the system from reservoir ν

$$\dot Q^{(\nu)} = \mathrm{Tr} \left\{ (H_S - \mu_\nu N_S) (\mathcal{L}^{(\nu)} \rho) \right\} \,. \tag{3.22}$$

We note that this is not a derivation of the first law. Rather, we have postulated it and used it to classify the individual currents. These definitions remain sensible when H_S is time-dependent.

Furthermore, we assume that also in case of slow time-dependent driving one has that the dissipators $\mathcal{L}^{(\nu)}(t)$ drag towards the **time-local** Gibbs state

$$\mathcal{L}^{(\nu)}(t) \frac{e^{-\beta_\nu (H_S(t) - \mu_\nu N_S)}}{Z} \equiv \mathcal{L}^{(\nu)}(t) \bar\rho^{(\nu)}(t) = 0 \,. \tag{3.23}$$

In particular, this implies that

$$\ln \bar{\rho}^{(\nu)}(t) = -\beta_\nu (H_S(t) - \mu_\nu N_S) - \ln Z \,, \tag{3.24}$$

where $\ln Z$ is just a number, such that $\mathrm{Tr}\left\{(\mathcal{L}^{(\nu)}\rho)\ln Z\right\} = 0$. Then, we can show the second law in non-equilibrium as follows

$$\begin{aligned} \dot{S}_{\mathrm{i}} &= \dot{S} - \sum_\nu \beta_\nu \dot{Q}^{(\nu)} \\ &= -\mathrm{Tr}\left\{\dot{\rho}\ln\rho\right\} + \sum_\nu \mathrm{Tr}\left\{[\mathcal{L}^{(\nu)}(t)\rho(t)]\ln\bar{\rho}^{(\nu)}(t)\right\} \\ &= -\sum_\nu \mathrm{Tr}\left\{[\mathcal{L}^{(\nu)}(t)\rho(t)][\ln\rho(t) - \ln\bar{\rho}^{(\nu)}(t)]\right\} \,, \end{aligned} \tag{3.25}$$

where we have used that $\dot{S} = -\mathrm{Tr}\left\{\dot{\rho}\ln\rho\right\} = -\sum_\nu \mathrm{Tr}\left\{(\mathcal{L}^{(\nu)}\rho)\ln\rho\right\}$, since the commutator term does not contribute. With view on Eq. (3.23), we can for each term in the summation use Spohn's inequality to conclude that the entropy production rate

$$\dot{S}_{\mathrm{i}} = \dot{S} - \sum_\nu \beta_\nu \dot{Q}^{(\nu)} \geq 0 \,. \tag{3.26}$$

This denotes the second law in presence of (slow) driving and multiple reservoirs. We stress that we have used only that the total Liouville superoperator is additive in the baths and probability conserving, and that the stationary state of each Lindblad superoperator is the local thermal equilibrium state, possibly depending on time.

We will now discuss some consequences of this second law.

3.4 Steady-State Dynamics

By steady-state we mean that the system density matrix has reached a stationary value, which will in general be a complicated nonequilibrium steady state. The term steady state also means that for the moment we neglect driving $H_S(t) \to H_S$, and the reservoirs only perform chemical work on the system and exchange heat with it – in other words, only matter and energy currents determine the thermodynamics of the model. Given a finite-dimensional Hilbert space and ergodic dynamics, the von-Neumann entropy of the system will saturate at some point $\dot{S} \to 0$ and the entropy production rate is given by the heat flows

$$\dot{S}_{\mathrm{i}} \to -\sum_\nu \beta_\nu \dot{Q}^{(\nu)} = -\sum_\nu \beta_\nu \left[I_E^{(\nu)} - \mu_\nu I_M^{(\nu)}\right] \geq 0 \,, \tag{3.27}$$

where $I_E^{(\nu)}$ and $I_M^{(\nu)}$ are the energy and matter currents entering the system from reservoir ν, respectively. Naturally, we see that the entropy production has to vanish when all the currents vanish (e.g. at a global equilibrium state). Whereas energy and matter conservation imply equalities among the currents at steady state

$$\sum_\nu I_M^{(\nu)} = 0 \,, \qquad \sum_\nu I_E^{(\nu)} = 0 \,, \tag{3.28}$$

the positivity of entropy production imposes a further constraint among the currents, e.g. for a two-terminal system

$$\begin{aligned}\dot{S}_{\rm i} &= -\beta_L(I_E^{(L)} - \mu_L I_M^{(L)}) - \beta_R(I_E^{(R)} - \mu_R I_M^{(R)}) \\ &= (\beta_R - \beta_L)I_E + (\mu_L\beta_L - \mu_R\beta_R)I_M \geq 0\,, \end{aligned} \tag{3.29}$$

where we have introduced the currents from left to right $I_E = +I_E^{(L)} = -I_E^{(R)}$ and $I_M = +I_M^{(L)} = -I_M^{(R)}$.

We first discuss the case of equal temperatures $\beta = \beta_L = \beta_R$. The second law implies that

$$(\mu_L - \mu_R)I_M \geq 0\,, \tag{3.30}$$

which is nothing but the trivial statement that the current is always directed from a lead with large chemical potential towards the lead with smaller chemical potential.

Next, we consider equal chemical potentials $\mu_L = \mu_R = \mu$ but different temperatures. Then, our setup has to obey

$$(\beta_R - \beta_L)(I_E - \mu I_M) \geq 0\,, \tag{3.31}$$

where $I_E - \mu I_M$ can now be interpreted as the heat transferred from left to right. When $\beta_R > \beta_L$ (i.e., the left lead is hotter than the right one $T_L > T_R$), the second law just implies that $I_E - \mu I_M \geq 0$, i.e., the heat has to flow from left to right. Similarly, it has to revert sign when $\beta_R < \beta_L$. Altogether, this only tells us that heat always flows from hot to cold – another well-known statement of the second law of thermodynamics.

An interesting scenario arises when there are both a temperature and a potential gradient present, dragging to different directions. For a two-terminal system the second law reads

$$(\beta_R - \beta_L)I_E + (\mu_L\beta_L - \mu_R\beta_R)I_M \geq 0\,. \tag{3.32}$$

Then, it is possible to use a temperature gradient to drive a current against a potential bias, i.e., to perform work. In case of e.g. electrons driven against an electric bias, this would be called a **thermoelectric generator**. Without loss of generality we assume $\mu_L < \mu_R$ and $\beta_L < \beta_R$ (i.e., the left reservoir is hotter than the right one). The efficiency of this generator is then given by the ratio of the generated electric power $P = -I_M(\mu_L - \mu_R)$ divided by the heat entering the system from the hot reservoir

$$\begin{aligned}\eta &= \frac{-I_M(\mu_L - \mu_R)}{I_E - \mu_L I_M} = \frac{-(\beta_R - \beta_L)(\mu_L - \mu_R)I_M}{(\beta_R - \beta_L)I_E - (\beta_R - \beta_L)\mu_L I_M} \\ &= \frac{-(\beta_R - \beta_L)(\mu_L - \mu_R)I_M}{(\beta_R - \beta_L)I_E + (\mu_L\beta_L - \mu_R\beta_R)I_M - (\mu_L\beta_L - \mu_R\beta_R)I_M - (\beta_R - \beta_L)\mu_L I_M} \\ &\leq \frac{-(\beta_R - \beta_L)(\mu_L - \mu_R)I_M}{-(\mu_L\beta_L - \mu_R\beta_R)I_M - (\beta_R - \beta_L)\mu_L I_M} = \frac{(\beta_R - \beta_L)(\mu_L - \mu_R)}{(\mu_L\beta_L - \mu_R\beta_R) + (\beta_R - \beta_L)\mu_L} \\ &= 1 - \frac{\beta_L}{\beta_R} = 1 - \frac{T_R}{T_L} = 1 - \frac{T_{\rm cold}}{T_{\rm hot}} = \eta_{\rm Carnot}\,. \end{aligned} \tag{3.33}$$

The efficiency of such a generator is bounded by Carnot efficiency, irrespective of the microscopic details. We note that our scenario is different from the classical Carnot or Otto cycles, since our reservoirs are coupled at all times to the system, but it is interesting to see that the same universal law holds.

Conversely, one may apply a potential gradient to a system and use it to let the heat flow against the usual direction. This can be used as a **refrigerator** by cooling a cold reservoir or as a **heat pump** by heating a hot reservoir. Keeping the previous conventions $\mu_L < \mu_R$ and $\beta_L < \beta_R$, let us take a closer look at the performance of such engines. For a refrigerator, we assume that there exists a regime of parameters where the heat entering the system from the cold reservoir is positive $\dot{Q}_{\rm cold} = -(I_E - \mu_R I_M) > 0$, which can only be driven by chemical or electric work injected into the system $\dot{W}_{\rm cons} = +(\mu_L - \mu_R) I_M > 0$. In this regime, we can compare the heat entering the system from the cold reservoir with the chemical work rate injected into the system (alternatively, the electric power consumed). This is commonly called coefficient of performance (COP)

$$\begin{aligned}
{\rm COP}_{\rm cooling} &= \frac{-(I_E - \mu_R I_M)}{(\mu_L - \mu_R) I_M} \\
&= \frac{-[(\beta_R - \beta_L) I_E + (\mu_L \beta_L - \mu_R \beta_R) I_M] + (\mu_L \beta_L - \mu_R \beta_R) I_M + (\beta_R - \beta_L) \mu_R I_M}{(\beta_R - \beta_L)(\mu_L - \mu_R) I_M} \\
&\leq \frac{+(\mu_L \beta_L - \mu_R \beta_R) I_M + (\beta_R - \beta_L) \mu_R I_M}{(\beta_R - \beta_L)(\mu_L - \mu_R) I_M} \\
&= \frac{\beta_L}{\beta_R - \beta_L} = \frac{T_R}{T_L - T_R} = \frac{T_{\rm cold}}{T_{\rm hot} - T_{\rm cold}} \,. \qquad (3.34)
\end{aligned}$$

A similar calculation holds for the case of heating, where we compare the heat entering the hot reservoir $\dot{Q}_{\rm hot} = -(I_E - \mu_L I_M) > 0$ with the consumed work rate $\dot{W}_{\rm cons} = +(\mu_L - \mu_R) I_M > 0$

$$\begin{aligned}
{\rm COP}_{\rm heating} &= \frac{-(I_E - \mu_L I_M)}{(\mu_L - \mu_R) I_M} \\
&\leq \frac{\beta_R}{\beta_R - \beta_L} = \frac{T_L}{T_L - T_R} = \frac{T_{\rm hot}}{T_{\rm hot} - T_{\rm cold}} \,. \qquad (3.35)
\end{aligned}$$

Exercise 29 (Coefficient of Performance)**.** *Calculate the upper bound on the coefficient of performance for heating.*

Conventional heat pumps for houses reach COPs in the order of four, i.e., with each kWh of electric energy one pumps on average four kWh of heat into the house. This explains their commercial use in some occasions despite the relatively hight cost of electric energy.

3.5 Example: The single-electron transistor

For the previously discussed example of the single-electron transistor with two reservoirs

$$H = \epsilon d^\dagger d + \sum_{\nu \in \{L,R\}} \left(t_{k\nu} d c_{k\nu}^\dagger + {\rm h.c.} \right) + \sum_{\nu \in \{L,R\}} \epsilon_{k\nu} c_{k\nu}^\dagger c_{k\nu} \qquad (3.36)$$

we had obtained that the dynamics of the populations $(P_0, P_1) = (\rho_{00}, \rho_{11})$ followed a simple rate equation, additive in the reservoirs

$$\mathcal{W} = \begin{pmatrix} -\Gamma_L f_L - \Gamma_R f_R & +\Gamma_L (1 - f_L) + \Gamma_R (1 - f_R) \\ +\Gamma_L f_L + \Gamma_R f_R & -\Gamma_L (1 - f_L) - \Gamma_R (1 - f_R) \end{pmatrix} . \qquad (3.37)$$

This implies for the currents from left to right

$$I_M = I_M^{(L)} = \frac{\Gamma_L \Gamma_R}{\Gamma_L + \Gamma_R}(f_L - f_R)\,, \qquad I_E = I_E^{(L)} = \epsilon I_M\,, \tag{3.38}$$

where ϵ denotes the dot level, at which the Fermi functions and tunneling rates are evaluated

$$f_\nu = \frac{1}{e^{\beta_\nu(\epsilon-\mu_\nu)}+1}\,, \qquad \Gamma_\nu = \Gamma_\nu(\epsilon) = 2\pi \sum_k |t_{k\nu}|^2 \delta(\epsilon - \epsilon_{k\nu})\,. \tag{3.39}$$

We can plot the currents versus the bias voltage at $\mu_L = +V/2$ and $\mu_R = -V/2$ to identify the regimes where the device acts as thermoelectric generator or refrigerator, see Fig. 3.2.

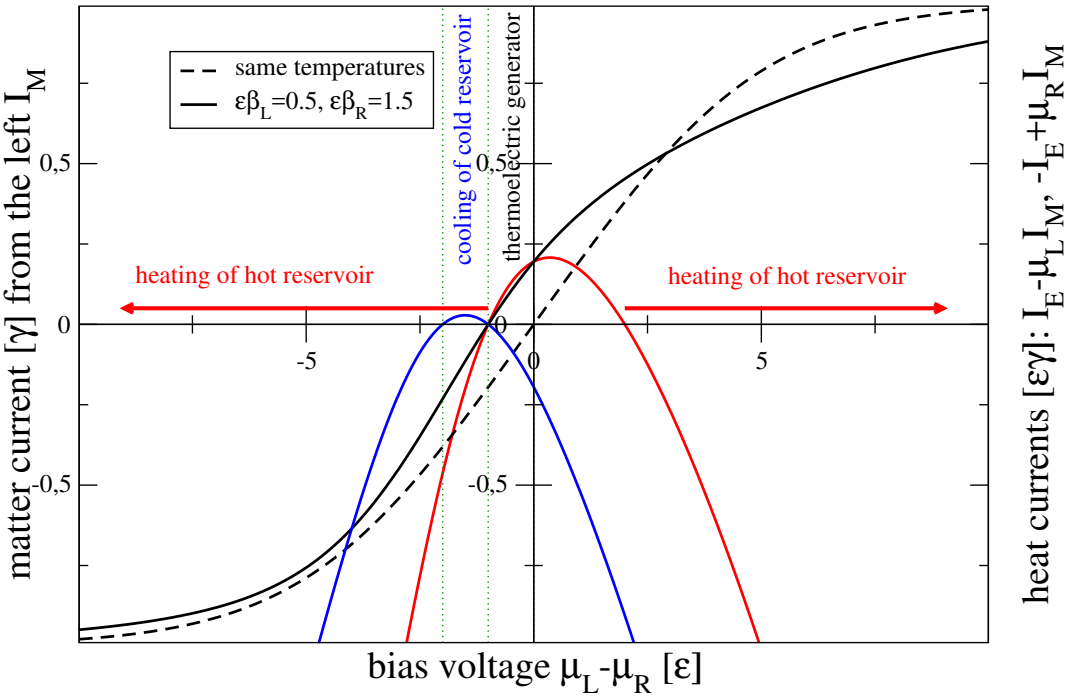

Figure 3.2: Plot of the matter current (solid black) and heat currents entering from left (solid red) and right (solid blue) versus bias voltage. The dashed black curve is a reference curve for equal temperatures $\epsilon\beta_\alpha = 1$. In particular for large bias voltages, both reservoirs are heated. However, since here the energy is mainly provided by the bias voltage across the system, it rather corresponds to a conventional heater than a heat pump. We also see that there is a region where $-I_M(\mu_L - \mu_R) > 0$, where the system acts as thermoelectric generator, and to the left of it there is a region where the cold right reservoir is cooled while simultaneously the hot left reservoir is heated (blue text). Here, the system acts as a true heat pump.

3.6 Example: The double quantum dot

We consider a double quantum dot with internal tunnel coupling T and Coulomb interaction U that is weakly coupled to two fermionic contacts via the rates Γ_L and Γ_R, see Fig. 3.3. The

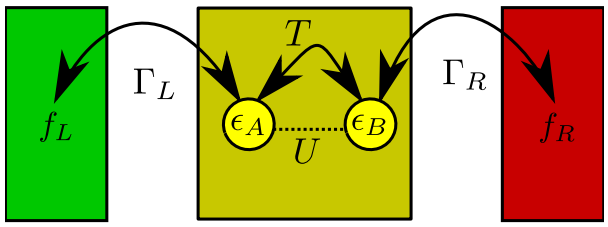

Figure 3.3: A double quantum dot (system) with on-site energies $\epsilon_{A/B}$ and internal tunneling amplitude T and Coulomb interaction U may host at most two electrons. It is weakly tunnel-coupled to two fermionic contacts via the rates $\Gamma_{L/R}$ at different thermal equilibria described by the Fermi distributions $f_{L/R}(\omega)$.

corresponding Hamiltonian reads

$$\begin{aligned}
\mathcal{H}_{\rm S} &= \epsilon_A d_A^\dagger d_A + \epsilon_B d_B^\dagger d_B + T\left(d_A d_B^\dagger + d_B d_A^\dagger\right) + U d_A^\dagger d_A d_B^\dagger d_B\,,\\
\mathcal{H}_{\rm B} &= \sum_k \epsilon_{kL} c_{kL}^\dagger c_{kL} + \sum_k \epsilon_{kR} c_{kR}^\dagger c_{kR}\,,\\
\mathcal{H}_{\rm I} &= \sum_k \left(t_{kL} d_A c_{kL}^\dagger + t_{kL}^* c_{kL} d_A^\dagger\right) + \sum_k \left(t_{kR} d_B c_{kR}^\dagger + t_{kR}^* c_{kR} d_B^\dagger\right)\,.
\end{aligned} \tag{3.40}$$

In contrast to simple rate equations, the internal tunneling T is not a transition rate but an amplitude, since it occurs at the level of the Hamiltonian. Furthermore, we note that strictly speaking we do not have a tensor product decomposition in the interaction Hamiltonian, as the coupling operators anti-commute, e.g.,

$$\{d, c_{kR}\} = 0\,. \tag{3.41}$$

We may however use the *Jordan-Wigner transform*, which decomposes the Fermionic operators in terms of Pauli matrices acting on different spins

$$\begin{aligned}
d_A &= \sigma^- \otimes \mathbf{1} \otimes \mathbf{1} \otimes \ldots \otimes \mathbf{1}\,, \qquad d_B = \sigma^z \otimes \sigma^- \otimes \mathbf{1} \otimes \ldots \otimes \mathbf{1}\,,\\
c_{kL} &= \sigma^z \otimes \sigma^z \otimes \underbrace{\sigma^z \otimes \ldots \otimes \sigma^z}_{k-1} \otimes \sigma^- \otimes \mathbf{1} \otimes \ldots \otimes \mathbf{1}\,,\\
c_{kR} &= \sigma^z \otimes \sigma^z \otimes \underbrace{\sigma^z \otimes \ldots \otimes \sigma^z}_{K_L} \otimes \underbrace{\sigma^z \otimes \ldots \otimes \sigma^z}_{k-1} \otimes \sigma^- \otimes \mathbf{1} \otimes \ldots \otimes \mathbf{1}
\end{aligned} \tag{3.42}$$

to map to a tensor-product decomposition of the interaction Hamiltonian, where $\sigma^\pm = \frac{1}{2}\left[\sigma^x \pm \mathrm{i}\sigma^y\right]$. The remaining operators follow from $(\sigma^+)^\dagger = \sigma^-$ and vice versa. This decomposition automatically obeys the fermionic anti-commutation relations such as e.g. $\left\{c_k, d^\dagger\right\} = 0$ and may therefore also be used to create a fermionic operator basis with computer algebra programs (e.g. use `KroneckerProduct` in Mathematica).

Exercise 30 (Jordan-Wigner transform)**.** *Show that for fermions distributed on N sites, the decomposition*

$$c_i = \underbrace{\sigma^z \otimes \ldots \otimes \sigma^z}_{i-1} \otimes \sigma^- \otimes \underbrace{\mathbf{1} \otimes \ldots \otimes \mathbf{1}}_{N-i}$$

preserves the fermionic anti-commutation relations

$$\{c_i, c_j\} = \mathbf{0} = \left\{c_i^\dagger, c_j^\dagger\right\}\,, \qquad \left\{c_i, c_j^\dagger\right\} = \delta_{ij}\mathbf{1}\,.$$

Show also that the fermionic Fock space basis $c_i^\dagger c_i \left|n_1,\ldots,n_N\right\rangle = n_i \left|n_1,\ldots,n_N\right\rangle$ *obeys* $\sigma_i^z \left|n_1,\ldots,n_N\right\rangle = (-1)^{n_i+1}\left|n_1,\ldots,n_N\right\rangle$.

Inserting the decomposition (3.42) in the Hamiltonian, we may simply use the relations

$$\begin{aligned}
(\sigma^x)^2 &= (\sigma^y)^2 = (\sigma^z)^2 = \mathbf{1}\,, \qquad \sigma^+\sigma^- = \frac{1}{2}\left[\mathbf{1}+\sigma^z\right]\,, \qquad \sigma^-\sigma^+ = \frac{1}{2}\left[\mathbf{1}-\sigma^z\right]\,,\\
\sigma^z\sigma^- &= -\sigma^-\,, \qquad \sigma^-\sigma^z = +\sigma^-\,, \qquad \sigma^z\sigma^+ = +\sigma^+\,, \qquad \sigma^+\sigma^z = -\sigma^+
\end{aligned} \tag{3.41}$$

to obtain a system of interacting spins

$$\begin{aligned}
\mathcal{H}_\mathrm{S} &= \epsilon_A \frac{1}{2}\left[\mathbf{1}+\sigma_A^z\right] + \epsilon_B \frac{1}{2}\left[\mathbf{1}+\sigma_B^z\right] + T\left[\sigma_A^-\sigma_B^+ + \sigma_A^+\sigma_B^-\right] + U\frac{1}{2}\left[\mathbf{1}+\sigma_A^z\right]\frac{1}{2}\left[\mathbf{1}+\sigma_B^z\right]\\
\mathcal{H}_\mathrm{B} &= \sum_k \epsilon_{kL}\frac{1}{2}\left[\mathbf{1}+\sigma_{kL}^z\right] + \sum_k \epsilon_{kR}\frac{1}{2}\left[\mathbf{1}+\sigma_{kR}^z\right]\\
\mathcal{H}_\mathrm{I} &= \sigma_A^-\sigma_B^z \otimes \sum_k t_{kL}\left[\prod_{k'<k}\sigma_{k'L}^z\right]\sigma_{kL}^+ + \sigma_A^+\sigma_B^z \otimes \sum_k t_{kL}^*\left[\prod_{k'<k}\sigma_{k'L}^z\right]\sigma_{kL}^-\\
&\quad + \sigma_B^- \otimes \sum_k t_{kR}\left[\prod_{k'}\sigma_{k'L}^z\right]\left[\prod_{k''<k}\sigma_{k''R}^z\right]\sigma_{kR}^+ + \sigma_B^+ \otimes \sum_k t_{kR}^*\left[\prod_{k'}\sigma_{k'L}^z\right]\left[\prod_{k''<k}\sigma_{k''R}^z\right]\sigma_{kR}^-
\end{aligned} \tag{3.42}$$

.

With this, we could proceed by simply viewing the Hamiltonian as a complicated total system of non-locally interacting spins. However, the order of operators in the nonlocal Jordan-Wigner transformation may be chosen as convenient without destroying the fermionic anticommutation relations. We may therefore also define new fermionic operators on the subspace of the system (first two sites, with reversed order) and the baths (all remaining sites with original order), respectively

$$\begin{aligned}
\tilde{d}_A &= \sigma^- \otimes \sigma^z\,, \qquad \tilde{d}_B = \mathbf{1}\otimes\sigma^-\,,\\
\tilde{c}_{kL} &= \underbrace{\sigma^z\otimes\ldots\otimes\sigma^z}_{k-1}\otimes\sigma^-\otimes\mathbf{1}\otimes\ldots\otimes\mathbf{1}\,,\\
\tilde{c}_{kR} &= \underbrace{\sigma^z\otimes\ldots\otimes\sigma^z}_{K_L}\otimes\underbrace{\sigma^z\otimes\ldots\otimes\sigma^z}_{k-1}\otimes\sigma^-\otimes\mathbf{1}\otimes\ldots\otimes\mathbf{1}\,.
\end{aligned} \tag{3.43}$$

These new operators obey fermionic anti-commutation relations in system and bath separately (e.g. $\{\tilde{d}_A,\tilde{d}_B\}=\mathbf{0}$ and $\{\tilde{c}_{kL},\tilde{c}_{k'L}\}=\mathbf{0}$), but act on different Hilbert spaces, such that system and bath operators do commute by construction (e.g. $[\tilde{d}_A,\tilde{c}_{kL}]=0$). In the new operator basis, the Hamiltonian appears as

$$\begin{aligned}
\mathcal{H}_\mathrm{S} &= \left[\epsilon_A\tilde{d}_A^\dagger\tilde{d}_A + \epsilon_B\tilde{d}_B^\dagger\tilde{d}_B + T\left(\tilde{d}_A\tilde{d}_B^\dagger + \tilde{d}_B\tilde{d}_A^\dagger\right) + U\tilde{d}_A^\dagger\tilde{d}_A\tilde{d}_B^\dagger\tilde{d}_B\right]\otimes\mathbf{1}\,,\\
\mathcal{H}_\mathrm{B} &= \mathbf{1}\otimes\left[\sum_k \epsilon_{kL}\tilde{c}_{kL}^\dagger\tilde{c}_{kL} + \sum_k \epsilon_{kR}\tilde{c}_{kR}^\dagger\tilde{c}_{kR}\right]\,,\\
\mathcal{H}_\mathrm{I} &= \tilde{d}_A\otimes\sum_k t_{kL}\tilde{c}_{kL}^\dagger + \tilde{d}_A^\dagger\otimes\sum_k t_{kL}^*\tilde{c}_{kL} + \tilde{d}_B\otimes\sum_k t_{kR}\tilde{c}_{kR}^\dagger + \tilde{d}_B^\dagger\otimes\sum_k t_{kR}^*\tilde{c}_{kR}\,,
\end{aligned} \tag{3.44}$$

which is the same (for this and some more special cases) as if we had ignored the anticommuting nature of the system and bath operators from the beginning.

We do now proceed by calculating the Fourier transforms of the bath correlation functions

$$\begin{aligned} \gamma_{12}(\omega) &= \Gamma_L(-\omega) f_L(-\omega)\,, \qquad \gamma_{21}(\omega) = \Gamma_L(+\omega)[1 - f_L(+\omega)]\,, \\ \gamma_{34}(\omega) &= \Gamma_R(-\omega) f_R(-\omega)\,, \qquad \gamma_{43}(\omega) = \Gamma_R(+\omega)[1 - f_R(+\omega)] \end{aligned} \tag{3.45}$$

with the continuum tunneling rates $\Gamma_\alpha(\omega) = 2\pi \sum_k |t_{k\alpha}|^2 \delta(\omega - \epsilon_{k\alpha})$ and Fermi functions $f_\alpha(\epsilon_{k\alpha}) = \left\langle c^\dagger_{k\alpha} c_{k\alpha} \right\rangle = \left[e^{\beta_\alpha(\epsilon_{k\alpha} - \mu_\alpha)} + 1\right]^{-1}$.

Exercise 31 (DQD bath correlation functions)**.** *Calculate the Fourier transforms (3.45) of the bath correlation functions for the double quantum dot, assuming that the reservoirs are in a thermal equilibrium state with inverse temperatures β_α and chemical potential μ_α.*

Next, we diagonalize the system Hamiltonian (in the Fock space basis)

$$\begin{aligned} E_0 &= 0\,, \qquad |v_0\rangle = |00\rangle\,, \\ E_- &= \epsilon - \sqrt{\Delta^2 + T^2}\,, \qquad |v_-\rangle \propto \left[\left(\Delta + \sqrt{\Delta^2 + T^2}\right)|10\rangle + T\,|01\rangle\right]\,, \\ E_+ &= \epsilon + \sqrt{\Delta^2 + T^2}\,, \qquad |v_+\rangle \propto \left[\left(\Delta - \sqrt{\Delta^2 + T^2}\right)|10\rangle + T\,|01\rangle\right]\,, \\ E_2 &= 2\epsilon + U\,, \qquad |v_2\rangle = |11\rangle\,, \end{aligned} \tag{3.46}$$

where $\Delta = (\epsilon_B - \epsilon_A)/2$ and $\epsilon = (\epsilon_A + \epsilon_B)/2$ and $|01\rangle = -\tilde{d}^\dagger_B |00\rangle$, $|10\rangle = \tilde{d}^\dagger_A |00\rangle$, and $|11\rangle = \tilde{d}^\dagger_B \tilde{d}^\dagger_A |00\rangle$. We have not symmetrized the coupling operators but to obtain the BMS limit, we may alternatively use Eqns. (2.89) and (2.90) when $\tau \to \infty$. Specifically, when we have no degeneracies in the system Hamiltonian ($\Delta^2 + T^2 > 0$), the master equation in the energy eigenbasis (where $a, b \in \{0, -, +, 2\}$) becomes a rate equation (2.52), where for non-hermitian coupling operators the transition rates from b to a are given by

$$\gamma_{ab,ab} = \sum_{\alpha\beta} \gamma_{\alpha\beta}(E_b - E_a) \langle a|\, A_\beta\, |b\rangle \langle a|\, A^\dagger_\alpha\, |b\rangle^* \,. \tag{3.47}$$

We may calculate the Liouvillians for the interaction with the left and right contact separately

$$\gamma_{ab,ab} = \gamma^L_{ab,ab} + \gamma^R_{ab,ab}\,, \tag{3.48}$$

since we are constrained to second order perturbation theory in the tunneling amplitudes. Since we have $\tilde{d}_A = A^\dagger_2 = A_1 = \tilde{d}_A$ and $\tilde{d}_B = A^\dagger_4 = A_3 = \tilde{d}_B$, we obtain for the left-associated dampening coefficients

$$\begin{aligned} \gamma^L_{ab,ab} &= \gamma_{12}(E_b - E_a)|\langle a|\, A_2\, |b\rangle|^2 + \gamma_{21}(E_b - E_a)|\langle a|\, A_1\, |b\rangle|^2\,, \\ \gamma^R_{ab,ab} &= \gamma_{34}(E_b - E_a)|\langle a|\, A_4\, |b\rangle|^2 + \gamma_{43}(E_b - E_a)|\langle a|\, A_3\, |b\rangle|^2\,. \end{aligned} \tag{3.49}$$

In the wideband (flatband) limit $\Gamma_{L/R}(\omega) = \Gamma_{L/R}$, we obtain for the nonvanishing transition rates

in the energy eigenbasis

$$\begin{aligned}
\gamma^L_{0-,0-} &= \Gamma_L\gamma_+[1-f_L(\epsilon-\sqrt{\Delta^2+T^2})]\,, \qquad \gamma^R_{0-,0-} = \Gamma_R\gamma_-[1-f_R(\epsilon-\sqrt{\Delta^2+T^2})]\,,\\
\gamma^L_{0+,0+} &= \Gamma_L\gamma_-[1-f_L(\epsilon+\sqrt{\Delta^2+T^2})]\,, \qquad \gamma^R_{0+,0+} = \Gamma_R\gamma_+[1-f_R(\epsilon+\sqrt{\Delta^2+T^2})]\,,\\
\gamma^L_{-2,-2} &= \Gamma_L\gamma_-[1-f_L(\epsilon+U+\sqrt{\Delta^2+T^2})]\,, \qquad \gamma^R_{-2,-2} = \Gamma_R\gamma_+[1-f_R(\epsilon+U+\sqrt{\Delta^2+T^2})]\,,\\
\gamma^L_{+2,+2} &= \Gamma_L\gamma_+[1-f_L(\epsilon+U-\sqrt{\Delta^2+T^2})]\,, \qquad \gamma^R_{+2,+2} = \Gamma_R\gamma_-[1-f_R(\epsilon+U-\sqrt{\Delta^2+T^2})]\,,\\
\gamma^L_{-0,-0} &= \Gamma_L\gamma_+f_L(\epsilon-\sqrt{\Delta^2+T^2})\,, \qquad \gamma^R_{-0,-0} = \Gamma_R\gamma_-f_R(\epsilon-\sqrt{\Delta^2+T^2})\,,\\
\gamma^L_{+0,+0} &= \Gamma_L\gamma_-f_L(\epsilon+\sqrt{\Delta^2+T^2})\,, \qquad \gamma^R_{+0,+0} = \Gamma_R\gamma_+f_R(\epsilon+\sqrt{\Delta^2+T^2})\,,\\
\gamma^L_{2-,2-} &= \Gamma_L\gamma_-f_L(\epsilon+U+\sqrt{\Delta^2+T^2})\,, \qquad \gamma^R_{2-,2-} = \Gamma_R\gamma_+f_R(\epsilon+U+\sqrt{\Delta^2+T^2})\,,\\
\gamma^L_{2+,2+} &= \Gamma_L\gamma_+f_L(\epsilon+U-\sqrt{\Delta^2+T^2})\,, \qquad \gamma^R_{2+,2+} = \Gamma_R\gamma_-f_R(\epsilon+U-\sqrt{\Delta^2+T^2})\,,
\end{aligned} \tag{3.50}$$

with the dimensionless coefficients

$$\gamma_\pm = \frac{1}{2}\left[1 \pm \frac{\Delta}{\sqrt{\Delta^2+T^2}}\right] \tag{3.51}$$

arising from the matrix elements of the system coupling operators. This rate equation can also be visualized with a network, see Fig. 3.4. We note that although both reservoirs drive all transitions,

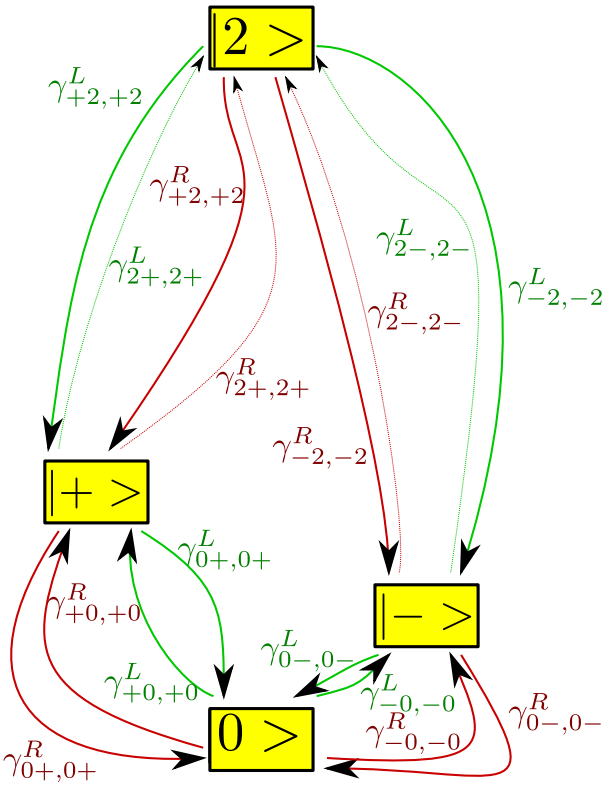

Figure 3.4: Configuration space of a serial double quantum dot coupled to two leads. Due to the hybridization of the two levels, electrons may jump directly from the left contact to right-localized modes and vice versa, such that in principle all transitions are driven by both contacts. However, the relative strength of the couplings is different, such that the two Liouillians have a different structure. In the Coulomb-blockade limit, transitions to the doubly occupied state are forbidden (thin dotted lines), such that – if the doubly occupied state is initially not occupied – the system dimension can be reduced.

their relative strength is different, and we do not have a simple situation as discussed previously in Eq. (3.5). Consequently, the stationary state of the rate equation cannot be written as some grand-canonical equilibrium state, which is most conveniently shown by disproving the relations $\bar\rho_{--}/\bar\rho_{00} = e^{-\beta(E_- - E_0-\mu)}$, $\bar\rho_{++}/\bar\rho_{00} = e^{-\beta(E_+-E_0-\mu)}$ and $\bar\rho_{++}/\bar\rho_{--} = e^{-\beta(E_+-E_-)}$.

As the simplest example of the resulting rate equation, we study the high-bias and Coulomb-blockade limit $f_{L/R}(\epsilon+U\pm\sqrt{\Delta^2+T^2}) \to 0$ and $f_L(\epsilon\pm\sqrt{\Delta^2+T^2}) \to 1$ and $f_R(\epsilon\pm\sqrt{\Delta^2+T^2}) \to 0$

when the onsite-energies are degenerate such that $\Delta \to 0$ (such that $\gamma_\pm \to 1/2$). This removes any dependence on the internal tunneling amplitude T. Consequently, derived quantities such as e.g. the current will not depend on T either and we would obtain a current even when $T \to 0$ (where we have a disconnected structure). However, precisely in this limit (i.e., $\Delta \to 0$ and $T \to 0$), the two levels E_- and E_+ become energetically degenerate, and a simple rate equation description is not applicable. The take-home message of this failure is that one should not use plug and play formulas without learning about their limits. Therefore, keeping in mind that $T \neq 0$, the resulting Liouvillian reads

$$\mathcal{L} = \frac{1}{2}\begin{pmatrix} -2\Gamma_L & \Gamma_R & \Gamma_R & 0 \\ \Gamma_L & -\Gamma_R & 0 & \Gamma_L+\Gamma_R \\ \Gamma_L & 0 & -\Gamma_R & \Gamma_L+\Gamma_R \\ 0 & 0 & 0 & -2(\Gamma_L+\Gamma_R) \end{pmatrix}, \tag{3.52}$$

where it becomes visible that the doubly occupied state will simply decay and may therefore – since we are interested in the long-term dynamics – be eliminated completely

$$\mathcal{L}_{\text{CBHB}} = \frac{1}{2}\begin{pmatrix} -2\Gamma_L & \Gamma_R & \Gamma_R \\ \Gamma_L & -\Gamma_R & 0 \\ \Gamma_L & 0 & -\Gamma_R \end{pmatrix}. \tag{3.53}$$

Exercise 32 (Stationary DQD currents)**.** *Calculate the stationary currents entering the right reservoir.*

At finite bias voltages, it becomes of course harder to calculate steady states and stationary currents. However, for low temperatures, the Fermi functions will behave similar to step functions, and the transport window becomes sharp. Then, by enlarging the bias voltage, the transport window is opened, and the currents will exhibit steps when a new transport channel is inside the transport window, see Fig. 3.5. A further obvious observation is that at zero bias voltage, we have

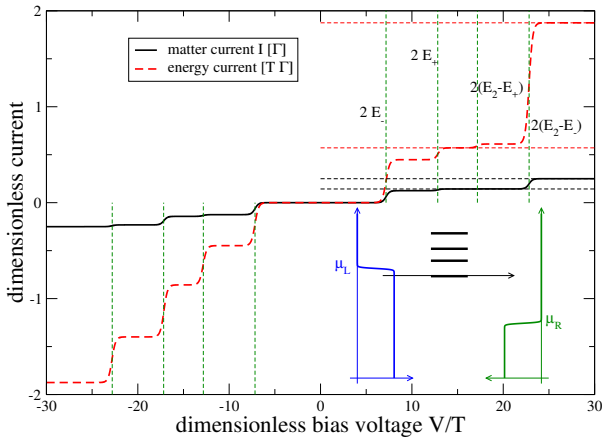

Figure 3.5: Plot of matter (solid black) and energy (dashed red) currents. At sufficiently low temperatures, the steps in the currents occur for positive bias voltage at $\mu_L = V/2 \in \{E_- - E_0, E_+ - E_0, E_2 - E_+, E_2 - E_-\}$. The inset displays the configuration of these transition energies relative to left (blue) and right (green) Fermi functions taken at $V = 10T$. Then, only the lowest transition energy (arrow) is inside the transport window, such that transport is dominated by transitions between $|-\rangle$ and $|0\rangle$. Other parameters have been chosen as $\mu_L = -\mu_R = V/2$, $\Gamma_L = \Gamma_R = \Gamma$, $\epsilon_A = 4T$, $\epsilon_B = 6T$,$U = 5T$, and $\beta T = 10$.

vanishing currents. This must happen only at equal temperatures. The entropy production in this case is fully determined by the matter current $\dot{S}_\text{i} = \beta(\mu_L - \mu_R)I_M$, where I_M denotes the current from left to right. Identifying $P = (\mu_L - \mu_R)I_M$ with the power dissipated by the device, the entropy production just becomes $\dot{S}_\text{i} = \beta P$.

3.7 Phonon-Assisted Tunneling

We consider here a three-terminal system, comprised as before of two quantum dots. The left dot is tunnel-coupled to the left lead, the right dot to the right, but in addition, tunneling between the dots is now triggered by a third (bosonic) reservoir that does not change the particle content. That is, without the bosonic reservoir (e.g. phonons or photons) the model would not support a steady state matter current – which is in contrast to the previous model

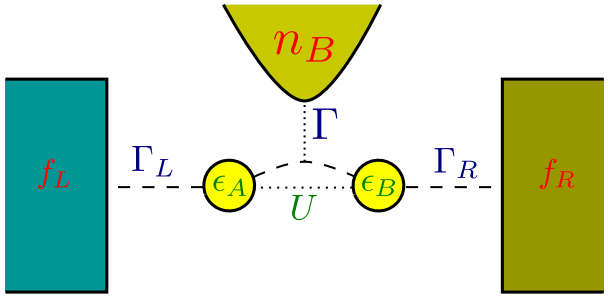

Figure 3.6: Sketch of two quantum dots that are separately tunnel-coupled to their adjacent reservoir in the conventional way by rates Γ_L and Γ_R. The mere Coulomb interaction U only allows for the exchange of energy between the dots, but with phonons present (rounded terminals), tunneling between A and B becomes possible (dotted and dashed). The device may act as a thermoelectric generator converting thermal gradients into power.

The system is described by the Hamiltonian

$$\mathcal{H}_{\rm S} = \epsilon_A d_A^\dagger d_A + \epsilon_B d_B^\dagger d_B + U d_A^\dagger d_A d_B^\dagger d_B \tag{3.54}$$

with on-site energies $\epsilon_A < \epsilon_B$ and Coulomb interaction U. Since there is no internal tunneling, its energy eigenstates coincide with the localized basis $|n_A, n_B\rangle$ with the dot occupations $n_A, n_B \in \{0, 1\}$. This structure makes it particularly simple to derive a master equation in rate equation representation. The jumps between states are triggered by the electronic tunneling Hamiltonians and the electron-phonon interaction

$$\begin{aligned}\mathcal{H}_{\rm I} &= \sum_k \left(t_{kL} d_A c_{kL}^\dagger + t_{kL}^* c_{kL} d_A^\dagger \right) + \sum_k \left(t_{kR} d_B c_{kR}^\dagger + t_{kR}^* c_{kR} d_B^\dagger \right) \\ &\quad + \left(d_A d_B^\dagger + d_B d_A^\dagger \right) \otimes \sum_q \left(h_q a_q + h_q^* a_q^\dagger \right) ,\end{aligned} \tag{3.55}$$

where $c_{k\alpha}$ are fermionic and a_q bosonic annihilation operators. The three reservoirs

$$\mathcal{H}_{\rm B} = \sum_k \epsilon_{kL} c_{kL}^\dagger c_{kL} + \sum_k \epsilon_{kR} c_{kR}^\dagger c_{kR} + \sum_q \omega_q a_q^\dagger q_q \tag{3.56}$$

are assumed to remain in separate thermal equilibrium states, such that the reservoir density matrix is assumed to be a product of the single density matrices. This automatically implies that the expectation value of linear combinations of the coupling operators vanishes. In the weak-coupling limit, the rate matrix will be additively decomposed into contributions resulting from the electronic (L, R) and bosonic (B) reservoirs $\mathcal{L} = \mathcal{L}_L + \mathcal{L}_R + \mathcal{L}_B$ From our results with the single-electron transistor, we may readily reproduce the rates for the electronic jumps. Ordering the basis as $\rho_{00,00}$, $\rho_{10,10}$, $\rho_{01,01}$, and $\rho_{11,11}$ and using for simplicity the wide-band limit $\Gamma_\alpha(\omega) \approx \Gamma_\alpha$

these read

$$\begin{aligned}\mathcal{L}_L &= \Gamma_L \begin{pmatrix} -f_L(\epsilon_A) & 1-f_L(\epsilon_A) & 0 & 0 \\ +f_L(\epsilon_A) & -[1-f_L(\epsilon_A)] & 0 & 0 \\ 0 & 0 & -f_L(\epsilon_A+U) & 1-f_L(\epsilon_A+U) \\ 0 & 0 & +f_L(\epsilon_A+U) & -[1-f_L(\epsilon_A+U)] \end{pmatrix} \\ \mathcal{L}_R &= \Gamma_R \begin{pmatrix} -f_R(\epsilon_B) & 0 & 1-f_R(\epsilon_B) & 0 \\ 0 & -f_R(\epsilon_B+U) & 0 & 1-f_R(\epsilon_B+U) \\ +f_R(\epsilon_B) & 0 & -[1-f_R(\epsilon_B)] & 0 \\ 0 & +f_R(\epsilon_B+U) & 0 & -[1-f_R(\epsilon_B+U)] \end{pmatrix}, \end{aligned} \tag{3.57}$$

where the electronic tunneling rates are as usual obtained via (in the wide-band limit) $\Gamma_\alpha \approx \Gamma_\alpha(\omega) = 2\pi \sum_k |t_{k\alpha}|^2 \delta(\omega - \epsilon_{k\alpha})$ from the microscopic tunneling amplitudes $t_{k\alpha}$. We note that the Fermi functions are evaluated at the energy difference of the jump to which they refer. Although energy may be transferred between the left and right junctions without the presence of phonons, it is not possible to transfer charges.

For the spin-boson example, we have also already calculated the correlation function for the phonons for a spin-boson model in Sec. 2.2.4. Since the reservoir coupling operator is identical, we may use our result from Eq. (2.107).

$$\gamma(\omega) = \Gamma(+\omega)\Theta(+\omega)[1+n_B(+\omega)] + \Gamma(-\omega)\Theta(-\omega)n_B(-\omega)\,, \tag{3.58}$$

where $\Gamma(\omega) = 2\pi \sum_k |h_k|^2 \delta(\omega - \omega_k)$ was the bosonic emission or absorption rate and $n_B(\omega)$ denoted the Bose-Einstein distribution function. For consistency, we just note that the KMS condition is obeyed. With this, we may readily evaluate the rates due to the phonon reservoirs, i.e., we have with $\Gamma = \Gamma(\epsilon_B - \epsilon_A)$

$$\mathcal{L}_B = \Gamma \begin{pmatrix} 0 & 0 & 0 & 0 \\ 0 & -n_B(\epsilon_B-\epsilon_A) & 1+n_B(\epsilon_B-\epsilon_A) & 0 \\ 0 & +n_B(\epsilon_B-\epsilon_A) & -[1+n_B(\epsilon_B-\epsilon_A)] & 0 \\ 0 & 0 & 0 & 0 \end{pmatrix}. \tag{3.59}$$

The rate matrices in Eqs. (3.57) and (3.59) can be used to determine all currents. We have a three terminal system, where the phonon terminal only allows for the exchange of energy, i.e., in total we can calculate five non-vanishing currents. With the conservation laws on matter and energy currents, we can at steady state eliminate two of these, and the entropy production becomes

$$\begin{aligned}\dot{S}_\mathrm{i} &= -\beta_\mathrm{ph} I_E^B - \beta_L(I_E^L - \mu_L I_M^L) - \beta_R(I_E^R - \mu_R I_M^R) \\ &= -\beta_\mathrm{ph} I_E^B - \beta_L(I_E^L - \mu_L I_M^L) + \beta_R(I_E^L + I_E^B - \mu_R I_M^L) \\ &= (\beta_R - \beta_\mathrm{ph}) I_E^B + (\beta_R - \beta_L) I_E^L + (\beta_L\mu_L - \beta_R\mu_R) I_M^L\,, \end{aligned} \tag{3.60}$$

which has the characteristic affinity-flux form. In usual electronic setups, the electronic temperatures will be the same $\beta_\mathrm{el} = \beta_L = \beta_R$, such that the entropy production further reduces to

$$\dot{S}_\mathrm{i} = (\beta_\mathrm{el} - \beta_\mathrm{ph}) I_E^B + \beta_\mathrm{el}(\mu_L - \mu_R) I_M^L \geq 0\,, \tag{3.61}$$

where we can identify the term $(\mu_L - \mu_R) I_M^L$ as a power consumed or produced by the device. Furthermore, we note that the device obeys the tight-coupling property: Every electron traversing

the system from left to right must absorb energy $\epsilon_B - \epsilon_A$ from the phonon reservoir $I_E^B = (\epsilon_B - \epsilon_A) I_M^L$. Therefore, the entropy production can also be written as

$$\dot{S}_\mathrm{i} = \left[(\beta_\mathrm{el} - \beta_\mathrm{ph})(\epsilon_B - \epsilon_A) + \beta_\mathrm{el}(\mu_L - \mu_R)\right] I_M^L \geq 0\,. \tag{3.62}$$

We note that the prefactor of the matter current vanishes at

$$V^* = \mu_L^* - \mu_R^* = \left(\frac{T_\mathrm{el}}{T_\mathrm{ph}} - 1\right)(\epsilon_B - \epsilon_A)\,. \tag{3.63}$$

Since the prefactor switches sign at this voltage, the matter current must vanish at this voltage, too – otherwise the entropy production would not be positive. Without calculation, we have therefore found that at bias voltage V^* the current must vanish.

Noting that the total entropy production is positive does not imply that all contributions are separately positive. Fig. 3.7 displays the current as a function of the bias voltage for different electronic and phonon temperature configurations. It is visible that at zero bias, the matter

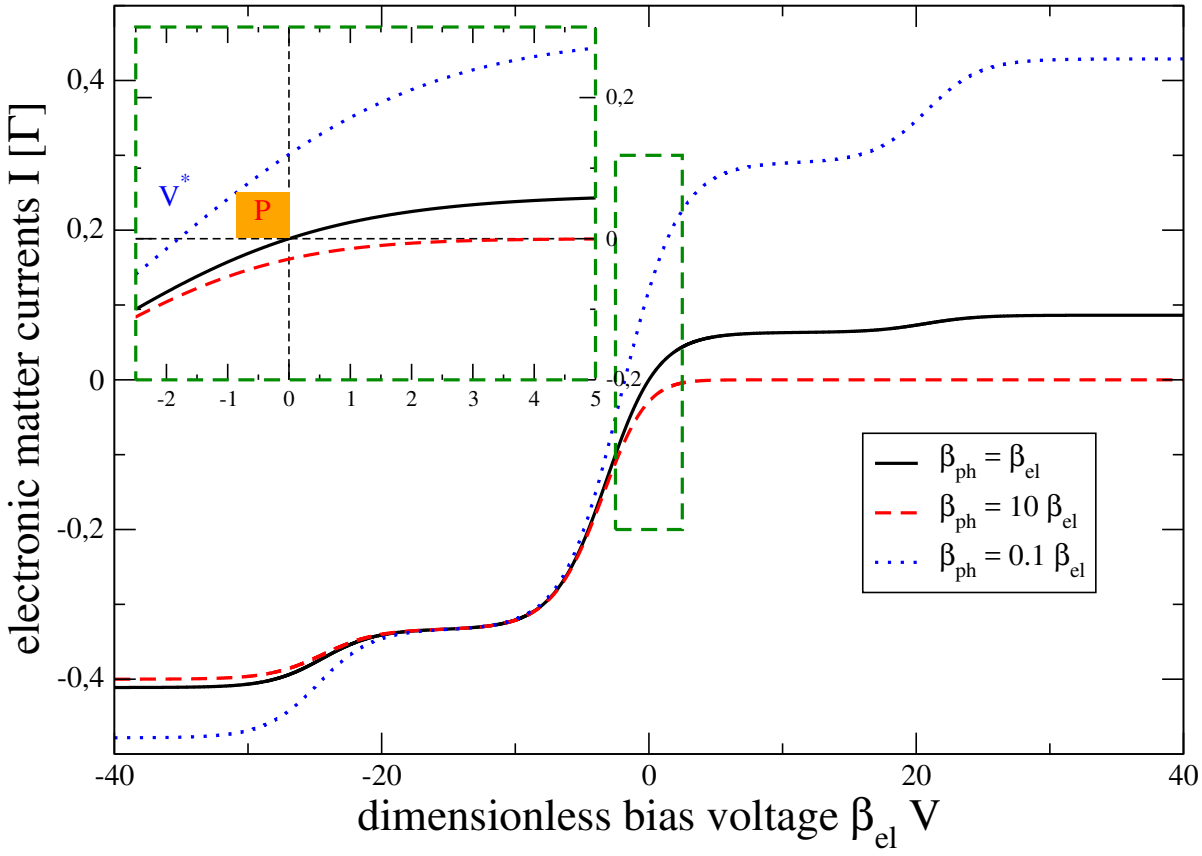

Figure 3.7: Electronic matter current in units of $\Gamma_L = \Gamma_R = \Gamma$ versus dimensionless bias voltage $\beta_\mathrm{el} V$. For low phonon temperatures $\beta_\mathrm{ph}(\epsilon_B - \epsilon_A) \gg 1$, the current cannot flow from left to right, such that the system acts as a rectifier (dashed red). For large phonon temperatures $\beta_\mathrm{ph}(\epsilon_B - \epsilon_A) \ll 1$, the energy driving the current against the bias (see zoomed inset) is supplied by the phonon bath. Other parameters: $\beta_\mathrm{el}\epsilon_B = 2$, $\beta_\mathrm{el}\epsilon_A = 0$, $\beta_\mathrm{el}U = 10$, $J_B = \Gamma$, $\beta_L = \beta_R = \beta_\mathrm{el}$, and $\mu_L = +V/2 = -\mu_R$.

current does not vanish when electron and phonon temperatures are not chosen equal.

3.7.1 Thermoelectric performance

We concentrate on the simple case discussed before and use $\beta_L = \beta_R = \beta_{\rm el}$ and $\beta_{\rm ph} = \beta_B$. In regions where the current runs against the bias, the power

$$P = -(\mu_L - \mu_R) I_M^L \tag{3.64}$$

becomes positive, and we can define an efficiency via

$$\eta = \frac{-(\mu_L - \mu_R) I_M^L}{\dot{Q}_{\rm in}} \Theta(P)\,, \tag{3.65}$$

where $\dot{Q}_{\rm in}$ is the heat entering the system from the hot reservoir. The purpose of the Heaviside function is just to avoid misinterpretations of the efficiency.

Consequently, when the phonon temperature is larger than the electron temperature $T_{\rm ph} > T_{\rm el}$, the input heat is given by the positive energy flow from the hot phonon bath into the system, such that – due to the tight-coupling property – the efficiency becomes trivially dependent on the bias voltage

$$\eta_{T_{\rm ph}>T_{\rm el}} = \frac{P}{I_E^B} \Theta(P) = -\frac{V}{\epsilon_B - \epsilon_A} \Theta(P)\,. \tag{3.66}$$

At first sight, one might think that this efficiency could become larger than one. It should be kept in mind however that it is only valid in regimes where the power (3.64) is positive, which limits the applicability of these efficiencies to voltages within $V = 0$ and $V = V^*$ from Eq. (3.63). The maximum efficiency is reached at $V = V^*$ and reads

$$\eta_{T_{\rm ph}>T_{\rm el}} < \eta_{\rm max} = 1 - \frac{T_{\rm el}}{T_{\rm ph}} = \eta_{\rm Ca}\,, \tag{3.67}$$

and is thus upper-bounded by Carnot efficiency

$$\eta_{\rm Ca} = 1 - \frac{T_{\rm cold}}{T_{\rm hot}}\,. \tag{3.68}$$

In the opposite case, where $T_{\rm ph} < T_{\rm el}$, the input heat is given by the sum of the energy currents entering from the hot electronic leads $\dot{Q}_{\rm in} = \dot{Q}^L + \dot{Q}^R = I_E^L + I_E^R + P = -I_E^B + P$, such that the efficiency becomes

$$\eta_{T_{\rm ph}<T_{\rm el}} = \frac{P}{-I_E^B + P} = \frac{(\mu_L - \mu_R)}{(\epsilon_B - \epsilon_A) + (\mu_L - \mu_R)} = \frac{1}{1 + \frac{\epsilon_B - \epsilon_A}{\mu_L - \mu_R}}\,, \tag{3.69}$$

which also trivially depends on the bias voltage. Inserting the maximum bias voltage with positive power in Eq. (3.63) we obtain the maximum efficiency

$$\eta_{T_{\rm ph}<T_{\rm el}} < \frac{1}{1 + \frac{1}{\frac{T_{\rm el}}{T_{\rm ph}} - 1}} = 1 - \frac{T_{\rm ph}}{T_{\rm el}}\,, \tag{3.70}$$

which is also just the Carnot efficiency.

Unfortunately, Carnot efficiencies are reached at vanishing current, i.e., at zero power. At these parameters, a thermoelectric device is useless. It is therefore more practical to consider the efficiency at maximum power. However, since the currents depend in a highly nonlinear fashion on all parameters (coupling constants, temperatures, chemical potentials, and system parameters), this becomes a numerical optimization problem – unless one restricts the analysis to the linear response regime.

Chapter 4

Full Counting Statistics

Previous definitions of currents were based on balances of the system and the phenomenologic identification of the change of the system observable (energy, particle number). This automatically implies that e.g. there is no contribution from the interaction. Sometimes one is also interested in more information beyond the mean values, i.e., the statistics of single jumps into the reservoir. In Full Counting Statistics (FCS) one is interested in the probability distribution $P_n(t)$ denoting the number of particles n transferred to a specific reservoir after time t. This can in principle be generalized to full energy counting statistics.

4.1 Phenomenologic Introduction

Suppose that by some method we can identify jump terms between different states in the master equation, i.e., we can separate the total dissipator as

$$\mathcal{L} = \mathcal{L}_0 + \mathcal{L}_1 \,, \tag{4.1}$$

where $\mathcal{L}_1$ denotes the jump term and $\mathcal{L}_0$ the jump-free evolution (containing the isolated dynamics of the system or un-monitored jumps). We would like to have an expansion of the total propagator $\mathcal{P}(t) = e^{\mathcal{L}t}$ that makes the number of such jumps explicit. We could go to some interaction picture, considering $\mathcal{L}_0$ as the free evolution and $\mathcal{L}_1$ as the perturbation. However, for our purposes it is more useful to consider the Laplace transform $\mathcal{P}(z) = \int_0^\infty \mathcal{P}(t) e^{-zt} dt$ of the propagator

$$\begin{aligned} \mathcal{P}(z) &= [z\mathbf{1} - \mathcal{L}_0 - \mathcal{L}_1]^{-1} = [(z\mathbf{1} - \mathcal{L}_0)(\mathbf{1} - (z\mathbf{1} - \mathcal{L}_0)^{-1}\mathcal{L}_1)]^{-1} \\ &= (\mathbf{1} - (z\mathbf{1} - \mathcal{L}_0)^{-1}\mathcal{L}_1)^{-1}(z\mathbf{1} - \mathcal{L}_0)^{-1} \,. \end{aligned} \tag{4.2}$$

At this time, it is useful to introduce the free propagator

$$\mathcal{P}_0(z) = [z\mathbf{1} - \mathcal{L}_0]^{-1} = \int_0^\infty e^{\mathcal{L}_0 t} e^{-zt} dt \,. \tag{4.3}$$

Using it, we can expand the full propagator as

$$\mathcal{P}(z) = \sum_{n=0}^{\infty} [\mathcal{P}_0(z)\mathcal{L}_1]^n \mathcal{P}_0(z) = \mathcal{P}_0(z) + \mathcal{P}_0(z)\mathcal{L}_1\mathcal{P}_0(z) + \mathcal{P}_0(z)\mathcal{L}_1\mathcal{P}_0(z)\mathcal{L}_1\mathcal{P}_0(z) + \dots \,. \tag{4.4}$$

We remark that the convolution property holds also for matrix-valued functions (provided we do not change their order)

$$\begin{aligned}\int_0^\infty dt e^{-zt}\int_0^t d\tau \mathcal{A}(t-\tau)\mathcal{B}(\tau) &= \int_0^\infty d\tau\int_\tau^\infty dt\mathcal{A}(t-\tau)e^{-zt}\mathcal{B}(\tau)\\ &= \int_0^\infty\left[\int_0^\infty dt'\mathcal{A}(t')e^{-zt'}\right]e^{-z\tau}\mathcal{B}(\tau)d\tau = \mathcal{A}(z)\mathcal{B}(z)\,. \quad (4.5)\end{aligned}$$

Here, we have exchanged in the first equality sign the integrals, using that the total integration region is the same. Applying this recursively, we can indeed show that (4.4) is equivalent to a convolution series

$$\begin{aligned}\mathcal{P}(t) &= e^{\mathcal{L}_0(t-0)} + \int_0^t e^{\mathcal{L}_0(t-t_1)}\mathcal{L}_1 e^{\mathcal{L}_0(t_1-0)}dt_1\\ &\quad + \int_0^t dt_2\int_0^{t_2} dt_1 e^{\mathcal{L}_0(t-t_2)}\mathcal{L}_1 e^{\mathcal{L}_0(t_2-t_1)}\mathcal{L}_1 e^{\mathcal{L}_0(t_1-0)} + \dots\,, \quad (4.6)\end{aligned}$$

which has the appealing interpretation that we have periods of free evolutions interrupted by single jump events, see Fig. 4.1.

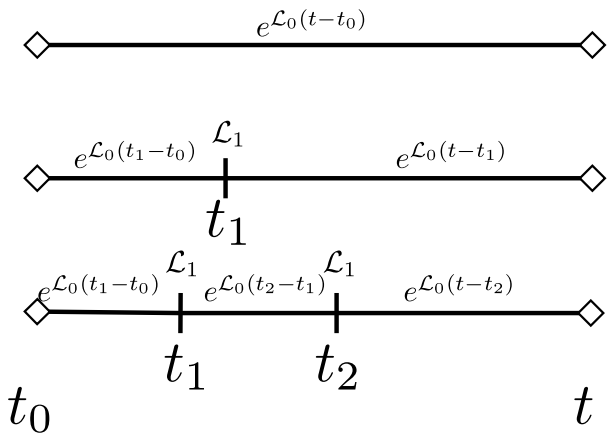

Figure 4.1: Illustration of the first three terms in the series expansion in Eq. (4.6). Periods of free evolution (lines) are interrupted by instantaneous jumps (marks). In the end, one has to integrate over all times at which jumps may occur.

Exercise 33 (Jump series expansion)**.** *Show that the expansion (4.6) can also be obtained in an interaction picture by using* $\rho(t) = e^{\mathcal{L}_0 t}\tilde{\rho}(t)$.

The benefit of this series expansion is that it yields a decomposition where we can readily write down the probabilities for n jump events during time t

$$P_n(t) = \mathrm{Tr}\left\{\int_0^t dt_n\dots\int_0^{t_2} dt_1 e^{\mathcal{L}_0(t-t_n)}\mathcal{L}_1\dots\mathcal{L}_1 e^{\mathcal{L}_0(t_2-t_1)}\mathcal{L}_1 e^{\mathcal{L}_0(t_1-0)}\rho_0\right\}\,, \quad (4.7)$$

which looks way more convenient in Laplace space

$$P_n(z) = \mathrm{Tr}\left\{\left[\mathcal{P}_0(z)\mathcal{L}_1\right]^n\mathcal{P}_0(z)\rho_0\right\}\,. \quad (4.8)$$

But suppose we are only given the full propagator $\mathcal{P}(t)$. Is there a convenient way to sort out only those contributions that have exactly n jump events? Taking the orthonormality relation

$$\frac{1}{2\pi}\int_{-\pi}^{+\pi} e^{+\mathrm{i}n\chi}e^{-\mathrm{i}m\chi}d\chi = \delta_{nm} \tag{4.9}$$

into account, it becomes quite obvious that one can infer the statistics of such jumps with following replacement

$$\mathcal{L}_1 \to \mathcal{L}_1 e^{+\mathrm{i}\chi}\,, \qquad \mathcal{L} \to \mathcal{L}(\chi) = \mathcal{L}_0 + \mathcal{L}_1 e^{+\mathrm{i}\chi} \tag{4.10}$$

in the full propagator $\mathcal{P}(\chi,t) = e^{\mathcal{L}(\chi)t}$. The new variable χ is conventionally called *counting field*. Then, we can use the orthonormality relation (4.9) to conclude

$$P_n(t) = \frac{1}{2\pi}\int_{-\pi}^{+\pi} \mathrm{Tr}\left\{\mathcal{P}(\chi,t)\rho_0\right\} e^{-\mathrm{i}n\chi}d\chi\,, \qquad P_n(z) = \frac{1}{2\pi}\int_{-\pi}^{+\pi} \mathrm{Tr}\left\{\mathcal{P}(\chi,z)\rho_0\right\} e^{-\mathrm{i}n\chi}d\chi\,. \tag{4.11}$$

The corresponding Moment-generating function is given by the Fourier transform of the probability distribution, and we can infer the definition below.

Def. 12 (Moment-Generating function)**.**

$$M(\chi,t) = \mathrm{Tr}\left\{e^{\mathcal{L}(\chi)t}\rho_0\right\}\,. \tag{4.12}$$

Once this function is known, all moments can be computed by differentiation with respect to the counting field

$$\left\langle n^k\right\rangle_t = \sum_n n^k P_n(t) = (-\mathrm{i}\partial_\chi)^k M(\chi,t)\Big|_{\chi=0}\,. \tag{4.13}$$

The cumulant-generating function is given by

$$C(\chi,t) = \ln M(\chi,t)\,, \tag{4.14}$$

and by differentiation with respect to the counting field all cumulants are recovered $\left\langle\left\langle n^k\right\rangle\right\rangle_t = (-\mathrm{i}\partial_\chi)^k C(\chi,t)\Big|_{\chi=0}$.

An easy way to see that moments can be obtained by differentiation with respect to the counting field χ is to consider Eq. (4.7) under the replacement $\mathcal{L}_1 \to \mathcal{L}_1 e^{+\mathrm{i}\chi}$. The total momeng-generating function (MGF) can be expanded as

$$M(\chi,t) = \sum_n e^{+\mathrm{i}n\chi}P_n(t)\,, \tag{4.15}$$

which is just the inverse Fourier transform (FT) of Eq. (4.11). This makes it quite obvious that $\left\langle n^k\right\rangle = (-\mathrm{i}\partial_\chi)^k M(\chi,t)\Big|_{\chi\to 0}$. Cumulants and Moments are of course related, we just summarize

relations for the lowest few cumulants

$$\begin{aligned}
\langle\langle n\rangle\rangle &= \langle n\rangle \,, \\
\langle\langle n^2\rangle\rangle &= \langle n^2\rangle - \langle n\rangle^2 \,, \\
\langle\langle n^3\rangle\rangle &= \langle n^3\rangle - 3\langle n\rangle\langle n^2\rangle + 2\langle n\rangle^3 \,, \\
\langle\langle n^4\rangle\rangle &= \langle n^4\rangle - 4\langle n\rangle\langle n^3\rangle - 3\langle n^2\rangle^2 + 12\langle n\rangle^2\langle n^2\rangle - 6\langle n\rangle^4 \,.
\end{aligned} \tag{4.16}$$

Obviously, the first two cumulants are just the **mean** and **width** of the probability distribution. For unimodal distributions, the third cumulant (skewness) and the fourth cumulant (kurtosis) describe the shape of the distribution near its maximum. In contrast to moments, higher cumulants are inert when a trivial transformation such as a simple shift is performed on a probability distribution.

4.1.1 Multiple jumps

So how is it then possible to count different jumps? In principle, we can base this on the already existing expansion. By further splitting the free Liouvillian $\mathcal{L}_0 = \mathcal{L}_{00} + \mathcal{L}_2$ we would obtain the decomposition

$$\mathcal{P}_0(z) = \sum_{m=0}^{\infty} \left[\mathcal{P}_{00}(z)\mathcal{L}_2\right]^n \mathcal{L}_2 \,, \tag{4.17}$$

which we can insert in Eq. (4.4). The first terms of the resulting expansion would read

$$\begin{aligned}
\mathcal{P}(z) &= \mathcal{P}_{00}(z) + \mathcal{P}_{00}(z)\mathcal{L}_1\mathcal{P}_{00}(z) + \mathcal{P}_{00}(z)\mathcal{L}_2\mathcal{P}_{00}(z) \\
&\quad + \mathcal{P}_{00}(z)\mathcal{L}_1\mathcal{P}_{00}(z)\mathcal{L}_1\mathcal{P}_{00}(z) + \mathcal{P}_{00}(z)\mathcal{L}_2\mathcal{P}_{00}(z)\mathcal{L}_2\mathcal{P}_{00}(z) \\
&\quad + \mathcal{P}_{00}(z)\mathcal{L}_1\mathcal{P}_{00}(z)\mathcal{L}_2\mathcal{P}_{00}(z) + \mathcal{P}_{00}(z)\mathcal{L}_2\mathcal{P}_{00}(z)\mathcal{L}_1\mathcal{P}_{00}(z) + \ldots \,.
\end{aligned} \tag{4.18}$$

This becomes pretty involved very soon, and a diagrammatic representation is more useful, see Fig. 4.2. However, we see that with the replacement $\mathcal{L}_1 \to \mathcal{L}_1 e^{+\mathrm{i}\chi}$ and $\mathcal{L}_2 \to \mathcal{L}_2 e^{+\mathrm{i}\xi}$ the probability

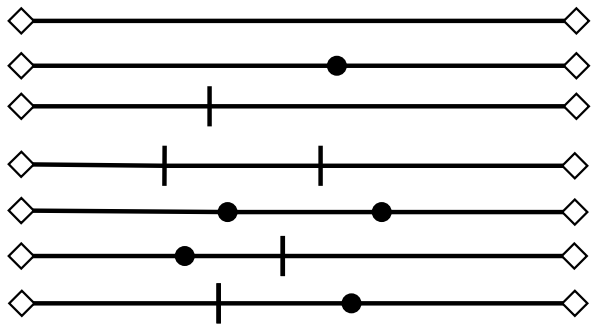

Figure 4.2: Illustration of the first 7 terms in the series expansion in Eq. (4.18). Periods of free evolution (lines) are interrupted by instantaneous jumps of the first (marks) or second (balls) type. In practice, many diagrams may vanish as e.g. for a system hosting at most one electron one will not observe two electrons jumping out subsequently.

of getting n jumps of type $\mathcal{L}_1$ and m jumps of type $\mathcal{L}_2$ can be obtained via

$$P_{nm}(z) = \frac{1}{2\pi}\int_{-\pi}^{+\pi} d\chi \frac{1}{2\pi}\int_{-\pi}^{+\pi} d\xi \mathrm{Tr}\left\{\mathcal{P}(\chi,\xi,z)\rho_0\right\} e^{-\mathrm{i}n\chi} e^{-\mathrm{i}m\xi} \,. \tag{4.19}$$

An important special case arises when we are interested in all trajectories that only lead to a net difference. For example, we may be interested in counting the outgoing jumps of a particle ($\mathcal{L}_+$) and subtract the ingoing jumps ($\mathcal{L}_-$) of the same particle type. Then, we can simply use the decomposition $\mathcal{L}(\chi) = \mathcal{L}_0 + e^{+\mathrm{i}\chi}\mathcal{L}_+ + e^{-\mathrm{i}\chi}\mathcal{L}_-$, i.e., we use $\xi = -\chi$. Performing the integral over $d\chi$ now reconstructs all trajectories with the correct net number $n = n_1 - n_2$.

4.1.2 Cumulant dynamics

The clear advantage of the description by cumulants however lies in the fact that the long-term evolution of the cumulant-generating function is usually given by the dominant eigenvalue of the Liouvillian

$$\mathcal{C}(\chi, t) \approx \lambda(\chi) t \,, \tag{4.20}$$

where $\lambda(\chi)$ is the (uniqueness assumed) eigenvalue of the Liouvillian that vanishes at zero counting field $\lambda(0) = 0$. For this reason, the dominant eigenvalue is also interpreted as the cumulant-generating function of the stationary current. We recall that the Liouville superoperator is in general non-hermitian and may not have a spectral representation. Nevertheless, we can represent it in Jordan Block form

$$\mathcal{L}(\chi) = Q(\chi)\mathcal{L}_J(\chi)Q^{-1}(\chi) \,, \tag{4.21}$$

where $Q(\chi)$ is a (non-unitary) similarity matrix and $\mathcal{L}_J(\chi)$ contains the eigenvalues of the Liouvillian on its diagonal – distributed in blocks with a size corresponding to the eigenvalue multiplicity. We assume that there exists one stationary state $\bar{\rho}$, i.e., one eigenvalue $\lambda(\chi)$ with $\lambda(0) = 0$ and that all other eigenvalues have a larger negative real part near $\chi = 0$. Then, we use this decomposition in the matrix exponential to estimate its long-term evolution

$$\begin{aligned}
\mathcal{M}(\chi, t) &= \mathrm{Tr}\left\{e^{\mathcal{L}(\chi)t}\rho_0\right\} = \mathrm{Tr}\left\{e^{Q(\chi)\mathcal{L}_J(\chi)Q^{-1}(\chi)t}\rho_0\right\} = \mathrm{Tr}\left\{Q(\chi)e^{\mathcal{L}_J(\chi)t}Q^{-1}(\chi)\rho_0\right\} \\
&\to \mathrm{Tr}\left\{Q(\chi)\begin{pmatrix} e^{\lambda(\chi)\cdot t} & & & \\ & 0 & & \\ & & \ddots & \\ & & & 0 \end{pmatrix}Q^{-1}(\chi)\rho_0\right\} \\
&= e^{\lambda(\chi)\cdot t}\mathrm{Tr}\left\{Q(\chi)\begin{pmatrix} 1 & & & \\ & 0 & & \\ & & \ddots & \\ & & & 0 \end{pmatrix}Q^{-1}(\chi)\rho_0\right\} = e^{\lambda(\chi)t}c(\chi)
\end{aligned} \tag{4.22}$$

with some polynomial $c(\chi)$ depending on the matrix $Q(\chi)$. This implies that the cumulant-generating function

$$\mathcal{C}(\chi, t) = \ln \mathcal{M}(\chi, t) = \lambda(\chi)t + \ln c(\chi) \approx \lambda(\chi)t \tag{4.23}$$

becomes linear in $\lambda(\chi)$ for large times. Therefore, for large times, the cumulants can be conveniently determined once the dominant eigenvalue of the Liouvillian is known.

4.1.3 Example: The single-electron transistor

We will illustrate these findings with the simple rate equation of the SET with two junctions

$$\mathcal{L} = \begin{pmatrix} -\Gamma_L f_L & +\Gamma_L(1-f_L) \\ +\Gamma_L f_L & -\Gamma_L(1-f_L) \end{pmatrix} + \begin{pmatrix} -\Gamma_R f_R & +\Gamma_R(1-f_R) \\ +\Gamma_R f_R & -\Gamma_R(1-f_R) \end{pmatrix} . \tag{4.24}$$

For such rate equations, we can naturally interpret the off-diagonal matrix elements as jump terms. Counting, for example the particles entering the system from the left as positive and leaving to the left as negative, we would get the generalized Liouvillian

$$\mathcal{L}(\chi) = \begin{pmatrix} -\Gamma_L f_L & +\Gamma_L(1-f_L)e^{-\mathrm{i}\chi} \\ +\Gamma_L f_L e^{+\mathrm{i}\chi} & -\Gamma_L(1-f_L) \end{pmatrix} + \begin{pmatrix} -\Gamma_R f_R & +\Gamma_R(1-f_R) \\ +\Gamma_R f_R & -\Gamma_R(1-f_R) \end{pmatrix} . \tag{4.25}$$

The full moment-generating function can be obtained by exponentiating this matrix, but we can also consider its dominant eigenvalue (simpler). Here we will for simplicity only discuss the infinite bias regime $f_L \to 1$ and $f_R \to 0$. Then, we get two eigenvalues

$$\lambda_\pm(\chi) = \frac{1}{2}\left(-\Gamma_L - \Gamma_R \pm \sqrt{(\Gamma_L-\Gamma_R)^2 + 4e^{+\mathrm{i}\chi}\Gamma_L\Gamma_R}\right) , \tag{4.26}$$

and it is visible that $\lambda_+(0) = 0$, such that $\lambda(\chi) = \lambda_+(\chi)$ is the sought-after generating function for the cumulants. In the long-time limit, the first cumulants become

$$\begin{aligned} \langle\langle n \rangle\rangle &= \frac{\Gamma_L\Gamma_R}{\Gamma_L+\Gamma_R} t\,, \\ \left\langle\left\langle n^2 \right\rangle\right\rangle &= \frac{\Gamma_L\Gamma_R}{\Gamma_L+\Gamma_R} \frac{\Gamma_L^2+\Gamma_R^2}{(\Gamma_L+\Gamma_R)^2} t\,, \\ \left\langle\left\langle n^3 \right\rangle\right\rangle &= \frac{\Gamma_L\Gamma_R}{\Gamma_L+\Gamma_R} \frac{\Gamma_L^4 - 2\Gamma_L^3\Gamma_R + 6\Gamma_L^2\Gamma_R^2 - 2\Gamma_L\Gamma_R^3 + \Gamma_R^4}{(\Gamma_L+\Gamma_R)^4} t \end{aligned} \tag{4.27}$$

Exercise 34 (Cumulants)**.** *Show that the above formulas hold.*

Alternatively, we can count different things, e.g. the jumps over the right junction, the total number of outgoing or ingoing jumps, the total number of jumps etc.

Exercise 35 (Total number of jumps at infinite bias)**.** *Calculate the long-term cumulant-generating function in the infinite bias limit $f_L \to 1$ and $f_R \to 0$ for the probability $P_n(t)$ of measuring n jumps in total. How is the first cumulant related to the current?*

For example, one may be interested in the total number of jumps when the dot is only coupled to a single equilibrium reservoir

$$\mathcal{L}(\chi) = \Gamma \begin{pmatrix} -f & +(1-f)e^{+\mathrm{i}\chi} \\ +f e^{+\mathrm{i}\chi} & -1+f \end{pmatrix} . \tag{4.28}$$

The dominant eigenvalue is given by

$$\lambda(\chi) = \frac{\Gamma}{2}\left(-1 + \sqrt{1 - 4\left(1-e^{+2\mathrm{i}\chi}\right) f(1-f)}\right) . \tag{4.29}$$

From it, we can determine the average value of total jumps for long times

$$\langle n\rangle = 2\Gamma t f(1-f) \leq \frac{\Gamma t}{2}\,. \tag{4.30}$$

One concludes that the average number of jumps vanishes at zero temperature (where $f \in [0,1]$) at becomes maximal at infinite temperature (where $f \to 1/2$).

4.2 Derivation with virtual detectors

There exist many cases where we have some physical process that we can clearly identify on the level of a given Hamiltonian but possibly not on the level of a Liouville superoperator. For example, we may consider to monitor our single electron transistor with a point contact. If we only look at jumps of the dot, we may not infer from them the statistics of the point contact particles. However, given a microscopic model, we may phenomenologically identify terms which we might want to count. Technically, such problems can still be handled with a quantum master equation by introducing a **virtual detector** at the level of the interaction Hamiltonian. Suppose that in the interaction Hamiltonian we can identify terms associated with a change of the tracked obervable in the reservoir

$$\mathcal{H}_{\rm I} = A_+ \otimes B_+ + A_- \otimes B_- + \sum_{\alpha\neq\{+,-\}} A_\alpha \otimes B_\alpha\,, \tag{4.31}$$

where e.g. B_+ increases and B_- decreases the reservoir particle number. We now artificially extend the system Hilbert space by adding a virtual detector

$$\begin{aligned} \mathcal{H}_{\rm S} &\to \mathcal{H}_{\rm S}\otimes\mathbf{1}\,, \qquad \mathcal{H}_{\rm B}\to\mathcal{H}_{\rm B} \\ \mathcal{H}_{\rm I} &\to + \left[A_+\otimes D^\dagger\right]\otimes B_+ + \left[A_-\otimes D\right]\otimes B_- + \sum_{\alpha\neq\{+,-\}}\left[A_\alpha\otimes\mathbf{1}\right]\otimes B_\alpha\,, \end{aligned} \tag{4.32}$$

where

$$D = \sum_n |n\rangle\langle n+1|\,, \qquad D^\dagger = \sum_n |n+1\rangle\langle n| \tag{4.33}$$

are the detector operators, and $-\infty < n < +\infty$ is an integer number. Here $|n\rangle$ are the eigenstates of the detector, and we see that $D^\dagger|n\rangle = |n+1\rangle$ and $D|n\rangle = |n-1\rangle$. This obviously also implies that $DD^\dagger = D^\dagger D = \mathbf{1}$. We see that each time a B_+ event occurs, the detector changes its state from n to $n+1$ and reduces it when a B_- event occurs. Such a detector is ideal in the sense that it does not have its own energy content (its own Hamiltonian vanishes). Therefore, it will be called **virtual detector** here. The detector operators in the interaction Hamiltonian can also be viewed as bookkeeping operators that simply facilitate the correct identification of terms in the master equation. We can now formally consider the detector as part of the system and derive the master equation. Since there is no direct interaction between the original system and the detector, the eigenbasis of both system and detector is now given by $|a,n\rangle = |a\rangle\otimes|n\rangle$, and we may derive e.g. the coarse-graining master equation or the BMS master equation in the usual way. When we decompose the system density matrix as

$$\rho(t) = \sum_n \rho^{(n)}(t)\otimes|n\rangle\langle n|\,, \tag{4.34}$$

we can interpret $\rho^{(n)}(t)$ as the system density matrix conditional on detector state n. By using that

$$\begin{aligned} \langle n|\, DA_-\rho A_+ D^\dagger\, |n\rangle &= A_-\rho^{(n+1)}A_+\,, \\ \langle n|\, D^\dagger A_+\rho A_- D\, |n\rangle &= A_+\rho^{(n-1)}A_- \end{aligned} \tag{4.35}$$

we can reduce the resulting master equation to a form like

$$\dot\rho^{(n)} = \mathcal{L}_0\rho^{(n)} + \mathcal{L}_+\rho^{(n-1)} + \mathcal{L}_-\rho^{(n+1)}\,. \tag{4.36}$$

The coarse-graining master equation in Box 11 for example shows that such conditioned master equations can be readily derived. This form now provides a natural decomposition into no-jump ($\mathcal{L}_0$), and jumps into and out of the system ($\mathcal{L}_\pm$). We can re-introduce the counting field by performing a discrete Fourier transform

$$\rho(\chi,t) = \sum_n e^{+\mathrm{i}n\chi}\rho^{(n)}(t)\,, \tag{4.37}$$

which recovers the generalized Liouville superoperator

$$\mathcal{L}(\chi) = \mathcal{L}_0 + \mathcal{L}_- e^{-\mathrm{i}\chi} + \mathcal{L}_+ e^{+\mathrm{i}\chi}\,. \tag{4.38}$$

4.2.1 Example: single resonant level

As the most trivial application we consider a quantum dot coupled to a single lead

$$\begin{aligned} H &= \epsilon d^\dagger d + \sum_k \left(t_k d c_k^\dagger + t_k^* c_k d^\dagger\right) + \sum_k \epsilon_k c_k^\dagger c_k \\ &\to \epsilon d^\dagger d + d\otimes B^\dagger \otimes \sum_k t_k d c_k^\dagger + d^\dagger \otimes B \otimes \sum_k t_k^* c_k + \sum_k \epsilon_k c_k^\dagger c_k\,, \end{aligned} \tag{4.39}$$

where we have tacitly performed the tensor-product mapping and also introduced the virtual detector in the second line. The system coupling operators become

$$A_1 = d\otimes B^\dagger\,, \qquad A_2 = d^\dagger\otimes B\,, \tag{4.40}$$

and the reservoir correlation functions read

$$C_{12}(\tau) = \frac{1}{2\pi}\int \Gamma(\omega)f(\omega)e^{+\mathrm{i}\omega\tau}d\omega\,, \qquad C_{21}(\tau) = \frac{1}{2\pi}\int \Gamma(\omega)[1-f(\omega)]e^{-\mathrm{i}\omega\tau}d\omega\,. \tag{4.41}$$

Now, we can for example consider the coarse-graining master equation from Def. 11

$$\begin{aligned} \dot{\boldsymbol{\rho}} &= -\mathrm{i}\left[\frac{1}{2\mathrm{i}\tau}\int_0^\tau dt_1 dt_2 \mathrm{sgn}(t_1-t_2)\left(C_{12}(t_1-t_2)e^{-\mathrm{i}\epsilon(t_1-t_2)}dd^\dagger + C_{21}(t_1-t_2)e^{+\mathrm{i}\epsilon(t_1-t_2)}d^\dagger d\right),\boldsymbol{\rho}\right] \\ &\quad + \frac{1}{\tau}\int_0^\tau dt_1 dt_2 C_{12}(t_1-t_2)e^{-\mathrm{i}\epsilon(t_1-t_2)}\left[(d^\dagger\otimes B)\boldsymbol{\rho}(d\otimes B^\dagger) - \frac{1}{2}\left\{dd^\dagger,\boldsymbol{\rho}\right\}\right] \\ &\quad + \frac{1}{\tau}\int_0^\tau dt_1 dt_2 C_{21}(t_1-t_2)e^{+\mathrm{i}\epsilon(t_1-t_2)}\left[(d\otimes B^\dagger)\boldsymbol{\rho}(d^\dagger\otimes B) - \frac{1}{2}\left\{d^\dagger d,\boldsymbol{\rho}\right\}\right], \end{aligned} \tag{4.42}$$

where we have used that $BB^\dagger = B^\dagger B = \mathbf{1}$. Now, inserting a decomposition of the form

$$\boldsymbol{\rho} = \sum_n \boldsymbol{\rho}^{(\boldsymbol{n})}(t) \otimes |n\rangle \langle n| \tag{4.43}$$

and sandwiching the equation with the states $\langle n| \dots |n\rangle$ we obtain a conditional (or n-resolved) master equation for the dot alone

$$\begin{aligned}
\dot{\boldsymbol{\rho}}^{(\boldsymbol{n})} &= -\mathrm{i}\left[\frac{1}{2\mathrm{i}\tau}\int_0^\tau dt_1 dt_2 \mathrm{sgn}(t_1-t_2)\left(C_{12}(t_1-t_2)e^{-\mathrm{i}\epsilon(t_1-t_2)}dd^\dagger + C_{21}(t_1-t_2)e^{+\mathrm{i}\epsilon(t_1-t_2)}d^\dagger d\right), \boldsymbol{\rho}^{(\boldsymbol{n})}\right] \\
&\quad + \frac{1}{\tau}\int_0^\tau dt_1 dt_2 C_{12}(t_1-t_2)e^{-\mathrm{i}\epsilon(t_1-t_2)}\left[d^\dagger \boldsymbol{\rho}^{(\boldsymbol{n+1})} d - \frac{1}{2}\left\{dd^\dagger, \boldsymbol{\rho}^{(\boldsymbol{n})}\right\}\right] \\
&\quad + \frac{1}{\tau}\int_0^\tau dt_1 dt_2 C_{21}(t_1-t_2)e^{+\mathrm{i}\epsilon(t_1-t_2)}\left[d\boldsymbol{\rho}^{(\boldsymbol{n-1})} d^\dagger - \frac{1}{2}\left\{d^\dagger d, \boldsymbol{\rho}^{(\boldsymbol{n})}\right\}\right] .
\end{aligned} \tag{4.44}$$

Upon discrete Fourier transformation, this yields

$$\begin{aligned}
\dot{\boldsymbol{\rho}}(\chi,t) &= -\mathrm{i}\left[\frac{1}{2\mathrm{i}\tau}\int_0^\tau dt_1 dt_2 \mathrm{sgn}(t_1-t_2)\left(C_{12}(t_1-t_2)e^{-\mathrm{i}\epsilon(t_1-t_2)}dd^\dagger + C_{21}(t_1-t_2)e^{+\mathrm{i}\epsilon(t_1-t_2)}d^\dagger d\right), \boldsymbol{\rho}(\chi,t)\right] \\
&\quad + \frac{1}{\tau}\int_0^\tau dt_1 dt_2 C_{12}(t_1-t_2)e^{-\mathrm{i}\epsilon(t_1-t_2)}\left[d^\dagger \boldsymbol{\rho}(\chi,t) e^{-\mathrm{i}\chi} d - \frac{1}{2}\left\{dd^\dagger, \boldsymbol{\rho}(\chi,t)\right\}\right] \\
&\quad + \frac{1}{\tau}\int_0^\tau dt_1 dt_2 C_{21}(t_1-t_2)e^{+\mathrm{i}\epsilon(t_1-t_2)}\left[d\boldsymbol{\rho}(\chi,t) e^{+\mathrm{i}\chi} d^\dagger - \frac{1}{2}\left\{d^\dagger d, \boldsymbol{\rho}(\chi,t)\right\}\right] .
\end{aligned} \tag{4.45}$$

Upon using that

$$\begin{aligned}
\lim_{\tau\to\infty}\frac{1}{\tau}\int_0^\tau dt_1 dt_2 C_{12}(t_1-t_2)e^{-\mathrm{i}\epsilon(t_1-t_2)} &= \Gamma(\epsilon) f(\epsilon) , \\
\lim_{\tau\to\infty}\frac{1}{\tau}\int_0^\tau dt_1 dt_2 C_{21}(t_1-t_2)e^{+\mathrm{i}\epsilon(t_1-t_2)} &= \Gamma(\epsilon)[1-f(\epsilon)] ,
\end{aligned} \tag{4.46}$$

we see that we recover the rate equation with counting fields we had phenomenologically introduced before

$$\frac{d}{dt}\begin{pmatrix} \rho_{00} \\ \rho_{11} \end{pmatrix} = \Gamma(\epsilon)\begin{pmatrix} -f(\epsilon) & +(1-f(\epsilon))e^{+\mathrm{i}\chi} \\ +f(\epsilon)e^{-\mathrm{i}\chi} & -(1-f(\epsilon))\rho_{11} \end{pmatrix} . \tag{4.47}$$

We note that the difference in sign arises from our convention that particles entering the reservoirs should be counted positive.

4.2.2 Example: SET monitored by a point contact

High-precision tests of counting statistics have been performed with a quantum point contact that is capacitively coupled to a single-electron transistor [9]. The Hamiltonian of the system depicted in Fig. 4.3 reads

$$\begin{aligned}
\mathcal{H}_\mathrm{S} &= \epsilon d^\dagger d , \\
\mathcal{H}_\mathrm{B} &= \sum_k \epsilon_{kL} c_{kL}^\dagger c_{kL} + \sum_k \epsilon_{kL} c_{kR}^\dagger c_{kR} + \sum_k \varepsilon_{kL}\gamma_{kL}^\dagger\gamma_{kL} + \sum_k \varepsilon_{kL}\gamma_{kR}^\dagger\gamma_{kR} , \\
\mathcal{H}_\mathrm{I} &= \left[\sum_k t_{kL} d c_{kL}^\dagger + \sum_k t_{kR} d c_{kR}^\dagger + \mathrm{h.c.}\right] + \left[\sum_{kk'}\left(t_{kk'} + d^\dagger d\tau_{kk'}\right)\gamma_{kL}\gamma_{k'R}^\dagger + \mathrm{h.c.}\right] ,
\end{aligned} \tag{4.48}$$

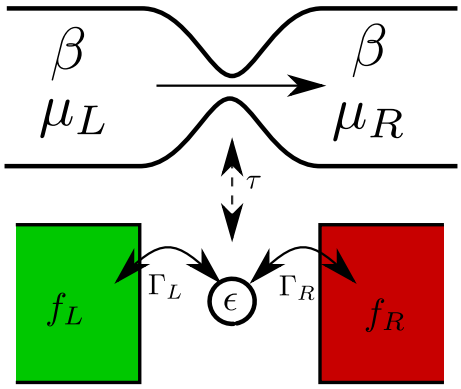

Figure 4.3: Sketch of a quantum point contact (in fact, a two component bath with the components held at different chemical potential) monitoring a single electron transistor. The tunneling through the quantum point contact is modified when the SET is occupied.

where ϵ denotes the dot level, $c_{k\alpha}$ annihilate electrons on SET lead α and $\gamma_{k\alpha}$ are the annihilation operators for the QPC lead α. The QPC baseline tunneling amplitude is given by $t_{kk'}$ and describes the scattering of and electron from mode k in the left lead to mode k' in the right QPC contact. When the nearby SET is occupied it is modified to $t_{kk'} + \tau_{kk'}$, where $\tau_{kk'}$ represents the change of the tunneling amplitude.

We will derive a master equation for the dynamics of the SET due to the interaction with the QPC and the two SET contacts. In addition, we are interested not only in the charge counting statistics of the SET but also the QPC. The Liouvillian for the SET-contact interaction is well known and has been stated previously (we insert counting fields at the right lead to count charges traversing the SET from left to right)

$$\mathcal{L}_{\mathrm{SET}}(\chi) = \begin{pmatrix} -\Gamma_L f_L - \Gamma_R f_R & +\Gamma_L(1-f_L) + \Gamma_R(1-f_R)e^{+\mathrm{i}\chi} \\ +\Gamma_L f_L + \Gamma_R f_R e^{-\mathrm{i}\chi} & -\Gamma_L(1-f_L) - \Gamma_R(1-f_R) \end{pmatrix} . \tag{4.49}$$

We will therefore derive the dissipator for the SET-QPC interaction separately. To keep track of the tunneled QPC electrons, we insert a virtual detector operator in the respective tunneling Hamiltonian

$$\begin{aligned} \mathcal{H}_{\mathrm{I}}^{\mathrm{QPC}} &= \sum_{kk'} \left(t_{kk'}\mathbf{1} + d^\dagger d \tau_{kk'}\right) B^\dagger \gamma_{kL}\gamma_{k'R}^\dagger + \sum_{kk'} \left(t_{kk'}^*\mathbf{1} + d^\dagger d \tau_{kk'}^*\right) B \gamma_{k'R}\gamma_{kL}^\dagger \\ &= \mathbf{1}\otimes B^\dagger \otimes \sum_{kk'} t_{kk'}\gamma_{kL}\gamma_{k'R}^\dagger + \mathbf{1}\otimes B \otimes \sum_{kk'} t_{kk'}^*\gamma_{k'R}\gamma_{kL}^\dagger \\ &\quad + d^\dagger d \otimes B^\dagger \otimes \sum_{kk'} \tau_{kk'}\gamma_{kL}\gamma_{k'R}^\dagger + d^\dagger d \otimes B \otimes \sum_{kk'} \tau_{kk'}^*\gamma_{k'R}\gamma_{kL}^\dagger . \end{aligned} \tag{4.50}$$

Note that we have implicitly performed the mapping to a tensor product representation of the fermionic operators, which is unproblematic here as between SET and QPC no particle exchange takes place and the electrons in the QPC and the SET may be treated as different particle types. To simplify the system, we assume that the change of tunneling amplitudes affects all modes in the same manner, i.e., $\tau_{kk'} = \tilde{\tau} t_{kk'}$, which enables us to combine some coupling operators

$$\mathcal{H}_{\mathrm{I}}^{\mathrm{QPC}} = \left[\mathbf{1} + \tilde{\tau} d^\dagger d\right] \otimes B^\dagger \otimes \sum_{kk'} t_{kk'}\gamma_{kL}\gamma_{k'R}^\dagger + \left[\mathbf{1} + \tilde{\tau}^* d^\dagger d\right] \otimes B \otimes \sum_{kk'} t_{kk'}^*\gamma_{k'R}\gamma_{kL}^\dagger . \tag{4.51}$$

The evident advantage of this approximation is that only two correlation functions have to be computed. We can now straightforwardly (since the baseline tunneling term is not included in the bath Hamiltonian) map to the interaction picture

$$B_1(\tau) = \sum_{kk'} t_{kk'}\gamma_{kL}\gamma^\dagger_{k'R}e^{-\mathrm{i}(\varepsilon_{kL}-\varepsilon_{k'R})\tau}\,, \qquad B_2(\tau) = \sum_{kk'} t^*_{kk'}\gamma_{k'R}\gamma^\dagger_{kL}e^{+\mathrm{i}(\varepsilon_{kL}-\varepsilon_{k'R})\tau}\,. \tag{4.52}$$

For the first bath correlation function we obtain

$$\begin{aligned} C_{12}(\tau) &= \sum_{kk'}\sum_{\ell\ell'} t_{kk'}t^*_{\ell\ell'}e^{-\mathrm{i}(\varepsilon_{kL}-\varepsilon_{k'R})\tau}\left\langle\gamma_{kL}\gamma^\dagger_{k'R}\gamma_{\ell'R}\gamma^\dagger_{\ell L}\right\rangle \\ &= \sum_{kk'}|t_{kk'}|^2e^{-\mathrm{i}(\varepsilon_{kL}-\varepsilon_{k'R})\tau}\left[1-f_L(\varepsilon_{kL})\right]f_R(\varepsilon_{k'R}) \\ &= \frac{1}{2\pi}\int\int T(\omega,\omega')\left[1-f_L(\omega)\right]f_R(\omega')e^{-\mathrm{i}(\omega-\omega')\tau}d\omega d\omega'\,, \end{aligned} \tag{4.53}$$

where we have introduced $T(\omega,\omega') = 2\pi\sum_{kk'}|t_{kk'}|^2\delta(\omega-\varepsilon_{kL})\delta(\omega-\varepsilon_{k'R})$. Note that in contrast to previous tunneling rates, this quantity is dimensionless. The integral factorizes when $T(\omega,\omega')$ factorizes (or when it is flat $T(\omega,\omega')=t$).

In this case, the correlation function $C_{12}(\tau)$ is expressed as a product in the time domain, such that its Fourier transform will be given by a convolution integral

$$\begin{aligned} \gamma_{12}(\Omega) &= \int C_{12}(\tau)e^{+\mathrm{i}\Omega\tau}d\tau \\ &= t\int d\omega d\omega'\left[1-f_L(\omega)\right]f_R(\omega')\delta(\omega-\omega'-\Omega) \\ &= t\int\left[1-f_L(\omega)\right]f_R(\omega-\Omega)d\omega\,. \end{aligned} \tag{4.54}$$

For the other correlation function, we have

$$\gamma_{21}(\Omega) = t\int f_L(\omega)\left[1-f_R(\omega+\Omega)\right]d\omega\,. \tag{4.55}$$

Exercise 36 (Correlation functions for the QPC)**.** *Show the validity of Eqns. (4.55).*

The structure of the Fermi functions demonstrates that the shift Ω can be included in the chemical potentials. Therefore, we consider integrals of the type

$$I = \int f_1(\omega)\left[1-f_2(\omega)\right]d\omega\,. \tag{4.56}$$

At zero temperature, these should behave as $I \approx (\mu_1-\mu_2)\Theta(\mu_1-\mu_2)$, where $\Theta(x)$ denotes the Heaviside-Θ function, which follows from the structure of the integrand, see Fig. 4.4. For finite temperatures, the value of the integral can also be calculated, for simplicity we constrain ourselves to the (experimentally relevant) case of equal temperatures ($\beta_1=\beta_2=\beta$), for which we obtain

$$\begin{aligned} I &= \int\frac{1}{\left(e^{\beta(\mu_2-\omega)}+1\right)\left(e^{-\beta(\mu_1-\omega)}+1\right)}d\omega \\ &= \lim_{\delta\to\infty}\int\frac{1}{\left(e^{\beta(\mu_2-\omega)}+1\right)\left(e^{-\beta(\mu_1-\omega)}+1\right)}\frac{\delta^2}{\delta^2+\omega^2}d\omega\,, \end{aligned} \tag{4.57}$$

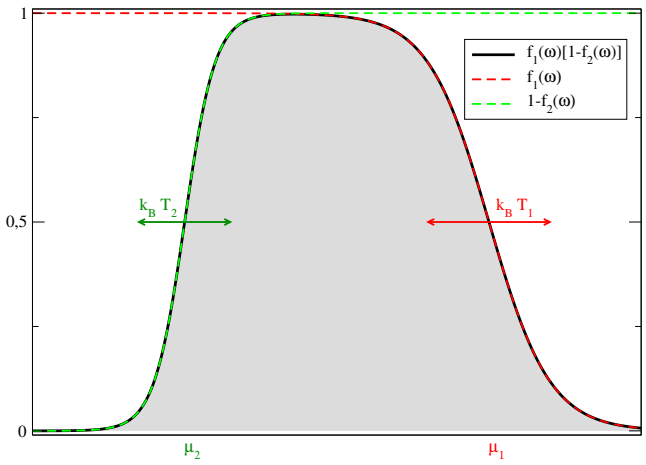

Figure 4.4: Integrand in Eq. (4.56). At zero temperature at both contacts, we obtain a product of two step functions and the area under the curve is given by the difference $\mu_1 - \mu_2$ as soon as $\mu_1 > \mu_2$ (and zero otherwise).

where we have introduced the Lorentzian-shaped regulator to enforce convergence. By identifying the poles of the integrand

$$\begin{aligned} \omega^*_{\pm} &= \pm \mathrm{i}\delta\,, \\ \omega^*_{1,n} &= \mu_1 + \mathrm{i}\frac{\pi}{\beta}(2n+1)\,, \\ \omega^*_{2,n} &= \mu_2 + \mathrm{i}\frac{\pi}{\beta}(2n+1)\,, \end{aligned} \tag{4.58}$$

where $n \in \{0, \pm 1, \pm 2, \pm 3, \ldots$ we can solve the integral by using the residue theorem, see also Fig. 4.5 for the integration contour. Finally, we obtain for the integral

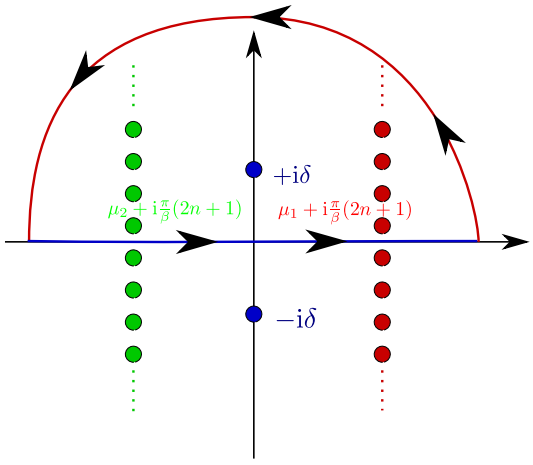

Figure 4.5: Poles and integration contour for Eq. (4.56) in the complex plane. The integral along the real axis (blue line) closed by an arc (red curve) in the upper complex plane, along which (due to the regulator) the integrand vanishes sufficiently fast.

$$\begin{aligned} I &= 2\pi\mathrm{i} \lim_{\delta\to\infty} \Big\{ \mathrm{Res}\, f_1(\omega)\,[1-f_2(\omega)]\, \frac{\delta^2}{\delta^2+\omega^2}\Big|_{\omega=+\mathrm{i}\delta} + \sum_{n=0}^{\infty} \mathrm{Res}\, f_1(\omega)\,[1-f_2(\omega)]\, \frac{\delta^2}{\delta^2+\omega^2}\Big|_{\omega=\mu_1+\mathrm{i}\frac{\pi}{\beta}(2n+1)} \\ &\quad + \sum_{n=0}^{\infty} \mathrm{Res}\, f_1(\omega)\,[1-f_2(\omega)]\, \frac{\delta^2}{\delta^2+\omega^2}\Big|_{\omega=\mu_2+\mathrm{i}\frac{\pi}{\beta}(2n+1)} \Big\} \\ &= \frac{\mu_1-\mu_2}{1-e^{-\beta(\mu_1-\mu_2)}}\,, \end{aligned} \tag{4.59}$$

which automatically obeys the simple zero-temperature ($\beta \to \infty$) limit. With the replacements

$\mu_1 \to \mu_R + \Omega$ and $\mu_2 \to \mu_L$, we obtain for the first bath correlation function

$$\gamma_{12}(\Omega) = t\frac{\Omega - V}{1 - e^{-\beta(\Omega - V)}}\,, \tag{4.60}$$

where $V = \mu_L - \mu_R$ is the QPC bias voltage. Likewise, with the replacements $\mu_1 \to \mu_L$ and $\mu_2 \to \mu_R - \Omega$, the second bath correlation function becomes

$$\gamma_{21}(\Omega) = t\frac{\Omega + V}{1 - e^{-\beta(\Omega + V)}}\,. \tag{4.61}$$

Now we can calculate the transition rates in our system (containing the virtual detector and the quantum dot) for a non-degenerate system spectrum. However, now the detector is part of our system. Therefore, the system state is not only characterized by the number of charges on the SET dot $a \in \{0, 1\}$ but also by the number of charges n that have tunneled through the QPC and have thereby changed the detector state

$$\dot\rho_{(a,n)(a,n)} = \sum_{b,m} \gamma_{(a,n)(b,m),(a,n)(b,m)}\rho_{(b,m)(b,m)} - \left[\sum_{b,m} \gamma_{(b,m)(a,n),(b,m)(a,n)}\right]\rho_{(a,n)(a,n)}\,. \tag{4.62}$$

Shortening the notation by omitting the double-indices we may also write

$$\dot\rho^{(n)}_{aa} = \sum_{b,m} \gamma_{(a,n),(b,m)}\rho^{(m)}_{bb} - \left[\sum_{b,m} \gamma_{(b,m),(a,n)}\right]\rho^{(n)}_{aa}\,, \tag{4.63}$$

where $\rho^{(n)}_{aa} = \rho_{(a,n),(a,n)}$ and $\gamma_{(a,n),(b,m)} = \gamma_{(a,n)(a,n),(b,m)(b,m)}$. It is evident that the coupling operators $A_1 = (\mathbf{1} + \tilde\tau d^\dagger d) \otimes B^\dagger$ and $A_2 = (\mathbf{1} + \tilde\tau^* d^\dagger d) \otimes B$ only allow for sequential tunneling through the QPC at lowest order (i.e., $m = n \pm 1$) and do not induce transitions between different dot states (i.e., $a = b$), such that the only non-vanishing contributions may arise for

$$\begin{aligned}
\gamma_{(0,n)(0,n+1)} &= \gamma_{12}(0)\,\langle 0,n|\,A_2\,|0,n+1\rangle\,\langle 0,n|\,A_1^\dagger\,|0,n+1\rangle^* = \gamma_{12}(0)\,,\\
\gamma_{(0,n)(0,n-1)} &= \gamma_{21}(0)\,\langle 0,n|\,A_1\,|0,n-1\rangle\,\langle 0,n|\,A_2^\dagger\,|0,n-1\rangle^* = \gamma_{21}(0)\,,\\
\gamma_{(1,n)(1,n+1)} &= \gamma_{12}(0)\,\langle 1,n|\,A_2\,|1,n+1\rangle\,\langle 1,n|\,A_1^\dagger\,|1,n+1\rangle^* = \gamma_{12}(0)|1+\tilde\tau|^2\,,\\
\gamma_{(1,n)(1,n-1)} &= \gamma_{21}(0)\,\langle 1,n|\,A_1\,|1,n-1\rangle\,\langle 1,n|\,A_2^\dagger\,|1,n-1\rangle^* = \gamma_{21}(0)|1+\tilde\tau|^2\,.
\end{aligned} \tag{4.64}$$

The remaining terms just account for the normalization.

Exercise 37 (Normalization terms)**.** *Compute the remaining rates*

$$\sum_m \gamma_{(0,m)(0,m),(0,n)(0,n)}\,, \qquad \text{and} \qquad \sum_m \gamma_{(1,m)(1,m),(1,n)(1,n)}$$

explicitly.

Adopting the notation of conditional master equations, this leads to the connected system

$$\begin{aligned}
\dot\rho^{(n)}_{00} &= \gamma_{12}(0)\rho^{(n+1)}_{00} + \gamma_{21}(0)\rho^{(n-1)}_{00} - [\gamma_{12}(0) + \gamma_{21}(0)]\,\rho^{(n)}_{00}\\
\dot\rho^{(n)}_{11} &= |1+\tilde\tau|^2\gamma_{12}(0)\rho^{(n+1)}_{11} + |1+\tilde\tau|^2\gamma_{21}(0)\rho^{(n-1)}_{11} - |1+\tilde\tau|^2\,[\gamma_{12}(0) + \gamma_{21}(0)]\,\rho^{(n)}_{11}\,,
\end{aligned} \tag{4.64}$$

such that after Fourier transformation with the counting field ξ for the QPC, we obtain the following dissipator

$$\mathcal{L}_{\rm QPC}(\xi) = \begin{pmatrix} \left[\gamma_{21}\left(e^{+{\rm i}\xi}-1\right)+\gamma_{12}\left(e^{-{\rm i}\xi}-1\right)\right] & 0 \\ 0 & |1+\tilde{\tau}|^2\left[\gamma_{21}\left(e^{+{\rm i}\xi}-1\right)+\gamma_{12}\left(e^{-{\rm i}\xi}-1\right)\right] \end{pmatrix}, \tag{4.65}$$

which could not have been deduced directly from a Liouvillian for the SET alone. More closely analyzing the Fourier transforms of the bath correlation functions

$$\begin{aligned} \gamma_{21} &= \gamma_{21}(0) = t\frac{V}{1-e^{-\beta V}}, \\ \gamma_{12} &= \gamma_{12}(0) = t\frac{V}{e^{+\beta V}-1} \end{aligned} \tag{4.66}$$

we see that for sufficiently large QPC bias voltages $V \to \infty$, transport becomes unidirectional: One contribution becomes linear in the voltage $\gamma_{21} \to tV$ and the other one is exponentially suppressed $\gamma_{12} \to 0$. Despite the unusual form of the tunneling rates we see that they obey the usual detailed balance relations

$$\frac{\gamma_{21}}{\gamma_{12}} = e^{+\beta V}. \tag{4.67}$$

The sum of both Liouvillians (4.49) and (4.65) constitutes the total dissipator

$$\mathcal{L}(\chi,\xi) = \mathcal{L}_{\rm SET}(\chi) + \mathcal{L}_{\rm QPC}(\xi), \tag{4.68}$$

which can be used to calculate the probability distributions for tunneling through both transport channels (QPC and SET).

Exercise 38 (QPC current)**.** *Show that the stationary state of the SET is unaffected by the additional QPC dissipator and calculate the stationary current through the QPC for Liouvillian (4.68).*

When we consider the case $\{\Gamma_L,\Gamma_R\} \ll \{tV, |1+\tilde{\tau}|tV\}$, we approach a bistable system, where for a nearly stationary SET the QPC transmits many charges. Then, the QPC current measured at finite times will be large when the SET dot is empty and reduced otherwise. In this case, the counting statistics approaches the case of telegraph noise. When the dot is empty or filled throughout respectively, the current can easily be determined as

$$I_0 = \left[\gamma_{21}(0)-\gamma_{12}(0)\right], \qquad I_1 = |1+\tilde{\tau}|^2\left[\gamma_{21}(0)-\gamma_{12}(0)\right]. \tag{4.69}$$

For finite time intervals Δt, the number of electrons tunneling through the QPC Δn is determined by the probability distribution

$$P_{\Delta n}(\Delta t) = \frac{1}{2\pi}\int_{-\pi}^{+\pi} {\rm Tr}\left\{e^{\mathcal{L}(0,\xi)\Delta t - {\rm i}\Delta n\xi}\rho(t)\right\} d\xi, \tag{4.70}$$

where $\rho(t)$ represents the initial density matrix. This quantity can e.g. be evaluated numerically. When Δt is not too large (such that the stationary state is not really reached) and not too small

(such that there are sufficiently many particles tunneling through the QPC to meaningfully define a current), a continuous measurement of the QPC current maps to a fixed-point iteration as follows: Measuring a certain particle number corresponds to a projection, i.e., the system-detector density matrix is projected to a certain measurement outcome which occurs with the probability $P_{\Delta n}(\Delta t)$

$$\rho = \sum_n \rho^{(n)} \otimes |n\rangle \langle n| \overset{m}{\to} \frac{\rho^{(m)}}{\mathrm{Tr}\,\{\rho^{(m)}\}} \,. \tag{4.71}$$

It is now essential to use the density matrix after the measurement as the initial state for the next iteration. This ensures that e.g. after measuring a large current it is in the next step more likely to measure a large current than a low current. Consequently, the ratio of measured particles divided by measurement time gives a current estimate $I(t) \approx \frac{\Delta n}{\Delta t}$ for the time interval. Such current trajectories are used to track the full counting statistics through quantum point contacts, see Fig. 4.6 In this way, the QPC acts as a detector for the counting statistics of the SET circuit.

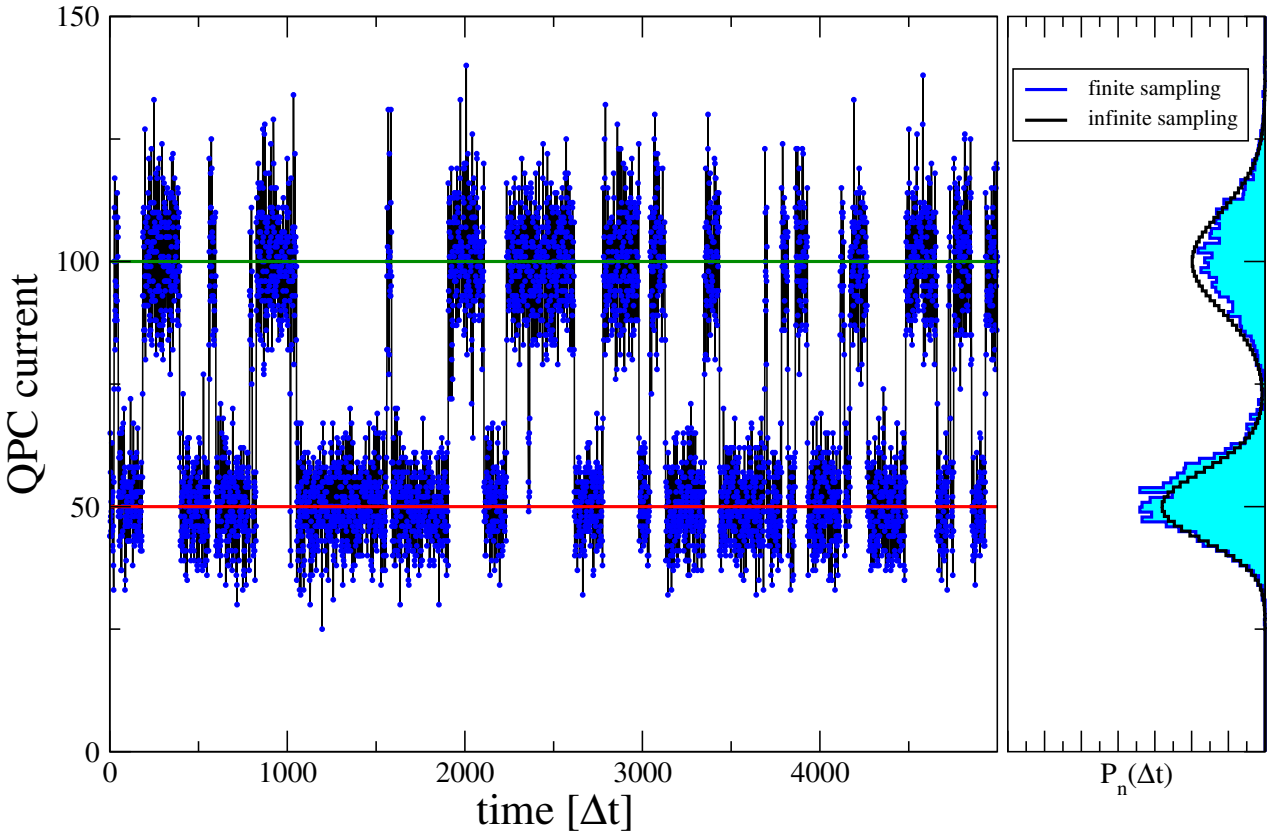

Figure 4.6: Numerical simulation of the time-resolved QPC current for a fluctuating dot occupation. At infinite SET bias, the QPC current allows to reconstruct the full counting statistics of the SET, since each current blip from low (red line) to high (green line) current corresponds to an electron leaving the SET to its right junction. Parameters: $\Gamma_L \Delta t = \Gamma_R \Delta t = 0.01$, $\gamma_{12}(0) = |1+\tilde{\tau}|^2 \gamma_{12}(0) = 0$, $\gamma_{21}(0) = 100.0$, $|1+\tilde{\tau}|^2 \gamma_{21}(0) = 50.0$, $f_L = 1.0$, $f_R = 0.0$. The right panel shows the corresponding probability distribution $P_n(\Delta t)$ versus $n = I\Delta t$, where the blue curve is sampled from the left panel and the black curve is the theoretical limit for infinitely long times.

Finally, we note that for an SET, a QPC only acts as a reliable detector when the SET transport

is unidirectional (large bias).

4.2.3 Example: Pure-Dephasing Model

As another example where the counting statistics cannot be deduced from the system dynamics, we revisit the pure-dephasing limit of the spin-boson model

$$H = \Omega\sigma^z + \sigma^z \otimes \sum_k \left(h_k b_k + h_k^* b_k^\dagger\right) + \sum_k \omega_k b_k^\dagger b_k \,. \tag{4.72}$$

If we wish to count the total number of particles radiated into the reservoir, we introduce virtual detector operators and generalize the Hamiltonian to

$$H = \Omega\sigma^z + \sigma^z \otimes B \otimes \sum_k h_k b_k + \sigma^z \otimes B^\dagger \otimes h_k^* b_k^\dagger + \sum_k \omega_k b_k^\dagger b_k \,, \tag{4.73}$$

from which we can infer the system coupling operators

$$A_1 = \sigma^z \otimes B^\dagger \,, \qquad A_2 = \sigma^z \otimes B \,. \tag{4.74}$$

We note that these are time-independent in the interaction picture $\boldsymbol{A_i}(t) = A_i$. Furthermore, the reservoir correlation functions become

$$\begin{aligned} C_{12}(\tau) &= \frac{1}{2\pi}\int_0^\infty \Gamma(\omega)[1+n_B(\omega)]e^{-\mathrm{i}\omega\tau}d\omega \,, \\ C_{21}(\tau) &= \frac{1}{2\pi}\int_{-\infty}^0 \Gamma(-\Omega)n_B(-\Omega)e^{-\mathrm{i}\omega\tau}d\omega \,. \end{aligned} \tag{4.75}$$

From these expressions, we can read off their Fourier transforms

$$\gamma_{21}(\omega) = \Theta(-\omega)\Gamma(-\omega)n_B(-\omega) \,, \qquad \gamma_{12}(\omega) = \Theta(+\omega)\Gamma(+\omega)[1+n_B(+\omega)] \,. \tag{4.76}$$

The coupling operators are evidently not hermitian. Therefore, we recall the coarse-graining Liouvillian from Def. 11. With $\sigma_z^2 = \mathbf{1}$ we see that we can ignore the Lamb-shift contribution, and the coarse-graining master equation becomes

$$\begin{aligned} \dot{\boldsymbol{\rho}} &= \frac{1}{2\pi\tau}\int_0^\tau dt_1 \int_0^\tau dt_2 \int d\omega\Theta(\omega)\Gamma(\omega)[1+n_B(\omega)]e^{-\mathrm{i}\omega(t_1-t_2)}\left[(\sigma^z\otimes B)\boldsymbol{\rho}(\sigma^z\otimes B^\dagger) - \boldsymbol{\rho}\right] \\ &\quad + \frac{1}{2\pi\tau}\int_0^\tau dt_1 \int_0^\tau dt_2 \int d\omega\Theta(-\omega)\Gamma(-\omega)n_B(-\omega)e^{-\mathrm{i}\omega(t_1-t_2)}\left[(\sigma^z\otimes B^\dagger)\boldsymbol{\rho}(\sigma^z\otimes B) - \boldsymbol{\rho}\right] \end{aligned} \tag{4.77}$$

In contrast to Eq. (2.113) we have split the two terms in the dissipator since we count one as particle-creating and the other one as particle annihilating in the reservoir. Performing the temporal integrations we obtain

$$\begin{aligned} \dot{\boldsymbol{\rho}} &= \gamma_-(\tau)\left[e^{-\mathrm{i}\chi}\sigma^z\boldsymbol{\rho}\sigma^z - \boldsymbol{\rho}\right] + \gamma_+(\tau)\left[e^{+\mathrm{i}\chi}\sigma^z\boldsymbol{\rho}\sigma^z - \boldsymbol{\rho}\right] \,, \\ \gamma_+(\tau) &= \int \Theta(\omega)\Gamma(\omega)[1+n_B(\omega)]\frac{\tau}{2\pi}\mathrm{sinc}^2\left[\frac{\omega\tau}{2}\right]d\omega \,, \\ \gamma_-(\tau) &= \int \Theta(-\omega)\Gamma(-\omega)n_B(-\omega)\frac{\tau}{2\pi}\mathrm{sinc}^2\left[\frac{\omega\tau}{2}\right]d\omega \,. \end{aligned} \tag{4.78}$$

Eventually, we can write this as Liouville superoperator with counting fields on the diagonals

$$\begin{aligned}
\dot{\boldsymbol{\rho}}_{\mathbf{00}} &= \left[\gamma_-(\tau)(e^{-\mathrm{i}\chi}-1)+\gamma_+(\tau)(e^{+\mathrm{i}\chi}-1)\right]\boldsymbol{\rho}_{\mathbf{00}}\,,\\
\dot{\boldsymbol{\rho}}_{\mathbf{11}} &= \left[\gamma_-(\tau)(e^{-\mathrm{i}\chi}-1)+\gamma_+(\tau)(e^{+\mathrm{i}\chi}-1)\right]\boldsymbol{\rho}_{\mathbf{11}}\,,\\
\dot{\boldsymbol{\rho}}_{\mathbf{01}} &= -\left[\gamma_-(\tau)(e^{-\mathrm{i}\chi}+1)+\gamma_+(\tau)(e^{+\mathrm{i}\chi}+1)\right]\boldsymbol{\rho}_{\mathbf{01}}\,,\\
\dot{\boldsymbol{\rho}}_{\mathbf{00}} &= -\left[\gamma_-(\tau)(e^{-\mathrm{i}\chi}+1)+\gamma_+(\tau)(e^{+\mathrm{i}\chi}+1)\right]\boldsymbol{\rho}_{\mathbf{10}}\,.
\end{aligned} \tag{4.79}$$

When setting the counting field to zero, we recover Eq. (2.113). Since this is diagonal, we can easily exponentiate the Liouvillian, and the cumulant-generating function becomes at finite times

$$C(\chi,\tau)=\left[\gamma_-(\tau)(e^{-\mathrm{i}\chi}-1)+\gamma_+(\tau)(e^{+\mathrm{i}\chi}-1)\right]\tau\,. \tag{4.80}$$

Interestingly, the cumulant generating function does not depend on the initial state of the system in this particular example. With this, the first cumulant becomes

$$\begin{aligned}
\langle\langle N\rangle\rangle_\tau &= (-\mathrm{i}\partial_\chi)\,\mathrm{Tr}\left\{e^{\mathcal{L}_\tau(\chi)\tau}\rho_0\right\}\big|_{\chi\to 0}=\left[\gamma_+(\tau)-\gamma_-(\tau)\right]\tau\\
&= \int_0^\infty \Gamma(\omega)\frac{\tau^2}{2\pi}\mathrm{sinc}^2\left[\frac{\omega\tau}{2}\right]d\omega=\frac{2}{\pi}\int_0^\infty\frac{\Gamma(\omega)}{\omega^2}\sin^2\left(\frac{\omega\tau}{2}\right)d\omega\,.
\end{aligned} \tag{4.81}$$

We see that this becomes completely independent of the initial state of the system and also of the thermal properties of the reservoir. Similarly, we get for the second cumulant

$$\begin{aligned}
\left\langle\left\langle N^2\right\rangle\right\rangle_\tau &= \left[\gamma_+(\tau)+\gamma_-(\tau)\right]\tau=\int_0^\infty\Gamma(\omega)[1+2n_B(\omega)]\frac{\tau^2}{2\pi}\mathrm{sinc}^2\left[\frac{\omega\tau}{2}\right]d\omega\\
&= \frac{2}{\pi}\int_0^\infty\frac{\Gamma(\omega)[1+2n_B(\omega)]}{\omega^2}\sin^2\left(\frac{\omega\tau}{2}\right)d\omega\,.
\end{aligned} \tag{4.82}$$

Whereas the mean does not depend on the thermal properties of the reservoirs, the second cumulant does. We should therefore try to confirm this result independently.

Exact solution

To solve the pure-dephasing spin-boson problem exactly for the evolution of reservoir observables, we now consider the Heisenberg equations of motion. The reservoir modes evolve according to

$$\dot{b}_k=+\mathrm{i}[H,b_k]=-\mathrm{i}h_k^*\sigma^z-\mathrm{i}\omega_k b_k(t)\,. \tag{4.83}$$

Since σ^z is constant in the Heisenberg picture, this is readily solved by

$$b_k(t)=e^{-\mathrm{i}\omega_k t}b_k+\frac{h_k^*}{\omega_k}\left(e^{-\mathrm{i}\omega_k t}-1\right)\sigma^z\,, \tag{4.84}$$

and similar for the hermitian conjugate operator. Therefore, the exact expectation value of the particle number in the reservoir becomes

$$\begin{aligned}
\langle N\rangle_t &= \sum_k\mathrm{Tr}\left\{\left(e^{+\mathrm{i}\omega_k t}b_k^\dagger+\frac{h_k}{\omega_k}\left(e^{+\mathrm{i}\omega_k t}-1\right)\sigma^z\right)\left(e^{-\mathrm{i}\omega_k t}b_k+\frac{h_k^*}{\omega_k}\left(e^{-\mathrm{i}\omega_k t}-1\right)\sigma^z\right)\rho_S^0\otimes\rho_B^0\right\}\\
&= \langle N\rangle_0+\sum_k\frac{|h_k|^2}{\omega^2}[2-2\cos(\omega t)]\,.
\end{aligned} \tag{4.85}$$

This change arises from the interaction. The change in the particle number can be compared with our previous result

$$\Delta N(t) = \frac{1}{2\pi}\int \frac{\Gamma(\omega)}{\omega^2} 4\sin^2\left[\frac{\omega t}{2}\right] d\omega\,, \tag{4.86}$$

and we see that the coarse-graining current matches the exact solution when the coarse-graining time is chosen dynamically with the physical time $\tau = t$.

Now, we consider the second moment

$$\begin{aligned}
\left\langle N^2\right\rangle_t &= \sum_{kq} \mathrm{Tr}\Big\{ \left(e^{+\mathrm{i}\omega_k t} b_k^\dagger + \frac{h_k}{\omega_k}\left(e^{+\mathrm{i}\omega_k t}-1\right)\sigma^z\right)\left(e^{-\mathrm{i}\omega_k t} b_k + \frac{h_k^*}{\omega_k}\left(e^{-\mathrm{i}\omega_k t}-1\right)\sigma^z\right)\times \\
&\quad \times \left(e^{+\mathrm{i}\omega_q t} b_q^\dagger + \frac{h_q}{\omega_q}\left(e^{+\mathrm{i}\omega_q t}-1\right)\sigma^z\right)\left(e^{-\mathrm{i}\omega_q t} b_q + \frac{h_q^*}{\omega_q}\left(e^{-\mathrm{i}\omega_q t}-1\right)\sigma^z\right)\rho_S^0\otimes\rho_B^0\Big\} \\
&= \left\langle N^2\right\rangle_0 + \sum_{kq}\frac{|h_k|^2}{\omega_k^2}[2-2\cos(\omega_k t)]\frac{|h_q|^2}{\omega_q^2}[2-2\cos(\omega_q t)] \\
&\quad +2\left\langle N\right\rangle_0 \sum_k \frac{|h_k|^2}{\omega_k^2}[2-2\cos(\omega_k t)] + \sum_k [1+2n_B(\omega_k)]\frac{|h_k|^2}{\omega_k^2}[2-2\cos(\omega_k t)]\,.
\end{aligned} \tag{4.87}$$

Putting things together we construct the second cumulant

$$\left\langle\left\langle N^2\right\rangle\right\rangle_t = \sum_k [1+2n_B(\omega_k)]\frac{|h_k|^2}{\omega_k^2}[2-2\cos(\omega_k t)] = \frac{2}{\pi}\int_0^\infty \frac{\Gamma(\omega)}{\omega^2}[1+2n_B(\omega)]\sin^2\left(\frac{\omega t}{2}\right) d\omega\,. \tag{4.88}$$

Also the second cumulant agrees with the exact solution.

4.3 Waiting times and Full Counting Statistics

We will also briefly discuss the relation between full counting statistics and waiting times, see also Ref. [10]. Suppose we have a decomposition of the Liouville superoperator into n jump terms

$$\mathcal{L} = \mathcal{L}_0 + \mathcal{L}_1 + \ldots + \mathcal{L}_n\,, \tag{4.89}$$

where $\mathcal{L}_i$ describes a jump of type i. With the FCS, we can ask for the probabilities of having n_i jumps of type i during a time interval Δt. In contrast, a waiting time distribution $P(\tau)$ denotes the distribution of times between two events. A trivial example of a waiting time distribution can be easily constructed from the FCS by asking for the average waiting time for the first jump to occur. The probability of observing no jump from $t_0 = 0$ up to time t is given by $P_0(t) = \mathrm{Tr}\left\{e^{\mathcal{L}_0 t}\rho_0\right\}$. Then, one can easily show that $P(\tau) = -\dot{P}_0(\tau) = -\mathrm{Tr}\left\{\mathcal{L}_0 e^{\mathcal{L}_0\tau}\rho_0\right\}$ is the distribution of waiting times. Since we always have $P(\tau) \geq 0$ and $\int_0^\infty P(\tau)d\tau = -P_0(\infty) + P_0(0) = 1$, this is a valid probability distribution. The starting event here is the beginning of the observation, and the final event is the first observed jump.

However, the waiting time problem can be formulated much more generally. For example, we can ask for the waiting time distribution between two successive jump events, i.e., for the time between a jump of type i followed by a jump of type j. This will of course depend on the initial state, such that to avoid ambiguities one usually chooses it to be the steady state $\rho_0 = \bar{\rho}$, obeying $\mathcal{L}\bar{\rho} = 0$. We also note that we assume that there exists only one steady state.

First, to meaningfully define the waiting time distribution, we have to ask ourselves about the density matrix after the first jump has occurred. From the probability $P_1^i(t)$ of observing a single jump of type i during Δt

$$P_1^i(\Delta t) = \int_{t_0}^{t_0+\Delta t} \mathrm{Tr}\left\{e^{\mathcal{L}_0(t_0+\Delta t-t_1)}\mathcal{L}_i e^{\mathcal{L}_0(t_1-t_0)}\bar{\rho}\right\} dt_1 \tag{4.90}$$

we can infer that as $\Delta t \to 0$, the probability becomes $P_n^i(\Delta t) \to \Delta t \mathrm{Tr}\left\{\mathcal{L}_i\bar{\rho}\right\}$, and the corresponding density matrix right after the jump becomes

$$\rho^{(i)} = \frac{\Delta t \mathcal{L}_i\bar{\rho}}{\Delta t \mathrm{Tr}\left\{\mathcal{L}_i\bar{\rho}\right\}} = \frac{\mathcal{L}_i\bar{\rho}}{\mathrm{Tr}\left\{\mathcal{L}_i\bar{\rho}\right\}}\,. \tag{4.91}$$

Here, we have normalized by the probability of this particular jump. We can now take this as the initial state and ask for the probability that no second jump of any type occurs up to time t

$$P_0^i(t) = \mathrm{Tr}\left\{e^{\mathcal{L}_0 t}\rho^{(i)}\right\}\,. \tag{4.92}$$

The corresponding waiting time distribution would – in complete analogy to our previous arguments – be given by $P^i(\tau) = -\mathrm{Tr}\left\{\mathcal{L}_0 e^{\mathcal{L}_0\tau}\rho^{(i)}\right\}$, but our sought-after final event is not the end of the observations, but should be the observation of a second jump. We can also write down the un-normalized density matrix for this trajectory, defined by an initial jump of type i, followed by a jump-free evolution up to time τ

$$\rho^{(0,i)}(\tau) = e^{\mathcal{L}_0\tau}\rho^{(i)}\,. \tag{4.93}$$

Now, observing a jump of type j at time τ yields the conditional density matrix

$$\rho^{(j,i)}(\tau) = \mathcal{L}_j e^{\mathcal{L}_0\tau}\rho^{(i)}\,, \tag{4.94}$$

and the corresponding probability is given by the trace of this expression. This leads to the definition below.

Def. 13 (Waiting time distribution)**.** *For a Liouvillian decomposition $\mathcal{L} = \mathcal{L}_0 + \sum_{i=1}^n \mathcal{L}_i$ with jump terms $\mathcal{L}_i$ and steady state $\mathcal{L}\bar{\rho} = 0$, the waiting time distribution between an initial jump of type i and a successive jump of type j is defined as*

$$w_{ji}(\tau) = \frac{\mathrm{Tr}\left\{\mathcal{L}_j e^{\mathcal{L}_0\tau}\mathcal{L}_i\bar{\rho}\right\}}{\mathrm{Tr}\left\{\mathcal{L}_i\bar{\rho}\right\}}\,. \tag{4.95}$$

The waiting times defined this way are positive when our probability interpretation of the Dyson series holds. However, they are not always normalized to one, since a jump i may not necessarily be followed by a jump j.

For example, we can consider the single resonant level with the splitting $\mathcal{L} = \mathcal{L}_0 + \mathcal{L}_1 + \mathcal{L}_2$, where

$$\mathcal{L}_0 = \Gamma\begin{pmatrix} -f & 0 \\ 0 & -(1-f) \end{pmatrix}, \qquad \mathcal{L}_1 = \Gamma\begin{pmatrix} 0 & 0 \\ f & 0 \end{pmatrix}, \qquad \mathcal{L}_2 = \Gamma\begin{pmatrix} 0 & 1-f \\ 0 & 0 \end{pmatrix}. \tag{4.96}$$

The steady state of the full Liouvillian is given by $\bar{\rho} = (1-f, f)^T$. Then, we can compute the waiting time distributions

$$w(\tau) = \begin{pmatrix} 0 & \Gamma f e^{-\Gamma f \tau} \\ \Gamma(1-f)e^{-\Gamma(1-f)\tau} & 0 \end{pmatrix} . \tag{4.97}$$

This trivially shows that it is not possible to observe two successive jumps of the same type in this system, it can only hold a single electron. Consequently, we also observe that these waiting time distributions are normalized.

For completeness, we also revisit the SET in the infinite bias regime with the splitting

$$\mathcal{L}_0 = \begin{pmatrix} -\Gamma_L & 0 \\ 0 & -\Gamma_R \end{pmatrix} , \qquad \mathcal{L}_1 = \begin{pmatrix} 0 & 0 \\ +\Gamma_L & 0 \end{pmatrix} , \qquad \mathcal{L}_2 = \begin{pmatrix} 0 & +\Gamma_R \\ 0 & 0 \end{pmatrix} . \tag{4.98}$$

The steady state is given by $\rho = (\Gamma_R, \Gamma_L)^T/(\Gamma_L + \Gamma_R)$, and the waiting time distributions become

$$w(\tau) = \begin{pmatrix} 0 & \Gamma_L e^{-\Gamma_L \tau} \\ \Gamma_R e^{-\Gamma_R \tau} & 0 \end{pmatrix} . \tag{4.99}$$

These are precisely the waiting time distributions that could be extracted from Fig. 4.6. Here, $\Gamma_L e^{-\Gamma_L \tau}$ is the distributions for the empty dot, and $\Gamma_R e^{-\Gamma_R \tau}$ corresponds to the filled dot.

4.4 General Microscopic Derivation

Sometimes, we are interested not only in the number of particles but also e.g. in the energy transferred into the reservoir. Then, it is less clear how one would proceed with a virtual detector approach. Alternatively, one could be interested in other observables of the reservoir, where at the level of the Hamiltonian it is not immediately apparent how these reservoir observables are changed by individual terms. Therefore, we also consider another microscopic way of deriving generalized master equations here. At this point, we only assume that the observable of interest $\hat{O}$ commutes with the reservoir Hamiltonian $[\hat{O}, H_B] = 0$. The observable in the reservoir can already initially take infinite values – after all, a reservoir can contain an infinite amount of particles. To say by how much the observable has changed, we have to define a reference, which can be done with an initial measurement.

We therefore employ the spectral decomposition of the observable

$$\hat{O} = \sum_\ell O_\ell \left|\ell\right\rangle \left\langle\ell\right| . \tag{4.100}$$

The initial measurement projects the bath density matrix to

$$\bar{\rho}_B \xrightarrow{\ell} \frac{\left|\ell\right\rangle \left\langle\ell\right| \bar{\rho}_B \left|\ell\right\rangle \left\langle\ell\right|}{P_\ell} = \frac{\bar{\rho}_B^{(\ell)}}{P_\ell} , \tag{4.101}$$

where $P_\ell = \mathrm{Tr}\left\{\left|\ell\right\rangle \left\langle\ell\right| \bar{\rho}_B\right\}$ denotes the probability for the outcome ℓ to be obtained in the first measurement. Since we only measure a reservoir observable, this does not affect the system density matrix. The initial value O_ℓ is now our reference point with respect to which we define the change. Since we do not only want a generating function specific to a certain initial value, we perform a weighted average over all outcomes to define the moment-generating function

$$M(\chi, t) = \sum_\ell \mathrm{Tr}\left\{ e^{\mathrm{i}\chi(\hat{O}-O_\ell)} \boldsymbol{U}(t) \rho_S^0 \otimes \bar{\rho}_B^{(\ell)} \boldsymbol{U}^\dagger(t) \right\} , \tag{4.102}$$

where we see that the probability P_ℓ has cancelled due to the weighted average. We note that this equation has been written down in the interaction picture, where due to our assumption the reservoir observable did not pick up a time dependence. Clearly, computing derivatives with respect to χ pulls down powers of $(\hat{O} - O_\ell)$ in the usual way.

We now evaluate the moment-generating function as

$$\begin{aligned} M(\chi,t) &= \sum_\ell \mathrm{Tr}\left\{e^{+\mathrm{i}(\hat{O}-O_\ell)\chi}\boldsymbol{U}(t)\rho_S^0\otimes\rho_B^{(\ell)}\boldsymbol{U}^\dagger(t)\right\} \\ &= \sum_\ell \mathrm{Tr}\left\{e^{+\mathrm{i}\hat{O}\frac{\chi}{2}}\boldsymbol{U}(t)e^{-\mathrm{i}O_\ell\frac{\chi}{2}}\rho_S^0\otimes\rho_B^{(\ell)}e^{-\mathrm{i}O_\ell\frac{\chi}{2}}\boldsymbol{U}^\dagger(t)e^{+\mathrm{i}\hat{O}\frac{\chi}{2}}\right\} \\ &= \sum_\ell \mathrm{Tr}\left\{e^{+\mathrm{i}\hat{O}\frac{\chi}{2}}\boldsymbol{U}(t)e^{-\mathrm{i}\hat{O}\frac{\chi}{2}}\rho_S^0\otimes e^{+\mathrm{i}(\hat{O}-O_\ell)\frac{\chi}{2}}\rho_B^{(\ell)}e^{+\mathrm{i}(\hat{O}-O_\ell)\frac{\chi}{2}}e^{-\mathrm{i}\hat{O}\frac{\chi}{2}}\boldsymbol{U}^\dagger(t)e^{+\mathrm{i}\hat{O}\frac{\chi}{2}}\right\} \\ &= \sum_\ell \mathrm{Tr}\left\{e^{+\mathrm{i}\hat{O}\frac{\chi}{2}}\boldsymbol{U}(t)e^{-\mathrm{i}\hat{O}\frac{\chi}{2}}\rho_S^0\otimes\rho_B^{(\ell)}e^{-\mathrm{i}\hat{O}\frac{\chi}{2}}\boldsymbol{U}^\dagger(t)e^{+\mathrm{i}\hat{O}\frac{\chi}{2}}\right\} \\ &= \mathrm{Tr}\left\{\boldsymbol{U}_{+\frac{\chi}{2}}(t)\rho_0\otimes\left(\sum_\ell\bar{\rho}_B^{(\ell)}\right)\boldsymbol{U}^\dagger_{-\frac{\chi}{2}}(t)\right\} = \mathrm{Tr}\left\{\boldsymbol{U}_{+\frac{\chi}{2}}(t)\rho_0\otimes\bar{\rho}_B\boldsymbol{U}^\dagger_{-\frac{\chi}{2}}(t)\right\} \end{aligned} \tag{4.103}$$

Here, we have used that O_ℓ is just a number (first line) and also that $e^{\mathrm{i}(\hat{O}-O_\ell)\chi/2}\bar{\rho}_B^{(\ell)}e^{\mathrm{i}(\hat{O}-O_\ell)\chi/2} = \bar{\rho}_B^{(\ell)}$ by construction, cf. Eq. (4.101). Instead of the usual bath density matrix, we have now used its averaged initial value after the projection $\bar{\rho}_B = \sum_\ell |\ell\rangle\langle\ell|\,\bar{\rho}_B\,|\ell\rangle\langle\ell|$. Depending on measurement and initial state, this may or may not have any effect on the statistics. Eventually, this defines a generalized time evolution operator

$$\boldsymbol{U}_{+\frac{\chi}{2}}(t) = e^{+\mathrm{i}\hat{O}\frac{\chi}{2}}\boldsymbol{U}(t)e^{-\mathrm{i}\hat{O}\frac{\chi}{2}}\,. \tag{4.104}$$

This obeys the same initial condition as the normal time evolution operator, and from $\dot{\boldsymbol{U}}(t) = -\mathrm{i}\boldsymbol{H_I}(t)\boldsymbol{U}(t)$ we can conclude that

$$\dot{\boldsymbol{U}}_{+\frac{\chi}{2}}(t) = -\mathrm{i}e^{+\mathrm{i}\hat{O}\frac{\chi}{2}}\boldsymbol{H_I}(t)e^{-\mathrm{i}\hat{O}\frac{\chi}{2}}\boldsymbol{U}_{+\frac{\chi}{2}}(t) = -\mathrm{i}\boldsymbol{H_I}\left(\frac{\chi}{2},t\right)\boldsymbol{U}_{+\frac{\chi}{2}}(t)\,. \tag{4.105}$$

This defines a generalized interaction Hamiltonian

$$\boldsymbol{H_I}\left(\frac{\chi}{2},t\right) = e^{+\mathrm{i}\hat{O}\frac{\chi}{2}}\boldsymbol{H_I}(t)e^{-\mathrm{i}\hat{O}\frac{\chi}{2}} = \sum_\alpha \boldsymbol{A_\alpha}(t)\otimes e^{+\mathrm{i}\hat{O}\frac{\chi}{2}}\boldsymbol{B_\alpha}(t)e^{-\mathrm{i}\hat{O}\frac{\chi}{2}}\,, \tag{4.106}$$

and with an analogous calculation, we obtain

$$\dot{\boldsymbol{U}}^\dagger_{-\frac{\chi}{2}} = +\mathrm{i}\boldsymbol{U}^\dagger_{-\frac{\chi}{2}}\boldsymbol{H_I}\left(\frac{-\chi}{2},t\right)\,. \tag{4.107}$$

In Eqns. (2.78) and (2.79) this then simply implies

$$\begin{aligned} \boldsymbol{U}_{+\frac{\chi}{2}}(t) &= \mathbf{1} - \mathrm{i}\int_0^t \boldsymbol{\mathcal{H}_I}\left(+\frac{\chi}{2},t_1\right)dt_1 - \int_0^t dt_1dt_2\boldsymbol{\mathcal{H}_I}\left(+\frac{\chi}{2},t_1\right)\boldsymbol{\mathcal{H}_I}\left(+\frac{\chi}{2},t_2\right)\Theta(t_1-t_2) + \dots\,, \\ \boldsymbol{U}^\dagger_{-\frac{\chi}{2}}(t) &= \mathbf{1} + \mathrm{i}\int_0^t \boldsymbol{\mathcal{H}_I}\left(-\frac{\chi}{2},t_1\right)dt_1 - \int_0^t dt_1dt_2\boldsymbol{\mathcal{H}_I}\left(-\frac{\chi}{2},t_1\right)\boldsymbol{\mathcal{H}_I}\left(-\frac{\chi}{2},t_2\right)\Theta(t_2-t_1) + \end{aligned} \tag{4.108}$$

Based on this evolution, we can now follow e.g. the coarse-graining derivation of a master equation with using only minor modifications. Using the same assumptions as in Sec. 2.2.3 (vanishing of first order, initially factorizing state) we get

$$\begin{aligned} t\mathcal{L}_t\rho_S^0 &= +\int_0^t dt_1 dt_2 \mathrm{Tr_B}\left\{\boldsymbol{\mathcal{H}_I}\left(+\frac{\chi}{2},t_2\right)\rho_S^0\otimes\bar{\bar{\rho}}_B\boldsymbol{\mathcal{H}_I}\left(-\frac{\chi}{2},t_1\right)\right\} \\ &\quad -\int_0^t dt_1 dt_2\Theta(t_1-t_2)\mathrm{Tr_B}\left\{\boldsymbol{\mathcal{H}_I}\left(+\frac{\chi}{2},t_1\right)\boldsymbol{\mathcal{H}_I}\left(+\frac{\chi}{2},t_2\right)\rho_S^0\otimes\bar{\bar{\rho}}_B\right\} \\ &\quad -\int_0^t dt_1 dt_2\Theta(t_2-t_1)\mathrm{Tr_B}\left\{\rho_S^0\otimes\bar{\bar{\rho}}_B\boldsymbol{\mathcal{H}_I}\left(-\frac{\chi}{2},t_1\right)\boldsymbol{\mathcal{H}_I}\left(-\frac{\chi}{2},t_1\right)\right\} \\ &= \sum_{\alpha\beta}\int_0^t dt_1 dt_2\Big[C^\chi_{\alpha\beta}(t_1,t_2)\boldsymbol{A_\beta}(t_2)\rho_S^0\boldsymbol{A_\alpha}(t_1) \\ &\quad -C^0_{\alpha\beta}(t_1,t_2)\Theta(t_1-t_2)\boldsymbol{A_\alpha}(t_1)\boldsymbol{A_\beta}(t_2)\rho_S^0 - C^0_{\alpha\beta}(t_1,t_2)\Theta(t_2-t_1)\rho_S^0\boldsymbol{A_\alpha}(t_1)\boldsymbol{A_\beta}(t_2)\Big]. \end{aligned} \tag{4.109}$$

In the last line, we have used that e.g. $\mathrm{Tr_B}\left\{e^{+\mathrm{i}\hat{O}\chi}\boldsymbol{B_\alpha}(t_1)e^{-\mathrm{i}\hat{O}\chi}e^{+\mathrm{i}\hat{O}\chi}\boldsymbol{B_\alpha}(t_2)e^{-\mathrm{i}\hat{O}\chi}\bar{\bar{\rho}}_B\right\} = C^0_{\alpha\beta}(t_1,t_2)$. Furthermore, we defined the generalized correlation function.

Def. 14 (Generalized Correlation Function)**.** *The generalized reservoir correlation function is defined as*

$$C^\chi_{\alpha\beta}(t_1,t_2) = \mathrm{Tr}\left\{e^{-\mathrm{i}\hat{O}\frac{\chi}{2}}\boldsymbol{B_\alpha}(t_1)e^{+\mathrm{i}\hat{O}\frac{\chi}{2}}e^{+\mathrm{i}\hat{O}\frac{\chi}{2}}\boldsymbol{B_\beta}(t_2)e^{-\mathrm{i}\hat{O}\frac{\chi}{2}}\bar{\bar{\rho}}_B\right\}. \tag{4.110}$$

If in addition $[H_B,\bar{\bar{\rho}}_B]=0$*, this simplifies with* $\tau = t_1 - t_2$

$$C^\chi_{\alpha\beta}(\tau) = \mathrm{Tr}\left\{e^{-\mathrm{i}\hat{O}\chi}\boldsymbol{B_\alpha}(\tau)e^{+\mathrm{i}\hat{O}\chi}B_\beta\bar{\bar{\rho}}_B\right\} \tag{4.111}$$

This definition can be used to complete the coarse-graining master equation to the counting-field dependent case

Def. 15 (Generalized CG Master Equation)**.** *An interaction Hamiltonian of the form* $\mathcal{H}_\mathrm{I} = \sum_\alpha A_\alpha\otimes B_\alpha$ *with reservoir observable* $\hat{O}$ *leads in the interaction picture to the generalized master equation*

$$\begin{aligned} \dot{\boldsymbol{\rho}}_\mathbf{S} &= -\mathrm{i}\left[\frac{1}{2\mathrm{i}\tau}\int_0^\tau dt_1\int_0^\tau dt_2\sum_{\alpha\beta}C^0_{\alpha\beta}(t_1,t_2)\mathrm{sgn}(\mathrm{t}_1-\mathrm{t}_2)\boldsymbol{A_\alpha}(\mathrm{t}_1)\boldsymbol{A_\beta}(\mathrm{t}_2),\boldsymbol{\rho_S}\right] \\ &\quad +\frac{1}{\tau}\int_0^\tau dt_1\int_0^\tau dt_2\sum_{\alpha\beta}\left[C^\chi_{\alpha\beta}(t_1,t_2)\boldsymbol{A_\beta}(t_2)\boldsymbol{\rho_S}\boldsymbol{A_\alpha}(t_1) - \frac{C^0_{\alpha\beta}(t_1,t_2)}{2}\left\{\boldsymbol{A_\alpha}(t_1)\boldsymbol{A_\beta}(t_2),\boldsymbol{\rho_S}\right\}\right]. \end{aligned} \tag{4.112}$$

As with the virtual detectors, we see that the counting-field dependence only affects the terms with the density matrix in the middle.

4.4.1 Example: SRL energy current

Let us consider the energy current entering the single resonant level (SRL). The Hamiltonian reads (we implicitly use the mapping to tensor products)

$$H = \epsilon d^\dagger d + d \otimes \sum_k h_k c_k^\dagger + d^\dagger \otimes \sum_k h_k^* c_k + \sum_k \epsilon_k c_k^\dagger c_k \,. \tag{4.113}$$

We define $B_1 = \sum_k h_k c_k^\dagger$ and $B_2 = B_1^\dagger$. If we are interested in the energy entering the reservoir, the observable obviously commutes with the reservoir density matrix, when this is held at a Gibbs state. Furthermore, since the bath density matrix is already diagonal in the measurement basis, we have $\bar{\bar{\rho}}_B = \bar{\rho}_B$. The generalized correlation functions then become

$$\begin{aligned} C_{12}^\chi(\tau) &= \frac{1}{2\pi}\int \Gamma(\omega) f(\omega) e^{-\mathrm{i}\omega\chi} e^{+\mathrm{i}\omega\tau} d\omega = \frac{1}{2\pi}\int \Gamma(-\omega) f(-\omega) e^{+\mathrm{i}\omega\chi} e^{-\mathrm{i}\omega\tau}\,, \\ C_{21}^\chi(\tau) &= \frac{1}{2\pi}\int \Gamma(\omega)[1-f(\omega)] e^{+\mathrm{i}\omega\chi} e^{-\mathrm{i}\omega\tau}\,. \end{aligned} \tag{4.114}$$

From this, we can read off the Fourier transforms of the correlation functions

$$\gamma_{12}^\chi(\omega) = \Gamma(-\omega) f(-\omega) e^{+\mathrm{i}\omega\chi}\,, \qquad \gamma_{21}^\chi(\omega) = \Gamma(+\omega)[1-f(+\omega)] e^{+\mathrm{i}\omega\chi}\,. \tag{4.115}$$

When we want to evaluate the rate equation, we get for the transition rates

$$\gamma_{ab,ab} = \sum_{\alpha\beta} \gamma_{\alpha\beta}(E_b - E_a) \langle a| A_\beta |b\rangle \langle a| A_\alpha^\dagger |b\rangle^*\,, \tag{4.116}$$

which in our case become dependent on the counting field

$$\gamma_{01,01}^\chi = \gamma_{21}^\chi(+\epsilon) = \Gamma(\epsilon)[1-f(\epsilon)] e^{+\mathrm{i}\epsilon\chi}\,, \qquad \gamma_{10,10}^\chi = \gamma_{12}^\chi(-\epsilon) = \Gamma(\epsilon) f(\epsilon) e^{-\mathrm{i}\epsilon\chi}\,, \tag{4.117}$$

and our generalized rate matrix becomes

$$\mathcal{L}(\chi) = \Gamma(\epsilon) \begin{pmatrix} -f(\epsilon) & +[1-f(\epsilon)] e^{+\mathrm{i}\epsilon\chi} \\ +f(\epsilon) e^{-\mathrm{i}\epsilon\chi} & -[1-f(\epsilon)] \end{pmatrix}. \tag{4.118}$$

These are precisely the differences we would have guessed from a rate equation representation. The sign convention here has been chosen such that currents count positively when they enter the reservoir. Note however, that there exist examples where a microscopic derivation is required to obtain a consistent treatment, see below.

4.4.2 Example: pure dephasing model

We revisit the pure dephasing model

$$H = \Omega\sigma^z + \sigma^z \otimes \sum_k \left(h_k b_k + h_k^* b_k^\dagger \right) + \sum_k \omega_k b_k^\dagger b_k \tag{4.119}$$

and consider the total energy radiated into the reservoir, such that $\hat{O} = \sum_k \omega_k b_k^\dagger b_k$. Again we have $\bar{\bar{\rho}}_B = \bar{\rho}_B$, and the additional benefit is now that we can get away with a single correlation function

$$\begin{aligned} C^\chi(\tau) &= \mathrm{Tr}_\mathrm{B}\left\{ e^{-\mathrm{i}H_B\chi} \sum_k \left(h_k b_k e^{-\mathrm{i}\omega_k\tau} + h_k^* b_k^\dagger e^{+\mathrm{i}\omega_k\tau} \right) e^{+\mathrm{i}H_B\chi} \sum_q \left(h_q b_q + h_q^* b_q^\dagger \right) \bar{\rho}_B \right\} \\ &= \sum_k |h_k|^2 \left[e^{+\mathrm{i}\omega_k\chi} e^{-\mathrm{i}\omega_k\tau} [1 + n_B(\omega_k)] + e^{-\mathrm{i}\omega_k\chi} e^{+\mathrm{i}\omega_k\tau} n_B(\omega_k) \right] \\ &= \frac{1}{2\pi} \int_0^\infty \Gamma(\omega) \left[e^{+\mathrm{i}\omega\chi} e^{-\mathrm{i}\omega\tau} [1 + n_B(\omega)] + e^{-\mathrm{i}\omega\chi} e^{+\mathrm{i}\omega\tau} n_B(\omega) \right] d\omega \\ &= \frac{1}{2\pi} \int d\omega e^{-\mathrm{i}\omega\tau} \left[\Theta(\omega)\Gamma(\omega)[1 + n_B(\omega)] e^{+\mathrm{i}\omega\chi} + \Theta(-\omega)\Gamma(-\omega) n_B(-\omega) e^{+\mathrm{i}\omega\chi} \right] . \end{aligned} \tag{4.120}$$

With $\sigma_z^2 = \mathbf{1}$ we can again ignore the Lamb-shift contribution, and the coarse-graining master equation (4.112) becomes

$$\begin{aligned} \dot{\boldsymbol{\rho}} &= \frac{1}{2\pi\tau} \int_0^\tau dt_1 \int_0^\tau dt_2 \int d\omega \Theta(\omega)\Gamma(\omega)[1 + n_B(\omega)] e^{-\mathrm{i}\omega(t_1 - t_2)} \left[e^{+\mathrm{i}\omega\chi} \sigma^z \boldsymbol{\rho} \sigma^z - \boldsymbol{\rho} \right] \\ &\quad + \frac{1}{2\pi\tau} \int_0^\tau dt_1 \int_0^\tau dt_2 \int d\omega \Theta(-\omega)\Gamma(-\omega) n_B(-\omega) e^{-\mathrm{i}\omega(t_1 - t_2)} \left[e^{+\mathrm{i}\omega\chi} \sigma^z \boldsymbol{\rho} \sigma^z - \boldsymbol{\rho} \right] . \end{aligned} \tag{4.121}$$

We can also write this as

$$\begin{aligned} \dot{\boldsymbol{\rho}} &= [\gamma_-(\chi,\tau)\sigma^z \boldsymbol{\rho} \sigma^z - \gamma_-(0,\tau)\boldsymbol{\rho}] + [\gamma_+(\chi,\tau)\sigma^z \boldsymbol{\rho} \sigma^z - \gamma_+(0,\tau)\boldsymbol{\rho}] , \\ \gamma_+(\chi,\tau) &= \int \Theta(\omega)\Gamma(\omega)[1 + n_B(\omega)] e^{+\mathrm{i}\omega\chi} \frac{\tau}{2\pi} \mathrm{sinc}^2\left[\frac{\omega\tau}{2} \right] d\omega , \\ \gamma_-(\chi,\tau) &= \int \Theta(-\omega)\Gamma(-\omega) n_B(-\omega) e^{+\mathrm{i}\omega\chi} \frac{\tau}{2\pi} \mathrm{sinc}^2\left[\frac{\omega\tau}{2} \right] d\omega . \end{aligned} \tag{4.122}$$

As before with the particle counting in Eq. (4.79), this Liouvillian is diagonal

$$\begin{aligned} \dot{\boldsymbol{\rho}}_{\mathbf{00}} &= [\gamma_-(\chi,\tau) - \gamma_-(0,\tau) + \gamma_+(\chi,\tau) - \gamma_+(0,\tau)] \boldsymbol{\rho}_{\mathbf{00}} , \\ \dot{\boldsymbol{\rho}}_{\mathbf{11}} &= [\gamma_-(\chi,\tau) - \gamma_-(0,\tau) + \gamma_+(\chi,\tau) - \gamma_+(0,\tau)] \boldsymbol{\rho}_{\mathbf{11}} , \\ \dot{\boldsymbol{\rho}}_{\mathbf{01}} &= -[\gamma_-(\chi,\tau) + \gamma_-(0,\tau) + \gamma_+(\chi,\tau) + \gamma_+(0,\tau)] \boldsymbol{\rho}_{\mathbf{01}} , \\ \dot{\boldsymbol{\rho}}_{\mathbf{00}} &= -[\gamma_-(\chi,\tau) + \gamma_-(0,\tau) + \gamma_+(\chi,\tau) + \gamma_+(0,\tau)] \boldsymbol{\rho}_{\mathbf{10}} , \end{aligned} \tag{4.123}$$

and the cumulant-generating function becomes $\mathcal{C}(\chi,\tau) = [\gamma_-(\chi,\tau) - \gamma_-(0,\tau) + \gamma_+(\chi,\tau) - \gamma_+(0,\tau)]\tau$. When setting the counting field to zero, we also recover Eq. (2.113). The mean energy for example becomes

$$\begin{aligned} E(\tau) &= \int \Theta(\omega)\omega\Gamma(\omega)[1 + n_B(\omega)] \frac{\tau^2}{2\pi} \mathrm{sinc}^2\left(\frac{\omega\tau}{2} \right) d\omega + \int \Theta(-\omega)\omega\Gamma(-\omega) n_B(-\omega) \frac{\tau^2}{2\pi} \mathrm{sinc}^2\left(\frac{\omega\tau}{2} \right) d\omega \\ &= \int_0^\infty \omega\Gamma(\omega) \frac{\tau^2}{2\pi} \mathrm{sinc}^2\left(\frac{\omega\tau}{2} \right) d\omega = \frac{2}{\pi} \int_0^\infty \frac{\Gamma(\omega)}{\omega} \sin^2\left(\frac{\omega\tau}{2} \right) d\omega . \end{aligned} \tag{4.124}$$

To obtain the exact solution for the radiated energy, we can use the same approach as in Eq. (4.84), i.e., the exact Heisenberg picture dynamics. Then, the expectation value of the reservoir

energy becomes

$$\begin{aligned}\langle E\rangle_t &= \sum_k \omega_k \mathrm{Tr}\left\{\left(e^{+\mathrm{i}\omega_k t}b_k^\dagger + \frac{h_k}{\omega_k}\left(e^{+\mathrm{i}\omega_k t}-1\right)\sigma^z\right)\left(e^{-\mathrm{i}\omega_k t}b_k + \frac{h_k^*}{\omega_k}\left(e^{-\mathrm{i}\omega_k t}-1\right)\sigma^z\right)\rho_S^0\otimes\rho_B^0\right\} \\ &= \langle E\rangle_0 + \sum_k \frac{|h_k|^2}{\omega_k}[2-2\cos(\omega_k t)] = \langle E\rangle_0 + \frac{2}{\pi}\int_0^\infty \frac{\Gamma(\omega)}{\omega}\sin^2\left(\frac{\omega t}{2}\right)d\omega\,, \end{aligned} \tag{4.125}$$

and we see that the difference agrees exactly with our previously computed mean value for coarse-graining, derived using energy counting fields

Exercise 39 (Energetic noise)**.** *Show that also for the second cumulant of the radiated energy the results from the generalized coarse-graining master equation and the exact solution agree*

$$\left\langle\left\langle E^2\right\rangle\right\rangle = \frac{2}{\pi}\int_0^\infty \Gamma(\omega)[1+2n_B(\omega)]\sin^2\left(\frac{\omega t}{2}\right)d\omega\,. \tag{4.126}$$

4.5 Symmetries

4.5.1 Mathematical Motivation

The probability distribution $P_n(t)$ is given by the inverse Fourier transform of the moment-generating function

$$P_n(t) = \frac{1}{2\pi}\int_{-\pi}^{+\pi}\mathcal{M}(\chi,t)e^{-\mathrm{i}n\chi}d\chi = \frac{1}{2\pi}\int_{-\pi}^{+\pi}e^{\mathcal{C}(\chi,t)-\mathrm{i}n\chi}d\chi\,. \tag{4.127}$$

Accordingly, a symmetry in the cumulant-generating function (or moment-generating function) of the form

$$\mathcal{C}(-\chi,t) = \mathcal{C}(+\chi+\mathrm{i}\alpha,t) \tag{4.128}$$

leads to a symmetry of the probabilities

$$\begin{aligned}\frac{P_{+n}(t)}{P_{-n}(t)} &= \frac{\frac{1}{2\pi}\int_{-\pi}^{+\pi}e^{\mathcal{C}(\chi,t)-\mathrm{i}n\chi}d\chi}{\frac{1}{2\pi}\int_{-\pi}^{+\pi}e^{\mathcal{C}(\chi,t)+\mathrm{i}n\chi}d\chi} = \frac{\int_{-\pi}^{+\pi}e^{\mathcal{C}(\chi,t)-\mathrm{i}n\chi}d\chi}{\int_{-\pi}^{+\pi}e^{\mathcal{C}(-\chi,t)-\mathrm{i}n\chi}d\chi} \\ &= \frac{\int_{-\pi}^{+\pi}e^{\mathcal{C}(\chi,t)-\mathrm{i}n\chi}d\chi}{\int_{-\pi}^{+\pi}e^{\mathcal{C}(\chi+\mathrm{i}\alpha,t)-\mathrm{i}n\chi}d\chi} = \frac{\int_{-\pi}^{+\pi}e^{\mathcal{C}(\chi,t)-\mathrm{i}n\chi}d\chi}{\int_{-\pi+\mathrm{i}\alpha}^{+\pi+\mathrm{i}\alpha}e^{\mathcal{C}(\chi,t)-\mathrm{i}n[\chi-\mathrm{i}\alpha]}d\chi} \\ &= \frac{\int_{-\pi}^{+\pi}e^{\mathcal{C}(\chi,t)-\mathrm{i}n\chi}d\chi}{e^{-n\alpha}\int_{-\pi}^{+\pi}e^{\mathcal{C}(\chi,t)-\mathrm{i}n\chi}d\chi} \\ &= e^{+n\alpha}\,, \end{aligned} \tag{4.129}$$

where we have used in the last step that the counting field always enters as a function of $e^{\pm\mathrm{i}\chi}$. This automatically implies that $\mathcal{C}(-\pi+\mathrm{i}\sigma,t) = \mathcal{C}(+\pi+\mathrm{i}\sigma,t)$ for all real numbers σ, such that

we can add two further integration paths from $-\pi$ to $-\pi + \mathrm{i}\alpha$ and from $+\pi + \mathrm{i}\alpha$ to $+\pi$ to the integral in the denominator. The value of the cumulant-generating function along these paths is the same, such that due to the different integral orientation there is no net change. Finally, using analyticity of the integrand, we deform the integration contour in the denominator, leaving two identical integrals in numerator and denominator. Note that the system may be very far from thermodynamic equilibrium but still obey a symmetry of the form (4.128), which leads to a fluctuation theorem of the form (4.129) being valid far from equilibrium.

As example, we consider the SET. The characteristic polynomial $\mathcal{D}(\chi) = |\mathcal{L}(\chi) - \lambda \mathbf{1}|$ of the Liouvillian (4.25) and therefore also all eigenvalues obeys the symmetry

$$\mathcal{D}(-\chi) = \mathcal{D}\left(+\chi + \mathrm{i}\ln\left[\frac{f_L(1-f_R)}{(1-f_L)f_R}\right]\right) = \mathcal{D}\left(\chi + \mathrm{i}\left[(\beta_R - \beta_L)\,\epsilon + \beta_L\mu_L - \beta_R\mu_R\right]\right). \tag{4.130}$$

Exercise 40 (Eigenvalue Symmetry)**.** *(1 points)*
Compute the characteristic polynomial of the Liouvillian (4.25) and confirm the symmetry (4.130).

which leads to the fluctuation theorem

$$\lim_{t\to\infty} \frac{P_{+n}(t)}{P_{-n}(t)} = e^{n[(\beta_R-\beta_L)\epsilon + \beta_L\mu_L - \beta_R\mu_R]}. \tag{4.131}$$

We note that the exponent does not depend on the microscopic details of the model (Γ_α) but only on thermodynamic quantities. Indeed, we had computed the entropy production rate for this model before

$$\dot{S}_\mathrm{i} = \left[(\beta_R - \beta_L)\,\epsilon + \beta_L\mu_L - \beta_R\mu_R\right], \tag{4.132}$$

such that in the exponent, we simply have the integrated entropy production.

We would obtain the same result for a DQD coupled to two terminals. For equal temperatures, this becomes

$$\lim_{t\to\infty} \frac{P_{+n}(t)}{P_{-n}(t)} = e^{n\beta V}, \tag{4.133}$$

which directly demonstrates that the average current

$$I = \frac{d}{dt}\langle n(t)\rangle = \frac{d}{dt}\sum_{n=-\infty}^{+\infty} nP_n(t) = \sum_{n=1}^{\infty} n\left[P_{+n}(t) - P_{-n}(t)\right] = \sum_{n=1}^{\infty} nP_n(t)\left[1 - e^{-n\beta V}\right] \tag{4.134}$$

always follows the voltage. We can interpret the exponent in Eq. (4.131) in terms of the entropy that has been produced: The quantity $n\epsilon$ describes the energy that has traversed the SET for large times, and consequently, the term in the exponent approximates the entropy production, which is for large times simply proportional to the number of particles that have travelled from left to right

$$\Delta S_\mathrm{i} \approx (\beta_R - \beta_L)\, n\epsilon + (\beta_L\mu_L - \beta_R\mu_R)\, n. \tag{4.135}$$

Therefore, we can interpret the fluctuation theorem also as a stochastic manifestation of the second law

$$\frac{P(+\Delta S_\mathrm{i})}{P(-\Delta S_\mathrm{i})} = e^{+\Delta S_\mathrm{i}}. \tag{4.136}$$

Here, trajectories with a negative entropy production $\Delta S_{\rm i}$ are not forbidden. They are just less likely to occur than their positive-production counterparts, such that – on average – the second law is always obeyed.

The SET has the property of **tight coupling** between enery and matter currents: Every electron carries the same energy. For more general systems, where this property is not present, one still obtains a fluctuation theorem for the entropy production. Then, the combined counting statistics of energy and matter currents is necessary to obtain it. Furthermore, one will for an n-terminal system need $2n$ counting fields to quantify the entropy production. In the long-term limit, one can use conservation laws, such that the maximum number of counting fields is given by $2n-2$, which can be further reduced when one has further symmetries (like tight-coupling).

4.5.2 Microscopic discussion for multiple counting fields

In general, we can decide to count matter and energy exchanges with all N junctions of our model. Then, our Liouvillian depends on counting fields for both matter and energy at all these junctions $\mathcal{L} \to \mathcal{L}(\boldsymbol{\chi}, \boldsymbol{\xi})$, where $\boldsymbol{\chi} = (\chi_1, \ldots, \chi_N)$ denotes the matter and $\boldsymbol{\xi} = (\xi_1, \ldots, \xi_N)$ the energy counting fields. Let us further assume that our model leads to an additive rate equation

$$\dot{P}_a = \sum_\nu \sum_{b\neq a} \gamma_{ab}^{(\nu)} e^{+\mathrm{i}(N_a - N_b)\chi_\nu} e^{+\mathrm{i}(E_a - E_b)\xi_\nu} P_b - \sum_\nu \sum_{b\neq a} \gamma_{ba}^{(\nu)} P_a \,. \tag{4.137}$$

Here, γ_{ab} denotes the rate from b to a and E_a and N_a denote the corresponding energies and particle numbers. We have inserted the particle counting field χ_ν and energy counting field ξ_ν for exchanges with reservoir ν adopting the convention that contributions entering the system are counted positively. The rates obey the detailed balance property (2.60)

$$\frac{\gamma_{ab}^{(\nu)}}{\gamma_{ba}^{(\nu)}} = e^{\beta_\nu[(E_b - E_a) - \mu_\nu(N_b - N_a)]} \,. \tag{4.138}$$

Writing this in matrix notation

$$\dot{\boldsymbol{P}} = \mathcal{W}(\boldsymbol{\chi}, \boldsymbol{\xi}) \boldsymbol{P} \,, \tag{4.139}$$

we note that the counting fields would only enter the off-diagonal entries due to our assumptions. Then, we can show the following symmetry relation

$$\mathcal{W}^T(-\boldsymbol{\chi} - \mathrm{i}\boldsymbol{A}, -\boldsymbol{\xi} - \mathrm{i}\boldsymbol{B}) = \mathcal{W}(\boldsymbol{\chi}, \boldsymbol{\xi}) \,, \; \boldsymbol{B} = (\beta_1, \ldots, \beta_N)^T \;, \; \boldsymbol{A} = -(\mu_1\beta_1, \ldots, \mu_N\beta_N)^T \;, \tag{4.140}$$

where T denotes the transpose. In components, this means (we do assume $a \neq b$)

$$\begin{aligned} \gamma_{ba}^{(\nu)} e^{+\mathrm{i}(-\chi_\nu - \mathrm{i}A_\nu)(N_b - N_a)} e^{+\mathrm{i}(-\xi_\nu - \mathrm{i}B_\nu)(E_b - E_a)} &= \gamma_{ab}^{(\nu)} e^{+\beta_\nu(E_a - E_b)} e^{-\beta_\nu\mu_\nu(N_a - N_b)} \times \\ &\quad \times e^{-\mathrm{i}(-\chi_\nu - \mathrm{i}A_\nu)(N_a - N_b)} e^{-\mathrm{i}(-\xi_\nu - \mathrm{i}B_\nu)(E_a - E_b)} \\ &\overset{!}{=} \gamma_{ab,ab}^{(\nu)} e^{+\mathrm{i}\chi_\nu(N_a - N_b)} e^{+\mathrm{i}\xi_\nu(E_a - E_b)} \,. \end{aligned} \tag{4.141}$$

In the first equality sign, we have inserted the local detailed balance relation specific to reservoir ν. Now, solving for the coefficients we see that this is fulfilled when $A_\nu = -\mu_\nu\beta_\nu$ and $B_\nu = \beta_\nu$, proving our relation (4.140).

This symmetry transfers to the long-term cumulant-generating function. The eigenvalues $\lambda_\alpha(\boldsymbol{\chi},\boldsymbol{\xi})$ of the rate matrix solve the characteristic polynomial at all $\boldsymbol{\chi}$ and $\boldsymbol{\xi}$

$$|\mathcal{W}(\boldsymbol{\chi},\boldsymbol{\xi}) - \lambda_\alpha(\boldsymbol{\chi},\boldsymbol{\xi})| = 0\,. \tag{4.142}$$

Evaluating this at shifted values we see that

$$\begin{aligned} &|\mathcal{W}(-\boldsymbol{\chi} - \mathrm{i}\boldsymbol{A}, -\boldsymbol{\xi} - \mathrm{i}\boldsymbol{B}) - \lambda_\alpha(-\boldsymbol{\chi} - \mathrm{i}\boldsymbol{A}, -\boldsymbol{\xi} - \mathrm{i}\boldsymbol{B})\cdot\mathbf{1}| \\ &= \left|\mathcal{W}^T(-\boldsymbol{\chi} - \mathrm{i}\boldsymbol{A}, -\boldsymbol{\xi} - \mathrm{i}\boldsymbol{B}) - \lambda_\alpha(-\boldsymbol{\chi} - \mathrm{i}\boldsymbol{A}, -\boldsymbol{\xi} - \mathrm{i}\boldsymbol{B})\cdot\mathbf{1}\right| \\ &= |\mathcal{W}(\boldsymbol{\chi},\boldsymbol{\xi}) - \lambda_\alpha(-\boldsymbol{\chi} - \mathrm{i}\boldsymbol{A}, -\boldsymbol{\xi} - \mathrm{i}\boldsymbol{B})\cdot\mathbf{1}|\,, \end{aligned} \tag{4.143}$$

where we have used that the eigenvalues do not change under transposition for an arbitrary quadratic matrix. Therefore, the eigenvalues and in particular the long-term cumulant-generating function inherit this symmetry

$$\lim_{t\to\infty} C(-\boldsymbol{\chi} - \mathrm{i}\boldsymbol{A}, -\boldsymbol{\xi} - \mathrm{i}\boldsymbol{B}, t) = \lim_{t\to\infty} C(\boldsymbol{\chi},\boldsymbol{\xi},t)\,. \tag{4.144}$$

Before, we have learned for the example that a symmetry relation of the form $C(-\chi - \mathrm{i}\alpha, t) = C(+\chi, t)$ implies a fluctuation theorem of the form $P_{+n}(t)/P_{-n}(t) = e^{-n\alpha}$. Now, applying this to $2N$ dimensions, we conclude

$$\lim_{t\to\infty} \frac{P_{+\boldsymbol{\Delta N},+\boldsymbol{\Delta E}}(t)}{P_{-\boldsymbol{\Delta N},-\boldsymbol{\Delta E}}(t)} = e^{-(\boldsymbol{\Delta E}\cdot\boldsymbol{B} + \boldsymbol{\Delta N}\cdot\boldsymbol{A})} = e^{-\sum_\nu \beta_\nu[\Delta E_\nu - \mu_\nu \Delta N_\nu]}\,. \tag{4.145}$$

In the exponent, we recognize the integrated entropy change of the reservoirs, which in the long-term limit becomes the entropy production. Therefore, the interpretation of the above formula is as follows: Each trajectory with an exchange of $\boldsymbol{\Delta N}$ particles and an energy of $\boldsymbol{\Delta E}$ is associated with an entropy production of $\Delta_{\mathrm{i}} S = -\sum_\nu \beta_\nu\,[\Delta E_\nu - \mu_\nu \Delta N_\nu]$. Then, the fluctuation theorem corresponds to a stochastic formulation of the second law

Def. 16 (Crooks fluctuation theorem)**.** *A stochastic formulation of the second law is given by Crooks fluctuation theorem*

$$\frac{P_{+\Delta_{\mathrm{i}} S}}{P_{-\Delta_{\mathrm{i}} S}} = e^{+\Delta_{\mathrm{i}} S}\,, \tag{4.146}$$

where $\Delta_{\mathrm{i}} S$ is the total entropy production.

The Crooks relation [11] is more quantitative than the average statement of the second law discussed before.

4.5.3 Symmetries in the coarse-graining master equation

Assume that we are given a generalized coarse-graining master equation as in Def. 15.

$$\begin{aligned} \dot{\boldsymbol{\rho}}_{\mathbf{S}} \;=\; & -\mathrm{i}\left[\frac{1}{2\mathrm{i}\tau}\int_0^\tau dt_1 \int_0^\tau dt_2 \sum_{\alpha\beta} C^0_{\alpha\beta}(t_1,t_2)\mathrm{sgn}(\mathrm{t}_1 - \mathrm{t}_2)\boldsymbol{A}_{\boldsymbol{\alpha}}(\mathrm{t}_1)\boldsymbol{A}_{\boldsymbol{\beta}}(\mathrm{t}_2), \boldsymbol{\rho}_{\mathbf{S}}\right] \\ & + \frac{1}{\tau}\int_0^\tau dt_1 \int_0^\tau dt_2 \sum_{\alpha\beta}\left[C^\xi_{\alpha\beta}(t_1,t_2)\boldsymbol{A}_{\boldsymbol{\beta}}(t_2)\boldsymbol{\rho}_{\mathbf{S}}\boldsymbol{A}_{\boldsymbol{\alpha}}(t_1) - \frac{C^0_{\alpha\beta}(t_1,t_2)}{2}\left\{\boldsymbol{A}_{\boldsymbol{\alpha}}(t_1)\boldsymbol{A}_{\boldsymbol{\beta}}(t_2), \boldsymbol{\rho}_{\mathbf{S}}\right\}\right]. \end{aligned} \tag{4.147}$$

We further assume that the reservoir density matrix commutes with the bath Hamiltonian and that the tracked observable is the energy of the reservoir $\hat{O} = H_B$, such that ξ denotes an energy counting field of the reservoir. This does imply that $\bar{\bar{\rho}}_B = \bar{\rho}_B$, and the generalized correlation function can be written as the conventional correlation function

$$C^{\xi}_{\alpha\beta}(t_1, t_2) = C_{\alpha\beta}(t_1 - t_2 - \xi)\,. \tag{4.148}$$

We can evaluate this equation in the basis where the time-dependent density matrix is diagonal $\rho = \sum_j P_j \left|j\right\rangle \left\langle j\right|$. This basis will for finite τ in general **not** coincide with the system energy eigenbasis. Then, the transition rate from j to i at coarse-graining time τ is only given by the jump term

$$\begin{aligned} R^{\tau}_{ij}(\xi) &= \frac{1}{\tau}\int_0^{\tau} dt_1 \int_0^{\tau} dt_2 \sum_{\alpha\beta} C_{\alpha\beta}(t_1 - t_2 - \xi) \left\langle i\right| \boldsymbol{A_\beta}(t_2) \left|j\right\rangle \left\langle j\right| \boldsymbol{A_\alpha}(t_1) \left|i\right\rangle \\ &= \int d\omega \sum_{\alpha\beta} \gamma_{\alpha\beta}(\omega) e^{+\mathrm{i}\omega\xi} \frac{1}{2\pi\tau} \int_0^{\tau} dt_1 \int_0^{\tau} dt_2 e^{-\mathrm{i}\omega(t_1 - t_2)} \left\langle i\right| \boldsymbol{A_\beta}(t_2) \left|j\right\rangle \left\langle j\right| \boldsymbol{A_\alpha}(t_1) \left|i\right\rangle \\ &= \int R^{\tau}_{ij,+\omega} e^{+\mathrm{i}\omega\xi} d\omega\,. \end{aligned} \tag{4.149}$$

The rate $R^{\tau}_{ij,+\omega}$ describes at coarse-graining time τ the processes fro a system transition from $j \to i$ that go along with a reservoir energy change $+\omega$.

To allow for the description of particle exchange processes, we can generalize this by a particle counting field for the reservoir

$$R^{\tau}_{ij}(\chi, \xi) = \int R^{\tau}_{ij,+\omega} e^{+\mathrm{i}(N_j - N_i)\chi} e^{+\mathrm{i}\omega\xi} d\omega\,. \tag{4.150}$$

Here, we have assumed that the total particle number is conserved, such that a process $j \to i$ in the system must imply the opposite particle change $N_j - N_i$ in the reservoir. This is not a severe restriction, as $\left|j\right\rangle$ still does not need to coincide with the energy eigenbasis of the system. Conservation of the total particle number $[H_I, N_S + N_B] = 0$ implies that the eigenstates of system and reservoir can be grouped in blocks with a defined particle number. For reservoirs with a chemical potential and interactions supporting conservation of the total particle number, we had found before that the KMS relation generalizes, see Eq. (2.59)

$$\sum_{\bar{\alpha}} A_{\bar{\alpha}} C_{\alpha\bar{\alpha}}(\tau) = \sum_{\bar{\alpha}} e^{+\beta\mu N_S} A_{\bar{\alpha}} e^{-\beta\mu N_S} C_{\bar{\alpha}\alpha}(-\tau - \mathrm{i}\beta)\,. \tag{4.151}$$

Simply Fourier-transforming this equation yields

$$\sum_{\bar{\alpha}} A_{\bar{\alpha}} \gamma_{\alpha\bar{\alpha}}(\omega) = \sum_{\bar{\alpha}} e^{+\beta\mu N_S} A_{\bar{\alpha}} e^{-\beta\mu N_S} \gamma_{\bar{\alpha}\alpha}(-\omega) e^{+\beta\omega}\,. \tag{4.152}$$

From this, we can conclude

$$\begin{aligned}
\frac{R^\tau_{ij,+\omega}}{R_{ji,-\omega}} &= \frac{\sum_{\alpha\beta}\gamma_{\alpha\beta}(\omega)\frac{1}{2\pi\tau}\int_0^\tau dt_1\int_0^\tau dt_2 e^{-\mathrm{i}\omega(t_1-t_2)}\langle i|\boldsymbol{A}_{\boldsymbol{\beta}}(t_2)|j\rangle\langle j|\boldsymbol{A}_{\boldsymbol{\alpha}}(t_1)|i\rangle}{\sum_{\alpha\beta}\gamma_{\alpha\beta}(-\omega)\frac{1}{2\pi\tau}\int_0^\tau dt_1\int_0^\tau dt_2 e^{+\mathrm{i}\omega(t_1-t_2)}\langle j|\boldsymbol{A}_{\boldsymbol{\beta}}(t_2)|i\rangle\langle i|\boldsymbol{A}_{\boldsymbol{\alpha}}(t_1)|j\rangle} \\
&= \frac{\sum_{\alpha\beta}\gamma_{\alpha\beta}(\omega)\int_0^\tau dt_1\int_0^\tau dt_2 e^{-\mathrm{i}\omega(t_1-t_2)}\langle i|\boldsymbol{A}_{\boldsymbol{\beta}}(t_2)|j\rangle\langle j|\boldsymbol{A}_{\boldsymbol{\alpha}}(t_1)|i\rangle}{\sum_{\alpha\beta}\gamma_{\beta\alpha}(-\omega)\int_0^\tau dt_1\int_0^\tau dt_2 e^{-\mathrm{i}\omega(t_1-t_2)}\langle j|\boldsymbol{A}_{\boldsymbol{\alpha}}(t_1)|i\rangle\langle i|\boldsymbol{A}_{\boldsymbol{\beta}}(t_2)|j\rangle} \\
&= \frac{\sum_{\alpha\beta}\gamma_{\alpha\beta}(\omega)\int_0^\tau dt_1\int_0^\tau dt_2 e^{-\mathrm{i}\omega(t_1-t_2)}\langle i|\boldsymbol{A}_{\boldsymbol{\beta}}(t_2)|j\rangle\langle j|\boldsymbol{A}_{\boldsymbol{\alpha}}(t_1)|i\rangle}{e^{-\beta\omega}\sum_{\alpha\beta}\gamma_{\alpha\beta}(\omega)\int_0^\tau dt_1\int_0^\tau dt_2 e^{-\mathrm{i}\omega(t_1-t_2)}\langle j|e^{+\beta\mu N_S}\boldsymbol{A}_{\boldsymbol{\alpha}}(t_1)e^{-\beta\mu N_S}|i\rangle\langle i|\boldsymbol{A}_{\boldsymbol{\beta}}(t_2)|j\rangle} \\
&= e^{+\beta[\omega-\mu(N_j-N_i)]}\,. \qquad (4.153)
\end{aligned}$$

We stress again that $N_j - N_i = -(N_i - N_j)$ is the reservoir particle change when the system undergoes the transition $j \to i$. This is similar to our detailed balance relation used before. We can therefore conclude the symmetry relation

$$R^\tau_{ji}(-\chi - \mathrm{i}\beta\mu, -\xi + \mathrm{i}\beta) = R^\tau_{ij}(\chi,\xi)\,, \qquad (4.154)$$

which implies the fluctuation theorem (now for multiple counting fields and multiple reservoirs, assuming an additive decomposition of all rates such that the symmetries prevail)

$$\lim_{t\to\infty}\frac{P_{+\boldsymbol{\Delta N},+\boldsymbol{\Delta E}}}{P_{-\boldsymbol{\Delta N},-\boldsymbol{\Delta E}}} = e^{+\sum_\nu \beta_\nu(\Delta E_\nu - \mu_\nu \Delta N_\nu)}\,. \qquad (4.155)$$

Comparing this to Eq. (4.145), we see that there is a different sign in the exponent. This comes from our different way of counting. Making the fluctuation theorem explicit e.g. for two terminals

$$\lim_{t\to\infty}\frac{P_{+\Delta N_L,+\Delta E_L,+\Delta N_R,+\Delta E_R}}{P_{-\Delta N_L,-\Delta E_L,-\Delta N_R,-\Delta E_R}} = e^{\beta_L(\Delta E_L-\mu_L\Delta N_L)+\beta_R(\Delta E_R-\mu_R\Delta N_R)} \qquad (4.156)$$

we can consider the limit where $\Delta N_L \approx -\Delta N \approx +\Delta N_R$ and $\Delta E_L \approx -\Delta E \approx +\Delta E_R$ to conclude for these trajectories (counting positive when transfers from left to right occur)

$$\frac{P_{+\Delta N,+\Delta E}}{P_{-\Delta N,-\Delta E}} \to e^{(\beta_R-\beta_L)\Delta E+(\beta_L\mu_L-\beta_R\mu_R)\Delta N}\,, \qquad (4.157)$$

which agrees with our previous results.

Chapter 5

Periodically driven systems

In the previous chapters, we have treated mainly undriven systems, and if driving was considered, we assumed it to be so slow that the previous approximations would go through. This resulted in trivial time-dependencies: In the Liouvillian, simply the time-dependent Hamiltonian had to be used. In general, time-dependent systems are notoriously difficult to solve already for closed quantum systems. There are only the treatable cases of an adiabatic evolution (this one also includes Hamiltonians obeying $[H(t_1), H(t_2)] = 0$) and the case of periodic driving, where $H(t + T) = H(t)$ with period T. Here, we will investigate how the master eqution for a periodically driven system Hamiltonian should be derived. Thereby, we will allow for driven system Hamiltonians and driven interactions, but will leave the reservoir time-independent. The latter constraint comes from the fact that we would like to keep the reservoirs at equilibrium states throughout, which would be incompatible with fast driving.

5.1 Floquet treatment of closed systems

For a closed system $\left|\dot{\Psi}\right\rangle = -\mathrm{i}H(t)\left|\Psi\right\rangle$ with periodic $H(t) = H(t + T)$ we can write the time evolution operator $\dot{U} = -\mathrm{i}H(t)U(t)$ from initial time t_1 to final time t always as a product of operators

$$U(t, t_1) = e^{-\mathrm{i}K_{t_0}(t)} e^{-\mathrm{i}\bar{H}_{t_0}\cdot(t-t_1)} e^{+\mathrm{i}K_{t_0}(t_1)}\,, \tag{5.1}$$

where the **kick operator** $K_{t_0}(T)$ inherits the periodicity of the Hamiltonian and vanishes at $K_{t_0}(t_0 + nT) = \mathbf{0}$ for integer n. Note that the kick operator is a function of time, we will try to mark products with a dot. This implies that the stroboscopic evolution between full periods is just given by the **Floquet Hamiltonian** $U(t_0 + nT, t_0) = e^{-\mathrm{i}\bar{H}_{t_0} nT}$. We note that both Floquet Hamiltonian and kick operator depend on the initial time t_0 which should therefore be specified. Furthermore, they are both not uniquely defined, adding integer multiples of $2\pi\mathbf{1}$ does not change the dynamics. Here, we will be interested in $t_0 = 0$ and also take the initial time to be the same $t_1 = 0$. With this choice (and by dropping the indices we conventionally refer to this choice), we have

$$U(t, 0) = U(t) = U_{\mathrm{kick}}(t) e^{-\mathrm{i}\bar{H}t}\,, \tag{5.2}$$

where we have that the kick operator is unitary, periodic $U_{\mathrm{kick}}(t) = U_{\mathrm{kick}}(t + T)$, and vanishes at multiples of the period $U_{\mathrm{kick}}(nT) = \mathbf{1}$. In what follows, we will only need the properties of the

decomposition above, for a more general discussion see Ref. [12]. To illustrate these concepts, we will consider simple examples below.

5.1.1 General properties

From the periodicity of the kick operator we can conclude that the transformation into the Heisenberg picture (which for an open system becomes the interaction picture) can be written in a special form

$$U^\dagger(t)AU(t) = e^{+\mathrm{i}\bar{H}t}U^\dagger_{\mathrm{kick}}(t)\hat{A}U_{\mathrm{kick}}(t)e^{-\mathrm{i}\bar{H}t} = \sum_{n=-\infty}^{+\infty} e^{+\mathrm{i}\bar{H}t}\hat{A}_n e^{\mathrm{i}n\Omega t}e^{-\mathrm{i}\bar{H}t}\,, \tag{5.3}$$

where we have used that $U^\dagger_{\mathrm{kick}}(t)\hat{A}U_{\mathrm{kick}}(t)$ has the periodicity of the original driving and can therefore be expanded in a Fourier series

$$\hat{A}_n = \frac{\Omega}{2\pi}\int_{-T/2}^{+T/2} U^\dagger_{\mathrm{kick}}(t)\hat{A}U_{\mathrm{kick}}(t)e^{-\mathrm{i}n\Omega t}dt\,, \qquad T = \frac{2\pi}{\Omega}\,. \tag{5.4}$$

Inserting the eigenbasis of the Floquet Hamiltonian $\bar{H}\,|a\rangle = E_a\,|a\rangle$, we can further write

$$U^\dagger(t)AU(t) = \sum_{ab}\sum_n \hat{A}^{ab}_n e^{\mathrm{i}(E_a - E_b + n\Omega)t}\,. \tag{5.5}$$

The energy differences $E_a - E_b$ are also called Bohr frequencies of the Floquet Hamiltonian, and the operators in the sum are given by

$$\hat{A}^{ab}_n = |a\rangle\langle a|\,\hat{A}_n\,|b\rangle\langle b|\,. \tag{5.6}$$

5.1.2 Train of δ-kicks

Here, we consider a simple time-dependence of the form

$$H(t) = H_0 + V\sum_{n=0}^{\infty}\delta(t - \frac{2n+1}{2}T)\,, \tag{5.7}$$

with some constant Hamiltonian H_0 and a periodically acting perturbation V, which is ultrastrong and ultrashort acting at $T/2, 3T/2, 5T/2, \ldots$. We have chosen the kick to act in the middle of the observation interval in order to avoid ambiguities. To get the time evolution during a δ-kick, we can integrate

$$U_\delta = \lim_{\epsilon\to 0}\hat{T}\exp\left\{-\mathrm{i}\int_{T/2-\epsilon}^{T/2+\epsilon} H(t')dt'\right\} = \lim_{\epsilon\to 0}\exp\left\{-\mathrm{i}\int_{T/2-\epsilon}^{T/2+\epsilon}\frac{V}{2\epsilon}dt'\right\} = e^{-\mathrm{i}V}\,. \tag{5.8}$$

Here, we have approximated $\delta(x) = \lim_{\epsilon\to 0}\Theta(x+\epsilon)\Theta(\epsilon - x)/(2\epsilon)$, and for small enough ϵ the influence of H_0 can be safely neglected. The time-dependence can therefore be modelled as piecewise-constant, we can construct the time evolution operator from

$$U(t,0) = \begin{cases} e^{-\mathrm{i}H_0 t} & : \quad 0 < t < T/2 \\ e^{-\mathrm{i}H_0(t-T/2)}e^{-\mathrm{i}V}e^{-\mathrm{i}H_0 T/2} & : \quad T/2 < t < 3T/2 \\ e^{-\mathrm{i}H_0(t-3T/2)}e^{-\mathrm{i}V}e^{-\mathrm{i}H_0 T}e^{-\mathrm{i}V}e^{-\mathrm{i}H_0 T/2} & : \quad 3T/2 < t < 5T/2 \\ \vdots & \end{cases}\,. \tag{5.9}$$

This form arises since during the kick operation we can completely neglect the influence of H_0, and the δ-function can be approximated by a very fast time-dependent turning on and off of $V \to Vg(t)$, which does of course commute with itself. We can therefore conclude for the Floquet Hamiltonian for the initial time $t_0 = 0$

$$U(T) = e^{-\mathrm{i}H_0T/2}e^{-\mathrm{i}V}e^{-\mathrm{i}H_0T/2} \equiv e^{-\mathrm{i}\bar{H}T} \,. \tag{5.10}$$

From this form we already see that $\bar{H}$ is some sort of average Hamiltonian that has to act for the full period to obtain the same result as the time-dependent one. Note that the terminus average should not be used literally as in general $\bar{H} \neq \frac{1}{T}\int_0^T H(t)dt$. However, when $[V, H_0] = 0$ we do indeed see that the average Hamiltonian can be computed by the conventional average.

From comparing the time evolution at arbitrary time (note that $\Delta t < T/2$ though)

$$U(nT + \Delta t) = e^{-\mathrm{i}H_0\Delta t}\left[e^{-\mathrm{i}H_0T/2}e^{-\mathrm{i}V}e^{-\mathrm{i}H_0T/2}\right]^n = e^{-\mathrm{i}H_0\Delta t}e^{+\mathrm{i}\bar{H}\Delta t}e^{-\mathrm{i}\bar{H}(nT+\Delta t)} \tag{5.11}$$

we conclude that the kick operator is for $0 < \Delta t < T/2$ defined by

$$U_{\text{kick}}(nT + \Delta t) = U_{\text{kick}}(\Delta t) = e^{-\mathrm{i}H_0\Delta t}e^{+\mathrm{i}\bar{H}\Delta t} \,. \tag{5.12}$$

From this expression we can already see that $U_{\text{kick}}(0) = \mathbf{1}$. Similarly, we can look at the evolution during the second half of the period

$$\begin{aligned} U(nT + T/2 + \Delta t) &= e^{-\mathrm{i}H_0\Delta t}e^{-\mathrm{i}V}e^{-\mathrm{i}H_0T/2}e^{-\mathrm{i}\bar{H}nT} \\ &= e^{-\mathrm{i}H_0\Delta t}e^{-\mathrm{i}V}e^{-\mathrm{i}H_0T/2}e^{+\mathrm{i}\bar{H}(T/2+\Delta t)}e^{-\mathrm{i}\bar{H}(nT+T/2+\Delta t)} \,, \end{aligned} \tag{5.13}$$

which defines the kick operator during the second half

$$U_{\text{kick}}(+T/2 + \Delta t) = e^{-\mathrm{i}H_0\Delta t}e^{-\mathrm{i}V}e^{-\mathrm{i}H_0T/2}e^{+\mathrm{i}\bar{H}(T/2+\Delta t)} \,. \tag{5.14}$$

This expression tells us that $U_{\text{kick}}(T) = \mathbf{1}$ as well.

To make the example more explicit, we consider in the following

$$H_0 = \frac{\omega}{2}\sigma^z \,, \qquad V = \lambda\sigma^x \,. \tag{5.15}$$

This implies that

$$e^{-\mathrm{i}\alpha H_0} = \cos(\frac{\alpha\omega}{2})\mathbf{1} - \mathrm{i}\sin(\frac{\alpha\omega}{2})\sigma^z \,, \qquad e^{-\mathrm{i}V} = \cos(\lambda)\mathbf{1} - \mathrm{i}\sin(\lambda)\sigma^x \,. \tag{5.16}$$

The exponential of the Floquet Hamiltonian is then given by

$$e^{-\mathrm{i}\bar{H}T} = e^{-\mathrm{i}H_0T/2}e^{-\mathrm{i}V}e^{-\mathrm{i}H_0T/2} = \cos(\lambda)\cos(\omega T/2)\mathbf{1} - \mathrm{i}\cos(\lambda)\sin(\omega T/2)\sigma^z - \mathrm{i}\sin(\lambda)\sigma^x \,. \tag{5.17}$$

To obtain the Floquet Hamiltonian, we have to take the logarithm of that matrix, which demonstrates the difficulties. Even more specific, when $\omega T = \pi$, some terms cancel and we obtain for the Floquet Hamiltonian

$$\bar{H}_{\omega T=\pi} = \frac{\omega}{2}\cos(\lambda)\sigma^z + \frac{\omega}{2}\sin(\lambda)\sigma^x \,. \tag{5.18}$$

It is interesting to see that by the application of a diagonal Hamiltonian and a δ-kick we obtain an effective evolution that is rotated. The kick operator would then be calculated in a similar fashion.

To sum up, we can for this example calculate the Floquet operators because we can write down the full time evolution operator. Already for simple systems, finding the Floquet Hamiltonian and kick operator is quite involved.

5.1.3 Driven two-level system

Another popular example that is simple to treat is the driven two-level system

$$H(t) = \frac{\omega}{2}\sigma^z + P\sigma^+ e^{-\mathrm{i}\Omega t} + P^*\sigma^- e^{+\mathrm{i}\Omega t}\,. \tag{5.19}$$

We can use the rotation

$$V(t) = e^{-\mathrm{i}\Omega/2\sigma^z t} \tag{5.20}$$

on the complete Hamiltonian to move into a time-independent frame.

Then, we get

$$V^\dagger(t)\sigma^z V(t) = \sigma^z\,, \qquad V^\dagger(t)\sigma^\pm V(t) = \sigma^\pm e^{\pm\mathrm{i}\Omega t}\,. \tag{5.21}$$

Therefore, applying this to the Schrödinger equation $|\Psi\rangle = V(t)\left|\tilde{\Psi}\right\rangle$ transforms it into a time-independent frame

$$-\mathrm{i}\frac{\Omega}{2}\sigma^z V(t)\left|\tilde{\Psi}\right\rangle + V(t)\left|\dot{\tilde{\Psi}}\right\rangle \;=\; -\mathrm{i}HV(t)\left|\tilde{\Psi}\right\rangle\,, \tag{5.22}$$

which we can rewrite as

$$\left|\dot{\tilde{\Psi}}\right\rangle = \left[-\mathrm{i}V^\dagger(t)HV(t) + \mathrm{i}\frac{\Omega}{2}\sigma^z\right]\left|\tilde{\Psi}\right\rangle = -\mathrm{i}\left[\left(\frac{\omega-\Omega}{2}\right)\sigma^z + P\sigma^+ + P^*\sigma^-\right]\left|\tilde{\Psi}\right\rangle\,. \tag{5.23}$$

In this frame, the Hamiltonian is time-independent, and by exponentiating it we obtain the corresponding time evolution operator. Inserting the original transformation, therefore time evolution operator in the original frame is given by

$$U(t) = e^{-\mathrm{i}\frac{\Omega}{2}\sigma^z t} e^{-\mathrm{i}\left[\left(\frac{\omega-\Omega}{2}\right)\sigma^z + P\sigma^+ + P^*\sigma^-\right]t}\,. \tag{5.24}$$

Correspondingly, the Floquet Hamiltonian can be obtained by looking at times $t = T = \frac{2\pi}{\Omega}$. Then, we get

$$\begin{aligned}
U(T) &= \exp\left\{-\mathrm{i}\pi\sigma^z\right\}\exp\left\{-\mathrm{i}\left[\left(\frac{\omega-\Omega}{2}\right)\sigma^z + P\sigma^+ + P^*\sigma^-\right]\frac{2\pi}{\Omega}\right\}\\
&= -\exp\left\{-\mathrm{i}\left[\left(\frac{\omega-\Omega}{2}\right)\sigma^z + P\sigma^+ + P^*\sigma^-\right]\frac{2\pi}{\Omega}\right\}\\
&= \exp\left\{-\mathrm{i}\left[\left(\frac{\omega-\Omega}{2}\right)\sigma^z + P\sigma^+ + P^*\sigma^-\right]\frac{2\pi}{\Omega} + \mathrm{i}\pi\mathbf{1}\right\}\\
&= \exp\left\{-\mathrm{i}\left[\left(\frac{\omega-\Omega}{2}\right)\sigma^z + P\sigma^+ + P^*\sigma^- - \frac{\Omega}{2}\mathbf{1}\right]\frac{2\pi}{\Omega}\right\}\,.
\end{aligned} \tag{5.25}$$

From this, we can directly read off the Floquet Hamiltonian

$$\bar{H} = \left(\frac{\omega-\Omega}{2}\right)\sigma^z + P\sigma^+ + P^*\sigma^- - \frac{\Omega}{2}\mathbf{1}\,. \tag{5.26}$$

Clearly, this is not the conventional average Hamiltonian (which would not have terms proportional to P and P^*). To find the kick operator, we proceed with this result

$$U(t) = V(t)e^{-\mathrm{i}\frac{\Omega t}{2}\mathbf{1}}e^{-\mathrm{i}\bar{H}t} = e^{-\mathrm{i}\Omega t/2(\sigma^z+\mathbf{1})}e^{-\mathrm{i}\bar{H}t}\,, \tag{5.27}$$

which leaves us with

$$U_{\mathrm{kick}}(t) = e^{-\mathrm{i}\Omega t/2(\sigma^z+\mathbf{1})} = \begin{pmatrix} e^{-\mathrm{i}\Omega t} & 0\\ 0 & 1\end{pmatrix}\,, \tag{5.28}$$

from which we can clearly see the periodicity.

5.1.4 Driven cavity

Let us consider the example before with bosonic operators

$$H(t) = \omega a^\dagger a + P e^{+\mathrm{i}\Omega t} a + P^* e^{-\mathrm{i}\Omega t} a^\dagger \,. \tag{5.29}$$

As before, we can find a unitary transformation that moves into a frame $|\Psi\rangle = e^{-\mathrm{i}\Omega a^\dagger a t} \left|\tilde{\Psi}\right\rangle = V(t) \left|\tilde{\Psi}\right\rangle$, where the Hamiltonian becomes time-independent

$$\left|\dot{\tilde{\Psi}}\right\rangle = -\mathrm{i} V^\dagger(t)[H(t) - \Omega a^\dagger a] V(t) \left|\tilde{\Psi}\right\rangle = -\mathrm{i}[(\omega - \Omega) a^\dagger a + P a + P^* a^\dagger] \left|\tilde{\Psi}\right\rangle \,. \tag{5.30}$$

We can therefore write the full time evolution operator in the original frame as

$$U(t) = e^{-\mathrm{i}\Omega a^\dagger a t} e^{-\mathrm{i}[(\omega-\Omega) a^\dagger a + P a + P^* a^\dagger] t} \,. \tag{5.31}$$

Therefore,

$$U(2\pi/\Omega) = e^{-\mathrm{i}2\pi a^\dagger a} e^{-\mathrm{i}[(\omega-\Omega) a^\dagger a + P a + P^* a^\dagger] T} = e^{-\mathrm{i}[(\omega-\Omega) a^\dagger a + P a + P^* a^\dagger] T} = e^{-\mathrm{i}\bar{H} T} \,, \tag{5.32}$$

where we have used that $e^{-\mathrm{i}2\pi a^\dagger a} = \mathbf{1}$. This can be seen e.g. by evaluating the operator in the Fock space basis. Then, we can read off the Floquet Hamiltonian

$$\bar{H} = (\omega - \Omega) a^\dagger a + P a + P^* a^\dagger \tag{5.33}$$

and the kick operator

$$U_{\mathrm{kick}}(t) = e^{-\mathrm{i}\Omega a^\dagger a t} \,. \tag{5.34}$$

5.1.5 Application: Generalized RWAs

The RWA neglects rapidly oscillating terms in a suitable regime. Let as assume we are given a driven system of the form

$$H(t) = H_0 + H_1 \cos(\Omega t) \,, \tag{5.35}$$

where H_0 denotes the undriven (static) part of the Hamiltonian and H_1 is periodically modulated. The naive RWA approximation would simply average over one period $T = 2\pi/\Omega$, which would yield

$$H(t) \overset{\Omega\to\infty}{\to} \frac{1}{T} \int_0^T H(t) dt = H_0 \,. \tag{5.36}$$

This is the brute-force RWA approximation that we have used e.g. in the derivation of the quantum-optical master equation, where it was called secular approximation. However, if the driving frequency is finite, we can improve on this estimate by transforming into an interaction picture with respect to H_1. In this picture, the relevant Hamiltonian becomes

$$\tilde{H}(t) \;=\; e^{+\mathrm{i}\int_0^t \cos(\Omega t') dt' H_1} H_0 e^{-\mathrm{i}\int_0^t \cos(\Omega t') dt' H_1} = e^{+\mathrm{i}\sin(\Omega t)/\Omega H_1} H_0 e^{-\mathrm{i}\sin(\Omega t)/\Omega H_1} \,, \tag{5.37}$$

where we have used that the driven part of the Hamiltonian commutes with itself at different times, such that the time ordering need not be applied. The Hamiltonian is thus still time-dependent, but by performing the RWA approximation in this frame

$$\tilde{H}(t) \to \frac{1}{T}\int_0^T \tilde{H}(t)dt\,, \tag{5.38}$$

we would get a time-independent approximation. Then, the total time evolution operator could be approximated as

$$U(t) \approx \exp\left\{-\mathrm{i}\frac{\sin(\Omega t)}{\Omega}H_1\right\}\exp\left\{-\mathrm{i}\left[\frac{1}{T}\int_0^T \tilde{H}(t')dt'\right]t\right\}\,, \tag{5.39}$$

and the quality of this truncation depends on the microscopic details. From the periodicity of the first term, we can identify this as the first approximation to the kick operator

$$U_{\text{kick}}(t) \approx \exp\left\{-\mathrm{i}\frac{\sin(\Omega t)}{\Omega}H_1\right\}\,, \tag{5.40}$$

and consequently, we have found an approximation to the Floquet Hamiltonian

$$\bar{H} \approx \frac{1}{T}\int_0^T \tilde{H}(t)dt \tag{5.41}$$

as a conventional average over the Hamiltonian in the interaction picture (but not the original picture).

We can exemplify this for a simple two-level system

$$H(t) = \frac{\omega}{2}\sigma^z + \lambda\sigma^x\cos(\Omega t)\,. \tag{5.42}$$

Since this has a small Hilbert space, we can solve it numerically exact. But for now, we calculate the Hamiltonian in the transformed frame

$$\begin{aligned}
\tilde{H}(t) &= e^{+\mathrm{i}\sin(\Omega t)/\Omega H_1}H_0 e^{+\mathrm{i}\sin(\Omega t)/\Omega H_1} \\
&= \left[\cos\left(\lambda\frac{\sin(\Omega t)}{\Omega}\right) + \mathrm{i}\sin\left(\lambda\frac{\sin(\Omega t)}{\Omega}\right)\sigma^x\right]H_0\left[\cos\left(\lambda\frac{\sin(\Omega t)}{\Omega}\right) - \mathrm{i}\sin\left(\lambda\frac{\sin(\Omega t)}{\Omega}\right)\sigma^x\right] \\
&= \cos\left(2\frac{\lambda}{\Omega}\sin(\Omega t)\right)\frac{\omega}{2}\sigma^z + \sin\left(2\frac{\lambda}{\Omega}\sin(\Omega t)\right)\frac{\omega}{2}\sigma^y\,.
\end{aligned} \tag{5.43}$$

The zero-frequency component of this Hamiltonian becomes

$$\bar{H} \approx \frac{1}{T}\int_0^T \tilde{H}(t)dt = \mathcal{J}_0\left(2\frac{\lambda}{\Omega}\right)\frac{\omega}{2}\sigma^z\,, \tag{5.44}$$

where $\mathcal{J}_0(z)$ denotes the Bessel function of the first kind, defined by the differential equation $z^2\mathcal{J}_n''(z) + z\mathcal{J}_n'(z) + (z^2 - n^2)\mathcal{J}_n(z) = 0$. Our improved version of the time evolution operator would therefore read

$$U(t) \approx \exp\left\{-\mathrm{i}\sin(\Omega t)\frac{\lambda}{\Omega}\sigma^x\right\}\exp\left\{-\mathrm{i}\mathcal{J}_0\left(2\frac{\lambda}{\Omega}\right)\frac{\omega}{2}\sigma^z t\right\}\,. \tag{5.45}$$

To compute the full numerical solution technically, we use the Heisenberg picture, where

$$\frac{d}{dt}\langle\sigma^\alpha\rangle = \mathrm{Tr}\left\{U^\dagger(t)\left[\mathrm{i}H(t),\sigma^\alpha\right]U(t)\rho_0\right\}\ , \tag{5.46}$$

to obtain a closed set of differential equations for the operator expectation values

$$\begin{aligned}
\frac{d}{dt}\langle\sigma^x\rangle &= -\omega\langle\sigma^y\rangle\ , \\
\frac{d}{dt}\langle\sigma^y\rangle &= -2\lambda\cos(\Omega t)\langle\sigma^z\rangle + \omega\langle\sigma^x\rangle\ , \\
\frac{d}{dt}\langle\sigma^z\rangle &= +2\lambda\cos(\Omega t)\langle\sigma^y\rangle\ .
\end{aligned} \tag{5.47}$$

This set can be solved numerically and thereby yields the true solution of the dynamics in terms of all relevant expectation values. For most real-world problems we will not be able to calculate such an exact benchmark solution.

We can compare the effects of performing the RWA in the original frame and in the frame defined by the driving with the exact solution, see Fig. 5.1. We see that the naive RWA approximation

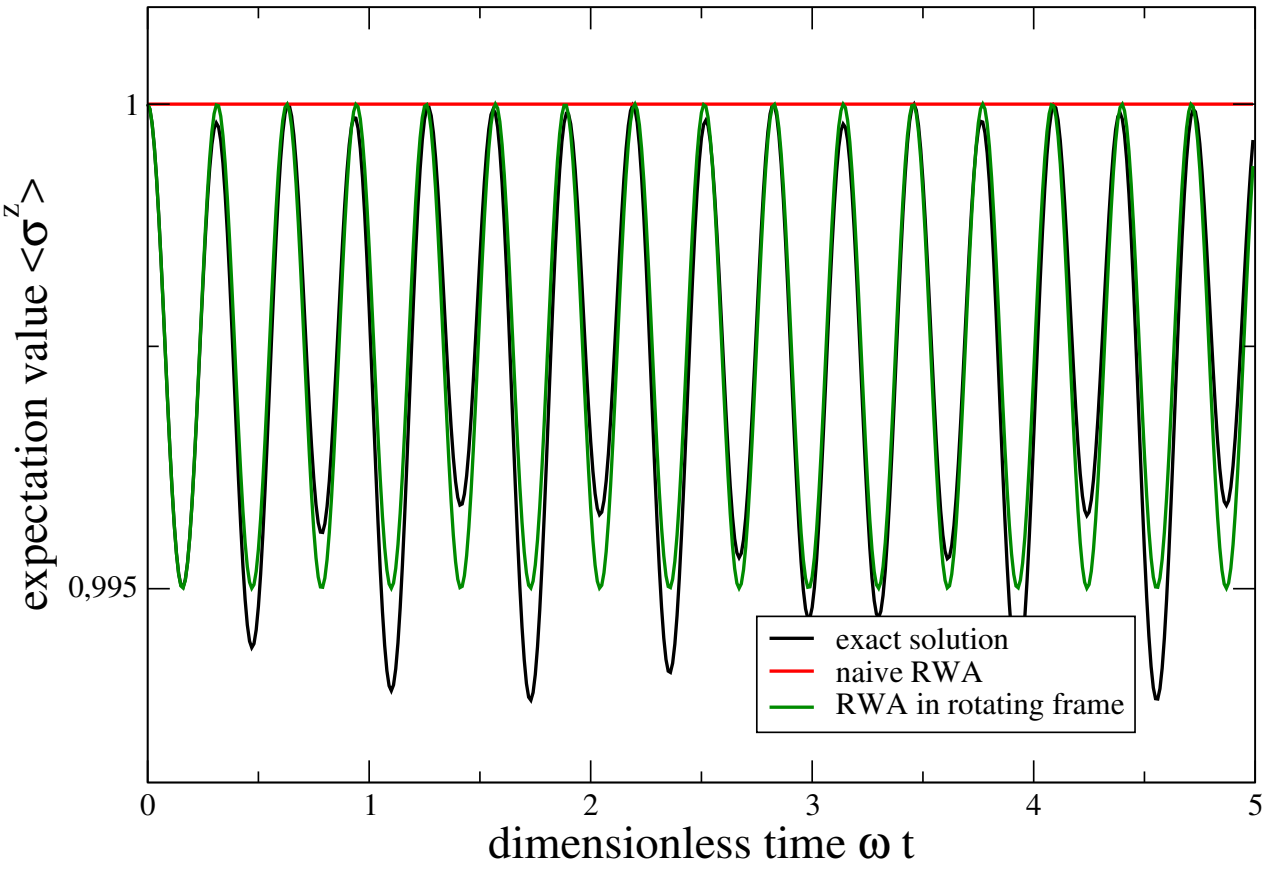

Figure 5.1: Expectation value for σ^z versus time for the exact solution (black), the RWA approximation in the original frame (red), and the RWA approximation in the comoving frame (green).

leaves the $\langle\sigma^z\rangle$ constant. In contrast, by applying the RWA approximation in the comoving frame, the dynamics of the exact solution is reproduced much better. However, we also see that it is

still far from perfect. Therefore, we could gain further improvements by switching to yet another comoving frame, applying the same methodology as before in the original Schrödinger frame. This would require to include at least the first non-vanishing Fourier components

$$\begin{aligned}\tilde{H}_{-1}e^{-\mathrm{i}\Omega t}+\tilde{H}_{+1}e^{+\mathrm{i}\Omega t} &= \frac{1}{T}\int_0^T \tilde{H}(t')e^{+\mathrm{i}\Omega t'}dt'e^{-\mathrm{i}\Omega t}+\frac{1}{T}\int_0^T \tilde{H}(t')e^{-\mathrm{i}\Omega t'}dt'e^{+\mathrm{i}\Omega t}\\ &= \mathcal{J}_1\left(\frac{2\lambda}{\Omega}\right)\omega\sin(\Omega t)\sigma^y \end{aligned} \tag{5.48}$$

in the next transformation.

5.2 Floquet treatment of open systems

Now we imagine our driven system coupled to a bath, where we allow also for driven interactions $H(t)=H_S(t)+H_I(t)+H_B$ in general, but let us first review the standard case.

5.2.1 Standard Floquet treatment

In the standard treatment, we only consider a periodically driven system

$$H(t)=H_S(t)+H_I+H_B\,,\qquad H_S(t+T)=H_S(t)\,. \tag{5.49}$$

Essentially, the derivation of the master equation follows conceptionally the same steps as in Sec. 2.2.1, see e.g. Ref. [13] The only difference is that for a driven system, the transformation into the interaction picture is much more involved

$$\begin{aligned}\boldsymbol{A_\alpha}(t) &= \left[\hat{T}e^{-\mathrm{i}\int_0^t H_S(t')dt'}\right]^\dagger A_\alpha\left[\hat{T}e^{-\mathrm{i}\int_0^t H_S(t')dt'}\right]\\ &= \sum_n\sum_{ab}A_\alpha^{n,ab}e^{+\mathrm{i}(E_a-E_b+n\Omega)t}=\sum_n\sum_\omega A_\alpha^{n,\omega}e^{+\mathrm{i}(\omega+n\Omega)t}\,,\end{aligned} \tag{5.50}$$

where the ω are the Bohr frequencies of the Floquet Hamiltonian, which we have only introduced to shorten the notation. Here, we have implicitly used the Floquet decomposition by applying Eq. (5.5). We see that the transition frequencies of the system are no longer relevant, but rather the transition frequencies of the Floquet Hamiltonian, supplemented by integer multiples of the driving. Floquet theory essentially just tells us that such a decomposition does exist, but it does not provide help to obtain this decomposition. In this section, we will assume that we have found the operators $A_\alpha^{n,\omega}$. We can perform the Born and Markov approximations as usual and can therefore directly start with Eq. (2.30)

$$\begin{aligned}\dot{\boldsymbol{\rho}}_{\mathbf{S}} &= -\int_0^\infty \mathrm{Tr}_\mathrm{B}\left\{[\boldsymbol{\mathcal{H}}_\mathbf{I}(t),[\boldsymbol{\mathcal{H}}_\mathbf{I}(t-\tau),\boldsymbol{\rho}_\mathbf{S}(t)\otimes\bar{\rho}_\mathrm{B}]]\right\}d\tau \qquad (5.51)\\ &= -\int_0^\infty\sum_{\alpha\beta}\sum_{nn'}\sum_{\omega\omega'}\mathrm{Tr}_\mathrm{B}\left\{\left[A_\alpha^{n\omega}e^{+\mathrm{i}(\omega+n\Omega)t}\boldsymbol{B}_{\boldsymbol{\alpha}}(t),\left[A_\beta^{n'\omega'}e^{+\mathrm{i}(\omega'+n'\Omega)(t-\tau)}\boldsymbol{B}_{\boldsymbol{\beta}}(t-\tau),\boldsymbol{\rho}_\mathbf{S}(t)\otimes\bar{\rho}_\mathrm{B}\right]\right]\right\}d\tau\,.\end{aligned}$$

The standard way to perform the secular approximation is now to assume in addition that the driving is fast, keeping in the equation above only the terms where the resonance conditions

$\omega' = -\omega$ and $n' = -n$ are fulfilled separately. This yields

$$\begin{aligned}
\dot{\boldsymbol{\rho}}_{\mathbf{S}} &= -\int_0^\infty \sum_{\alpha\beta}\sum_n\sum_\omega \mathrm{Tr}_{\mathrm{B}}\left\{\left[A_\alpha^{n\omega}\boldsymbol{B}_{\boldsymbol{\alpha}}(t),\left[A_\beta^{-n,-\omega}e^{+\mathrm{i}(\omega+n\Omega)\tau}\boldsymbol{B}_{\boldsymbol{\beta}}(t-\tau),\boldsymbol{\rho}_{\mathbf{S}}(t)\otimes\bar{\rho}_{\mathrm{B}}\right]\right]\right\}d\tau \\
&= -\sum_{\alpha\beta}\sum_n\sum_\omega\int_0^\infty d\tau e^{+\mathrm{i}(\omega+n\Omega)\tau}\Big[+A_\alpha^{+n,+\omega}A_\beta^{-n,-\omega}\boldsymbol{\rho}_{\mathbf{S}}(t)C_{\alpha\beta}(+\tau) \\
&\quad -A_\alpha^{+n,+\omega}\boldsymbol{\rho}_{\mathbf{S}}(t)A_\beta^{-n,-\omega}C_{\beta\alpha}(-\tau)-A_\beta^{-n,-\omega}\boldsymbol{\rho}_{\mathbf{S}}(t)A_\alpha^{+n,+\omega}C_{\alpha\beta}(+\tau) \\
&\quad +\boldsymbol{\rho}_{\mathbf{S}}(t)A_\beta^{-n,-\omega}A_\alpha^{+n,+\omega}C_{\beta\alpha}(-\tau)\Big] \\
&= +\sum_{\alpha\beta}\sum_n\sum_\omega\Big[-A_\alpha^{+n,+\omega}A_\beta^{-n,-\omega}\boldsymbol{\rho}_{\mathbf{S}}(t)\Gamma_{\alpha\beta}(+\omega+n\Omega) \\
&\quad +A_\alpha^{+n,+\omega}\boldsymbol{\rho}_{\mathbf{S}}(t)A_\beta^{-n,-\omega}\Gamma^*_{\alpha\beta}(-\omega-n\Omega)+A_\beta^{-n,-\omega}\boldsymbol{\rho}_{\mathbf{S}}(t)A_\alpha^{+n,+\omega}\Gamma_{\alpha\beta}(+\omega+n\Omega) \\
&\quad -\boldsymbol{\rho}_{\mathbf{S}}(t)A_\beta^{-n,-\omega}A_\alpha^{+n,+\omega}\Gamma^*_{\alpha\beta}(-\omega-n\Omega)\Big], \qquad (5.52)
\end{aligned}$$

where we have introduced as in standard discussions our half-sided Fourier transforms and used that $C_{\alpha\beta}(-\tau) = C^*_{\alpha\beta}(+\tau)$ for hermitian coupling operators. Expressing them as before in hermitian and anti-hermitian parts via $\Gamma_{\alpha\beta}(\omega) = 1/2\gamma_{\alpha\beta}(\omega) + 1/2\sigma_{\alpha\beta}(\omega)$, we eventually get the Floquet master equation.

Def. 17 (Floquet master equation)**.** *For a decomposition of the (hermitian) system coupling operators* $\boldsymbol{A}_{\boldsymbol{\alpha}}(t) = \sum_n\sum_\omega A_\alpha^{n,\omega}e^{+\mathrm{i}(\omega+n\Omega)t}$*, the Floquet master equation becomes*

$$\begin{aligned}
\dot{\boldsymbol{\rho}}_{\mathbf{S}} &= -\mathrm{i}\left[\sum_{\alpha\beta}\sum_n\sum_\omega\frac{1}{2\mathrm{i}}\sigma_{\alpha\beta}(\omega+n\Omega)A_\alpha^{+n,+\omega}A_\beta^{-n,-\omega},\boldsymbol{\rho}_{\mathbf{S}}\right] \\
&\quad +\sum_{\alpha\beta}\sum_n\sum_\omega\gamma_{\alpha\beta}(\omega+n\Omega)\left[A_\beta^{-n,-\omega}\boldsymbol{\rho}_{\mathbf{S}}A_\alpha^{+n,+\omega}-\frac{1}{2}\left\{A_\alpha^{+n,+\omega}A_\beta^{-n,-\omega},\boldsymbol{\rho}_{\mathbf{S}}\right\}\right]. \qquad (5.53)
\end{aligned}$$

Here, ω *are the Bohr frequencies of the Floquet Hamiltonian.*

We see that we can not in general expect the system to thermalize, not even in the Floquet Hamiltonian basis, since the KMS relations encoded in the correlation functions involve transitions with an additional shifts $n\Omega$ [14]. In order to derive this master equation, we had – on top of the usual Born, Markov, and secular approximation – a fast driving assumption $\Omega \to \infty$ (to motivate the separate cancellation of phase factors). Finally, when the coupling operators are hermitian, we can relate $A_\alpha^{n,\omega} = (A_\alpha^{-n,-\omega})^\dagger$. For such a system, it is less obvious how one should define the energy counting. Indeed, there is ample evidence that microscopically-derived counting fields need to be used to obtain a consistent thermodynamic description [15].

5.2.2 Coarse-graining treatment

To avoid the aforementioned fast-driving assumption, we recall the coarse-graining method from Def. 15, using that $[H_B, \bar{\bar{\rho}}_B] = 0$ and that we count the energy of the reservoir with the counting

field ξ

$$\begin{aligned}\dot{\boldsymbol{\rho}}_{\mathbf{S}} &= -\mathrm{i}\left[\frac{1}{2\mathrm{i}\tau}\int_0^\tau dt_1\int_0^\tau dt_2\sum_{\alpha\beta}C^0_{\alpha\beta}(t_1-t_2)\mathrm{sgn}(\mathrm{t}_1-\mathrm{t}_2)\boldsymbol{A}_{\boldsymbol{\alpha}}(\mathrm{t}_1)\boldsymbol{A}_{\boldsymbol{\beta}}(\mathrm{t}_2),\boldsymbol{\rho}_{\mathbf{S}}\right] \\ &+\frac{1}{\tau}\int_0^\tau dt_1\int_0^\tau dt_2\sum_{\alpha\beta}\left[C^0_{\alpha\beta}(t_1-t_2-\xi)\boldsymbol{A}_{\boldsymbol{\beta}}(t_2)\boldsymbol{\rho}_{\mathbf{S}}\boldsymbol{A}_{\boldsymbol{\alpha}}(t_1)-\frac{C^0_{\alpha\beta}(t_1-t_2)}{2}\left\{\boldsymbol{A}_{\boldsymbol{\alpha}}(t_1)\boldsymbol{A}_{\boldsymbol{\beta}}(t_2),\boldsymbol{\rho}_{\mathbf{S}}\right\}\right].\end{aligned} \tag{5.54}$$

Here, we did not use any assumption on the system coupling operators, i.e., the whole scheme is applicable also when we drive our system or our system coupling operators (i.e., the interaction Hamiltonian) periodically. Indeed, for a static system Hamiltonian with a periodically driven coupling to the system

$$H(t)=H_S+\sum_\alpha A_\alpha(t)\otimes B_\alpha(t)+H_B\,,\qquad A_\alpha(t+T)=A_\alpha(t)\,, \tag{5.55}$$

we could also switch to the interaction picture, where the system coupling operators would assume the familiar form

$$\boldsymbol{A}_{\boldsymbol{\alpha}}(t)=\sum_n\sum_{\tilde{\omega}}A^{n,\tilde{\omega}}_\alpha e^{+\mathrm{i}(\tilde{\omega}+n\Omega)t}\,. \tag{5.56}$$

Then however, the $\tilde{\omega}$ would be the transition frequencies of H_S. We therefore simply start from the above general decomposition, leaving at present open whether we drive system or interaction Hamiltonian. We can insert the inverse Fourier transforms

$$C^0_{\alpha\beta}(\tau)=\frac{1}{2\pi}\int\gamma^0_{\alpha\beta}(\omega)e^{-\mathrm{i}\omega\tau}d\omega\,,\qquad C^0_{\alpha\beta}(\tau)\mathrm{sgn}(\tau)=\frac{1}{2\pi}\int\sigma^0_{\alpha\beta}(\omega)e^{-\mathrm{i}\omega\tau}d\omega \tag{5.57}$$

to perform the temporal integrals. As before, we hereby employ

$$\frac{1}{2\pi\tau}\int_0^\tau\int_0^\tau e^{-\mathrm{i}\omega(t_1-t_2)}e^{+\mathrm{i}\alpha t_1}e^{-\mathrm{i}\beta t_2}dt_1dt_2=\frac{\tau}{2\pi}e^{+\mathrm{i}(\alpha-\beta)\tau/2}\mathrm{sinc}\left[(\alpha-\omega)\frac{\tau}{2}\right]\mathrm{sinc}\left[(\beta-\omega)\frac{\tau}{2}\right]\,, \tag{5.58}$$

which eventually yields

$$\begin{aligned}\dot{\boldsymbol{\rho}}_{\mathbf{S}} &= -\mathrm{i}\int d\omega\sum_{\alpha\beta}\sigma^0_{\alpha\beta}(\omega)\frac{\tau}{4\pi\mathrm{i}}\sum_{nn'}\sum_{\tilde{\omega},\tilde{\omega}'}e^{+\mathrm{i}(\tilde{\omega}+n\Omega-\tilde{\omega}'-n'\Omega)\tau/2}\times \\ &\times\mathrm{sinc}\left[(\tilde{\omega}+n\Omega-\omega)\frac{\tau}{2}\right]\mathrm{sinc}\left[(\tilde{\omega}'+n'\Omega-\omega)\frac{\tau}{2}\right]\left[A^{+n,+\tilde{\omega}}_\alpha A^{-n',-\tilde{\omega}'}_\beta,\boldsymbol{\rho}_{\mathbf{S}}\right] \\ &+\int d\omega\sum_{\alpha\beta}\gamma^0_{\alpha\beta}(\omega)\frac{\tau}{2\pi}\sum_{nn'}\sum_{\tilde{\omega},\tilde{\omega}'}e^{+\mathrm{i}(\tilde{\omega}+n\Omega-\tilde{\omega}'-n'\Omega)\tau/2}\mathrm{sinc}\left[(\tilde{\omega}+n\Omega-\omega)\frac{\tau}{2}\right]\mathrm{sinc}\left[(\tilde{\omega}'+n'\Omega-\omega)\frac{\tau}{2}\right] \\ &\times\left[e^{+\mathrm{i}\omega\xi}A^{-n',-\tilde{\omega}'}_\beta\boldsymbol{\rho}_{\mathbf{S}}A^{+n,+\tilde{\omega}}_\alpha-\frac{1}{2}\left\{A^{+n,+\tilde{\omega}}_\alpha A^{-n',-\tilde{\omega}'}_\beta,\boldsymbol{\rho}_{\mathbf{S}}\right\}\right].\end{aligned} \tag{5.59}$$

For fixed τ, we can consider the asymptotics of this master equation. When the driving is very fast $\Omega\to\infty$, we will only keep the terms where $n'=n$, and subsequently taking $\tau\to\infty$ reproduces the Floquet master equation (5.53). In contrast, when the driving is very slow $\Omega\to 0$, we can neglect the Ω-dependence in the sinc- and exponential functions and absorb the dependence via $A^{\tilde{\omega}}_\alpha=\sum_n A^{n,\tilde{\omega}}_\alpha$, which would reproduce our previous coarse-graining master equation, but now with $\tilde{\omega}$ denoting the transition frequencies of the Floquet Hamiltonian. However, for slow driving $\Omega\to 0$, the Floquet Hamiltonian falls back to the original system Hamiltonian, such that we reproduce the known dynamics of an open two-level system. The general dynamics for finite Ω is hard to estimate, we will therefore discuss only specific cases here.

5.2.3 Commuting driving

We consider the case where the driving commutes with the interaction

$$\begin{aligned} H(t) &= \frac{\omega}{2}\sigma^z + P\sigma^+ e^{-\mathrm{i}\Omega t} + P^*\sigma^- e^{+\mathrm{i}\Omega t} \\ &\quad + \left(P\sigma^+ e^{-\mathrm{i}\Omega t} + P^*\sigma^- e^{+\mathrm{i}\Omega t}\right) \otimes \sum_k (h_k b_k + h_k^* b_k^\dagger) + \sum_k \omega_k b_k^\dagger b_k \,. \end{aligned} \tag{5.60}$$

Here, both the system part and the interaction are driven, but in a completely synchronous way, such the system part of the driving and the interaction part commute at the same times. In addition, it has the advantage that we can compute the Floquet Hamiltonian exactly without approximation. The time evolution operator for the system was found to be (5.24)

$$U(t) = e^{-\mathrm{i}\frac{\Omega}{2}\sigma^z t} e^{-\mathrm{i}\left[\left(\frac{\omega-\Omega}{2}\right)\sigma^z + P\sigma^+ + P^*\sigma^-\right]t} \,, \tag{5.61}$$

such that it is not difficult to transform the system coupling operator into the interaction picture

$$\begin{aligned} \boldsymbol{A}(t) &= U^\dagger(t)\left(P\sigma^+ e^{-\mathrm{i}\Omega t} + P^*\sigma^- e^{+\mathrm{i}\Omega t}\right) U(t) \\ &= e^{+\mathrm{i}\left[\left(\frac{\omega-\Omega}{2}\right)\sigma^z + P\sigma^+ + P^*\sigma^-\right]t} \left(P\sigma^+ + P^*\sigma^-\right) e^{-\mathrm{i}\left[\left(\frac{\omega-\Omega}{2}\right)\sigma^z + P\sigma^+ + P^*\sigma^-\right]t} \\ &= e^{+\mathrm{i}\bar{H}t}\left(P\sigma^+ + P^*\sigma^-\right) e^{-\mathrm{i}\bar{H}t} \,. \end{aligned} \tag{5.62}$$

From this expression we see that the time-dependence of the coupling operator in the interaction picture is trivially given only by the transition frequencies of the Floquet Hamiltonian, such that in our general expansion (5.5) only the $n = 0$-term survives. For such a case, we can follow the usual derivation of the master equation, with the coupling operator in the Schrödinger picture replaced by $A \to (P\sigma^+ + P^*\sigma^-)$ and the system Hamiltonian replaced by the Floquet Hamiltonian (5.26)

$$\bar{H} = \left(\frac{\omega - \Omega}{2}\right)\sigma^z + P\sigma^+ + P^*\sigma^- - \frac{\Omega}{2}\mathbf{1} \,. \tag{5.63}$$

These will then assume the form of a simple rate equation in the energy eigenbasis of the Floquet Hamiltonian $\bar{H}\,|\bar{a}\rangle = \bar{E}_a\,|\bar{a}\rangle$ instead of the system Hamiltonian

$$\dot{\rho}_{aa} = \sum_b \gamma_{ab,ab}\rho_{bb} - \sum_b \gamma_{ba,ba}\rho_{aa} \,, \tag{5.64}$$

with the transition rate

$$\gamma_{ab,ab} = \gamma(\bar{E}_b - \bar{E}_a)\left|\langle\bar{a}|\left(P\sigma^+ + P^*\sigma^-\right)|\bar{b}\rangle\right|^2 . \tag{5.65}$$

Since the reservoir correlation function for this model $\gamma(\omega) = \Gamma(\omega)[1 + n_B(\omega)]$ obeys the KMS relations, the steady state of this master equation will be a Gibbs state in the Floquet basis. This result can be shown to hold [14] when first, the Hamiltonian of the system is bounded and second, the driving Hamiltonian commutes with itself at different times, and third, the driving commutes with the interaction. Although our example does not support the second condition, it also yields thermalization in the Floquet eigenbasis. Below we will see that this case is very specific.

5.2.4 Example: Open driven Two-Level system

We revisit our example of a driven two-level system, which is now coupled to a reservoir of bosonic oscillators

$$H(t) = \frac{\omega}{2}\sigma^z + P\sigma^+ e^{-\mathrm{i}\Omega t} + P^*\sigma^- e^{+\mathrm{i}\Omega t} + \sigma^x \sum_k (h_k b_k + h_k^* b_k^\dagger) + \sum_k \omega_k b_k^\dagger b_k \,. \tag{5.66}$$

We have already derived the time-evolution operator for the system in Eq. (5.24), which yields

$$\begin{aligned}
\boldsymbol{\sigma^x}(t) &= U^\dagger(t)\sigma^x U(t) \\
&= e^{+\mathrm{i}\left[\left(\frac{\omega-\Omega}{2}\right)\sigma^z + P\sigma^+ + P^*\sigma^-\right]t} e^{+\mathrm{i}\frac{\Omega}{2}\sigma^z t}\sigma^x e^{-\mathrm{i}\frac{\Omega}{2}\sigma^z t} e^{-\mathrm{i}\left[\left(\frac{\omega-\Omega}{2}\right)\sigma^z + P\sigma^+ + P^*\sigma^-\right]t} \\
&= e^{+\mathrm{i}\left[\left(\frac{\omega-\Omega}{2}\right)\sigma^z + P\sigma^+ + P^*\sigma^-\right]t} \left[\cos(\Omega t)\sigma^x + \sin(\Omega t)\sigma^y\right] e^{-\mathrm{i}\left[\left(\frac{\omega-\Omega}{2}\right)\sigma^z + P\sigma^+ + P^*\sigma^-\right]t} \\
&= e^{+\mathrm{i}\left[\left(\frac{\omega-\Omega}{2}\right)\sigma^z + P\sigma^+ + P^*\sigma^-\right]t} \left[e^{+\mathrm{i}\Omega t}\sigma^+ + e^{-\mathrm{i}\Omega t}\sigma^-\right] e^{-\mathrm{i}\left[\left(\frac{\omega-\Omega}{2}\right)\sigma^z + P\sigma^+ + P^*\sigma^-\right]t} \\
&= e^{+\mathrm{i}\bar{H}t}\left[e^{+\mathrm{i}\Omega t}\sigma^+ + e^{-\mathrm{i}\Omega t}\sigma^-\right] e^{-\mathrm{i}\bar{H}t} \,.
\end{aligned} \tag{5.67}$$

Here, the phase factors resulting from the shift of the Floquet Hamiltonian in Eq. (5.26) and kick operator would cancel in any case, and we also see already that only the $n = \pm 1$ terms contribute. The transition energies of the Floquet Hamiltonian become

$$\tilde{\omega} \in \left\{0, \pm\sqrt{(\omega-\Omega)^2 + 4|P|^2}\right\} = \{0, \pm\omega^*\} \,, \tag{5.68}$$

and we again note that both Bohr frequencies and eigenvectors are invariant with respect to trivial shifts of the Hamiltonian. We can now proceed by representing the coupling operators in eigenstates of the Floquet Hamiltonian $\bar{H}\,|a\rangle = E_a\,|a\rangle$, which we do directly in Eq. (5.54)

$$\begin{aligned}
\dot{\boldsymbol{\rho}}_\mathbf{S} &= -\mathrm{i}\left[\frac{1}{2\mathrm{i}\tau}\int_0^\tau dt_1 \int_0^\tau dt_2 C^0(t_1-t_2)\mathrm{sgn}(\mathrm{t}_1-\mathrm{t}_2)\boldsymbol{\sigma^x}(\mathrm{t}_1)\boldsymbol{\sigma^x}(\mathrm{t}_2), \boldsymbol{\rho}_\mathbf{S}\right] \qquad (5.69) \\
&\quad + \frac{1}{\tau}\int_0^\tau dt_1 \int_0^\tau dt_2 \left[C^0(t_1-t_2-\xi)\boldsymbol{\sigma^x}(t_2)\boldsymbol{\rho}_\mathbf{S}\boldsymbol{\sigma^x}(t_1) - \frac{C^0(t_1-t_2)}{2}\left\{\boldsymbol{\sigma^x}(t_1)\boldsymbol{\sigma^x}(t_2), \boldsymbol{\rho}_\mathbf{S}\right\}\right] \\
&= -\mathrm{i}\int d\omega\sigma(\omega)\frac{1}{4\pi\mathrm{i}\tau}\int_0^\tau dt_1\int_0^\tau dt_2 e^{-\mathrm{i}\omega(t_1-t_2)}\sum_{abc} e^{+\mathrm{i}(E_a-E_b)t_1}e^{+\mathrm{i}(E_b-E_c)t_2} \times \\
&\quad \times (e^{+\mathrm{i}\Omega t_1}\sigma^+_{ab} + e^{-\mathrm{i}\Omega t_1}\sigma^-_{ab})(e^{+\mathrm{i}\Omega t_2}\sigma^+_{bc} + e^{-\mathrm{i}\Omega t_2}\sigma^-_{bc})\left[|a\rangle\langle c|, \boldsymbol{\rho}_\mathbf{S}\right] \\
&\quad + \int d\omega\gamma(\omega)e^{+\mathrm{i}\omega\xi}\frac{1}{2\pi\tau}\int_0^\tau dt_1\int_0^\tau dt_2 e^{-\mathrm{i}\omega(t_1-t_2)}\sum_{abcd} e^{+\mathrm{i}(E_a-E_b)t_2}e^{+\mathrm{i}(E_c-E_d)t_1} \times \\
&\quad \times (e^{+\mathrm{i}\Omega t_2}\sigma^+_{ab} + e^{-\mathrm{i}\Omega t_2}\sigma^-_{ab})(e^{+\mathrm{i}\Omega t_1}\sigma^+_{cd} + e^{-\mathrm{i}\Omega t_1}\sigma^-_{cd})\,|a\rangle\langle b|\,\boldsymbol{\rho}_\mathbf{S}\,|c\rangle\langle d| \\
&\quad - \int d\omega\gamma(\omega)\frac{1}{4\pi\tau}\int_0^\tau dt_1\int_0^\tau dt_2 e^{-\mathrm{i}\omega(t_1-t_2)}\sum_{abc} e^{+\mathrm{i}(E_a-E_b)t_1}e^{+\mathrm{i}(E_b-E_c)t_2} \times \\
&\quad \times (e^{+\mathrm{i}\Omega t_1}\sigma^+_{ab} + e^{-\mathrm{i}\Omega t_1}\sigma^-_{ab})(e^{+\mathrm{i}\Omega t_2}\sigma^+_{bc} + e^{-\mathrm{i}\Omega t_2}\sigma^-_{bc})\left\{|a\rangle\langle c|, \boldsymbol{\rho}_\mathbf{S}\right\} \,. \qquad (5.70)
\end{aligned}$$

Here, we recall again that

$$\begin{aligned}\frac{1}{2\pi\tau}\int_0^\tau dt_1\int_0^\tau dt_2 e^{-\mathrm{i}(\omega-\alpha_1)t_1}e^{+\mathrm{i}(\omega-\alpha_2)t_2} &= \frac{\tau}{2\pi}e^{+\mathrm{i}(\alpha_1-\alpha_2)\tau/2}\mathrm{sinc}\left[(\omega-\alpha_1)\frac{\tau}{2}\right]\mathrm{sinc}\left[(\omega-\alpha_2)\frac{\tau}{2}\right]\\ &\overset{\tau\to\infty}{\to} \delta_{\alpha_1,\alpha_2}\delta(\omega-\alpha_1)\,. \end{aligned} \tag{5.71}$$

For finite coarse-graining times τ, we simply have to keep all terms, but for large τ we only need to keep those satisfying the resonance conditions

$$\begin{aligned}\dot{\boldsymbol{\rho}}_{\mathbf{S}} &= -\mathrm{i}\int d\omega\sigma(\omega)\frac{1}{2\mathrm{i}}\sum_{abc}\left[|a\rangle\langle c|\,,\boldsymbol{\rho}_{\mathbf{S}}\right]\times\\ &\times\Big[\delta_{E_a-E_b+\Omega,E_c-E_b-\Omega}\delta(\omega-E_a+E_b-\Omega)\sigma^+_{ab}\sigma^+_{bc}\\ &\quad+\delta_{E_a-E_b+\Omega,E_c-E_b+\Omega}\delta(\omega-E_a+E_b-\Omega)\sigma^+_{ab}\sigma^-_{bc}\\ &\quad+\delta_{E_a-E_b-\Omega,E_c-E_b-\Omega}\delta(\omega-E_a+E_b+\Omega)\sigma^-_{ab}\sigma^+_{bc}\\ &\quad+\delta_{E_a-E_b-\Omega,E_c-E_b+\Omega}\delta(\omega-E_a+E_b+\Omega)\sigma^-_{ab}\sigma^-_{bc}\Big]\\ &+\int d\omega\gamma(\omega)e^{+\mathrm{i}\omega\xi}\sum_{abcd}|a\rangle\langle b|\,\boldsymbol{\rho}_{\mathbf{S}}\,|c\rangle\langle d|\times\\ &\times\Big[\delta_{E_c-E_d+\Omega,E_b-E_a-\Omega}\delta(\omega+E_a-E_b+\Omega)\sigma^+_{ab}\sigma^+_{cd}\\ &\quad+\delta_{E_c-E_d+\Omega,E_b-E_a+\Omega}\delta(\omega+E_a-E_b-\Omega)\sigma^-_{ab}\sigma^+_{cd}\\ &\quad+\delta_{E_c-E_d-\Omega,E_b-E_a-\Omega}\delta(\omega+E_a-E_b+\Omega)\sigma^+_{ab}\sigma^-_{cd}\\ &\quad+\delta_{E_c-E_d-\Omega,E_b-E_a+\Omega}\delta(\omega+E_a-E_b-\Omega)\sigma^-_{ab}\sigma^-_{cd}\Big]\\ &-\frac{1}{2}\int d\omega\gamma(\omega)\sum_{abc}\left\{|a\rangle\langle c|\,,\boldsymbol{\rho}_{\mathbf{S}}\right\}\times\\ &\times\Big[\delta_{E_a-E_b+\Omega,E_c-E_b-\Omega}\delta(\omega-E_a+E_b-\Omega)\sigma^+_{ab}\sigma^+_{bc}\\ &\quad+\delta_{E_a-E_b+\Omega,E_c-E_b+\Omega}\delta(\omega-E_a+E_b-\Omega)\sigma^+_{ab}\sigma^-_{bc}\\ &\quad+\delta_{E_a-E_b-\Omega,E_c-E_b-\Omega}\delta(\omega-E_a+E_b+\Omega)\sigma^-_{ab}\sigma^+_{bc}\\ &\quad+\delta_{E_a-E_b-\Omega,E_c-E_b+\Omega}\delta(\omega-E_a+E_b+\Omega)\sigma^-_{ab}\sigma^-_{bc}\Big]\,, \end{aligned} \tag{5.72}$$

which can be further simplified. Let us look at the interesting case of fast driving $\Omega\gg\omega^*$. We furthermore use that the spectrum of the Floquet Hamiltonian is non-degenerate, e.g. $\delta_{E_a,E_c}=\delta_{ac}$

to obtain

$$\begin{aligned}
\dot{\boldsymbol{\rho}}_{\mathbf{S}} &= -\mathrm{i}\int d\omega\sigma(\omega)\frac{1}{2\mathrm{i}}\sum_{abc}\left[|a\rangle\langle c|,\boldsymbol{\rho}_{\mathbf{S}}\right]\times \\
&\times\Big[+\delta_{ac}\delta(\omega-E_a+E_b-\Omega)\sigma^+_{ab}\sigma^-_{bc}+\delta_{ac}\delta(\omega-E_a+E_b+\Omega)\sigma^-_{ab}\sigma^+_{bc}\Big] \\
&+\int d\omega\gamma(\omega)e^{+\mathrm{i}\omega\xi}\sum_{abcd}|a\rangle\langle b|\boldsymbol{\rho}_{\mathbf{S}}|c\rangle\langle d|\times \\
&\times\Big[+\delta_{E_c-E_d,E_b-E_a}\delta(\omega+E_a-E_b-\Omega)\sigma^-_{ab}\sigma^+_{cd}+\delta_{E_c-E_d,E_b-E_a}\delta(\omega+E_a-E_b+\Omega)\sigma^+_{ab}\sigma^-_{cd}\Big] \\
&-\frac{1}{2}\int d\omega\gamma(\omega)\sum_{abc}\left\{|a\rangle\langle c|,\boldsymbol{\rho}_{\mathbf{S}}\right\}\times \\
&\times\Big[+\delta_{ac}\delta(\omega-E_a+E_b-\Omega)\sigma^+_{ab}\sigma^-_{bc}+\delta_{ac}\delta(\omega-E_a+E_b+\Omega)\sigma^-_{ab}\sigma^+_{bc}\Big]. \qquad (5.73)
\end{aligned}$$

Evaluating this in the eigenbasis of the Floquet Hamiltonian, we get with $\rho_i=\langle i|\boldsymbol{\rho}_{\mathbf{S}}|i\rangle$ a simple rate equation of the form

$$\dot{\rho}_i=\sum_j R_{ij}(\xi)\rho_j-\sum_j R_{ji}(0)\rho_i\,, \qquad (5.74)$$

where the rates are given by

$$R_{ij}(\xi) = \sigma^-_{ij}\sigma^+_{ji}\gamma(E_j-E_i+\Omega)e^{+\mathrm{i}\xi(E_j-E_i+\Omega)}+\sigma^+_{ij}\sigma^-_{ji}\gamma(E_j-E_i-\Omega)e^{+\mathrm{i}\xi(E_j-E_i-\Omega)}\,. \qquad (5.75)$$

Note that these are actual rates, as $\sigma^\mp_{ij}\sigma^\pm_{ji}=|\langle i|\sigma^\mp|j\rangle|^2\geq 0$ and for this coupling we had previously computed $\gamma(\omega)=\Gamma(\omega)[1+n_B(\omega)]$ with spectral coupling density $\Gamma(-\omega)=-\Gamma(+\omega)$ and Bose distribution $n_B(\omega)=[e^{\beta\omega}-1]^{-1}$. This rate equation can now be treated with our usual formalism. We observe however a few non-standard things.

First, we see that to evaluate the energy current, we need to consider the energy differences of the Floquet Hamiltonian instead those of the original one and furthermore, they become shifted by multiples of the driving frequency (here just $\pm\Omega$). In particular, the diagonal entries of this rate equation may carry counting fields. Therefore, in short, a microscopic treatment of the counting field derivation is absolutely necessary.

Second, we see that the usual detailed balance relations do not even hold in the Floquet basis

$$\frac{R_{ij}(0)}{R_{ji}(0)}\neq e^{\beta(E_j-E_i)}\,. \qquad (5.76)$$

Consequently, the steady state is not a Gibbs state in the Floquet basis, which can be related to the fact that the Hamiltonians of the driving $P\sigma^+e^{-\mathrm{i}\omega t}+\mathrm{h.c.}$ and the coupling to the bath $\sigma^x\otimes B$ do not commute [14].

Third, we see that the generalized relations we demonstrated generally for the coarse-graining method do hold also in this specific case

$$\begin{aligned}
R_{ji}(-\xi+\mathrm{i}\beta) &= \sigma^-_{ji}\sigma^+_{ij}\gamma(E_i-E_j+\Omega)e^{+\mathrm{i}(-\xi+\mathrm{i}\beta)(E_i-E_j+\Omega)}+\sigma^+_{ji}\sigma^-_{ij}\gamma(E_i-E_j-\Omega)e^{+\mathrm{i}(-\xi+\mathrm{i}\beta)(E_i-E_j-\Omega)} \\
&= \sigma^-_{ij}\sigma^+_{ji}\gamma(E_j-E_i+\Omega)e^{-\beta(E_j-E_i+\Omega)}e^{+\mathrm{i}(-\xi+\mathrm{i}\beta)(E_i-E_j-\Omega)} \\
&\quad +\sigma^+_{ij}\sigma^-_{ji}\gamma(E_j-E_i-\Omega)e^{-\beta(E_j-E_i-\Omega)}e^{+\mathrm{i}(-\xi+\mathrm{i}\beta)(E_i-E_j+\Omega)} \\
&= R_{ij}(+\xi)\,, \qquad (5.77)
\end{aligned}$$

where we have used the simple KMS relation (without particle exchange) $\gamma(-\omega) = \gamma(\omega)e^{-\beta\omega}$. Therefore, with the energy exchange correctly defined, we again obtain a fluctuation theorem in presence of periodic driving

$$\lim_{t\to\infty} \frac{P_{+\omega}(t)}{P_{-\omega}(t)} = e^{+\beta\omega}\,, \tag{5.78}$$

where ω denotes the energy of the bath.

Finally, we note that due to energy conservation (first law), the work rate done on the system due to the driving must be given by minus the heat current entering the system from the reservoir.

5.2.5 Upgrade: Two-terminal driven Two-Level system

We can couple our driven system to two reservoirs $\nu \in \{L, R\}$

$$H(t) = \frac{\omega}{2}\sigma^z + P\sigma^+ e^{-\mathrm{i}\Omega t} + P^*\sigma^- e^{+\mathrm{i}\Omega t} + \sigma^x \sum_{k\nu}(h_{k\nu}b_{k\nu} + h^*_{k\nu}b^\dagger_{k\nu}) + \sum_{k\nu}\omega_{k\nu}b^\dagger_{k\nu}b_{k\nu}\,. \tag{5.79}$$

All previous calculations go through, we just get additive rates

$$\dot\rho_i = \sum_\nu \sum_j R^{(\nu)}_{ij}(\xi_\nu)\rho_j - \sum_\nu\sum_j R^{(\nu)}_{ji}(0)\rho_i\,, \tag{5.80}$$

where the rates are now explicitly given by

$$\begin{aligned} R^{(\nu)}_{ij}(\xi_\nu) \;=\; & \left|\sigma^-_{ij}\right|^2 \Gamma_\nu(E_j - E_i + \Omega)[1 + n_\nu(E_j - E_i + \Omega)]e^{+\mathrm{i}\xi_\nu(E_j - E_i + \Omega)} \\ & + \left|\sigma^+_{ij}\right|^2 \Gamma_\nu(E_j - E_i - \Omega)[1 + n_\nu(E_j - E_i - \Omega)]e^{+\mathrm{i}\xi(E_j - E_i - \Omega)}\,. \end{aligned} \tag{5.81}$$

The currents into the individual reservoirs however are now no longer conserved. Instead, the first law reads at steady state

$$\dot W = -I^{(L)}_E - I^{(R)}_E\,. \tag{5.82}$$

In contrast, without driving, the energy currents would approach

$$\bar I^{(L)}_E = -\bar I^{(R)}_E = \frac{\Gamma_L(\omega)\Gamma_R(\omega)}{\Gamma_L(\omega)[1 + 2n_L(\omega)] + \Gamma_R(\omega)[1 + 2n_R(\omega)]}\omega[n_L(\omega) - n_R(\omega)]\,. \tag{5.83}$$

This is illustrated in Fig. 5.2, exemplified for a spectral coupling density of the form

$$\Gamma_\nu(\omega) = \frac{4\Gamma_\nu\omega\delta^2_\nu\epsilon_\nu}{\omega^4 + 2\omega^2(\delta_\nu - \epsilon_\nu)(\delta_\nu + \epsilon_\nu) + (\delta^2_\nu + \epsilon^2_\nu)^2} = -\Gamma_\nu(-\omega)\,. \tag{5.84}$$

One can see that finite driving strength implies a mismatch between the energy currents. From the individual symmetry of the generalized rates $R_{ij}(\xi_L, \xi_R) = R^{(L)}_{ij}(\xi_L) + R^{(R)}_{ij}(\xi_R)$,

$$R_{ji}(-\xi_L + \mathrm{i}\beta_L, -\xi_R + \mathrm{i}\beta_R) \;=\; R_{ij}(+\xi_L, +\xi_R) \tag{5.85}$$

we do thus get a fluctuation theorem, which can however not be expressed by only looking at the heat exchanged with one reservoir.

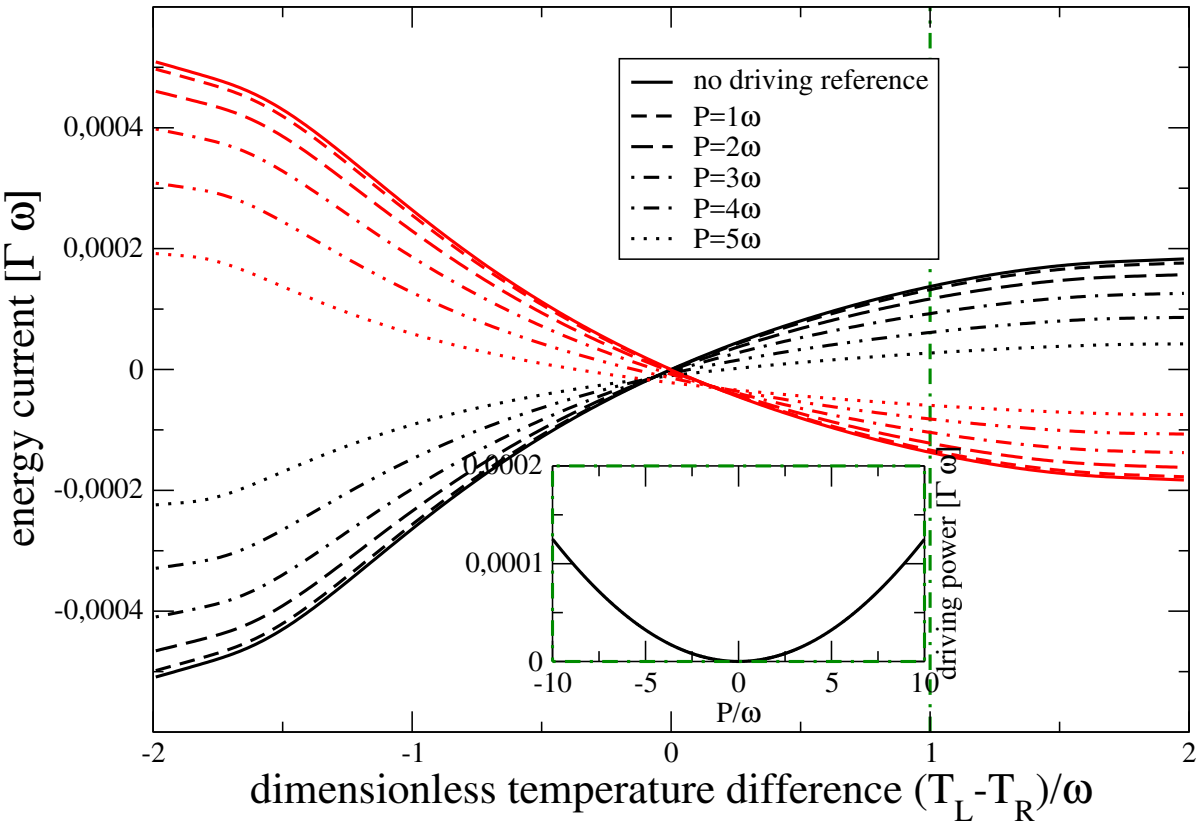

Figure 5.2: Plot of the energy currents entering the system from the left (black) and right (red) reservoirs for different values of the driving amplitude P (legend). Without driving ($P = 0$, solid), the currents reproduce Eq. (5.83), such that their sum must cancel. For finite driving, the observed mismatch $P = -I_E^{(L)} - I_E^{(R)}$ denotes the work performed on the system (inset taken at $T_L - T_R = \omega$, vertical dash-dotted line). Parameters: $\Gamma_\nu = \Gamma$, $(T_L + T_R)/(2\omega) = 1$, $\epsilon_L = 10\omega$, $\epsilon_R = 20\omega$, $\delta_L = \delta_R = \omega$, $\Omega = 100\omega$.

5.2.6 Driven cavity master equation

Let us consider the example before with bosonic operators

$$H(t) = \omega a^\dagger a + P e^{+\mathrm{i}\Omega t} a + P^* e^{-\mathrm{i}\Omega t} a^\dagger + (a + a^\dagger) \otimes \sum_k (h_k b_k + h_k^* b_k^\dagger) + \sum_k \omega_k b_k^\dagger b_k \,. \tag{5.86}$$

In Eq. (5.31), we had already derived the time evolution operator of the system, such that now, we want to investigate how the coupling operators transfer into the interaction picture

$$\begin{aligned} \boldsymbol{a}(t) &= e^{+\mathrm{i}[(\omega-\Omega)a^\dagger a + Pa + P^* a^\dagger]t} e^{+\mathrm{i}\Omega a^\dagger a t} a e^{-\mathrm{i}\Omega a^\dagger a t} e^{-\mathrm{i}[(\omega-\Omega)a^\dagger a + Pa + P^* a^\dagger]t} \\ &= e^{-\mathrm{i}\Omega t} e^{+\mathrm{i}[(\omega-\Omega)a^\dagger a + Pa + P^* a^\dagger]t} a e^{-\mathrm{i}[(\omega-\Omega)a^\dagger a + Pa + P^* a^\dagger]t} \\ &= e^{-\mathrm{i}\Omega t} \tilde{a}(t) \,. \end{aligned} \tag{5.87}$$

For the new operator we get the differential equation

$$\dot{\tilde{a}} = -\mathrm{i}(\omega - \Omega)\tilde{a}(t) - \mathrm{i}P^* \mathbf{1} \,, \tag{5.88}$$

which we would like to solve with the initial condition $\tilde{a}(0) = a$. Eventually, we get

$$\tilde{a}(t) = e^{-\mathrm{i}(\omega-\Omega)t} a - \frac{P^*}{\omega - \Omega} \left(1 - e^{-\mathrm{i}(\omega-\Omega)t}\right) \,. \tag{5.89}$$

Exercise 41 (Check)**.** *Reproduce the solution above.*

Combining this with our previous calculations we eventually get

$$\begin{aligned}\boldsymbol{a}(t) &= e^{-\mathrm{i}\Omega t}\left[e^{-\mathrm{i}(\omega-\Omega)t}a - \frac{P^*}{\omega-\Omega}\left(1-e^{-\mathrm{i}(\omega-\Omega)t}\right)\right] = e^{-\mathrm{i}\omega t}a - \frac{P^*}{\omega-\Omega}\left(e^{-\mathrm{i}\Omega t}-e^{-\mathrm{i}\omega t}\right)\\ &= e^{-\mathrm{i}\omega t}\left[a+\frac{P^*}{\omega-\Omega}\right] - \frac{P^*}{\omega-\Omega}e^{-\mathrm{i}\Omega t}\\ &= e^{-\mathrm{i}\omega t}b - \frac{P^*}{\omega-\Omega}e^{-\mathrm{i}\Omega t}\,, \end{aligned} \tag{5.90}$$

which can be expressed by a displaced annihilation operator b, which obviously satisfies the same commutation relations. We note that this remains well-defined also at resonant driving $\Omega \to \omega$, but then $\boldsymbol{a}(t)$ grows linearly in time. Therefore, perturbation theory is no longer applicable for (near) resonant driving. The Bohr frequencies of the Floquet Hamiltonian are integer multiples of $(\omega-\Omega)$, such that we have reproduced the usual Floquet representation of the coupling operator.

Exercise 42 (Bohr frequencies)**.** *Compute the transition frequencies of the Floquet Hamiltonian* $\bar{H} = (\omega-\Omega)a^\dagger a + Pa + P^*a^\dagger$.

Therefore, our total coupling operator becomes

$$\boldsymbol{A}(t) = e^{-\mathrm{i}\omega t}b + e^{+\mathrm{i}\omega t}b^\dagger - \frac{P^*}{\omega-\Omega}e^{-\mathrm{i}\Omega t} - \frac{P}{\omega-\Omega}e^{+\mathrm{i}\Omega t}\,. \tag{5.91}$$

These are the ones we need to use in our coarse-graining master equation

$$\begin{aligned}\dot{\boldsymbol{\rho}}_{\mathbf{S}} &= -\mathrm{i}\left[\frac{1}{2\mathrm{i}\tau}\int_0^\tau dt_1\int_0^\tau dt_2 C^0(t_1-t_2)\mathrm{sgn}(\mathrm{t}_1-\mathrm{t}_2)\boldsymbol{A}(\mathrm{t}_1)\boldsymbol{A}(\mathrm{t}_2),\boldsymbol{\rho}_{\mathbf{S}}\right]\\ &\quad + \frac{1}{\tau}\int_0^\tau dt_1\int_0^\tau dt_2\left[C^0(t_1-t_2-\xi)\boldsymbol{A}(t_2)\boldsymbol{\rho}_{\mathbf{S}}\boldsymbol{A}(t_1) - \frac{C^0(t_1-t_2)}{2}\left\{\boldsymbol{A}(t_1)\boldsymbol{A}(t_2),\boldsymbol{\rho}_{\mathbf{S}}\right\}\right]\\ &\equiv -\mathrm{i}\left[\frac{1}{2\mathrm{i}}\int d\bar{\omega}\sigma(\bar{\omega})\eta_1(\tau),\boldsymbol{\rho}_{\mathbf{S}}\right] + \int d\bar{\omega}\gamma(\bar{\omega})\left[e^{+\mathrm{i}\bar{\omega}\xi}\eta_2(\tau,\boldsymbol{\rho}_{\mathbf{S}}) - \frac{1}{2}\left\{\eta_1(\tau),\boldsymbol{\rho}_{\mathbf{S}}\right\}\right]. \end{aligned} \tag{5.92}$$

Here, we have defined

$$\begin{aligned}\eta_1(\tau) &= \frac{1}{2\pi\tau}\int_0^\tau dt_1dt_2e^{-\mathrm{i}\bar{\omega}(t_1-t_2)}\left[e^{-\mathrm{i}\omega t_1}b + e^{+\mathrm{i}\omega t_1}b^\dagger - \frac{P^*}{\omega-\Omega}e^{-\mathrm{i}\Omega t_1} - \frac{P}{\omega-\Omega}e^{+\mathrm{i}\Omega t_1}\right]\times\\ &\quad\times\left[e^{-\mathrm{i}\omega t_2}b + e^{+\mathrm{i}\omega t_2}b^\dagger - \frac{P^*}{\omega-\Omega}e^{-\mathrm{i}\Omega t_2} - \frac{P}{\omega-\Omega}e^{+\mathrm{i}\Omega t_2}\right]\\ \eta_2(\tau,\boldsymbol{\rho}_{\mathbf{S}}) &= \frac{1}{2\pi\tau}\int_0^\tau dt_1dt_2e^{-\mathrm{i}\bar{\omega}(t_1-t_2)}\left[e^{-\mathrm{i}\omega t_2}b + e^{+\mathrm{i}\omega t_2}b^\dagger - \frac{P^*}{\omega-\Omega}e^{-\mathrm{i}\Omega t_2} - \frac{P}{\omega-\Omega}e^{+\mathrm{i}\Omega t_2}\right]\boldsymbol{\rho}_{\mathbf{S}}\times\\ &\quad\left[e^{-\mathrm{i}\omega t_1}b + e^{+\mathrm{i}\omega t_1}b^\dagger - \frac{P^*}{\omega-\Omega}e^{-\mathrm{i}\Omega t_1} - \frac{P}{\omega-\Omega}e^{+\mathrm{i}\Omega t_1}\right] \end{aligned} \tag{5.93}$$

Very fast driving

To obtain a simple discussion, let us first consider the limit of very fast driving $\Omega \gg \omega$ and large coarse-graining times $\tau \to \infty$, where we can directly neglect many terms in $\eta_1(\tau)$ and $\eta_2(\tau, \boldsymbol{\rho}_{\mathbf{S}})$, namely all those that are of $\mathcal{O}\{\Omega^{-1}\}$. This yields by invoking the relations (5.71) for the coefficients

$$\begin{aligned} \eta_1(\tau) &\approx \frac{\tau}{2\pi}\mathrm{sinc}^2\left[(\bar{\omega}+\omega)\frac{\tau}{2}\right] bb^\dagger + \frac{\tau}{2\pi}\mathrm{sinc}^2\left[(\bar{\omega}-\omega)\frac{\tau}{2}\right] b^\dagger b\,, \\ \eta_2(\tau, \boldsymbol{\rho}_{\mathbf{S}}) &\approx \frac{\tau}{2\pi}\mathrm{sinc}^2\left[(\bar{\omega}+\omega)\frac{\tau}{2}\right] b^\dagger \boldsymbol{\rho}_{\mathbf{S}} b + \frac{\tau}{2\pi}\mathrm{sinc}^2\left[(\bar{\omega}-\omega)\frac{\tau}{2}\right] b \boldsymbol{\rho}_{\mathbf{S}} b^\dagger\,. \end{aligned} \tag{5.94}$$

Eventually, we get for $\tau \to \infty$ and using that in this limit $b \approx a$ the simple master equation

$$\begin{aligned} \dot{\boldsymbol{\rho}}_{\mathbf{S}} &= -\mathrm{i}\left[\frac{1}{2\mathrm{i}}\left[\sigma(-\omega)aa^\dagger + \sigma(+\omega)a^\dagger a, \boldsymbol{\rho}_{\mathbf{S}}\right]\right] \\ &\quad +\gamma(+\omega)\left[e^{+\mathrm{i}\omega\xi} a\boldsymbol{\rho}_{\mathbf{S}}a^\dagger - \frac{1}{2}\left\{a^\dagger a, \boldsymbol{\rho}_{\mathbf{S}}\right\}\right] + \gamma(-\omega)\left[e^{-\mathrm{i}\omega\xi} a^\dagger\boldsymbol{\rho}_{\mathbf{S}}a - \frac{1}{2}\left\{aa^\dagger, \boldsymbol{\rho}_{\mathbf{S}}\right\}\right]\,. \end{aligned} \tag{5.95}$$

Upon neglecting the Lamb-shift $\sigma(\omega) \to 0$ and considering the zero-temperature limit $\gamma(\omega) \to \Gamma(\omega)$ and $\gamma(-\omega) \to 0$, this reduces to

$$\dot{\boldsymbol{\rho}}_{\mathbf{S}} = \Gamma(\omega)\left[e^{+\mathrm{i}\omega\xi} a\boldsymbol{\rho}_{\mathbf{S}}a^\dagger - \frac{1}{2}\left\{a^\dagger a, \boldsymbol{\rho}_{\mathbf{S}}\right\}\right]\,. \tag{5.96}$$

Finally, we can switch back to the Schrödinger picture (using the same fast driving assumptions that we have already used, this only amounts to adding the commutator with the system Hamiltonian, and we get

$$\dot{\rho}_{\mathrm{S}} = -\mathrm{i}\left[\omega a^\dagger a + Pe^{+\mathrm{i}\Omega t}a + P^* e^{-\mathrm{i}\Omega t}a^\dagger, \rho_{\mathrm{S}}\right] + \Gamma(\omega)\left[e^{+\mathrm{i}\omega\xi} a\rho_{\mathrm{S}}a^\dagger - \frac{1}{2}\left\{a^\dagger a, \rho_{\mathrm{S}}\right\}\right]\,. \tag{5.97}$$

Up to the necessary replacements $P \to P/2$ and $\Gamma(\omega) \to \gamma$ (compare the different system Hamiltonians), we recover the phenomenologically introduced master equation from our introduction (1.38) when in addition $\xi \to 0$.

Let us in this simple case compute the microscopically derived energy current, adopting the convention that it counts positively when leaving the reservoir

$$\begin{aligned} I_E(t) &= +\mathrm{i}\partial_\chi \frac{d}{dt}\mathrm{Tr}\left\{e^{\mathcal{L}(\chi)t}\rho_0\right\}\Big|_{\chi=0} = (+\mathrm{i}\partial_\chi)\mathrm{Tr}\left\{\mathcal{L}(\chi)e^{\mathcal{L}(\chi)t}\rho_0\right\}\Big|_{\chi=0} \\ &= +\mathrm{i}\mathrm{Tr}\left\{\mathcal{L}'(0)e^{\mathcal{L}(0)t}\rho_0\right\} + \mathrm{i}\mathrm{Tr}\left\{\mathcal{L}(0)\left(\partial_\chi e^{\mathcal{L}(\chi)t}\Big|_{\chi=0}\right)\rho_0\right\} \\ &= +\mathrm{i}\mathrm{Tr}\left\{\mathcal{L}'(0)\rho(t)\right\} = -\omega\Gamma(\omega)\mathrm{Tr}\left\{a^\dagger a\rho(t)\right\}\,. \end{aligned} \tag{5.98}$$

For large times, we have shown that this will approach a stationary value.

Alternatively, we could have computed the energy current entering the system with the phenomenologic approach of Eq. (3.19)

$$\begin{aligned} I_E^{\mathrm{ph}}(t) &= \mathrm{Tr}\left\{H_S(t)\Gamma(\omega)\left[a\rho_{\mathrm{S}}a^\dagger - \frac{1}{2}\left\{a^\dagger a, \rho_{\mathrm{S}}\right\}\right]\right\} \\ &= \Gamma(\omega)\mathrm{Tr}\left\{\left[\omega a^\dagger a + Pe^{+\mathrm{i}\Omega t}a + P^* e^{-\mathrm{i}\Omega t}a^\dagger\right]\left[a\rho_{\mathrm{S}}a^\dagger - \frac{1}{2}\left\{a^\dagger a, \rho_{\mathrm{S}}\right\}\right]\right\} \\ &= -\omega\Gamma(\omega)\mathrm{Tr}\left\{a^\dagger a\rho(t)\right\} - \frac{P\Gamma(\omega)}{2}e^{+\mathrm{i}\Omega t}\mathrm{Tr}\left\{a\rho(t)\right\} - \frac{P^*\Gamma(\omega)}{2}e^{-\mathrm{i}\Omega t}\mathrm{Tr}\left\{a^\dagger\rho(t)\right\}\,. \end{aligned} \tag{5.99}$$

The expectation values of a and $a^\dagger$ do not vanish (see one of our early exercises), such that the two currents do not agree $I_E(t) \neq I_E^{\rm ph}(t)$. This should not be too surprising, as the basis of the first current was the negative energy change in the reservoir, whereas the basis of the second is the positive energy change in the system. Their long-term integral however should not differ (the interaction Hamiltonian should not host ever-increasing amounts of energy), and indeed we see that by averaging over one period the two currents would coincide, since all expectation values in the above equation approach stationary values.

Very slow Driving

Now, we consider the limit of very slow driving $\Omega \ll \omega$, where we get approximately

$$\begin{aligned}
\eta_1(\tau) &\approx \frac{\tau}{2\pi}\mathrm{sinc}^2\left[(\bar\omega+\omega)\frac{\tau}{2}\right] bb^\dagger + \frac{\tau}{2\pi}\mathrm{sinc}^2\left[(\bar\omega-\omega)\frac{\tau}{2}\right] b^\dagger b + \frac{\tau}{2\pi}\mathrm{sinc}^2\left[\bar\omega\frac{\tau}{2}\right]\frac{(P+P^*)^2}{(\omega-\Omega)^2}\,,\\
\eta_2(\tau,\boldsymbol{\rho}_{\mathbf{S}}) &\approx \frac{\tau}{2\pi}\mathrm{sinc}^2\left[(\bar\omega+\omega)\frac{\tau}{2}\right] b^\dagger\boldsymbol{\rho}_{\mathbf{S}} b + \frac{\tau}{2\pi}\mathrm{sinc}^2\left[(\bar\omega-\omega)\frac{\tau}{2}\right] b\boldsymbol{\rho}_{\mathbf{S}} b^\dagger\\
&\quad + \frac{\tau}{2\pi}\mathrm{sinc}^2\left[\bar\omega\frac{\tau}{2}\right]\frac{(P+P^*)^2}{(\omega-\Omega)^2}\boldsymbol{\rho}_{\mathbf{S}}\,. \qquad (5.100)
\end{aligned}$$

All the terms proportional to the identity vanish in the master equation for large coarse-graining times τ, and we obtain

$$\begin{aligned}
\dot{\boldsymbol{\rho}}_{\mathbf{S}} &= -\mathrm{i}\left[\frac{\sigma(-\omega)}{2\mathrm{i}}bb^\dagger + \frac{\sigma(+\omega)}{2\mathrm{i}}b^\dagger b, \boldsymbol{\rho}_{\mathbf{S}}\right]\\
&\quad + \gamma(+\omega)\left[e^{+\mathrm{i}\omega\xi}b\boldsymbol{\rho}_{\mathbf{S}}b^\dagger - \frac{1}{2}\left\{b^\dagger b, \boldsymbol{\rho}_{\mathbf{S}}\right\}\right] + \gamma(-\omega)\left[e^{-\mathrm{i}\omega\xi}b^\dagger\boldsymbol{\rho}_{\mathbf{S}}b - \frac{1}{2}\left\{bb^\dagger, \boldsymbol{\rho}_{\mathbf{S}}\right\}\right]\,. \qquad (5.101)
\end{aligned}$$

In the limit of slow driving, we can approximate $b \approx a + \frac{P^*}{\omega}$, and we see that the resulting master equation is not the same as the one that we used phenomenologically. The full transformation into the interaction picture was given by

$$U(t) = e^{-\mathrm{i}\Omega a^\dagger a t}e^{-\mathrm{i}\left[(\omega-\Omega)a^\dagger a + Pa + P^*a^\dagger\right]t}\,, \qquad (5.102)$$

from which we get for the inverse transformation

$$\begin{aligned}
U(t)aU^\dagger(t) &= e^{-\mathrm{i}\Omega a^\dagger a t}\left[ae^{+\mathrm{i}(\omega-\Omega)t} + \frac{P^*}{(\omega-\Omega)}\left(e^{+\mathrm{i}(\omega-\Omega)t}-1\right)\right]e^{+\mathrm{i}\Omega a^\dagger a t}\\
&= ae^{+\mathrm{i}\omega t} + \frac{P^*}{(\omega-\Omega)}\left(e^{+\mathrm{i}(\omega-\Omega)t}-1\right)\,,\\
U(t)bU^\dagger(t) &= e^{+\mathrm{i}\omega t}\left[a + \frac{P^*}{\omega-\Omega}e^{-\mathrm{i}\Omega t}\right] \approx e^{+\mathrm{i}\omega t}\left[a + \frac{P^*}{\omega}e^{-\mathrm{i}\Omega t}\right]\,. \qquad (5.103)
\end{aligned}$$

This implies that in the original Schrödinger picture, we get (neglecting the Lamb-shift $\sigma(\pm\omega) \to 0$)

$$\begin{aligned}
\dot{\rho}_{\rm S} &= -{\rm i}\left[\omega a^\dagger a + Pae^{+{\rm i}\Omega t} + P^* a^\dagger e^{-{\rm i}\Omega t}, \rho_{\rm S}\right] \\
&\quad +\gamma(+\omega)\left[e^{+{\rm i}\omega\xi}\left(a + \frac{P^*}{\omega}e^{-{\rm i}\Omega t}\right)\rho_{\rm S}\left(a^\dagger + \frac{P}{\omega}e^{+{\rm i}\Omega t}\right) - \frac{1}{2}\left\{\left(a^\dagger + \frac{P}{\omega}e^{+{\rm i}\Omega t}\right)\left(a + \frac{P^*}{\omega}e^{-{\rm i}\Omega t}\right), \rho_{\rm S}\right\}\right] \\
&\quad +\gamma(-\omega)\left[e^{-{\rm i}\omega\xi}\left(a^\dagger + \frac{P}{\omega}e^{+{\rm i}\Omega t}\right)\rho_{\rm S}\left(a + \frac{P^*}{\omega}e^{-{\rm i}\Omega t}\right) - \frac{1}{2}\left\{\left(a + \frac{P^*}{\omega}e^{-{\rm i}\Omega t}\right)\left(a^\dagger + \frac{P}{\omega}e^{+{\rm i}\Omega t}\right), \rho_{\rm S}\right\}\right] \\
&= -{\rm i}\left[\omega c^\dagger(t)c(t), \rho_{\rm S}\right] \qquad (5.104) \\
&\quad +\gamma(+\omega)\left[e^{+{\rm i}\omega\xi}c(t)\rho_{\rm S}c^\dagger(t) - \frac{1}{2}\left\{c^\dagger(t)c(t), \rho_{\rm S}\right\}\right] + \gamma(-\omega)\left[e^{-{\rm i}\omega\xi}c^\dagger(t)\rho_{\rm S}c(t) - \frac{1}{2}\left\{c(t)c^\dagger(t), \rho_{\rm S}\right\}\right],
\end{aligned}$$

where we have defined $c(t) = a + \frac{P^*}{\omega}e^{-{\rm i}\Omega t}$ (in the Hamiltonian, the commutator with the identity will always vanish). We note that $c(t)$ obeys the canonical commutation relations. We further see that for slow driving, the master equation always tends to equilibrate in the time-dependent Gibbs state of the system, i.e., $\rho(t) \propto e^{-\beta\omega c^\dagger(t)c(t)}$ is a time-local stationary state of the master equation, and the framework of Sec. 3.3 applies.

We can now compare the microscopic and phenomenologic currents. The microscopic energy current of the reservoir becomes (we use the convention that it counts positive when leaving the reservoir)

$$\begin{aligned}
I_E(t) &= {\rm i}{\rm Tr}\left\{\mathcal{L}'(0)\rho_{\rm S}(t)\right\} \\
&= \omega\gamma(-\omega){\rm Tr}\left\{c(t)c^\dagger(t)\rho_{\rm S}(t)\right\} - \omega\gamma(+\omega){\rm Tr}\left\{c^\dagger(t)c(t)\rho_{\rm S}(t)\right\}. \qquad (5.105)
\end{aligned}$$

Similarly, the phenomenologic energy current entering the system yields

$$\begin{aligned}
I_E^{\rm ph}(t) &= \omega\gamma(+\omega){\rm Tr}\left\{c^\dagger(t)c(t)\left[c(t)\rho_{\rm S}c^\dagger(t) - \frac{1}{2}\left\{c^\dagger(t)c(t), \rho_{\rm S}\right\}\right]\right\} \\
&\quad +\omega\gamma(-\omega){\rm Tr}\left\{c^\dagger(t)c(t)\left[c^\dagger(t)\rho_{\rm S}c(t) - \frac{1}{2}\left\{c(t)c^\dagger(t), \rho_{\rm S}\right\}\right]\right\} \\
&= -\omega\gamma(+\omega){\rm Tr}\left\{c^\dagger(t)c(t)\rho_{\rm S}\right\} + \omega\gamma(-\omega){\rm Tr}\left\{c(t)c^\dagger(t)\rho_{\rm S}\right\}. \qquad (5.106)
\end{aligned}$$

Therefore, we see that for slow driving, the microscopic energy current out of the reservoir and the phenomenologic energy current entering the system coincide $I_E^{\rm ph}(t) = I_E(t)$.

Chapter 6

Feedback control

6.1 External feedback

In this section, we will first discuss theoretical approaches to continuous feedback control schemes. Repeated measurements are performed on the system, and conditioned control actions are then applied. The presented schemes are by far not complete but already cover some quite useful overview of feedback schemes.

6.1.1 Piecewise-Constant feedback

Closed-loop (or feedback) control means that the system is monitored (either continuously or at certain times) and that the result of these measurements is fed back by changing some parameter of the system. Under measurement with outcome m (an index characterizing the possible outcomes), the density matrix transforms as

$$\rho \xrightarrow{m} \frac{M_m \rho M_m^\dagger}{\mathrm{Tr}\left\{M_m^\dagger M_m \rho\right\}}\,, \tag{6.1}$$

and the probability at which this outcome occurs is given by $\mathrm{Tr}\left\{M_m^\dagger M_m \rho\right\} = \mathrm{Tr}\left\{M_m \rho M_m^\dagger\right\}$. This can also be written in superoperator notation ($\mathcal{M}_m\rho \hat{=} M_m \rho M_m^\dagger$)

$$\rho \xrightarrow{m} \frac{\mathcal{M}_m \rho}{\mathrm{Tr}\left\{\mathcal{M}_m \rho\right\}}\,. \tag{6.2}$$

Let us assume that conditioned on the measurement result m at time t, we apply a propagator for the time interval Δt. Then, a measurement result m at time t provided, the density matrix at time $t + \Delta t$ will be given by

$$\rho^{(m)}(t + \Delta t) = e^{\mathcal{L}^{(m)}\Delta t} \frac{\mathcal{M}_m \rho}{\mathrm{Tr}\left\{\mathcal{M}_m \rho\right\}}\,. \tag{6.3}$$

However, to obtain an effective description of the density matrix evolution, we have to average over all measurement outcomes – where we have to weight each outcome by the corresponding probability

$$\rho(t + \Delta t) = \sum_m \mathrm{Tr}\left\{\mathcal{M}_m \rho(t)\right\} e^{\mathcal{L}^{(m)}\Delta t} \frac{\mathcal{M}_m \rho}{\mathrm{Tr}\left\{\mathcal{M}_m \rho\right\}} = \sum_m e^{\mathcal{L}_m \Delta t} \mathcal{M}_m \rho(t)\,. \tag{6.4}$$

Note that this is an iteration scheme and not a conventional master equation. More generally – not constraining the conditioned dynamics to Lindblad evolutions – one could also write

$$\rho(t+\Delta t) = \sum_m \mathcal{K}^{(m)}(\Delta t)\mathcal{M}_m\rho(t)\,, \tag{6.5}$$

where $\mathcal{K}^{(m)}(\Delta t)\rho \hat{=} \sum_\alpha K_\alpha^{(m)}(\Delta t)\rho K_\alpha^{(m)\dagger}(\Delta t)$ with $\sum_\alpha K_\alpha^{(m)\dagger}K_\alpha^{(m)} = \mathbf{1}$ is a conditioned Kraus map. Furthermore, the conditioned Liouvillian $\mathcal{L}^{(m)}$ or the Kraus map $\mathcal{K}^{(m)}$ may well depend on the time t (at which the measurement is performed) as long as it is constant during the interval $[t, t+\Delta t]$, and on the width of the time interval Δt.

Continuous feedback limit

Expanding now the exponential of the Liouvillian in the limit of a continuous feedback control scheme $\Delta t \to 0$, we obtain

$$\rho(t+\Delta t) = \sum_m \mathcal{M}_m\rho(t) + \Delta t \sum_m \mathcal{L}_m\mathcal{M}_m\rho(t)\,. \tag{6.6}$$

In particular, when $\sum_m \mathcal{M}_m = \mathbf{1}$ holds, we can form a difference quotient on the l.h.s., which as $\Delta t \to 0$ yields an effective Liouvillian under feedback control

$$\mathcal{L}_{\rm fb}\rho = \lim_{\Delta t\to 0}\frac{\rho(t+\Delta t)-\rho(t)}{\Delta t} = \sum_m \mathcal{L}_m\mathcal{M}_m\,. \tag{6.7}$$

Def. 18 (Weak measurement feedback Liouvillian)**.** *For measurement superoperators obeying* $\sum_m \mathcal{M}_m = \mathbf{1}$ *the effective continuous feedback master equation reads*

$$\mathcal{L}_{\rm fb} = \sum_m \mathcal{L}_m\mathcal{M}_m\,, \tag{6.8}$$

where $\mathcal{L}_m$ *is the conditional Lindblad evolution and* $\mathcal{M}_m$ *describes the measurement action corresponding to outcome* m*.*

Unfortunately, the condition $\sum_m \mathcal{M}_m = \mathbf{1}$ will only hold for special cases. Physically, this results from the fact that a quantum measurement always has an effect on the system – independent of whether conditioned control actions or not take place. When it does not hold, an effective Liouvillian under feedback control does not exist, and the evolution is described rather by an iteration of the form (6.4) or (6.5). However, very often a weaker condition can be fulfilled, namely that the measurement superoperators have projector properties

$$\mathcal{M}_m\mathcal{M}_n = \mathcal{M}_m\delta_{mn}\,. \tag{6.9}$$

From this, we can conclude that

$$\frac{\sum_m \mathcal{M}_m\rho(t+\Delta t) - \sum_m \mathcal{M}_m\rho(t)}{\Delta t} = \sum_n \mathcal{M}_n \sum_m \mathcal{L}_m\mathcal{M}_m\rho(t)\,, \tag{6.10}$$

which we can turn into a master equation for the projected part of the density matrix

$$\tilde{\rho}(t) = \sum_m \mathcal{M}_m \rho(t)\,. \tag{6.11}$$

We can furthermore again insert this sum of all superoperators at the right of each superoperator $\mathcal{M}_m$, since $\mathcal{M}_m = \mathcal{M}_m \sum_n \mathcal{M}_n$, without changing the dynamics. This defines an effective feedback master equation for projective measurements.

Def. 19 (Feedback Liouvillian for projective measurements)**.** *For projective measurements $\mathcal{M}_m\mathcal{M}_n = \mathcal{M}_m\delta_{mn}$, the projected density matrix $\bar{\rho} = \sum_n \mathcal{M}_n\rho$ obeys the feedback master equation*

$$\dot{\tilde{\rho}} = \mathcal{L}_{\rm fb}\tilde{\rho}\,, \qquad \mathcal{L}_{\rm fb} = \sum_n \mathcal{M}_n \sum_m \mathcal{L}_m\mathcal{M}_m\,. \tag{6.12}$$

We note that $\mathcal{L}_{\rm fb}$ typically only acts in a particular subspace. When considered for the full system, it will become multistable. For example, considering projective measurements $\mathcal{M}_m\rho \hat{=} |m\rangle\langle m|\,\rho\,|m\rangle\langle m|$, and one particular stationary state $\mathcal{L}_{\rm fb}\bar{\rho} = 0$, we see that we can add arbitrary coherences $\bar{\rho}' = \bar{\rho} + \sum_{n\neq m}\alpha_{nm}|n\rangle\langle m|$, and will obtain another stationary state $\mathcal{L}_{\rm fb}\bar{\rho}' = 0$, since these additional terms will vanish under the projective measurements.

6.1.2 Wiseman-Milburn feedback

A special case of the weak measurement feedback discussed before arises when we consider bipartite systems, composed of subsystems A and B, where we perform strong projective measurements only on the subsystem B. From the perspective of the total system, such measurements will not be fully projective and will therefore appear as weak measurements. Let us therefore denote the density matrix of the compound system by

$$\sigma(t) = \sum_{nm} \rho^{(nm)}(t) \otimes |n\rangle\langle m|\,, \tag{6.13}$$

where the $|n\rangle$ label a particular basis in the Hilbert space of subsystem B, and correspondingly, $\rho^{(nm)}(t)$ is a conditional density matrix in subsystem A. Furthermore, we will assume that the diagonal conditional density matrices $\rho^{(n)}(t) \equiv \rho^{(nn)}(t)$ follow a conditional master equation

$$\dot{\rho}^{(n)}(t) = \mathcal{L}_0\rho^{(n)}(t) + \mathcal{L}_+\rho^{(n-1)}(t) + \mathcal{L}_-\rho^{(n+1)}(t)\,, \tag{6.14}$$

which occurs, for example, quite naturally in problems of Full Counting Statistics, cf. Sec. 4. In this case, n actually denotes the excitations counted in a detector, which may be, for example, the number of photons emitted by a cavity or the number of electrons that have passed through a quantum dot system or a QPC. We recall that given a decomposition in terms of counting fields, such an n-resolved master equation may be obtained by performing an inverse Fourier transform

$$\rho^{(n)}(t) = \frac{1}{2\pi}\int_{-\pi}^{+\pi} \rho(\chi,t)e^{-{\rm i}n\chi}d\chi\,, \tag{6.15}$$

and by tracing over the ancilla (detector) states we recover the density matrix of the system

$$\rho(t) = \mathrm{Tr}_\mathrm{D}\left\{\sigma(t)\right\} = \sum_n \rho^{(n)}(t)\,. \tag{6.16}$$

We assume that at time t, we can write the total density matrix as $\sigma(t) = \rho(t) \otimes |0\rangle\langle 0|$, i.e., $\rho^{(nm)}(t) = \delta_{n0}\delta_{m0}\rho(t)$, which simply means that we reset our counting variable to zero after each measurement or that we use a new ancilla variable after every measurement. Then, we write the total density matrix at time $t + \Delta t$ as (neglecting terms of order Δt^2)

$$\begin{aligned}
\sigma(t+\Delta t) &= \sigma(t) + \Delta t \sum_{nm} \dot\rho^{(nm)}(t) \otimes |n\rangle\langle m| \\
&= \rho(t)\otimes|0\rangle\langle 0| + \Delta t \sum_n \dot\rho^{(n)}(t)\otimes|n\rangle\langle n| + \Delta t \sum_{n\neq m} \dot\rho^{(nm)}(t)\otimes|n\rangle\langle m| \\
&= \rho(t)\otimes|0\rangle\langle 0| + \Delta t \sum_n \left[\mathcal{L}_0\rho^{(n)}(t) + \mathcal{L}_+\rho^{(n-1)}(t) + \mathcal{L}_-\rho^{(n+1)}(t)\right]\otimes|n\rangle\langle n| \\
&\quad + \Delta t \sum_{n\neq m} \dot\rho^{(nm)}(t)\otimes|n\rangle\langle m| \\
&= \rho(t)\otimes|0\rangle\langle 0| + \Delta t\left[\mathcal{L}_0\rho(t)\otimes|0\rangle\langle 0| + \mathcal{L}_+\rho(t)\otimes|+1\rangle\langle +1| + \mathcal{L}_-\rho(t)\otimes|-1\rangle\langle -1|\right] \\
&\quad + \Delta t \sum_{n\neq m} \dot\rho^{(nm)}(t)\otimes|n\rangle\langle m|\,.
\end{aligned} \tag{6.17}$$

Here, the neglect of higher-order terms means that we consider times Δt that are so short that at most a single particle can be detected in the detector. Now, we perform a **projective** measurement of the ancilla (the particles counted by the detector) and compute the effective action of this process (dissipation plus subsequent measurement) on the reduced density matrix

$$\begin{aligned}
\mathcal{P}_0(\Delta t)\rho(t) &\equiv \mathrm{Tr}_\mathrm{D}\left\{|0\rangle\langle 0|\,\sigma(t+\Delta t)\,|0\rangle\langle 0|\right\} = \left[\mathbf{1} + \mathcal{L}_0\Delta t\right]\rho(t)\,, \\
\mathcal{P}_{-1}(\Delta t)\rho(t) &\equiv \mathrm{Tr}_\mathrm{D}\left\{|-1\rangle\langle -1|\,\sigma(t+\Delta t)\,|-1\rangle\langle -1|\right\} = \mathcal{L}_-\Delta t\rho(t)\,, \\
\mathcal{P}_{+1}(\Delta t)\rho(t) &\equiv \mathrm{Tr}_\mathrm{D}\left\{|+1\rangle\langle +1|\,\sigma(t+\Delta t)\,|+1\rangle\langle +1|\right\} = \mathcal{L}_+\Delta t\rho(t)\,.
\end{aligned} \tag{6.18}$$

We see that the effective propagation superoperators only approximately add up to the identity. Here, this occurs as they also contain effects of dissipation.

The basic idea of Wiseman-Milburn feedback is now to perform an instantaneous unitary rotation right after the measurement outcome $\pm$:

$$\mathcal{U}_\pm = U_\pm \rho U_\pm^\dagger\,, \tag{6.19}$$

which can be implemented as a δ-kick on the Hamiltonian $U = e^{-\mathrm{i}V}$, see Sec. 5.1.2. Upon not measuring any change of the ancilla variable (the particle detector), no control action is performed. Consequently, the feedback iteration for the density matrix becomes

$$\begin{aligned}
\rho(t+\Delta t) &= \left[\mathcal{P}_0(\Delta t) + \mathcal{U}_-\mathcal{P}_-(\Delta t) + \mathcal{U}_+\mathcal{P}_+(\Delta t)\right]\rho(t) \\
&= \left[\mathbf{1} + \Delta t\left(\mathcal{L}_0 + \mathcal{U}_+\mathcal{L}_+ + \mathcal{U}_-\mathcal{L}_-\right)\right]\rho(t)\,,
\end{aligned} \tag{6.20}$$

which yields the Wiseman-Milburn feedback Liouvillian [3].

Def. 20 (Wisemen-Milburn feedback Liouvillian)**.** *The Wiseman-Milburn Liouvillian reads*

$$\mathcal{L}_{\rm fb} = \mathcal{L}_0 + \mathcal{U}_+\mathcal{L}_+ + \mathcal{U}_-\mathcal{L}_- \,, \tag{6.21}$$

where $\mathcal{U}_\pm\rho \hat{=} U_\pm \rho U_\pm^\dagger$ *denotes the unitary control action and* $\mathcal{L}_\pm$ *the jump terms associated with particle increase (+) or decrease (-) in the detector.*

The major difference in the derivation in comparison to the previous section was that we assumed that the measurement could take finite time to complete. During this time, dissipation acts on the measured system even in absence of any control actions.

6.1.3 Application: Stabilization of Fock states

We start from the master equation of a cavity coupled to a thermal bath

$$\begin{aligned}\dot\rho &= -\mathrm{i}\left[\Omega a^\dagger a, \rho\right] \\ &\quad +\Gamma(1+n_B)\left[e^{+\mathrm{i}\chi} a\rho a^\dagger - \frac{1}{2}\left\{a^\dagger a, \rho\right\}\right] + \Gamma n_B\left[e^{-\mathrm{i}\chi} a^\dagger\rho a - \frac{1}{2}\left\{aa^\dagger, \rho\right\}\right] ,\end{aligned} \tag{6.22}$$

which we have already presented in Sec. 1.3.1, and which is here just equipped with an additional counting field χ for the number of emitted or absorbed photons. Without any measurements and feedback, the stationary state of this master equation is just a statistical mixture of energy eigenstates. In particular at large temperatures, this is not a pure state but highly mixed.

Now, acting with different unitary operations whenever a photon is emitted U_+ (simple detection with a click of a photo-detector) or absorbed from the system (this is more difficult, we would need to shine light on the system and then infer the absorption from the absence of a click in a photodetector placed on the other side), we would obtain the effective feedback master equation

$$\begin{aligned}\dot\rho &= -\mathrm{i}\left[\Omega a^\dagger a, \rho\right] \\ &\quad +\Gamma(1+n_B)\left[U_+ a\rho a^\dagger U_+^\dagger - \frac{1}{2}\left\{a^\dagger a, \rho\right\}\right] + \Gamma n_B\left[U_- a^\dagger\rho a U_-^\dagger - \frac{1}{2}\left\{aa^\dagger, \rho\right\}\right] \\ &= -\mathrm{i}H_{\rm eff}\rho + \mathrm{i}\rho H_{\rm eff}^\dagger + \Gamma(1+n_B)U_+ a\rho a^\dagger U_+^\dagger + \Gamma n_B U_- a^\dagger\rho a U_- \,,\end{aligned} \tag{6.23}$$

where we have defined the **effective non-Hermitian Hamiltonian**

$$H_{\rm eff} = \Omega a^\dagger a - \mathrm{i}\frac{\Gamma}{2}(1+n_B)a^\dagger a - \mathrm{i}\frac{\Gamma}{2}n_B aa^\dagger \,. \tag{6.24}$$

Clearly, the Fock states are eigenstates of $H_{\rm eff}$

$$\begin{aligned} H_{\rm eff}\left|m\right\rangle &= \Omega m - \mathrm{i}\frac{\Gamma}{2}(1+n_B)m - \mathrm{i}\frac{\Gamma}{2}n_B(1+m) \,, \\ \left\langle m\right| H_{\rm eff}^\dagger &= \Omega m + \mathrm{i}\frac{\Gamma}{2}(1+n_B)m + \mathrm{i}\frac{\Gamma}{2}n_B(1+m) \,. \end{aligned} \tag{6.25}$$

We can now ask what unitary operations one needs to apply to stabilize a particular particle number eigenstate $\bar\rho = \left|m\right\rangle\left\langle m\right|$. Inserting this in the master equation yields the condition

$$\begin{aligned} 0 &= \left[-\Gamma(1+n_B)m - \Gamma n_B(1+m)\right]\left|m\right\rangle\left\langle m\right| \\ &\quad +\Gamma(1+n_B)mU_+\left|m-1\right\rangle\left\langle m-1\right|U_+^\dagger + \Gamma n_B(m+1)U_-\left|m+1\right\rangle\left\langle m+1\right|U_-^\dagger \,, \end{aligned} \tag{6.26}$$

which can be fulfilled by unitary control operations obeying

$$U_+ |m-1\rangle = |m\rangle \ , \qquad U_- |m+1\rangle = |m\rangle \ . \tag{6.27}$$

There are many unitaries fulfilling this condition, but their actual implementation may be hard. Generally, the decomposition into an effective non-hermitian Hamiltonian and its eigenstates may be helpful to find suitable control actions for obtaining pure stationary states [16].

6.2 Maxwell's demon

Maxwell invented his famous demon as a thought experiment to demonstrate that thermodynamics is a macroscopic effective theory: An intelligent being (the demon) living in a box is measuring the speed of molecules of some gas in the box. An initial thermal distribution of molecules implies that the molecules have different velocities. The demon measures the velocities and inserts an impermeable wall whenever the the molecule is too fast or lets it pass into another part of the box when it is slow. As time progresses, this would lead to a sorting of hot and cold molecules, and the temperature difference could be exploited to perform work.

This is nothing but a feedback (closed-loop) control scheme: The demon performs a measurement (is the molecule slow or fast) and then uses the information to perform an appropriate control action on the system (inserting a wall or not). Classically, the insertion of a wall requires in the idealized case no work, such that only information is used to create a temperature gradient. However, the Landauer principle states that with each bit of information erased, heat of at least $k_B T \ln(2)$ is dissipated into the environment. To remain functionable, the demon must at some point start to delete the information, which leads to the dissipation of heat. The dissipated heat will exceed the energy obtainable from the thermal gradient.

6.2.1 Phenomenology of an electronic setup

An analog of a Maxwell demon may be implemented in an electronic context: There, an experimentalist takes the role of the demon. The box is replaced by the SET (including the contacts), on which by a nearby QPC a measurement of the dot state (simply empty or filled) is performed. Depending on the measurement outcome, the tunneling rates are modified in time in a piecewise constant manner: When there is no electron on the dot, the left tunneling rate Γ_L is increased (low barrier) and the right tunneling rate Γ_R is decreased (high barrier). The opposite is done when there is an electron on the dot, see Fig. 6.1. Thus, the only difference in comparison to the previous chapter is that now **information of the system state is used to modify the tunneling rates**. Very simple considerations already demonstrate that with this scheme, it will be possible to transport electrons against an existing bias only with time-dependent tunneling rates. When one junction is completely decoupled $\Gamma_{L/R}^{\min} \to 0$, this will completely rectify the transport from left to right also against the bias (if the bias is finite). In the following, we will address the statistics of this device.

The first step is to identify an effective evolution equation for the density matrix accounting for measurement and control. A measurement of a low QPC current will imply – compare Eq. (4.71) – that the system is most likely filled, whereas a large QPC current indicates an empty SET dot. In the idealized limit of no measurement errors, this simply corresponds to a projection

$$M_E = |0\rangle \langle 0| \ , \qquad M_F = |1\rangle \langle 1| \tag{6.28}$$

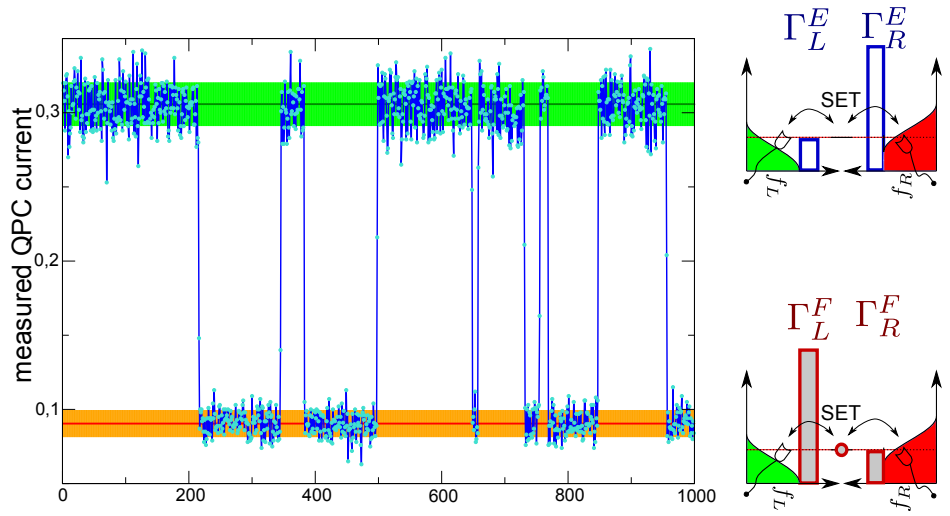

Figure 6.1: Sketch of the feedback scheme: For a filled dot (low QPC current), the left tunneling rate is minimal and the right tunneling rate is maximal and vice-versa for an empty dot. The dot level itself is not changed.

onto the empty and filled SET dot states, respectively. In the full space (ordering the density matrix as $(\rho_{00}, \rho_{11}, \rho_{01}, \rho_{10})^T$ these have superoperator representations (defining $\mathcal{M}_\sigma \rho \hat{=} M_\sigma \rho M_\sigma^\dagger$) as

$$\mathcal{M}_E = \begin{pmatrix} 1 & 0 & 0 & 0 \\ 0 & 0 & 0 & 0 \\ 0 & 0 & 0 & 0 \\ 0 & 0 & 0 & 0 \end{pmatrix}, \qquad \mathcal{M}_F = \begin{pmatrix} 0 & 0 & 0 & 0 \\ 0 & 1 & 0 & 0 \\ 0 & 0 & 0 & 0 \\ 0 & 0 & 0 & 0 \end{pmatrix}, \tag{6.29}$$

and we see that $\mathcal{M}_E + \mathcal{M}_F \neq \mathbf{1}$. Similarly, the dissipators for the SET exhibit the same block structure separating the evolution of coherences and populations

$$\mathcal{L}_{E/F} = \begin{pmatrix} \bar{\mathcal{L}}_{E/F} & \mathbf{0} \\ \mathbf{0} & \mathcal{L}_{E/F}^{\text{coh}} \end{pmatrix}. \tag{6.30}$$

Therefore, due to the common block structure of the individual dissipators and the measurement superoperators we can reduce the dynamics to the populations only, where with

$$\bar{\mathcal{M}}_E = \begin{pmatrix} 1 & 0 \\ 0 & 0 \end{pmatrix}, \qquad \bar{\mathcal{M}}_F = \begin{pmatrix} 0 & 0 \\ 0 & 1 \end{pmatrix} \tag{6.31}$$

we indeed have $\bar{\mathcal{M}}_E + \bar{\mathcal{M}}_F = \mathbf{1}$. Therefore, for a continuous measurement and feedback control loop, the effective population Liouvillian under feedback control becomes

$$\mathcal{L}_{\text{eff}} = \bar{\mathcal{L}}^{(E)} \bar{\mathcal{M}}_E + \bar{\mathcal{L}}^{(F)} \bar{\mathcal{M}}_F \tag{6.32}$$

Note that this can be performed with and without counting fields. Taking into account the diagonal structure of the projection superoperators, this simply implies that the effective Liouvillian under feedback has the first column from the Liouvillian conditioned on an empty dot and the second column from the Liouvillian conditioned on the filled dot

$$\mathcal{L}_{\text{eff}}(\chi_L, \chi_R) = \begin{pmatrix} -\Gamma_L^E f_L - \Gamma_R^E f_R & +\Gamma_L^F (1-f_L) e^{+\mathrm{i}\chi_L} + \Gamma_R^F (1-f_R) e^{+\mathrm{i}\chi_R} \\ +\Gamma_L^E f_L e^{-\mathrm{i}\chi_L} + \Gamma_R^E f_R e^{-\mathrm{i}\chi_R} & -\Gamma_L^F (1-f_L) - \Gamma_R^F (1-f_R) \end{pmatrix}. \tag{6.33}$$

Evidently, it still obeys trace conservation but now the tunneling rates in the two columns are different ones.

Exercise 43 (Current at zero bias)**.** *(1 points)*
Calculate the feedback-current at zero bias $f_L = f_R = f$ in dependence on f. What happens at zero temperatures, where $f \to \{0, 1\}$?

The effective Liouvillian describes the average evolution of trajectories under continuous monitoring and feedback. The validity of the effective description can be easily checked by calculating Monte-Carlo solutions as follows:

Starting e.g. with a filled dot, the probability to jump out e.g. to the right lead during the small time interval Δt reads $P^{(F)}_{\text{out,R}} = \Gamma^F_R(1-f_R)\Delta t$. Similarly, we can write down the probabilities to jump out to the left lead and also the probabilities to jump onto an empty dot from either the left or right contact

$$\begin{aligned} P^{(F)}_{\text{out,R}} &= \Gamma^F_R(1-f_R)\Delta t\,, \qquad P^{(F)}_{\text{out,L}} = \Gamma^F_L(1-f_L)\Delta t\,, \\ P^{(E)}_{\text{in,R}} &= \Gamma^E_R f_R \Delta t\,, \qquad P^{(E)}_{\text{in,L}} = \Gamma^E_L f_L \Delta t\,. \end{aligned} \tag{6.34}$$

Naturally, these jump probabilities also uniquely determine the change of the particle number on either contact. The remaining probability is simply the one that no jump occurs during Δt. A Monte-Carlo simulation is obtained by drawing a random number and choosing one out of three possible outcomes for empty (jumping in from left contact, from right contact, or remaining empty) and for a filled (jumping out to left contact, to right contact, or remaining filled) dot. Repeating the procedure several times yields a single trajectory for $n(t)$, $n_L(t)$, and $n_R(t)$. The ensemble average of many such trajectories agrees perfectly with the solution of the effective feedback master equation

$$\begin{aligned} \langle n\rangle_t &= \text{Tr}\left\{d^\dagger d e^{\mathcal{L}_{\text{eff}}(0,0)t}\rho_0\right\}\,, \\ \langle n_L\rangle_t &= (-\mathrm{i}\partial_\chi)\,\text{Tr}\left\{e^{\mathcal{L}_{\text{eff}}(\chi,0)t}\rho_0\right\}\big|_{\chi=0}\,, \\ \langle n_R\rangle_t &= (-\mathrm{i}\partial_\chi)\,\text{Tr}\left\{e^{\mathcal{L}_{\text{eff}}(0,\chi)t}\rho_0\right\}\big|_{\chi=0}\,, \end{aligned} \tag{6.35}$$

see Fig. 6.2. To compare with the case without feedback, we parametrize the change of tunneling rates by dimensionless constants

$$\Gamma^E_L = e^{\delta^E_L}\Gamma_L\,, \qquad \Gamma^E_R = e^{\delta^E_R}\Gamma_R\,, \qquad \Gamma^F_L = e^{\delta^F_L}\Gamma_L\,, \qquad \Gamma^F_R = e^{\delta^F_R}\Gamma_R\,, \tag{6.36}$$

where $\delta^\beta_\alpha \to 0$ reproduces the case without feedback and $\delta^\beta_\alpha > 0 (< 0)$ increases (decreases) the tunneling rate to contact α conditioned on dot state β. The general current can directly be calculated as

$$I = \frac{f_L(1-f_R)\Gamma^E_L\Gamma^F_R - (1-f_L)f_R\Gamma^F_L\Gamma^E_R}{\Gamma^E_L f_L + \Gamma^F_L(1-f_L) + \Gamma^E_R f_R + \Gamma^F_R(1-f_R)}\,, \tag{6.37}$$

which reduces to the conventional current (3.38) without feedback when $\Gamma^\beta_\alpha \to \Gamma_\alpha$. For finite feedback strength however, this will generally induce a non-vanishing current at zero bias, see Fig. 6.3. In our idealized setup, this current is only generated by the information on whether the

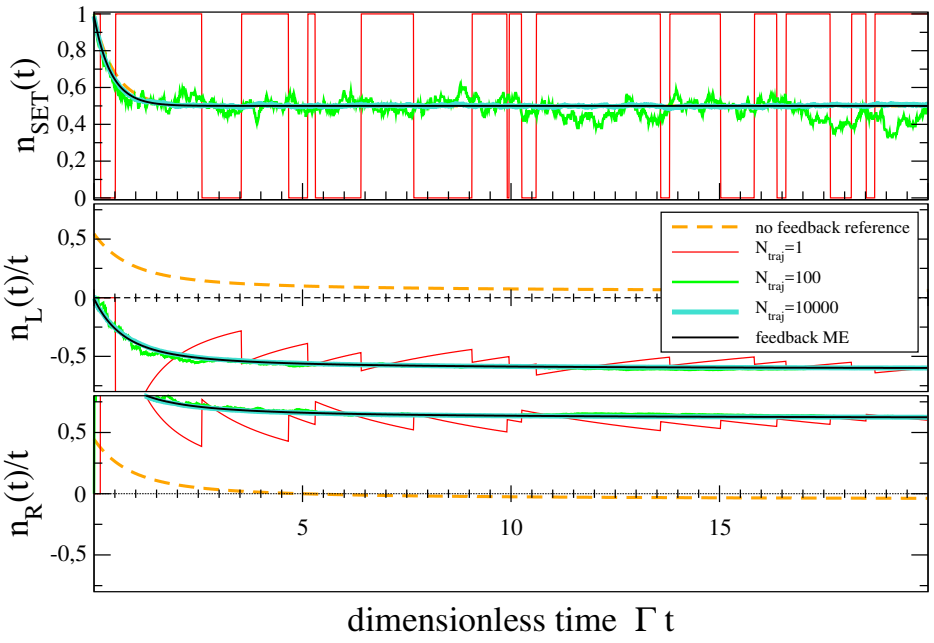

Figure 6.2: Comparison of a single (thin red curve with jumps, same realization in all panels) and the average of 100 (medium thickness, green) and 10000 (bold smooth curve, turquoise) trajectories with the solution from the effective feedback master equation (thin black) for the dot occupation (top), the number of particles on the left (middle), and the number of particles on the right (bottom). The average of the trajectories converges to the effective feedback master equation result. The reference curve without feedback (dashed orange) may be obtained by using vanishing feedback parameters and demonstrates that the direction of the current may actually be reversed via sufficiently strong feedback. Parameters: $\Gamma_L = \Gamma_R \equiv \Gamma$, $f_L = 0.45$, $f_R = 0.55$, $\delta_L^E = \delta_R^F = 1.0$, $\delta_R^E = \delta_L^F = -10.0$, and $\Gamma\Delta t = 0.01$.

dot is occupied or empty – hence the interpretation as a Maxwell demon. When the contacts are held at equal temperatures $\beta_L = \beta_R = \beta$, this raises the question for the maximum power

$$P = -IV \tag{6.38}$$

generated by the device.

In what follows, we will consider symmetric feedback characterized by a single parameter

$$\delta_L^E = \delta_R^F = -\delta_L^F = -\delta_R^E = +\delta\,, \tag{6.39}$$

where $\delta > 0$ favors transport from left to right and $\delta < 0$ transport from right to left and also symmetric bare tunneling rates $\Gamma = \Gamma_L = \Gamma_R$. With these assumptions, it is easy to see that for large feedback strengths $\delta \gg 1$, the current simply becomes

$$I \to \Gamma e^{\delta} \frac{f_L(1-f_R)}{f_L + (1-f_R)}\,. \tag{6.40}$$

To determine the maximum power, we would have to maximize with respect to left and right chemical potentials μ_L and μ_R, the lead temperature β and the dot level ϵ. However, as these

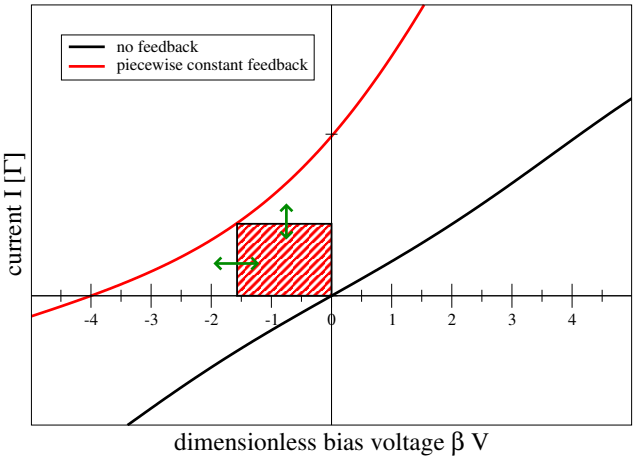

Figure 6.3: Current voltage characteristics for finite feedback strength $\delta = 1$ (red curve) and without feedback $\delta = 0$ (black curve). For finite feedback, the current may point in the other direction than the voltage leading to a positive power $P = -IV$ (shaded region) generated by the device.

parameters only enter implicitly in the Fermi functions, it is more favorable to use that for equal temperatures

$$\beta(\mu_L - \mu_R) = \beta V = \ln\left[\frac{f_L(1-f_R)}{(1-f_L)f_R}\right], \tag{6.41}$$

such that we can equally maximize

$$P = -IV = \frac{1}{\beta}(-I\beta V) \to \frac{\Gamma e^{\delta}}{\beta}\left[-\frac{f_L(1-f_R)}{f_L+(1-f_R)}\ln\left(\frac{f_L(1-f_R)}{(1-f_L)f_R}\right)\right]. \tag{6.42}$$

The term in square brackets can now be maximized numerically with respect to the parameters f_L and f_R in the range $0 \leq f_{L/R} \leq 1$, such that one obtains for the maximum power at strong feedback

$$P \leq k_{\mathrm{B}}T\Gamma e^{\delta}0.2785 \qquad \text{at} \qquad f_L = 0.2178 \qquad f_R = 0.7822\,. \tag{6.43}$$

The average work extracted from the SET circuit between two QPC measurement points at t and $t + \Delta t$ is therefore given by

$$\langle W\rangle \leq k_{\mathrm{B}}T\Gamma e^{\delta}\Delta t 0.2785\,. \tag{6.44}$$

We can contrast this with the heat dissipated in the QPC circuit to perform the measurement. Naively, to perform feedback efficiently, it is required that the QPC sampling rate is fast enough that all state changes of the SET are faithfully detected (no tunneling charges are missed). This requires that $\Gamma e^{\delta}\Delta t < 1$. Therefore, we can refine the upper bound for the average work

$$W \leq k_{\mathrm{B}}T0.2785\,. \tag{6.45}$$

This has to be contrasted with the Landauer principle, which states that for each deleted bit in the demons brain (each QPC data point enconding high current or low current) heat of

$$Q \geq k_{\mathrm{B}}T\ln(2) \approx k_{\mathrm{B}}T0.6931 \tag{6.46}$$

is dissipated. These rough estimates indicate that the second law does not appear to be violated.

Finally, we use our knowledge of Full Counting Statistics to investigate the fluctuation theorem. The conventional fluctuation theorem for the SET at equal temperatures

$$\frac{P_{+n}(t)}{P_{-n}(t)} = e^{n\beta V} \tag{6.47}$$

is modified in presence of feedback. Since the Liouvillian still contains the counting fields in the conventional way, simply the factor in the exponential, but not the dependence on the number of tunneled electrons n is changed. To evaluate the FT, we identify symmetries in the cumulant-generating function (or alternatively the eigenvalues of the Liouvillian)

$$\begin{aligned}
\lambda(-\chi) &= \lambda\left(+\chi + \mathrm{i}\ln\left[\frac{\Gamma_L^E\Gamma_R^F}{\Gamma_L^F\Gamma_R^E}\frac{f_L(1-f_R)}{(1-f_L)f_R}\right]\right) \\
&= \lambda\left(+\chi + \mathrm{i}\ln\left[e^{+4\delta}\frac{f_L(1-f_R)}{(1-f_L)f_R}\right]\right) = \lambda\left(+\chi + \mathrm{i}\ln\left[e^{+4\delta}e^{\beta V}\right]\right) \\
&= \lambda(+\chi + \mathrm{i}(4\delta + \beta V))\,.
\end{aligned} \tag{6.48}$$

Exercise 44 (Fluctuation theorem under feedback)**.** *Show the validity of this equation.*

From this symmetry of the cumulant-generating function we obtain for the fluctuation theorem under feedback

$$\lim_{t\to\infty}\frac{P_{+n}(t)}{P_{-n}(t)} = e^{n(\beta V + 4\delta)} = e^{n\beta(V-V^*)}\,, \tag{6.49}$$

where $V^* = -4\delta/\beta$ denotes the voltage at which the current (under feedback) vanishes.

If our previous investigations we had found that the fluctuation theorems are related to the entropy production. Now, in addition to the expected entropy production $\Delta_\mathrm{i}S = n\beta V$ we find an additional contribution, which one could – lacking a microscopic description of the feedback mechanism – interpret as an information term modifying the entropy balance of the system in presence of feedback.

Exercise 45 (Vanishing feedback current)**.** *(1 points)*
Show for equal temperatures that the feedback current vanishes when $V = V^* = -4\delta/\beta$.

The fact that the estimates concerning the second law are rather vague result from the missing physical implementation of the control loop. In our model, it could be anything, even represented by a human being pressing a button whenever the QPC current changes. The entropy produced by such a humanoid implementation of the control loop would by far exceed the local entropy reduction manifested by a current running against the bias. Below, we will therefore investigate these questions in greater detail.

6.2.2 Conventional entropy production in rate equations

In this section, we will mathematically treat rate equations of the form

$$\dot{P}_a = \sum_\nu \sum_b W_{ab}^{(\nu)} P_b\,, \tag{6.50}$$

where $W_{ab}^{(\nu)}$ is the transition rate from state b to state a and ν denotes a reservoir which triggers the particular transition. Naturally, conservation of probabilities implies that $\sum_a W_{ab}^{(\nu)} = 0$ for all a and for each reservoir ν, such that the diagonal elements are fixed via

$$W_{aa}^{(\nu)} = -\sum_{b\neq a} W_{ba}^{(\nu)} \,. \tag{6.51}$$

Having in mind that each reservoir is kept at a certain equilibrium, we also postulate the existence of a local detailed balance condition for each reservoir. This implies that the ratio of forward and backward transition rates between states i and j that are triggered by reservoir ν obey

$$\frac{W_{ji}^{(\nu)}}{W_{ij}^{(\nu)}} = e^{-\beta_\nu[(E_j-E_i)-\mu_\nu(N_j-N_i)]} \,, \tag{6.52}$$

where β_ν and μ_ν denote inverse temperature and chemical potential of the corresponding reservoir, and E_i and N_i denote energy and particle number of the state i, respectively. The above relation follows naturally from the extension of the KMS condition to systems with chemical potentials and is – as we have seen – automatically fulfilled for a large number of microscopically derived models.

Then, the Shannon entropy of the system

$$S = -\sum_i P_i(t) \ln P_i(t) \tag{6.53}$$

obeys the balance equation

$$\begin{aligned}
\dot{S} &= -\frac{d}{dt}\sum_i P_i \ln P_i = -\sum_i \dot{P}_i \ln P_i \\
&= -\sum_{ij}\sum_\nu W_{ij}^{(\nu)} P_j \ln\left(P_i \frac{W_{ji}^{(\nu)}}{P_j W_{ij}^{(\nu)}} \frac{P_j W_{ij}^{(\nu)}}{W_{ji}^{(\nu)}}\right) \\
&= +\sum_{ij}\sum_\nu W_{ij}^{(\nu)} P_j \ln\left(\frac{W_{ij}^{(\nu)} P_j}{W_{ji}^{(\nu)} P_i}\right) + \sum_{ij}\sum_\nu W_{ij}^{(\nu)} P_j \ln\left(\frac{W_{ji}^{(\nu)}}{W_{ij}^{(\nu)}} \frac{1}{P_j}\right) \\
&= \underbrace{+\sum_{ij}\sum_\nu W_{ij}^{(\nu)} P_j \ln\left(\frac{W_{ij}^{(\nu)} P_j}{W_{ji}^{(\nu)} P_i}\right)}_{\geq 0} + \sum_{ij}\sum_\nu W_{ij}^{(\nu)} P_j \underbrace{\ln\left(\frac{W_{ji}^{(\nu)}}{W_{ij}^{(\nu)}}\right)}_{-\beta_\nu[(E_j-E_i)-\mu_\nu(N_j-N_i)]} \,.
\end{aligned} \tag{6.54}$$

In the above lines, we have simply used trace conservation $\sum_i W_{ij}^{(\nu)} = 0$ and finally the local detailed balance property (6.52). This property enables us to identify in the long-term limit the second term as energy and matter currents. When multiplied by the inverse temperature of the corresponding reservoir, they would combine to an entropy flow, which motivates the definition below.

Def. 21 (Entropy Flow). *For a rate equation satisfying detailed balance, the entropy flow from reservoir ν is defined as*

$$\begin{aligned}\dot{S}_{\mathrm{e}}^{(\nu)} &= \sum_{ij} W_{ij}^{(\nu)} P_j \ln \frac{W_{ji}^{(\nu)}}{W_{ij}^{(\nu)}} = +\sum_{ij} W_{ij}^{(\nu)} P_j \left[-\beta_\nu[(E_j - E_i) - \mu_\nu(N_j - N_i)]\right] \\ &= \beta_\nu \left(I_E^{(\nu)} - \mu_\nu I_M^{(\nu)}\right), \end{aligned} \tag{6.55}$$

where energy currents $I_E^{(\nu)}$ and matter currents $I_M^{(\nu)}$ associated to reservoir ν count positive when entering the system.

The remaining contribution corresponds to a production term [17]. We note that it is always positive, which can be deduced from the formal similarity to the Kullback-Leibler divergence of two probability distributions or – more directly – using the Logarithmic Sum Inequality.

Exercise 46 (Logarithmic Sum Inequality). *Show that for non-negative a_i and b_i*

$$\sum_{i=1}^{n} a_i \ln \frac{a_i}{b_i} \geq a \ln \frac{a}{b}$$

with $a = \sum_i a_i$ and $b = \sum_i b_i$.

Its positivity is perfectly consistent with the second law of thermodynamics, and we therefore identify the remaining contribution as entropy production.

Def. 22 (Entropy Production). *For a rate equation, the average entropy production is defined as*

$$\dot{S}_{\mathrm{i}} = \sum_{ij}\sum_{\nu} W_{ij}^{(\nu)} P_j \ln\left(\frac{W_{ij}^{(\nu)} P_j}{W_{ji}^{(\nu)} P_i}\right) \geq 0\,. \tag{6.55}$$

It is always positive and at steady state balanced by the entropy flow.

When the dimension of the system's Hilbert space is finite and the rate equation approaches a stationary state, its Shannon entropy will also approach a constant value $\dot{S} = 0$. Therefore, at steady state the entropy production in the system must be balanced by the entropy flow through its terminals

$$\dot{S}_{\mathrm{i}} = -\dot{S}_{\mathrm{e}} = -\sum_{\nu} \beta_\nu \left(I_E^{(\nu)} - \mu_\nu I_M^{(\nu)}\right). \tag{6.56}$$

The above formula conveniently relates the entropy production to energy and matter currents from the terminals into the system. Evidently, the entropy production is thus related to heat currents $\dot{Q}^{(\nu)} = I_E^{(\nu)} - \mu_\nu I_M^{(\nu)}$, which can be determined from a master equation by means of the Full Counting Statistics.

Below, we will show that the above definitions are consistent with what we had before when the Liouville superoperators $\mathcal{L}^{(\nu)}$ have a block structure separating the evolution of coherences and populations, i.e., when in the energy eigenbasis we have

$$H\left|i\right\rangle = E_i\left|i\right\rangle\,, \qquad N\left|i\right\rangle = N_i\left|i\right\rangle\,, \qquad \left\langle i\right|\mathcal{L}^{(\nu)}\rho\left|i\right\rangle = \sum_j W_{ij}^{(\nu)}\left\langle j\right|\rho\left|j\right\rangle\,. \tag{6.57}$$

For this, it is helpful to note that the trace of a product of two matrices can be written as terms only arising from products of the diagonal terms and terms composed of products from off-diagonal terms

$$\mathrm{Tr}\left\{AB\right\} = \sum_{i,j} A_{ij}B_{ji} = \sum_i A_{ii}B_{ii} + \sum_{i\neq j} A_{ij}B_{ji}\,, \tag{6.58}$$

which also implies that traces of products of a diagonal matrix A and an off-diagonal matrix B will always vanish.

For a full Lindblad master equation we defined the energy current entering the system in Eq. (3.11). It can be written as (we drop for simplicity all time dependencies)

$$\begin{aligned} I_E^{(\nu)} &= \mathrm{Tr}\left\{H(\mathcal{L}^{(\nu)}\rho)\right\} = \sum_i E_i(\mathcal{L}^{(\nu)}\rho)_{ii} = \sum_{ij} E_i W_{ij}^{(\nu)}\rho_{jj} \\ &= \sum_{i\neq j} E_i W_{ij}^{(\nu)}\rho_{jj} - \sum_{i\neq j} E_i W_{ji}^{(\nu)}\rho_{ii} = \sum_{ij}(E_i - E_j)W_{ij}^{(\nu)}\rho_{jj}\,, \end{aligned} \tag{6.59}$$

which is the same as the energy current based on the rate equation when we identify $P_j = \rho_{jj}$. In complete analogy, we find for the matter current defined in Eq. (3.13)

$$I_M^{(\nu)} = \mathrm{Tr}\left\{N(\mathcal{L}^{(\nu)}\rho)\right\} = \sum_{ij}(N_i - N_j)W_{ij}^{(\nu)}\rho_{jj}\,. \tag{6.60}$$

This proves that the definitions for the currents based on the rate equation and on the master equation coincide when the master equation assumes block form separating coherences and populations in the system energy eigenbasis.

Now, we consider the entropy production rate defined in Eq. (3.25)

$$\dot{S}_{\mathrm{i}}^{\mathrm{Sp}} = -\sum_\nu \mathrm{Tr}\left\{[\mathcal{L}^{(\nu)})\rho][\ln\rho - \ln\bar{\rho}^{(\nu)}]\right\} = \sum_\nu \dot{S}_{\mathrm{i}}^{\mathrm{Sp},\nu}\,. \tag{6.61}$$

For simplicity of notation, we introduce the projection to the diagonal elements of the matrix A in the system energy eigenbasis as a superoperator

$$\mathcal{P}A = \sum_i \left|i\right\rangle\left\langle i\right|A\left|i\right\rangle\left\langle i\right|\,. \tag{6.62}$$

From this, we can conclude that an individual reservoir-specific term in the Spohn entropy production rate $\dot{S}_{\mathrm{i}}^{\mathrm{Sp}} \geq 0$ can be written as

$$\begin{aligned} \dot{S}_{\mathrm{i}}^{\mathrm{Sp},\nu} &= -\mathrm{Tr}\left\{(\mathcal{P}\mathcal{L}^{(\nu)}\rho)\mathcal{P}[\ln\rho - \ln\bar{\rho}^{(\nu)}]\right\} - \mathrm{Tr}\left\{((1-\mathcal{P})\mathcal{L}^{(\nu)}\rho)(1-\mathcal{P})[\ln\rho - \ln\bar{\rho}^{(\nu)}]\right\} \\ &= -\mathrm{Tr}\left\{(\mathcal{P}\mathcal{L}^{(\nu)}\rho)\mathcal{P}[\ln\rho - \ln\bar{\rho}^{(\nu)}]\right\} - \mathrm{Tr}\left\{((1-\mathcal{P})\mathcal{L}^{(\nu)}\rho)(1-\mathcal{P})\ln\rho\right\} \\ &= -\mathrm{Tr}\left\{(\mathcal{P}\mathcal{L}^{(\nu)}\rho)\mathcal{P}[\ln\mathcal{P}\rho - \ln\bar{\rho}^{(\nu)}]\right\} - \mathrm{Tr}\left\{((1-\mathcal{P})\mathcal{L}^{(\nu)}\rho)(1-\mathcal{P})\ln\rho\right\} \\ &\quad +\mathrm{Tr}\left\{(\mathcal{P}\mathcal{L}^{(\nu)}\rho)\mathcal{P}[\ln\mathcal{P}\rho - \ln\rho]\right\} \\ &= -\mathrm{Tr}\left\{(\mathcal{P}\mathcal{L}^{(\nu)}\rho)\mathcal{P}[\ln\mathcal{P}\rho - \ln\bar{\rho}^{(\nu)}]\right\} \\ &\quad +\mathrm{Tr}\left\{((1-\mathcal{P})\mathcal{L}^{(\nu)}\rho)(1-\mathcal{P})[\ln\mathcal{P}\rho - \ln\rho]\right\} + \mathrm{Tr}\left\{(\mathcal{P}\mathcal{L}^{(\nu)}\rho)\mathcal{P}[\ln\mathcal{P}\rho - \ln\rho]\right\} \\ &= -\mathrm{Tr}\left\{(\mathcal{L}^{(\nu)}\mathcal{P}\rho)[\ln\mathcal{P}\rho - \ln\bar{\rho}^{(\nu)}]\right\} - \mathrm{Tr}\left\{(\mathcal{L}^{(\nu)}\rho)[\ln\rho - \ln\mathcal{P}\rho]\right\}\,, \end{aligned} \tag{6.63}$$

where in the second step we have used that $\bar{\rho}^{(\nu)}$ (and its logarithm) is diagonal in the energy eigenbasis in which we evaluate the trace. In the last step, we have used again the previous decomposition into diagonal and off-diagonal contributions. Furthermore, we also used that $\mathcal{P}\mathcal{L} = \mathcal{L}\mathcal{P}$ (block form of the Liouvillian). Therefore, we see that the entropy production additively splits into a part arising from the dynamics of the populations and another part coming from the dynamics of the coherences.

The first term for the populations can be written as

$$\begin{aligned}
\dot{S}_{\mathrm{i}}^{1,\nu} &= -\mathrm{Tr}\left\{(\mathcal{L}^{(\nu)}\mathcal{P}\rho)[\ln \mathcal{P}\rho - \ln \bar{\rho}^{(\nu)}]\right\} = -\sum_{ij} W_{ij}^{(\nu)} P_j \left[\ln P_i - \ln \bar{P}_i^{(\nu)}\right] \\
&= -\sum_{ij} W_{ij}^{(\nu)} P_j \ln P_i + \sum_{ij} W_{ij}^{(\nu)} P_j \ln \bar{P}_i^{(\nu)} = +\sum_{ij} W_{ij}^{(\nu)} P_j \ln \frac{P_j}{P_i} + \sum_{ij} W_{ij}^{(\nu)} P_j \ln \frac{\bar{P}_i^{(\nu)}}{\bar{P}_j^{(\nu)}} \\
&= \sum_{ij} W_{ij}^{(\nu)} P_j \ln \frac{P_j}{P_i}\frac{\bar{P}_i^{(\nu)}}{\bar{P}_j^{(\nu)}} = \sum_{ij} W_{ij}^{(\nu)} P_j \ln \frac{P_j W_{ij}^{(\nu)}}{P_i W_{ji}^{(\nu)}}\,, \qquad (6.64)
\end{aligned}$$

where we have used that $\sum_i W_{ij}^{(\nu)} = 0$ and eventually that $\frac{\bar{P}_i^{(\nu)}}{\bar{P}_j^{(\nu)}} = \frac{W_{ij}^{(\nu)}}{W_{ji}^{(\nu)}}$. We see that it exactly reproduces the entropy production rate for rate equation in Def. 22.

Finally, we discuss the coherences. From the contractivity of completely positive trace-preserving maps [7] we can show that

$$D(e^{\mathcal{L}\Delta t}\rho(t)|e^{\mathcal{L}\Delta t}\mathcal{P}\rho(t)) \leq D(\rho(t)|\mathcal{P}\rho(t)) \qquad (6.65)$$

that one can as $\Delta t \to 0$ obtain an inequality of the form

$$\dot{S}_{\mathrm{i}}^{2,\nu} = -\mathrm{Tr}\left\{(\mathcal{L}^{(\nu)}\rho(t))[\ln \rho(t) - \ln \mathcal{P}\rho(t)]\right\} \geq 0\,. \qquad (6.66)$$

Exercise 47 (Entropy production of coherent decay)**.** *Show that under the assumptions discussed in this section, the above inequality holds. You may want to use that (why)* $\mathrm{Tr}\left\{(e^{\mathcal{L}\Delta t}\rho)\ln e^{\mathcal{L}\Delta t}\mathcal{P}\rho\right\} = \mathrm{Tr}\left\{(e^{\mathcal{L}\Delta t}\mathcal{P}\rho)\ln e^{\mathcal{L}\Delta t}\mathcal{P}\rho\right\}$.

This proves that for the standard quantum-optical master equation, the total master equation entropy production $\dot{S}_{\mathrm{i}}^{\mathrm{Sp}} = \sum_\nu \left[\dot{S}_{\mathrm{i}}^{1,\nu} + \dot{S}_{\mathrm{i}}^{2,\nu}\right]$ decomposes into two separately positive terms, one describing the evolution of the populations only – with the usual entropy production for rate equations remaining in general finite at large times – and another transient term containing the entropic contributions stemming from the decay of the coherences.

6.2.3 Entropic analysis of rate equations with feedback

We will in this section discuss the necessary modifications in the entropy production rate in rate equations that are subject to feedback control actions. The control actions will be allowed to change both the tunneling rates [18] and the energies of the system [19].

We now consider a feedback conditioned on the system being in state j. Physically, this means that some external controller monitors the state of the system, and upon detecting the system in

state j, it immediately changes the system properties accordingly: The energies of all levels i are **without delay** changed to $E_i^{(j)}$ and also the transition rates due to reservoir ν from j to other states are changed to $W_{ij}^{(j,\nu)}$. Then, the rate equation under feedback becomes

$$\dot{P}_i = \sum_\alpha \sum_j W_{ij}^{(j,\alpha)} P_j \,. \tag{6.67}$$

As we will see, one can distinguish between changes of bare tunneling rates and changes of the energy levels. Whereas the first type leaves the energetics of the system invariant but changes the entropy and is for this reason also called Maxwell demon feedback [18], changing the energy levels modifies both the energetic and entropic balances. It can therefore also not be considered a simple work source.

During a jump $j \to i$ (where the system particle number changes according to $\Delta N_{ij} = N_i - N_j$), the energy balance of the system becomes $\Delta E_{ij} = (E_i^{(j)} - E_j^{(j)}) + (E_i^{(i)} - E_i^{(j)})$, where the first contribution is exchanged with the reservoir and contributes to the heat via $\Delta Q_{ij} = (E_i^{(j)} - E_j^{(j)}) - \mu(N_i - N_j)$, and the second describes feedback energy ΔE_{fb} injected into the system from the control action following immediately thereafter, see also Fig. 6.4 for an illustration. This enables us to

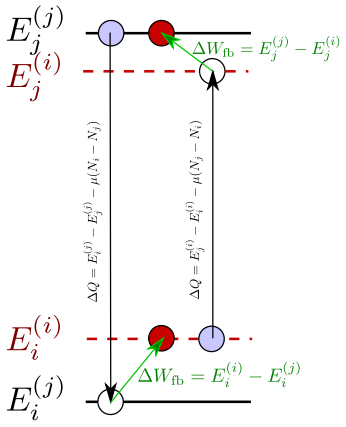

Figure 6.4: Sketch of the energetic balance for the transition from from state $j \to i$ (left) and from state $i \to j$ (right) subject to feedback control applied immediately thereafter. The initial transition (blue to hollow circles) leads to the exchange of heat between system and reservoir (vertical terms). Immediately thereafter, the control action changes the energy levels (hollow to filled red circes), thereby injecting energy into the system if the level is occupied.

write the energy and particle currents entering the system from reservoir ν as

$$\begin{aligned} I_E^{(\nu)} &= \sum_{ij} (E_i^{(j)} - E_j^{(j)}) W_{ij}^{(j,\nu)} P_j \,, \\ I_M^{(\nu)} &= \sum_{ij} (N_i - N_j) W_{ij}^{(j,\nu)} P_j \,. \end{aligned} \tag{6.68}$$

The energy injected in the system with the feedback actions can be similarly computed

$$I_E^{\mathrm{fb}} = \sum_\nu \sum_{ij} (E_i^{(i)} - E_i^{(j)}) W_{ij}^{(j,\nu)} P_j \,, \tag{6.69}$$

and together we find for the total change of the system energy $E = \sum_i E_i^{(i)} P_i$

$$\begin{aligned}
\dot{E} &= \sum_{ij}\sum_{\nu} E_i^{(i)} W_{ij}^{(j,\nu)} P_j \\
&= \sum_{\nu}\sum_{i\neq j} E_i^{(i)} W_{ij}^{(j,\nu)} P_j - \sum_{\nu}\sum_{i\neq j} E_i^{(i)} W_{ji}^{(i,\nu)} P_i \\
&= \sum_{\nu}\sum_{i,j} (E_i^{(i)} - E_j^{(j)}) W_{ij}^{(j,\nu)} P_j = \left(\sum_{\nu} I_E^{(\nu)}\right) + I_E^{\mathrm{fb}} \\
&= \sum_{\nu} \mu_\nu I_M^{(\nu)} + I_E^{\mathrm{fb}} + \sum_{\nu} (I_E^{(\nu)} - \mu_\nu I_M^{(\nu)}) \,. \qquad (6.70)
\end{aligned}$$

This is the first law of thermodynamics, where in the last line we can identify the chemical work done on the system, the energy injected from the feedback, and the heat currents entering from the reservoirs.

We can also consider the evolution of the systems Shannon entropy $S = -\sum_i P_i \ln P_i$, where we get from algebraic manipulations [2]

$$\begin{aligned}
\dot{S} &= -\sum_i \dot{P}_i \ln P_i = \dot{S}_{\mathrm{i}} + \dot{S}_{\mathrm{e}} \,, \\
\dot{S}_{\mathrm{i}} &= \sum_{\nu}\sum_{ij} W_{ij}^{(j,\nu)} P_j \ln\left(\frac{W_{ij}^{(j,\nu)} P_j}{W_{ji}^{(i,\nu)} P_i}\right) \geq 0 \,, \\
\dot{S}_{\mathrm{e}} &= \sum_{\nu}\sum_{ij} W_{ij}^{(j,\nu)} P_j \ln\left(\frac{W_{ji}^{(i,\nu)}}{W_{ij}^{(j,\nu)}}\right) . \qquad (6.71)
\end{aligned}$$

Here, the positivity of the entropy production rate $\dot{S}_{\mathrm{i}}$ follows from mathematical terms (it has the form of a relative entropy), and the second term $\dot{S}_{\mathrm{e}}$ can from the conventional detailed balance relation (6.52) in absence of feedback be identified as the negative entropy change in the reservoirs. However, the feedback changes the detailed balance relation in a way which we phenomenologically parametrize as

$$\frac{W_{ji}^{(i,\nu)}}{W_{ij}^{(j,\nu)}} = e^{\beta_\nu[(E_i^{(j)} - E_j^{(j)}) - \mu_\nu(N_i - N_j)]} e^{-\Delta_{ij}^{(\nu)}} e^{-\sigma_{ij}^{(\nu)}} \,. \qquad (6.72)$$

Here, the first term is associated with the entropy change of the reservoirs, indeed we can recover the heat flow from the reservoirs into the system from it. The second term $\Delta_{ij}^{(\nu)}$ parametrizes changes of the transition rates that are not associated with energetic changes in the system. Consequently, it must not depend on the reservoir temperatures. Finally, the term $\sigma_{ij}^{(\nu)}$ gathers all remaining influences of the feedback. By distinguishing between $\Delta_{ij}^{(\nu)}$ and $\sigma_{ij}^{(\nu)}$ we have presupposed that an unambiguous discrimination between these feedback effects is possible. Inserting this decomposition into the "entropy flow" term we obtain

$$\begin{aligned}
\dot{S}_{\mathrm{e}} &= \sum_{\nu} \beta_\nu \dot{Q}^{(\nu)} - \mathcal{I}_1 - \mathcal{I}_2 \,, \\
\mathcal{I}_1 &= \sum_{\nu}\sum_{ij} W_{ij}^{(j,\nu)} P_j \Delta_{ij}^{(\nu)} \,, \\
\mathcal{I}_2 &= \sum_{\nu}\sum_{ij} W_{ij}^{(j,\nu)} P_j \sigma_{ij}^{(\nu)} \,. \qquad (6.73)
\end{aligned}$$

Solving for the entropy production, we can express it as

$$\dot{S}_{\rm i} = \dot{S} - \sum_\nu \beta_\nu \dot{Q}^{(\nu)} + \mathcal{I}_1 + \mathcal{I}_2 \geq 0\,. \tag{6.74}$$

This is the second law of thermodynamics in presence of a non-equilibrium environment and feedback control.

At steady state, $\dot{S} \to 0$, and the usual inequality for the currents $-\sum_\nu \beta_\nu \dot{Q}^{(\nu)} \geq 0$ is modified by two effective currents. The first one $\mathcal{I}_1$ is associated with feedback actions that have no direct impact on the energetics, whereas the second one takes the energetic feedback actions into account. We note here that these information currents are just an effective description (for example, they can become negative), since we have not made the implementation of the feedback loop explicit in our treatment but remain at a phenomenologic level. If that is done for a microscopic treatment of the detector [20], it is possible to link the effective information current with the time-derivative of the mutual information between controlled system and detector device [21, 22].

Depending on the regime, one may identify contributions to the total entropy production rate (6.74) which are negative. These always need to be compensated by the other, positive contributions, which enables one to define information-theoretic efficiencies that are upper-bounded by one.

6.2.4 Our example: Maxwell's demon

For error-free feedback the average feedback rate matrix becomes (for simplicity without counting fields)

$$\mathcal{L}_{\rm fb} = \sum_\nu \begin{pmatrix} -\Gamma_\nu^E f_\nu^E & +\Gamma_\nu^F[1-f_\nu^F] \\ +\Gamma_\nu^E f_\nu^E & -\Gamma_\nu^F[1-f_\nu^F] \end{pmatrix}. \tag{6.75}$$

Here, the piecewise-constant driving leads to two possible values of the SET tunneling rates $\Gamma_\nu \to \Gamma_\nu^{E/F}$ and also of the system Hamiltonian ($\epsilon \to \epsilon^{E/F}$). Since the dot parameters in the description only enter implicitly, we described the latter by conditional Fermi functions $f_\nu \to f_\nu^{E/F}$. With such a feedback scheme, one will in general inject both energy and information into the system, which can be consistently treated on the local level.

Assuming the conditioned dot Hamiltonian as $H_S = \epsilon_{E/F} d^\dagger d$, the empty dot has energies $E_0^{(0)} = 0$ and $E_1^{(0)} = \epsilon_E$, and when filled, the system has energies $E_0^{(1)} = 0$ and $E_1^{(1)} = \epsilon_F$. Therefore, we can identify the heat entering the system from reservoir ν during a jump out of the system as $\Delta Q_{\rm out}^{(\nu)} = E_0^{(1)} - E_1^{(1)} - \mu_\nu(N_0 - N_1) = -\epsilon_F + \mu$ and for a jump into the system as $\Delta Q_{\rm in}^{(\nu)} = E_1^{(0)} - E_0^{(0)} - \mu_\nu(N_1 - N_0) = +\epsilon_E - \mu$, leading to an overall heat current of

$$\begin{aligned} \dot{Q}^{(\nu)} &= -(\epsilon_F - \mu_\nu)\mathcal{L}_{\rm fb}^{01,\nu} P_1 + (\epsilon_E - \mu_\nu)\mathcal{L}_{\rm fb}^{10,\nu} P_0 \\ &= I_E^{(\nu)} - \mu_\nu I_M^{(\nu)}\,, \end{aligned} \tag{6.76}$$

which also defines energy $I_E^{(\nu)}$ and matter $I_M^{(\nu)}$ currents entering the system from reservoir ν

$$\begin{aligned} I_E^{(\nu)} &= \epsilon_E \mathcal{L}_{\rm fb}^{10,\nu} P_0 - \epsilon_F \mathcal{L}_{\rm fb}^{01,\nu} P_1 = \epsilon_E \Gamma_\nu^E f_\nu^E P_0 - \epsilon_F \Gamma_\nu^F (1-f_\nu^F) P_1\,, \\ I_M^{(\nu)} &= \mathcal{L}_{\rm fb}^{10,\nu} P_0 - \mathcal{L}_{\rm fb}^{01,\nu} P_1 = \Gamma_\nu^E f_\nu^E P_0 - \Gamma_\nu^F (1-f_\nu^F) P_1\,, \end{aligned} \tag{6.77}$$

and we see that they are no longer tightly coupled. A similar result holds if also the energy of the empty state is changed by the feedback. We can show that the energy change of the system is

balanced by the energy currents entering the system from both reservoirs and the energy current injected by the feedback

$$I_E^{\rm fb} = (\epsilon_F - \epsilon_E) \sum_\nu \mathcal{L}_{\rm fb}^{10,\nu} P_0 \,. \tag{6.78}$$

To discuss the entropic balance, we can with Eq. (6.75) write the ratio of backward- and forward rates for each reservoir as

$$\begin{aligned} \frac{\mathcal{L}_{\rm fb}^{01,\nu}}{\mathcal{L}_{\rm fb}^{10,\nu}} &= \frac{\Gamma_\nu^F}{\Gamma_\nu^E} \frac{1-f_\nu^F}{f_\nu^E} = \left(\frac{1-f_\nu^E}{f_\nu^E}\right) \left[\frac{\Gamma_\nu^F}{\Gamma_\nu^E}\right] \left\{\frac{1-f_\nu^F}{1-f_\nu^E}\right\} , \\ \frac{\mathcal{L}_{\rm fb}^{10,\nu}}{\mathcal{L}_{\rm fb}^{01,\nu}} &= \frac{\Gamma_\nu^E}{\Gamma_\nu^F} \frac{f_\nu^E}{1-f_\nu^F} = \left(\frac{f_\nu^F}{1-f_\nu^F}\right) \left[\frac{\Gamma_\nu^E}{\Gamma_\nu^F}\right] \left\{\frac{f_\nu^E}{f_\nu^F}\right\} , \end{aligned} \tag{6.79}$$

where we see from $(1-f_\nu^E)/f_\nu^E = e^{+\beta_\nu(\epsilon_E-\mu_\nu)}$ and $f_\nu^F/(1-f_\nu^F) = e^{-\beta_\nu(\epsilon_F-\mu_\nu)}$ that the terms in round parentheses $(\ldots)$ will when inserted in the "entropy flow" term

$$\dot{S}_{\rm e}^{(\nu)} = \sum_{ij} W_{ij}^{(j,\nu)} P_j \ln \frac{W_{ji}^{(i,\nu)}}{W_{ij}^{(j,\nu)}} \tag{6.80}$$

compose the entropy change in the reservoirs $-\beta_\nu \dot{Q}^{(\nu)}$, compare Eq. (6.76). The terms in square brackets $[\ldots]$ are a pure Maxwell-demon contribution [18] in the sense that they only affect the entropic balance directly, and the terms in curly brackets $\{\ldots\}$ describe the influence on the feedback energy injection on the entropic balance. We therefore define the feedback parameters

$$\begin{aligned} \Delta_{01}^{(\nu)} &= \ln \frac{\Gamma_\nu^F}{\Gamma_\nu^E} , \qquad \Delta_{10}^{(\nu)} = \ln \frac{\Gamma_\nu^E}{\Gamma_\nu^F} , \\ \sigma_{01}^{(\nu)} &= \ln \frac{f_\nu^F}{f_\nu^E} , \qquad \sigma_{10}^{(\nu)} = \ln \frac{1-f_\nu^E}{1-f_\nu^F} , \end{aligned} \tag{6.81}$$

compare also Eq. (6.72). We see that the information contribution of the feedback obeys $\Delta_{01}^{(\nu)} = -\Delta_{10}^{(\nu)}$ and the energetic contribution obeys $\sigma_{01}^{(\nu)}\sigma_{10}^{(\nu)} = \beta_\nu(\epsilon_E - \epsilon_F)$. With these, the "entropy flow" term becomes modified by information currents $\dot{S}_{\rm e} = \sum_\nu \beta_\nu \dot{Q}^{(\nu)} - \mathcal{I}_1 - \mathcal{I}_2$, of which the first reads explicitly

$$\begin{aligned} \mathcal{I}_1 &= \sum_\nu \left[\mathcal{L}_{\rm fb}^{01,\nu} P_1 - \mathcal{L}_{\rm fb}^{10,\nu} P_0\right] \ln \frac{\Gamma_\nu^F}{\Gamma_\nu^E} = -\sum_\nu \ln \frac{\Gamma_\nu^F}{\Gamma_\nu^E} I_M^{(\nu)} \\ &\to \left(\ln \frac{\Gamma_R^F}{\Gamma_R^E} - \ln \frac{\Gamma_L^F}{\Gamma_L^E}\right) I_M = I_M \ln \left[\frac{\Gamma_L^E \Gamma_R^F}{\Gamma_L^F \Gamma_R^E}\right] . \end{aligned} \tag{6.82}$$

Above, it is visible that the individual contributions to the information current $\mathcal{I}_1$ are tightly coupled to the matter current. At steady state, we have conservation of the matter currents $I_M = I_M^{(L)} = -I_M^{(R)}$, such that also the total information current is tightly coupled to the matter current.

Looking at the second information current we see that

$$\mathcal{I}_2 = \sum_\nu \left[\mathcal{L}_{\rm fb}^{01,\nu} P_1 \ln \frac{f_\nu^F}{f_\nu^E} + \mathcal{L}_{\rm fb}^{10,\nu} P_0 \ln \frac{1-f_\nu^E}{1-f_\nu^F}\right] . \tag{6.83}$$

and from the first law also conservation of the individual energy currents and the feedback energy current $I_E^{(L)} + I_E^{(R)} + I_E^{\rm fb} = 0$.

Inserting these in the steady-state entropy production rate $\dot{S}_{\rm i} = -\dot{S}_{\rm e}$ we find that at equal temperatures $\beta = \beta_L = \beta_R$ the second law reads

$$\dot{S}_{\rm i} \to \beta(\mu_L - \mu_R) I_M + \mathcal{I}_1 + \beta I_E^{\rm fb} + \mathcal{I}_2 \geq 0\,. \tag{6.84}$$

Here, the first term contains the produced electric power $P = -(\mu_L - \mu_R) I_M$, which without feedback would always be negative. The second term contains the purely informational contribution of the feedback to the entropic balance. The third term quantifies how the difference of left and right energy currents $I_E^{(L)} + I_E^{(R)} = -I_E^{\rm fb}$ affects the heat exchanged with the reservoirs. If the feedback does not affect the energy levels ($\epsilon_E = \epsilon_F$), this term will naturally vanish. Finally, the last term describes the effect of the feedback level driving on the entropic balance. Since the level driving also enters the entropic balance, we cannot interpret this simply as work on the system.

For simplicity, we can parametrize the tunneling rates using only a single parameter

$$\begin{aligned} \Gamma_L^F &= \Gamma e^{+\delta}\,, \qquad \Gamma_R^F = \Gamma e^{-\delta}\,, \\ \Gamma_L^E &= \Gamma e^{-\delta}\,, \qquad \Gamma_R^E = \Gamma e^{+\delta}\,, \end{aligned} \tag{6.85}$$

which will for $\delta > 0$ favor transport from right to left. This will not change the energetics, but the entropic balance is affected by the information current $\mathcal{I}_1$. When we similarly parametrize the changes of the dot level as

$$\epsilon_F = \epsilon e^{+\Delta}\,, \qquad \epsilon_E = \epsilon e^{-\Delta}\,, \tag{6.86}$$

this will for $\Delta \neq 0$ inject energy into the system via feedback operations. This secondary type of feedback will not only modify the energy balance (first law), visible in an imbalance between left and right energy currents $I_E^{(L)} \neq -I_E^{(R)}$. In addition, it also affects the entropic balance via both a modification of the heat flow and the information current $\mathcal{I}_2$. These effects are illustrated in Fig. 6.5.

It is clearly visible that neglecting the feedback completely, one may observe an apparent violation of the second law (dashed and solid red curves). The unconscious injection of energy may lead to a significant increase of the overall produced power (solid red curve) but also implies an apparent violation of the second law under Maxwell-demon feedback (solid green curve). By contrast, the full entropy production rate (6.84) is always positive as expected (black curves).

Finally, we turn to the integral fluctuation theorem for entropy production. Formally, we get a fluctuation theorem for the probabilities of transferred particles from left to right, since the when we equip Eq. (6.75) with counting fields, we get

$$\mathcal{L}_{\rm fb}(\chi) = \begin{pmatrix} -\Gamma_L^E f_L^E & +\Gamma_L^F [1 - f_L^F] e^{-{\rm i}\chi} \\ +\Gamma_L^E f_L^E e^{+{\rm i}\chi} & -\Gamma_L^F [1 - f_L^F] \end{pmatrix} + \begin{pmatrix} -\Gamma_R^E f_R^E & +\Gamma_R^F [1 - f_R^F] \\ +\Gamma_R^E f_R^E & -\Gamma_R^F [1 - f_R^F] \end{pmatrix}. \tag{6.87}$$

In the long-term cumulant-generating function we obtain the symmetry

$$C\,(-\chi, t) = C\,(+\chi + {\rm i}\alpha, t)\,, \qquad \alpha = \ln \frac{f_L^E (1 - f_R^F) \Gamma_L^E \Gamma_R^F}{(1 - f_L^F) f_R^E \Gamma_L^F \Gamma_R^E}\,, \tag{6.88}$$

which leads to a fluctuation theorem of the form

$$\lim_{t\to\infty} \frac{P_{+n}(t)}{P_{-n}(t)} = e^{+n\alpha}\,. \tag{6.89}$$

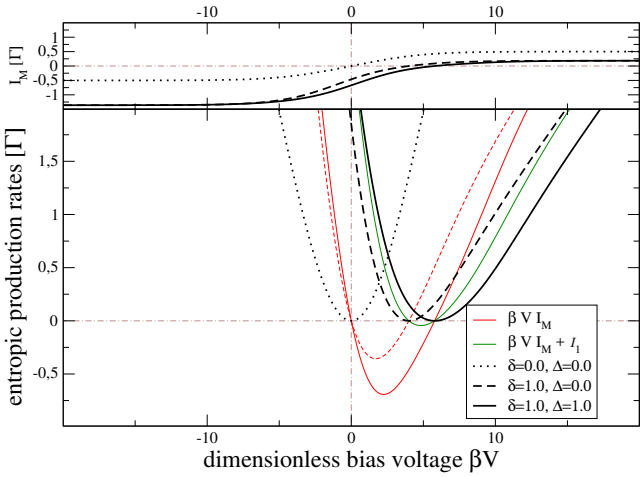

Figure 6.5: Plot of the matter current from left to right (top) and contributions to the total entropy production rate (6.84) (bottom) for situations without feedback $\delta = \Delta = 0$ (dotted), with Maxwell-demon feedback $\delta = +1.0$, $\Delta = 0$ (dashed), and with energy-injecting feedback $\delta = \Delta = +1.0$ (solid). With feedback active (dashed and solid), we see that the matter current at equilibrium $V = 0$ becomes negative and remains negative for a small region $0 < V < V^*$, where the device produces positive power $P = -VI_M$ either using only information ($\Delta = 0$) or information and energy injection ($\Delta \neq 0$). Red thin curves of similar style denote the naive entropy production rate $\beta(\mu_L - \mu_R)I_M = -\beta P$ that one would conjecture in ignorance of any feedback actions taken. Green thin curves of similar style denote the naive entropy production rate $-\beta(\mu_L - \mu_R)I_M + \mathcal{I}_1$ that one would conjecture when assuming that the feedback does not affect the energy levels. The black curves denote the true entropy production rate, which is positive in all parameter regimes. Dash-dotted lines just serve for orientation. Other parameters: $\beta\epsilon = 1$.

When $f_\nu^E = f_\nu^F$, we indeed recover our previous fluctuation theorem (6.49). In this case, we have indeed the total entropy production in the exponent. However, when the feedback injects energy into the system $f_\nu^E \neq f_\nu^F$, we have already found that the average entropy production is no longer tightly coupled to the matter current and can therefore not be simply proportional to the total number of particles travelling through the system. The observed symmetry is then just a purely mathematical one – actually a fluctuation theorem is observed for any fluctuating two-level system, regardless of any detailed balance relation.

6.3 Coherent/Autonomous feedback

In contrast to external feedback loops, we can augment a quantum system by replacing the measurement, signal processing, and control actions by a single auxiliary system, which we add to the original quantum system. The controller and the original quantum systems are then treated in an all-inclusive fashion. Typically, such setups are less flexible, since the control protocoll cannot just be changed by altering classical parts of the feedback loop. However, they offer more understanding on the thermodynamics as the complete feedback loop can be treated as part of the system.

6.3.1 An autonomous version of a Maxwell demon

Consider a single-electron transistor as before now capacitively interacting with another quantum dot, which is coupled to its own reservoir as depicted in Fig. 6.6. The system Hamiltonian of this

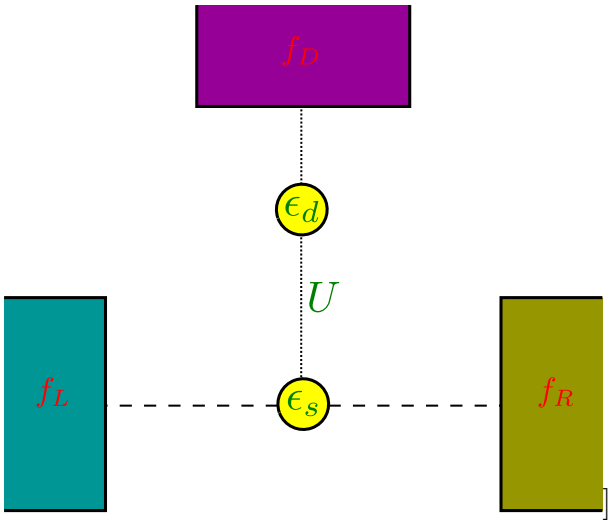

Figure 6.6: Sketch of an SET (bottom circuit) that is capacitively coupled via the Coulomb interaction U to another quantum dot. The additional quantum dot is tunnel-coupled to its own reservoir with Fermi function f_D. Since the associated stationary matter current vanishes, only energy can be transferred across this junction (dotted line).

three-terminal system reads

$$\mathcal{H}_{\mathrm{S}} = \epsilon_d c_d^\dagger c_d + \epsilon_s c_s^\dagger c_s + U c_d^\dagger c_d c_s^\dagger c_s \,, \tag{6.90}$$

where ϵ_s and ϵ_d denote the on-site energies of the SET dot and the demon dot, respectively, whereas U denotes the Coulomb interaction between the two dots. The system dot is tunnel-coupled to left and right leads, whereas the demon dot is tunnel-coupled to its junction only

$$\mathcal{H}_{\mathrm{I}} = \sum_k \left(t_{kL} c_s c_{kL}^\dagger + t_{kL}^* c_{kL} c_s^\dagger \right) + \sum_k \left(t_{kR} c_s c_{kR}^\dagger + t_{kR}^* c_{kR} c_s^\dagger \right) + \sum_k \left(t_{kd} c_d c_{kd}^\dagger + t_{kd}^* c_{kL} c_d^\dagger \right) \,. \tag{6.91}$$

Furthermore, all the junctions are modeled as non-interacting fermions

$$\mathcal{H}_{\mathrm{B}} = \sum_{\nu \in \{L,R,d\}} \sum_k \epsilon_{k\nu} c_{k\nu}^\dagger c_{k\nu} \,. \tag{6.92}$$

Treating the tunneling amplitudes perturbatively and fixing the reservoirs at thermal equilibrium states we derive the standard quantum-optical master equation, compare also Def. 7. Importantly, we do not apply the popular wide-band limit here (which would mean to approximate $\Gamma_\nu(\omega) \approx \Gamma_\nu$). In the energy eigenbasis of $\mathcal{H}_{\mathrm{S}}$ – further-on denoted by $|\rho\sigma\rangle$ where $\rho \in \{E, F\}$ describes the systems dot state and $\sigma \in \{0, 1\}$ denotes the state of the demon dot (both either empty or filled, respectively) – the populations obey a simple rate equation defined by Eq. (2.52). Denoting the populations by $p_{\rho\sigma} = \langle \rho\sigma | \, \rho \, | \rho\sigma \rangle$, the rate equation $\dot{P} = \mathcal{L}P$ in the ordered basis $P = (p_{0E}, p_{1E}, p_{0F}, p_{1F})^T$ decomposes into the contributions due to the different reservoirs

$\mathcal{L} = \mathcal{L}_D + \mathcal{L}_L + \mathcal{L}_R$, which read

$$\begin{aligned}
\mathcal{L}_D &= \begin{pmatrix} -\Gamma_D f_D & +\Gamma_D(1-f_D) & 0 & 0 \\ +\Gamma_D f_D & -\Gamma_D(1-f_D) & 0 & 0 \\ 0 & 0 & -\Gamma_D^U f_D^U & +\Gamma_D^U(1-f_D^U) \\ 0 & 0 & +\Gamma_D^U f_D^U & -\Gamma_D^U(1-f_D^U) \end{pmatrix}, \\
\mathcal{L}_\alpha &= \begin{pmatrix} -\Gamma_\alpha f_\alpha & 0 & +\Gamma_\alpha(1-f_\alpha) & 0 \\ 0 & -\Gamma_\alpha^U f_\alpha^U & 0 & +\Gamma_\alpha^U(1-f_\alpha^U) \\ +\Gamma_\alpha f_\alpha & 0 & -\Gamma_\alpha(1-f_\alpha) & 0 \\ 0 & +\Gamma_\alpha^U f_\alpha^U & 0 & -\Gamma_\alpha^U(1-f_\alpha^U) \end{pmatrix}, \qquad \alpha \in \{L,R\}\,, \qquad (6.93)
\end{aligned}$$

where we have used the abbreviations $\Gamma_\alpha = \Gamma_\alpha(\epsilon_s)$ and $\Gamma_\alpha^U = \Gamma_\alpha(\epsilon_s + U)$ for $\alpha \in \{L, R\}$ and $\Gamma_D = \Gamma_D(\epsilon_d)$ and $\Gamma_D^U = \Gamma_D(\epsilon_d + U)$ for the tunneling rates and similarly for the Fermi functions $f_\alpha = f_\alpha(\epsilon_s)$, $f_\alpha^U = f_\alpha(\epsilon_s + U)$, $f_D = f_D(\epsilon_d)$, and $f_D^U = f_D(\epsilon_d + U)$, respectively. We note that all contributions separately obey local-detailed balance relations. Closer inspection of the rates in Eq. (6.93) reveals that these rates could have been guessed without any microscopic derivation. For example, the transition rate from state $|1E\rangle$ to state $|0E\rangle$ is just given by the bare tunneling rate for the demon junction Γ_D multiplied by the probability to find a free space in the terminal at transition frequency ϵ_d. Similarly, the transition rate from state $|1F\rangle$ to state $|0F\rangle$ corresponds to an electron jumping out of the demon dot to its junction, this time, however, transporting energy of $\epsilon_d + U$. We have ordered our basis such that the upper left block of $\mathcal{L}_D$ describes the dynamics of the demon dot conditioned on an empty system dot, whereas the lower block accounts for the dynamics conditioned on a filled system.

As a whole, the system respects the second law of thermodynamics. We demonstrate this by analyzing the entropy production by means of the Full Counting Statistics. In order to avoid having to trace six counting fields, we note that the system obeys three conservation laws, since the two dots may only exchange energy but not matter

$$I_M^{(L)} + I_M^{(R)} = 0\,, \qquad I_M^{(D)} = 0\,, \qquad I_E^{(L)} + I_E^{(R)} + I_E^{(D)} = 0\,, \qquad (6.94)$$

where $I_E^{(\nu)}$ and $I_M^{(\nu)}$ denote energy and matter currents to terminal ν, respectively. Therefore, three counting fields should in general suffice to completely track the full entropy production in the long-term limit. For simplicity however, we compute the entropy production for the more realistic case of equal temperatures at the left and right SET junction $\beta = \beta_L = \beta_R$. Technically, this is conveniently performed by balancing with the entropy flow and using the conservation laws

$$\begin{aligned}
\dot{S}_\mathrm{i} &= -\dot{S}_\mathrm{e} = -\sum_\nu \beta^{(\nu)}(I_E^{(\nu)} - \mu^{(\nu)} I_M^{(\nu)}) \\
&= -\beta(I_E^{(L)} - \mu_L I_M^{(L)} + I_E^{(R)} - \mu_R I_M^{(R)}) - \beta_D I_E^{(D)} \\
&= (\beta - \beta_D) I_E^{(D)} - \beta(\mu_L - \mu_R) I_M^{(R)}\,. \qquad (6.95)
\end{aligned}$$

Thus, we conclude that for equal temperatures left and right it should even suffice to track e.g. only the energy transferred to the demon junction and the particles to the right lead. Therefore, we introduce counting fields for the demon (ξ) and for the particles transferred to the left junctions

(χ), and the counting-field dependent rate equation becomes

$$\begin{aligned}
\mathcal{L}_D(\xi) &= \begin{pmatrix} -\Gamma_D f_D & +\Gamma_D(1-f_D)e^{+\mathrm{i}\xi\epsilon_d} & 0 & 0 \\ +\Gamma_D f_D e^{-\mathrm{i}\xi\epsilon_d} & -\Gamma_D(1-f_D) & 0 & 0 \\ 0 & 0 & -\Gamma_D^U f_D^U & +\Gamma_D^U(1-f_D^U)e^{+\mathrm{i}\xi(\epsilon_d+U)} \\ 0 & 0 & +\Gamma_D^U f_D^U e^{-\mathrm{i}\xi(\epsilon_d+U)} & -\Gamma_D^U(1-f_D^U) \end{pmatrix}, \\
\mathcal{L}_R(\chi) &= \begin{pmatrix} -\Gamma_R f_R & 0 & +\Gamma_R(1-f_R)e^{+\mathrm{i}\chi} & 0 \\ 0 & -\Gamma_R^U f_R^U & 0 & +\Gamma_R^U(1-f_R^U)e^{+\mathrm{i}\chi} \\ +\Gamma_R f_R e^{-\mathrm{i}\chi} & 0 & -\Gamma_R(1-f_R) & 0 \\ 0 & +\Gamma_R^U f_R^U e^{-\mathrm{i}\chi} & 0 & -\Gamma_R^U(1-f_R^U) \end{pmatrix}. \qquad (6.96)
\end{aligned}$$

These counting fields can now be used to reconstruct the statistics of energy and matter transfer. The currents can be obtained by performing suitable derivatives of the rate matrix. For example, the energy current to the demon is given by $I_E^{(D)} = -\mathrm{i}\mathrm{Tr}\left\{\partial_\xi \mathcal{L}(\xi,0)|_{\xi=0}\,\bar{\rho}\right\}$, where $\bar{\rho}$ is the steady state $\mathcal{L}(0,0)\bar{\rho}=0$.

To test the fluctuation theorem, we calculate the characteristic polynomial

$$\begin{aligned}
\mathcal{D}(\xi,\chi) &= |\mathcal{L}(\xi,\chi)-\lambda\mathbf{1}| \\
&= (L_{11}-\lambda)(L_{22}-\lambda)(L_{33}-\lambda)(L_{44}-\lambda) \\
&\quad -(L_{11}-\lambda)(L_{22}-\lambda)L_{34}(\xi)L_{43}(\xi) - (L_{11}-\lambda)(L_{33}-\lambda)L_{24}(\chi)L_{42}(\chi) \\
&\quad -(L_{22}-\lambda)(L_{44}-\lambda)L_{13}(\chi)L_{31}(\chi) - (L_{33}-\lambda)(L_{44}-\lambda)L_{12}(\xi)L_{21}(\xi) \\
&\quad +L_{12}(\xi)L_{21}(\xi)L_{34}(\xi)L_{43}(\xi) + L_{13}(\chi)L_{31}(\chi)L_{24}(\chi)L_{42}(\chi) \\
&\quad -L_{12}(\xi)L_{24}(\chi)L_{31}(\chi)L_{43}(\xi) - L_{13}(\chi)L_{21}(\xi)L_{34}(\xi)L_{42}(\chi) \\
&= (L_{11}-\lambda)(L_{22}-\lambda)(L_{33}-\lambda)(L_{44}-\lambda) \\
&\quad -(L_{11}-\lambda)(L_{22}-\lambda)L_{34}(0)L_{43}(0) - (L_{11}-\lambda)(L_{33}-\lambda)L_{24}(\chi)L_{42}(\chi) \\
&\quad -(L_{22}-\lambda)(L_{44}-\lambda)L_{13}(\chi)L_{31}(\chi) - (L_{33}-\lambda)(L_{44}-\lambda)L_{12}(0)L_{21}(0) \\
&\quad +L_{12}(0)L_{21}(0)L_{34}(0)L_{43}(0) + L_{13}(\chi)L_{31}(\chi)L_{24}(\chi)L_{42}(\chi) \\
&\quad -L_{12}(\xi)L_{24}(\chi)L_{31}(\chi)L_{43}(\xi) - L_{13}(\chi)L_{21}(\xi)L_{34}(\xi)L_{42}(\chi)\,, \qquad (6.97)
\end{aligned}$$

where L_{ij} simply denote the matrix elements of the rate matrix $\mathcal{L}$. We note the symmetries

$$\begin{aligned}
L_{13}(-\chi) &= \frac{1-f_L}{f_L} L_{31}\left(+\chi + \mathrm{i}\ln\frac{f_L(1-f_R)}{(1-f_L)f_R}\right) = \frac{1-f_L}{f_L} L_{31}\left(+\chi + \mathrm{i}\beta(\mu_L-\mu_R)\right), \\
L_{24}(-\chi) &= \frac{1-f_L^U}{f_L^U} L_{42}\left(+\chi + \mathrm{i}\ln\frac{f_L^U(1-f_R^U)}{(1-f_L^U)f_R^U}\right) = \frac{1-f_L^U}{f_L^U} L_{42}\left(+\chi + \mathrm{i}\beta(\mu_L-\mu_R)\right), \\
L_{12}(-\xi) &= L_{21}\left(+\xi + \frac{\mathrm{i}}{\epsilon_d}\ln\frac{1-f_D}{f_D}\right) = L_{21}\left(+\xi + \frac{\mathrm{i}}{\epsilon_d}\beta_D(\epsilon_d-\mu_D)\right), \\
L_{34}(-\xi) &= L_{43}\left(+\xi + \frac{\mathrm{i}}{\epsilon_d+U}\ln\frac{1-f_D^U}{f_D^U}\right) = L_{43}\left(+\xi + \frac{\mathrm{i}}{\epsilon_d+U}\beta_D(\epsilon_d+U-\mu_D)\right), \qquad (6.98)
\end{aligned}$$

which can be used to show that the full characteristic polynomial obeys the symmetry

$$\mathcal{D}(-\xi,-\chi) = \mathcal{D}(\xi + \mathrm{i}(\beta_D-\beta)/U, \chi + \mathrm{i}\beta(\mu_L-\mu_R))\,. \qquad (6.99)$$

This symmetry implies – when monitoring the energy current to the demon e_D and the number of electrons transferred to the right junction n_R – for the corresponding probability distribution the

fluctuation theorem

$$\lim_{t\to\infty}\frac{P_{+\Delta n_S,+\Delta e_D}}{P_{-\Delta n_S,-\Delta e_D}} = e^{(\beta_D-\beta)\Delta e_D+\beta(\mu_L-\mu_R)\Delta n_S}\,. \tag{6.100}$$

Instead of determining the continuous energy emission distribution, we could alternatively have counted the discrete number of electrons entering the demon dot at energy ϵ_D and leaving it at energy ϵ_D+U. Since this process leads to a net energy extraction of energy U from the system, the corresponding matter current is tightly coupled to the energy current across the demon junction, i.e., their number would be related to the energy via $\Delta e_D = n_D U$. Comparing the value in the exponent of Eq. (6.100) with the average expectation value of the entropy production in Eq. (6.95), we can also – roughly speaking – interpret the fluctuation theorem as the ratio of probabilities for trajectories with a positive and negative entropy production.

In addition, we identify $P = (\mu_L-\mu_R)I_M^{(R)} = -(\mu_L-\mu_R)I_M^{(L)}$ as the power generated by the device, which – when the current flows against the bias – may yield a negative contribution βP to the overall entropy production. In these parameter regimes however, the negative contribution $\beta(\mu_L-\mu_R)I_M^{(R)}$ must be over-balanced by the second term $(\beta-\beta_D)I_E^{(D)}$, which clearly requires – when the demon reservoir is colder than the SET reservoirs $\beta_D > \beta_S$ – that the energy current flows out of the demon $I_E^{(D)} < 0$. As a whole, the system therefore just converts a thermal gradient between the two subsystems into power: A fraction of the heat coming from the hot SET leads is converted into power, and the remaining fraction is dissipated as heat at the cold demon junction. The corresponding efficiency for this conversion can be constructed from the output power $P = -(\mu_L-\mu_R)I_M^{(L)}$ and the input heat $\dot{Q}_L+\dot{Q}_R = -I_E^{(D)} - (\mu_L-\mu_R)I_M^{(L)} = \dot{Q}_{\rm diss}+P$, where $\dot{Q}_{\rm diss} = -I_E^{(D)}$ is the heat dissipated into the demon reservoir. Using that $\dot{S}_{\rm i}\geq 0$ we find that the efficiency – which of course is only useful in parameter regimes where the power is positive $\beta(\mu_L-\mu_R)I_M^{(R)} > 0$ – is upper-bounded by Carnot efficiency

$$\eta = \frac{P}{\dot{Q}_{\rm diss}+P} \leq 1-\frac{T_D}{T} = \eta_{\rm Car}\,. \tag{6.101}$$

For practical applications a large efficiency is not always sufficient. For example, a maximum efficiency at zero power output would be quite useless. Therefore, it has become common standard to first maximize the power output of the device and then compute the corresponding efficiency at maximum power. Due to the nonlinearity of the underlying equations, this may be a difficult numerical optimization problem. To reduce the number of parameters, we assume that $f_D^U = 1-f_D$ (which is the case when $\epsilon_D = \mu_D - U/2$) and $f_L^U = 1-f_R$ as well as $f_R^U = 1-f_L$ (which for $\beta_L=\beta_R=\beta$ is satisfied when $\epsilon_S = 1/2(\mu_L+\mu_R)-U/2$), see also the left panel of Fig. 6.7. Furthermore, we parametrize the modification of the tunneling rates by a single parameter via

$$\begin{aligned}
\Gamma_L &= \Gamma\frac{e^{+\delta}}{\cosh(\delta)}\,, \qquad \Gamma_L^U = \Gamma\frac{e^{-\delta}}{\cosh(\delta)}\\
\Gamma_R &= \Gamma\frac{e^{-\delta}}{\cosh(\delta)}\,, \qquad \Gamma_R^U = \Gamma\frac{e^{+\delta}}{\cosh(\delta)}
\end{aligned} \tag{6.102}$$

to favor transport in a particular direction. We have inserted the normalization by $\cosh(\delta)$ to keep the tunneling rates finite as the feedback strength δ is increased. Trivially, at $\delta=0$ we recover symmetric unperturbed tunneling rates and when $\delta\to\infty$, transport will be completely rectified. The matter current from left to right in the limit where the demon dot is much faster than the

SET ($\Gamma_D \to \infty$ and $\Gamma_D^U \to \infty$) becomes

$$I_M^{(L)} = \frac{\Gamma}{2}\left[f_L - f_R + \tanh(\delta)\,(f_L + f_R - 2f_D)\right] . \tag{6.103}$$

Similarly, we obtain for the energy current to the demon

$$I_E^{(D)} = \frac{\Gamma U}{2}\left[f_L + f_R - 2f_D + (f_L - f_R)\tanh(\delta)\right] , \tag{6.104}$$

which determines the dissipated heat. These can be converted into an efficiency solely expressed by Fermi functions when we use that

$$\begin{aligned} \beta(\mu_L - \mu_R) &= \ln\left(\frac{f_L(1-f_R)}{(1-f_L)f_R}\right) , \\ \beta U &= \ln\left(\frac{f_R(1-f_R^U)}{(1-f_R)f_R^U}\right) \to \ln\left(\frac{f_R f_L}{(1-f_R)(1-f_L)}\right) , \end{aligned} \tag{6.105}$$

which can be used to write the efficiency of heat to power conversion as

$$\eta = \frac{P}{\dot{Q}_{\rm diss} + P} = \frac{1}{1 + \frac{\beta \dot{Q}_{\rm diss}}{\beta P}} = \frac{1}{1 + \frac{\ln\left(\frac{f_R f_L}{(1-f_R)(1-f_L)}\right)(f_L + f_R - 2f_D + (f_L - f_R)\tanh(\delta))}{\ln\left(\frac{f_L(1-f_R)}{(1-f_L)f_R}\right)(f_L - f_R + (f_L + f_R - 2f_D)\tanh(\delta))}} , \tag{6.106}$$

which is also illustrated in Fig. 6.7.

Beyond these average considerations, the qualitative action of the device may also be understood at the level of single trajectories, see Fig. 6.8. It should be noted that at the trajectory level, all possible trajectories are still allowed, even though ones with positive total entropy production must on average dominate. As a whole, the system thereby merely converts a temperature gradient (cold demon, hot system) into useful power (current times voltage).

6.3.2 Local View: A Feedback-Controlled Device

An experimentalist having access only to the SET circuit would measure a positive generated power, conserved particle currents $I_M^{(L)} + I_M^{(R)} = 0$, but possibly a slight mismatch of left and right energy currents $I_E^{(L)} + I_E^{(R)} = -I_E^{(D)} \neq 0$. This mismatch could not fully account for the generated power, since for any efficiency $\eta > 1/2$ in Fig. 6.8 we have $\left|I_E^{(D)}\right| < P$. Therefore, the experimentalist would conclude that his description of the system by energy and matter flows is not complete and he might suspect Maxwell's demon at work. Here, we will make the reduced dynamics of the SET dot alone more explicit by deriving a reduced rate equation.

We can evidently write the rate equation defined by Eqs. (6.93) as $\dot{P}_\alpha = \mathcal{L}_{\alpha\alpha'} P_{\alpha'}$. Here, $\alpha \in \{E0, E1, F0, F1\}$ labels the energy eigenstates of the total system composed by the single dot and the demon dot. Resolving these two degrees of freedom $\alpha = (ij)$, where $i \in \{E, F\}$ and $j \in \{0, 1\}$, we can equivalently write $\dot{P}_{ij} = \mathcal{L}_{ij,i'j'} P_{i'j'}$, where i and j label the system (i) and detector/demon (j) degrees of freedom, respectively. If we discard the dynamics of the demon dot by tracing over its degrees of freedom $P_i = \sum_j P_{ij}$, we formally arrive at a non-Markovian evolution equation for the populations of the SET dot.

$$\dot{P}_i = \sum_{i'}\sum_{jj'} \mathcal{L}_{ij,i'j'} P_{i'j'} = \sum_{i'}\left[\sum_{jj'} \mathcal{L}_{ij,i'j'} \frac{P_{i'j'}}{P_{i'}}\right] P_{i'} = \mathcal{W}_{ii'}(t) P_{i'} . \tag{6.107}$$

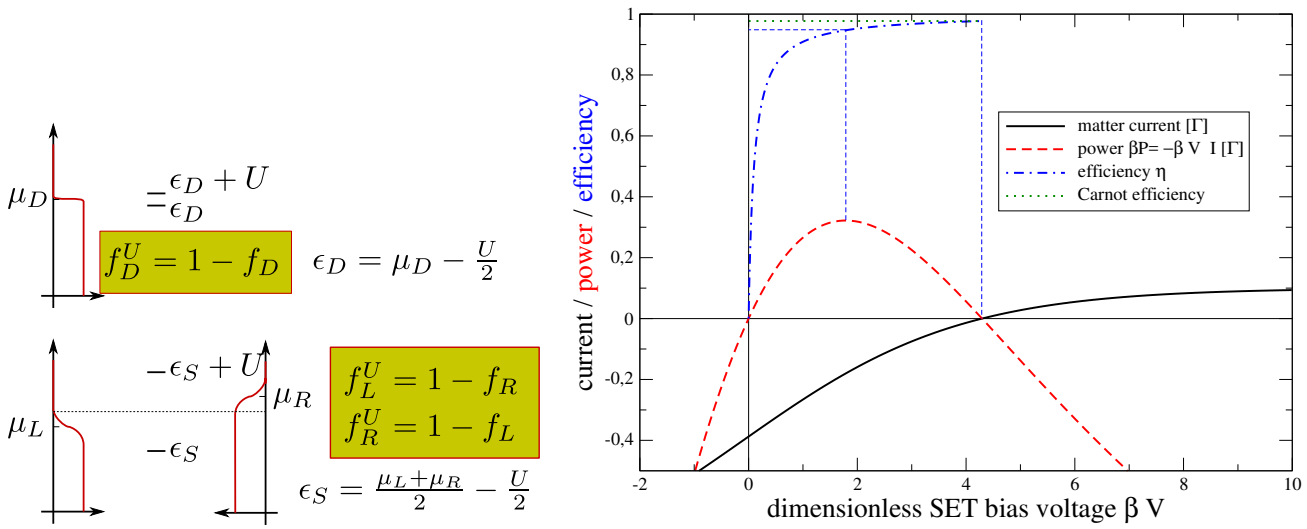

Figure 6.7:
Left: Sketch of the assumed configurations of chemical potentials, which imply at $\beta_L = \beta_R$ relations between the Fermi functions.
Right: Plot of current (solid black, in units of Γ), dimensionless power $\beta V I$ (dashed red, in units of Γ), and efficiency η (dash-dotted blue) versus dimensionless bias voltage. At equilibrated bias (origin), the efficiency vanishes by construction, whereas it reaches Carnot efficiency (dotted green) at the new equilibrium, i.e., at zero power. At maximum power however, the efficiency still closely approaches the Carnot efficiency. Parameters: $\delta = 100$, tunneling rates parametrized as in Eq. (6.102), $f_D = 0.9 = 1 - f_D^U$, $\beta\epsilon_S = -0.05 = -\beta(\epsilon_S + U)$, such that the Carnot efficiency becomes $\eta_{\text{Carnot}} = 1 - (\beta U)/(\beta_D U) \approx 0.977244$.

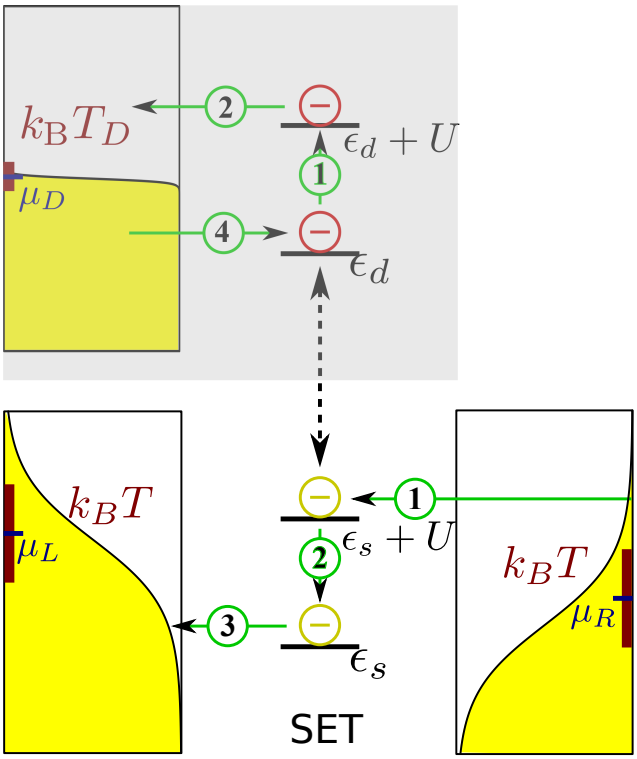

Figure 6.8: Level sketch of the setup. Shaded yellow regions represent occupied levels in the leads with chemical potentials and temperatures indicated. Central horizontal lines represent transition energies of system and demon dot, respectively. When the other dot is occupied, the bare transition frequency of every system is shifted by the Coulomb interaction U. The shown trajectory then becomes likely in the suggested Maxwell-demon mode: Initially, the SET is empty and the demon dot is filled. When $\Gamma_R^U \gg \Gamma_L^U$, the SET dot is most likely first filled from the left lead, which shifts the transition frequency of the demon (1). When the bare tunneling rates of the demon are much larger than that of the SET, the demon dot will rapidly equilibrate by expelling the electron to its associated reservoir (2) before a further electronic jump at the SET may occur. At the new transition frequency, the SET electron is more likely to escape first to the left than to the right when $\Gamma_L \gg \Gamma_R$ (3). Now, the demon dot will equilibrate again by filling with an electron (4) thus restoring the initial state. In essence, an electron is transferred against the bias through the SET circuit while in the demon system an electron enters at energy ϵ_d and leaves at energy $\epsilon_d + U$ leading to a net transfer of U from the demon into its reservoir.

This equation is non-Markovian, since to solve for the time-dependent rates $\mathcal{W}_{ii'}$ we would need to integrate over the solution of the full rate equation, which implies that they depend on the values of the system of the past. However, we may identify $\frac{P_{i'j'}}{P_{i'}}$ as the conditional probability of the demon being in state j' provided the system is in state i'.

Direct inspection of the rates suggests that when we assume the limit where the bare rates of the demon system are much larger than the SET tunneling rates, these conditional probabilities will assume their conditioned stationary values much faster than the SET dynamics. In this limit, the dynamics is mainly dominated by transitions between just two mesostates instead of the original four states. These mesostates are associated to either a filled or an empty system quantum dot, respectively. We may hence arrive again at a Markovian description by approximating

$$P_{j'|i} = \frac{P_{i'j'}}{P_{i'}} \to \frac{\bar{P}_{i'j'}}{\bar{P}_{i'}}\,, \tag{6.108}$$

which yields the coarse-grained rate matrix

$$\mathcal{W}_{ii'} = \sum_{jj'} \mathcal{L}_{ij,i'j'} \frac{\bar{P}_{i'j'}}{\bar{P}_{i'}}\,. \tag{6.109}$$

For the model at hand, the stationary conditional probabilities become in the limit where $\Gamma_D^{(U)} \gg \Gamma_{L/R}^{(U)}$

$$\begin{aligned} P_{0|E} &= \frac{\bar{P}_{E0}}{\bar{P}_E} = 1 - f_D\,, \qquad P_{1|E} = \frac{\bar{P}_{E1}}{\bar{P}_E} = f_D\,, \\ P_{0|F} &= \frac{\bar{P}_{F0}}{\bar{P}_F} = 1 - f_D^U\,, \qquad P_{1|F} = \frac{\bar{P}_{F1}}{\bar{P}_F} = f_D^U\,, \end{aligned} \tag{6.110}$$

and just describe the fact that – due to the time-scale separation – the demon dot immediately reaches a thermal stationary state that depends on the occupation of the SET dot. The temperature and chemical potential of the demon reservoir determine if and how well the demon dot – which can be envisaged as the demon's memory capable of storing just one bit – captures the actual state of the system dot. For example, for high demon temperatures it will be roughly independent on the system dots occupation as $f_D \approx f_D^U \approx 1/2$. At very low demon temperatures however, and if the chemical potential of the demon dot is adjusted such that $\epsilon_d - \mu_D < 0$ and $\epsilon_d + U - \mu_D > 0$, the demon dot will nearly accurately (more formally when $\beta_D U \gg 1$) track the system occupation, since $f_D \to 1$ and $f_D^U \to 0$. Then, the demon dot will immediately fill when the SET dot is emptied and its electron will leave when the SET dot is filled. It thereby faithfully detects the state of the SET. In the presented model, the demon temperature thereby acts as a source of error in the demon's measurement of the system's state. In addition, the model at hand allows to investigate the detector backaction on the probed system, which is often neglected. Here, this backaction is essential, and we will now investigate it by analyzing the reduced dynamics in detail.

The coarse-grained probabilities P_E and P_F of finding the SET dot empty or filled, respectively, obey the rate equation dynamics

$$\mathcal{L} = \begin{pmatrix} -L_{FE} & +L_{EF} \\ +L_{FE} & -L_{EF} \end{pmatrix} \tag{6.111}$$

with the coarse-grained rates

$$\begin{aligned} L_{EF} &= L_{E0,F0}\frac{\bar{P}_{F0}}{\bar{P}_F} + L_{E1,F1}\frac{\bar{P}_{F1}}{\bar{P}_F} \\ &= \left[\Gamma_L(1-f_L)+\Gamma_R(1-f_R)\right](1-f_D^U) + \left[\Gamma_L^U(1-f_L^U)+\Gamma_R^U(1-f_R^U)\right] f_D^U\,, \\ L_{FE} &= L_{F0,E0}\frac{\bar{P}_{E0}}{\bar{P}_E} + L_{F1,E1}\frac{\bar{P}_{E1}}{\bar{P}_E} \\ &= \left[\Gamma_L f_L+\Gamma_R f_R\right](1-f_D) + \left[\Gamma_L^U f_L^U+\Gamma_R^U f_R^U\right] f_D\,. \end{aligned} \tag{6.112}$$

We note that a naive experimenter – not aware of the demon interacting with the SET circuit – would attribute the rates in the coarse-grained dynamics to just two reservoirs: $\mathcal{L} = \mathcal{L}_L + \mathcal{L}_R$ with the rates $\mathcal{L}_{EF}^{(\alpha)} = (1-f_D^U)\Gamma_\alpha(1-f_\alpha) + f_D^U\Gamma_\alpha^U(1-f_\alpha^U)$ and $\mathcal{L}_{FE}^{(\alpha)} = (1-f_D)\Gamma_\alpha f_\alpha + f_D\Gamma_\alpha^U f_\alpha^U$. Thus, when the SET is not sensitive to the demon state $\Gamma_{L/R}^U \approx \Gamma_{L/R}$ and $f_{L/R}^U \approx f_{L/R}$, local detailed balance is restored, and we recover the conventional SET rate equation.

We note that the matter current

$$I_M^{(\nu)} = L_{EF}^{(\nu)}\bar{P}_F - \mathcal{L}_{FE}^{(\nu)}\bar{P}_E \tag{6.113}$$

is conserved $I_M^{(L)} = -I_M^{(R)}$, such that the entropy production becomes

$$\begin{aligned} \dot{S}_\mathrm{i} &= \sum_{\nu\in\{L,R\}} L_{EF}^{(\nu)}\bar{P}_F \ln\left(\frac{\mathcal{L}_{EF}^{(\nu)}\bar{P}_F}{\mathcal{L}_{FE}^{(\nu)}\bar{P}_E}\right) + \mathcal{L}_{FE}^{(\nu)}\bar{P}_E \ln\left(\frac{\mathcal{L}_{FE}^{(\nu)}\bar{P}_E}{\mathcal{L}_{EF}^{(\nu)}\bar{P}_F}\right) \\ &= \sum_{\nu\in\{L,R\}} \left(L_{EF}^{(\nu)}\bar{P}_F - \mathcal{L}_{FE}^{(\nu)}\bar{P}_E\right) \ln\left(\frac{\mathcal{L}_{EF}^{(\nu)}\bar{P}_F}{\mathcal{L}_{FE}^{(\nu)}\bar{P}_E}\right) \\ &= I_M^{(L)} \ln\left(\frac{\mathcal{L}_{EF}^{(L)}\mathcal{L}_{FE}^{(R)}}{\mathcal{L}_{FE}^{(L)}\mathcal{L}_{EF}^{(R)}}\right) = I_M^{(L)}\mathcal{A}\,, \end{aligned} \tag{6.114}$$

and is thus representable in a simple flux-affinity form. Similarly, we note that if we would count particle transfers from the left to the right reservoir, the following fluctuation theorem would hold

$$\frac{P_{+n}}{P_{-n}} = e^{n\mathcal{A}}\,, \tag{6.115}$$

and the fact that these fluctuations could in principle be resolved demonstrates that the affinity in the entropy production is a meaningful and measurable quantity. Without the demon dot, the conventional affinity of the SET would simply be given by

$$\mathcal{A}_0 = \ln\left(\frac{(1-f_L)f_R}{f_L(1-f_R)}\right) = \beta_L(\epsilon-\mu_L) - \beta_R(\epsilon-\mu_R)\,, \tag{6.116}$$

and ignoring the physical implementation of the demon, we can interpret the modification of the entropy production due to the demon as an additional information current that is tightly coupled to the particle current

$$\dot{S}_\mathrm{i} = I_M^{(L)}\mathcal{A}_0 + I_M^{(L)}(\mathcal{A}-\mathcal{A}_0) = \dot{S}_\mathrm{i}^{(0)} + \mathcal{I}\,. \tag{6.117}$$

When the demon temperature is lowered such that $\beta_D U \gg 1$ and its chemical potential is adjusted such that $f_D \to 1$ and $f_D^U \to 0$, the affinity becomes

$$\mathcal{A} = \ln\left(\frac{\Gamma_L(1-f_L)\Gamma_R^U f_R^U}{\Gamma_L^U f_L^U \Gamma_R(1-f_R)}\right) = \ln\left(\frac{\Gamma_L\Gamma_R^U}{\Gamma_L^U\Gamma_R}\right) + \ln\left(\frac{f_L f_R^U}{f_L^U f_R}\right) + \mathcal{A}_0\,. \tag{6.118}$$

The last term on the right-hand side is simply the affinity without the demon dot. The first two terms quantify the modification of the affinity. The pure limit of a Maxwell demon is reached, when the energetic backaction of the demon on the SET is negligible, i.e., when $f_L^U \approx f_L$ and $f_R^U \approx f_R$, which requires comparably large SET temperatures $\beta_{L/R}U \ll 1$. Of course, to obtain any nontrivial effect, it is still necessary to keep non-flat tunneling rates $\Gamma_{L/R}^U \neq \Gamma_{L/R}$, and in this case one recovers the case discussed in the previous section – identifying Γ_α^E with Γ_α and Γ_α^F with Γ_α^U.

6.4 Further feedback applications

6.4.1 Suppression of Noise

The simplest model to study the suppression of noise in counting statistics [23] is that of a single junction. Such a junction could be physically implemented by a QPC

$$H = \sum_k \epsilon_{kL} c_{kL}^\dagger c_{kL} + \sum_k \epsilon_{kR} c_{kR}^\dagger c_{kR} + \sum_{kk'}\left[t_{kk'} c_{kL} c_{k'R}^\dagger + t_{kk'}^* c_{k'R} c_{kL}^\dagger\right]\,, \tag{6.119}$$

where $c_{k\alpha}$ are fermionic annihilation operators for electrons in mode k and lead α. The tunneling process from an electron of the left lead in mode k to the mode k' of the right lead is described by the term $t_{kk'} c_{kL} c_{k'R}^\dagger$, whereas the inverse process is described by the hermitian conjugate term. We have treated this model before – as a detector measuring the charge of a single electron transistor, compare Sec. 4.2.2. We can therefore simply consider the limit where the single-electron transistor is empty throughout, such that the QPC dynamics is not affected by it. Then, one as in the small tunneling limit the equation

$$\dot{P}_n = +\gamma P_{n-1}(t) + \bar{\gamma} P_{n+1} - [\gamma + \bar{\gamma}]\, P_n(t)\,, \tag{6.120}$$

where $P_n(t)$ denotes the probability to have n particles passed the junction after time t. Here, the forward and backward tunneling rates are microscopically linked to the QPC parameters, compare Eq. (4.66)

$$\gamma \;=\; t\frac{V}{1-e^{-\beta V}}\,, \qquad \bar{\gamma} = t\frac{V}{e^{+\beta V}-1}\,, \tag{6.121}$$

where t denotes the bare transition function of the QPC, β its inverse temperature, and V the bias voltage applied accross the QPC. We see that for $V > 0$, we have transport from left to right, whereas for $V < 0$ the current is reversed. Thereby, all the microscopic information contained in the tunneling amplitudes $t_{kk'}$ and the lead occupations $f_\alpha(\omega)$ is compressed only in the two tunneling rates γ and $\bar{\gamma}$, see Fig. 6.9. Thus, one may be changing the bias voltage modify these tunneling rates.

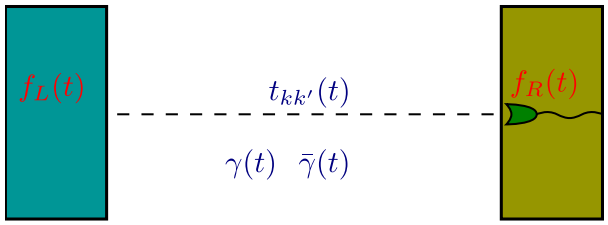

Figure 6.9: Sketch of a single junction between two reservoirs, characterized by their Fermi functions f_α and tunneling amplitudes $t_{kk'}$. The time-dependent microscopic parameters just enter into the time-dependent left-to-right and right-to-left tunneling rates $\gamma(t)$ and $\bar{\gamma}(t)$, respectively. The piecewise-constant time-dependence may either follow a predefined protocol (open-loop control) or can be conditioned on a measurement result (feedback control). The system in this case is given by a virtual detector that counts the net number of particles transferred from left to right.

Dynamics in absence of control

First let us consider the time-independent case. After Fourier transformation $P(\chi,t) = \sum_n P_n(t) e^{+in\chi}$, the n-resolved equation becomes

$$\dot{P}(\chi,t) = \left[\gamma(e^{+i\chi}-1) + \bar{\gamma}(e^{-i\chi}-1)\right] P(\chi,t)\,. \tag{6.122}$$

This is thus in perfect agreement with what we had for the QPC statistics in Eq. (4.65). With the initial condition $P(\chi,0) = 1$ it is solved by

$$P(\chi,t) = \exp\left\{\left[\gamma(e^{+i\chi}-1) + \bar{\gamma}(e^{-i\chi}-1)\right] t\right\}\,. \tag{6.123}$$

Exercise 48 (Cumulants)**.** *Show that the cumulants of the probability distribution $P_n(t)$ are given by*

$$\left\langle\left\langle n^k \right\rangle\right\rangle = \left[\gamma + (-1)^k \bar{\gamma}\right] t\,,$$

and can thus be understood as two counter-propagating Poissonian distributions.

This initial condition is chosen because we assume that at time $t = 0$, no particle has crossed the junction $P_n(0) = \delta_{n,0}$. The probability to count n particles after time t can be obtained from the inverse Fourier transform

$$P_n(t) = \frac{1}{2\pi}\int_{-\pi}^{+\pi} \exp\left\{\left[\gamma(e^{+i\chi}-1) + \bar{\gamma}(e^{-i\chi}-1)\right] t\right\} e^{-in\chi} d\chi\,. \tag{6.123}$$

This probability can for this one-dimensional model be calculated analytically even in the case of

bidirectional transport

$$\begin{aligned} P_n(t) &= e^{-(\gamma+\bar{\gamma})t} \sum_{a,b=0}^{\infty} \frac{(\gamma t)^a}{a!} \frac{(\bar{\gamma} t)^b}{b!} \frac{1}{2\pi} \int_{-\pi}^{+\pi} e^{+\mathrm{i}(a-b-n)\chi} d\chi \\ &= e^{-(\gamma+\bar{\gamma})t} \sum_{a,b=0}^{\infty} \frac{(\gamma t)^a}{a!} \frac{(\bar{\gamma} t)^b}{b!} \delta_{a-b,n} \\ &= e^{-(\gamma+\bar{\gamma})t} \begin{cases} \sum_{a=n}^{\infty} \frac{(\gamma t)^a}{a!} \frac{(\bar{\gamma} t)^{a-n}}{(a-n)!} & : \quad n \geq 0 \\ \sum_{a=0}^{\infty} \frac{(\gamma t)^a}{a!} \frac{(\bar{\gamma} t)^{a-n}}{(a-n)!} & : \quad n < 0 \end{cases} \\ &= e^{-(\gamma+\bar{\gamma})t} \left(\frac{\gamma}{\bar{\gamma}} \right)^{n/2} \mathcal{J}_n(2\sqrt{\gamma\bar{\gamma}} t) \,, \end{aligned} \tag{6.124}$$

where $\mathcal{J}_n(x)$ denotes a modified Bessel function of the first kind – defined as the solution of $z^2 \mathcal{J}_n''(z) + z\mathcal{J}_n'(z) - (z^2 + n^2)\mathcal{J}_n(z) = 0$. In the unidirectional transport limit, this reduces to a normal Poissonian distribution

$$\lim_{\bar{\gamma} \to 0} P_n(t) = \begin{cases} e^{-\gamma t} \frac{(\gamma t)^n}{n!} & : \quad n \geq 0 \\ 0 & : \quad n < 0 \end{cases} . \tag{6.125}$$

Exercise 49 (Poissonian limit)**.** *Show that a Poissonian distribution arises in the unidirectional transport limit.*

We further note that the moment-generating function just trivially given by $M(\chi, t) = P(\chi, t)$, and correspondingly the cumulant-generating function assumes the simple form

$$C(\chi, t) = \gamma t(e^{+\mathrm{i}\chi} - 1) + \bar{\gamma} t(e^{-\mathrm{i}\chi} - 1) \,, \tag{6.126}$$

which now also holds for finite times and not only for large times. We see that this is just the independent superposition of two counter-propagating Poissonian processes with cumulants γt and $\bar{\gamma} t$.

In the following, we will – mainly for simplicity – consider only the unidirectional transport limit by demanding that the bias voltage is always large enough such that the reverse tunneling process is negligible $\bar{\gamma} \to 0$.

Open-Loop Control

Now we consider the case of a time-dependent rate $\gamma \to \gamma(t)$ with a piecewise-constant time dependence. Just for simplicity, we will constrain ourselves to unidirectional transport $\bar{\gamma} = 0$ as shown in Fig. 6.10, where the time-dependence of $\gamma(t)$ is well approximated by a piecewise-constant protocol. We assume that the parameter γ is changed at regular time intervals Δt, such that the control protocol is fully characterized by the sequence $\{\gamma_1, \gamma_2, \ldots\}$. The fact that the model is scalar (has no internal structure) implies that the system has no internal memory, and the initial state for each interval is therefore just that no particle has crossed the junction. Consequently, the probability distribution of measuring particles in the α-th time interval is completely independent

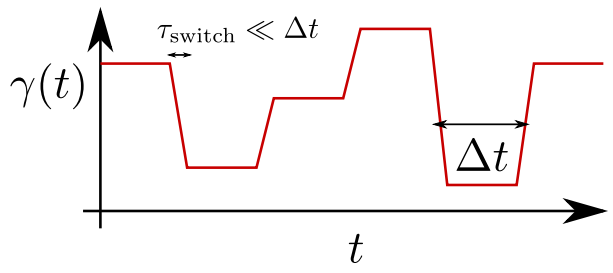

Figure 6.10: Time-dependent tunneling rate which is (nearly) piecewise constant during the intervals Δt. In the model, we neglect the switching time τ_{switch} completely.

from the outcome of the interval $\alpha - 1$. If we denote the cumulant during the interval Δt in the α-th interval by $\left\langle\left\langle n^k \right\rangle\right\rangle_\alpha$, we find for the average over all time intervals

$$\langle\langle \bar{n^k} \rangle\rangle = \frac{1}{N}\sum_{\alpha=1}^{N} \left\langle\left\langle n^k \right\rangle\right\rangle_\alpha = \frac{1}{N}\sum_{\alpha=1}^{N} \gamma_\alpha \Delta t = \langle\gamma\rangle\, \Delta t\,, \tag{6.127}$$

i.e., all average cumulants are simply described by the time-averaged tunneling rate Regardless of the actual form of the protocol, one therefore always obtains a Poissonian distribution. In conclusion, piecewise-constant open loop control applied to a single junction will not substantially alter its dynamics.

Closed-Loop control

For simplicity, we again consider here the unidirectional transport limit, which is described by

$$\dot{P}_n = \gamma P_{n-1} - \gamma P_n\,. \tag{6.128}$$

The parameter γ describes the speed at which the resulting Poissonian distribution

$$P_n(\Delta t) = \begin{cases} e^{-\gamma\Delta t}\frac{(\gamma\Delta t)^n}{n!} & : \quad n \geq 0 \\ 0 & : \quad n < 0 \end{cases} \tag{6.129}$$

moves towards larger n. This however, also goes along with a spread of the distribution: Its width $\sigma = \sqrt{C_2} = \sqrt{\langle n^2\rangle - \langle n\rangle^2}$ increases as $\sigma \propto t^{1/2}$. When we arrange the probabilities in an infinite-dimensional vector, the rate matrix appears band-diagonal

$$\frac{d}{dt}\begin{pmatrix} \vdots \\ P_{n-1} \\ P_n \\ \vdots \end{pmatrix} = \begin{pmatrix} \ddots & & & \\ \ddots & -\gamma & & \\ & +\gamma & -\gamma & \\ & & \ddots & \ddots \end{pmatrix}\begin{pmatrix} \vdots \\ P_{n-1} \\ P_n \\ \vdots \end{pmatrix} = \boldsymbol{\mathcal{L}}\boldsymbol{P}\,. \tag{6.130}$$

For the initial state $P_n(0) = \delta_{n,0}$ we have written the solution to the above equation explicitly in terms of a Poissonian distribution (6.129). Using the translational invariance in n and linearity of the equations, we can therefore write the general solution explicitly as

$$\begin{pmatrix} P_0(t+\Delta t) \\ P_1(t+\Delta t) \\ P_2(t+\Delta t) \\ \vdots \\ P_n(t+\Delta t) \\ \vdots \end{pmatrix} = e^{-\gamma\Delta t}\begin{pmatrix} 1 & & & \\ \gamma\Delta t & 1 & & \\ \frac{(\gamma\Delta t)^2}{2} & \gamma\Delta t & 1 & \\ \vdots & \vdots & \ddots & \ddots \\ \frac{(\gamma\Delta t)^n}{n!} & \frac{(\gamma\Delta t)^{n-1}}{(n-1)!} & \cdots & \cdots \\ \vdots & \vdots & & \end{pmatrix}\begin{pmatrix} P_0(t) \\ P_1(t) \\ P_2(t) \\ \vdots \\ P_n(t) \\ \vdots \end{pmatrix} = e^{\mathcal{L}\Delta t}\boldsymbol{P}(t)\,, \tag{6.131}$$

which takes the form $\boldsymbol{P}(t+\Delta t) = \mathcal{P}(\Delta t)\boldsymbol{P}(t) = e^{\mathcal{L}\Delta t}\boldsymbol{P}(t)$ with the infinite-dimensional propagation matrix $\mathcal{P}(\Delta t)$.

Exercise 50 (Probability conservation)**.** *Show that the above introduced propagator* $\mathcal{P}(\Delta t)$*preserves the sum of all probabilities, i.e., that* $\sum_n P_n(t+\Delta t) = \sum_n P_n(t)$.

We have found previously that an open-loop control scheme does not drastically modify the probability distribution of tunneled particles. We do now consider regular measurements of the number of tunneled particles being performed at time intervals Δt. The major difference to our previous considerations is now that we modify the tunneling rate γ dependent on the measured number of tunneled particles. Measurement of n tunneled particles can be described by a projective measurement of the density matrix. In super-operator notation, the matrix elements of the corresponding projector just read

$$(\mathcal{M}_n)_{ij} = \delta_{i,n}\delta_{j,n}\,. \tag{6.132}$$

Conditioning the following propagator on the measurement result $\mathcal{P}(\Delta t) \to \mathcal{P}_n(\Delta t)$ via switching the tunneling rate dependent on the measurement outcome, the effective propagator under feedback control becomes

$$\mathcal{P}_{\rm fb}(\Delta t) = \sum_n \mathcal{P}_n(\Delta t)\mathcal{M}_n\,. \tag{6.133}$$

Making everything explicit, the propagation matrix becomes

$$\mathcal{P}_{\rm fb}(\Delta t) = \begin{pmatrix} e^{-\gamma_0\Delta t} & & & \\ e^{-\gamma_0\Delta t}(\gamma_0\Delta t) & e^{-\gamma_1\Delta t} & & \\ e^{-\gamma_0\Delta t}\frac{(\gamma_0\Delta t)^2}{2} & e^{-\gamma_1\Delta t}(\gamma_1\Delta t) & e^{-\gamma_2\Delta t} & \\ \vdots & \vdots & \vdots & \ddots \\ e^{-\gamma_0\Delta t}\frac{(\gamma_0\Delta t)^n}{n!} & e^{-\gamma_1\Delta t}\frac{(\gamma_1\Delta t)^{n-1}}{(n-1)!} & e^{-\gamma_2\Delta t}\frac{(\gamma_2\Delta t)^{n-2}}{(n-2)!} & \cdots \\ \vdots & \vdots & \vdots & \ddots \end{pmatrix}. \tag{6.134}$$

The vector of probabilities under feedback evolves according to the iteration scheme $\boldsymbol{P}(t+\Delta t) = \mathcal{P}_{\rm fb}(\Delta t)\boldsymbol{P}(t)$. Formally, every column thus corresponds to a different Poissonian process with tunneling rate γ_n.

Exercise 51 (Effective Feedback Propagator)**.** *Show the validity of Eq. (6.134).*

One could now calculate even the full dynamics of cumulants for very large measurement intervals Δt [2]. However, here we will mainly only discuss the continuous feedback limit as $\Delta t \to 0$. Using that $\sum_n \mathcal{M}_n = \mathbf{1}$, we get the effective feedback Liouvillian

$$\mathcal{L}_{\rm fb} = \sum_{n=0}^{\infty}\mathcal{L}_n\mathcal{M}_n = \begin{pmatrix} -\gamma_0 & & & \\ +\gamma_0 & -\gamma_1 & & \\ & +\gamma_1 & -\gamma_2 & \\ & & \ddots & \ddots \end{pmatrix}, \tag{6.135}$$

which can also be written in the form

$$\dot{P}_n = +\gamma_{n-1}P_{n-1} - \gamma_n P_n \,. \tag{6.136}$$

We see that translational invariance is broken, such that simply using a discrete Fourier transform $P(\chi,t) = \sum_n P_n(t)e^{+\mathrm{i}n\chi}$ will not lead to a simple generalized master equation as in absence of feedback. Instead, it will lead to partial differential equations that can only be solved with significant effort.

The feedback protocol is now defined when one decides what action to perform in response to measuring a certain number of particles at time t, i.e., in allowing for time and particle-resolved tunneling rates $\gamma_n(t)$. We first define the time-dependent first two cumulants

$$C_1(t) = \sum_n nP_n(t)\,, \qquad C_2(t) = \sum_n n^2 P_n(t) - C_1^2(t)\,, \tag{6.137}$$

which yields for the first cumulant the differential equation

$$\dot{C}_1 = \sum_n n\left[\gamma_{n-1}P_{n-1} - \gamma_n P_n\right] = \sum_n \left[(n+1)\gamma_n P_n - n\gamma_n P_n\right] = \sum_n \gamma_n P_n = \langle\gamma_n\rangle_t \,. \tag{6.138}$$

From a similar calculation, we get the time derivative of the second cumulant

$$\begin{aligned}\dot{C}_2 &= \sum_n n^2\left[\gamma_{n-1}P_{n-1} - \gamma_n P_n\right] - 2C_1(t)\dot{C}_1 = \sum_n (2n+1)\,\gamma_n P_n - 2C_1(t)\dot{C}_1 \\ &= \langle\gamma_n\rangle_t\left[1 - 2C_1(t)\right] + 2\,\langle n\gamma_n\rangle_t \,.\end{aligned} \tag{6.139}$$

Below, we discuss different feedback realizations.

Linear Feedback

Linear feedback of the form

$$\gamma_n(t) = \gamma\left[1 - g(n - \gamma t)\right] \tag{6.140}$$

with the feedback parameters $g > 0$ and $\gamma > 0$ is much simpler to evaluate analytically. It can be thought of an approximation of a general feedback scheme. Of course, the above scheme formally allows for negative rates when $n \gg \gamma_0 t$. In reality however, the probability for such a process is exponentially suppressed for sufficiently large times, since for large times the width of a Poissonian process is sufficiently smaller than its mean value $\sigma/\mu = 1/\sqrt{\gamma t}$. The objective of the feedback is to increase the tunneling rate when the number of particles is below γt and to decrease the tunneling rate when it is above γt. Thereby, slow trajectories are sped up, and fast trajectories are slowed down.

The linear feedback scheme has the advantage that the equations for the cumulant evolutions close. In particular, the first cumulant evolves according to

$$\dot{C}_1 = \gamma\left[1 + g\gamma t\right] - g\gamma C_1(t)\,, \tag{6.141}$$

which for the initial condition $C_1(0) = 0$ has the particularly simple solution $C_1(t) = \gamma t$. Inserting this in the evolution equation of the second cumulant, we get

$$\begin{aligned}\dot{C}_2 &= \gamma[1 - 2\gamma t] + 2\,\langle n\gamma_n\rangle_t = \gamma[1 - 2\gamma t] + 2\left[\langle n\rangle\,\gamma(1 + g\gamma t) - g\gamma\left\langle n^2\right\rangle\right] \\ &= \gamma[1 - 2\gamma t] + 2\left[\gamma t(1 + g\gamma t)\gamma - g\gamma(C_2(t) + (\gamma t)^2)\right] \\ &= \gamma[1 - 2gC_2(t)]\,.\end{aligned} \tag{6.142}$$

This coupled set of differential equations admits for the initial conditions $C_1(0) = 0$ and $C_2(0) = 0$ the simple solution [23]

$$C_1(t) = \gamma t\,, \qquad C_2(t) = \frac{1 - e^{-2g\gamma t}}{2g}\,, \tag{6.143}$$

which shows a continuous evolution towards a constant width of $\bar{\sigma} = \sqrt{\lim_{t\to\infty} C_2(t)} = \frac{1}{\sqrt{2g}}$.

Freezing the second cumulant of otherwise stochastic processes has many interesting applications. For example, many processes with a stochastic fluctuating work load might profit from a smoothed evolution if control may be applied. In an electronic context, a stabilized width of the electronic counting statistics could help to improve the standard of the electric current [24].

Exponential Feedback

The linear feedback is simple to treat but has the disadvantage that negative rates may in principle occur. Next, we consider an exponential feedback scheme

$$\gamma_n(t) = \gamma e^{\alpha(\gamma t - n)}\,. \tag{6.144}$$

This for $\alpha > 0$ also tends to slow down fast trajectories ($n > \gamma t$) and to speed up slow trajectories ($n < \gamma t$) by decreasing or increasing the tunneling rate. However, we see that in contrast to the previous scheme the rate is always positive. We cannot solve the general dynamics anymore, but we can start from a Gaussian distribution

$$P_n(t) = \frac{1}{\sqrt{2\pi}\sigma} e^{-\frac{(n-\mu)^2}{2\sigma^2}} \tag{6.145}$$

and then look how the feedback affects the distribution. We stress that at present, μ and σ are unknown. When $\gamma t \gg \sigma$, we can replace the summation over n by an integral over $x = n$, where we see immediately that the distribution is properly normalized. Evaluating everything by integrals, we get

$$\dot{C}_1 = \langle \gamma_n \rangle \approx \int \gamma e^{\alpha(\gamma t - x)} \frac{1}{\sqrt{2\pi}\sigma} e^{-\frac{(x-\mu)^2}{2\sigma^2}} dx = \gamma \exp\left\{ \frac{\alpha}{2} \left(\alpha\sigma^2 + 2\gamma t - 2\mu \right) \right\}\,. \tag{6.146}$$

Therefore, demanding that the first cumulant grows linearly with $\dot{C}_1 = \gamma$ we obtain the constraint

$$\mu = \gamma t + \sigma^2 \alpha/2\,. \tag{6.147}$$

The solution for the first cumulant could with the appropriate initial condition then be $C_1(t) = \mu = \gamma t + \sigma^2\alpha/2$. We can insert this in the evolution equation for the second cumulant

$$\begin{aligned} \dot{C}_2 &= \dot{C}_1 \left[1 - 2C_1(t)\right] + 2 \left\langle n\gamma_n \right\rangle_t = \gamma \left[1 - 2C_1(t)\right] + 2 \int \gamma x e^{\alpha(\gamma t - x)} \frac{1}{\sqrt{2\pi}\sigma} e^{-\frac{(x-\mu)^2}{2\sigma^2}} dx \\ &= \gamma \left[1 - 2C_1(t)\right] + 2\gamma^2 t - \gamma\alpha\sigma^2 = \gamma[1 - \alpha\sigma^2]\,. \end{aligned} \tag{6.148}$$

Therefore, in order to stabilize a Gaussian with width σ, we need to adjust the feedback protocol parameter as

$$\alpha = \frac{1}{2\sigma^2}\,. \tag{6.149}$$

6.4.2 Qubit stabilization

Qubits – any quantum-mechanical two-level system that can be prepared in a superposition of its two states $|0\rangle$ and $|1\rangle$ – are at the heart of quantum computers with great technological promises. The major obstacle to be overcome to build a quantum computer is decoherence: Qubits prepared in pure superposition states (as required for performing quantum computation) tend to decay into a statistical mixture when coupled to a destabilizing reservoir (of which there is an abundance in the real world). Here, we will approach the decoherence with a quantum master equation and use feedback control to act against the decay of coherences.

The system is described by

$$\begin{aligned} \mathcal{H}_{\mathrm{S}} &= \frac{\Omega}{2}\sigma^z\,, \qquad \mathcal{H}_{\mathrm{B}}^{(1)} = \sum_k \omega_{k1} b_{k1}^\dagger b_{k1}\,, \qquad \mathcal{H}_{\mathrm{B}}^{(2)} = \sum_k \omega_{k2} b_{k2}^\dagger b_{k2} \\ \mathcal{H}_{\mathrm{I}}^{(1)} &= \sigma^z \otimes \sum_k \left[h_{k1} b_{k1} + h_{k1}^* b_{k1}^\dagger\right]\,, \qquad \mathcal{H}_{\mathrm{I}}^{(2)} = \sigma^x \otimes \sum_k \left[h_{k2} b_{k2} + h_{k2}^* b_{k2}^\dagger\right]\,, \end{aligned} \tag{6.150}$$

where σ^α represent the Pauli matrices and b_k bosonic annihilation operators. We assume that the two bosonic baths are independent, such that we can calculate the dissipators separately. We have already calculated the Fourier-transform of the bath correlation function for such coupling operators. When we analytically continue the spectral coupling density to negative frequencies as $J(-\omega) = -J(+\omega)$, it can also be written as

$$\gamma(\omega) = J(\omega)\left[1 + n(\omega)\right]\,. \tag{6.151}$$

Since it obeys the KMS condition we may expect thermalization of the qubits density matrix with the bath temperature. Note that due to the divergence of $n(\omega)$ at $\omega \to 0$, it is favorable to use an Ohmic spectral density such as e.g.

$$J(\omega) = J_0 \omega e^{-\omega/\omega_c}\,, \tag{6.152}$$

which grants an existing limit $\gamma(0)$. For the two interaction Hamiltonians chosen, we can make the corresponding coefficients explicit

coefficient	A: pure dephasing $A = \sigma^z$	B: dissipation $A = \sigma^x$
$\gamma_{00,00}$	$+\gamma(0)$	0
$\gamma_{00,11}$	$-\gamma(0)$	0
$\gamma_{11,00}$	$-\gamma(0)$	0
$\gamma_{11,11}$	$+\gamma(0)$	0
$\gamma_{01,01}$	0	$\gamma(+\Omega)$
$\gamma_{10,10}$	0	$\gamma(-\Omega)$
σ_{00}	$\frac{\sigma(0)}{2\mathrm{i}}$	$\frac{\sigma(-\Omega)}{2\mathrm{i}}$
σ_{11}	$\frac{\sigma(0)}{2\mathrm{i}}$	$\frac{\sigma(+\Omega)}{2\mathrm{i}}$

and rewrite the corresponding Liouvillian in the ordering $\rho_{00}, \rho_{11}, \rho_{01}, \rho_{10}$ as a superoperator (fur-

ther abbreviating $\gamma_{0/\pm} = \gamma(0/\pm\Omega)$, $\Sigma = \sigma_{00} - \sigma_{11}$)

$$\begin{aligned}
\mathcal{L}_A &= \begin{pmatrix} 0 & 0 & 0 & 0 \\ 0 & 0 & 0 & 0 \\ 0 & 0 & -2\gamma_0 - \mathrm{i}\Omega & 0 \\ 0 & 0 & 0 & -2\gamma_0 + \mathrm{i}\Omega \end{pmatrix} \\
\mathcal{L}_B &= \begin{pmatrix} -\gamma_- & +\gamma_+ & 0 & 0 \\ +\gamma_- & -\gamma_+ & 0 & 0 \\ 0 & 0 & -\frac{\gamma_- + \gamma_+}{2} - \mathrm{i}(\Omega + \Sigma) & 0 \\ 0 & 0 & 0 & -\frac{\gamma_- + \gamma_+}{2} + \mathrm{i}(\Omega + \Sigma) \end{pmatrix} .
\end{aligned} \tag{6.153}$$

Both Liouvillians lead to a decay of coherences with a rate (we assume $\Omega > 0$)

$$\begin{aligned}
\gamma_A &= 2\gamma_0 = 2 \lim_{\omega \to 0} J(\omega) \left[1 + n(\omega)\right] = 2\frac{J_0}{\beta} = 2 J_0 k_\mathrm{B} T \,, \\
\gamma_B &= \frac{\gamma_- + \gamma_+}{2} = \frac{1}{2}\left[J(\Omega)[1 + n(\Omega)] + J(-\Omega)[1 + n(-\Omega)]\right] = \frac{1}{2}\left[J(\Omega)[1 + n(\Omega)] + J(\Omega) n(\Omega)\right] \\
&= \frac{1}{2} J(\Omega) \coth\left[\frac{\Omega}{2 k_\mathrm{B} T}\right] ,
\end{aligned} \tag{6.154}$$

which both scale proportional to T for large bath temperatures. Therefore, the application of either Liouvillian or a superposition of both will in the high-temperature limit simply lead to rapid decoherence. The same can be expected from a turnstyle (open-loop control), where the Liouvillians act one at a time following a pre-defined protocol.

The situation changes however, when measurement results are used to determine which Liouvillian is acting. We choose to act with Liouvillian $\mathcal{L}_A$ throughout and to turn on Liouvillian $\mathcal{L}_B$ in addition – multiplied by a dimensionless feedback parameter $\alpha \geq 0$ – when a certain measurement result is obtained. Given a measurement with just two outcomes, the effective propagator is then given by

$$\mathcal{P}(\Delta t) = e^{\mathcal{L}_A \Delta t} \mathcal{M}_1 + e^{(\mathcal{L}_A + \alpha \mathcal{L}_B)\Delta t} \mathcal{M}_2 \,, \tag{6.155}$$

where $\mathcal{M}_i$ are the superoperators corresponding to the action of the measurement operators $M_i \rho M_i^\dagger$ on the density matrix. First, to obtain any nontrivial effect (coupling between coherences and populations), the measurement superoperators should not have the same block structure as the Liouvillians. Therefore, we consider a projective measurement of the σ^x expectation value

$$M_1 = \frac{1}{2}\left[\mathbf{1} + \sigma^x\right] , \qquad M_2 = \frac{1}{2}\left[\mathbf{1} - \sigma^x\right] . \tag{6.156}$$

These projection operators obviously fulfil the completeness relation $M_1^\dagger M_1 + M_2^\dagger M_2 = \mathbf{1}$. The superoperators corresponding to $M_i \rho M_i^\dagger$ are also orthogonal projectors

$$\mathcal{M}_1 = \frac{1}{4}\begin{pmatrix} 1 & 1 & 1 & 1 \\ 1 & 1 & 1 & 1 \\ 1 & 1 & 1 & 1 \\ 1 & 1 & 1 & 1 \end{pmatrix} , \qquad \mathcal{M}_2 = \frac{1}{4}\begin{pmatrix} 1 & 1 & -1 & -1 \\ 1 & 1 & -1 & -1 \\ -1 & -1 & 1 & 1 \\ -1 & -1 & 1 & 1 \end{pmatrix} . \tag{6.157}$$

Exercise 52 (Measurement superoperators)**.** *(1 points)*
Show the correspondence between M_i and $\mathcal{M}_i$ in the above equations.

However, they are not complete in this higher-dimensional space $\mathcal{M}_1 + \mathcal{M}_2 \neq \mathbf{1}$. Since the measurement superoperators do not have the same block structure as the Liouvillians, we cannot expect a simple rate equation description to hold anymore.

Without feedback ($\alpha = 0$), it is easy to see that the measurements still have an effect in contrast to an evolution without measurements

$$\frac{1}{2}\begin{pmatrix} 1 & 1 & 0 & 0 \\ 1 & 1 & 0 & 0 \\ 0 & 0 & e^{-(2\gamma_0+\mathrm{i}\Omega)\Delta t} & e^{-(2\gamma_0+\mathrm{i}\Omega)\Delta t} \\ 0 & 0 & e^{-(2\gamma_0-\mathrm{i}\Omega)\Delta t} & e^{-(2\gamma_0-\mathrm{i}\Omega)\Delta t} \end{pmatrix} = e^{\mathcal{L}_A \Delta t}\left(\mathcal{M}_1 + \mathcal{M}_2\right) \neq$$

$$e^{\mathcal{L}_A \Delta t} = \begin{pmatrix} 1 & 0 & 0 & 0 \\ 0 & 1 & 0 & 0 \\ 0 & 0 & e^{-(2\gamma_0+\mathrm{i}\Omega)\Delta t} & 0 \\ 0 & 0 & 0 & e^{-(2\gamma_0-\mathrm{i}\Omega)\Delta t} \end{pmatrix}. \tag{6.158}$$

This may have significant consequences – even without dissipation ($\gamma_0 = 0$) and without feedback ($\alpha = 0$): The repeated application of the propagator for measurement without feedback ($\gamma_0 = 0$ and $\alpha = 0$) yields

$$\left[e^{\mathcal{L}_A \Delta t}\left(\mathcal{M}_1 + \mathcal{M}_2\right)\right]^n = \frac{1}{2}\begin{pmatrix} 1 & 1 & 0 & 0 \\ 1 & 1 & 0 & 0 \\ 0 & 0 & e^{-\mathrm{i}\Omega\Delta t}\cos^{n-1}(\Omega\Delta t) & e^{-\mathrm{i}\Omega\Delta t}\cos^{n-1}(\Omega\Delta t) \\ 0 & 0 & e^{+\mathrm{i}\Omega\Delta t}\cos^{n-1}(\Omega\Delta t) & e^{+\mathrm{i}\Omega\Delta t}\cos^{n-1}(\Omega\Delta t) \end{pmatrix}. \tag{6.159}$$

Exercise 53 (Repeated measurements)**.** *(1 points)*
Show the validity of the above equation.

In contrast, without the measurements we have for repeated application of the propagator simply

$$\left[e^{\mathcal{L}_A \Delta t}\right]^n = e^{\mathcal{L}_A n \Delta t}. \tag{6.160}$$

When we now consider the limit $n \to \infty$ and $\Delta t \to 0$ but $n\Delta t = t$ remaining finite, it becomes obvious that the no-measurement propagator for $\gamma_0 = 0$ simply describes coherent evolution. In contrast, when the measurement frequency becomes large enough, the measurement propagator in Eq. (6.158) approaches

$$\left[e^{\mathcal{L}_A \Delta t}\left(\mathcal{M}_1 + \mathcal{M}_2\right)\right]^n = \frac{1}{2}\begin{pmatrix} 1 & 1 & 0 & 0 \\ 1 & 1 & 0 & 0 \\ 0 & 0 & 1 & 1 \\ 0 & 0 & 1 & 1 \end{pmatrix} \tag{6.161}$$

and thereby freezes the eigenstates of the measurement superoperators, e.g. $\bar{\rho} = \frac{1}{2}\left[|0\rangle + |1\rangle\right]\left[\langle 0| + \langle 1|\right]$. This effect is known as Quantum-Zeno effect (a watched pot never boils) and occurs when measurement operators and system Hamiltonian do not commute and the evolution between measurements is unitary (here $\gamma_0 = 0$). When the evolution between measurements is an open one ($\gamma_0 > 0$), the Quantum-Zeno effect cannot be used to stabilize the coherences, which becomes evident from the propagator in Eq. (6.158).

With feedback ($\alpha > 0$) however, the effective propagator $\mathcal{P}(\Delta t)$ does not have the Block structure anymore. It can be used to obtain a fixed-point iteration for the density matrix

$$\rho(t + \Delta t) = \mathcal{P}(\Delta t)\rho(t)\,. \tag{6.162}$$

Here, we cannot even for small Δt approximate the evolution by another effective Liouvillian, since $\lim_{\Delta t \to 0} \mathcal{W}(\Delta t) \neq \mathbf{1}$. Instead, one can analyze the eigenvector of $\mathcal{W}(\Delta t)$ with eigenvalue 1 as the (in a stroboscopic sense) stationary state. It is more convenient however to consider the expectation values of $\langle \sigma^i \rangle_t$ that fully characterize the density matrix via

$$\rho_{00} = \frac{1 + \langle \sigma^z \rangle}{2}\,, \qquad \rho_{11} = \frac{1 - \langle \sigma^z \rangle}{2}\,, \qquad \rho_{01} = \frac{\langle \sigma^x \rangle - \mathrm{i}\,\langle \sigma^y \rangle}{2}\,, \qquad \rho_{10} = \frac{\langle \sigma^x \rangle + \mathrm{i}\,\langle \sigma^y \rangle}{2}\,. \tag{6.163}$$

Note that decoherence therefore implies vanishing expectation values of $\langle \sigma^x \rangle \to 0$ and $\langle \sigma^y \rangle \to 0$ in our setup. Converting the iteration equation for the density matrix into an iteration equation for the expectation values of Pauli matrices we obtain

$$\begin{aligned}
\langle \sigma^x \rangle_{t+\Delta t} &= \frac{e^{-2\gamma_0 \Delta t}}{2}\left\{(1 + \langle \sigma^x \rangle_t)\cos(\Omega \Delta t) - (1 - \langle \sigma^x \rangle_t)\, e^{-(\gamma_- + \gamma_+)\alpha \Delta t/2} \cos\left[(\Omega + \alpha(\Omega + \Sigma))\,\Delta t\right]\right\} \\
\langle \sigma^y \rangle_{t+\Delta t} &= \frac{e^{-2\gamma_0 \Delta t}}{2}\left\{(1 + \langle \sigma^x \rangle_t)\sin(\Omega \Delta t) - (1 - \langle \sigma^x \rangle_t)\, e^{-(\gamma_- + \gamma_+)\alpha \Delta t/2} \sin\left[(\Omega + \alpha(\Omega + \Sigma))\,\Delta t\right]\right\} \\
\langle \sigma^z \rangle_{t+\Delta t} &= \frac{(\gamma_+ - \gamma_-)\,(1 - \langle \sigma^x \rangle_t)}{2(\gamma_- + \gamma_+)}\left(1 - e^{-(\gamma_- + \gamma_+)\alpha \Delta t}\right)\,,
\end{aligned} \tag{6.164}$$

which (surprisingly) follow just the expectation values $\langle \sigma^x \rangle_t$ on the r.h.s. The first of the above equations can be expanded for small Δt to yield

$$\frac{\langle \sigma^x \rangle_{t+\Delta t} - \langle \sigma^x \rangle_t}{\Delta t} = -\frac{1}{4}\left[8\gamma_0 + \alpha\,(\gamma_- + \gamma_+)\right]\langle \sigma^x \rangle_t + \frac{1}{4}\alpha\,(\gamma_- + \gamma_+) + \mathcal{O}\{\Delta t\}\,. \tag{6.165}$$

When $\Delta t \to 0$, this becomes a differential equation with the stationary state

$$\langle \bar{\sigma}^x \rangle = \frac{\alpha(\gamma_- + \gamma_+)}{8\gamma_0 + \alpha(\gamma_- + \gamma_+)}\,, \tag{6.166}$$

which approaches 1 for large values of α. Taking into account the large-temperature expansions for the dampening coefficients

$$\gamma_0 = J_0 k_\mathrm{B} T\,, \qquad \gamma_- + \gamma_+ \approx 2J_0 e^{-\Omega/\omega_c} k_\mathrm{B} T\,, \tag{6.167}$$

we see that this stabilization effect also holds at large temperatures – a sufficiently strong (and perfect) feedback provided. An initially coherent superposition is thus not only stabilized, but also emerges when the scheme is initialized in a completely mixed state. Also for finite Δt, the fixed-point iteration yields sensible evolution for the expectation values of the Pauli matrices, see Fig. 6.11.

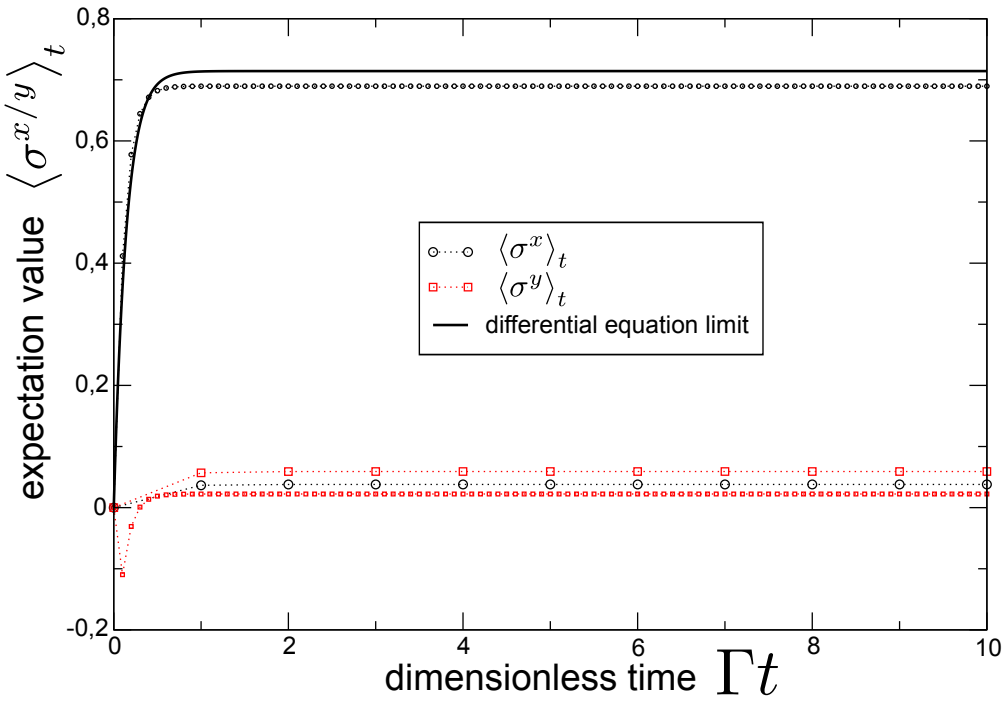

Figure 6.11: Expectation values of the Pauli matrices for finite feedback strength $\alpha = 10$ and finite stepsize Δt (spacing given by symbols). For large Δt, the fixed point is nearly completely mixed. For small Δt, the curve for $\langle \sigma^x \rangle_t$ approaches the differential equation limit (solid line), but the curve for $\langle \sigma^y \rangle_t$ approaches 0. For $\gamma_- = \gamma_+$, the iteration for $\langle \sigma^z \rangle_t$ vanishes throughout. Thin dotted lines only serve to guide the eye, i.e., the expectation values between measurements (symbols) may be different. Parameters: $\gamma_- = \gamma_+ = \gamma_0 = \Gamma$, $\Omega \Delta t = \in \{1, 0.1\}$, and $\Sigma \Delta t \in \{0.5, 0.05\}$.

6.5 Feedback as back-action: Relaxation Dynamics

So far, control has only affected the interaction (e.g. tunneling rates) or the system (projective measurements or time-dependent system parameters). A direct change of the reservoir parameters would normally be hard to describe (and to achieve experimentally), since here fast changes would usually drive the reservoir out of equilibrium. A third possibility that is usually not explored is to force the reservoirs into a maximum entropy state subject to the side constraint of varying energy and matter content. In our master equation, this would simply mean that the reservoir inverse temperature β_ν and chemical potential μ_ν are allowed to be time-dependent

$$\bar{\rho}_B = \bigotimes_\nu \frac{e^{-\beta_\nu(t)\left[H_B^{(\nu)} - \mu_\nu(t) N_B^{(\nu)}\right]}}{\mathrm{Tr}\left\{ e^{-\beta_\nu(t)\left[H_B^{(\nu)} - \mu_\nu(t) N_B^{(\nu)}\right]} \right\}} . \tag{6.168}$$

To determine the value of the inverse temperature β_ν and the chemical potential μ_ν, one can determine these consistently from calculating the energy and matter currents between system and reservoir ν. We will call such reservoirs that are actually influenced by the presence of the system **meso-reservoirs** to stress that they are not supposed to be infinitely large.

For a thermal reservoir state, the total particle number in the reservoir ν is represented as

$$N_\nu = \sum_k \left\langle c^\dagger_{k\nu} c_{k\nu} \right\rangle = \sum_k f(\omega_{k\nu}) = \frac{1}{2\pi} \int \mathcal{D}_\nu(\omega) f_\nu(\omega) d\omega \,, \tag{6.169}$$

where $f_\nu(\omega)$ (depending implicitly on inverse temperature β_ν and chemical potential μ_ν) can be a Fermi or Bose distribution – depending on the type of the reservoir. Here, the quantity

$$\mathcal{D}_\nu(\omega) = 2\pi \sum_k \delta(\omega - \omega_{k\nu}) \tag{6.170}$$

is the spectral density of the reservoir, it should not be confused with the spectral coupling density $\Gamma_\nu(\omega) = 2\pi \sum_k |t_{k\nu}| \delta(\omega - \omega_{k\nu})$, as the latter is also influenced determined by the coupling between system and reservoir, whereas the former is a pure reservoir property and remains well-defined in absence of any coupling. In an analogous fashion we can obtain the energy contained in the reservoir

$$E_\nu = \frac{1}{2\pi} \int \mathcal{D}_\nu(\omega) \omega f_\nu(\omega) d\omega \,. \tag{6.171}$$

Total conservation of charge and energy implies that given charge and energy currents into the reservoir

$$\begin{aligned} \dot{N}_\nu &= -I^{(\nu)}_M = \frac{\partial N_\nu}{\partial \mu_\nu} \dot{\mu}_\nu + \frac{\partial N_\nu}{\partial \beta_\nu} \frac{d\beta_\nu}{dT_\nu} \dot{T}_\nu \,, \\ \dot{E}_\nu &= -I^{(\nu)}_E = \frac{\partial E_\nu}{\partial \mu_\nu} \dot{\mu}_\nu + \frac{\partial E_\nu}{\partial \beta_\nu} \frac{d\beta_\nu}{dT_\nu} \dot{T}_\nu \,, \end{aligned} \tag{6.172}$$

one can calculate the change of reservoir charge and energy. Here however, we will be interested in the change of reservoir temperature and chemical potential, for which we can obtain a differential equation by solving the above equations for $\dot{\mu}_\nu$ and $\dot{T}_\nu$. For example, in case of fermions, we can first solve for

$$\begin{aligned} \frac{\partial N_\nu}{\partial \mu_\nu} &= \frac{1}{2\pi} \int \mathcal{D}_\nu(\omega) f_\nu(\omega)[1 - f_\nu(\omega)] d\omega \beta_\nu = \mathcal{I}_1 \beta_\nu \,, \\ \frac{\partial N_\nu}{\partial \beta_\nu} &= -\frac{1}{2\pi} \int \mathcal{D}_\nu(\omega) f_\nu(\omega)[1 - f_\nu(\omega)](\omega - \mu_\nu) d\omega = -\mathcal{I}_2 \,, \\ \frac{\partial E_\nu}{\partial \mu_\nu} &= \frac{1}{2\pi} \int \mathcal{D}_\nu(\omega) \omega f_\nu(\omega)[1 - f_\nu(\omega)] d\omega \beta_\nu = (\mathcal{I}_2 + \mu_\nu \mathcal{I}_1) \beta_\nu \,, \\ \frac{\partial E_\nu}{\partial \beta_\nu} &= -\frac{1}{2\pi} \int \mathcal{D}_\nu(\omega) \omega f_\nu(\omega)[1 - f_\nu(\omega)](\omega - \mu_\nu) d\omega = -\mathcal{I}_3 - \mu_\nu \mathcal{I}_2 \,. \end{aligned} \tag{6.173}$$

Here, we have defined three integrals

$$\begin{aligned} \mathcal{I}_1 &= \frac{1}{2\pi} \int \mathcal{D}_\nu(\omega) f(\omega)[1 - f_\nu(\omega)] d\omega \,, \qquad \mathcal{I}_2 = \frac{1}{2\pi} \int \mathcal{D}_\nu(\omega)(\omega - \mu_\nu) f_\nu(\omega)[1 - f_\nu(\omega)] d\omega \,, \\ \mathcal{I}_3 &= \frac{1}{2\pi} \int \mathcal{D}_\nu(\omega)(\omega - \mu_\nu)^2 f_\nu(\omega)[1 - f_\nu(\omega)] d\omega \,, \end{aligned} \tag{6.174}$$

which in the wide-band limit $\mathcal{D}_\nu(\omega) = 2\pi D_\nu$ can be solved exactly

$$\mathcal{I}_1 = \frac{D_\nu}{\beta_\nu} = D_\nu T_\nu \,, \qquad \mathcal{I}_2 = 0 \,, \qquad \mathcal{I}_3 = \frac{\pi^2}{3} \frac{D_\nu}{\beta^3_\nu} = \frac{\pi^2}{3} D_\nu T^3_\nu \,. \tag{6.175}$$

Exercise 54 (Fermi integrals)**.** *Show validity of Eq. (6.175). You might want to use that*

$$\int_0^\infty \frac{\ln^2(x)}{(x+1)^2} = \frac{\pi^2}{3}\,. \tag{6.176}$$

From these, we obtain a simple relation between currents and thermodynamic parameters

$$\begin{pmatrix} -I_M^{(\nu)} \\ -I_E^{(\nu)} \end{pmatrix} = D_\nu \begin{pmatrix} 1 & 0 \\ \mu & \frac{\pi^2}{3} T_\nu \end{pmatrix} \begin{pmatrix} \dot{\mu}_\nu \\ \dot{T}_\nu \end{pmatrix}. \tag{6.177}$$

We can directly invert the matrix containing the heat and charge capacities to solve for the first derivatives

$$\begin{pmatrix} \dot{\mu}_\nu \\ \dot{T}_\nu \end{pmatrix} = \frac{1}{D_\nu} \begin{pmatrix} 1 & 0 \\ -\frac{3}{\pi^2}\frac{\mu_\nu}{T_\nu} & \frac{3}{\pi^2}\frac{1}{T_\nu} \end{pmatrix} \begin{pmatrix} -I_M^{(\nu)} \\ -I_E^{(\nu)} \end{pmatrix}. \tag{6.178}$$

Although we have represented this using a matrix, we stress that the resulting ODE is highly nonlinear, since the currents may themselves depend in a highly nonlinear fashion on the reservoir temperature. Any reasonable two-terminal setup should realistically obey particle conservation $I_M^R + I_M^L = 0$ and also energy conservation $I_E^R + I_E^L = 0$. This will in general lead to conserved quantities respected by the system of coupled differential equations.

A useful example is the single-electron transistor that has been treated previously. Here, we have two reservoirs with temperatures T_L, T_R and chemical potentials μ_L and μ_R, respecively. When these are connected via a single quantum dot, the current (counting positive if directed from left to right) reads

$$J_M = \gamma\left[f_L(\epsilon) - f_R(\epsilon)\right], \qquad J_E = \epsilon J_M\,, \tag{6.179}$$

where γ encodes details of the coupling strength to the respective reservoirs into a single factor and where ϵ was the on-site energy of the quantum dot. The so-called tight-coupling property $J_E = \epsilon J_M$ follows from the fact that a single quantum dot only has a single transition frequency ϵ. This can be compared with a more complicated structure, e.g. two quantum dots connecting the two reservoirs in parallel without direct interaction. Then, the currents have the structure

$$\begin{aligned} J_M &= \gamma_1\left[f_L(\epsilon_1) - f_R(\epsilon_1)\right] + \gamma_2\left[f_L(\epsilon_2) - f_R(\epsilon_2)\right], \\ J_E &= \epsilon_1\gamma_1\left[f_L(\epsilon_1) - f_R(\epsilon_1)\right] + \epsilon_2\gamma_2\left[f_L(\epsilon_2) - f_R(\epsilon_2)\right]. \end{aligned} \tag{6.180}$$

These do not exhibit the tight-coupling property $J_E \neq \epsilon J_M$ – unless the ϵ_i are equal. Nevertheless, also here global equilibrium $\mu_L = \mu_R$ and $\beta_L = \beta_R$ will evidently lead to vanishing currents and therefore to fixed points. Now, by initializing the system e.g. with a temperature gradient in the absence of a charge gradient it is possible to generate (at least temporally) a voltage, i.e., to extract work. The temporal evolution of such a system is depicted in Fig. 6.12. It is visible that in the tight-coupling limit, it is possible to convert e.g. an initial temperature gradient into work (a persistent voltage). However, it should realistically be kept in mind that the tight-coupling property is never exactly fulfilled and relaxation into final equilibrium may thus be expected. Nevertheless, even these more realistic systems show a distinct timescale separation between initial charge separation

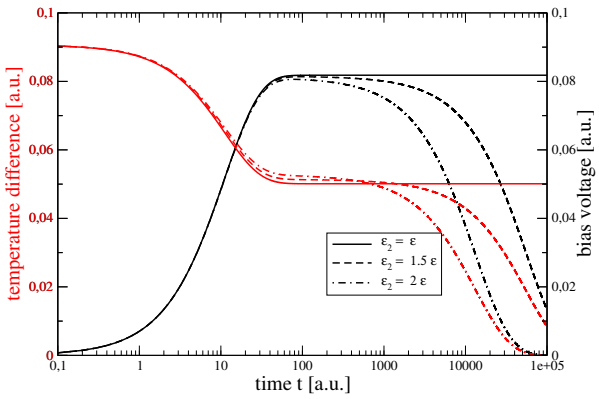

Figure 6.12: Temporal evolution of the bias voltage $V(t)$ (black) and the temperature difference $T_L - T_R$ (red) for different ratios of channel energies $\epsilon_2 = \alpha\epsilon = \epsilon_1$ (solid, dashed, and dash-dotted, respectively). After an initial evolution phase the system reaches a pseudo-equilibrium that is persistent only for $\epsilon_1 = \epsilon_2$ (solid curves). Whenever the channel energies are different, the pseudo-equilibrium eventually relaxes to thermal equilibrium. During the pseudo-equilibrium phase (intermediate plateaus), part of the initial temperature gradient has been converted into a voltage.

and discharging of the system. It should be noted that the proposed equilibration dynamics for a meso-reservoir would at steady state be similar to a Büttiker probe [25]. There however, such probe reservoirs are attached to systems to enforce dephasing behaviour, with temperatures and potentials fixed to yield vanishing local energy and matter currents. They would correspond to the steady-state dynamics of the meso-reservoir presented here.

Clearly, such equilibration processes are observed in many classical objects of finite size: A cold and a hot object (possibly also differently charged) will – when being put into contact – after some time assume a common temperature and common potential, i.e., the behaviour predicted by these phenomenologic equations is not unreasonable. One may therefore ask what kind of microscopic processes could actually induce the situation enforced by postulating Eq. (6.168). One possibility could be the existence of a super-bath enforcing the time-dependent equilibrium state on the meso-reservoir. However, such a coupling would have to be comparably strong and should be strange in the sense that it must not exchange energy and matter with the meso-reservoir – otherwise it would lead to additional terms in our balance equations. An interaction type that would not change the energy- and matter balance for the meso-reservoir would be a pure-dephasing interaction. This would safely remove all off-diagonal elements from the meso-reservoir density matrix. However, it remains questionable then how the proper Boltzmann distribution can be generated along the diagonals, as slight perturbations induced by the system would immediately be damped away from the super-reservoir.

Alternatively, we could imagine the reservoir to be given by an interacting Hamiltonian H_B^I. In computing correlation functions, we could then approximate the true dynamics as $e^{-\mathrm{i}H_B^I t}\rho_B^0 e^{+\mathrm{i}H_B^I t} \approx \frac{e^{-\beta H_B}}{Z_B}$, which means that the dynamics of the interacting system could be approximately interpreted as thermal, similar to principles of canonical typicality [26].

Chapter 7

Non-equilibrium beyond leading order

To understand the limit within which master equations are valid, it is quite instructive to compare the master equation results against exactly solvable models. Unfortunately, such models are quite rare. With a formal exact solution, one can study non-equilibrium setups and transport in a regime where the coupling between system and reservoir becomes strong and/or non-Markovian. They are therefore quite useful to define the limits of our perturbative appraoches.

In the lecture, we have already treated an exactly solvable variant of the spin-boson model: The pure dephasing limit, cf. Sec. 4.4.2. However, to obtain a pure non-equilibrium setting at steady state, it is necessary to go beyond pure-dephasing limits.

In this chapter, we will discuss representatives of exactly solvable models: First, we consider a non-interacting fermionic transport model, where the Hamiltonian can be written as a quadratic form of fermionic annihilation and creation operators. We note that when the fermionic operators are replaced by bosonic ones, we again end up with a bosonic transport model that also allows for a non-perturbative solution of a nonequilibrium steady state [27].

7.1 Quantum Dot coupled to two fermionic leads

As one of the simplest fermionic models, we consider a single electron transistor (SET): The system, bath, and interaction Hamiltonians are given by

$$\begin{aligned} \mathcal{H}_{\rm S} &= \epsilon d^\dagger d\,, \qquad \mathcal{H}_{\rm B} = \sum_k \epsilon_{kL} c_{kL}^\dagger c_{kL} + \sum_k \epsilon_{kR} c_{kR}^\dagger c_{kR}\,, \\ \mathcal{H}_{\rm I} &= \sum_k \left(t_{kL} d c_{kL}^\dagger + t_{kL}^* c_{kL} d^\dagger \right) + \sum_k \left(t_{kR} d c_{kR}^\dagger + t_{kR}^* c_{kR} d^\dagger \right)\,, \end{aligned} \tag{7.1}$$

where d is a fermionic annihilation operator on the dot and $c_{k\nu}$ are fermionic annihilation operators of an electron in the k-th mode of lead ν. Obviously, this corresponds to a quadratic fermionic Hamiltonian, which can in principle be solved exactly by various methods such as e.g. non-equilibrium Greens functions [28] or even the equation-of-motion approach [29]. Such quadratic models are useful to study exact transport properties [30] or exact master equations [31].

7.1.1 Heisenberg Picture Dynamics

To be as self-contained as possible, we here simply compute the Heisenberg equations of motion for the system and bath annihilation operators (we denote operators in the Heisenberg picture by

boldface symbols)

$$\begin{aligned} \dot{\boldsymbol{d}} &= -\mathrm{i}\epsilon\boldsymbol{d} + \mathrm{i}\sum_k \left[t_{kL}^* \boldsymbol{c_{kL}} + t_{kR}^* \boldsymbol{c_{kR}}\right] , \\ \dot{\boldsymbol{c_{kL}}} &= -\mathrm{i}\epsilon_{kL}\boldsymbol{c_{kL}} + \mathrm{i}t_{kL}\boldsymbol{d} , \qquad \dot{\boldsymbol{c_{kR}}} = -\mathrm{i}\epsilon_{kR}\boldsymbol{c_{kR}} + \mathrm{i}t_{kR}\boldsymbol{d} . \end{aligned} \tag{7.2}$$

Surprisingly, this system is already closed and we obtain its solution by performing a Laplace transform [32]

$$\begin{aligned} z\tilde{d}(z) - d &= -\mathrm{i}\epsilon\tilde{d}(z) + \mathrm{i}\sum_k \left[t_{kL}^* \tilde{c}_{kL}(z) + t_{kR}^* \tilde{c}_{kR}(z)\right] , \\ z\tilde{c}_{kL}(z) - c_{kL} &= -\mathrm{i}\epsilon_{kL}\tilde{c}_{kL}(z) + \mathrm{i}t_{kL}\tilde{d}(z) , \qquad z\tilde{c}_{kR}(z) - c_{kR} = -\mathrm{i}\epsilon_{kR}\tilde{c}_{kR}(z) + \mathrm{i}t_{kR}\tilde{d}(z) . \end{aligned} \tag{7.3}$$

In the above equations, we can eliminate the operators $\tilde{c}_{kL}(z)$ and $\tilde{c}_{kR}(z)$. This yields for the dot annihilation operator

$$\tilde{d}(z) = \frac{d + \mathrm{i}\sum_k \left(\frac{t_{kL}^* c_{kL}}{z+\mathrm{i}\epsilon_{kL}} + \frac{t_{kR}^* c_{kR}}{z+\mathrm{i}\epsilon_{kR}}\right)}{z + \mathrm{i}\epsilon + \sum_k \left(\frac{|t_{kL}|^2}{z+\mathrm{i}\epsilon_{kL}} + \frac{|t_{kR}|^2}{z+\mathrm{i}\epsilon_{kR}}\right)} \equiv \tilde{f}(z)d + \sum_k \left(\tilde{g}_{kL}(z)c_{kL} + \tilde{g}_{kR}(z)c_{kR}\right) , \tag{7.4}$$

where we have introduced the functions $\tilde{g}_{k\nu}(z)$ and $\tilde{f}(z)$. This expression also yields the solution for the operators of the right lead modes

$$\tilde{c}_{k\nu}(z) = \frac{1}{z + \mathrm{i}\epsilon_{k\nu}} c_{k\nu} + \frac{\mathrm{i}t_{k\nu}}{z + \mathrm{i}\epsilon_{k\nu}} \tilde{d}(z) . \tag{7.5}$$

Inverting the Laplace transform may now be achieved by identifying the poles and applying the residue theorem. In the wide-band limit discussed below, this becomes particularly simple.

7.1.2 Stationary Occupation

The time-dependent occupation $n(t) = \left\langle d^\dagger(t)d(t)\right\rangle$ is found by inverting the Laplace transform. For the moment we do it formally and already perform the expectation value

$$\begin{aligned} n(t) &= \left\langle \left[f^*(t)d^\dagger + \sum_k \left(g_{kL}^*(t)c_{kL}^\dagger + g_{kR}^*(t)c_{kR}^\dagger\right)\right] \left[f(t)d + \sum_k \left(g_{kL}(t)c_{kL} + g_{kR}(t)c_{kR}\right)\right] \right\rangle \\ &= |f(t)|^2 n_0 + \sum_k \left(|g_{kL}(t)|^2 f_L(\epsilon_{kL}) + |g_{kR}(t)|^2 f_R(\epsilon_{kR})\right) , \end{aligned} \tag{7.6}$$

where we have used a product state as an initial one

$$\rho_0 = \rho_{\mathrm{S}}^0 \frac{e^{-\beta_L(H_L - \mu_L N_L)}}{Z_L} \frac{e^{-\beta_R(H_R - \mu_R N_R)}}{Z_R} \tag{7.7}$$

with the lead Hamiltonians $H_\nu = \sum_k \epsilon_{k\nu} c_{k\nu}^\dagger c_{k\nu}$ and the lead particle numbers $N_\nu = \sum_k c_{k\nu}^\dagger c_{k\nu}$. These eventually yield the only non-vanishing expectation values $n_0 = \left\langle d^\dagger d\right\rangle$ and $f_\nu(\epsilon_{k\nu}) = \left\langle c_{k\nu}^\dagger c_{k\nu}\right\rangle$. Inverse lead temperatures β_ν and chemical potentials μ_ν thereby only enter implicitly in

the Fermi functions. Therefore, to find the exact solution for the time-dependent dot occupation, we have to find the inverse Laplace transform of

$$\begin{aligned}\tilde{f}(z) &= \frac{1}{z+\mathrm{i}\epsilon+\sum_k\left(\frac{|t_{kL}|^2}{z+\mathrm{i}\epsilon_{kL}}+\frac{|t_{kR}|^2}{z+\mathrm{i}\epsilon_{kR}}\right)}\,,\\ \tilde{g}_{k\nu}(z) &= \frac{\mathrm{i}t^*_{k\nu}}{[z+\mathrm{i}\epsilon_{k\nu}]\left[z+\mathrm{i}\epsilon+\sum_k\left(\frac{|t_{kL}|^2}{z+\mathrm{i}\epsilon_{kL}}+\frac{|t_{kR}|^2}{z+\mathrm{i}\epsilon_{kR}}\right)\right]}\,,\end{aligned} \tag{7.8}$$

which heavily depends on the number of modes and their distribution in the reservoir. Any system with a finite number of reservoir modes, for example, will exhibit recurrences to the initial state.

Only systems with a continuous spectrum of reservoir modes can be expected to yield a stationary system state. To obtain that limit, we for simplicity assume $N+1$ modes in each reservoir $-N/2 \le k \le +N/2$. These are distributed over the energies as $\epsilon_{k\nu} = k\Omega/\sqrt{N}$ and assumed to couple weaker to the dot as their momentum increases

$$|t_{k\nu}|^2 = \frac{\Omega}{2\pi\sqrt{N}}\frac{\Gamma_\nu\delta_\nu^2}{(k\Omega/\sqrt{N})^2+\delta_\nu^2}\,. \tag{7.9}$$

Letting the number of reservoir modes N go to infinity, we can replace the summation in the denominators by a continuous integral

$$\begin{aligned}\tilde{f}(z) &\approx \frac{1}{z+\mathrm{i}\epsilon+\int\frac{1}{2\pi}\left(\frac{\Gamma_L\delta_L^2}{\omega^2+\delta_L^2}+\frac{\Gamma_R\delta_R^2}{\omega^2+\delta_R^2}\right)\frac{1}{z+\mathrm{i}\omega}d\omega} = \frac{1}{z+\mathrm{i}\epsilon+\frac{1}{2}\left(\frac{\Gamma_L\delta_L}{z+\delta_L}+\frac{\Gamma_R\delta_R}{z+\delta_R}\right)}\,,\\ \tilde{g}_{k\nu}(z) &\approx \frac{\mathrm{i}t^*_{k\nu}}{(z+\mathrm{i}\epsilon_{k\nu})\left[z+\mathrm{i}\epsilon+\int\frac{1}{2\pi}\left(\frac{\Gamma_L\delta_L^2}{\omega^2+\delta_L^2}+\frac{\Gamma_R\delta_R^2}{\omega^2+\delta_R^2}\right)\frac{1}{z+\mathrm{i}\omega}d\omega\right]}\\ &= \frac{1}{[z+\mathrm{i}\epsilon_{k\nu}]\left[z+\mathrm{i}\epsilon+\frac{1}{2}\left(\frac{\Gamma_L\delta_L}{z+\delta_L}+\frac{\Gamma_R\delta_R}{z+\delta_R}\right)\right]}\,.\end{aligned} \tag{7.10}$$

We note that this transfer from a discrete to a continuous spectrum of reservoir modes is commonly performed formally by introducing the energy-dependent tunneling rates

$$\Gamma_\nu(\omega) = 2\pi\sum_k |t_{k\nu}|^2\delta(\omega-\epsilon_{k\nu})\,. \tag{7.11}$$

Here, we have thereby assumed a Lorentzian-shaped tunneling rate [33]

$$\Gamma_\nu(\omega) = \frac{\Gamma_\nu\delta_\nu^2}{\omega^2+\delta_\nu^2}\,. \tag{7.12}$$

The simple pole structure of such tunneling rates renders analytic calculations simple. Superpositions of many Lorentzian shapes with shifted centers may approximate quite general tunneling rates [34].

To obtain sufficiently simple results, we assume the wide-band limit $\delta_\nu \to \infty$ (within which the tunneling rates are flat), where one obtains the simple expression

$$\begin{aligned}\tilde{f}(z) &\to \frac{1}{z+\mathrm{i}\epsilon+(\Gamma_L+\Gamma_R)/2}\,,\\ \tilde{g}_{k\nu}(z) &\to \frac{\mathrm{i}t^*_{k\nu}}{(z+\mathrm{i}\epsilon_{k\nu})\,[z+\mathrm{i}\epsilon+(\Gamma_L+\Gamma_R)/2]}\,.\end{aligned} \tag{7.13}$$

Inserting the inverse Laplace transforms of these expressions

$$\begin{aligned} f(t) &\to e^{-\mathrm{i}\epsilon t}e^{-\Gamma t/2}\,, \\ g_{k\nu}(t) &\to \frac{t^*_{k\nu}\left(e^{-\mathrm{i}\epsilon t}e^{-\Gamma t/2}-e^{-\mathrm{i}\epsilon_{k\nu}t}\right)}{\epsilon_{k\nu}-\epsilon+\mathrm{i}\Gamma/2} \end{aligned} \tag{7.14}$$

(with $\Gamma \equiv \Gamma_L + \Gamma_R$) into Eq. (7.6) we obtain by switching to a continuum representation

$$\begin{aligned} n(t) &= e^{-\Gamma t}n_0 + \sum_k \sum_\nu |t_{k\nu}|^2 f_\nu(\epsilon_{k\nu}) 4 \frac{1-2e^{-\Gamma t/2}\cos[(\epsilon_{k\nu}-\epsilon)t]+e^{-\Gamma t}}{\Gamma^2+4(\epsilon_{k\nu}-\epsilon)^2} \\ &= e^{-\Gamma t}n_0 + \sum_\nu \int d\omega \Gamma_\nu f_\nu(\omega) \frac{4}{2\pi} \frac{1-2e^{-\Gamma t/2}\cos[(\omega-\epsilon)t]+e^{-\Gamma t}}{\Gamma^2+4(\omega-\epsilon)^2}\,. \end{aligned} \tag{7.15}$$

The long-term limit can – due to $\Gamma \geq 0$ – be read off easily, and the stationary occupation becomes

$$\bar{n} = \sum_\nu \int d\omega \Gamma_\nu f_\nu(\omega) \frac{2}{\pi} \frac{1}{\Gamma^2+4(\omega-\epsilon)^2}\,. \tag{7.16}$$

With the above formula for the stationary occupation valid for the wide-band limit, one can easily demonstrate the following:

At infinite bias $f_L(\omega) = 1$ and $f_R(\omega) = 0$, the stationary occupation approaches $\bar{n} \to \Gamma_L/(\Gamma_L + \Gamma_R)$, regardless of the coupling strength. A similar result is of course obtained for reverse infinite bias where $\bar{n} \to \Gamma_R/(\Gamma_L + \Gamma_R)$.

When the quantum dot is coupled weakly to a single bath only (e.g. $\Gamma_R(\omega) = 0$), the stationary occupation approaches the Fermi distribution of the coupled lead, evaluated at the dot energy (e.g. $\bar{n} = f_L(\epsilon) + \mathcal{O}\{\Gamma_L\}$). This implies that for weak coupling to an equilibrium reservoir, the system will equilibrate with the temperature and chemical potential of the reservoir, consistent with what one expects from a master equation approach.

When the dot is coupled weakly to both reservoirs, the stationary state approaches

$$\bar{n} \to \frac{\Gamma_L f_L(\epsilon) + \Gamma_R f_R(\epsilon)}{\Gamma_L + \Gamma_R}\,, \tag{7.17}$$

which is also obtained within a master equation approach, compare Sec. 3.5.

Exercise 55 (Weak Coupling Limit)**.** *Show that Eq. (7.16) reduces in the weak coupling limit to Eq. (7.17 by using a representation of the Dirac-Delta distribution*

$$\delta(x) = \lim_{\epsilon\to 0} \frac{1}{\pi}\frac{\epsilon}{x^2+\epsilon^2}\,.$$

In contrast, for the strong-coupling limit, the stationary occupation will be suppressed $\bar{n} \to 0$, as the exact solution for the stationary state is no longer localized on the dot.

7.1.3 Stationary Current

The stationary current from left to right through the SET can be defined as the long-term limit of the change of particle numbers at the right lead

$$I = \lim_{t\to\infty} \frac{d}{dt} \left\langle \sum_k c_{kR}^\dagger c_{kR} \right\rangle , \tag{7.17}$$

which we can evaluate in the Heisenberg picture as we did for the stationary occupation. Using Eq. (7.5), the right lead modes can be written as

$$\begin{aligned} \tilde{c}_{kR}(z) &= \frac{\mathrm{i}t_{kR}}{(z+\mathrm{i}\epsilon_{kR})(z+\mathrm{i}\epsilon+\Gamma/2)} d + \frac{1}{z+\mathrm{i}\epsilon_{kR}} c_{kR} \\ &\quad - \sum_q \frac{t_{kR}t_{qL}^*}{(z+\mathrm{i}\epsilon_{kR})(z+\mathrm{i}\epsilon_{qL})(z+\mathrm{i}\epsilon+\Gamma/2)} c_{qL} \\ &\quad - \sum_q \frac{t_{kR}t_{qR}^*}{(z+\mathrm{i}\epsilon_{kR})(z+\mathrm{i}\epsilon_{qR})(z+\mathrm{i}\epsilon+\Gamma/2)} c_{qR} \,. \end{aligned} \tag{7.18}$$

Now, performing the inverse Laplace transform and neglecting all transient dynamics, we obtain the asymptotic evolution of the annihilation operators in the Heisenberg picture

$$\begin{aligned} \boldsymbol{c}_{kR}(t) \;\to\; & \left(-\frac{t_{kR} e^{-\mathrm{i}\epsilon_{kR}t}}{\epsilon_{kR}-\epsilon+\mathrm{i}\Gamma/2} \right) d + e^{-\mathrm{i}\epsilon_{kR}t} c_{kR} \\ & + \sum_q \frac{t_{kR}t_{qL}^*}{\epsilon_{kR}-\epsilon_{qL}} \left(\frac{e^{-\mathrm{i}\epsilon_{qL}t}}{\epsilon_{qL}-\epsilon+\mathrm{i}\Gamma/2} - \frac{e^{-\mathrm{i}\epsilon_{kR}t}}{\epsilon_{kR}-\epsilon+\mathrm{i}\Gamma/2} \right) c_{qL} \\ & + \sum_q \frac{t_{kR}t_{qR}^*}{\epsilon_{kR}-\epsilon_{qR}} \left(\frac{e^{-\mathrm{i}\epsilon_{qR}t}}{\epsilon_{qR}-\epsilon+\mathrm{i}\Gamma/2} - \frac{e^{-\mathrm{i}\epsilon_{kR}t}}{\epsilon_{kR}-\epsilon+\mathrm{i}\Gamma/2} \right) c_{qR} \,. \end{aligned} \tag{7.19}$$

The occupation of the right lead therefore becomes

$$\begin{aligned} N_R \;\to\; & \sum_k \frac{|t_{kR}|^2}{(\epsilon_{kR}-\epsilon)^2+\Gamma^2/4} n_0 + N_R^0 \\ & - \sum_{kq} \left[\frac{t_{kR}t_{qR}^*}{\epsilon_{kR}-\epsilon_{qR}} e^{+\mathrm{i}\epsilon_{kR}t} \left(\frac{e^{-\mathrm{i}\epsilon_{qR}t}}{\epsilon_{qR}-\epsilon+\mathrm{i}\Gamma/2} - \frac{e^{-\mathrm{i}\epsilon_{kR}t}}{\epsilon_{kR}-\epsilon+\mathrm{i}\Gamma/2} \right) \delta_{kq} f_R(\epsilon_{kR}) + \mathrm{h.c.} \right] \\ & + \sum_{kq} \frac{|t_{kR}|^2|t_{qL}|^2}{(\epsilon_{kR}-\epsilon_{qL})^2} \left(\frac{e^{+\mathrm{i}\epsilon_{qL}t}}{\epsilon_{qL}-\epsilon-\mathrm{i}\Gamma/2} - \frac{e^{+\mathrm{i}\epsilon_{kR}t}}{\epsilon_{kR}-\epsilon-\mathrm{i}\Gamma/2} \right) \\ & \quad \times \left(\frac{e^{-\mathrm{i}\epsilon_{qL}t}}{\epsilon_{qL}-\epsilon+\mathrm{i}\Gamma/2} - \frac{e^{-\mathrm{i}\epsilon_{kR}t}}{\epsilon_{kR}-\epsilon+\mathrm{i}\Gamma/2} \right) f_L(\epsilon_{qL}) \\ & + \sum_{kq} \frac{|t_{kR}|^2|t_{qR}|^2}{(\epsilon_{kR}-\epsilon_{qR})^2} \left(\frac{e^{+\mathrm{i}\epsilon_{qR}t}}{\epsilon_{qR}-\epsilon-\mathrm{i}\Gamma/2} - \frac{e^{+\mathrm{i}\epsilon_{kR}t}}{\epsilon_{kR}-\epsilon-\mathrm{i}\Gamma/2} \right) \\ & \quad \times \left(\frac{e^{-\mathrm{i}\epsilon_{qR}t}}{\epsilon_{qR}-\epsilon+\mathrm{i}\Gamma/2} - \frac{e^{-\mathrm{i}\epsilon_{kR}t}}{\epsilon_{kR}-\epsilon+\mathrm{i}\Gamma/2} \right) f_R(\epsilon_{qR}) \,. \end{aligned} \tag{7.20}$$

The first term is just triggered by the initial occupation of the dot, and the second term corresponds to the initial occupation of the right lead. These terms are just constant and cannot contribute to

the current, which however is different for all other terms. Introducing the tunneling rates in the wide-band limit $\Gamma_\nu \approx \Gamma_\nu(\omega) = \sum_k |t_{k\nu}|^2 \delta(\omega - \epsilon_{k\nu})$, we can represent the right lead occupation by integrals

$$\begin{aligned} N_R \;\to\; & \frac{1}{2\pi}\int d\omega \frac{\Gamma_R}{(\omega-\epsilon)^2+\Gamma^2/4} n_0 + N_R^0 - \frac{1}{2\pi}\int d\omega \Gamma_R f_R(\omega)\left[\frac{4+4\mathrm{i}\omega t - 2t(\Gamma+2\mathrm{i}\epsilon)}{(2\omega+\mathrm{i}\Gamma-2\epsilon)^2} + \text{h.c.}\right] \\ & + \frac{1}{4\pi^2}\int d\omega d\omega' \left(\Gamma_L\Gamma_R f_L(\omega') + \Gamma_R^2 f_R(\omega')\right) \frac{1}{(\omega-\omega')^2}\left|\frac{e^{-\mathrm{i}\omega' t}}{\omega'-\epsilon+\mathrm{i}\Gamma/2} - \frac{e^{-\mathrm{i}\omega t}}{\omega-\epsilon+\mathrm{i}\Gamma/2}\right|^2 \end{aligned} \tag{7.21}$$

Whereas the first two terms are constant and do not contribute to the current, all other terms yield a non-vanishing contribution. The long-term limit of the time-derivative of the very last term is a bit involved to determine. It can be found, for example, by using properties of the Laplace transform. To evaluate the current, we therefore consider the limit

$$\begin{aligned} F(\omega') \;\equiv\; & \lim_{t\to\infty}\frac{d}{dt}\int d\omega \frac{1}{(\omega-\omega')^2}\left|\frac{e^{-\mathrm{i}\omega' t}}{\omega'-\epsilon+\mathrm{i}\Gamma/2} - \frac{e^{-\mathrm{i}\omega t}}{\omega-\epsilon+\mathrm{i}\Gamma/2}\right|^2 \\ =\; & \lim_{z\to 0} z\int_0^\infty dt e^{-zt}\frac{d}{dt}\int d\omega \frac{1}{(\omega-\omega')^2}\left|\frac{e^{-\mathrm{i}\omega' t}}{\omega'-\epsilon+\mathrm{i}\Gamma/2} - \frac{e^{-\mathrm{i}\omega t}}{\omega-\epsilon+\mathrm{i}\Gamma/2}\right|^2 \\ =\; & \frac{8\pi}{\Gamma^2+4(\omega'-\epsilon)^2}\,, \end{aligned} \tag{7.22}$$

which with its Lorentzian shape converges for small Γ towards a Dirac-Delta distribution. The current becomes

$$\begin{aligned} I \;=\; & -\frac{1}{\pi}\int d\omega \Gamma_R f_R(\omega)\frac{\Gamma/2}{(\omega-\epsilon)^2+(\Gamma/2)^2} + \frac{1}{\pi\Gamma}\int d\omega \left(\Gamma_L\Gamma_R f_L(\omega) + \Gamma_R^2 f_R(\omega)\right)\frac{\Gamma/2}{(\omega-\epsilon)^2+(\Gamma/2)^2} \\ =\; & \frac{\Gamma_L\Gamma_R}{\Gamma_L+\Gamma_R}\int d\omega \left[f_L(\omega) - f_R(\omega)\right]\frac{1}{\pi}\frac{\Gamma/2}{(\omega-\epsilon)^2+(\Gamma/2)^2}\,. \end{aligned} \tag{7.23}$$

Alternatively, this expression can also be derived by evaluating the expectation value of the current operator directly $I = \mathrm{i}\sum_k t_{kR}\left\langle \boldsymbol{c}_{\boldsymbol{kR}}^\dagger(t)\boldsymbol{d}(t)\right\rangle + \text{h.c.}$. The integrals in the above expression can be solved analytically by analysis in the complex plane, but here we will be content with the above integral representation, which can also be found using non-equilibrium Greens functions [28]. For consistency, we note that the current is antisymmetric under exchange of left and right leads as expected.

In the weak-coupling limit $\Gamma \to 0$, the current reduces to

$$I \;=\; \frac{\Gamma_L\Gamma_R}{\Gamma_L+\Gamma_R}\left[f_L(\epsilon) - f_R(\epsilon)\right]\,, \tag{7.24}$$

which at equal temperatures left and right implies that the current always flows from the lead with larger chemical potential to the one with lower chemical potential.

Exercise 56 (Weak-Coupling Limit)**.** *Show that Eq. (7.24) follows from Eq. (7.23) when* $\Gamma \to 0$.

Finally, we note further that, in the infinite bias limit ($f_L(\omega) \to 1$ and $f_R(\omega) \to 0$), the current becomes $I = \Gamma_L\Gamma_R/(\Gamma_L+\Gamma_R)$, which is independent of the coupling strength and also consistent

with Eq. (7.24). We have already seen that the master equation approach applied to the same problem reproduces Eq. (7.24) and therefore coincides with the exact result in the infinite bias limit.

Fig. 7.1 demonstrates the effect of increasing but symmetric coupling strengths $\Gamma_L = \Gamma_R = \gamma$ on the current. Whereas the weak-coupling result is well approximated when $\beta\gamma \ll 1$, one may

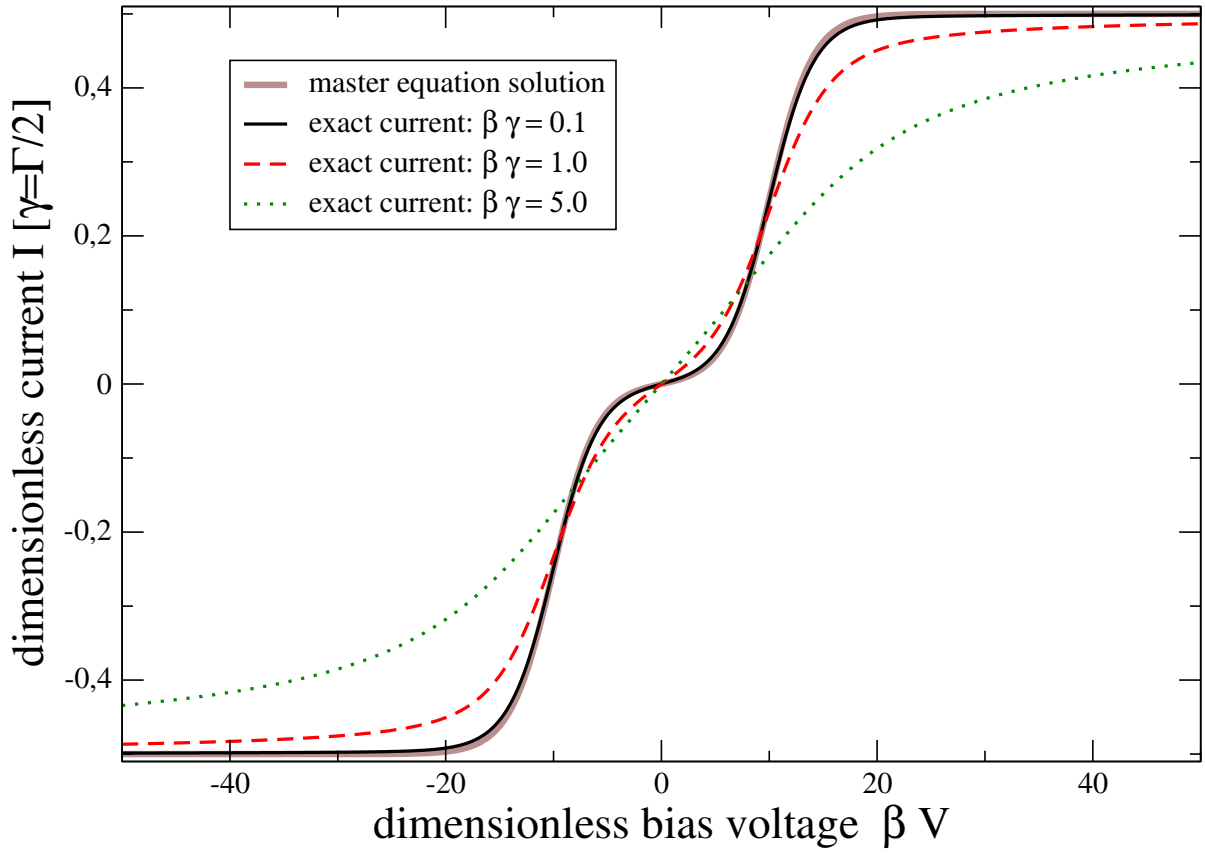

Figure 7.1: Plot of the electronic matter current (in units of $\gamma = \Gamma_L = \Gamma_R = \Gamma/2$) versus the bias voltage for symmetric tunneling rates and equal electronic temperatures $\beta_L = \beta_R = \beta$ and dot level $\beta\epsilon = 5$. For small coupling strength, exact (black solid) and master equation solution (brown bold) coincide for all bias voltages. For stronger couplings (red dashed and green dotted, respectively), the determination of the dot level ϵ from the current is no longer possible.

observe significant deviations for strong couplings. In the shown example, spectroscopy of the dot level ϵ via detecting steps in the $I-V$ characteristics is therefore only possible in the weak-coupling limit.

7.2 Quantum point contact

We have treated the point contact model

$$H = \sum_k \epsilon_{kL} c_{kL}^\dagger c_{kL} + \sum_k \epsilon_{kR} c_{kR}^\dagger c_{kR} + \sum_{kk'} \left(t_{kk'} c_{kL} c_{k'R}^\dagger + t_{kk'}^* c_{k'R} c_{kL}^\dagger \right) \tag{7.25}$$

before, see Sec. 4.2.2, where we used the tunneling rate

$$T(\omega,\omega') = 2\pi \sum_{kk'} |t_{kk'}|^2 \delta(\omega - \epsilon_{kL})\delta(\omega' - \epsilon_{k'R})\,. \tag{7.26}$$

Since the total Hamiltonian is a quadratic function of fermionic annihilation and creation operators, we can use in principle the very same methods as before to solve this model exactly. The Heisenberg equations of motion for the full system become

$$\begin{aligned} \dot{\boldsymbol{c}}_{kL} &= -\mathrm{i}\epsilon_{kL}\boldsymbol{c}_{kL} + \mathrm{i}\sum_{k'} t^*_{kk'}\boldsymbol{c}_{k'R}\,, \\ \dot{\boldsymbol{c}}_{kR} &= -\mathrm{i}\epsilon_{kR}\boldsymbol{c}_{kR} + \mathrm{i}\sum_{k'} t_{k'k}\boldsymbol{c}_{k'L}\,. \end{aligned} \tag{7.27}$$

However, the general solution will be quite involved, and we therefore just sketch the approach to highlight the difficulties. To see what we are aiming for, we write down the time derivative of the particle number in the left reservoir

$$\dot{\boldsymbol{N}}_L = \sum_k \left[\dot{\boldsymbol{c}}^\dagger_{kL}\boldsymbol{c}_{kL} + \boldsymbol{c}^\dagger_{kL}\dot{\boldsymbol{c}}_{kL}\right] = \sum_{kk'} \left[\mathrm{i}t^*_{kk'}\boldsymbol{c}^\dagger_{kL}\boldsymbol{c}_{k'R} - \mathrm{i}t_{kk'}\boldsymbol{c}^\dagger_{k'R}\boldsymbol{c}_{kL}\right]\,. \tag{7.28}$$

As the expectation value of this operator yields the current, it is also called current operator.

Low-dimensional toy model

We simplify the QPC Hamiltonian by assuming homogeneous energies and factorizing tunneling rates

$$\epsilon_{k\nu} = \epsilon_\nu\,, \qquad t_{kk'} = t_k t_{k'}\,. \tag{7.29}$$

With these assumptions, we can define the operators

$$\boldsymbol{C_L} = \sum_k t_k \boldsymbol{c_{kL}}\,, \qquad \boldsymbol{C_R} = \sum_k t^*_k \boldsymbol{c_{kR}}\,. \tag{7.30}$$

We get that the Heisenberg equations (7.27) close in these operators

$$\dot{\boldsymbol{C_L}} = -\mathrm{i}\epsilon_L \boldsymbol{C_L} + \mathrm{i}\left(\sum_k |t_k|^2\right)\boldsymbol{C_R}\,, \qquad \dot{\boldsymbol{C_R}} = -\mathrm{i}\epsilon_R \boldsymbol{C_R} + \mathrm{i}\left(\sum_k |t_k|^2\right)\boldsymbol{C_L}\,. \tag{7.31}$$

That is, simply exponentiating the matrix we obtain a solution for these operators

$$\begin{pmatrix} \boldsymbol{C_L} \\ \boldsymbol{C_R} \end{pmatrix} = \exp\left\{\begin{pmatrix} -\mathrm{i}\epsilon_L & \mathrm{i}\left(\sum_k |t_k|^2\right) \\ \mathrm{i}\left(\sum_k |t_k|^2\right) & -\mathrm{i}\epsilon_R \end{pmatrix} t\right\}\begin{pmatrix} C^0_L \\ C^0_R \end{pmatrix} = \begin{pmatrix} g_{LL}(t)C^0_L + g_{LR}(t)C^0_R \\ g_{RL}(t)C^0_L + g_{RR}(t)C^0_R \end{pmatrix}, \tag{7.32}$$

where the initial non-vanishing expectation values are

$$\left\langle C^{0\dagger}_L C^0_L\right\rangle = \sum_k |t_k|^2 f_L(\epsilon_{kL})\,, \qquad \left\langle C^{0\dagger}_R C^0_R\right\rangle = \sum_k |t_k|^2 f_R(\epsilon_{kR})\,. \tag{7.33}$$

Furthermore, we can express the current in these operators as well

$$\begin{aligned}
\left\langle \dot{\boldsymbol{N}}_{\boldsymbol{L}} \right\rangle &= \mathrm{i}\left\langle \boldsymbol{C}_{\boldsymbol{L}}^{\dagger}\boldsymbol{C}_{\boldsymbol{R}} \right\rangle - \mathrm{i}\left\langle \boldsymbol{C}_{\boldsymbol{R}}^{\dagger}\boldsymbol{C}_{\boldsymbol{L}} \right\rangle \\
&= \mathrm{i}g_{LL}^{*}(t)g_{RL}(t)\sum_k |t_k|^2 f_L(\epsilon_{kL}) + \mathrm{i}g_{LR}^{*}(t)g_{RR}(t)\sum_k |t_k|^2 f_R(\epsilon_{kR}) + \mathrm{h.c.} \\
&= \left[\mathrm{i}g_{LL}(-t)g_{RL}(t) - \mathrm{i}g_{LL}(t)g_{RL}(-t)\right]\sum_k |t_k|^2 f_L(\epsilon_{kL}) \\
&\quad + \left[\mathrm{i}g_{LR}(-t)g_{RR}(t) - \mathrm{i}g_{LR}(t)g_{RR}(-t)\right]\sum_k |t_k|^2 f_R(\epsilon_{kR}) \\
&= 2T\frac{\sin\left(t\sqrt{(\epsilon_L-\epsilon_R)^2+4T^2}\right)}{\sqrt{(\epsilon_L-\epsilon_R)^2+4T^2}}\sum_k |t_k|^2\left[f_R(\epsilon_{kR}) - f_L(\epsilon_{kR})\right], \qquad (7.34)
\end{aligned}$$

where we have used $T = \sum_k |t_k|^2$. This quantity will oscillate back and forth between the reservoirs, since we have essentially reduced our model to the interaction of just two modes, which will of course just display the coherent evolution.

Heisenberg Equations of Motion

Laplace-transforming the Heisenberg equations, we get (we adopt the convention that when we omit the Laplace transform variable, the operators correspond to the initial condition and are therefore just the normal Schrödinger picture operators)

$$\begin{aligned}
(s+\mathrm{i}\epsilon_{kL})c_{kL}(s) &= c_{kL} + \mathrm{i}\sum_{k'} t_{kk'}^{*}c_{k'R}(s), \\
(s+\mathrm{i}\epsilon_{kR})c_{kR}(s) &= c_{kR} + \mathrm{i}\sum_{k'} t_{k'k}c_{k'L}(s). \qquad (7.35)
\end{aligned}$$

The algebraic structure of these equations would allow one to eliminate e.g. the right modes. However, this would not help much as after their elimination, the left modes would couple among themselves. Therefore, we write the above equation as an algebraic matrix problem

$$G(s)\begin{pmatrix} \vdots \\ c_{kL}(s) \\ \vdots \\ \vdots \\ c_{kR}(s) \\ \vdots \end{pmatrix} = \begin{pmatrix} \vdots \\ c_{kL} \\ \vdots \\ \vdots \\ c_{kR} \\ \vdots \end{pmatrix},$$

$$G(s) = \begin{pmatrix} \ddots & \mathbf{0} & \mathbf{0} & & \vdots & \\ \mathbf{0} & s+\mathrm{i}\epsilon_{kL} & \mathbf{0} & \dots & -\mathrm{i}t_{kk'}^{*} & \dots \\ \mathbf{0} & \mathbf{0} & \ddots & & \vdots & \\ & \vdots & & \ddots & \mathbf{0} & \mathbf{0} \\ \dots & -\mathrm{i}t_{k'k} & \dots & \mathbf{0} & s+\mathrm{i}\epsilon_{kR} & \mathbf{0} \\ & \vdots & & \mathbf{0} & \mathbf{0} & \ddots \end{pmatrix} = \begin{pmatrix} G_{0L}(s) & -\mathrm{i}T^{\dagger} \\ -\mathrm{i}T & G_{0R}(s) \end{pmatrix} \qquad (7,36)$$

We we can solve by inverting the matrix $G(s)$

$$\boldsymbol{c}(s) = G^{-1}(s)\boldsymbol{c}\,, \tag{7.37}$$

or in the time-domain by exponentiating the matrix $\boldsymbol{c}(t) = e^{-G(0)t}\boldsymbol{c}$. While this can be easily done numerically for a finite number of reservoir modes, it becomes more challenging for a continuum of modes.

However, we can perturbatively expand the inverse of the full propagator in the tunneling matrix elements to any desired order

$$\begin{aligned} G^{-1}(s) &= G_0^{-1}(s) + G_0^{-1}(s)G_1G_0^{-1}(s) + G_0^{-1}(s)G_1G_0^{-1}(s)G_1G_0^{-1}(s) + \dots \\ &= \begin{pmatrix} G_{0L}^{-1}(s) & \mathbf{0} \\ \mathbf{0} & G_{0R}^{-1}(s) \end{pmatrix} + \begin{pmatrix} G_{0L}^{-1}(s) & \mathbf{0} \\ \mathbf{0} & G_{0R}^{-1}(s) \end{pmatrix} \begin{pmatrix} \mathbf{0} & -\mathrm{i}T^\dagger \\ -\mathrm{i}T & \mathbf{0} \end{pmatrix} \begin{pmatrix} G_{0L}^{-1}(s) & \mathbf{0} \\ \mathbf{0} & G_{0R}^{-1}(s) \end{pmatrix} + \dots \\ &= \begin{pmatrix} G_{0L}^{-1}(s) & \mathbf{0} \\ \mathbf{0} & G_{0R}^{-1}(s) \end{pmatrix} + \begin{pmatrix} \mathbf{0} & -\mathrm{i}G_{0L}^{-1}(s)T^\dagger G_{0R}^{-1}(s) \\ -\mathrm{i}G_{0R}^{-1}(s)TG_{0L}^{-1}(s) & \mathbf{0} \end{pmatrix} + \dots \end{aligned} \tag{7.38}$$

This implies for the fermionic operators

$$\begin{aligned} c_{kL}(s) &= \frac{c_{kL}}{s+\mathrm{i}\epsilon_{kL}} - \mathrm{i}\sum_{k'} \frac{t_{kk'}^*}{(s+\mathrm{i}\epsilon_{kL})(s+\mathrm{i}\epsilon_{k'R})} c_{k'R} + \dots\,, \\ c_{kR}(s) &= \frac{c_{kR}}{s+\mathrm{i}\epsilon_{kR}} - \mathrm{i}\sum_{k'} \frac{t_{k'k}}{(s+\mathrm{i}\epsilon_{kR})(s+\mathrm{i}\epsilon_{k'L})} c_{k'L} + \dots\,, \end{aligned} \tag{7.39}$$

and for the inverse Laplace transforms

$$\begin{aligned} \boldsymbol{c_{kL}}(t) &= e^{-\mathrm{i}\epsilon_{kL}t}c_{kL} + \sum_{k'} \frac{t_{kk'}^*\left(e^{-\mathrm{i}\epsilon_{kL}t} - e^{-\mathrm{i}\epsilon_{k'R}t}\right)}{\epsilon_{kL}-\epsilon_{k'R}} c_{k'R} + \dots\,, \\ \boldsymbol{c_{kR}}(t) &= e^{-\mathrm{i}\epsilon_{kR}t}c_{kR} + \sum_{k'} \frac{t_{k'k}\left(e^{-\mathrm{i}\epsilon_{kR}t} - e^{-\mathrm{i}\epsilon_{k'L}t}\right)}{\epsilon_{kR}-\epsilon_{k'L}} c_{k'L} + \dots \end{aligned} \tag{7.40}$$

Eventually inserting this in the expression for the current we get

$$\begin{aligned} I &= -\mathrm{i}\sum_{kk'} |t_{kk'}|^2 \frac{e^{+\mathrm{i}(\epsilon_{kL}-\epsilon_{k'R})t}-1}{\epsilon_{k'R}-\epsilon_{kL}} \left[f_L(\epsilon_{kL}) - f_R(\epsilon_{k'R})\right] + \text{h.c.} \\ &= -2\sum_{kk'} |t_{kk'}|^2 \frac{\sin\left[(\epsilon_{kL}-\epsilon_{k'R})t\right]}{\epsilon_{kL}-\epsilon_{k'R}} \left[f_L(\epsilon_{kL}) - f_R(\epsilon_{k'R})\right] \\ &= -\frac{1}{\pi}\int d\omega d\omega' T(\omega,\omega') \frac{\sin\left[(\omega-\omega')t\right]}{\omega-\omega'} \left[f_L(\omega) - f_R(\omega')\right] \\ &\overset{t\to\infty}{\to} -\int T(\omega,\omega)\left[f_L(\omega) - f_R(\omega)\right] d\omega = -\int T(\omega)\left[f_L(\omega) - f_R(\omega)\right] d\omega\,, \end{aligned} \tag{7.41}$$

where we have used that

$$\lim_{t\to\infty} \frac{\sin\left[(\omega-\omega')t\right]}{\omega-\omega'} = \pi\delta(\omega-\omega')\,. \tag{7.42}$$

Up to the sign originating from the consideration of the left junction, this is identical with the perturbative treatment that we had before: According to Eq. (4.65), the current from left to right for a stand-alone QPC becomes

$$\begin{aligned} I &= \gamma_{21}(0) - \gamma_{12}(0) = \int \left[C_{21}(\tau) - C_{12}(\tau)\right] d\tau \\ &= \int d\omega d\omega' T(\omega,\omega') \left[f_L(\omega)[1-f_R(\omega')] - [1-f_L(\omega)]f_R(\omega')\right] \delta(\omega-\omega') \\ &= \int d\omega T(\omega,\omega) \left[f_L(\omega) - f_R(\omega)\right] . \end{aligned} \tag{7.43}$$

However, we could now in principle go beyond this leading order by systematically going to higher order in our expansion (7.38). This however would only lead to higher-order corrections to the transmission function of the QPC $T(\omega) = T(\omega,\omega) + \dots$ but would not change the way in which the Fermi functions enter. The fact that the matter current (and similar the energy current) can be expressed as a frequency integral over a difference of lead occupations times a transmission function is well-known as Landauer formula [35]. It demonstrates that beyond the leading order master equation, the system does not only transmit at a specific frequency but admits tunneling at all frequencies. For the considered example of the QPC there is already at the lowest perturbative order tunneling at all frequencies because in this model there is no actual system.

Last, we state that the most general expression for the fermionic operators for a non-interacting system obeying conservation of the total particle number would be

$$\boldsymbol{c_{kL}}(t) = \sum_{k'} g^{LL}_{kk'}(t) c_{k'L} + \sum_{k'} g^{LR}_{kk'}(t) c_{k'R} , \qquad \boldsymbol{c_{kR}}(t) = \sum_{k'} g^{RL}_{kk'}(t) c_{k'L} + \sum_{k'} g^{RR}_{kk'}(t) c_{k'R} , \tag{7.44}$$

where $g^{\alpha\beta}_{kk'}(t)$ are functions that can be determined in each case separately. Their Laplace transforms are given by the components of the Greens function

$$G^{-1}(s) = \begin{pmatrix} g^{LL}(s) & g^{LR}(s) \\ g^{RL}(s) & g^{RR}(s) \end{pmatrix} , \tag{7.45}$$

which can be determined e.g. perturbatively (this section) or exactly (last section). With this, one can express arbitrary expectation values in terms of components of the Greens function.

7.3 Phonon-Coupled Single electron transistor

As before, we consider a quantum dot model that is additionally coupled to phonons. To keep the analysis simple however, we follow Ref. [36] by considering an SET that is coupled to one, many, or even a continuum of phonon modes as depicted in Fig. 7.2.

7.3.1 Model

The SET Hamiltonian is as before given by

$$H_{\text{SET}} = \epsilon d^\dagger d + \sum_{\nu\in\{L,R\}} \sum_k \left[\epsilon_{k\nu} c^\dagger_{k\nu} c_{k\nu} + t_{k\nu} d c^\dagger_{k\nu} + t^*_{k\nu} c_{k\nu} d^\dagger\right] . \tag{7.46}$$

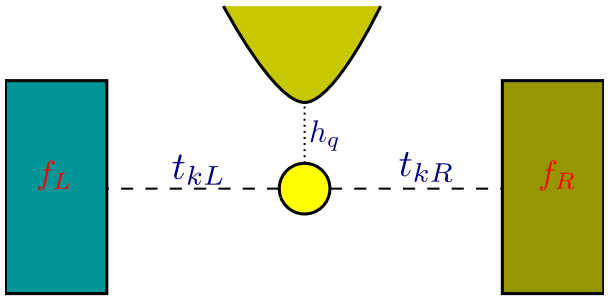

Figure 7.2: Sketch of a single-electron transistor that is capacitively coupled to a phonon reservoir. The interaction in the original Hamiltonian is of the pure dephasing type, i.e., the system energy will not be changed. A conventional master equation treatment would therefore yield no effect on the SET dynamics due to the phonon reservoir.

In addition however, the central dot of the SET now interacts

$$\mathcal{H}_{\rm I} = d^\dagger d \otimes \sum_{q=1}^{Q} \left[h_q a_q + h_q^* a_q^\dagger \right] \tag{7.47}$$

with a phonon reservoir $\mathcal{H}_{\rm B}^{\rm ph} = \sum_q \omega_q a_q^\dagger a_q$ containing Q phonon modes. Obviously, the interaction commutes with the central dot part of the SET Hamiltonian. Therefore, if one would conventionally derive a master equation for the population dynamics of the central quantum dot, the additional phonon bath would not affect the populations of the central dot at all – the interaction is of pure-dephasing type.

In general however, this cannot be true: The interaction does not commute with the total SET Hamiltonian, and therefore one must expect the phonons to have some effect. Indeed, extensive calculations with only a single phonon mode whose dynamics is completely taken into account have revealed a strong suppression of the electronic current when strongly-coupled phonons are present. This phenomenon has been termed Franck-Condon blockade [37].

To treat such cases within a master equation approach, we apply a transformation to the full Hamiltonian $H' = UHU^\dagger$ with the unitary operator

$$U = \exp\left\{ d^\dagger d \sum_q \left(\frac{h_q^*}{\omega_q} a_q^\dagger - \frac{h_q}{\omega_q} a_q \right) \right\} \equiv e^{d^\dagger d A} \,. \tag{7.48}$$

The above transformation is known as polaron or Lang-Firzov transformation [38, 39]. Obviously, the electronic leads are unaffected by the transformation, since $U c_{k\nu} U^\dagger = c_{k\nu}$, and also the central dot part is inert $U d^\dagger d U^\dagger = d^\dagger d$. There are multiple ways of proving the following relations

$$\begin{aligned} U d U^\dagger &= d e^{-A} \,, \qquad U d^\dagger U^\dagger = d^\dagger e^{+A} \,, \\ U a_q U^\dagger &= a_q - \frac{h_q^*}{\omega_q} d^\dagger d \,, \qquad U a_q^\dagger U^\dagger = a_q^\dagger - \frac{h_q}{\omega_q} d^\dagger d \,. \end{aligned} \tag{7.49}$$

Exercise 57 (Polaron transformation)**.** *Show the validity of Eqs. (7.49).*

These immediately also imply the relation

$$U a_q^\dagger a_q U^\dagger = a_q^\dagger a_q - \frac{d^\dagger d}{\omega_q} \left(h_q a_q + h_q^* a_q^\dagger \right) + \frac{|h_q|^2}{\omega_q^2} d^\dagger d \,. \tag{7.50}$$

After the polaron transformation, the Hamiltonian therefore reads

$$\begin{aligned} H' &= \left(\epsilon - \sum_q \frac{|h_q|^2}{\omega_q}\right) d^\dagger d + \sum_{k\nu} \epsilon_{k\nu} c_{k\nu}^\dagger c_{k\nu} + \sum_q \omega_q a_q^\dagger a_q \\ &\quad + \sum_{k\nu} \left(t_{k\nu} d c_{k\nu}^\dagger e^{-A} + t_{k\nu}^* c_{k\nu} d^\dagger e^{+A} \right) , \end{aligned} \tag{7.51}$$

and thereby admits a new decomposition into system and bath Hamiltonians, see also Fig. 7.3. Most obvious, we observe a shift of the electronic level $\epsilon \to \epsilon' = \epsilon - \sum_q \frac{|h_q|^2}{\omega_q}$. Second, the electronic

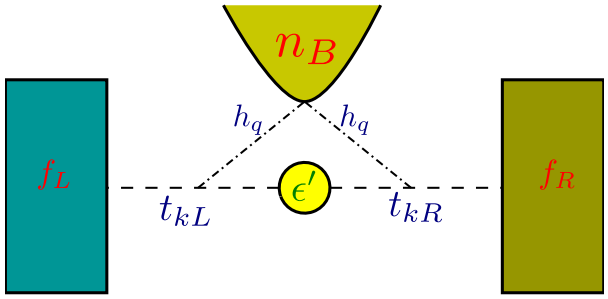

Figure 7.3: After the polaron transformation, direct coupling between the central quantum dot and the phonons in Fig. 7.2 is transformed to the electronic tunnel couplings. The electron-phonon coupling may be treated non-perturbatively (dash-dotted lines) when the electronic tunnel couplings are treated perturbatively (dashed lines).

tunneling terms between central dot and the adjacent leads now become dressed by exponential operators

$$\mathcal{H}_{\rm I}' = \sum_{k\nu} \left[t_{k\nu} d c_{k\nu}^\dagger e^{-\sum_q \left(\frac{h_q^*}{\omega_q} a_q^\dagger - \frac{h_q}{\omega_q} a_q \right)} + t_{k\nu}^* c_{k\nu} d^\dagger e^{+\sum_q \left(\frac{h_q^*}{\omega_q} a_q^\dagger - \frac{h_q}{\omega_q} a_q \right)} \right] , \tag{7.52}$$

which demonstrates that every single electronic jump from the central dot to the leads may now trigger multiple phonon emissions or absorptions. This implies that a perturbative treatment in $t_{k\nu}$ still enables for a non-perturbative treatment of the phonon absorption and emission amplitudes h_q. Furthermore, this leads to the somewhat non-standard situation that already in the interaction Hamiltonian one has now operators from different reservoirs occurring in a product, which implies interesting properties for the correlation functions.

7.3.2 Reservoir equilibrium in the polaron picture

Before we proceed further by deriving a master equation in the displaced polaron frame, we remark that the solution from the displaced frame has to be transformed back to the original picture. A rate equation in the displaced frame implies that the full density matrix in the polaron frame is given by a product state of system and reservoir, where the phonon reservoir density matrix is given by the thermal equilibrium state $\rho'(t) = \rho_{\rm S}'(t) \bar{\rho}_{\rm B}^{(L)} \bar{\rho}_{\rm B}^{(R)} \frac{e^{-\beta_{\rm ph} \mathcal{H}_{\rm B}'}}{Z_{\rm ph}'}$. The transformation back to the initial frame is given by the inverse polaron transformation

$$\begin{aligned} \rho(t) &= U^\dagger \rho'(t) U = U^\dagger \rho_{\rm S}'(t) \bar{\rho}_{\rm B}^{(L)} \bar{\rho}_{\rm B}^{(R)} U U^\dagger \frac{e^{-\beta_{\rm ph} \mathcal{H}_{\rm B}'}}{Z_{\rm ph}'} U \\ &= U^\dagger \rho_{\rm S}'(t) U \bar{\rho}_{\rm B}^{(L)} \bar{\rho}_{\rm B}^{(R)} \frac{e^{-\beta_{\rm ph} U^\dagger \mathcal{H}_{\rm B}' U}}{Z_{\rm ph}'} , \end{aligned} \tag{7.53}$$

where we have used that the polaron transformation (7.48) leaves the electronic reservoirs untouched. When the system density matrix does not exhibit coherences $\rho'_{\mathrm{S}}(t) = P_E(t)dd^\dagger + P_F(t)d^\dagger d$, the unitary transformation will leave it untouched, such that only the reservoir part will be modified. With $\mathcal{H}'_{\mathrm{B}} = \sum_q \omega_q a_q^\dagger a_q$ we can with the inverse transformations of Eq. (7.49)

$$\begin{aligned} U^\dagger \mathcal{H}'_{\mathrm{B}} U &= \sum_q \omega_q a_q^\dagger a_q + d^\dagger d \otimes \sum_q \left(h_q a_q + h_q^* a_q^\dagger\right) + \sum_q \frac{|h_q|^2}{\omega_q} d^\dagger d \\ &= d^\dagger d \otimes \sum_q \left(\omega_q a_q^\dagger a_q + h_q a_q + h_q^* a_q^\dagger + \frac{|h_q|^2}{\omega_q}\mathbf{1}\right) + dd^\dagger \otimes \sum_q \omega_q a_q^\dagger a_q \end{aligned} \tag{7.54}$$

represent the operator in the exponential as a sum of commuting operators. Since for all operators $AB = BA = \mathbf{0}$ we have $e^{A+B} = e^A e^B$ we conclude

$$\begin{aligned} e^{-\beta_{\mathrm{ph}} U^\dagger \mathcal{H}'_{\mathrm{B}} U} &= e^{-\beta_{\mathrm{ph}} d^\dagger d \otimes \sum_q \omega_q (a_q^\dagger + h_q/\omega_q)(a_q + h_q^*/\omega_q)} e^{-\beta_{\mathrm{ph}} dd^\dagger \otimes \sum_q \omega_q a_q^\dagger a_q} \\ &= \left[\mathbf{1} + d^\dagger d \left(e^{-\beta_{\mathrm{ph}} \sum_q \omega_q (a_q^\dagger + h_q/\omega_q)(a_q + h_q^*/\omega_q)} - \mathbf{1}\right)\right] \left[\mathbf{1} + dd^\dagger \left(e^{-\beta_{\mathrm{ph}} \sum_q \omega_q a_q^\dagger a_q} - \mathbf{1}\right)\right] \\ &= d^\dagger d e^{-\beta_{\mathrm{ph}} \sum_q \omega_q (a_q^\dagger + h_q/\omega_q)(a_q + h_q^*/\omega_q)} + dd^\dagger e^{-\beta_{\mathrm{ph}} \sum_q \omega_q a_q^\dagger a_q} . \end{aligned} \tag{7.55}$$

Comparing with the initial Hamiltonian, the phonon part of the first term in the last line is nothing but the thermal phonon state under the side constraint that the SET dot is filled. Formally, this can be seen by replacing $d^\dagger d \to 1$ in Eq. (7.47). Similarly, the other term is the thermalized phonon state when the SET dot is empty. Therefore, preparing the reservoir in a thermal state in the polaron-transformed frame implies that in the original frame, the reservoir state is conditioned on the state of the system. Inserting the assumption that there are no coherences in the system $\rho'_{\mathrm{S}}(t) = P_E(t)dd^\dagger + P_F(t)d^\dagger d$, the full density matrix in the original frame becomes

$$\rho(t) = P_E(t) dd^\dagger \bar{\rho}_{\mathrm{B}}^{(L)} \bar{\rho}_{\mathrm{B}}^{(R)} \otimes \frac{e^{-\beta_{\mathrm{ph}} \sum_q \omega_q a_q^\dagger a_q}}{Z'_{\mathrm{ph}}} + P_F(t) d^\dagger d \bar{\rho}_{\mathrm{B}}^{(L)} \bar{\rho}_{\mathrm{B}}^{(R)} \otimes \frac{e^{-\beta_{\mathrm{ph}} \sum_q \omega_q (a_q^\dagger + h_q/\omega_q)(a_q + h_q^*/\omega_q)}}{Z'_{\mathrm{ph}}} \tag{7.56}$$

Therefore, when the SET dot is occupied, the phonon state is given by a displaced thermal state, whereas when the SET dot is empty, it is just given by the thermal state corresponding to the original phonon Hamiltonian. The phonon dynamics thereby follows the system state immediately, which goes beyond the conventional Born approximation.

7.3.3 Polaron Rate Equation for discrete phonon modes

In the transformed frame, we do now proceed to derive a rate equation for the SET dot populations. We choose to count the phonons emitted into the phonon bath, to test the applicability of the counting field formalism. Here, we will use $N_{\mathrm{ph}} = \sum_q a_q^\dagger a_q$ as the reservoir observable of interest. Identifying the bath coupling operators in the interaction Hamiltonian (7.52) as

$$B_{1\nu} = \sum_k t_{k\nu} c_{k\nu}^\dagger e^{-A} , \qquad B_{2\nu} = \sum_k t_{k\nu}^* c_{k\nu} e^{+A} \tag{7.57}$$

it becomes quite obvious that the reservoir correlation functions will now simultaneously contain contributions from electronic and phonon reservoirs. Recalling the definition 14 of the generalized

correlation function, we obtain a simple product form between electronic and phononic contributions

$$\begin{aligned} C_{12}^{\nu,\chi}(\tau) &= \langle \boldsymbol{B_{1\nu}}(\tau) B_{2\nu} \rangle = C_{12,\mathrm{el}}^{\nu}(\tau) C_{12,\mathrm{ph}}^{\chi}(\tau)\,, \\ C_{21}^{\nu,\chi}(\tau) &= \langle \boldsymbol{B_{2\nu}}(\tau) B_{1\nu} \rangle = C_{21,\mathrm{el}}^{\nu}(\tau) C_{21,\mathrm{ph}}^{\chi}(\tau)\,. \end{aligned} \tag{7.58}$$

Here, the electronic contributions are just the conventional ones known from the SET

$$\begin{aligned} C_{12,\mathrm{el}}^{\nu}(\tau) &= \sum_k |t_{k\nu}|^2 f_\nu(\epsilon_{k\nu}) e^{+\mathrm{i}\epsilon_{k\nu}\tau} = \frac{1}{2\pi}\int \Gamma_\nu(-\omega) f_\nu(-\omega) e^{-\mathrm{i}\omega\tau} d\omega\,, \\ C_{21,\mathrm{el}}^{\nu}(\tau) &= \sum_k |t_{k\nu}|^2 [1-f_\nu(\epsilon_{k\nu})] e^{-\mathrm{i}\epsilon_{k\nu}\tau} = \frac{1}{2\pi}\int \Gamma_\nu(\omega) [1-f_\nu(\omega)] e^{-\mathrm{i}\omega\tau} d\omega\,. \end{aligned} \tag{7.59}$$

In contrast, the phonon contributions are given by

$$C_{12,\mathrm{ph}}^{\chi}(\tau) = \left\langle e^{-\mathrm{i}N_{\mathrm{ph}}\chi} e^{-\boldsymbol{A}(\tau)} e^{+\mathrm{i}N_{\mathrm{ph}}\chi} e^{+A} \right\rangle\,, \qquad C_{21,\mathrm{ph}}^{\chi}(\tau) = \left\langle e^{-\mathrm{i}N_{\mathrm{ph}}\chi} e^{+\boldsymbol{A}(\tau)} e^{+\mathrm{i}N_{\mathrm{ph}}\chi} e^{-A} \right\rangle\,, \tag{7.60}$$

with the phonon operator in the interaction picture

$$\boldsymbol{A}(\tau) = \sum_q \left(\frac{h_q^*}{\omega_q} a_q^\dagger e^{+\mathrm{i}\omega_q\tau} - \frac{h_q}{\omega_q} a_q e^{-\mathrm{i}\omega_q\tau} \right)\,. \tag{7.61}$$

We note that by $h_q \to -h_q$, we transform $C_{12,\mathrm{ph}}^{\chi}(\tau) \to C_{21,\mathrm{ph}}^{\chi}(\tau)$, such that we actually only need to calculate one correlation function. To calculate phonon contribution to the correlation function, we can exploit that (with $\boldsymbol{A}^\chi(\tau) = e^{-\mathrm{i}N_{\mathrm{ph}}\chi}\boldsymbol{A}(\tau)e^{+\mathrm{i}N_{\mathrm{ph}}\chi}$)

$$[\boldsymbol{A}^\chi(\tau), A] = 2\mathrm{i}\sum_q \frac{|h_q|^2}{\omega_q^2}\sin(\omega_q\tau - \chi) \tag{7.62}$$

is just a number, which implies – using the Baker-Campbell-Hausdorff relation

$$\begin{aligned} e^{-\boldsymbol{A}^\chi(\tau)} e^{+A} &= e^{A - \boldsymbol{A}^\chi(\tau) - 1/2[\boldsymbol{A}^\chi(\tau), A]} \\ &= e^{\sum_q \left(\frac{h_q^*}{\omega_q} a_q^\dagger (1-e^{+\mathrm{i}(\omega_q\tau-\chi)}) - \frac{h_q}{\omega_q} a_q (1-e^{-\mathrm{i}(\omega_q\tau-\chi)}) \right)} e^{-\mathrm{i}\sum_q \frac{|h_q|^2}{\omega_q^2}\sin(\omega_q\tau-\chi)}\,. \end{aligned} \tag{7.63}$$

For a thermal reservoir, the phonon correlation function can be written as a product of single-mode correlation functions $C_{12,\mathrm{ph}}^{\chi}(\tau) = \prod_{q=1}^{Q} C_{12,\mathrm{ph}}^{\chi,q}(\tau)$, where the single mode contributions read

$$\begin{aligned} C_{\mathrm{ph}}^{\chi,q}(\tau) &= \left\langle e^{\frac{h_q^*}{\omega_q} a_q^\dagger (1-e^{+\mathrm{i}(\omega_q\tau-\chi)}) - \frac{h_q}{\omega_q} a_q (1-e^{-\mathrm{i}(\omega_q\tau-\chi)})} e^{-\mathrm{i}\frac{|h_q|^2}{\omega_q^2}\sin(\omega_q\tau-\chi)} \right\rangle \\ &= \left\langle e^{\frac{h_q^*}{\omega_q} a_q^\dagger (1-e^{+\mathrm{i}(\omega_q\tau-\chi)})} e^{-\frac{h_q}{\omega_q} a_q (1-e^{-\mathrm{i}(\omega_q\tau-\chi)})} \right\rangle e^{-\frac{|h_q|^2}{\omega_q^2}(1-e^{-\mathrm{i}(\omega_q\tau-\chi)})}\,. \end{aligned} \tag{7.64}$$

By expanding the exponentials, we can evaluate the expectation value for thermal states, where

the probability of having n quanta in the mode q is given by $P_n = (1-e^{-\beta_{\rm ph}\omega_q})e^{-n\beta_{\rm ph}\omega_q}$ as

$$\begin{aligned}\left\langle e^{\alpha_q^* a_q^\dagger} e^{-\alpha_q a_q}\right\rangle &= \sum_{n,m=0}^{\infty} \frac{(\alpha_q^*)^n}{n!}\frac{(-\alpha_q)^m}{m!}\sum_{\ell=0}^{\infty} P_\ell \langle\ell|\,(a_q^\dagger)^n (a_q)^m\,|\ell\rangle \\ &= \sum_{n=0}^{\infty}\frac{(-1)^n|\alpha_q|^{2n}}{(n!)^2}\sum_{\ell=0}^{\infty} P_\ell \langle\ell|\,(a_q^\dagger)^n(a_q)^n\,|\ell\rangle = \sum_{\ell=0}^{\infty} P_\ell \sum_{n=0}^{\ell}\frac{(-1)^n|\alpha_q|^{2n}}{(n!)^2}\frac{\ell!}{(\ell-n)!} \\ &= \sum_{\ell=0}^{\infty} P_\ell \mathcal{L}_\ell(|\alpha_q|^2) = e^{-|\alpha_q|^2 n_B^q} \end{aligned} \tag{7.65}$$

with the Bose distribution $n_B^q = [e^{\beta_{\rm ph}\omega_q}-1]^{-1}$ and Legendre polynomials, defined by the Rodriguez formula [40]

$$\mathcal{L}_n(x) = \frac{1}{2^n n!}\frac{d^n}{dx^n}\left[x^2-1\right]^n . \tag{7.66}$$

The single-mode contributions thus become with $\alpha_q = \frac{h_q}{\omega_q}(1-e^{-{\rm i}(\omega_q\tau-\chi)})$

$$C_{\rm ph}^{\chi,q}(\tau) = \exp\left\{\frac{|h_q|^2}{\omega_q^2}\left[e^{-{\rm i}(\omega_q\tau-\chi)}(1+n_B^q)+e^{+{\rm i}(\omega_q\tau-\chi)}n_B^q-(1+2n_B^q)\right]\right\}, \tag{7.67}$$

such that finally, we obtain for the phonon correlation function

$$C_{12,{\rm ph}}^{\chi}(\tau) = \exp\left\{\sum_q \frac{|h_q|^2}{\omega_q^2}\left[e^{-{\rm i}(\omega_q\tau-\chi)}(1+n_B^q)+e^{+{\rm i}(\omega_q\tau-\chi)}n_B^q-(1+2n_B^q)\right]\right\}. \tag{7.68}$$

The fact that the transformation $h_q \to -h_q$ leaves this result invariant implies that the phonon contribution is always the same in Eq. (7.58), such that we can drop the indices 12 and 21. Furthermore, we see that the phonon counting field occurs at the positions where one might have intuitively expected them. We note that the phonon correlation function obeys the KMS condition.

Exercise 58 (KMS condition)**.** *Show that the phonon correlation function (7.68) obeys the KMS condition* $C(\tau) = C(-\tau - {\rm i}\beta_{\rm ph})$

The observation that in the phonon correlation function (7.67) the terms proportional to $(1+n_B^q)$ correspond to the emission of a phonon into the phonon reservoir and terms proportional to n_B^q alone are responsible for the absorption of a phonon from the reservoir enables one to derive the full phonon counting statistics from the model. Formally expanding the single mode correlation function into multiple emission (m') and absorption (m) events we would obtain a decomposition in the net number of phonon absorbtions by the phonon bath $n = m'-m$, where $C_{\rm ph}^{\chi,q}(\tau) = \sum_{n=-\infty}^{+\infty} C_{\rm ph}^{q,n}(\tau)e^{in\chi}$, and $C_{\rm ph}^{q,n}(\tau) = \frac{1}{2\pi}\int_{-\pi}^{+\pi} C_{\rm ph}^{\chi,q}(\tau)e^{-in\chi}d\chi$ can be determined by the inverse Fourier transform. In particular, using that

$$C_{\rm ph}^{q}(\tau) = e^{-\frac{|h_q|^2}{\omega_q^2}(1+2n_B^q)}\sum_{m,m'=0}^{\infty}\left(\frac{|h_q|^2}{\omega_q^2}\right)^{m+m'}\frac{(n_B^q)^m(1+n_B^q)^{m'}}{m!m'!}e^{+{\rm i}(m-m')\omega_q\tau} \tag{7.69}$$

one can show that by introducing the net number of phonon absorptions by the phonon bath $n = m' - m$, the correlation function can be represented as (below, we drop the counting field $\chi \to 0$, since we have an interpretation for each term)

$$C^q_{\rm ph}(\tau) = \sum_{n=-\infty}^{+\infty} e^{-{\rm i}n\omega_q\tau} e^{-\frac{|h_q|^2}{\omega_q^2}(1+2n_B^q)} \left(\frac{1+n_B^q}{n_B^q}\right)^{\frac{n}{2}} \mathcal{J}_n\left(2\frac{|h_q|^2}{\omega_q^2}\sqrt{n_B^q(1+n_B^q)}\right), \tag{7.70}$$

where $\mathcal{J}_n(x)$ denotes the modified Bessel function of the first kind [40] – defined by the solution of the differential equation $z^2\mathcal{J}_n''(z) + z\mathcal{J}_n'(z) - (z^2+n^2)\mathcal{J}_n(z) = 0$. Introducing for multiple modes the notation $\boldsymbol{n} = (n_1, \ldots, n_Q)$, $\boldsymbol{\omega} = (\omega_1, \ldots, \omega_Q)$, we therefore have for the full multi-mode phonon correlation function the representation

$$\begin{aligned} C_{\rm ph}(\tau) &= \sum_{\boldsymbol{n}} e^{-{\rm i}\boldsymbol{n}\cdot\boldsymbol{\omega}\tau} \prod_{q=1}^{Q} \left[e^{-\frac{|h_q|^2}{\omega_q^2}(1+2n_B^q)} \left(\frac{1+n_B^q}{n_B^q}\right)^{\frac{n_q}{2}} \mathcal{J}_{n_q}\left(2\frac{|h_q|^2}{\omega_q^2}\sqrt{n_B^q(1+n_B^q)}\right)\right] \\ &= \sum_{\boldsymbol{n}} e^{-{\rm i}\boldsymbol{n}\cdot\boldsymbol{\omega}\tau} C^{\boldsymbol{n}}_{\rm ph}\,, \end{aligned} \tag{7.71}$$

where the simple exponential prefactor enables to calculate the Fourier transform of the full correlation function. In particular if only a single phonon mode is present, this enables a simple calculation of the Fourier transform of the complete electron-phonon correlation function

$$\begin{aligned} \gamma^\nu_{12}(\omega) &= \sum_{\boldsymbol{n_\nu}} \gamma^\nu_{12,{\rm el}}(\omega - \boldsymbol{n_\nu}\cdot\boldsymbol{\omega}) C^{\boldsymbol{n_\nu}}_{\rm ph} = \sum_{\boldsymbol{n_\nu}} \gamma^\nu_{12,\boldsymbol{n_\nu}}(\omega)\,, \\ \gamma^\nu_{21}(\omega) &= \sum_{\boldsymbol{n_\nu}} \gamma^\nu_{21,{\rm el}}(\omega - \boldsymbol{n_\nu}\cdot\boldsymbol{\omega}) C^{\boldsymbol{n_\nu}}_{\rm ph} = \sum_{\boldsymbol{n_\nu}} \gamma^\nu_{21,\boldsymbol{n_\nu}}(\omega)\,. \end{aligned} \tag{7.72}$$

Here, the terms $\gamma^\nu_{12,\boldsymbol{n_\nu}}$ are interpreted as the emission of $\boldsymbol{n_\nu}$ phonons into the phonon reservoir whilst an electron jumps from lead ν onto the SET dot, whereas $\gamma^\nu_{21,\boldsymbol{n_\nu}}$ accounts for the emission of $\boldsymbol{n_\nu}$ when an electron is emitted to lead ν. Now, the bosonic KMS relation

$$C^{-\boldsymbol{n_\nu}}_{\rm ph} = e^{-\beta_{\rm ph}\boldsymbol{n_\nu}\cdot\boldsymbol{\omega}} C^{+\boldsymbol{n_\nu}}_{\rm ph} \tag{7.73}$$

together with properties of the Fermi functions implies a KMS-type relation for the full correlation function

$$\gamma^\nu_{12,+\boldsymbol{n_\nu}}(-\omega) = e^{-\beta_\nu(\omega-\mu_\nu+\boldsymbol{n_\nu}\cdot\boldsymbol{\omega})} e^{+\beta_{\rm ph}\boldsymbol{n_\nu}\cdot\boldsymbol{\omega}} \gamma^\nu_{21,-\boldsymbol{n_\nu}}(+\omega)\,, \tag{7.74}$$

which now involves both the electronic and phononic temperatures.

Exercise 59 (KMS condition)**.** *Show the validity of relation (7.74).*

However, we note that when these temperatures are equal, the usual local detailed balance relations are reproduced. Deriving a secular-type rate equation for the dot occupation is now straightforward, the probabilities for finding the dot empty or filled are governed by the rate matrix

$$\mathcal{L} = \sum_{\nu\in\{L,R\}} \sum_{\boldsymbol{n_\nu}} \begin{pmatrix} -\gamma^\nu_{12,\boldsymbol{n_\nu}}(-\epsilon') & +\gamma^\nu_{21,-\boldsymbol{n_\nu}}(+\epsilon') \\ +\gamma^\nu_{12,\boldsymbol{n_\nu}}(-\epsilon') & -\gamma^\nu_{21,-\boldsymbol{n_\nu}}(+\epsilon') \end{pmatrix},$$

where $\gamma^{\nu}_{12,\boldsymbol{n_\nu}}(-\epsilon')$ denotes the rate for an electron jumping onto the SET dot from lead ν whilst simultaneously emitting $\boldsymbol{n_\nu}$ phonons of the various modes into the phonon reservoir. Correspondingly, $\gamma^{\nu}_{21,-\boldsymbol{n_\nu}}(+\epsilon')$ denotes the rate for the inverse process. Having identified the rates for the various involved processes, we can proceed by introducing counting fields. For a three-terminal system with the phononic junction only allowing for energy exchange and with conservation laws on the total energy and particle number we can expect three counting fields to be sufficient for tracking the full entropy production. These can – for example – be the matter transfer from left to right and the energy emitted to the phonon bath counted separately for electronic jumps, such that we have the counting-field dependent version

$$\begin{aligned}\mathcal{L}(\chi,\xi_L,\xi_R) &= \begin{pmatrix} -\gamma^{L}_{12,\boldsymbol{n_L}}(-\epsilon') & +\gamma^{L}_{21,-\boldsymbol{n_L}}(+\epsilon')e^{-\mathrm{i}\boldsymbol{n_L}\cdot\Omega\xi_L} \\ +\gamma^{L}_{12,\boldsymbol{n_L}}(-\epsilon')e^{+\mathrm{i}\boldsymbol{n_L}\cdot\Omega\xi_L} & -\gamma^{L}_{21,-\boldsymbol{n_L}}(+\epsilon') \end{pmatrix} \\ &+ \begin{pmatrix} -\gamma^{R}_{12,\boldsymbol{n_R}}(-\epsilon') & +\gamma^{R}_{21,-\boldsymbol{n_R}}(+\epsilon')e^{+\mathrm{i}\chi}e^{-\mathrm{i}\boldsymbol{n_R}\cdot\Omega\xi_R} \\ +\gamma^{R}_{12,\boldsymbol{n_R}}(-\epsilon')e^{-\mathrm{i}\chi}e^{+\mathrm{i}\boldsymbol{n_R}\cdot\Omega\xi_R} & -\gamma^{L}_{21,-\boldsymbol{n_R}}(+\epsilon') \end{pmatrix},\end{aligned}$$

which enables one to reconstruct all energy and matter currents and thus the full entropy flow.

Here, we will first investigate the impact of the phonon presence on the electronic matter current. If one is only interested in the electronic current, we may set $\xi_L = \xi_R = 0$. The transition rates in the above Liouvillian become particularly simple in the case of a single phonon mode

$$\begin{aligned}\gamma^{\nu}_{12,+n}(-\epsilon') &= \Gamma_\nu(\epsilon'+n\Omega)f_\nu(\epsilon'+n\Omega)e^{-\Lambda(1+2n_B)}\left(\frac{1+n_B}{n_B}\right)^{\frac{n}{2}}\mathcal{J}_n\left(2\Lambda\sqrt{n_B(1+n_B)}\right), \\ \gamma^{\nu}_{21,-n}(+\epsilon') &= \Gamma_\nu(\epsilon'+n\Omega)[1-f_\nu(\epsilon'+n\Omega)]e^{-\Lambda(1+2n_B)}\left(\frac{n_B}{1+n_B}\right)^{\frac{n}{2}}\mathcal{J}_n\left(2\Lambda\sqrt{n_B(1+n_B)}\right) \quad (7.75)\end{aligned}$$

where $\Lambda = \frac{|h|^2}{\Omega_q^2}$ denotes the dimensionless coupling strength to the single phonon mode which is occupied according to $n_B = [e^{\beta_{\mathrm{ph}}\Omega}-1]^{-1}$. The resulting electronic matter current is depicted in Fig. 7.4. Surprisingly, the simple 2×2 rate matrix predicts many signatures in the electronic current. For example, in the electronic matter current one can read off the renormalized dot level at sufficiently low electronic temperatures. In addition however, low temperatures also allow to determine the phonon frequency from the width of the multiple plateaus.

7.3.4 Thermodynamic interpretation

The present rate equation does not directly fit the scheme in Sec. 6.2.2, since the contribution of the three reservoirs to the rates is not additive. Nevertheless, an interpretation in terms of stochastic thermodynamics is possible.

The strong modification of the electronic current is due to the fact that the phonons allow for processes that would normally be forbidden, see Fig. 7.5 In the trajectory in the figure, first an electron jumps in from the left lead to the initially empty SET whilst absorbing two phonons. The change of the system energy by $\Delta E = +\epsilon' = \Delta E_L + \Delta E_{\mathrm{ph}}$ is supplied by both the left lead $\Delta E_L = \epsilon' - 2\Omega$ and the phonon bath $\Delta E_{\mathrm{ph}} = +2\Omega$. In the second step, the electron leaves the dot towards the right lead whilst again absorbing three phonons. Again, the change of the system energy by $-\epsilon'$ is supplied by the right lead $\Delta E_R = -(\epsilon'+3\Omega)$ and the phonon both $\Delta E_{rmph} = +3\Omega$. These energy and matter transfers can be used to construct the total heat exchanged between the reservoirs and thereby also the total entropy production in the steady state.

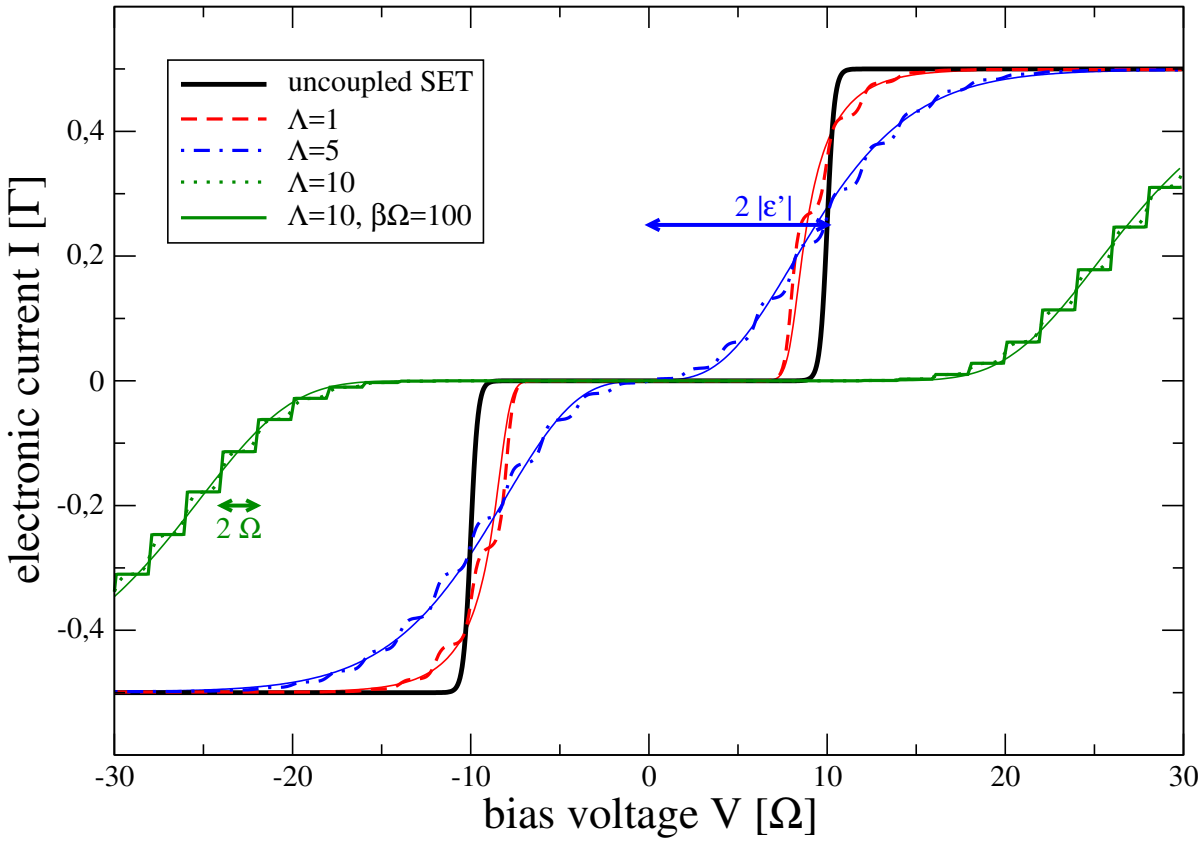

Figure 7.4: Electronic matter current versus bias voltage applied to the SET for vanishing (bold black) and increasing (dashed red, dash-dotted blue, and dotted green, respectively) coupling strengths $\Lambda = |h|^2/\Omega^2 = J_0$ to a single phonon mode of frequency Ω (bold curves) or to a continuum of phonon modes distributed according to an ohmic model (thin solid curves in background). The Franck-Condon blockade can within this model be understood in terms of a renormalization of the effective dot level $\epsilon' = \epsilon - \Lambda\Omega$, which – when $\Lambda\Omega \gg \epsilon$ will lead to current suppression. Furthermore, the steps in the electronic current observed for sufficiently low temperatures (solid green) admit for the transport spectroscopy of the phonon frequency Ω. In the multi-mode case (thin solid curves, for $\omega_c = \Omega$ and $J_0 = \Lambda$), current suppression due to the level renormalization is also observed but the steps in the current are no longer visible. Other parameters: $\Gamma_L = \Gamma_R = \Gamma$, $\beta_L = \beta_R = \beta_{\rm ph} = \beta$, $\beta\Omega = 10$ (except the thin green curve), $\epsilon = 5\Omega$, $J_0 = \Lambda$, $\omega_c = \Omega$.

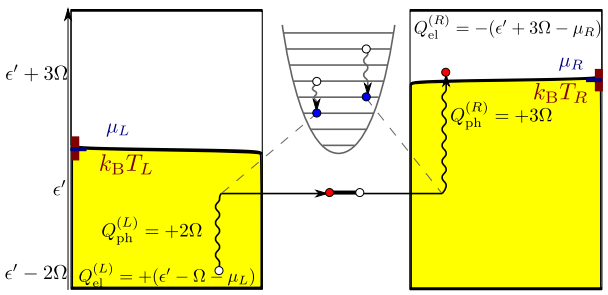

Figure 7.5: Sketch of the energetics of the problem for a single phonon mode, slightly adapted from Ref. [36]. For sufficiently low electronic temperatures, the dot level has to be between μ_L and μ_R to allow for transport, such that an electronic transfer from left to right would be extremely unlikely for the depicted situation. With phonons at sufficiently large temperature however, it is possible to realize trajectories where the missing energy is supplied by the phonon bath. The indicated heat transfers from reservoirs into the system allow for a complete reconstruction of the entropy flows even for single trajectories.

To relate the thermodynamic interpretation more to the modified local detailed balance relation, let us now for simplicity restrict ourselves to the case of a single phonon mode (the generalization to multiple modes is also possible). Formally, the rates corresponding to emission or absorption of different phonon numbers enter additively in Eq. (7.75). This enables one to see the phonon reservoir as a whole collection of infinitely many virtual phonon reservoirs that admit only for the emission or absorption of a certain number of phonons with the same frequency each time an electron is transferred across the SET junctions. This view enables one to adopt the definition 21 of the entropy flow, where the index ν labeling the reservoir may now assume infinitely many values $\nu \to (\nu, n)$, where $\nu \in \{L, R\}$ denotes the junction across which an electron is transferred and n denotes the virtual phonon reservoir from or to which only n phonons may be absorbed or emitted at once. Recalling that $\mathcal{L}_{EF}^{(\nu,n)}$ denotes the rate for an electron to leave the dot towards lead ν whilst absorbing n phonons from the reservoir and $\mathcal{L}_{FE}^{(\nu,n)}$ the rate of the inverse process, i.e., for an electron to enter the dot from lead ν whilst emitting n phonons into the reservoir, the local detailed balance relation becomes – with the rates in Eq. (7.75)

$$\begin{aligned} \ln\left(\frac{\mathcal{L}_{FE}^{(\nu,n)}}{\mathcal{L}_{EF}^{(\nu,n)}}\right) &= \ln\left(\frac{\gamma_{12,+n}(-\epsilon')}{\gamma_{21,-n}(+\epsilon')}\right) = \ln\left[\frac{f_\nu(\epsilon'+n\Omega)}{1-f_\nu(\epsilon'+n\Omega)}\left(\frac{1+n_B}{n_B}\right)^n\right] \\ &= \ln\left[e^{-\beta_\nu(\epsilon'+n\Omega-\mu_\nu)}e^{+n\beta_{\rm ph}\Omega}\right] = -\beta_\nu(\epsilon'+n\Omega-\mu_\nu)+\beta_{\rm ph}n\Omega\,, \end{aligned} \tag{7.76}$$

such that the entropy flow from the virtual reservoir (recall that $\nu \to (\nu, n)$) becomes

$$\begin{aligned} \dot{S}_{\rm e}^{(\nu,n)} &= \mathcal{L}_{EF}^{(\nu,n)}\bar{P}_F \ln\left(\frac{\mathcal{L}_{FE}^{(\nu,n)}}{\mathcal{L}_{EF}^{(\nu,n)}}\right) + \mathcal{L}_{FE}^{(\nu,n)}\bar{P}_E \ln\left(\frac{\mathcal{L}_{EF}^{(\nu,n)}}{\mathcal{L}_{FE}^{(\nu,n)}}\right) \\ &= \left[\mathcal{L}_{EF}^{(\nu,n)}\bar{P}_F - \mathcal{L}_{FE}^{(\nu,n)}\bar{P}_E\right]\ln\left(\frac{\mathcal{L}_{FE}^{(\nu,n)}}{\mathcal{L}_{EF}^{(\nu,n)}}\right) \\ &= \beta_\nu(I_E^{(\nu,n)} - \mu_\nu I_M^{(\nu,n)}) + \beta_{\rm ph} I_E^{(n,\nu,{\rm ph})} = \dot{S}_{\rm e,el}^{(\nu,n)} + \dot{S}_{\rm e,ph}^{(\nu,n)}\,, \end{aligned} \tag{7.77}$$

which is additive in electronic and phononic contributions. Here, we have introduced the energy flows corresponding to the emission or absorption of n phonons. The total energy flows are given

by

$$\begin{aligned} I_E^{\nu} &= \sum_n I_E^{(\nu,n)} = \sum_n \left[\gamma_{12,+n}(-\epsilon')\bar{P}_E - \gamma_{21,-n}(+\epsilon')\bar{P}_F\right](\epsilon' + n\Omega)\,, \\ I_E^{\mathrm{ph}} &= \sum_n \left[I_E^{(n,L,\mathrm{ph})} + I_E^{(n,R,\mathrm{ph})}\right] = \sum_n \sum_\nu \left[\gamma_{21,-n}(+\epsilon')\bar{P}_F - \gamma_{12,+n}(-\epsilon')\bar{P}_R\right] n\Omega\,, \end{aligned} \tag{7.78}$$

whereas the total electronic matter current from lead ν is given by

$$I_M^{\nu} = \sum_n I_E^{(\nu,n)} = \sum_n \left[\gamma_{12,+n}(-\epsilon')\bar{P}_E - \gamma_{21,-n}(+\epsilon')\bar{P}_F\right]\,. \tag{7.79}$$

Similarly, the total entropy flow from the electronic leads is obtained by summing over all different n, and the total entropy flow from the phonon reservoirs is obtained by summing over the contributions from different n and different ν

$$\begin{aligned} \dot{S}_{\mathrm{e}}^{(\nu)} &= \sum_n \dot{S}_{\mathrm{e,el}}^{(\nu,n)} \\ \dot{S}_{\mathrm{e}}^{\mathrm{ph}} &= \sum_n \left(\dot{S}_{\mathrm{e,ph}}^{(L,n)} + \dot{S}_{\mathrm{e,ph}}^{(R,n)}\right)\,. \end{aligned} \tag{7.80}$$

Altogether, the system obeys the laws of thermodynamics, which results in an overall positive entropy production. Consequently, we just note here that it is possible to verify a fluctuation theorem for entropy production, i.e., for $P_{n,e_{\mathrm{ph}}^L,e_{\mathrm{ph}}^R}(t)$ denoting the probability for trajectories with n electrons having traversed the SET from left to right and having emitted energy $e_{\mathrm{ph}}^L = \boldsymbol{n_L}\cdot\boldsymbol{\omega}$ to the phonon reservoir during electronic jumps over the left and energy $e_{\mathrm{ph}}^R = \boldsymbol{n_R}\cdot\boldsymbol{\omega}$ during jumps over the right barrier. In detail, it reads [36]

$$\lim_{t\to\infty} \frac{P_{+n,+e_{\mathrm{ph}}^L,+e_{\mathrm{ph}}^R}(t)}{P_{-n,-e_{\mathrm{ph}}^L,-e_{\mathrm{ph}}^R}(t)} = e^{[(\beta_R-\beta_L)\epsilon' + (\beta_L\mu_L - \beta_R\mu_R)]n + (\beta_{\mathrm{ph}}-\beta_L)e_{\mathrm{ph}}^L + (\beta_{\mathrm{ph}}-\beta_R)e_{\mathrm{ph}}^R}\,, \tag{7.81}$$

and it is straightforward to see that it reduces to the conventional fluctuation theorem when all temperatures are equal.

Disregarding the phonon counting statistics, we note that the system also obeys a fluctuation theorem involving the electronic transfer statistics only

$$\lim_{t\to\infty} \frac{P_{+n}(t)}{P_{-n}(t)} = e^{n\mathcal{A}_{\mathrm{eff}}}\,, \tag{7.82}$$

where the effective affinity $\mathcal{A}_{\mathrm{eff}}$ is however not related to the entropy production, it does, for example, depend on the details of the coupling.

7.3.5 Polaron Rate Equation for continuum phonon modes

Also for a continuum of phonon modes it is possible to obtain a master equation representation. Here, we directly represent the phonon correlation function (7.68), taking a counting field for the energy of the phonon reservoir into account. This then yields

$$C_{\mathrm{ph}}^{\xi}(\tau) = \exp\left\{\int_0^\infty d\omega \frac{J(\omega)}{\omega^2}\left[e^{-\mathrm{i}\omega(\tau-\xi)}(1+n_B(\omega)) + e^{+\mathrm{i}\omega(\tau-\xi)}n_B(\omega) - (1+2n_B(\omega))\right]\right\}\,, \tag{7.83}$$

where we have introduced the spectral density $J(\omega) = \sum_q |h_q|^2 \delta(\omega - \omega_q)$, and ξ is a counting field responsible for the energy of the phonon reservoir. When we choose the common ohmic parametrization $J(\omega) = J_0 \omega e^{-\omega/\omega_c}$ with dimensionless coupling strength J_0 and cutoff frequency ω_c, the integral can be solved exactly. Writing the Bose-Einstein distributions as a geometric series and resumming all separate integral contribution, we finally obtain for the phonon correlation function

$$C_{\rm ph}^{\xi}(\tau) = \left[\frac{\Gamma\left(\frac{1+\beta_{\rm ph}\omega_c + {\rm i}(\tau-\xi)\omega_c}{\beta_{\rm ph}\omega_c}\right)\Gamma\left(\frac{1+\beta_{\rm ph}\omega_c - {\rm i}(\tau-\xi)\omega_c}{\beta_{\rm ph}\omega_c}\right)}{\Gamma^2\left(\frac{1+\beta_{\rm ph}\omega_c}{\beta_{\rm ph}\omega_c}\right)(1+{\rm i}(\tau-\xi)\omega_c)} \right]^{J_0} , \tag{7.84}$$

where $\Gamma(x) = \int_0^\infty t^{x-1} e^{-t} dt$ denotes the Γ-function. The observation that $C_{\rm ph}^{\xi}(\tau) = C_{\rm ph}(\tau - \xi)$ (generally true for energy counting and an initial state that is diagonal in the energy eigenbasis) leads to the relation

$$\gamma_{\rm ph}^{\xi}(\omega) = e^{+{\rm i}\omega\xi}\gamma_{\rm ph}(\omega) . \tag{7.85}$$

We note from Eq. (7.83) that for particular parametrizations of the spectral coupling density one can expect that for large times the phonon correlation functions may remain finite $\lim_{t\to\infty} C_{\rm ph}(\tau) \neq 0$. However, the total correlation function is given by a product of electronic (which decay) and phonon correlation functions. Its Fourier transform (that enters the rates) can be calculated numerically from a convolution integral

$$\begin{aligned} \gamma_{12}^{\nu,\xi_\nu}(-\epsilon') &= \frac{1}{2\pi}\int d\omega \Gamma_\nu(-\omega) f_\nu(-\omega)\gamma_{\rm ph}(-\epsilon'-\omega)e^{-{\rm i}(\epsilon'+\omega)\xi_\nu} , \\ \gamma_{21}^{\nu,\xi_\nu}(+\epsilon') &= \frac{1}{2\pi}\int d\omega \Gamma_\nu(+\omega)[1-f_\nu(+\omega)]\gamma_{\rm ph}(+\epsilon'-\omega)e^{+{\rm i}(\epsilon'-\omega)\xi_\nu} , \end{aligned} \tag{7.86}$$

and enters in this case a rate matrix of the form

$$\mathcal{L}(\chi,\xi_L,\xi_R) = \begin{pmatrix} -\gamma_{12}^L(-\epsilon') & +\gamma_{21}^{L,\xi_L}(+\epsilon') \\ +\gamma_{12}^{L,\xi_L}(-\epsilon') & -\gamma_{21}^L(+\epsilon') \end{pmatrix} + \begin{pmatrix} -\gamma_{12}^R(-\epsilon') & +\gamma_{21}^{R,\xi_R}(+\epsilon')e^{+{\rm i}\chi} \\ +\gamma_{12}^{R,\xi_R}(-\epsilon')e^{-{\rm i}\chi} & -\gamma_{21}^R(+\epsilon') \end{pmatrix} , \tag{7.87}$$

from which the electronic matter current can be directly deduced. With the choices $J_0 = \frac{|h|^2}{\Omega^2}$ and $\omega_c = \Omega$ the electronic current is for high temperatures quite similar as if one would have only a single phonon mode. Also the symmetries are similar to that of Eq. (7.75), and a similar fluctuation theorem arises from that. The crucial difference however is that at low temperatures, the phonon plateaus are no longer visible – compare the thin solid versus the bold curves in Fig. 7.4. Since for the continuum model many different phonon frequencies contribute, this is expected. Interestingly however, the current suppression due to the presence of the phonons (Franck-Condon blockade) is also visible for a continuum of phonon modes.

7.4 $P(E)$ theory

Under the widely used secular approximation, energy exchanged between system and reservoir tends to be conserved individually. With the previously discussed example, we have a model where a part of the energy of an electron entering from an electronic lead is unrecoverably dissipated as heat into the phonon reservoir, such that only a fraction of that energy will actually arrive in the system. Here, we will provide general arguments to show that under specific conditions, a total fluctuation theorem will exist.

7.4.1 Conventional transition rates

We denote the energy levels of the system under consideration by E_i and their corresponding particle numbers by N_i. Here, i runs over all states of the system Hilbert space. Phenomenologically, we find that the reservoir-triggered conventional transition rate from system state j to system state i

$$R_{ij} = \Gamma_{ij} Q(E_i - E_j) \tag{7.88}$$

is given by a product of a bare tunneling rate Γ_{ij} and the probability $Q(E_i - E_j)$ that the reservoir allows for such a jump.

In particular, for fermionic jumps one has

$$Q(E_i - E_j) = \delta_{N_i - N_j, +1} f(E_i - E_j) + \delta_{N_i - N_j, -1}[1 - f(E_j - E_i)] \tag{7.89}$$

with Fermi functions

$$f(\omega) = \frac{1}{e^{\beta(\omega-\mu)} + 1} \tag{7.90}$$

described by reservoir temperature β and chemical potential μ. The first term in Eq. (7.89) describes the probability that to jump in, one first has to have a particle at resonant energy $E_i - E_j$ in the reservoir. To jump out, the energy slot at $E_j - E_i$ must be free (note the sign difference).

On the other hand, for bosonic jumps one would have

$$Q(E_i - E_j) = \delta_{N_i - N_j, +1} n(E_i - E_j) + \delta_{N_i - N_j, -1}[1 + n(E_j - E_i)] \tag{7.91}$$

with Bose function

$$n(\omega) = \frac{1}{e^{\beta(\omega-\mu)} - 1}\,, \tag{7.92}$$

where we have to obey the side constraint $\mu < \omega$.

In either case, these examples just demonstrate that a detailed balance condition is obeyed by the reservoir

$$\frac{Q(E_i - E_j)}{Q(E_j - E_i)} = e^{-\beta(E_i - E_j - \mu)}\,, \tag{7.93}$$

which in the following we will assume to be generally fulfilled. We note that with $\Gamma_{ij} = \Gamma_{ji}$ this transfers to the rate as

$$\frac{R_{ij}}{R_{ji}} = e^{-\beta(E_i - E_j - \mu)}\,. \tag{7.94}$$

7.4.2 Hidden Reservoir

To generalize this, we imagine an unspecified hidden reservoir able to inject energy into the system with each transfer between system and visible reservoir. This would mean that the transition between reservoir and system can be seen as an inelastic scattering event, where the hidden reservoir contributes energy E. Let the probability distribution for this energy contribution be denoted by

$P(E) \geq 0$ with $\int P(E)dE = 1$. Furthermore, we postulate the detailed balance property for the hidden reservoirs [41]

$$\frac{P(+E)}{P(-E)} = e^{\beta_H E} \tag{7.95}$$

with some inverse temperature β_H of the hidden reservoir. Assuming independence of the processes, the transition rate for this particular process would then be given by

$$R_{ij}^{+E} = \Gamma_{ij} Q(E_i - E_j + E) P(+E)\,, \tag{7.96}$$

and the rate for the inverse process would become

$$R_{ji}^{-E} = \Gamma_{ji} Q(E_j - E_i - E) P(-E)\,. \tag{7.97}$$

We note that for the energy-resolved rates we have the generalized relation

$$\frac{R_{ij}^{+E}}{R_{ji}^{-E}} = e^{-\beta(E_i - E_j + E - \mu)} e^{+\beta_H E}\,, \tag{7.98}$$

which recovers the original detailed balance relation (7.94) when $\beta_H = \beta$.

However, the total rates would be given by an integral

$$R_{ij} = \Gamma_{ij} \int Q(E_i - E_j + E) P(+E) dE\,, \tag{7.99}$$

and they will not obey detailed balance relations.

7.4.3 Currents

The rate (7.96) has the interpretation that to induce an energy change $E_i - E_j$ in the system, the conventional reservoir contributes energy $E_i - E_j + E$, where the fraction $-E$ is however absorbed in the hidden reservoir. We now allow for the possibility of multiple reservoirs (to support stationary currents) by replacing $R_{ij} \to R_{ij}^{(\nu)}$. As the hidden reservoir does not absorb or emit any particles, the steady-state matter current entering the system from reservoir ν is defined as usual

$$I_M^{(\nu)} = \sum_{ij} (N_i - N_j) R_{ij}^{(\nu)} \bar{P}_j\,, \tag{7.100}$$

where $\bar{P}_j$ denotes the system steady-state population in state j. However, the energy current into the system

$$I_E^{(\nu)} = \sum_{ij} (E_i - E_j) R_{ij}^{(\nu)} \bar{P}_j \tag{7.101}$$

now splits into two contributions $I_E^{(\nu)} = I_E^{(\nu),R} + I_E^{(\nu),H}$, where

$$I_E^{(\nu),R} = \sum_{ij} \int (E_i - E_j + E) R_{ij}^{(\nu),+E} dE \bar{P}_j\,, \qquad I_E^{(\nu),H} = \sum_{ij} \int (-E) R_{ij}^{(\nu)+E} dE \bar{P}_j \tag{7.102}$$

denote the fractions entering the system from the original reservoir and the hidden reservoir, respectively. Naively, we may also guess that the entropy production rate now in the long-term limit is again balanced by the matter and energy currents. Now for multiple real and hidden reservoirs ν, the entropy production rate would become at steady state (hypothesis)

$$\dot{S}_{\rm i} \to -\sum_\nu \beta_\nu \left(I_E^{\nu,R} - \mu_\nu I_M^\nu \right) - \sum_\nu \beta_{H,\nu} I_E^{\nu,H} \geq 0\,. \tag{7.103}$$

7.4.4 Entropic Balance

We start from a rate equation of the form

$$\dot{P}_i = \sum_\nu \sum_j R_{ij}^{(\nu)} P_j \tag{7.104}$$

with energy-resolved rates specific to tunneling processes between system and

$$R_{ij}^{(\nu)} = \int R_{ij,+E}^{(\nu)} dE \tag{7.105}$$

describing a transition $j \to i$ in the system while the hidden reservoir absorbs energy E. We note that the hidden reservoir can be different for each tunnel junction. In what follows, we will just require probability conservation

$$\sum_i R_{ij}^{(\nu)} = 0 \tag{7.106}$$

and a generalized local detailed balance condition

$$\frac{R_{ij,+E}^{(\nu)}}{R_{ji,-E}^{(\nu)}} = e^{-\beta_\nu[E_i - E_j + E - \mu_\nu(N_i - N_j)]} e^{+\beta_\nu^H E} \tag{7.107}$$

to hold. Here, β_ν and μ_ν denote inverse temperature and chemical potential of reservoir ν, and β_ν^H is the inverse temperature of the hidden reservoir associated to junction ν. Taking the time derivative of the systems Shannon entropy $S = -\sum_i P_i \ln P_i$ we get

$$\begin{aligned}
\dot{S} &= -\sum_i \dot{P}_i \ln P_i = -\sum_{ij}\sum_\nu \int dE R_{ij,+E}^{(\nu)} P_j \ln\left(\frac{R_{ji,-E}^{(\nu)} P_i}{R_{ij,+E}^{(\nu)} P_j} \frac{R_{ij,+E}^{(\nu)} P_j}{R_{ji,-E}^{(\nu)}}\right) \\
&= +\sum_{ij}\sum_\nu \int dE R_{ij,+E}^{(\nu)} P_j \ln\left(\frac{R_{ij,+E}^{(\nu)} P_j}{R_{ji,-E}^{(\nu)} P_i}\right) + \sum_{ij}\sum_\nu \int dE R_{ij,+E}^{(\nu)} P_j \ln\left(\frac{R_{ji,-E}^{(\nu)}}{R_{ij,+E}^{(\nu)} P_j}\right) \\
&= +\sum_{ij}\sum_\nu \int dE R_{ij,+E}^{(\nu)} P_j \ln\left(\frac{R_{ij,+E}^{(\nu)} P_j}{R_{ji,-E}^{(\nu)} P_i}\right) + \sum_{ij}\sum_\nu \int dE R_{ij,+E}^{(\nu)} P_j \ln\left(\frac{R_{ji,-E}^{(\nu)}}{R_{ij,+E}^{(\nu)}}\right) \\
&= +\sum_{ij}\sum_\nu \int dE R_{ij,+E}^{(\nu)} P_j \ln\left(\frac{R_{ij,+E}^{(\nu)} P_j}{R_{ji,-E}^{(\nu)} P_i}\right) \\
&\quad +\sum_{ij}\sum_\nu \int dE R_{ij,+E}^{(\nu)} P_j \left\{\beta_\nu[E_i - E_j + E - \mu_\nu(N_i - N_j)] - \beta_\nu^H E\right\} \\
&= +\sum_{ij}\sum_\nu \int dE R_{ij,+E}^{(\nu)} P_j \ln\left(\frac{R_{ij,+E}^{(\nu)} P_j}{R_{ji,-E}^{(\nu)} P_i}\right) + \sum_\nu \left\{\beta_\nu[I_E^{(\nu)} - \mu_\nu I_M^{(\nu)}] + \beta_\nu^H I_E^{(\nu),H}\right\}.
\end{aligned} \tag{7.108}$$

In the first equality sign we have jused used the trace conservation $\sum_i \dot{P}_i = 0$, in the third line we used that the term with an individual $\ln(P_j)$ would vanish due to the trace conservation as well, and in the fourth equation we have inserted the generalized KMS relation specific for each reservoir. Finally, we identify the entropy flow in terms of the heat currents entering the system

$$\dot{S}_{\rm e} = \sum_\nu \left\{\beta_\nu[I_E^{(\nu)} - \mu_\nu I_M^{(\nu)}] + \beta_\nu^H I_E^{(\nu),H}\right\} \tag{7.109}$$

and also the entropy production rate

$$\dot{S}_{\mathrm{i}} = \sum_{ij} \sum_{\nu} \int dE R^{(\nu)}_{ij,+E} P_j \ln \left(\frac{R^{(\nu)}_{ij,+E} P_j}{R^{(\nu)}_{ji,-E} P_i} \right) . \tag{7.110}$$

To show its positivity, we generalize the logarithmic sum inequality

$$\sum_i a_i \ln \frac{a_i}{b_i} \geq a \ln \frac{a}{b} , \qquad a = \sum_i a_i , \quad b = \sum_i b_i \tag{7.111}$$

to double summations and integrals

$$\int dE \sum_{ij} a^E_{ij} \ln \frac{a^E_{ij}}{b^E_{ij}} \geq a \ln \frac{a}{b} , \qquad a = \int dE \sum_{ij} a^E_{ij} , \quad b = \int dE \sum_{ij} b^E_{ij} . \tag{7.112}$$

Then, identifying $a^E_{ij} = R^{(\nu)}_{ij,+E} P_j$ and $b^E_{ij} = R^{(\nu)}_{ji,-E} P_i$ we obtain that $a = b$, and consequently, as $a \geq 0$ for each reservoir ν, this bounds the entropy production rate

$$\dot{S}_{\mathrm{i}} = \sum_{\nu} \dot{S}^{(\nu)}_{\mathrm{i}} \geq 0 , \tag{7.113}$$

which also holds in far-from-equilibrium regimes.

Furthermore, we note that if we introduce counting fields via

$$\mathcal{L}_{ij} = \sum_{\nu} \int dE R^{(\nu)}_{ij,+E} e^{+\mathrm{i}\chi_\nu (N_i - N_j)} e^{+\mathrm{i}\xi_\nu (E_i - E_j + E)} e^{-\mathrm{i}\lambda_\nu E} \tag{7.114}$$

in the off-diagonal matrix elements of the Liouvillian, we obtain a symmetry of the form

$$\mathcal{L}(-\chi_\nu, -\xi_\nu, -\lambda_\nu) = \mathcal{L}^\dagger (+\chi_\nu + \mathrm{i}\beta_\nu \mu_\nu, +\xi_\nu - \mathrm{i}\beta_\nu, +\lambda_\nu - \mathrm{i}\beta^H_\nu) . \tag{7.115}$$

As the eigenvalues of a matrix are not changed by transposition and as the long-term cumulant-generating function is given by the dominant eigenvalue of $\mathcal{L}$, it follows that

$$\mathcal{C}(-\chi_\nu, -\xi_\nu, -\lambda_\nu) = \mathcal{C}(+\chi_\nu + \mathrm{i}\beta_\nu \mu_\nu, +\xi_\nu - \mathrm{i}\beta_\nu, +\lambda_\nu - \mathrm{i}\beta^H_\nu) . \tag{7.116}$$

This in turn will imply that a fluctuation theorem exists for large times. Actually, one can prove that a modified fluctuation theorem exists also for short times, but this will have to take the changes of the system entropy into account.

7.5 A non-perturbative form for entropy production

A recent paper by M. Esposito nicely discusses general properties of entropy production that hold independent of the used master equation approaches [42]. We start from a setting where both system and interaction Hamiltonians are allowed to be time-dependent

$$H(t) = H_S(t) + \sum_{\nu} H^{(\nu)}_I(t) + \sum_{\nu} H^{(\nu)}_B . \tag{7.117}$$

Initially, we assume that the system and reservoirs are uncorrelated, and that the reservoirs are initially at thermal equilibrium states

$$\rho(0) = \rho_S(0) \bigotimes_\nu \bar{\rho}_B^{(\nu)} , \qquad \bar{\rho}_B^{(\nu)} = \frac{e^{-\beta_\nu (H_B^{(\nu)} - \mu_\nu N_B^{(\nu)})}}{Z_\nu} , \tag{7.118}$$

where Z_ν and $N_B^{(\nu)}$ denote partition function and reservoir particle number of reservoir ν, respectively. We will only assume this at the initial time, but not for $t > 0$. In fact, the treatment is so general that the reservoirs can be arbitrarily small, they can even consist of single qubits and they can move arbitrarily far away from any product state during the evolution. The only formal requirement is that they are initially represented as a thermal equilibrium state.

Since the evolution of the total system is unitary, the total entropy is a constant of motion, yielding the relation

$$-\mathrm{Tr}\left\{\rho(t)\ln\rho(t)\right\} = -\mathrm{Tr}\left\{\rho(0)\ln\rho(0)\right\} = -\mathrm{Tr_S}\left\{\rho_S(0)\ln\rho_S(0)\right\} - \sum_\nu \mathrm{Tr}_\nu \left\{\bar{\rho}_B^{(\nu)} \ln \bar{\rho}_B^{(\nu)}\right\} , \tag{7.119}$$

where we have used that for an initial product state it is additive in system and reservoir contributions. Now, we introduce the local reduced density matrices of system and reservoirs

$$\rho_S(t) = \mathrm{Tr}_{\{\nu\}}\left\{\rho(t)\right\} , \qquad \rho_\nu(t) = \mathrm{Tr}_{\mathrm{S},\nu'\neq\nu}\left\{\rho(t)\right\} , \tag{7.120}$$

and turn to the entropy of the system

$$S(t) = -\mathrm{Tr_S}\left\{\rho_S(t)\ln\rho_S(t)\right\} . \tag{7.121}$$

We see that its initial value is related to the full entropy of the system via

$$S(0) = -\mathrm{Tr}\left\{\rho(t)\ln\rho(t)\right\} + \sum_\nu \mathrm{Tr}_\nu \left\{\bar{\rho}_B^{(\nu)} \ln \bar{\rho}_B^{(\nu)}\right\} . \tag{7.122}$$

Its change can therefore be written as

$$\begin{aligned}
\Delta S(t) &= S(t) - S(0) \\
&= -\mathrm{Tr_S}\left\{\rho_S(t)\ln\rho_S(t)\right\} + \mathrm{Tr}\left\{\rho(t)\ln\rho(t)\right\} - \sum_\nu \mathrm{Tr}_\nu \left\{\bar{\rho}_B^{(\nu)} \ln \bar{\rho}_B^{(\nu)}\right\} \\
&= -\mathrm{Tr}\left\{\rho(t)\ln\rho_S(t)\right\} + \mathrm{Tr}\left\{\rho(t)\ln\rho(t)\right\} - \sum_\nu \mathrm{Tr}_\nu \left\{\bar{\rho}_B^{(\nu)} \ln \bar{\rho}_B^{(\nu)}\right\} \\
&= -\mathrm{Tr}\left\{\rho(t)\ln\rho_S(t)\bigotimes_\nu \bar{\rho}_B^{(\nu)}\right\} + \mathrm{Tr}\left\{\rho(t)\ln\rho(t)\right\} + \sum_\nu \mathrm{Tr}_\nu \left\{\left[\rho_\nu(t) - \bar{\rho}_B^{(\nu)}\right] \ln \bar{\rho}_B^{(\nu)}\right\} \\
&= D\left(\rho(t)\Big|\Big|\rho_S(t)\bigotimes_\nu \bar{\rho}_B^{(\nu)}\right) - \sum_\nu \beta_\nu \mathrm{Tr}_\nu \left\{\left[\rho_\nu(t) - \bar{\rho}_B^{(\nu)}\right]\left[H_B^{(\nu)} - \mu_\nu N_B^{(\nu)}\right]\right\} ,
\end{aligned} \tag{7.123}$$

where the first term is nothing but the distance – expressed in terms of the quantum relative entropy, compare Eq. (2.64) – between the actual state of the full density matrix and the product state. It is positive and vanishes if and only if the system and bath density matrices are not entangled, it will be denoted as the entropy production

$$\Delta_{\mathrm{i}} S(t) = D\left(\rho(t)\Big|\Big|\rho_S(t)\bigotimes_\nu \bar{\rho}_B^{(\nu)}\right) \geq 0 . \tag{7.124}$$

We see that the entropy production is large when the distance between the actual state and the product state is large, such that it can be seen as quantifying the correlations between system and reservoir. For finite-size reservoirs, recurrences can occur, and the entropy production can behave periodically. We therefore note that its production rate need not be positive. In particular, for periodically evolving systems we must observe times where $\frac{d}{dt}\Delta_{\rm i}S(t) < 0$.

By contrast, the second term can be identified as the entropy flow

$$\begin{aligned}\Delta_e S(t) &= -\sum_\nu \beta_\nu \mathrm{Tr}_\nu \left\{ \left[\rho_\nu(t) - \bar{\rho}_B^{(\nu)}\right] \left[H_B^{(\nu)} - \mu_\nu N_B^{(\nu)}\right]\right\} \\ &= \sum_\nu \beta_\nu \Delta Q_\nu(t)\,, \end{aligned} \tag{7.125}$$

where the the heat flowing from the reservoir ν into the system is defined as

$$\Delta Q_\nu(t) = \left\langle H_B^{(\nu)} - \mu_\nu N_B^{(\nu)}\right\rangle_0 - \left\langle H_B^{(\nu)} - \mu_\nu N_B^{(\nu)}\right\rangle_t . \tag{7.126}$$

7.5.1 Entropy production rate

We can solve Eq. (7.123) for the entropy production

$$\Delta_{\rm i}S(t) = S(t) - S(0) - \sum_\nu \beta_\nu \Delta Q_\nu(t)\,. \tag{7.127}$$

Performing a time derivative on both sides yields

$$\frac{d}{dt}\Delta_{\rm i}S(t) = \dot{S}(t) - \sum_\nu \beta_\nu \Delta \dot{Q}_\nu(t)\,, \tag{7.128}$$

where $\dot{Q}_\nu(t)$ now denotes the heat current entering the system from reservoir ν. In general, this quantity will not be positive. However, assuming evolution under a Lindblad form, we know that also the entropy production rate $\frac{d}{dt}\Delta_{\rm i}S(t) \to \dot{S}_{\rm i} \geq 0$ is positive, compare Sec. 3.3.

7.5.2 Example: Steady-state entropy production in the SET

For exactly solvable models such as the SET, we usually do not have direct access on the entropy production. However, we can express it by the entropy change of the system and the heat leaving the reservoirs

$$\Delta_{\rm i}S(t) = \Delta S(t) + \sum_\nu \left[\left\langle H_B^{(\nu)} - \mu_\nu N_B^{(\nu)}\right\rangle_t - \left\langle H_B^{(\nu)} - \mu_\nu N_B^{(\nu)}\right\rangle_0\right] . \tag{7.129}$$

For large times, the system reaches a stationary state, i.e., $\Delta S(t)$ assumes a constant value, which however is negligibly small in comparison to the other terms, which grow linearly in time. In particular, the difference between the reservoir energies and particle numbers at time t and the initial time will be given by

$$\left\langle H_B^{(\nu)}\right\rangle_t - \left\langle H_B^{(\nu)}\right\rangle_0 \approx -tI_E^{(\nu)}\,, \qquad \left\langle N_B^{(\nu)}\right\rangle_t - \left\langle N_B^{(\nu)}\right\rangle_0 \approx -tI_M^{(\nu)}\,, \tag{7.130}$$

where we have introduced the energy and matter currents entering the system from reservoir ν. We had already obtained an exact expression for the matter current, compare Eq. (7.23), but the calculation for the energy current is completely analogous, yielding

$$\begin{aligned} I_E^{(L)} &= I_E = \int \omega \left[f_L(\omega) - f_R(\omega)\right] T(\omega) d\omega = -I_E^{(R)} \\ I_M^{(L)} &= I_M = \int \left[f_L(\omega) - f_R(\omega)\right] T(\omega) d\omega = -I_M^{(R)} , \end{aligned} \tag{7.131}$$

where $T(\omega) \geq 0$ denotes a transmission function [27]. Neglecting the finite constant contributions, we obtain for the long-term entropy production

$$\begin{aligned} \Delta_{\rm i} S(t) &\approx t \left[-(\beta_L - \beta_R) I_E + (\beta_L \mu_L - \beta_R \mu_R) I_M\right] \\ &= t \int T(\omega) \left[(\beta_L \mu_L - \beta_R \mu_R) - (\beta_L - \beta_R)\omega\right] \left[f_L(\omega) - f_R(\omega)\right] d\omega . \end{aligned} \tag{7.132}$$

We can now examine the integrand more closely. Using that $T(\omega) > 0$, we find its only root at $\beta_L(\bar{\omega} - \mu_L) = \beta_R(\bar{\omega} - \mu_R)$. Furthermore, the first two derivatives become

$$\begin{aligned} \frac{d}{d\omega} \left[(\beta_L \mu_L - \beta_R \mu_R) - (\beta_L - \beta_R)\omega\right] \left[f_L(\omega) - f_R(\omega)\right] \Big|_{\omega=\bar{\omega}} &= 0 , \\ \frac{d^2}{d\omega^2} \left[(\beta_L \mu_L - \beta_R \mu_R) - (\beta_L - \beta_R)\omega\right] \left[f_L(\omega) - f_R(\omega)\right] \Big|_{\omega=\bar{\omega}} &= \frac{(\beta_L - \beta_R)^2}{1 + \cosh\left[\frac{\beta_L \beta_R (\mu_L - \mu_R)}{\beta_L - \beta_R}\right]} \geq 0 . \end{aligned} \tag{7.133}$$

This proves that the root of the integrand is actually a minimum of the integrand, and therefore the integrand is non-negative throughout. From this, we directly see that the second law is fulfilled at steady state

$$\Delta_{\rm i} S(t) \approx t \int T(\omega) \left[(\beta_L \mu_L - \beta_R \mu_R) - (\beta_L - \beta_R)\omega\right] \left[f_L(\omega) - f_R(\omega)\right] d\omega \geq 0 . \tag{7.134}$$

7.5.3 Example: Transient entropy production for pure-dephasing

We had solved the pure dephasing version of the spin-boson model

$$H = \Omega \sigma^z + \lambda \sigma^z \otimes \sum_k \left(h_k b_k + h_k^* b_k^\dagger\right) + \sum_k \omega_k b_k^\dagger b_k . \tag{7.135}$$

before. For the system, we would in the eigenbasis of σ^z simply obtain stationary populations and decaying coherences

$$|\rho_{01}|(t) = e^{-f(t)} \left|\rho_{01}^0\right| , \qquad f(t) = \frac{4}{\pi} \int_0^\infty \Gamma(\omega) \frac{\sin^2(\omega t/2)}{\omega^2} \coth\left(\frac{\beta\omega}{2}\right) d\omega , \tag{7.136}$$

compare Eq. (2.102). To benchmark our master equation approaches we had also calculated the change of the reservoir energy

$$\Delta E(t) = \frac{2}{\pi} \int_0^\infty \frac{\Gamma(\omega)}{\omega} \sin^2\left(\frac{\omega t}{2}\right) d\omega \tag{7.137}$$

see Eq. (4.125), and the change of the reservoir particle number

$$\Delta N(t) = \frac{2}{\pi}\int_0^\infty \frac{\Gamma(\omega)}{\omega^2}\sin^2\left(\frac{\omega t}{2}\right)d\omega \tag{7.138}$$

compare Eq. (4.85). For a single reservoir, Eq. (7.123) becomes

$$\Delta_{\rm i} S(t) = S(t) - S(0) + \beta\left[\Delta E(t) - \mu\Delta N(t)\right]. \tag{7.139}$$

Using that $\Delta E(t) > 0$, $\Delta N(t) > 0$, and for bosons $\mu \leq 0$ (actually, we would normally drop it for photons), we can already conclude that the second term is separately positive. Also, if we would let $t \to \infty$, the final density matrix of the system would be diagonal, such that we can conclude that $S(\infty) - S(0) > 0$, but does this hold for all times? Parametrizing the density matrix by the occupation ρ_{11} and the time-dependent coherence $\rho_{01}(t)$, its von-Neumann entropy becomes

$$\begin{aligned} S(t) = &-\frac{1}{2}\left[1 - \sqrt{(1-2\rho_{11})^2 + 4|\rho_{01}(t)|^2}\right]\ln\frac{1}{2}\left[1 - \sqrt{(1-2\rho_{11})^2 + 4|\rho_{01}(t)|^2}\right] \\ &-\frac{1}{2}\left[1 + \sqrt{(1-2\rho_{11})^2 + 4|\rho_{01}(t)|^2}\right]\ln\frac{1}{2}\left[1 + \sqrt{(1-2\rho_{11})^2 + 4|\rho_{01}(t)|^2}\right]. \end{aligned} \tag{7.140}$$

Using that as time increases, the coherences become smaller $|\rho_{01}(t)|^2 = e^{-2f(t)}|\rho_{01}^0|^2$, we find (in the regime $0 \leq (1-2\rho_{11})^2 + 4|\rho_{01}(t)|^2 \leq 1$ that is allowed for a valid density matrix), that $S(t) = -(1-x)/2\ln(1-x)/2 - (1+x)/2\ln(1+x)/2$ is a monotonously decaying function when $\sqrt{(1-2\rho_{11})^2 + 4|\rho_{01}(t)|^2} = x \in [0,1]$. Therefore, we conclude $S(t) > S(0)$, and consequently

$$\Delta_{\rm i} S(t) = S(t) - S(0) + \beta\left[\Delta E(t) - \mu\Delta N(t)\right] \geq 0\,, \tag{7.141}$$

confirming the validity of the second law or – depending on the perspective – the validity of our exact solution.

7.6 Reaction-coordinate treatment

Conventional master equation approaches typically work well when the coupling is small and when the Markovian approximation fits well. This implies rapidly decaying correlation functions and consequently, their Fourier transforms should be relatively flat. In the examples we discussed, these Fourier transforms were given by products of spectral coupling densities and Bose-Einstein or Fermi-Dirac distribution functions. Therefore, one may expect the conventional master equation to work well when the spectral coupling density is flat and also the temperature of the reservoir is high. In this section, we will discuss an approach that is applicable at high temperatures but very peaked spectral densities.

7.6.1 Bogoliubov transformation

Many physical problems are represented in the language of second quantization, using fermionic or bosonic annihilation and creation operators. These obey canonical commutation or anticommutation relations, respectively. Here, we just show that using a unitary transformation, we can map to new operators of the same type whilst preserving the canonical commutation relations.

We start with bosons, which obey the commutation relations

$$[a_k, a_{k'}^\dagger] = \delta_{kk'}\,, \qquad [a_k, a_{k'}] = 0\,. \tag{7.142}$$

The Bogoliubov transformation expands these operators in a new set of operators

$$a_k = \sum_q u_{kq} b_q\,, \qquad a_k^\dagger = \sum_q u_{kq}^* b_q^\dagger\,, \tag{7.143}$$

where the complex-valued coefficients u_{kq} are matrix elements of a unitary matrix, obeying the relation

$$\sum_{k'} u_{kk'} u_{qk'} = \delta_{kq}\,. \tag{7.144}$$

Then, the transformation is of course invertible, and we can show that the commutation relations are preserved, the only non-trivial one being

$$[a_k, a_{k'}^\dagger] = \sum_{qq'} u_{kq} u_{k'q'}^* [b_q, b_{q'}^\dagger] = \sum_q u_{kq} u_{k'q}^* = \delta_{kk'}\,. \tag{7.145}$$

The same holds for Fermions, with their anticommutation relations being

$$\{c_k, c_{k'}^\dagger\} = \delta_{kk'}\,, \qquad \{c_k, c_{k'}\} = 0\,. \tag{7.146}$$

We also find that any unitary transformation

$$c_k = \sum_q u_{kq} d_q\,, \qquad c_k^\dagger = \sum_q u_{kq}^* d_q^\dagger \tag{7.147}$$

will preserve the canonical anticommutation relations, the only non-trivial one being

$$\{c_k, c_{k'}^\dagger\} = \sum_{qq'} u_{kq} u_{k'q'}^* \{d_q, d_{q'}^\dagger\} = \sum_q u_{kq} u_{k'q}^* = \delta_{kk'}\,. \tag{7.148}$$

Such mappings are useful to bring e.g. a Hamiltonian into diagonal form, where its spectrum can be conventiently calculated, e.g.

$$\epsilon_1 c_1^\dagger c_1 + \epsilon_2 c_2^\dagger c_1 + T c_1^\dagger c_2 + T^* c_2^\dagger c_1 = \tilde{\epsilon}_1 d_1^\dagger d_1 + \tilde{\epsilon}_2 d_2^\dagger d_2\,. \tag{7.149}$$

This maps two coupled units into two decoupled ones. However, Bogoliubov mappings can also be used to change the structure of the Hamiltonian in a desired way, changing our definition of system and reservoir, see Fig. 7.6. In what we use below, the requirement is that the Hamiltonian of the interaction is linear in the reservoir creation and annihilation operators and that the reservoir consists of independent fermions or bosons.

7.6.2 Example: Mapping for a finite bosonic reservoir

Let us as an example consider the spin-boson model, described by the full Hamiltonian

$$H \;=\; \frac{\omega}{2}\sigma^z + \sigma^x \sum_k \left(h_k b_k + h_k^* b_k^\dagger\right) + \sum_k \omega_k b_k^\dagger b_k\,. \tag{7.150}$$

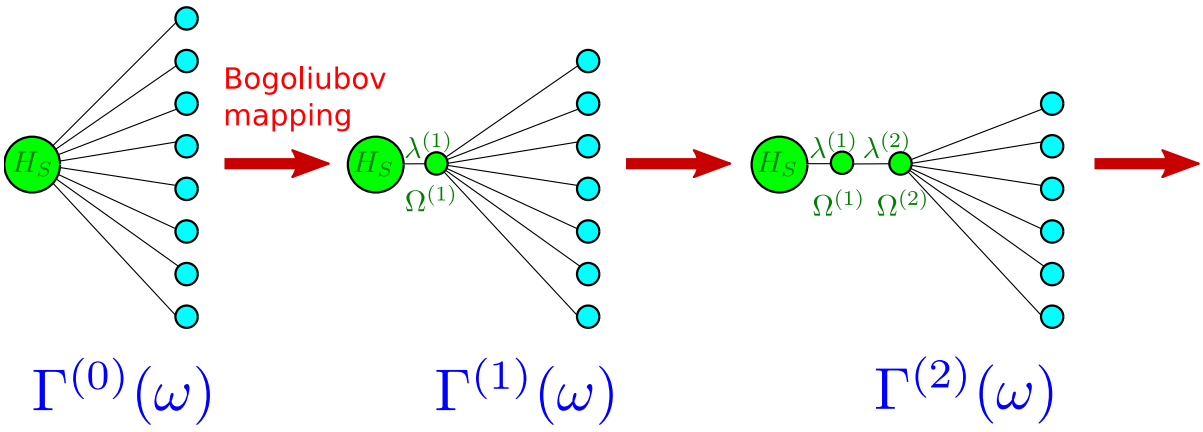

Figure 7.6: Sketch of the principle of Bogoliubov mappings to treat Non-Markovian system-reservoir interactions. Initially (left), the coupling between system and reservoir may not admit a Markovian treatment. Successive Bogoliubov transformations enable one to transfer degrees of freedom into the system, with the aim that the transformed coupling admits a Markovian treatment.

We will demonstrate that we can map this Hamiltonian into

$$\begin{aligned} H &= \frac{\omega}{2}\sigma^z + \sigma^x(\lambda a + \lambda^* a^\dagger) + \Omega a^\dagger a + \sum_{k>1}\left(H_k a a_k^\dagger + H_k^* a^\dagger a_k\right) + \sum_{k>1}\Omega_k a_k^\dagger a_k \\ &= \frac{\omega}{2}\sigma^z + |\lambda|\sigma^x(\tilde{a} + \tilde{a}^\dagger) + \Omega\tilde{a}^\dagger\tilde{a} + \sum_{k>1}\left(H_k\tilde{a}\tilde{a}_k^\dagger + H_k^*\tilde{a}^\dagger\tilde{a}_k\right) + \sum_{k>1}\Omega_k\tilde{a}_k^\dagger\tilde{a}_k\,. \end{aligned} \tag{7.151}$$

Here, we have in the last step only absorbed a phase in the bosonic operators of both supersystem and residual reservoir. This demonstrates that it completely suffices to consider $\lambda > 0$, i.e., its phase does not contain any physics in case of a single terminal.

The Bogoliubov transform simply maps to a new set of bosonic annihilation and creation operators. Mathematically, it can be written with a priori unknown coefficients $u_{kk'}$ as

$$b_k = u_{k1}a + \sum_{q>1} u_{kq}a_q\,, \tag{7.152}$$

and similarly for the creation operators. Here, we have split the first mode (later-on interpreted as reaction coordinate) from the others (the residual oscillators) also in notation, since the reaction coordinate will be treated as part of the system. The fact that the transformed operators have to obey bosonic commutation relations leads to the requirement

$$\delta_{kk'} = u_{k1}u_{k'1}^* + \sum_{q>1} u_{kq}u_{k'q}^*\,, \tag{7.153}$$

i.e., the transformation needs to be unitary. However, in addition we demand that this transformation maps the Hamiltonian into the simpler form of Eq. (7.151). This leads to additional equations. In particular, the constraint that $\sum_k(h_k b_k + h_k^* b_k^\dagger) = \lambda a + \lambda^* a^\dagger$ can be fulfilled by the equations

$$\begin{aligned} 0 &= \sum_k u_{kq}h_k\,, \qquad \forall q > 1\,, \\ \lambda &= \sum_k u_{k1}h_k\,. \end{aligned} \tag{7.154}$$

Finally, we have to fulfil the constraint $\sum_k \omega_k b_k^\dagger b_k = \Omega a^\dagger a + \sum_{q>1}(H_q a a_q^\dagger + H_q^* a^\dagger a_q) + \sum_{q>1}\Omega_q a_q^\dagger a_q$. This yields the equations

$$\begin{aligned} \Omega &= \sum_k \omega_k |u_{k1}|^2 \,, \\ \delta_{qq'}\Omega_q &= \sum_k \omega_k u_{kq}^* u_{kq'} \qquad \forall q, q' > 1 \,, \\ H_q &= \sum_k \omega_k u_{k1} u_{kq}^* \qquad \forall q > 1 \,. \end{aligned} \tag{7.155}$$

However, since we do not demand specific values for λ, Ω, and H_q, the three equations do not represent constraints but rather link the parameters of the transformed model with the original ones.

The only constraints to be fulfilled are therefore

$$\begin{aligned} 0 &= \sum_k u_{kq} h_k \,, \qquad \forall q > 1 \,, \\ \delta_{qq'}\Omega_q &= \sum_k \omega_k u_{kq}^* u_{kq'} \qquad \forall q, q' > 1 \,, \end{aligned} \tag{7.156}$$

where we have to demand that $\Omega_q \geq 0$ to ensure for thermodynamic stability. We will argue that such a solution will always exist. Arranging the elements of the original coupling and of the unknown coefficients in vectors

$$|h\rangle = \frac{1}{\sqrt{\sum_k |h_k|^2}} \begin{pmatrix} h_1^* \\ \vdots \\ h_K^* \end{pmatrix} \,, \qquad |u_q\rangle = \begin{pmatrix} u_{1q} \\ \vdots \\ u_{Kq} \end{pmatrix} \,, \tag{7.157}$$

we see that the first relation can be written as an orthogonality constraint of the form $\langle h|u_q\rangle = 0$ for $q > 1$. The second equation looks like an orthogonality relation between eigenvectors, except that the additional orthogonality constraint has to be respected. We can therefore fulfil both equations by defining the $|u_q\rangle$ as the eigenvectors of a matrix

$$\begin{aligned} H_{\text{eff}} |u_q\rangle &= \Omega_q |u_q\rangle \,, \\ H_{\text{eff}} &= (\mathbf{1} - |h\rangle\langle h|) \begin{pmatrix} \omega_1 & & \\ & \ddots & \\ & & \omega_K \end{pmatrix} (\mathbf{1} - |h\rangle\langle h|) \,. \end{aligned} \tag{7.158}$$

This matrix is hermitian and has thus real eigenvalues. Furthermore, its eigenvalues are non-negative, as it is obtained from a projection of a positive definite matrix. Of course, also the unitarity of the transformation is then respected. Clearly, the first eigenvector with eigenvalue $\Omega_1 = 0$ is $|u_1\rangle = |h\rangle$. Such transformations rather serve as proof-of-principle here, since one will in practice rather be interested in the continuum limit, where the explicit numerical diagonalizion becomes intractable.

However, even in the continuum limit we can determine the parameters of the supersystem without explicit numerical diagonalization, i.e., solely from knowing the spectral density of the

original model

$$\begin{aligned} |\lambda|^2 &= \sum_k |h_k|^2 \to \frac{1}{2\pi}\int \Gamma^{(0)}(\omega)d\omega\,, \\ \Omega &= \sum_k \omega_k |u_{k1}|^2 = \sum_k \omega_k \frac{|h_k|^2}{\sum_{k'}|h_{k'}|^2} = \frac{\sum_k \omega_k |h_k|^2}{|\lambda|^2} \to \frac{\frac{1}{2\pi}\int \omega\Gamma^{(0)}(\omega)d\omega}{\frac{1}{2\pi}\int \Gamma^{(0)}(\omega)d\omega}\,. \end{aligned} \tag{7.159}$$

We note that these two relations must generally hold for unitary transformations of the form $b_k = \sum_{k'} u_{kk'} a_{k'}$ (tacitly identifying $b_1 = b$). The first ist just a consequence of $[b, b^\dagger] = 1$, whereas the second follows from inverting the transformation and comparing the reservoir Hamiltonian. Also in case of fermions they hold correspondingly. It remains to relate the spectral density of the transformed model with the original spectral density.

7.6.3 Mappings for continuous reservoirs

Initial mapping for bosonic reservoirs

The general starting point is the Hamiltonian

$$H = H_S + S \otimes \sum_k \left(h_k a_k + h_k^* a_k^\dagger \right) + \sum_k \omega_k a_k^\dagger a_k\,, \tag{7.160}$$

where H_S is an arbitrary system Hamiltonian (containing e.g. interactions etc.), and $S = S^\dagger$ is a hermitian operator that acts exclusively in the Hilbert space of the system. In contrast, the a_k are bosonic annihilation operators annihilating mode k in the reservoir with energy ω_k and emission amplitude h_k. The Heisenberg equations of motion tell us

$$\begin{aligned} \dot{A} &= \mathrm{i}[H_S, A] + \mathrm{i}[S, A] \otimes \sum_k \left(h_k a_k + h_k^* a_k^\dagger \right) \equiv \mathrm{i}S_1 + \mathrm{i}S_2 \otimes \sum_k \left(h_k a_k + h_k^* a_k^\dagger \right)\,, \\ \dot{a}_k &= -\mathrm{i}\omega_k a_k - \mathrm{i}h_k^* S\,. \end{aligned} \tag{7.161}$$

The equation for the reservoir creation operators can be obtained by hermitian conjugation. We introduce the Fourier-transformed operators (this has technically the advantage that we need not deal with initial conditions)

$$a_k(z) = \int a_k(t) e^{+\mathrm{i}zt} dt \qquad : \qquad \Im z > 0\,, \tag{7.162}$$

and similar for all system operators. Note however that we follow the convention to introduce the same transformation for annihilation and creation operators, which means that in the following, when transferring results from annihilation operators towards creation operators, For a product of two operators we will then encounter a convolution

$$\int f(t)g(t)e^{+\mathrm{i}zt}dt = \frac{1}{2\pi}\int f(z')g(z-z')dz'\,, \tag{7.163}$$

which in the equations of motion then implies

$$\begin{aligned} \mathrm{i}zA(z) &= \mathrm{i}S_1(z) + \mathrm{i}\frac{1}{2\pi}\int S_2(z') \otimes \sum_k \left(h_k a_k(z-z') + h_k^* a_k^\dagger(z-z') \right) dz'\,, \\ \mathrm{i}z a_k(z) &= -\mathrm{i}\omega_k a_k(z) - \mathrm{i}h_k^* S(z)\,. \end{aligned} \tag{7.164}$$

Solving the second equation for $a_k(z) = \frac{-h_k^*}{z+\omega_k} S(z)$, and similarly for the creation operator $a_k^\dagger(z) = \frac{-h_k}{z+\omega_k} S(z)$ and inserting this in the first equation we get an equation valid for the system only

$$\begin{aligned} zA(z) &= S_1(z) - \frac{1}{2\pi}\int S_2(z')\sum_k \left(\frac{|h_k|^2}{z-z'+\omega_k} + \frac{|h_k|^2}{z-z'+\omega_k}\right) S(z-z')dz' \\ &= S_1(z) - \frac{1}{2\pi}\int S_2(z')\frac{1}{\pi}\int d\omega \left(\frac{\Gamma^{(0)}(\omega)}{z-z'+\omega}\right) S(z-z')dz' \\ &= S_1(z) - \frac{1}{2\pi}\int S_2(z')W^{(0)}(z'-z)S(z-z')dz' \,. \end{aligned} \tag{7.165}$$

In the last step, we have introduced the Cauchy-Hilbert transform of the spectral coupling density

$$W^{(n)}(z) = \frac{1}{\pi}\int \frac{\Gamma^{(n)}(\omega)}{\omega - z} d\omega \,. \tag{7.166}$$

Here, the index denotes the particular spectral coupling density, i.e., in our case $\Gamma^{(0)}(\omega) = 2\pi\sum_k |h_k|^2 \delta(\omega - \omega_k^0)$. The Cauchy-Hilbert transform can be inverted by performing a limit

$$\lim_{\epsilon\to 0^+} \Im W^{(n)}(\omega + \mathrm{i}\epsilon) = \frac{1}{\pi}\lim_{\epsilon\to 0^+}\int \frac{\Gamma^{(n)}(\omega')\epsilon}{(\omega'-\omega)^2+\epsilon^2} d\omega' = \Gamma^{(n)}(\omega) \,. \tag{7.167}$$

We will not solve the equation (7.165), not even knowing what the actual operators $S_1(z)$ and $S_2(z)$ are in our specific case.

Instead, we use that we can use that with our unitary mapping our Hamiltonian can be written as

$$H = H_S + \lambda S(b + b^\dagger) + \Omega b^\dagger b + \sum_k \left(H_k^* b b_k^\dagger + H_k b^\dagger b_k\right) + \sum_k \Omega_k b_k^\dagger b_k \,. \tag{7.168}$$

Here, H_S and S are the same operators as before, but b now annihilates a boson on the supersystem (composed now of system and **collective** or **reaction** coordinate) with new reaction coordinate energy Ω and supersystem-internal coupling λ. In particular, since we include the reaction coordinate dynamics into the system, one can treat the strong-coupling limit at the price of increasing the system dimension (which is strictly-speaking infinite in case of bosons). Furthermore, the b_k denote the modes of the **residual bath**, with transformed emission and absorbtion amplitudes H_k and renormalized energies Ω_k. We again derive the equations of motion in the Heisenberg picture

$$\begin{aligned} \dot{A} &= \mathrm{i}[H_S, A] + \mathrm{i}\lambda[S, A](b + b^\dagger) \equiv \mathrm{i}S_1 + \mathrm{i}S_2(b + b^\dagger) \,, \\ \dot{b} &= -\mathrm{i}\lambda S - \mathrm{i}\Omega b - \mathrm{i}\sum_k H_k b_k \,, \\ \dot{b}_k &= -\mathrm{i}H_k^* b - \mathrm{i}\Omega_k b_k \,. \end{aligned} \tag{7.169}$$

We apply the same Fourier transform, yielding

$$\begin{aligned} \mathrm{i}zA(z) &= \mathrm{i}S_1(z) + \frac{\mathrm{i}}{2\pi}\int S_2(z')\lambda\left[b(z-z') + b^\dagger(z-z')\right]dz' \,, \\ \mathrm{i}zb(z) &= -\mathrm{i}\lambda S(z) - \mathrm{i}\Omega b(z) - \mathrm{i}\sum_k H_k b_k(z) \,, \\ \mathrm{i}zb_k(z) &= -\mathrm{i}H_k^* b(z) - \mathrm{i}\Omega_k b_k(z) \,. \end{aligned} \tag{7.170}$$

We can solve the last equation

$$b_k(z) = \frac{-H_k^*}{z+\Omega_k} b(z) \tag{7.171}$$

and insert it in the second

$$zb(z) = -\lambda S(z) - \Omega b(z) + \sum_k \frac{|H_k|^2}{z+\Omega_k} b(z)\,, \tag{7.172}$$

which yields the solution

$$b(z) = \frac{-\lambda}{z+\Omega-\sum_k \frac{|H_k|^2}{z+\Omega_k}} S(z)\,. \tag{7.173}$$

With this solution, we eventually reconsider the first equation

$$\begin{aligned} zA(z) &= S_1(z) - \frac{1}{2\pi}\int S_2(z')2\left(\frac{\lambda^2}{z-z'+\Omega-\sum_k \frac{|H_k|^2}{z-z'+\Omega_k}}\right) S(z-z')dz' \\ &= S_1(z) - \frac{1}{2\pi}\int S_2(z')2\left(\frac{\lambda^2}{z-z'+\Omega-\frac{1}{2}W^{(1)}(z'-z)}\right) S(z-z')dz'\,. \end{aligned} \tag{7.174}$$

Comparing Eq. (7.174) with Eq. (7.165), we conclude

$$2\frac{\lambda^2}{\Omega-(z'-z)-\frac{1}{2}W^{(1)}(z'-z)} = W^{(0)}(z'-z)\,. \tag{7.175}$$

We solve this for

$$W^{(1)}(z) = 2\Omega - 2z - 4\frac{\lambda^2}{W^{(0)}(z)}\,, \tag{7.176}$$

and subsequently evaluate its imaginary part at $z = \omega + \mathrm{i}\epsilon$

$$\begin{aligned} \Gamma^{(1)}(\omega) &= \lim_{\epsilon\to 0^+} \Im W^{(1)}(\omega+\mathrm{i}\epsilon) = -4\lambda^2 \lim_{\epsilon\to 0^+} \Im \frac{1}{W^{(0)}(\omega+\mathrm{i}\epsilon)} \\ &= +4\lambda^2 \lim_{\epsilon\to 0^+} \frac{\Im W^{(0)}(\omega+\mathrm{i}\epsilon)}{|W^{(0)}(\omega+\mathrm{i}\epsilon)|^2} = 4\lambda^2 \frac{\Gamma^{(0)}(\omega)}{|W^{(0)}(\omega)|^2}\,. \end{aligned} \tag{7.177}$$

Therefore, to compute the spectral coupling density of the transformed Hamiltonian, we need to compute the Cauchy-Fourier transform of the old spectral density

$$\begin{aligned} \lim_{\epsilon\to 0^+} \left|W^{(n)}(\omega+\mathrm{i}\epsilon)\right|^2 &= \lim_{\epsilon\to 0^+} \left|\frac{1}{\pi}\int \frac{\Gamma^{(n)}(\omega')}{\omega'-\omega-\mathrm{i}\epsilon} d\omega'\right|^2 \\ &= \left[\frac{1}{\pi}\mathcal{P}\int \frac{\Gamma^{(n)}(\omega')}{\omega'-\omega} d\omega'\right]^2 + \left[\Gamma^{(n)}(\omega)\right]^2\,, \end{aligned} \tag{7.178}$$

where $\mathcal{P}$ denotes the Cauchy principal value. Altogether, we therefore obtain the mapping

$$\Gamma^{(1)}(\omega) = \frac{4\lambda^2\Gamma^{(0)}(\omega)}{\left[\frac{1}{\pi}\mathcal{P}\int \frac{\Gamma^{(0)}(\omega')}{\omega'-\omega} d\omega'\right]^2 + \left[\Gamma^{(0)}(\omega)\right]^2}\,. \tag{7.179}$$

The clear advantage is that we can now only use complex calculus to evaluate the next spectral coupling density from an old one.

Mapping for particle-conserving bosonic Hamiltonians

Let the mapping be given by

$$\begin{aligned} H &= H_S + a\sum_k h_k^* a_k^\dagger + a^\dagger \sum_k h_k a_k + \sum_k \omega_k a_k^\dagger a_k \\ &= H_S + \lambda^{(n)} a b^\dagger + \lambda^{(n)} a^\dagger b + \Omega^{(n)} b^\dagger b + b\sum_k H_k^* b_k^\dagger + b^\dagger \sum_k H_k b_k + \sum_k \Omega_k b_k^\dagger b_k \,. \end{aligned} \tag{7.180}$$

The Heisenberg equations become in the first representation

$$\dot{a} = \mathrm{i}[H_S, a] - \sum_k h_k a_k \equiv \mathrm{i}S_1 - \sum_k h_k a_k \,, \qquad \dot{a}_k = -\mathrm{i}h_k^* a - \mathrm{i}\omega_k a_k \,, \tag{7.181}$$

which upon Fourier-transformation, solving for the reservoir-mode and re-insertion into the first equation yields

$$z a(z) = S_1(z) + \frac{1}{2} W^{(n)}(-z) a(z) \,. \tag{7.182}$$

Similarly, the Heisenberg equations in the second representation read

$$\begin{aligned} \dot{a} &= \mathrm{i}[H_S, a] - \mathrm{i}\lambda^{(n)} b \equiv \mathrm{i}S_1 - \mathrm{i}\lambda^{(n)} b \,, \qquad \dot{b} = -\mathrm{i}\lambda^{(n)} a - \mathrm{i}\Omega^{(n)} b - \mathrm{i}\sum_k H_k b_k \,, \\ \dot{b}_k &= -\mathrm{i}H_k^* b - \mathrm{i}\Omega_k b_k \,. \end{aligned} \tag{7.183}$$

Upon Fourier-transforming, solving iteratively the last two equations and plugging the result into the first, we arrive at

$$z a(z) = S_1(z) + \frac{\left(\lambda^{(n)}\right)^2}{z + \Omega^{(n)} - \frac{1}{2} W^{(n+1)}(-z)} a(z) \,, \tag{7.184}$$

and comparing with the equation we had before we can again conclude that

$$\frac{1}{2} W^{(n)}(-z) = \frac{\left(\lambda^{(n)}\right)^2}{z + \Omega^{(n)} - \frac{1}{2} W^{(n+1)}(-z)} \,. \tag{7.185}$$

This is precisely the same relation we had before, such that the recursion relations for the spectral for the spectral densities

$$\Gamma^{(n)}(\omega) = 2\pi \sum_k |h_k|^2 \delta(\omega - \omega_k) \,, \qquad \Gamma^{(n+1)}(\omega) = 2\pi \sum_k |H_k|^2 \delta(\omega - \omega_k) \,, \tag{7.186}$$

and the renormalized coupling λ_n as well as the renormalized energy Ω_n the following relations hold

$$\begin{aligned} \lambda_n^2 &= \frac{1}{2\pi} \int \Gamma^{(n)}(\omega) d\omega \,, \qquad \Omega^n = \frac{1}{2\pi\lambda^2} \int \omega \Gamma^{(n)}(\omega) d\omega \,, \\ \Gamma^{(n+1)}(\omega) &= \frac{4\lambda_n^2 \Gamma^{(n)}(\omega)}{\left[\frac{1}{\pi}\mathcal{P}\int \frac{\Gamma^{(n)}(\omega')}{\omega' - \omega} d\omega'\right]^2 + \left[\Gamma^{(n)}(\omega)\right]^2} \,. \end{aligned} \tag{7.187}$$

The convergence properties of related recursion relations have been discussed in great detail [43].

The difference with the previous treatment is that the structure of the Hamiltonian (bosonic tunneling) is similar before and after the transformation, we just need to redefine system and reservoir. Therefore, it can be applied recursively. This way, we can understand Fig. 7.6 as the sequential application of multiple Bogoliubov transformations. However, this would in general be too tedious. Therefore, one would in practice prefer to truncate the resulting chain at some point, using a perturbative approach such as e.g. based on the master equation.

Mapping for fermionic tunneling Hamiltonians

For fermions everything works just as for bosons, we just replace in typical notation $h_k \to t_k$ and $H_k \to T_k$, but the same recursion relations and mappings hold. This can be easily understood as the equations of motions are for non-interacting fermions equivalent (up to a sign change in the amplitudes) as for non-interacting bosons. Using fermionic reaction coordinates has, however the clear advantage, that with an additional fermionic reaction coordinate, the dimension of the supersystem Hilbert space just doubles, whereas for bosons it is multiplied by infinity.

General properties of the recursion relations

We summarize that the recursion relations are valid for quite general bosonic and fermionic models that are linear in the bosonic and fermionic reservoir operators and which are mapped in to chains for particle-number-conserving hopping Hamiltonians.

Def. 23 (Martinazzo recursion relations)**.** *The couplings, energies, and spectral coupling densities transfer according to*

$$\begin{aligned} (\lambda^{(n)})^2 &= \frac{1}{2\pi}\int \Gamma^{(n)}(\omega)d\omega\,, \qquad \Omega^{(n)} = \frac{1}{2\pi(\lambda^{(n)})^2}\int \omega\Gamma^{(n)}(\omega)d\omega\,, \\ \Gamma^{(n+1)}(\omega) &= \frac{4\lambda_n^2\Gamma^{(n)}(\omega)}{\left[\frac{1}{\pi}\mathcal{P}\int\frac{\Gamma^{(n)}(\omega')}{\omega'-\omega}d\omega'\right]^2 + [\Gamma^{(n)}(\omega)]^2}\,. \end{aligned} \tag{7.188}$$

Table 7.1 provides some examples of spectral densities and their mappings. The functional form of the mapping implies that a hard cutoff will reproduce itself, such that convergence of all integrals is ensured. In particular, the last entry in Tab. 7.1 demonstrates that the limiting case of a semicircle

$$\Gamma^{(\infty)}(\omega) = \delta\sqrt{1-\left(\frac{\omega}{\delta}-\frac{\epsilon}{\delta}\right)^2}\Theta(\omega,\epsilon-\delta,\epsilon+\delta) \tag{7.189}$$

is a stationary point for mappings with a rigid cutoff. In contrast, the mapping suggested in Ref. [43] maps bosonic chains to a sequence of $x-x$ couplings, and the recursion relations are only formally similar, such that also the stationary spectral density is different.

7.6.4 General Properties: Stationary state of the supersystem

In the strong-coupling limit, we will no longer expect the local Gibbs state $e^{-\beta H_S}/Z_S$ to be the stationary state of the system. Rather, one will expect it to be given by the reduced density matrix

$\Gamma^{(n)}(\omega)$	$(\lambda^{(n)})^2$	$\Omega^{(n)}$	$\Gamma^{(n+1)}(\omega)$
$\Gamma\frac{\delta^2}{(\omega-\epsilon)^2+\delta^2}$	$\frac{\Gamma\delta}{2}$	ϵ	2δ
$\Gamma\frac{\delta^4}{[(\omega-\epsilon)^2+\delta^2]^2}$	$\frac{\Gamma\delta}{4}$	ϵ	$\frac{\delta(2\delta)^2}{(\omega-\epsilon)^2+(2\delta)^2}$
$\Gamma e^{-\frac{(\omega-\epsilon)^2}{\delta^2}}$	$\frac{\Gamma\delta}{2\sqrt{\pi}}$	ϵ	$\frac{2\delta e^{+\frac{(\omega-\epsilon)^2}{\delta^2}}}{\sqrt{\pi}\left[1-\mathrm{erf}^2\left(\mathrm{i}\frac{\omega-\epsilon}{\delta}\right)\right]}$
$\Gamma\Theta(\omega,\epsilon-\delta,\epsilon+\delta)$	$\frac{\Gamma\delta}{\pi}$	ϵ	$\frac{4\pi\delta}{\pi^2+4\mathrm{arctanh}^2\left(\frac{\epsilon-\omega}{\delta}\right)}\Theta(\omega,\epsilon-\delta,\epsilon+\delta)$
$\Gamma\left[1-\left(\frac{\omega}{\delta}-\frac{\epsilon}{\delta}\right)^2\right]\Theta(\omega,\epsilon-\delta,\epsilon+\delta)$	$\frac{2}{3}\frac{\Gamma\delta}{\pi}$	ϵ	$\frac{8\delta}{3\pi}\frac{1-\frac{(\omega-\epsilon)^2}{\delta^2}}{\frac{4\left(\delta(\omega-\epsilon)-(\omega+\delta-\epsilon)(\omega-\delta-\epsilon)\mathrm{arctanh}\left[\frac{\omega-\epsilon}{\delta}\right]\right)^2}{\pi^2\delta^4}+\left(1-\frac{(\omega-\epsilon)^2}{\delta^2}\right)^2}$
$\Gamma\sqrt{1-\left(\frac{\omega}{\delta}-\frac{\epsilon}{\delta}\right)^2}\Theta(\omega,\epsilon-\delta,\epsilon+\delta)$	$\frac{\Gamma\delta}{4}$	ϵ	$\delta\sqrt{1-\left(\frac{\omega}{\delta}-\frac{\epsilon}{\delta}\right)^2}\Theta(\omega,\epsilon-\delta,\epsilon+\delta)$

Table 7.1: Selected mappings for spectral densities, using $\Theta(x,a,b)=\Theta(x-a)\Theta(b-x)$ and $\mathrm{erf}(z)=\frac{2}{\sqrt{\pi}}\int_0^z e^{-t^2}dt$. As a rule of thumb, the width of the old density becomes the coupling strength of the new density, and only a hard cutoff will survive recursive transformations.

of the total Gibbs state

$$\bar{\rho}\approx \mathrm{Tr_B}\left\{\frac{e^{-\beta(H_S+H_B+H_I)}}{Z}\right\}, \tag{7.190}$$

which only when $H_I\to 0$ would coincide with the system-local Gibbs state. Since the reaction-coordinate mappings allow to to to arbitrarily strong coupling as long as the coupling between supersystem and residual reservoir is small, we can test whether the resulting stationary state in the supersystem is consistent with these assumptions.

When we apply the master equation formalism to the supersystem

$$H'_S=H_S+H_{RC}+H_{S,RC}\,, \tag{7.191}$$

composed of system and reaction coordinate, we know that for a single reservoir, the stationary state will approach the Gibbs state associated with the supersystem

$$\bar{\rho}'_S=\frac{e^{-\beta H'_S}}{\mathrm{Tr_{S,RC}}\left\{e^{-\beta H'_S}\right\}}\,. \tag{7.192}$$

We define a Hamiltonian of mean force

$$H^*=-\frac{1}{\beta}\ln\left(\frac{\mathrm{Tr_B}\left\{e^{-\beta(H_S+H_I+H_B)}\right\}}{\mathrm{Tr_B}\left\{e^{-\beta H_B}\right\}}\right). \tag{7.193}$$

It can be seen as an effective Hamiltonian for the system in the strong coupling limit. In the weak-coupling limit ($H_I\to 0$), we would get $H^*\to H_S$. By construction, the Hamiltonian of mean force obeys

$$\begin{aligned} e^{-\beta H^*} &= \frac{\mathrm{Tr_B}\left\{e^{-\beta(H_S+H_I+H_B)}\right\}}{\mathrm{Tr_B}\left\{e^{-\beta H_B}\right\}}=\frac{\mathrm{Tr_{RC,B'}}\left\{e^{-\beta(H'_S+H'_I+H'_B)}\right\}}{\mathrm{Tr_{RC,B'}}\left\{e^{-\beta(H_{RC}+H'_I+H'_B)}\right\}} \\ &\overset{H'_I\to 0}{\approx} \frac{\mathrm{Tr_{RC}}\left\{e^{-\beta H'_S}\right\}}{\mathrm{Tr_{RC}}\left\{e^{-\beta H_{RC}}\right\}}\,. \end{aligned} \tag{7.194}$$

This implies that the reduced steady state becomes

$$\bar{\rho}_S=\mathrm{Tr_{RC}}\left\{\bar{\rho}'_S\right\}=\frac{\mathrm{Tr_{RC}}\left\{e^{-\beta H'_S}\right\}}{\mathrm{Tr_{S,RC}}\left\{e^{-\beta H'_S}\right\}}\approx\frac{e^{\beta H^*}\mathrm{Tr_{RC}}\left\{e^{-\beta H_{RC}}\right\}}{\mathrm{Tr_{S,RC}}\left\{e^{-\beta H'_S}\right\}}=\frac{e^{\beta H^*}}{\mathrm{Tr}\left\{e^{\beta H^*}\right\}}\,. \tag{7.195}$$

7.6.5 Example: Single-Electron Transistor

According to the results of the previous section, the Hamiltonian for the SET

$$H = \epsilon d^\dagger d + \sum_\nu \sum_k \left(t_{k\nu} d c_{k\nu}^\dagger + t_{k\nu}^* c_{k\nu} d^\dagger \right) + \sum_\nu \sum_k \epsilon_{k\nu} c_{k\nu}^\dagger c_{k\nu} \,, \tag{7.196}$$

in addition characterized by a Lorentzian spectral coupling density

$$\Gamma_\nu^{(0)}(\omega) = 2\pi \sum_k |t_{k\nu}|^2 \delta(\omega - \epsilon_{k\nu}) = \frac{\Gamma_\nu \delta_\nu^2}{(\omega - \epsilon_\nu)^2 + \delta_\nu^2} \tag{7.197}$$

can therefore be mapped to a triple-quantum dot that is coupled to two leads (we introduce a separate reaction coordinate for each reservoir)

$$\begin{aligned} H &= \epsilon_L d_L^\dagger d_L + \epsilon d^\dagger d + \epsilon_R d_R^\dagger d_R + \sqrt{\frac{\Gamma_L \delta_L}{2}} \left(d d_L^\dagger + d_L d^\dagger \right) + \sqrt{\frac{\Gamma_R \delta_R}{2}} \left(d d_R^\dagger + d_R d^\dagger \right) \\ &\quad + \sum_\nu \sum_k \left(T_{k\nu} d_\nu d_{k\nu}^\dagger + T_{k\nu}^* d_{k\nu} d_\nu^\dagger \right) + \sum_\nu \sum_k \Omega_{k\nu} d_{k\nu}^\dagger d_{k\nu} \,. \end{aligned} \tag{7.198}$$

This second Hamiltonian is parametrized by the transformed spectral density

$$\Gamma_\nu^{(1)}(\omega) = 2\pi \sum_k |T_{k\nu}|^2 \delta(\omega - \Omega_{k\nu}) = 2\delta_\nu \,, \tag{7.199}$$

compare Tab. 7.1.

We can now treat the triple quantum dot as a system and apply the master equation formalism, provided that $\beta_\nu \delta_\nu \ll 1$. For a nonvanishing potential (or thermal) bias, we can compare the current obtained from the master equation treatment with the energy current from the exact solution [27] (compare also Sec. 7.1).

$$\begin{aligned} I_{\mathrm{M}} &= \int_{-\infty}^{\infty} G_{\mathrm{C}}(\omega) \left[f_{\mathrm{L}}(\omega) - f_{\mathrm{R}}(\omega) \right] S_{\mathrm{C}}(\omega) d\omega \,, \\ I_{\mathrm{E}} &= \int_{-\infty}^{\infty} \omega \cdot G_{\mathrm{C}}(\omega) \left[f_{\mathrm{L}}(\omega) - f_{\mathrm{R}}(\omega) \right] S_{\mathrm{C}}(\omega) d\omega \,, \end{aligned} \tag{7.200}$$

with the factors

$$\begin{aligned} G_{\mathrm{C}}(\omega) &= \frac{\Gamma_L^{(0)}(\omega) \Gamma_R^{(0)}(\omega)}{\Gamma(\omega)} \,, \\ S_{\mathrm{C}}(\omega) &= \frac{1}{\pi} \frac{\Gamma(\omega)/2}{(\Gamma(\omega)/2)^2 + \left[\omega - \epsilon - \Sigma(\omega) \right]^2} \,, \end{aligned} \tag{7.201}$$

and where $\Gamma(\omega) = \Gamma_L^{(0)}(\omega) + \Gamma_R^{(0)}(\omega)$ and $\Sigma(\omega) = \Sigma_{\mathrm{L}}(\omega) + \Sigma_{\mathrm{R}}(\omega)$ and

$$\Sigma_\nu(\omega) = \frac{1}{2\pi} \mathcal{P} \int_{-\infty}^{\infty} \frac{\Gamma_\nu^{(0)}(\omega')}{\omega - \omega'} d\omega' = \frac{\Gamma_\nu \delta_\nu (\omega - \epsilon_\nu)}{2 \left((\omega - \epsilon_\nu)^2 + \delta_\nu^2 \right)} \tag{7.202}$$

denotes a small correction to the system energy level (Lamb-shift).

The dependence of the energy current versus coupling strength is depicted in Fig. 7.7. For weak coupling strengths, the current is approximately linear, which agrees well with the master equation result. However, for intermediate coupling strengths the exact solution shows a turnover and saturates at infinite coupling strength. We see that the Lindblad-type secular master equation for the triple quantum dot fails spectactularly in the weak-coupling limit, whereas the secular master equation for the single quantum dot fails in the intermediate and strong coupling limit. Without the secular approximation, the Born-Markov master equation for the triple quantum dot performs farely well (with and without including imaginary parts in the half-sided FTs of the correlation functions). The failure of the secular approximation master equation for the triple quantum dot can be understood as for weak coupling $\Gamma_\alpha \to 0$, the system Hamiltonian becomes near degenerate for $\epsilon_L = \epsilon_R = \epsilon$. Then, the secular approximation is invalid.

7.6.6 Example: Pure dephasing model

We consider as initial Hamiltonian the pure dephasing model

$$H = \frac{\omega}{2}\sigma^z + \sigma^z \sum_{k\geq 1}(h_k b_k + h_k^* b_k^\dagger) + \sum_{k\geq 1}\omega_k b_k^\dagger b_k \,. \tag{7.203}$$

We had derived the exact solution for the change in the reservoir energy before, compare Eq. (4.125)

$$\Delta E(t) = \sum_k \frac{|h_k|^2}{\omega_k} 2[1-\cos(\omega_k t)] \,. \tag{7.204}$$

The total energy radiated into the reservoir can then be written as

$$\Delta E = \lim_{t\to\infty}\frac{1}{\pi}\int \Gamma(\omega)\frac{1-\cos(\omega t)}{\omega}d\omega = \frac{1}{\pi}\int\frac{\Gamma(\omega)}{\omega}d\omega \,. \tag{7.205}$$

The transient energy current into the reservoir therefore becomes

$$I_E = \frac{d}{dt}\Delta E(t) = \sum_k |h_k|^2 2\sin(\omega_k t) = \frac{1}{\pi}\int \Gamma^{(0)}(\omega)\sin(\omega t)d\omega \,. \tag{7.206}$$

As long as the initial reservoir state is diagonal in the reservoir Hamiltonian, this does not depend on its other characteristics (such as, e.g., temperature), and it describes a genuine quantum contribution resulting from the initial energy content of the interaction.

Using a reaction coordinate, we can map the model into

$$\begin{aligned} H &= \frac{\omega}{2}\sigma^z + \lambda\sigma^z(a+a^\dagger) + \Omega a^\dagger a \\ &\quad + a\sum_k H_k a_k^\dagger + a^\dagger \sum_k H_K^* a_k + \sum_k \Omega_k a_k^\dagger a_k \,. \end{aligned} \tag{7.207}$$

From the good experience with a Lorentzian functions we also would like to consider a Lorentzian-type density, but for bosons have the additional constraint that the density should rise at least linearly near the origin. From subtracting the Lorentzian with an inverted frequency we arrive at the parametrization

$$\Gamma^{(0)}(\omega) = 4\Gamma\frac{\delta^2\epsilon\omega}{((\omega-\epsilon)^2+\delta^2)\,((\omega+\epsilon)^2+\delta^2)} \,, \tag{7.208}$$

which vanishes linearly at the origin, and ϵ and δ still approximately assume the role of a mean and width, respectively.

The exact solution for the current then becomes

$$I_E(t) = \Gamma\delta e^{-\delta t}\sin(\epsilon t)\,. \tag{7.209}$$

Similarly, the total radiated energy becomes

$$\Delta E = \frac{\Gamma\delta\epsilon}{\delta^2+\epsilon^2}\,. \tag{7.210}$$

We obtain for the renormalized parameters of the supersystem

$$\lambda^2 = \frac{\Gamma\delta}{\pi}\arctan\left(\frac{\epsilon}{\delta}\right)\,, \qquad \Omega = \frac{\epsilon}{\frac{2}{\pi}\arctan\left(\frac{\epsilon}{\delta}\right)}\,. \tag{7.211}$$

For $\epsilon \gg \delta$, we can approximate $\arctan\left(\frac{\epsilon}{\delta}\right) \to \pi/2$, and we recover relations very similar to the previous case. The new spectral coupling density has to be calculated using the Martinazzo recursion relation (7.188). For brevity, we do not state it explicitly here, but again it vanishes linearly at $\Gamma^{(1)}(0) = 0$, and its height is now roughly controlled by δ and its width by ϵ.

We can now apply a master equation treatment for the system plus reaction coodinate, and compute the expectation value of the interaction energy

$$\Delta E_{\mathrm{i}}(t) = -\left\langle \lambda\sigma^z(a+a^\dagger)\right\rangle \tag{7.212}$$

between original system and reaction coordinate. Since this part of the Hamiltonian corresponds to the interaction Hamiltonian of the original model

$$\lambda\sigma^z(a+a^\dagger) = \sigma^z\sum_{k\geq 1}(h_k b_k + h_k^* b_k^\dagger)\,, \tag{7.213}$$

and the energy of the spin system does not change, it precisely corresponds to the energy radiated into the reservoir. However, we have to take care that the initial state of the spin and of the boson factorize

$$\rho'^0_S = \rho^0_S \otimes \rho^0_{RC}\,. \tag{7.214}$$

Furthermore, we have to fix the initial state of the reaction coordinate. In the regime where the master equation treatment of the supersystem is applicable, a reasonable choice is

$$\rho'^0_S = \rho^0_S \otimes \frac{e^{-\beta\Omega a^\dagger a}}{\mathrm{Tr}_{\mathrm{RC}}\left\{e^{-\beta\Omega a^\dagger a}\right\}}\,. \tag{7.215}$$

Finally, simulation of a bosonic quantum system within a Fock space representation requires a cutoff in the maximum number of bosonic quanta. Care should be taken that the bosonic cutoff is large enough by checking convergence of the results. Then, the RC method approaches the exact result pretty well. As sanity check, one can confirm that the solution does not depend on the initial state of the spin and not on the actual value of the initial temperature of the reaction coordinate.

In particular, we see in Fig. 7.8 that the oscillation frequency and amplitude of the exact solution is well reproduced by the RC method. We see that at short times the Lamb-shift is completely negligible, but at large times, keeping it, does improve the quality of the solution to an extent that it can hardly be distinguished from the exact result.

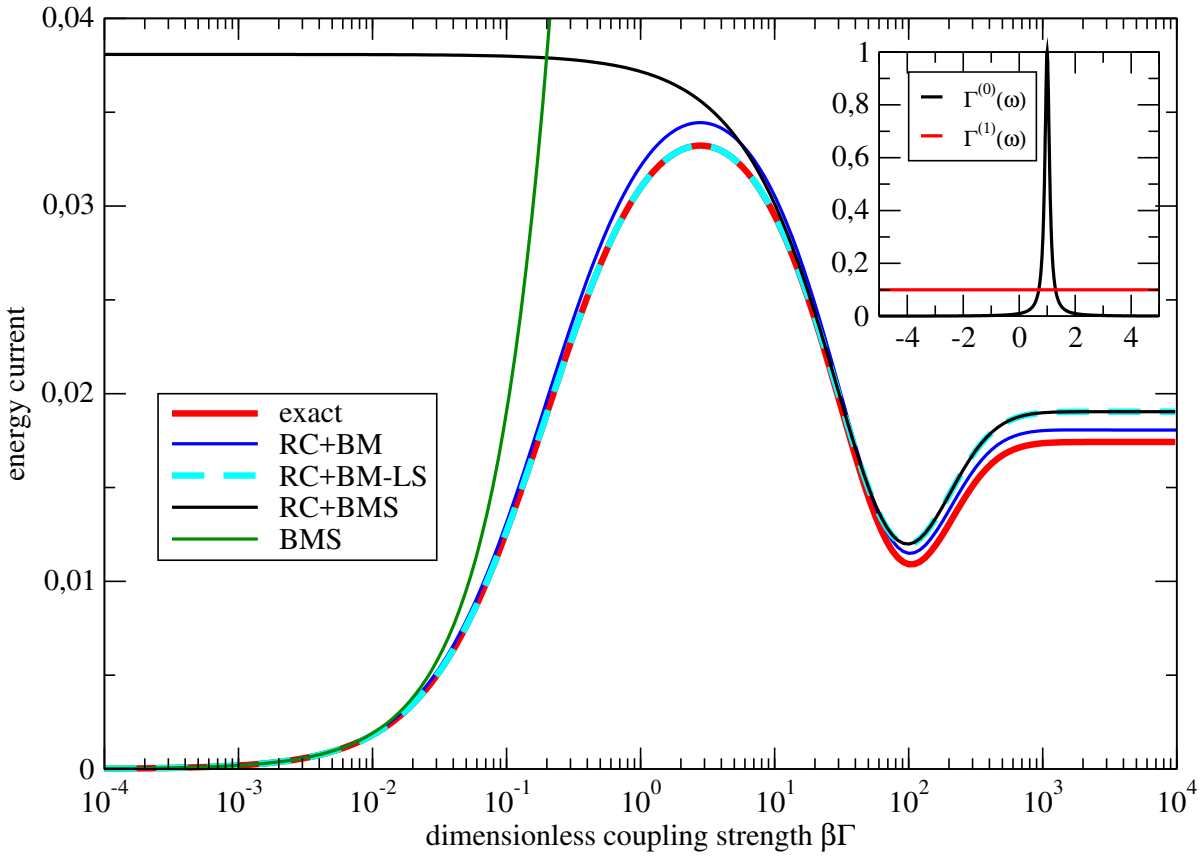

Figure 7.7: Plot of the energy currents computed using the naive secular master equation approach for the single dot (green), the exact solution (7.200) (red), the Born-Markov-Secular master equation for the triple quantum dot (black), and the Born-Markov master equation for the triple quantum dot (dark and light blue). In the strong-coupling limit, all triple quantum dot methods perform very well, where the naive master equation for the single dot fails completely. However, the secular approximation also predicts finite currents at vanishing coupling, which is nonsense. This results from the secular approximation, which becomes invalid in this regime. The Born-Markov approach does not have this problem (but does not guarantee a strictly positive definite density matrix or strictly consistent thermodynamics as it is not of Lindblad form). Finally, the dashed curve displays the result when the imaginary part of the half-sided FT's is just neglected. Parameters $\Gamma_L = \Gamma_R = \Gamma$, $\delta_L = \delta_R = 0.1$, $\epsilon_L = \epsilon_R = \epsilon = 1.0$, $\beta_L = \beta_R = 1.0$, $\mu_L = +1.0 = -\mu_R$.

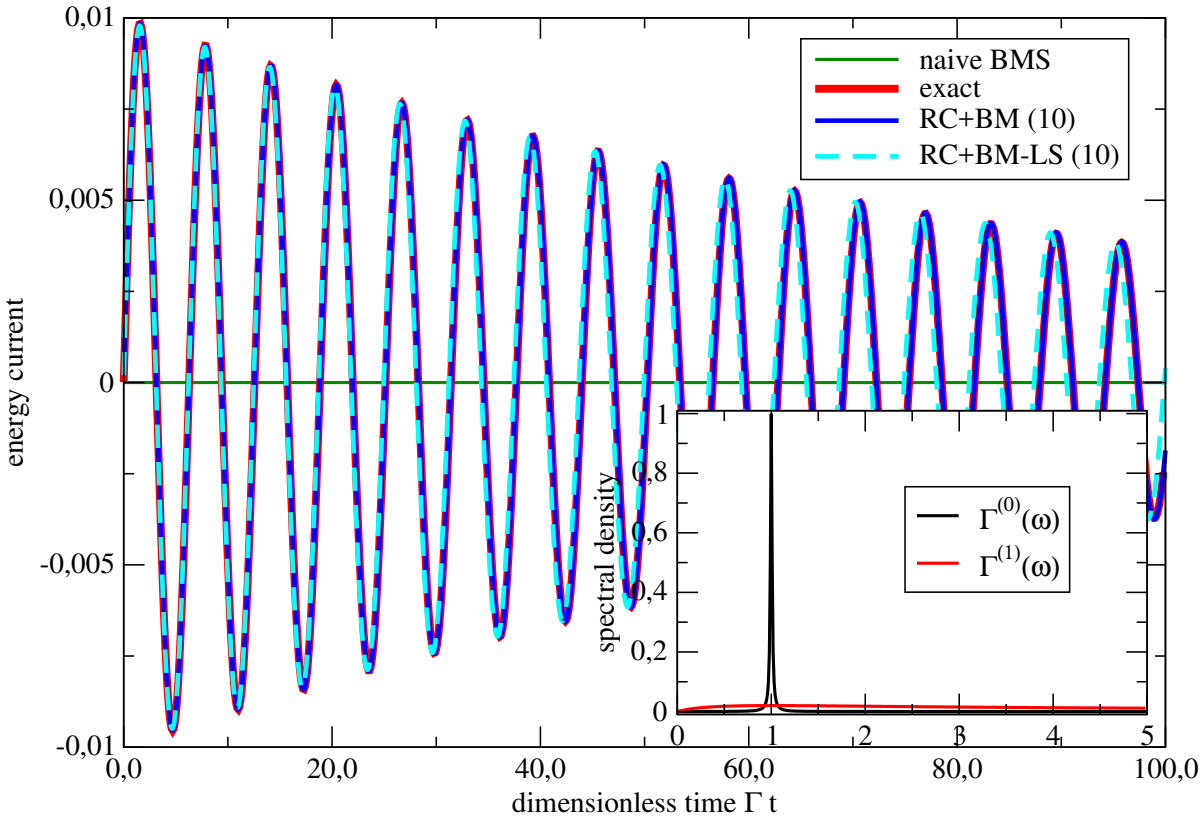

Figure 7.8: Plot of the time-dependent energy current entering the reservoir for the pure dephasing model. The RC method captures the initial phase quite well. Parameters: $\Gamma = 1$, $\delta = 0.01$, $\epsilon = 1$, $\beta = 100$, $\omega = 1$, $N_{\text{cut}} = 10$ ($N_{\text{cut}} = 15$ yields identical results).

Chapter 8

Selected nonequilibrium phenomena

8.1 The quantum Ising model in a transverse field

The quantum Ising chain in a transverse field for N spins

$$\mathcal{H}_{\mathrm{S}} = -g\sum_{i=1}^{N}\sigma_i^x - J\sum_{i=1}^{N}\sigma_i^z\sigma_{i+1}^z\,, \tag{8.1}$$

where g describes the coupling to an external magnetic field, J the inter-chain coupling to nearest neighbors, and periodic boundary conditions are assumed $\sigma_{N+1}^z \equiv \sigma_1^z$ is a paradigmatic model to describe quantum-critical behaviour [44]. The model is analytically diagonalizable for finite N and displays a second order quantum phase transition between a paramagnetic phase (for $g > J$) and a ferromagnetic one ($g < J$) [45].

We can introduce a dimensionless phase parameter by fixing $\Omega s = J$ and $\Omega(1-s) = g$ with energy scale Ω

$$\mathcal{H}_{\mathrm{S}} = -\Omega(1-s)\sum_{i=1}^{N}\sigma_i^x - \Omega s\sum_{i=1}^{N}\sigma_i^z\sigma_{i+1}^z\,. \tag{8.2}$$

The successive application of Jordan-Wigner, Fourier-, and Bogoliubov transform maps the system Hamiltonian into

$$\mathcal{H}'_{\mathrm{S}} = \sum_k \epsilon_k(\gamma_k^\dagger\gamma_k - 1/2)\,, \qquad k = \pm 1/2, \pm 3/2, \ldots, \pm(N-1)/2 \tag{8.3}$$

with fermionic annihilation operators γ_k that describe quasi-particles. Here, the quasi-momentum k may assume half-integer values, and the single-particle energies – that correspond to excitation energies of the full model – are defined by

$$\epsilon_k = 2\Omega\sqrt{(1-s)^2 + s^2 - 2s(1-s)\cos\left(\frac{2\pi k}{N}\right)}\,. \tag{8.4}$$

8.1.1 Exact Diagonalization of the closed system

The Jordan-Wigner transform (JWT)

$$\sigma_n^x = \mathbf{1} - 2c_n^\dagger c_n\,, \qquad \sigma_n^z = -(c_n + c_n^\dagger)\prod_{m=1}^{n-1}\left(\mathbf{1} - 2c_m^\dagger c_m\right) \tag{8.5}$$

maps the spin-1/2 Pauli matrices non-locally to fermionic operators c_m. Inserting the JWT into the Ising Hamiltonian, one has to treat the boundary term with special care

$$\begin{aligned} H &= -g\sum_{n=1}^{N}(\mathbf{1}-2c_n^\dagger c_n) - J\sum_{n=1}^{N-1}(c_n+c_n^\dagger)(c_{n+1}+c_{n+1}^\dagger)(\mathbf{1}-2c_n^\dagger c_n) \\ &\quad -J(c_N+c_N^\dagger)\left[\prod_{n=1}^{N-1}(\mathbf{1}-2c_n^\dagger c_n)\right](c_1+c_1^\dagger) \\ &= -g\sum_{n=1}^{N}(\mathbf{1}-2c_n^\dagger c_n) - J\sum_{n=1}^{N-1}(c_n^\dagger-c_n)(c_{n+1}^\dagger+c_{n+1}) \\ &\quad +J(c_N^\dagger-c_N)(c_1^\dagger+c_1)\left[\prod_{n=1}^{N}(\mathbf{1}-2c_n^\dagger c_n)\right], \end{aligned} \tag{8.6}$$

where we have extensively used the fermionic anticommutation relations. Introducing the projection operators on the subspaces with even (+) and odd (-) total number of fermion quasiparticles

$$\mathcal{P}^\pm \equiv \frac{1}{2}\left[\mathbf{1} \pm \prod_{m=1}^{N}(\mathbf{1}-2c_m^\dagger c_m)\right], \tag{8.7}$$

we may also write the Hamiltonian (8.6) $H = (\mathcal{P}^+ + \mathcal{P}^-)H(\mathcal{P}^+ + \mathcal{P}^-)$. It is straightforward to see that terms with different projectors and with $n < N$ vanish

$$\begin{aligned} 0 &= \mathcal{P}^+(\mathbf{1}-2c_n^\dagger c_n)\mathcal{P}^- = \mathcal{P}^-(\mathbf{1}-2c_n^\dagger c_n)\mathcal{P}^+, \\ 0 &= \mathcal{P}^+(c_n^\dagger-c_n)(c_{n+1}^\dagger+c_{n+1})\mathcal{P}^- = \mathcal{P}^-(c_n^\dagger-c_n)(c_{n+1}^\dagger+c_{n+1})\mathcal{P}^+. \end{aligned} \tag{8.8}$$

For the boundary terms one finds similarly

$$\begin{aligned} &(\mathcal{P}^+ + \mathcal{P}^-)(c_N^\dagger - c_N)(c_1^\dagger + c_1)\left[\prod_{n=1}^{N}(\mathbf{1}-2c_n^\dagger c_n)\right](\mathcal{P}^+ + \mathcal{P}^-) \\ &= (\mathcal{P}^+ + \mathcal{P}^-)(c_N^\dagger - c_N)(c_1^\dagger + c_1)(2\mathcal{P}^+ - \mathbf{1})(\mathcal{P}^+ + \mathcal{P}^-) \\ &= \mathcal{P}^+(c_N^\dagger - c_N)(c_1^\dagger + c_1)\mathcal{P}^+ - \mathcal{P}^-(c_N^\dagger - c_N)(c_1^\dagger + c_1)\mathcal{P}^-, \end{aligned} \tag{8.9}$$

such that we can finally write the Hamiltonian (8.6) as the sum of two non-interacting parts with either an even or an odd total number of fermionic quasiparticles

$$\begin{aligned} H &= \mathcal{P}^+H^+\mathcal{P}^+ + \mathcal{P}^-H^-\mathcal{P}^- \\ &= \mathcal{P}^+\left[-g\sum_{n=1}^{N}(\mathbf{1}-2c_n^\dagger c_n) - J\sum_{n=1}^{N}(c_n^\dagger-c_n)(c_{n+1}^\dagger+c_{n+1})\right]\mathcal{P}^+ \\ &\quad +\mathcal{P}^-\left[-g\sum_{n=1}^{N}(\mathbf{1}-2c_n^\dagger c_n) - J\sum_{n=1}^{N}(c_n^\dagger-c_n)(c_{n+1}^\dagger+c_{n+1})\right]\mathcal{P}^-. \end{aligned} \tag{8.10}$$

Note that this requires to define antiperiodic boundary conditions in the even (+) subspace $c_{N+1}^{(+)} \equiv -c_1^{(+)}$ and periodic boundary conditions in the odd (-) subspace $c_{N+1}^{(-)} \equiv +c_1^{(-)}$.

Since the even subspace is relevant to our model, we further seek to diagonalize the Hamiltonian

$$H^+ = -g\sum_{n=1}^{N}(\mathbf{1} - 2c_n^\dagger c_n) - J\sum_{n=1}^{N}(c_n^\dagger - c_n)(c_{n+1}^\dagger + c_{n+1}) \tag{8.11}$$

with antiperiodic boundary conditions $c_{N+1} = -c_1$. Translational invariance suggests to use the discrete Fourier transform (DFT, preserving the anticommutation relations due to its unitarity by construction)

$$c_n = \frac{e^{-i\pi/4}}{\sqrt{N}}\sum_k \tilde{c}_k e^{+ikn\frac{2\pi}{N}}\,, \tag{8.12}$$

which is a specific case of a Bogoliubov transformation. It is compatible with the antiperiodic boundary conditions when k takes half-integer values

$$k \in \{\pm\frac{1}{2}, \pm\frac{3}{2}, \pm\frac{5}{2}, \ldots\}\,, \qquad \text{where} \qquad |k| \leq \frac{N-1}{2} \tag{8.13}$$

(Note that the number of quasiparticles in the even subspace is the same e.g. for $N = 6$ and $N = 7$). The DFT maps the Hamiltonian into

$$H^+ \;=\; -gN\mathbf{1} + \sum_k \left\{2[g - J\cos(k2\pi/N)]\tilde{c}_k^\dagger\tilde{c}_k + J\sin(k2\pi/N)\left[\tilde{c}_k^\dagger\tilde{c}_{-k}^\dagger + \tilde{c}_{-k}\tilde{c}_k\right]\right\}\,. \tag{8.14}$$

Now, the observation that only positive and negative frequencies couple (conservation of one-dimensional quasi-momentum), suggests to use the reduced Bogoliubov transform

$$\tilde{c}_k = u_{+k}\gamma_{+k} + v_{-k}^*\gamma_{-k}^\dagger\,, \tag{8.15}$$

which mixes positive and negative momenta and where the a priori unknown coefficients have already been labeled suggestively (a more general ansatz would eventually of course yield the same solution). Since the new operators γ_k should be fermionic, we obtain from the orthonormality conditions

$$1 = |u_{+k}|^2 + |v_{-k}|^2\,, \qquad 0 = u_{+k}v_{+k}^* + u_{-k}v_{-k}^* = (v_{+k}^*, v_{-k}^*)\begin{pmatrix} u_{+k} \\ u_{-k}\end{pmatrix}\,. \tag{8.16}$$

Demanding that the Bogoliubov transform eliminates all non-diagonal terms (of the form $\gamma_{-k}\gamma_{+k}$ etc.) yields (by combining positive and negative k) the equation

$$\begin{aligned} 0 \;&=\; 2\left[g - J\cos\left(k\frac{2\pi}{N}\right)\right](u_{+k}v_{-k} - u_{-k}v_{+k}) + 2J\sin\left(k\frac{2\pi}{N}\right)(u_{-k}u_{+k} + v_{-k}v_{+k}) \\ &=\; (v_{-k}, u_{-k})\begin{pmatrix} +2\left[g - J\cos\left(k\frac{2\pi}{N}\right)\right] & +2J\sin\left(k\frac{2\pi}{N}\right) \\ +2J\sin\left(k\frac{2\pi}{N}\right) & -2\left[g - J\cos\left(k\frac{2\pi}{N}\right)\right]\end{pmatrix}\begin{pmatrix} u_{+k} \\ v_{+k}\end{pmatrix} \\ &\equiv\; (v_{-k}, u_{-k})\,\mathcal{M}\begin{pmatrix} u_{+k} \\ v_{+k}\end{pmatrix}\,. \end{aligned} \tag{8.17}$$

All equations can be fulfilled when we choose $(u_{+k}, v_{+k})^T$ as the normalized positive energy eigenstate of the matrix $\mathcal{M}$ with eigenvalue

$$\epsilon_k^+ = +2\sqrt{g^2 + J^2 - 2gJ\cos(k2\pi/N)} \equiv \epsilon_k \tag{8.18}$$

and $(v^*_{-k}, u^*_{-k})^T = (-v^*_{+k}, +u^*_{+k})^T$ as its negative energy eigenstate with eigenvalue $\epsilon^-_k = -2\sqrt{g^2 + J^2 - 2gJ\cos(k2\pi/N)}$. To be more explicit, we have

$$\begin{aligned} u_k &= \frac{g - J\cos(k2\pi/N) + \sqrt{g^2 + J^2 - 2gJ\cos(k2\pi/N)}}{\sqrt{\left[g - J\cos(k2\pi/N) + \sqrt{g^2 + J^2 - 2gJ\cos(k2\pi/N)}\right]^2 + \left[J\sin(k2\pi/N)\right]^2}}\,, \\ v_k &= \frac{J\sin(k2\pi/N)}{\sqrt{\left[g - J\cos(k2\pi/N) + \sqrt{g^2 + J^2 - 2gJ\cos(k2\pi/N)}\right]^2 + \left[J\sin(k2\pi/N)\right]^2}}\,. \end{aligned} \tag{8.19}$$

Using these solutions, we obtain when N is even

$$H^+ = \sum_k 2\sqrt{g^2 + J^2 - 2gJ\cos\left(k\frac{2\pi}{N}\right)}\left(\gamma^\dagger_k\gamma_k - \frac{1}{2}\right) = \sum_k \epsilon_k\left(\gamma^\dagger_k\gamma_k - \frac{1}{2}\right)\,, \tag{8.20}$$

which reproduces the single particle energies introduced before.

8.1.2 Equilibrium

We can write for the logarithm of the partition function

$$\begin{aligned} \ln Z(\beta) &= \ln \mathrm{Tr}\left\{e^{-\beta H}\right\} = \ln\prod_k\left(e^{+\beta\epsilon_k/2} + e^{-\beta\epsilon_k/2}\right) \\ &= \sum_k \ln\left[2\cosh\left(\frac{\beta\epsilon_k}{2}\right)\right] \\ &\to N\int_{-1/2}^{+1/2}\ln\left[2\cosh\left(\frac{\beta\epsilon(\kappa)}{2}\right)\right]d\kappa\,, \end{aligned} \tag{8.21}$$

where we have used an asymptotic convergence to an integral for large N in the last step and

$$\epsilon(\kappa) = 2\Omega\sqrt{(1-s)^2 + s^2 - 2s(1-s)\cos\left(2\pi\kappa\right)} \tag{8.22}$$

becomes a continuous band.

Now, the mean energy can be expressed by the derivative of the partition function with respect to the inverse temperature

$$\begin{aligned} \langle E\rangle &= \frac{\mathrm{Tr}\left\{He^{-\beta H}\right\}}{\mathrm{Tr}\left\{e^{-\beta H}\right\}} = \frac{-\partial_\beta Z(\beta)}{Z(\beta)} = -\partial_\beta \ln Z(\beta) \\ &= -N\int_{-1/2}^{+1/2}\frac{\epsilon(\kappa)}{2}\tanh\left(\frac{\beta\epsilon(\kappa)}{2}\right)d\kappa\,, \end{aligned} \tag{8.23}$$

and we see that at zero temperature $\beta \to \infty$ it simply becomes the ground state energy of the Ising model

$$\frac{\langle E\rangle}{N} \to -\int_{-1/2}^{+1/2}\frac{\epsilon(\kappa)}{2}d\kappa\,. \tag{8.24}$$

This integral can be solved exactly and leads to a discontinuity in the second derivative of the energy density with respect to the quantum-critical parameter.

The heat capacity is given by the derivative of the energy with respect to temperature

$$C = \frac{\partial \langle E \rangle}{\partial T} = \frac{\partial \langle E \rangle}{\partial \beta}\frac{\partial \beta}{\partial T} = -\beta^2 \frac{\partial \langle E \rangle}{\partial \beta} = +\beta^2 \frac{\partial^2 \ln Z(s,\beta)}{\partial \beta^2}\,. \tag{8.25}$$

For our model, we can therefore get an expression for the specific heat capacity (per chain length)

$$\frac{C}{N} = \int_{-1/2}^{+1/2} \frac{\left(\frac{\beta\epsilon(\kappa)}{2}\right)^2}{\cosh^2\left(\frac{\beta\epsilon(\kappa)}{2}\right)} d\kappa\,. \tag{8.26}$$

We can plot the heat capacity versus temperature and we see that away from the critical point ($s \neq 1/2$), it vanishes at low temperatures, i.e., injecting energy into the system immediately increases the temperature. At the critical point however, the spectrum becomes gapless, and the heat capacity is finite already at the smallest achievable temperatures. When we consider finite temperatures, the heat capacity vanishes for low temperatures in the gapped phase but rises above a certain critical temperature. This extends the zero-temperature phase diagram by a classical phase on top of the quantum phase, see Fig. 8.1.

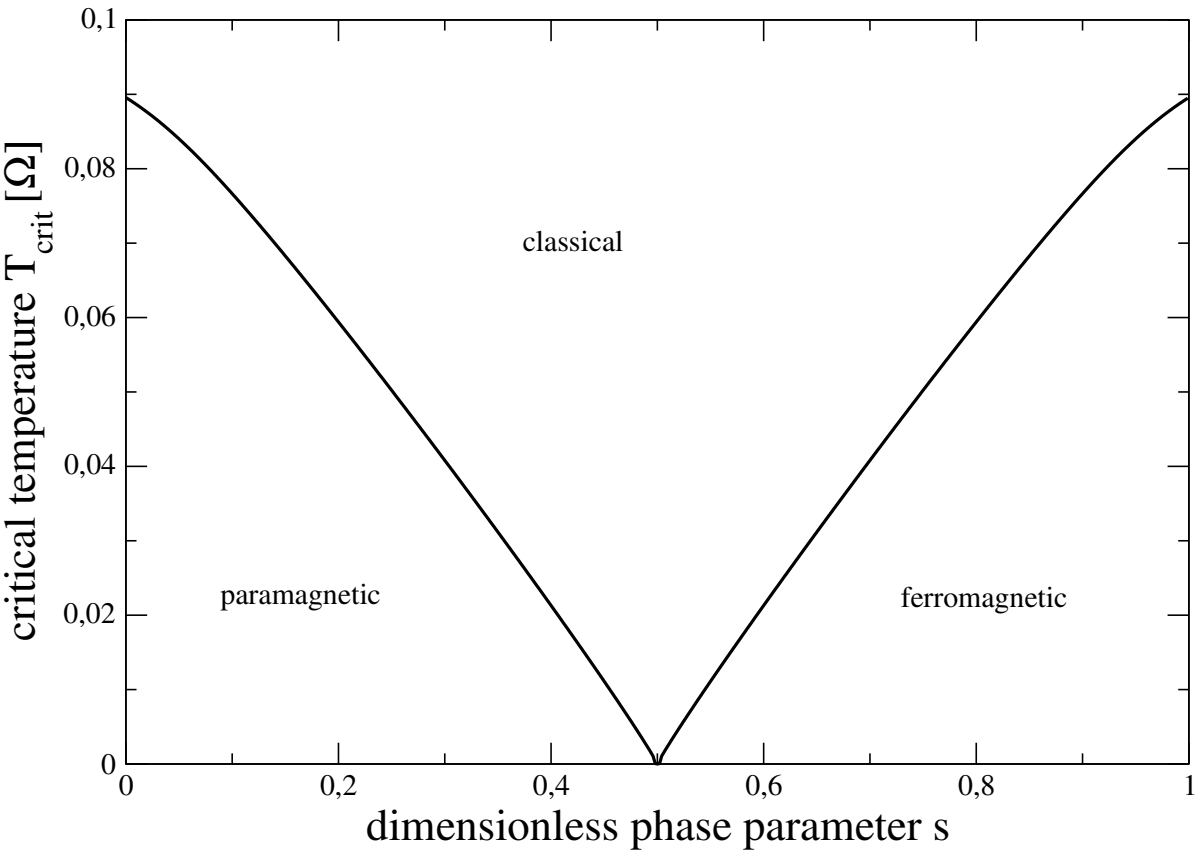

Figure 8.1: Plot of the critical temperature versus the paramagnetic-ferromagnetic transition parameter s. Below the curve, the heat capacity vanishes, whereas it becomes finite above the curve.

8.1.3 Non-Equilibrium

We can place the Ising model (8.1) in a nonequilibrium context by coupling it two two reservoirs, labeled source (S) and drain (D) in the following, using the collective coupling

$$H_I = J^x \otimes \sum_k \left(h_{kS} b_{kS} + h_{kS}^* b_{kS}^\dagger \right) + J^x \otimes \sum_k \left(h_{kD} b_{kD} + h_{kD}^* b_{kD}^\dagger \right) . \tag{8.27}$$

Since we have expressed the system Hamiltonian with non-interacting fermionic operators, it is useful to do the same with the interaction. Obviously, the used transformations do not affect the reservoir part, such that it suffices to transform $J_x = \sum_{i=1}^N \sigma_i^x$ with the very same transformations as before. Inserting the Jordan-Wigner-Transformation (8.5) yields

$$J_x = N\mathbf{1} - 2\sum_{n=1}^{N} c_n^\dagger c_n \, . \tag{8.28}$$

Furthermore, inserting the DFT (8.12) leads to

$$J_x = N\mathbf{1} - 2\sum_{k} \tilde{c}_k^\dagger \tilde{c}_k \, . \tag{8.29}$$

Finally, inserting the Bogoliubov transformation (8.15), replacing $k \to -k$ in some terms and exploiting that the coefficients (8.19) are real yields

$$J_x = N\mathbf{1} - 2\sum_{k} \left[|u_k|^2 \gamma_k^\dagger \gamma_k + |v_k|^2 \gamma_k \gamma_k^\dagger + u_k v_{-k} \left(\gamma_{+k}^\dagger \gamma_{-k}^\dagger + \gamma_{-k}\gamma_{+k} \right) \right] , \tag{8.30}$$

which by using the fermionic anticommutation relations is equivalent to

$$J^x \;=\; N\mathbf{1} - 2\sum_{k} \left[|v_k|^2 \mathbf{1} + \left(|u_k|^2 - |v_k|^2 \right) \gamma_k^\dagger \gamma_k + u_k v_{-k} \left(\gamma_{+k}^\dagger \gamma_{-k}^\dagger + \gamma_{-k}\gamma_{+k} \right) \right] , \tag{8.31}$$

where the coefficients are defined by $v_k \propto s \sin\left(\frac{2\pi k}{N}\right)$ and $u_k \propto \left[1 - s - s\cos\left(\frac{2\pi k}{N}\right) + \epsilon_k/(2\Omega)\right]$ subject to the normalization $|u_k|^2 + |v_k|^2 = 1$.

It is immediately visible that this type of interaction does not trigger transitions between the subspaces of even and odd quasiparticle number. We may therefore restrict our considerations completely to the subspace of even quasiparticle number. That is, out of the 2^n eigenstates which we can label as

$$|\boldsymbol{n}\rangle = \left| n_{-(N-1)/2}, \ldots, n_{-1/2}, n_{+1/2}, \ldots, n_{+(N-1)/2} \right\rangle \tag{8.32}$$

we can constrain ourselves to the ones that have an even total number of quasiparticles, of which there are just $2^{N/2}$. Furthermore, we see that – if at all – the interaction always creates pairs of quasi-particles with opposite quasi-momenta. Since the ground state has no quasi-particle pairs at all, the relevant subspace containing the total ground state and within which transitions are triggered by the interaction is given by the subspace of pairs of quasiparticles with opposite quasimomenta, i.e., we can constrain ourselves to the states

$$|\boldsymbol{n}\rangle = \left| n_{+(N-1)/2}, \ldots, n_{+1/2}, n_{+1/2}, \ldots, n_{+(N-1)/2} \right\rangle , \tag{8.33}$$

of which there are only $2^{N/2}$ (we have supposed before that N is even). In this subspace, the basis elements can be conveniently constructed from the ground state via

$$|\boldsymbol{n}\rangle = \left|n_{\frac{1}{2}}, n_{\frac{3}{2}}, \ldots, n_{\frac{N-1}{2}}\right\rangle \equiv \prod_{k>0} \left(\gamma_{+k}^{\dagger}\gamma_{-k}^{\dagger}\right)^{n_k} |0\rangle \ , \tag{8.34}$$

where $n_k \in \{0,1\}$ denotes the occupation of a quasi-particle pair with momenta $(+k,-k)$ such that $\left(\gamma_k^{\dagger}\gamma_k + \gamma_{-k}^{\dagger}\gamma_{-k}\right)|\boldsymbol{n}\rangle = 2n_k\,|\boldsymbol{n}\rangle$.

High-Dimensional Rate Equation.

Applying the standard master equation derivation in the relevant subspace, Eq. (8.34), (employing Born, Markov, and secular approximations in the standard way we have discussed) yields a rate equation

$$\dot{\rho}_{\boldsymbol{n}} = \sum_{\boldsymbol{m}} \left(\sum_{\alpha} \gamma^{\alpha}_{\boldsymbol{n}\boldsymbol{m}} \right) \rho_{\boldsymbol{m}} \tag{8.35}$$

for populations of the system energy eigenstates $\rho_{\boldsymbol{n}} \equiv \langle \boldsymbol{n}|\,\rho\,|\boldsymbol{n}\rangle$, where the transition rates $\gamma^{\alpha}_{\boldsymbol{n}\boldsymbol{m}}$ due to reservoir α admit only creation or annihilation of single quasi-particle pairs, see vertical lines in Fig. 8.2. Assuming thermal reservoir states, the transition rates ($\boldsymbol{n} \neq \boldsymbol{m}$) evaluate to $\gamma^{\alpha}_{\boldsymbol{n}\boldsymbol{m}} = \Gamma_{\alpha}(\Delta_{\boldsymbol{m}\boldsymbol{n}})\left[1 + n_{\alpha}(\Delta_{\boldsymbol{m}\boldsymbol{n}})\right]\left|\langle \boldsymbol{n}|\,J_x\,|\boldsymbol{m}\rangle\right|^2$ with energy differences $\Delta_{\boldsymbol{m}\boldsymbol{n}} \equiv E_{\boldsymbol{m}} - E_{\boldsymbol{n}}$ and system energies $E_{\boldsymbol{n}} = \sum_{k>0} \epsilon_k(2n_k - 1)$. The diagonal values $\gamma^{\alpha}_{\boldsymbol{n}\boldsymbol{n}}$ follow from trace conservation.

Using Eq. (8.35) and the rates $\gamma^{\alpha}_{\boldsymbol{n}\boldsymbol{m}}$, we obtain an analytical result for the non-equilibrium steady state solution. The stationary solution of the rate equation can even for non-equilibrium (different temperature) configurations be obtained using basically two ingredients. First, we note that the Fourier transforms of the bath correlation functions obey the usual Kubo-Martin-Schwinger conditions $\gamma_{\alpha}(-\omega) = e^{-\beta_{\alpha}\omega}\gamma_{\alpha}(+\omega)$, which lead when the system is coupled to only one bath (e.g. by setting $\Gamma_D(\omega) = 0$) to thermalization of the system with the temperature of the remaining reservoir (e.g. β_S^{-1}). Formally, such a thermal state is characterized by the ratio of diagonal elements to be

$$\frac{\bar{\rho}_{\boldsymbol{n}}}{\bar{\rho}_{\boldsymbol{m}}} = e^{-\beta(E_{\boldsymbol{n}} - E_{\boldsymbol{m}})} = \frac{n(E_{\boldsymbol{n}} - E_{\boldsymbol{m}})}{1 + n(E_{\boldsymbol{n}} - E_{\boldsymbol{m}})} \, , \tag{8.36}$$

where $n(\omega)$ corresponds to the Bose distribution of the connected reservoir. For coupling to multiple reservoirs we use that the occupations of the different reservoirs enter linearly and just weighted by the different tunneling rates to motivate the ansatz ($\Delta_{\boldsymbol{n}\boldsymbol{m}} \equiv E_{\boldsymbol{n}} - E_{\boldsymbol{m}}$)

$$\frac{\bar{\rho}_{\boldsymbol{n}}}{\bar{\rho}_{\boldsymbol{m}}} = \frac{\bar{n}(\Delta_{\boldsymbol{n}\boldsymbol{m}})}{1 + \bar{n}(\Delta_{\boldsymbol{n}\boldsymbol{m}})} \, , \qquad \bar{n}(\omega) \equiv \frac{\Gamma_S(\omega) n_S(\omega) + \Gamma_D(\omega) n_D(\omega)}{\Gamma_S(\omega) + \Gamma_D(\omega)} \, . \tag{8.37}$$

Indeed, one can easily prove for the rate equation

$$\begin{aligned} \dot{\rho}_{\boldsymbol{n}} \;=\; & \sum_{\boldsymbol{m}\neq\boldsymbol{n}} \sum_{\alpha} \Gamma_{\alpha}(\Delta_{\boldsymbol{m}\boldsymbol{n}})\left[1 + n_{\alpha}(\Delta_{\boldsymbol{m}\boldsymbol{n}})\right]\left|\langle \boldsymbol{n}|\,M_x\,|\boldsymbol{m}\rangle\right|^2 \rho_{\boldsymbol{m}} \\ & - \left(\sum_{\boldsymbol{m}\neq\boldsymbol{n}} \sum_{\alpha} \Gamma_{\alpha}(\Delta_{\boldsymbol{n}\boldsymbol{m}})\left[1 + n_{\alpha}(\Delta_{\boldsymbol{n}\boldsymbol{m}})\right]\left|\langle \boldsymbol{m}|\,M_x\,|\boldsymbol{n}\rangle\right|^2 \right) \rho_{\boldsymbol{n}} \end{aligned} \tag{8.38}$$

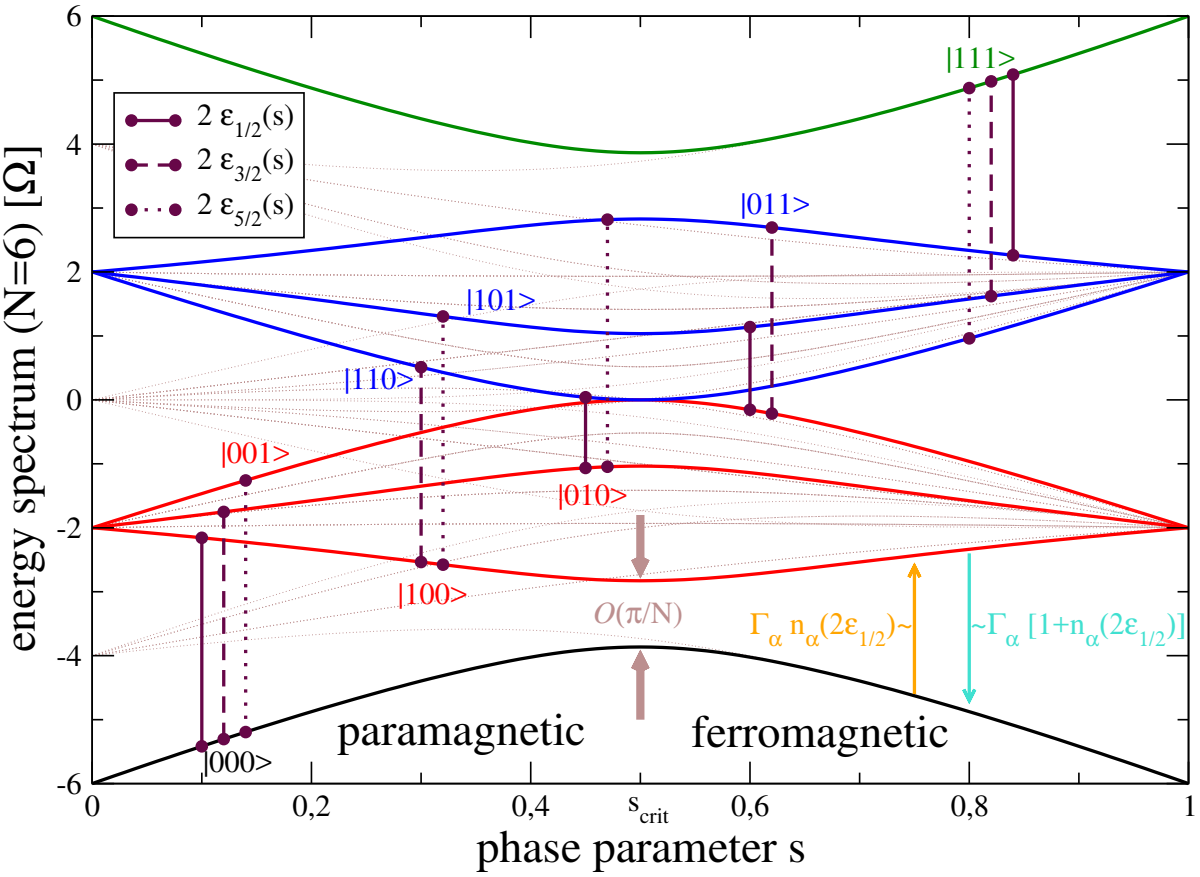

Figure 8.2: Spectrum of the Ising model for $N = 6$. The thin dotted curves belong to the subspace with an odd number of quasiparticles. Solid curves belong to the even subspace, and bold colored curves correspond to the subspace formed by pairs of quasiparticles with opposite quasimomenta. The vertical lines denote allowed transitions.

the validity of the stationary state by inserting

$$\bar{\rho}_{\boldsymbol{m}} = \frac{\bar{n}(\Delta_{\boldsymbol{mn}})}{1+\bar{n}(\Delta_{\boldsymbol{mn}})}\bar{\rho}_{\boldsymbol{n}} = \frac{\sum_\alpha \Gamma_\alpha(\Delta_{\boldsymbol{mn}}) n_\alpha(\Delta_{\boldsymbol{mn}})}{\sum_\alpha \Gamma_\alpha(\Delta_{\boldsymbol{mn}})\left[1+n_\alpha(\Delta_{\boldsymbol{mn}})\right]}\bar{\rho}_{\boldsymbol{n}} \tag{8.39}$$

and using that $\Gamma_\alpha(\Delta_{\boldsymbol{mn}}) = -\Gamma_\alpha(\Delta_{\boldsymbol{nm}})$ and $n_\alpha(\Delta_{\boldsymbol{mn}}) = -\left[1+n_\alpha(\Delta_{\boldsymbol{nm}})\right]$. By a sequence of pair annihilations – compare Fig. 8.2 – it therefore follows that any stationary occupation may be connected to the ground state occupation $\bar{\rho}_0$ via

$$\bar{\rho}_{\boldsymbol{n}} = \bar{\rho}_0 \prod_{k>0}\left(\frac{\bar{n}(2\epsilon_k)}{1+\bar{n}(2\epsilon_k)}\right)^{n_k} . \tag{8.40}$$

The latter is fixed by the normalization $\mathrm{Tr}\,\{\bar{\rho}_{\boldsymbol{n}}\} = 1$

$$1 = \bar{\rho}_0 \sum_{n_{1/2}=0}^{1} \cdots \sum_{n_{(N-1)/2}=0}^{1} \prod_{k>0}\left(\frac{\bar{n}(2\epsilon_k)}{1+\bar{n}(2\epsilon_k)}\right)^{n_k} = \bar{\rho}_0 \prod_{k>0}\left[\sum_{n_k=0}^{1}\left(\frac{\bar{n}(2\epsilon_k)}{1+\bar{n}(2\epsilon_k)}\right)^{n_k}\right] = \bar{\rho}_0 \prod_{k>0}\frac{1+2\bar{n}(2\epsilon_k)}{1+\bar{n}(2\epsilon_k)} \tag{8.41}$$

which eventually yields

$$\bar{\rho}_{\boldsymbol{n}} = \prod_{k>0}\frac{\left[\bar{n}(2\epsilon_k)\right]^{n_k}\left[1+\bar{n}(2\epsilon_k)\right]^{1-n_k}}{1+2\bar{n}(2\epsilon_k)} , \tag{8.42}$$

which is completely governed by an effective average bosonic occupation $\bar{n}(\omega) \equiv \frac{\sum_\alpha \Gamma_\alpha(\omega) n_\alpha(\omega)}{\sum_\alpha \Gamma_\alpha(\omega)}$. However, our system has more than one allowed transition frequency, which implies that the stationary state (8.42) is non-thermal (i.e., cannot be described by a single effective temperature) as soon as the reservoir temperatures are different $[n_S(\omega) \neq n_D(\omega)]$. We note that this non-equilibrium steady state for an interacting model holds for weak system-reservoir coupling only – opposed to results obtained for non-interacting models. Eq. (8.42) enables us to calculate the stationary values of the energy, the magnetization, and the current both for finite chain lengths and in the thermodynamic limit $N \to \infty$.

Energy

The stationary expectation value of the system energy then becomes

$$\begin{aligned} \left\langle \bar{E} \right\rangle &= \mathrm{Tr}\left\{\mathcal{H}_\mathrm{S}\bar{\rho}\right\} = \sum_{\boldsymbol{n}} \left\langle \boldsymbol{n}\right| \mathcal{H}_\mathrm{S} \left|\boldsymbol{n}\right\rangle \rho_{\boldsymbol{n}} = \sum_{k>0} \epsilon_k \sum_{\boldsymbol{n}} (2n_k - 1)\rho_{\boldsymbol{n}} \\ &= \sum_{k>0} \epsilon_k \sum_{n_k=0}^{1} \frac{[\bar{n}(2\epsilon_k)]^{n_k}\,[1+\bar{n}(2\epsilon_k)]^{1-n_k}}{1+2\bar{n}(2\epsilon_k)} (2n_k - 1) = \sum_{k>0} \frac{-\epsilon_k}{1+2\bar{n}(2\epsilon_k)}\,, \end{aligned} \tag{8.43}$$

where we have used that $\sum_{n_k=0}^{1} \frac{\bar{n}^{n_k}[1+\bar{n}]^{1-n_k}}{1+2\bar{n}} = 1$ holds for each k separately in the second line. In the thermodynamic limit ($N \to \infty$) and noting that all relevant quantities actually depend on $\kappa = k/N$, the sum is easily converted into an integral, and we arrive at

$$\bar{E} = \sum_{k>0} \frac{-\epsilon_k}{1+2\bar{n}(2\epsilon_k)} \overset{N\to\infty}{\to} N \int_0^{1/2} \frac{-\epsilon(\kappa)}{1+2\bar{n}(2\epsilon(\kappa))} d\kappa\,, \tag{8.44}$$

where we have introduced the continuum of system energies $\epsilon(\kappa) \equiv \epsilon_{(N\kappa)}$. At strictly zero temperature, where $\bar{n}(2\epsilon(\kappa)) = 0$, the system settles to the ground state, and the energy density can be expressed by a complete elliptic integral $E/N \to -\frac{2\Omega}{\pi}\mathcal{E}_E(4s(1-s))$, with a divergent second derivative at $s_\mathrm{crit} = 1/2$. This divergence, which reflects the usual ground state QPT criticality of the Ising chain, is also predictable from analyzing the analytic structure of the integrand in (8.44) at zero temperature. For finite temperature and also in non-equilibrium setups where $\bar{n}(2\epsilon(\kappa)) \neq 0$, the energy density remains analytic at the critical point.

Finally, we mention that at equilibrium, where $\bar{n}(\omega) = n(\omega)$, we can compare this with Eq. (8.23)

$$\begin{aligned} \langle E \rangle &= -N \int_{-1/2}^{+1/2} \frac{\epsilon(\kappa)}{2} \tanh\left(\frac{\beta\epsilon(\kappa)}{2}\right) d\kappa = -N \int_0^{1/2} \epsilon(\kappa) \tanh\left(\frac{\beta\epsilon(\kappa)}{2}\right) d\kappa \\ &= -N \int_0^{1/2} \frac{\epsilon(\kappa)}{1+2\bar{n}(\epsilon(\kappa))} d\kappa\,. \end{aligned} \tag{8.45}$$

Here, we have a difference in the denominator, which results from the fact that in Eq. (8.23) we have used the full subspace of an even number of quasiparticles, whereas here we have considered the subspace of pairs of quasiparticles with opposite quasimomentum. However, this discrepancy does not lead to drastic changes in the phase diagram. Since we can – up to a factor – transform the two expressions for the energy by a mere rescaling of Ω, the same phase diagram as depicted in Fig. 8.1 applies.

Magnetization

Similarly, we evaluate the diagonal matrix elements of the magnetization operator J^x

$$\begin{aligned} \langle \boldsymbol{n}| J_x |\boldsymbol{n}\rangle &= N - 4\sum_{k>0} |v_k|^2 - 4\sum_{k>0} \left(|u_k|^2 - |v_k|^2\right) n_k \\ &= N - 4\sum_{k>0} \left[|v_k|^2 + \left(1 - 2|v_k|^2\right) n_k\right] , \end{aligned} \tag{8.46}$$

which can be inserted in the stationary expectation value to yield

$$\begin{aligned} \left\langle \bar{J}_x \right\rangle &= \sum_{\boldsymbol{n}} \langle \boldsymbol{n}| J_x |\boldsymbol{n}\rangle \, \bar{\rho}_{\boldsymbol{n}} = N - 4\sum_{k>0} |v_k|^2 - 4\sum_{k>0} \left(1 - 2|v_k|^2\right) \sum_{n_k=0}^{1} n_k \frac{[\bar{n}(2\epsilon_k)]^{n_k} \, [1 + \bar{n}(2\epsilon_k)]^{1-n_k}}{1 + 2\bar{n}(2\epsilon_k)} \\ &= N - 4\sum_{k>0} |v_k|^2 - 4\sum_{k>0} \left(1 - 2|v_k|^2\right) \frac{\bar{n}(2\epsilon_k)}{1 + 2\bar{n}(2\epsilon_k)} = N - 4\sum_{k>0} \frac{|v_k|^2 + \bar{n}(2\epsilon_k)}{1 + 2\bar{n}(2\epsilon_k)} . \end{aligned} \tag{8.47}$$

Finally, the sum over k can similarly be converted into an integral. Furthermore, by inserting the coefficient (8.19) in the continuum representation and zero-temperature limit, we obtain for the magnetization density

$$\langle \bar{j}_x \rangle = \frac{\left\langle \bar{J}_x \right\rangle}{N} = 1 - 4\int_0^{1/2} v^2(\kappa) d\kappa = \frac{\mathcal{E}_E(4s(1-s)) + (1-2s)\mathcal{E}_K(4s(1-s))}{\pi(1-s)} , \tag{8.48}$$

where $\mathcal{E}_E(x)$ and $\mathcal{E}_K(x)$ denote the complete elliptic integral and the complete elliptic integral of the first kind, respectively.

Eventually, this results for large N in ($v(\kappa) \equiv v_{(Nk)}$)

$$\langle J_x \rangle \to N \left[1 - 4\int_0^{1/2} \frac{|v(\kappa)|^2 + \bar{n}(2\epsilon(\kappa))}{1 + 2\bar{n}(2\epsilon(\kappa))} d\kappa\right] . \tag{8.49}$$

At zero temperature, the integral is similarly solved by normal elliptic integrals and those of the first kind, which display a divergence in the first derivative of the magnetization density with respect to s. However, at finite temperature the magnetization density remains analytic, which is most evident in the trivial high-temperature case where $\bar{n}(2\epsilon(\kappa)) \to \infty$.

Heat Current

It is not too surprising that neither mean energy nor magnetization exhibit no sign of critical behaviour at $s = 1/2$, since at finite temperatures we are deeply within the classical phase. The more surprising it is that the heat current is even deeply withing the classical phase sensitive to the critical point.

This changes drastically, however, when we consider the heat current through the Ising chain from one reservoir to the other. The stationary current of bosons emitted to the drain can for example be obtained by inserting energy counting fields in the off-diagonal matrix elements of the rate equation matrix, i.e., to perform in Eq. (8.38) the replacements

$$\Gamma_D(\Delta_{\boldsymbol{mn}}) \left[1 + n_D(\Delta_{\boldsymbol{mn}})\right] \;\to\; \Gamma_D(\Delta_{\boldsymbol{mn}}) \left[1 + n_D(\Delta_{\boldsymbol{mn}})\right] e^{+\mathrm{i}\Delta_{\boldsymbol{mn}}\chi} , \tag{8.50}$$

which automatically takes into account that $\Delta_{\boldsymbol{mn}} > 0$ corresponds to emission into the drain and $\Delta_{\boldsymbol{mn}} < 0$ to absorption. Note that in the latter case one would use $\Gamma_D(-x)\left[1+n_D(-x)\right] = \Gamma_D(+x)n_D(+x)$. This upgrades the rate equation by a counting field $\dot{\rho} = \mathcal{L}(\chi)\rho$, and the stationary current can then be obtained with the stationary state by deriving the rate matrix with respect to the counting field χ

$$\begin{aligned}
I &= (-\mathrm{i})\mathrm{Tr}\left\{\mathcal{L}'(0)\bar{\rho}\right\} = \sum_{\boldsymbol{n}}\sum_{\boldsymbol{m}\neq\boldsymbol{n}} \Delta_{\boldsymbol{mn}}\Gamma_D(\Delta_{\boldsymbol{mn}})\left[1+n_D(\Delta_{\boldsymbol{mn}})\right]\left|\langle\boldsymbol{n}|\, M_x\,|\boldsymbol{m}\rangle\right|^2\bar{\rho}_{\boldsymbol{m}} \\
&= \sum_{\boldsymbol{nm}\,:\,\Delta_{\boldsymbol{mn}}>0} \Delta_{\boldsymbol{mn}}\Gamma_D(\Delta_{\boldsymbol{mn}})\left[1+n_D(\Delta_{\boldsymbol{mn}})\right]\left|\langle\boldsymbol{n}|\, M_x\,|\boldsymbol{m}\rangle\right|^2\bar{\rho}_{\boldsymbol{m}} \\
&\quad - \sum_{\boldsymbol{nm}\,:\,\Delta_{\boldsymbol{nm}}>0} \Delta_{\boldsymbol{nm}}\Gamma_D(\Delta_{\boldsymbol{nm}})n_D(\Delta_{\boldsymbol{nm}})\left|\langle\boldsymbol{n}|\, M_x\,|\boldsymbol{m}\rangle\right|^2\bar{\rho}_{\boldsymbol{m}} \\
&= \sum_{\boldsymbol{m}}\sum_{k>0}\left[2\epsilon_k m_k\Gamma_D(2\epsilon_k)\left[1+n_D(2\epsilon_k)\right](4u_kv_k)^2\,\bar{\rho}_{\boldsymbol{m}} - 2\epsilon_k(1-m_k)\Gamma_D(2\epsilon_k)n_D(2\epsilon_k)\,(4u_kv_k)^2\,\bar{\rho}_{\boldsymbol{m}}\right] \\
&= \sum_{k>0} 2\epsilon_k\Gamma_D(2\epsilon_k)(4u_kv_k)^2\sum_{\boldsymbol{m}}\left[m_k\left[1+n_D(2\epsilon_k)\right] - (1-m_k)n_D(2\epsilon_k)\right]\bar{\rho}_{\boldsymbol{m}} \\
&= \sum_{k>0} 2\epsilon_k\Gamma_D(2\epsilon_k)(4u_kv_k)^2\sum_{m_k=0}^{1}\left[m_k\left[1+n_D(2\epsilon_k)\right] - (1-m_k)n_D(2\epsilon_k)\right]\frac{\left[\bar{n}(2\epsilon_k)\right]^{m_k}\left[1+\bar{n}(2\epsilon_k)\right]^{1-m_k}}{1+2\bar{n}(2\epsilon_k)} \\
&= \sum_{k>0} 2\epsilon_k\Gamma_D(2\epsilon_k)(4u_kv_k)^2\frac{\bar{n}(2\epsilon_k)-n_D(2\epsilon_k)}{1+2\bar{n}(2\epsilon_k)} \\
&= \sum_{k>0} 2\epsilon_k(4u_kv_k)^2\frac{\Gamma_S(2\epsilon_k)\Gamma_D(2\epsilon_k)\left[n_S(2\epsilon_k)-n_D(2\epsilon_k)\right]}{\Gamma_S(2\epsilon_k)\left[1+2n_S(2\epsilon_k)\right]+\Gamma_D(2\epsilon_k)\left[1+2n_D(2\epsilon_k)\right]}\,, \qquad (8.51)
\end{aligned}$$

which with evaluating the prefactor $A_k \equiv 4u_kv_k$ from (8.19) becomes

$$\frac{I}{N} = 32\int_0^{1/2}\frac{s^2\Omega^2\sin^2(2\pi\kappa)}{\epsilon(\kappa)}\frac{\Gamma_S\Gamma_D[n_S(2\epsilon(\kappa))-n_D(2\epsilon(\kappa))]}{\Gamma_S[1+2n_S(2\epsilon(\kappa))]+\Gamma_D[1+2n_D(2\epsilon(\kappa))]}d\kappa \equiv \int_0^{1/2} j(s,\kappa)d\kappa \qquad (8.52)$$

At the critical point and for small κ, the integrand behaves as

$$\begin{aligned}
j(1/2,\kappa) &= \frac{8\pi\Omega(\beta_D-\beta_S)\Gamma_D\Gamma_S}{\Gamma_S\beta_D+\Gamma_D\beta_S}\kappa + \mathcal{O}\{\kappa^2\}\,, \\
\left.\frac{\partial}{\partial s}j(s,\kappa)\right|_{s=1/2} &= \frac{32\pi\Omega(\beta_D-\beta_S)\Gamma_D\Gamma_S}{\Gamma_S\beta_D+\Gamma_D\beta_S}\kappa + \mathcal{O}\{\kappa^2\}\,, \qquad (8.53)
\end{aligned}$$

which leads to divergence of the second derivative of the current at the critical point for all temperature configurations.

Analysis of the transition rates (e.g., by introducing energy counting fields as discussed before) yields our result for the current of net emitted bosons at the drain,

$$\begin{aligned}
I &= \sum_{\boldsymbol{n},\,\boldsymbol{m}}(E_{\boldsymbol{m}}-E_{\boldsymbol{n}})\gamma^D_{\boldsymbol{nm}}\bar{\rho}_{\boldsymbol{m}} \qquad (8.54) \\
&= \sum_{k>0}\frac{2\epsilon_kA_k^2\Gamma_S(2\epsilon_k)\Gamma_D(2\epsilon_k)\left[n_S(2\epsilon_k)-n_D(2\epsilon_k)\right]}{\Gamma_S(2\epsilon_k)\left[1+2n_S(2\epsilon_k)\right]+\Gamma_D(2\epsilon_k)\left[1+2n_D(2\epsilon_k)\right]},
\end{aligned}$$

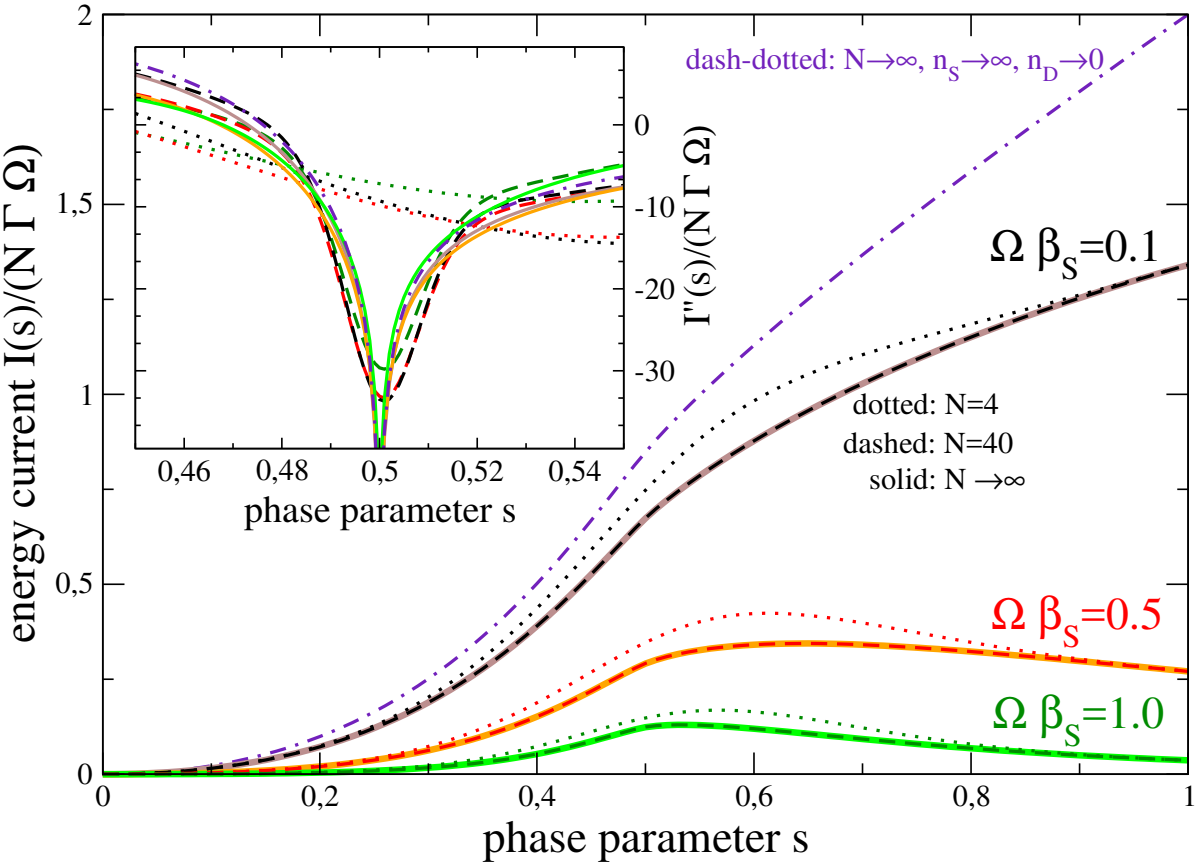

Figure 8.3: Renormalized energy current I and its second derivative w.r.t. s (inset) versus phase parameter s for different chain lengths $N = 4,\ 40,\ \infty$ (dotted, dashed, and bold solid, respectively) and for different source temperatures $\Omega\beta_S = 0.1, 0.5, 1.0$ (black/brown, red/orange, and dark/light green, respectively). The dash-dotted purple curve denotes the analytically accessible case of $n_D(\omega) \to 0$, $n_S(\omega) \to \infty$, and $N \to \infty$. Other parameters: $\Omega\beta_D = 10, \Gamma_S(\epsilon_k) = \Gamma_D(\epsilon_k) = \Gamma$.

where the second line follows after a straightforward calculation by inserting the stationary state and explicitly evaluating the transition rates. Here, we have introduced $A_k \equiv 4u_k v_k = \frac{4s\Omega}{\epsilon_k} \sin\left(\frac{2\pi k}{N}\right)$.

Evidently, the current is antisymmetric when $S \leftrightarrow D$, vanishes at equilibrium, and is positive when the source temperature exceeds the drain temperature [which implies $n_S(\omega) > n_D(\omega)$]. Most important however, in the thermodynamic limit $N \to \infty$ the current I directly reflects the signatures of the ground state quantum phase transition of the Ising chain. Formally, this correspondence is visible by the integral representation of I, which shows a divergence of its second derivative with respect to the phase parameter s at all temperatures, see Fig. 8.3. The second derivative of the integrand in the continuum version $I/N \equiv \int_0^{1/2} j(s,\kappa)d\kappa$ of Eq. (8.54) will at the critical point $s_{\rm crit} = 1/2$ for small κ diverge as

$$\left.\frac{\partial^2 j(s,\kappa)}{\partial s^2}\right|_{s=1/2} \approx -\frac{32\Omega\Gamma_S\Gamma_D(\beta_D-\beta_S)}{\pi(\Gamma_S\beta_D+\Gamma_D\beta_S)\kappa} + \mathcal{O}\{\kappa\}\,, \tag{8.55}$$

whilst the integrand itself and its first derivative remain finite. Even for the extreme non-equilibrium, infinite thermobias regime the heat current displays a divergence of the second derivative at $s_{\rm crit} = 1/2$, compare the dash-dotted curves in Fig. 8.3. This can even be seen in closed analyitic form, since in the infinite thermobias regime ($n_S(2\epsilon(\kappa)) \to \infty$ and $n_D(2\epsilon(\kappa)) \to 0$),

where (8.52) becomes

$$\begin{aligned}\frac{I}{N} &\rightarrow 16\Gamma_D(s\Omega)^2\int_0^{1/2}\frac{\sin^2(2\pi\kappa)}{\epsilon(\kappa)}d\kappa \\ &= \frac{4\Gamma_D\Omega}{3\pi(1-s)^2}\left[(1-2s(1-s))\mathcal{E}_E(4s(1-s))-(1-2s)^2\mathcal{E}_K(4s(1-s))\right], \end{aligned} \tag{8.56}$$

where $\mathcal{E}_E(x)$ represents the complete elliptic integral and $\mathcal{E}_K(x)$ the complete elliptic integral of the first kind.

8.2 Detection of charge fluctuations

Charge detectors are an important tool which we have used multiple times. Here, we will try to understand their effect on the system better and to link their presence with an effective description of quantum measurements. We will start from the point contact Hamiltonian

$$\begin{aligned}H_{\rm QPC} &= \sum_k \epsilon_{kL}\gamma_{kL}^\dagger\gamma_{kL}+\sum_k\epsilon_{kR}\gamma_{kR}^\dagger\gamma_{kR} \\ &\quad +(1-\delta d^\dagger d)\sum_{kk'}t_{kk'}\gamma_{kL}\gamma_{k'R}^\dagger+(1-\delta d^\dagger d)\sum_{kk'}t_{kk'}^*\gamma_{k'R}\gamma_{kL}^\dagger, \end{aligned} \tag{8.57}$$

where $t_{kk'}$ denotes the tunneling amplitude from mode k of the left QPC lead to mode k' of the right QPC lead. The prefactor $1-\delta d^\dagger d$ reduces ($0\leq\delta\leq 1$) these amplitudes when a nearby charge (we will specify it later) is present. For $\delta=0$, the QPC is insensitive to the nearby dot occupation, and $\delta\rightarrow 1$ means that transport through the QPC is completely blocked. We label our system coupling operators as $A_1=A_2=A=1-\delta d^\dagger d$ and for our reservoir we have $B_1=\sum_{kk'}t_{kk'}\gamma_{kL}\gamma_{k'R}^\dagger=B_2^\dagger$. Basically, we could have put these definitions into a single operator, but in Sec. 4.2.2, we have already computed the correlation functions for such a QPC model, and we can now add a counting field to the description counting positively all charges that enter the right QPC lead. Then, the Fourier transforms of the reservoir correlation functions become (compare Eqns. (4.60) and (4.61))

$$\begin{aligned}\gamma_{12}^\chi(\Omega) &= e^{-i\chi}t\int[1-f_L(\omega)]f_R(\omega-\Omega)d\omega=\frac{e^{-i\chi}t(\Omega-V)}{1-e^{-\beta(\Omega-V)}}, \\ \gamma_{21}^\chi(\Omega) &= e^{+i\chi}t\int f_L(\omega)f_R(\omega+\Omega)d\omega=\frac{e^{+i\chi}t(\Omega+V)}{1-e^{-\beta(\Omega+V)}}, \end{aligned} \tag{8.58}$$

where $t>0$ is some baseline transmission of the QPC, β its ambient temperature, and V the QPC bias voltage. Furthermore, according to Eq. (4.112), the coarse-graining dissipator can be written

as

$$\begin{aligned}
\dot{\boldsymbol{\rho}}_{\mathbf{S}} &= -\mathrm{i}\left[\frac{1}{2\mathrm{i}\tau}\int_0^\tau dt_1\int_0^\tau dt_2\sum_{\alpha\beta}C^0_{\alpha\beta}(t_1-t_2)\mathrm{sgn}(\mathrm{t}_1-\mathrm{t}_2)\boldsymbol{A}_{\boldsymbol{\alpha}}(\mathrm{t}_1)\boldsymbol{A}_{\boldsymbol{\beta}}(\mathrm{t}_2),\boldsymbol{\rho}_{\mathbf{S}}\right]\\
&\quad+\frac{1}{\tau}\int_0^\tau dt_1\int_0^\tau dt_2\sum_{\alpha\beta}\left[C^\chi_{\alpha\beta}(t_1-t_2)\boldsymbol{A}_{\boldsymbol{\beta}}(t_2)\boldsymbol{\rho}_{\mathbf{S}}\boldsymbol{A}_{\boldsymbol{\alpha}}(t_1)-\frac{C^0_{\alpha\beta}(t_1-t_2)}{2}\left\{\boldsymbol{A}_{\boldsymbol{\alpha}}(t_1)\boldsymbol{A}_{\boldsymbol{\beta}}(t_2),\boldsymbol{\rho}_{\mathbf{S}}\right\}\right]\\
&= -\mathrm{i}\left[\frac{1}{2\mathrm{i}2\pi\tau}\int_0^\tau dt_1\int_0^\tau dt_2\int d\omega\sigma^0_{\alpha\beta}(\omega)e^{-\mathrm{i}\omega(t_1-t_2)}\boldsymbol{A}_{\boldsymbol{\alpha}}(t_1)\boldsymbol{A}_{\boldsymbol{\beta}}(t_2),\boldsymbol{\rho}_{\mathbf{S}}\right]\\
&\quad+\frac{1}{2\pi\tau}\int_0^\tau dt_1\int_0^\tau dt_2\int d\omega e^{-\mathrm{i}\omega(t_1-t_2)}\sum_{\alpha\beta}\left[\gamma^\chi_{\alpha\beta}(\omega)\boldsymbol{A}_{\boldsymbol{\beta}}(t_2)\boldsymbol{\rho}_{\mathbf{S}}\boldsymbol{A}_{\boldsymbol{\alpha}}(t_1)-\frac{\gamma^0_{\alpha\beta}(\omega)}{2}\left\{\boldsymbol{A}_{\boldsymbol{\alpha}}(t_1)\boldsymbol{A}_{\boldsymbol{\beta}}(t_2),\boldsymbol{\rho}_{\mathbf{S}}\right\}\right].
\end{aligned}\tag{8.59}$$

In particular, we will be neglecting the Lamb-shift $\sigma^0_{\alpha\beta}(\omega)\to 0$ and will furthermore be interested in the infinite coarse-graining time limit $\tau\to\infty$, which effectively implements a secular approximation.

8.2.1 Single quantum dot

When the QPC couples only to a single quantum dot (SQD)

$$H_S=\epsilon d^\dagger d\,,\tag{8.60}$$

we see that the interaction commutes with the dot Hamiltonian, such that to lowest order (the dot may itself have further leads) no energy is exchanged between the QPC and the dot. For a single dot, the interaction picture dynamics is trivial $\boldsymbol{A}(t)=1-\delta d^\dagger d$, and the coarse-graining dissipator becomes for $\tau\to\infty$

$$\begin{aligned}
\dot{\boldsymbol{\rho}}_{\mathbf{S}} &= -\mathrm{i}\left[\frac{1}{2\mathrm{i}}\left(\sigma_{12}(0)+\sigma_{21}(0)\right)(1-\delta d^\dagger d)^2,\boldsymbol{\rho}_{\mathbf{S}}\right]\\
&\quad+\frac{tV}{e^{\beta V}-1}\left[e^{-\mathrm{i}\chi}(1-\delta d^\dagger d)\boldsymbol{\rho}_{\mathbf{S}}(1-\delta d^\dagger d)-\frac{1}{2}\left\{(1-\delta d^\dagger d)^2,\boldsymbol{\rho}_{\mathbf{S}}\right\}\right]\\
&\quad+\frac{tV}{1-e^{-\beta V}}\left[e^{+\mathrm{i}\chi}(1-\delta d^\dagger d)\boldsymbol{\rho}_{\mathbf{S}}(1-\delta d^\dagger d)-\frac{1}{2}\left\{(1-\delta d^\dagger d)^2,\boldsymbol{\rho}_{\mathbf{S}}\right\}\right].
\end{aligned}\tag{8.61}$$

As superpositions of states with different charge are not allowed for the SQD, the most general density matrix of a single dot can be written as $\boldsymbol{\rho}_{\mathbf{S}}(t)=P_0(t)\left|0\right\rangle\left\langle 0\right|+P_1(t)\left|1\right\rangle\left\langle 1\right|$, which obey the generalized master equation

$$\frac{d}{dt}\begin{pmatrix}P_0(t)\\P_1(t)\end{pmatrix}=\left(\gamma_{21}(e^{+\mathrm{i}\chi}-1)+\gamma_{12}(e^{-\mathrm{i}\chi}-1)\right)\begin{pmatrix}1&0\\0&(1-\delta)^2\end{pmatrix}\begin{pmatrix}P_0(t)\\P_1(t)\end{pmatrix}.\tag{8.62}$$

At vanishing counting field, the effect of the QPC vanishes completely. Writing the probabilities in a vector $\rho=(P_0,P_1)^T$, we can write this as

$$\dot\rho=\mathcal{L}_{\mathrm{dt}}(\chi)\rho\,,\qquad \mathcal{L}_{\mathrm{dt}}(\chi)=\left(\gamma_{21}(e^{+\mathrm{i}\chi}-1)+\gamma_{12}(e^{-\mathrm{i}\chi}-1)\right)\begin{pmatrix}1&0\\0&(1-\delta)^2\end{pmatrix}.\tag{8.63}$$

If no further leads change the occupation of the SQD, the prefactor directly encodes the cumulant-generating function of the QPC statistics, and we would get the two currents

$$I_E = \gamma_{21} - \gamma_{12} = tV\,, \qquad I_F = (1-\delta)^2\,(\gamma_{21} - \gamma_{12}) = (1-\delta)^2 tV\,, \tag{8.64}$$

depending on whether the dot is initially filled or empty, respectively. Similarly, we can compute the zero-frequency noise from the second derivative with respect to the counting field

$$S_E = \gamma_{21} + \gamma_{12} = tV\coth\left[\frac{\beta V}{2}\right]\,, \qquad S_F = (1-\delta)^2\,(\gamma_{21} + \gamma_{12}) = (1-\delta)^2 tV\coth\left[\frac{\beta V}{2}\right]\,. \tag{8.65}$$

For large bias voltage, we can approximate this by $\coth\left[\frac{\beta V}{2}\right] \to 1$, and the width of the current is just controlled by the bias voltage as well, such that transport becomes Poissonian. In contrast, for small bias voltage, the noise becomes $S_E \to 2t/\beta$ and $S_F \to (1-\delta)^2 S_E$, which is just linear in the temperature.

The Fano factor $F = S/|I|$ is therefore just given by

$$F_E = F_F = \coth\left[\frac{\beta V}{2}\right]\,, \tag{8.66}$$

and it is not dependent on the dot occupation. In particular, it reaches 1 (Poissonian transport, shot noise) when $V \to \infty$ and diverges as $2/(\beta V)$ for small bias voltage. However, when now the dot occupation is allowed to change in time, the dynamics becomes more interesting, see Fig. 8.4. To use the point contact as a detector, we require that during the measurement time Δt, the system does not change due to other processes. Then, the joint system-detector density matrix at time $t + \Delta t$ is given by

$$\sigma(t+\Delta t) = \sum_{nm} \rho^{(nm)}(t+\Delta t) \otimes |n\rangle\langle m|\,, \tag{8.67}$$

and by performing a projective measurement with the measurement operators $M_n = |0\rangle\langle n|$ we see that

$$M_n \sigma(t+\Delta t) M_n^\dagger = \rho^{(nn)}(t+\Delta t) \otimes |0\rangle\langle 0|\,. \tag{8.68}$$

To infer how a projective measurement of the detector charges affects the system density matrix, we consider its n-resolved version

$$\rho^{(n)}(t+\Delta t) = \frac{1}{2\pi}\int_{-\pi}^{+\pi} e^{\mathcal{L}(\chi)\Delta t} e^{-\mathrm{i}n\chi} d\chi \rho(t) = \mathcal{K}_n(\Delta t)\rho(t)\,. \tag{8.69}$$

When the bias voltage is large, transport becomes unidirectional, and we can simplify

$$\mathcal{L}_{\mathrm{dt}}(\chi) \to \gamma_{21}(e^{+\mathrm{i}\chi} - 1)\begin{pmatrix} 1 & 0 \\ 0 & (1-\delta)^2 \end{pmatrix}\,, \tag{8.70}$$

which enables us to compute all integrals explicitly

$$\rho^{(n)}(t+\Delta t) = \begin{pmatrix} \frac{\gamma_{21}^n \Delta t^n}{n!} e^{-\gamma_{21}\Delta t} & 0 \\ 0 & \frac{(1-\delta)^{2n}\gamma_{21}^n \Delta t^n}{n!} e^{-(1-\delta)^2\gamma_{21}\Delta t} \end{pmatrix} \rho(t) = \mathcal{K}_n(\Delta t)\rho(t)\,. \tag{8.71}$$

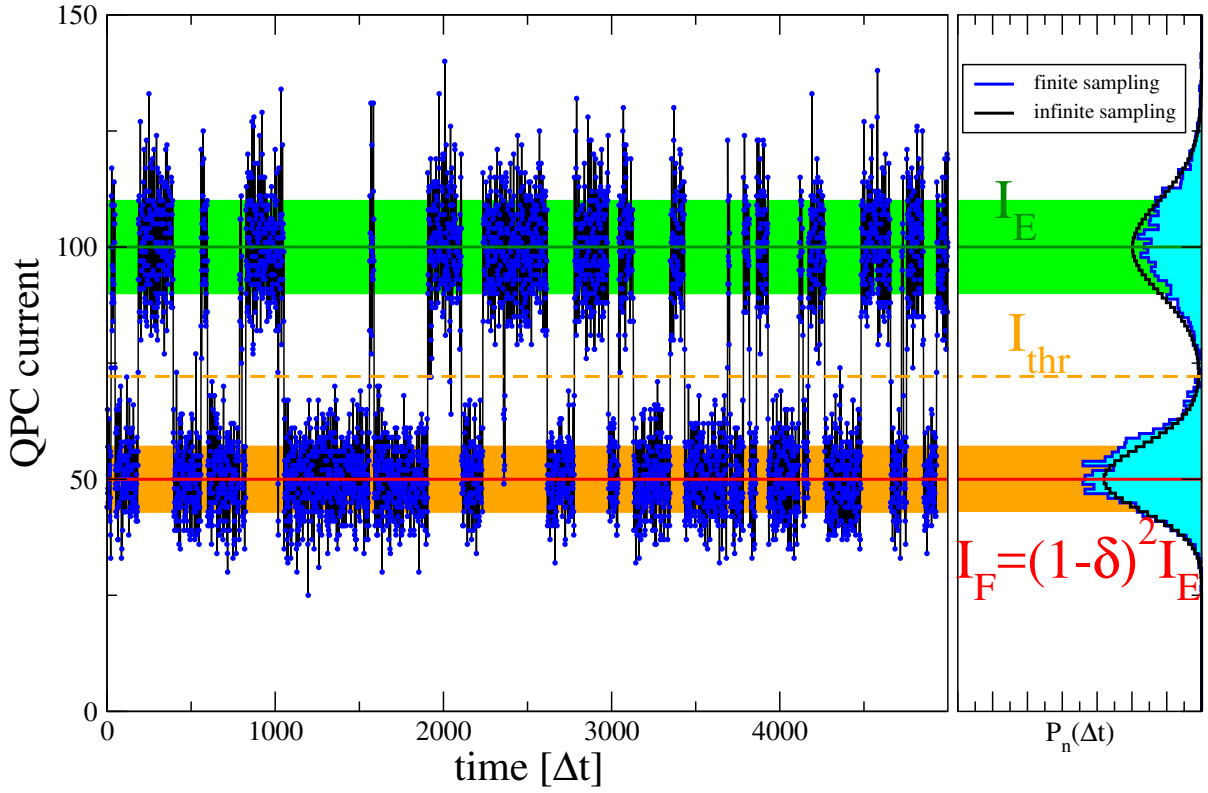

Figure 8.4: Left: Simulated QPC current – adapted from Fig. 4.6 – when the dot is allowed to experience slow occupation changes. Solid lines and shaded regions correspond to mean current $I_{E/F}$ and noise $\sqrt{S_{E/F}}$, respectively. To use the device as a detector discriminating empty and filled dot, a discrimination threshold (orange) needs to be chosen suitably. Right: Sampling of the trajectory on the left into a histogram (light color). The black curve would result for infinite sampling. By collecting all measurement outcomes above the threshold into the outcome empty (E) and all measurement outcomes below the threshold as corresponding to the outcome filled (F), one automatically implements a weak measurement on the system (allowing e.g. for the possibility of errors). Parameters as in Fig. 4.6.

These are just two Poissonian distributions moving at different pace: A fast one with cumulants $\gamma_{21}\Delta t$ for the empty dot and a slow one with cumulants $(1-\delta)^2\gamma_{21}\Delta t$. The propagator $\mathcal{K}_n(\Delta t)$ describes the effective action of measurement and interaction with the measurement device during Δt. Due to the normalization of the Poissonian distributions, we have $\sum_n \mathcal{K}_n = \mathbf{1}$, such that upon neglecting all measurement results, the measurement on the SQD has no effect. For large Δt, we can define a reasonable threshold such that $(1-\delta)^2\gamma_{21}\Delta t < n_{\rm th} < \gamma_{21}\Delta t$. We can calculate it analytically by solving for the n where Poissonian distributions are identical

$$\frac{(1-\delta)^{(2n)}(\gamma_{21}\Delta t)^n}{n!}e^{-(1-\delta)^2\gamma_{21}\Delta t} = \frac{(\gamma_{21}\Delta t)^n}{n!}e^{-\gamma_{21}\Delta t}\,, \tag{8.72}$$

which eventually yields

$$n_{\rm th} = \frac{-\delta(1-\delta/2)\gamma\Delta t}{\ln(1-\delta)}\,. \tag{8.73}$$

Now, by absorbing all measurement outcomes below the threshold into the outcome of a filled dot and the outcomes above the threshold into the outcome of an empty dot we get two measurement

superoperators, which have a simple parametrization

$$\mathcal{K}_E = \sum_{n\geq n_{\rm th}} \mathcal{K}_n(\Delta t) = \begin{pmatrix} 1-P^0_{\rm err} & 0 \\ 0 & P^1_{\rm err} \end{pmatrix}, \qquad \mathcal{K}_F = \sum_{n<n_{\rm th}} \mathcal{K}_n(\Delta t) = \begin{pmatrix} P^0_{\rm err} & 0 \\ 0 & 1-P^1_{\rm err} \end{pmatrix}. \quad (8.74)$$

For suitably chosen $n_{\rm th}$, these indeed approach projectors onto the empty or the filled state as for $\gamma\Delta t \to \infty$ we have $P_{\rm err} \to 0$.

8.2.2 Double quantum dot:Least-invasive measurement

Now, we consider a double quantum dot (DQD)

$$H_S = \epsilon(d_L^\dagger d_L + d_R^\dagger d_R) + T(d_L d_R^\dagger + d_R d_L^\dagger) + U d_L^\dagger d_L d_R^\dagger d_R\,, \quad (8.75)$$

with symmetric on-site energies ϵ, Coulomb interaction U, and tunneling amplitude T (generalizations are of course possible). We can immediately calculate the eigenvalues and eigenvectors of the system

$$\begin{aligned} |v_0\rangle &= |00\rangle\,, \qquad E_0 = 0\,, \\ \left|v_1^-\right\rangle &= \frac{1}{\sqrt{2}}\left[|01\rangle - |10\rangle\right], \qquad E_- = \epsilon - T\,, \\ \left|v_1^+\right\rangle &= \frac{1}{\sqrt{2}}\left[|01\rangle + |10\rangle\right], \qquad E_- = \epsilon + T\,, \\ |v_2\rangle &= |11\rangle\,, \qquad E_2 = 2\epsilon + U\,. \end{aligned} \quad (8.76)$$

If we only measure the left site occupation with the QPC (measuring on the right site is of course also possible), the system coupling operator in the Schrödinger picture becomes $A_1 = A_2 = 1 - \delta d_L^\dagger d_L$. However, in contrast to the SQD, the transformation into the interaction picture is less trivial

$$\begin{aligned} \boldsymbol{A}(t) &= \mathbf{1} - \delta e^{+{\rm i}H_S t} d_L^\dagger d_L e^{-{\rm i}H_S t} \\ &= \mathbf{1} - \delta\cos^2(Tt) d_L^\dagger d_L - \delta\sin^2(Tt) d_R^\dagger d_R - \delta\sin(Tt)\cos(Tt){\rm i}(d_L d_R^\dagger - d_R d_L^\dagger) \\ &\quad \mathbf{1} - \delta\frac{1}{4}\left[e^{+{\rm i}2Tt} - e^{-{\rm i}2Tt}\right](d_L d_R^\dagger - d_R d_L^\dagger) \\ &= \mathbf{1} - \delta\left[\frac{1}{4}d_L^\dagger d_L - \frac{1}{4}d_R^\dagger d_R + \frac{1}{4}(d_L d_R^\dagger - d_R d_L^\dagger)\right] e^{+2{\rm i}Tt} \\ &\quad -\delta\left[\frac{1}{4}d_L^\dagger d_L - \frac{1}{4}d_R^\dagger d_R - \frac{1}{4}(d_L d_R^\dagger - d_R d_L^\dagger)\right] e^{-2{\rm i}Tt} \\ &\quad -\delta\left[\frac{1}{2}d_L^\dagger d_L + \frac{1}{2}d_R^\dagger d_R\right] \\ &= A_+ e^{+2{\rm i}Tt} + A_- e^{-2{\rm i}Tt} + A_0\,, \end{aligned} \quad (8.77)$$

where we note that it does only depend on the internal DQD tunneling amplitude T. We can insert this in the coarse-graining dissipator, which under neglect of the Lamb-shift $\sigma_{\alpha\beta}(\omega) \to 0$ and in the unidirectional QPC transport limit $\gamma_{12}(\omega) \to 0$ becomes

$$\dot{\boldsymbol{\rho}}_{\mathbf{S}} = \frac{1}{2\pi\tau}\int_0^\tau dt_1 dt_2 \int d\omega e^{-{\rm i}\omega(t_1-t_2)}\gamma_{21}(\omega)\left[e^{+{\rm i}\chi}\boldsymbol{A}(t_2)\boldsymbol{\rho}_{\mathbf{S}}\boldsymbol{A}(t_1) - \frac{1}{2}\left\{\boldsymbol{A}(t_1)\boldsymbol{A}(t_2), \boldsymbol{\rho}_{\mathbf{S}}\right\}\right] \quad (8.78)$$

Out of the many contributions that arise when inserting the actual time-dependence of the system operator, we only keep those that survive in the limit $\tau \to \infty$, yielding

$$\begin{aligned}\dot{\boldsymbol{\rho}}_{\mathbf{S}} &= \gamma_{21}(+2T)\left[e^{+\mathrm{i}\chi}A_-\boldsymbol{\rho}_{\mathbf{S}}A_+ - \frac{1}{2}\{A_+A_-,\boldsymbol{\rho}_{\mathbf{S}}\}\right] + \gamma_{21}(-2T)\left[e^{+\mathrm{i}\chi}A_+\boldsymbol{\rho}_{\mathbf{S}}A_- - \frac{1}{2}\{A_-A_+,\boldsymbol{\rho}_{\mathbf{S}}\}\right] \\ &\quad +\gamma_{21}(0)\left[e^{+\mathrm{i}\chi}A_0\boldsymbol{\rho}_{\mathbf{S}}A_0 - \frac{1}{2}\{A_0A_0,\boldsymbol{\rho}_{\mathbf{S}}\}\right]. \end{aligned} \tag{8.79}$$

This dissipator looks quite different from the SQD dissipator. Phenomenologically, it can move charges between left and right dot and thereby change the charge configuration just by the physical back-action of the measurement. It induces dephasing in the energy eigenbasis of the system but also acts dissipatively, since it can exchange energy with the system, compare Fig. 8.5. The

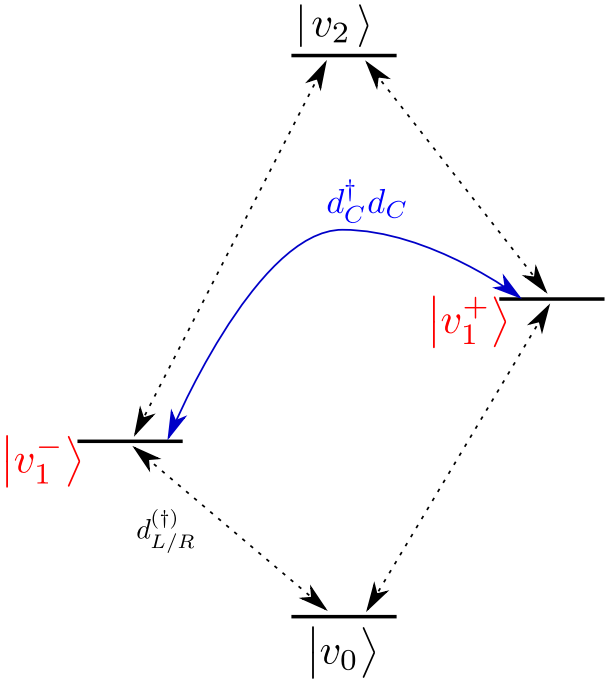

Figure 8.5: Sketch of the energy levels of the DQD. Tunnel-couplings to further leads from left and right dots may induce the dotted transitions, whereas the coupling to the QPC may only induce transition between the singly-charged states (solid blue) with energy difference $\Delta E = 2T$.

simplest case arises when we consider QPC transmissions that would not allow for energy exchange, which could e.g. be achieved by choosing a narrow transmission function for the QPC, such that $\gamma_{21}(+2T) = \gamma_{21}(-2T) = 0$. By doing so, we effectively forbid the detector to exchange energy with the system, as can be seen by realizing that $[H_S, A_0] = 0$. Then, the dissipator further simplifies

$$\dot{\boldsymbol{\rho}}_{\mathbf{S}} = +\gamma_{21}(0)\left[e^{+\mathrm{i}\chi}A_0\boldsymbol{\rho}_{\mathbf{S}}A_0 - \frac{1}{2}\{A_0A_0,\boldsymbol{\rho}_{\mathbf{S}}\}\right] = \left(e^{+\mathrm{i}\chi}\mathcal{J} + \mathcal{L}_0\right)\boldsymbol{\rho}_{\mathbf{S}}, \tag{8.80}$$

Evaluating this in the energy eigenbasis, this yields with $A_0 = \mathbf{1} - \delta/2 d_L^\dagger d_L - \delta/2 d_R^\dagger d_R$ the coupled equations (we abbreviate $\gamma = \gamma_{21}(0)$)

$$\begin{aligned}\dot{\rho}_{00} &= \gamma(e^{+\mathrm{i}\chi}-1)\rho_{00}, \\ \dot{\rho}_{--} &= \gamma(1-\delta/2)^2(e^{+\mathrm{i}\chi}-1)\rho_{--}, \\ \dot{\rho}_{++} &= \gamma(1-\delta/2)^2(e^{+\mathrm{i}\chi}-1)\rho_{++}, \\ \dot{\rho}_{22} &= \gamma(1-\delta)^2(e^{+\mathrm{i}\chi}-1)\rho_{22}, \\ \dot{\rho}_{-+} &= \gamma(1-\delta/2)^2(e^{+\mathrm{i}\chi}-1)\rho_{-+}, \\ \dot{\rho}_{+-} &= \gamma(1-\delta/2)^2(e^{+\mathrm{i}\chi}-1)\rho_{+-}. \end{aligned} \tag{8.81}$$

This means that the measurement damps the coherences in the energy eigenbasis – but leaves the coherences in the local (site-) basis. Without counting ($\chi \to 0$), there would be no effect of the measurement, not even dephasing. With counting, we have an additional dephasing in the energy eigenbasis due to the measurement. In this limit, the QPC makes no difference between an electron situated on the left or right dot, since it couples to the hybridized states. Consequently, in its cumulant-generating function we only see three different currents: $I_0 = \gamma$ for the empty DQD, $I_1 = \gamma(1-\delta/2)^2$ for the singly-charged DQD (coherences also contribute to this sector), and $I_2 = \gamma(1-\delta)^2$ for the doubly charged DQD. When the DQD is in addition coupled to electronic leads that lead to slow occupation changes, the allowed coherences ρ_{-+} and ρ_{+-} will be damped away, and the QPC will only switch between the three allowed current values, not at all resolving the location of the electron in the singly-charged sector. The switching between these currents is dictated by the rates which we have previously calculated for the DQD coupled to two leads, compare Eq. (3.50), such that the total Liouvillian can be written as

$$\mathcal{L}(\boldsymbol{\chi}, \boldsymbol{\xi}, \chi) = \mathcal{L}_{\mathrm{DQD}}(\boldsymbol{\chi}, \boldsymbol{\xi}) + \mathcal{L}_{\mathrm{dt}}(\chi)\,, \tag{8.82}$$

where $\mathcal{L}_{\mathrm{DQD}}(\boldsymbol{\chi}, \boldsymbol{\xi})$ denotes the DQD Liouvillian with counting fields describing the matter and energy transfers to left and right DQD leads, and where $\mathcal{L}_{\mathrm{dt}}(\chi)$ is defined by Eq. (8.81). The fact that the measurement is hardly invasive is also exemplified by the fact that the fluctuation theorem for the DQD, exemplified by an existing symmetry of the form, compare Eq. (4.140),

$$\mathcal{L}^T_{\mathrm{DQD}}(-\boldsymbol{\chi} - \mathrm{i}\boldsymbol{A}, -\boldsymbol{\xi} - \mathrm{i}\boldsymbol{B}) = \mathcal{L}_{\mathrm{DQD}}(\boldsymbol{\chi}, \boldsymbol{\xi})\,, \qquad \boldsymbol{A} = (-\mu_L\beta_L, -\mu_R\beta_R)\,, \qquad \boldsymbol{B} = (\beta_L, \beta_R)\,, \tag{8.83}$$

is not changed by the presence of the detector

$$\mathcal{L}^T(-\boldsymbol{\chi} - \mathrm{i}\boldsymbol{A}, -\boldsymbol{\xi} - \mathrm{i}\boldsymbol{B}, \chi) = \mathcal{L}(\boldsymbol{\chi}, \boldsymbol{\xi}, \chi)\,, \tag{8.84}$$

since the counting field of the latter only occurs on the diagonal. To interpret the outcome of the detector, we consider Fig. 8.6.

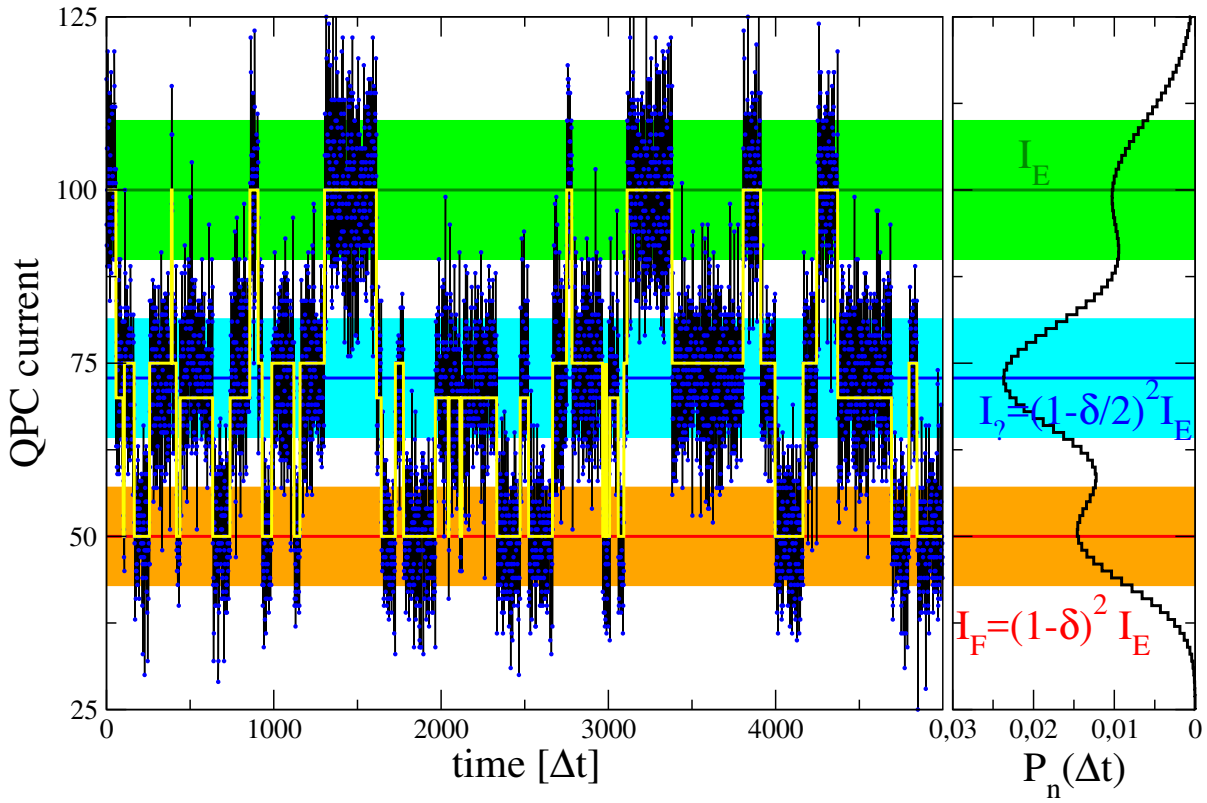

Figure 8.6: Left: Simulated QPC current when the DQD is allowed to experience slow occupation changes. Solid lines and shaded regions correspond to mean current and noise, respectively. The yellow curve depicts the actual state of the system, ordered from top to bottom values as $|v_0\rangle$, $|v_-\rangle$, $|v_+\rangle$, and $|v_2\rangle$, respectively. Right: Corresponding histogram for infinitely long sampling of the trajectory – calculated by computing the weighted average (for the chosen parameters we have $P_0 = P_- = P_+ = P_2 = 1/4$) of Poissonian distributions for the respective QPC currents. In contrast to Fig. 8.4, there are now three QPC currents observed, and two thresholds can be defined. By collecting all measurement outcomes above the upper threshold into the outcome empty (E) and all measurement outcomes below the lower threshold as corresponding to the outcome filled (F), we can implement the measurement superoperators as before. However, in addition there is now a third outcome (inconclusive). When measuring the medium current, the probability for the left dot to be occupied or empty is 1/2. Other parameters as in Fig. 4.6.

There, one can observe three currents, where the lowest one corresponds to a doubly filled DQD, and the highest one to an empty DQD. The intermediate current corresponds to a singly-charged DQD, where however due to the high symmetry we cannot resolve the location of the charge. Therefore, upon measuring this intermediate current, the probability to find the monitored empty or filled is just one half, respectively. This measurement outcome should therefore be termed inconclusive. The Liouvillian superoperators obey due to our special choice of operators $[\mathcal{J}, \mathcal{L}_0] = 0$. In this case, we can compute the effective measurement propagator exactly

$$\mathcal{K}_n(\Delta t) = \frac{1}{2\pi}\int_{-\pi}^{+\pi} e^{e^{+i\chi}\mathcal{J}\Delta t + \mathcal{L}_0\Delta t - in\chi} d\chi = \frac{\mathcal{J}^n \Delta t^n}{n!} e^{\mathcal{L}_0 \Delta t}\,, \tag{8.85}$$

and by defining the thresholds $n_1 < n_2$, we can define the measurement superoperators in the same

way as we did before

$$\mathcal{K}_E = \sum_{n\geq n_2} \mathcal{K}_n(\Delta t)\,, \qquad \mathcal{K}_? = \sum_{n_1<n<n_2} \mathcal{K}_n(\Delta t)\,, \qquad \mathcal{K}_F = \sum_{n\leq n_1} \mathcal{K}_n(\Delta t)\,. \tag{8.86}$$

In contrast to the single quantum dot however, the measurement – when performed on a singly-charged state – does not resolve the site of the electron. Furthermore, not considering the counting statistics of the QPC at all ($\chi \to 0$), we see that the associated Liouvillian vanishes and therefore we have

$$\mathcal{K}_E + \mathcal{K}_? + \mathcal{K}_F = \mathbf{1}\,, \tag{8.87}$$

a consequence of our simplifications.

Note that the equations would be more complicated if we allowed the QPC to exchange energy with the DQD system (e.g. finite $\gamma_{21}(\pm 2T)$, such that e.g. the blue transition in Fig. 8.5 would be allowed) or of we would make the DQD more asymmetric $\epsilon_L \neq \epsilon_R$. Then also the original fluctuation theorem would be modified, and depending on the system configuration one may also observe four different currents instead of three, allowing for the possibility to locate the electron.

8.2.3 Triple quantum dot:Least invasive measurement

Now, we consider a serial double quantum dot (TQD), which for simplicity we choose highly symmetric and in addition without Coulomb interaction

$$H_S = \epsilon(d_L^\dagger d_L + d_C^\dagger d_C + d_R^\dagger d_R) + T_L(d_L d_C^\dagger + d_C d_L^\dagger) + T_R(d_R d_C^\dagger + d_C d_R^\dagger)\,. \tag{8.88}$$

The spectrum of the TQD can in this simple case also be obtained analytically

$$\begin{aligned}
|v_0\rangle &= |000\rangle\,, \qquad E_0 = 0\,,\\
|v_1^-\rangle &= \frac{1}{\sqrt{2+2\frac{T_R^2}{T_L^2}}}|100\rangle - \frac{1}{\sqrt{2}}|010\rangle + \frac{1}{\sqrt{2+2\frac{T_L^2}{T_R^2}}}|001\rangle\,, \qquad E_1^- = \epsilon - \sqrt{T_L^2+T_R^2}\,,\\
|v_1^0\rangle &= -\sqrt{\frac{T_R^2}{T_L^2+T_R^2}}|100\rangle + \frac{1}{\sqrt{1+\frac{T_R^2}{T_L^2}}}|001\rangle\,, \qquad E_1^0 = \epsilon\,,\\
|v_1^+\rangle &= \frac{1}{\sqrt{2+2\frac{T_R^2}{T_L^2}}}|100\rangle + \frac{1}{\sqrt{2}}|010\rangle + \frac{1}{\sqrt{2+2\frac{T_L^2}{T_R^2}}}|001\rangle\,, \qquad E_1^+ = \epsilon + \sqrt{T_L^2+T_R^2}\,,\\
|v_2^-\rangle &= \frac{1}{\sqrt{2+2\frac{T_L^2}{T_R^2}}}|110\rangle - \frac{1}{\sqrt{2}}|101\rangle + \frac{1}{\sqrt{2+2\frac{T_R^2}{T_L^2}}}|011\rangle\,, \qquad E_2^- = 2\epsilon - \sqrt{T_L^2+T_R^2}\,,\\
|v_2^0\rangle &= -\sqrt{\frac{T_L^2}{T_L^2+T_R^2}}|110\rangle + \frac{1}{\sqrt{1+\frac{T_L^2}{T_R^2}}}|011\rangle\,, \qquad E_2^0 = 2\epsilon\,,\\
|v_2^+\rangle &= \frac{1}{\sqrt{2+2\frac{T_L^2}{T_R^2}}}|110\rangle + \frac{1}{\sqrt{2}}|101\rangle + \frac{1}{\sqrt{2+2\frac{T_R^2}{T_L^2}}}|011\rangle\,, \qquad E_2^+ = 2\epsilon + \sqrt{T_L^2+T_R^2}\,,\\
|v_3\rangle &= |111\rangle\,, \qquad E_3 = 3\epsilon\,.
\end{aligned} \tag{8.89}$$

We see that the splitting between states of equal charge that have a non-vanishing matrix element with the operator $d_C^\dagger d_C$ is $\Delta E = 2\sqrt{T_L^2+T_R^2}$.

When the point contact measures the central dot, i.e., $A_1 = A_2 = \mathbf{1} - \delta d_C^\dagger d_C$, the transformation into the interaction picture becomes

$$\begin{aligned}
\boldsymbol{A}(t) &= \mathbf{1} - \delta e^{+\mathrm{i}H_S t} d_C^\dagger d_C e^{-\mathrm{i}H_S t} \\
&= \mathbf{1} - \delta \frac{T_R^2}{T_L^2+T_R^2} \sin^2(t\sqrt{T_L^2+T_R^2}) d_R^\dagger d_R - \delta \frac{T_L^2}{T_L^2+T_R^2} \sin^2(t\sqrt{T_L^2+T_R^2}) d_L^\dagger d_L \\
&\quad -\delta \cos^2(t\sqrt{T_L^2+T_R^2}) d_C^\dagger d_C + \delta \frac{T_L T_R}{T_L^2+T_R^2} \sin^2(t\sqrt{T_L^2+T_R^2})(d_L d_R^\dagger + d_R d_L^\dagger) \\
&\quad +\delta \frac{\mathrm{i}T_L}{\sqrt{T_L^2+T_R^2}} \sin(t\sqrt{T_L^2+T_R^2}) \cos(t\sqrt{T_L^2+T_R^2})(d_L d_C^\dagger - d_C d_L^\dagger) \\
&\quad -\delta \frac{\mathrm{i}T_R}{\sqrt{T_L^2+T_R^2}} \sin(t\sqrt{T_L^2+T_R^2}) \cos(t\sqrt{T_L^2+T_R^2})(d_C d_R^\dagger - d_R d_C^\dagger) \\
&= A_- e^{-2\mathrm{i}t\sqrt{T_L^2+T_R^2}} + A_0 + A_+ e^{+2\mathrm{i}t\sqrt{T_L^2+T_R^2}} \,. \qquad (8.90)
\end{aligned}$$

Here, we have specifically

$$\begin{aligned}
A_0 &= \mathbf{1} - \delta \frac{T_R^2}{2(T_L^2+T_R^2)} d_R^\dagger d_R - \delta \frac{T_L^2}{2(T_L^2+T_R^2)} d_L^\dagger d_L - \delta \frac{1}{2} d_C^\dagger d_C + \delta \frac{T_L T_R}{2(T_L^2+T_R^2)}(d_L d_R^\dagger + d_R d_L^\dagger) \,, \\
A_- &= +\delta \frac{T_R^2}{4(T_L^2+T_R^2)} d_R^\dagger d_R + \delta \frac{T_L^2}{2(T_L^2+T_R^2)} d_L^\dagger d_L - \delta \frac{1}{4} d_C^\dagger d_C - \delta \frac{T_L T_R}{4(T_L^2+T_R^2)}(d_L d_R^\dagger + d_R d_L^\dagger) \\
&\quad -\delta \frac{T_L}{4\sqrt{T_L^2+T_R^2}}(d_L d_C^\dagger - d_C d_L^\dagger) + \delta \frac{T_R}{4\sqrt{T_L^2+T_R^2}}(d_C d_R^\dagger - d_R d_C^\dagger) \,, \\
A_+ &= +\delta \frac{T_R^2}{4(T_L^2+T_R^2)} d_R^\dagger d_R + \delta \frac{T_L^2}{2(T_L^2+T_R^2)} d_L^\dagger d_L - \delta \frac{1}{4} d_C^\dagger d_C - \delta \frac{T_L T_R}{4(T_L^2+T_R^2)}(d_L d_R^\dagger + d_R d_L^\dagger) \\
&\quad +\delta \frac{T_L}{4\sqrt{T_L^2+T_R^2}}(d_L d_C^\dagger - d_C d_L^\dagger) - \delta \frac{T_R}{4\sqrt{T_L^2+T_R^2}}(d_C d_R^\dagger - d_R d_C^\dagger) \,. \qquad (8.91)
\end{aligned}$$

The dissipator then becomes in the unidirectional transport limit (under neglect of Lamb-shift and taking $\tau \to \infty$)

$$\begin{aligned}
\dot{\boldsymbol{\rho}}_{\mathbf{S}} &= \gamma_{21}(+2\sqrt{T_L^2+T_R^2}) \left[e^{+\mathrm{i}\chi} A_- \boldsymbol{\rho}_{\mathbf{S}} A_+ - \frac{1}{2} \{A_+ A_-, \boldsymbol{\rho}_{\mathbf{S}}\} \right] \\
&\quad +\gamma_{21}(-2\sqrt{T_L^2+T_R^2}) \left[e^{+\mathrm{i}\chi} A_+ \boldsymbol{\rho}_{\mathbf{S}} A_- - \frac{1}{2} \{A_- A_+, \boldsymbol{\rho}_{\mathbf{S}}\} \right] \\
&\quad +\gamma_{21}(0) \left[e^{+\mathrm{i}\chi} A_0 \boldsymbol{\rho}_{\mathbf{S}} A_0 - \frac{1}{2} \{A_0 A_0, \boldsymbol{\rho}_{\mathbf{S}}\} \right] . \qquad (8.92)
\end{aligned}$$

The presence of the detector may now induce transitions between eigenstates of the same charge, Fig. 8.7.

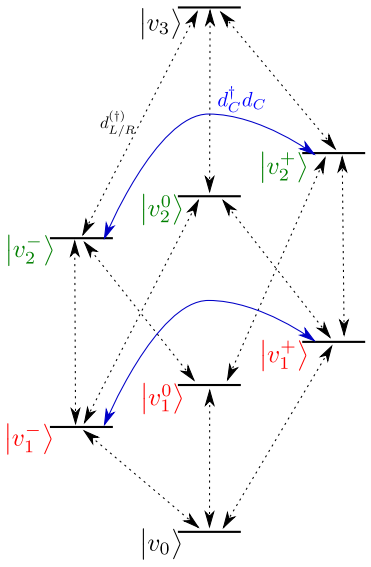

Figure 8.7: Sketch of the energy levels of the TQD. Tunnel-couplings to further leads from left and right dots may induce the dotted transitions, whereas the coupling to the QPC may only induce transition between the singly-charged states (solid blue) with energy difference $\Delta E = 2\sqrt{T_L^2 + T_R^2}$.

However, to obtain the least invasive detector we consider a limit where the detector does not inject energy, by considering the limit $\gamma_{21}(\pm 2\sqrt{T_L^2 + T_R^2}) \to 0$, i.e.,

$$\dot{\boldsymbol{\rho}}_{\mathbf{S}} \;=\; \gamma_{21}(0)\left[e^{+\mathrm{i}\chi} A_0 \boldsymbol{\rho}_{\mathbf{S}} A_0 - \frac{1}{2}\left\{A_0 A_0, \boldsymbol{\rho}_{\mathbf{S}}\right\}\right] . \tag{8.93}$$

That in this case the detector does not inject energy is also exemplified by the relation $[H_S, A_0] = 0$. However, now even in absence of counting $\xi \to 0$, the effect of the detector is non-trivial. In contrast to the DQD, the dissipator $\mathcal{L}(0)$ does not vanish. This is essentially due to the fact that the system energy eigenstates with a different occupation of the central dot have different energies, compare $|v_1^0\rangle$ with $|v_1^\pm\rangle$ and $|v_2^0\rangle$ with $|v_2^\pm\rangle$.

By sandwiching the dissipator, we get the following equations for the diagonal entries (for simplicity, we only state these as we assume that the coherences are damped away in the long-term limit by additional leads attached to the TQD left and right)

$$\begin{aligned}
\dot{\rho}_0 &= \gamma(e^{+\mathrm{i}\chi} - 1)\rho_0 \,, \\
\dot{\rho}_{10} &= \gamma(e^{+\mathrm{i}\chi} - 1)\rho_{10} \,, \\
\dot{\rho}_{1-} &= \gamma(1-\delta/2)^2(e^{+\mathrm{i}\chi} - 1)\rho_{1-} \,, \\
\dot{\rho}_{1+} &= \gamma(1-\delta/2)^2(e^{+\mathrm{i}\chi} - 1)\rho_{1+} \,, \\
\dot{\rho}_{2-} &= \gamma(1-\delta/2)^2(e^{+\mathrm{i}\chi} - 1)\rho_{2-} \,, \\
\dot{\rho}_{2+} &= \gamma(1-\delta/2)^2(e^{+\mathrm{i}\chi} - 1)\rho_{2+} \,, \\
\dot{\rho}_{20} &= \gamma(1-\delta)^2(e^{+\mathrm{i}\chi} - 1)\rho_{20} \,, \\
\dot{\rho}_3 &= \gamma(1-\delta)^2(e^{+\mathrm{i}\chi} - 1)\rho_3 \,.
\end{aligned} \tag{8.94}$$

The equations for the 12 allowed coherences are similar with one exception (not shown): As $\chi \to 0$, the QPC has a non-vanishing effect on some of the coherences. As with the DQD, we can identify three currents: $I_E = \gamma$, when the central dot is empty with certainty, $I_1 = \gamma(1-\delta/2)$, when the central dot is empty with probability 1/2, and $I_F = \gamma(1-\delta)^2$, when the central dot is filled with certainty. We can readily set up the BMS rate equation in the energy eigenbasis of the TQD

$$\dot{\rho}_{aa} = \sum_b \gamma_{ab,ab}\rho_{bb} - \sum_b \gamma_{ba,ba}\rho_{aa} \,, \qquad \gamma_{ab} = \sum_{\alpha\beta} \gamma_{\alpha\beta}(E_b - E_a)\,\langle a|\, A_\beta\,|b\rangle\,\langle a|\, A_\alpha^\dagger\,|b\rangle^* \,, \tag{8.95}$$

which for brevity we do not show explicitly here. Fig. 8.7 may serve as a guidance here, for example, the rate to relax from $|v_1^0\rangle$ to $|v_0\rangle$ is given by

$$R_{0,10} = \Gamma_L[1 - f_L(\epsilon)]\frac{T_R^2}{T_L^2 + T_R^2} + \Gamma_R[1 - f_R(\epsilon)]\frac{1}{1 + \frac{T_R^2}{T_L^2}}\,. \tag{8.96}$$

We can set up the full master equation as before, and, as the QPC counting field only enters on the diagonal, the same arguments as before apply, such that the TQD fluctuation theorem is not modified in this limit. In a similar fashion as for the DQD, we can also generate trajectories for the QPC current. The result (not shown) looks just as the curve with symbols in Fig. 8.6, and again the possibility of an inconclusive measurement result occurs. However, even when one measures e.g. a high current with sufficient confidence, one is not sure whether the TQD is actually in the state $|v_0\rangle$ or in the state $|v_1^0\rangle$. This limitation of measurement is something fundamental and related to the uncertainty relation.

From the results of the last two sections, we see that a minimally invasive detector (leading only to dephasing in the system energy eigenbasis) does not completely fulfil the purpose for which it was constructed: It measures populations of energy eigenstates instead of populations of sites, which need not always coincide and therefore induces an inconclusive outcome. Below, we will discuss a variant of the detector that measures the local occupation.

8.2.4 Strongly-coupled QPC

Suppose that we have as before a system-QPC interaction of the form

$$H_I = (\mathbf{1} - \delta d^\dagger d)\left[\sum_{kk'} t_{kk'}\gamma_{kL}\gamma_{k'R}^\dagger + \text{h.c.}\right]\,, \tag{8.97}$$

which is however strong in comparison to the system Hamiltonian. Then, it is more advisable to go to the interaction picture only with respect to the reservoir Hamiltonian, thereby treating H_I and H_S on equal footing. Essentially, this just means that we add the commutator with the system Hamiltonian in the dissipator and neglect the time-dependence of the system coupling operators in the derivation of the master equation, effectively implementing the so-called **singular coupling limit** [1]. Then, the dissipator for any system (SQD, DQD, TQD, ...) looks very similar to the dissipator for the single quantum dot (8.61), except that it is already in the Schrödinger picture

$$\begin{aligned}\dot{\rho_{\rm S}} &= -\mathrm{i}\,[H_S, \rho_{\rm S}] - \mathrm{i}\left[\frac{1}{2\mathrm{i}}\left(\sigma_{12}(0) + \sigma_{21}(0)\right)(1 - \delta d^\dagger d)^2, \rho_{\rm S}\right] \\ &\quad + \frac{tV}{e^{\beta V} - 1}\left[e^{-\mathrm{i}\chi}(1 - \delta d^\dagger d)\rho_{\rm S}(1 - \delta d^\dagger d) - \frac{1}{2}\left\{(1 - \delta d^\dagger d)^2, \rho_{\rm S}\right\}\right] \\ &\quad + \frac{tV}{1 - e^{-\beta V}}\left[e^{+\mathrm{i}\chi}(1 - \delta d^\dagger d)\rho_{\rm S}(1 - \delta d^\dagger d) - \frac{1}{2}\left\{(1 - \delta d^\dagger d)^2, \rho_{\rm S}\right\}\right]\,.\end{aligned} \tag{8.98}$$

Neglecting the Lamb-shift and considering the unidirectional QPC transport limit, it assumes the form

$$\mathcal{L}_{\rm dt}(\chi)\rho_{\rm S} = \gamma\left[e^{+\mathrm{i}\chi}(1 - \delta d^\dagger d)\rho_{\rm S}(1 - \delta d^\dagger d) - \frac{1}{2}\left\{(1 - \delta d^\dagger d)^2, \rho_{\rm S}\right\}\right] = e^{+\mathrm{i}\chi}\mathcal{J}\rho - \mathcal{J}_0\rho\,. \tag{8.99}$$

We see that by averaging over all particle measurement outcomes ($\chi \to 0$), we can write the dissipator as

$$\mathcal{L}_{\rm dt}(0)\rho_{\rm S} = -\gamma\frac{\delta^2}{2}\left[dd^\dagger\rho d^\dagger d + d^\dagger d\rho dd^\dagger\right] . \tag{8.100}$$

This just damps the coherences in the localized basis.

When the QPC is coupled to the central dot of a TQD that is in turn coupled to two leads as before, we can always represent the most general density matrix in the localized basis of the TQD as

$$\rho = \begin{pmatrix} \rho_{000,000} & & & & & & & & \\ & \rho_{100,100} & \rho_{100,010} & \rho_{100,001} & & & & & \\ & \rho_{010,100} & \rho_{010,010} & \rho_{010,001} & & & & & \\ & \rho_{001,100} & \rho_{001,010} & \rho_{001,001} & & & & & \\ & & & & \rho_{110,110} & \rho_{110,101} & \rho_{110,011} & & \\ & & & & \rho_{101,110} & \rho_{101,101} & \rho_{101,011} & & \\ & & & & \rho_{011,110} & \rho_{011,101} & \rho_{011,011} & & \\ & & & & & & & \rho_{111,111} & \end{pmatrix} . \tag{8.101}$$

Here, the coherences shown in red will be damped away when the dissipator is applied sufficiently often or strongly. However, the deleted coherences are very vital for transport: To lowest order, it is not possible for an electron to travel from the left dot to the right (e.g. from $|100\rangle$ to $|001\rangle$) and vice versa without populating these coherences shown in red. Therefore, when the central dot is monitored sufficiently often/strongly, the transport through it is completely blocked – a manifestation of the quantum Zeno effect.

Since for this dissipator we have $[\mathcal{J}, \mathcal{J}_0] = \mathbf{0}$, we can calculate the quantities for detection analytically

$$\mathcal{K}_n(\Delta t) = \frac{1}{2\pi}\int_{-\pi}^{+\pi} e^{\mathcal{L}_{\rm dt}(\chi)\Delta t - {\rm i}n\chi}d\chi = \frac{\mathcal{J}^n\Delta t^n}{n!}e^{-\mathcal{J}_0\Delta t} . \tag{8.102}$$

In particular, we use the identity

$$(\mathbf{1} - \delta d^\dagger d)^n = \left[dd^\dagger + (1-\delta)d^\dagger d\right]^n = dd^\dagger + (1-\delta)^n d^\dagger d . \tag{8.103}$$

to compute

$$\begin{aligned}
\mathcal{J}^n\rho &= \gamma^n \left[dd^\dagger + (1-\delta)^n d^\dagger d\right] \rho \left[dd^\dagger + (1-\delta)^n d^\dagger d\right] , \\
e^{-\mathcal{J}_0\Delta t}\rho &= \sum_{n=0}^{\infty} \frac{(-1)^n\gamma^n\Delta t^n}{2^n n!} \left[1-\delta d^\dagger d\right]^{2n} \rho \sum_{m=0}^{\infty} \frac{(-1)^m\gamma^m\Delta t^m}{2^m m!} \left[1-\delta d^\dagger d\right]^{2m} \\
&= \sum_{n=0}^{\infty} \frac{(-1)^n\gamma^n\Delta t^n}{2^n n!} \left[dd^\dagger + (1-\delta)^{2n} d^\dagger d\right] \rho \sum_{n=0}^{\infty} \frac{(-1)^m\gamma^m\Delta t^m}{2^m m!} \left[dd^\dagger + (1-\delta)^{2m} d^\dagger d\right]^m \\
&= \left[e^{-\gamma/2\Delta t} dd^\dagger + e^{-\gamma/2\Delta t(1-\delta)^2} d^\dagger d\right] \rho \left[e^{-\gamma/2\Delta t} dd^\dagger + e^{-\gamma/2\Delta t(1-\delta)^2} d^\dagger d\right] \\
&= e^{-\gamma\Delta t} dd^\dagger\rho dd^\dagger + e^{-\gamma(1-\delta)^2\Delta t} d^\dagger d\rho d^\dagger d + e^{-\gamma(1-\delta+\delta^2/2)\Delta t} \left(dd^\dagger\rho d^\dagger d + d^\dagger d\rho dd^\dagger\right) , \\
e^{+\mathcal{J}e^{+i\chi}\Delta t}\rho &= \sum_{n=0}^{\infty} \frac{\gamma^n\Delta t^n e^{+in\chi}}{n!} \left[dd^\dagger + (1-\delta)^n d^\dagger d\right] \rho \left[dd^\dagger + (1-\delta)^n d^\dagger d\right] \\
&= \sum_{n=0}^{\infty} \frac{\gamma^n\Delta t^n e^{in\chi}}{n!} \left[dd^\dagger\rho dd^\dagger + (1-\delta)^{2n} d^\dagger d\rho d^\dagger d + (1-\delta)^n \left(dd^\dagger\rho d^\dagger d + d^\dagger d\rho dd^\dagger\right)\right] \\
&= e^{+\gamma\Delta t e^{+i\chi}} dd^\dagger\rho dd^\dagger + e^{+\gamma\Delta t(1-\delta)^2 e^{+i\chi}} d^\dagger d\rho d^\dagger d + e^{+\gamma\Delta t(1-\delta)e^{+i\chi}} \left(dd^\dagger\rho d^\dagger d + d^\dagger d\rho dd^\dagger\right) .
\end{aligned} \tag{8.104}$$

In particular, from combining the last two identities we obtain for the action of the full dissipator

$$e^{\mathcal{L}_{\rm dt}(0)\Delta t}\rho = dd^\dagger\rho dd^\dagger + d^\dagger d\rho d^\dagger d + e^{-\gamma\Delta t\delta^2/2} \left(dd^\dagger\rho d^\dagger d + d^\dagger d\rho dd^\dagger\right) . \tag{8.105}$$

From this, we obtain that the exponential of this particular dissipator has a very similar action than the dissipator itself

$$\left(e^{\mathcal{L}_{\rm dt}(0)\Delta t} - \mathbf{1}\right)\rho = \left(e^{-\gamma\Delta t\delta^2/2} - 1\right) \left(dd^\dagger\rho d^\dagger d + d^\dagger d\rho dd^\dagger\right) = \frac{1-e^{-\gamma\Delta t\delta^2/2}}{\gamma\delta^2/2} \mathcal{L}_{\rm dt}(0)\rho . \tag{8.106}$$

This can be helpful to evaluate the energy change of the system during such a measurement of duration Δt

$$\Delta E = {\rm Tr}\left\{H_S \left(e^{\mathcal{L}_{\rm dt}(0)\Delta t} - \mathbf{1}\right)\rho\right\} = \frac{1-e^{-\gamma\Delta t\delta^2/2}}{\gamma\delta^2/2} {\rm Tr}\left\{H_S(\mathcal{L}_{\rm dt}(0)\rho)\right\} , \tag{8.107}$$

which enables to define a current

$$I_E^{\rm ms} = \frac{\Delta E}{\Delta t} = \frac{1-e^{-\alpha}}{\alpha} {\rm Tr}\left\{H_S(\mathcal{L}_{\rm dt}(0)\rho)\right\} , \qquad \alpha = \frac{\gamma\Delta t\delta^2}{2} . \tag{8.108}$$

For small α, this corresponds to the usual phenomenologically defined current, whereas for large α, this tends to zero. We also note that the prefactor is always smaller than one.

We can be more specific and ask for the system energy change for a specific measurement outcome

$$\Delta E_n = {\rm Tr}\left\{H_S \left(\frac{\mathcal{K}_n(\Delta t)\rho}{{\rm Tr}\left\{\mathcal{K}_n(\Delta t)\rho\right\}} - \rho\right)\right\} , \tag{8.109}$$

or – after having defined a suitable threshold to separate between just two outcomes (empty and filled) – for the average system energy change under measuring the outcome empty (E) or filled (F), respectively

$$\Delta E_E = \frac{1}{P_E} {\rm Tr}\left\{H_S(\mathcal{K}_E(\Delta t) - P_E)\rho\right\} , \qquad \Delta E_F = \frac{1}{P_F} {\rm Tr}\left\{H_S(\mathcal{K}_F(\Delta t) - P_F)\rho\right\} , \tag{8.110}$$

where $P_E = \mathrm{Tr}\,\{\mathcal{K}_E(\Delta t)\rho\}$ and $P_F = \mathrm{Tr}\,\{\mathcal{K}_F(\Delta t)\rho\}$, respectively. For these questions it is helpful to compute

$$\begin{aligned}\mathcal{K}_n(\Delta t)\rho &= \frac{(\gamma\Delta t)^n}{n!}e^{-\gamma\Delta t}dd^\dagger\rho dd^\dagger + \frac{(\gamma\Delta t(1-\delta)^2)^n}{n!}e^{-\gamma\Delta t(1-\delta)^2}d^\dagger d\rho d^\dagger d \\ &\quad + \frac{(\gamma\Delta t(1-\delta))^n}{n!}e^{-\gamma\Delta t(1-\delta)}e^{-\gamma\Delta t\delta^2/2}\left(dd^\dagger\rho d^\dagger d + d^\dagger d\rho dd^\dagger\right) . \end{aligned} \tag{8.111}$$

It may be convenient to parametrize such a measurement by just two dimensionless numbers $0 \ll y \ll x$

$$x = \gamma\Delta t\,, \qquad y = \gamma\Delta t(1-\delta)^2\,. \tag{8.112}$$

Then, we have

$$\sqrt{xy} = \gamma\Delta t(1-\delta)\,, \qquad \frac{\gamma\Delta t\delta^2}{2} = \frac{(\sqrt{x}-\sqrt{y})^2}{2}\,, \tag{8.113}$$

which completely defines the measurement superoperators. The measurement becomes strong (in the sense that it deletes coherences) when x and y are very different, and it also becomes error-free (projective) when both x and y are very large but different. It becomes completely non-invasive (after normalization), when $x = y$.

From summing up all outcomes up to a threshold $n_{\rm th}$, we get the propagator for the coarse-grained measurement result *filled*

$$\begin{aligned}\mathcal{K}_F\rho &= \frac{\Gamma(n_{\rm th}+1,\gamma\Delta t)}{\Gamma(n_{\rm th}+1)}dd^\dagger\rho dd^\dagger + \frac{\Gamma(n_{\rm th}+1,\gamma\Delta t(1-\delta)^2)}{\Gamma(n_{\rm th}+1)}d^\dagger d\rho d^\dagger d \\ &\quad + \frac{\Gamma(n_{\rm th}+1,\gamma\Delta t(1-\delta))}{\Gamma(n_{\rm th}+1)}e^{-\gamma\Delta t\delta^2/2}\left(dd^\dagger\rho d^\dagger d + d^\dagger d\rho dd^\dagger\right) , \end{aligned} \tag{8.114}$$

and from $\mathcal{K}_E + \mathcal{K}_F = e^{\mathcal{L}_{\rm dt}\Delta t}$ we conclude for the result *empty*

$$\begin{aligned}\mathcal{K}_E\rho &= \left(1 - \frac{\Gamma(n_{\rm th}+1,\gamma\Delta t)}{\Gamma(n_{\rm th}+1)}\right)dd^\dagger\rho dd^\dagger + \left(1 - \frac{\Gamma(n_{\rm th}+1,\gamma\Delta t(1-\delta)^2)}{\Gamma(n_{\rm th}+1)}\right)d^\dagger d\rho d^\dagger d \\ &\quad + \left(1 - \frac{\Gamma(n_{\rm th}+1,\gamma\Delta t(1-\delta))}{\Gamma(n_{\rm th}+1)}\right)e^{-\gamma\Delta t\delta^2/2}\left(dd^\dagger\rho d^\dagger d + d^\dagger d\rho dd^\dagger\right) . \end{aligned} \tag{8.115}$$

The function $f(n_{\rm th},x) \equiv \frac{\Gamma(n_{\rm th}+1,x)}{\Gamma(n_{\rm th}+1)}$ behaves similar to a Fermi function as a function of x, it is always between 0 and 1, in particular it is 1 when $x \ll n_{\rm th}$ and it is zero when $x \gg n_{\rm th}$. Its steepest descent is found at $x^* = n_{\rm th}$, for which an optimal value can also be expressed in terms of x and y

$$n_{\rm th} = \frac{x-y}{\ln\frac{x}{y}}\,. \tag{8.116}$$

With the additional suppression of coherences, these measurement superoperators indeed approach ideal projectors onto the empty or filled state, respectively. Furthermore, being the exponential of Lindblad evolutions, they preserve the density matrix properties (after normalization), i.e., they automatically implement a weak measurement of the occupation, with the limit $\gamma\Delta t\delta^2/2 \to \infty$ limit of a strong measurement (deleting the coherences).

We now consider a series of infinitesimally short measurements, parametrized only by x and y and performed at timesteps of $\Delta\tau > 0$, in between which the Liouvillian $\mathcal{L}_{\rm TQD}$ of a triple quantum dot shall be acting. The density matrix at time $t + \Delta\tau$ can then be iteratively obtained

$$\rho(t+\Delta\tau) = \frac{1}{P_n(x,y)} e^{\mathcal{L}_{\rm TQD}\Delta\tau} \mathcal{K}_n(x,y)\rho(t)\,, \qquad P_n(x,y) = {\rm Tr}\left\{\mathcal{K}_n(x,y)\rho(t)\right\}\,, \tag{8.117}$$

where $P_n(x,y)$ denotes the probability to measure n particles. We can now check how different measurement schemes affect the subsequent evolution [3], see Fig. 8.8. In the first three panels

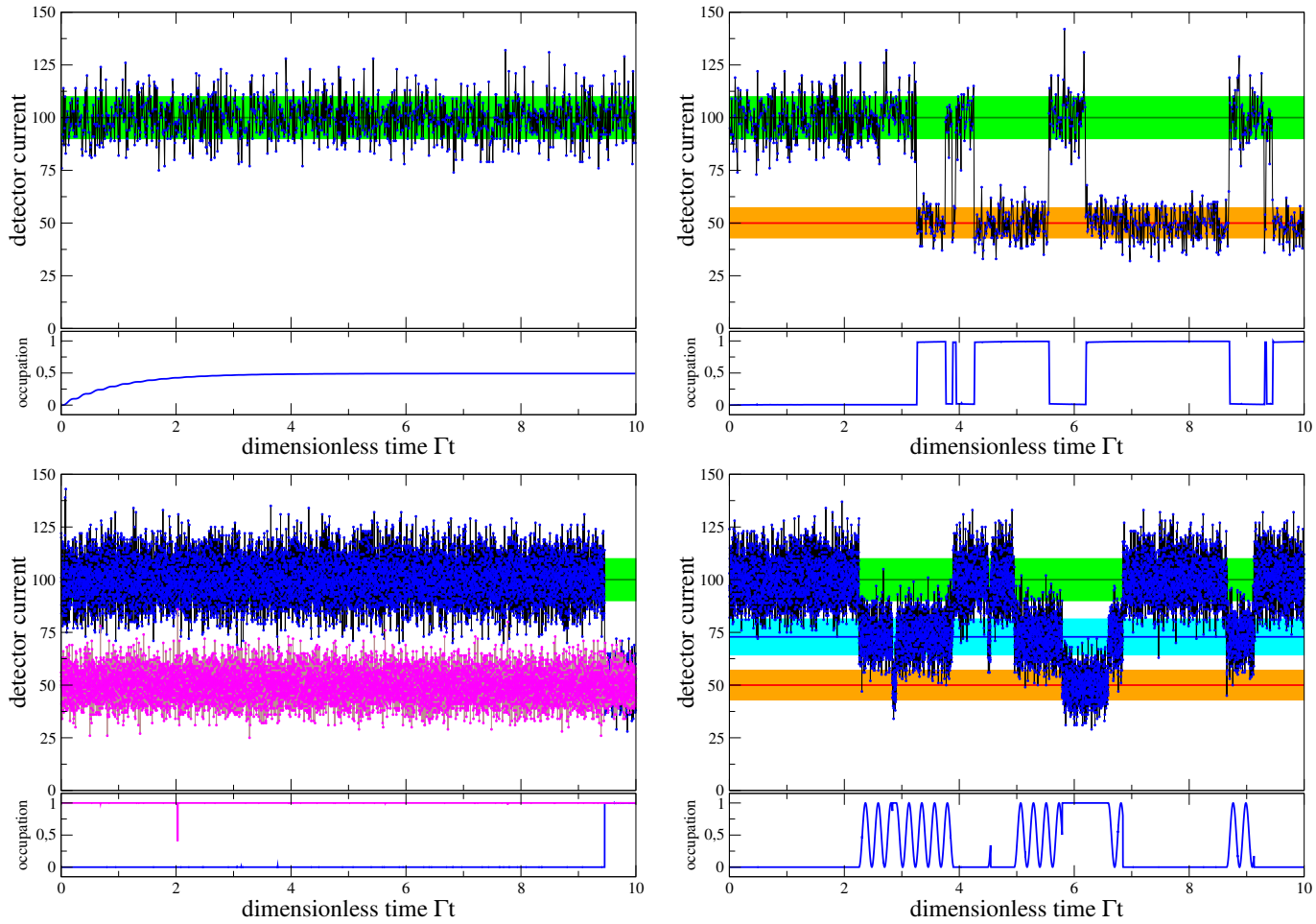

Figure 8.8: Plot of detector current trajectories (symbols) and system occupations (curves) for a completely insensitive detector (top left), an invasive detector (top right), an invasive detector which measures 10 times more frequently (bottom left, for different initial conditions) and a non-invasive QND detector which measures also very frequently but in the energy eigenbasis (bottom right). Parameters: $\Gamma_L = \Gamma_R = \Gamma$, $\beta_L = \beta_R = \beta$, $T_L = T_R = T$, $\beta\Gamma = 0.01$, $\beta T = 0.1$, $\beta\mu_L = +5 = -\beta\mu_R$, $\beta\epsilon = 1$, $x = 100$, $y = 50$ (top left: $y = 100$), $\Gamma\Delta t = 0.01$ (top panels), $\Gamma\Delta t = 0.001$ (bottom panels).

of Fig. 8.8 we consider a measurement in the site basis, derived within the singular-coupling limit, described by the exponential of Eq. (8.99). In the last (bottom right) panel we consider a non-invasive quantum non-demolishion (QND) measurement, described by the exponential of Eq. (8.93).

First, when $x = y$ (top left), the detector (here measuring in the local basis) is not sensitive to the system and it does not influence its dynamics. The detector statistics is just Poissonian and the system behaves as if it was not monitored. When the detector measures in the local basis (top right) and is sensitive to the system occupation, the repeated application of the measurement leads to the superposition of two Poissonian processes for the detector statistics, and projects the system density matrix, suppressing coherences. An even more frequent application of the measurement (bottom left) leads for an invasive detector to the suppression of coherences, quantum-Zeno trapping the population of the central dot, independent of the initial condition (blue and magenta). Significantly less jumps are observed. Finally, for measuring non-invasively in the energy eigenbasis (bottom right), a third, inconclusive, outcome is introduced in the detector statistics, during which the system evolves coherently as if it was decoupled from the leads.

Bibliography

[1] H.-P. Breuer and F. Petruccione. *The Theory of Open Quantum Systems*. Oxford University Press, Oxford, 2002.

[2] G. Schaller. *Open Quantum Systems Far from Equilibrium*, volume 881 of *Lecture Notes in Physics*. Springer, 2014.

[3] H. M. Wiseman and G. J. Milburn. *Quantum Measurement and Control*. Cambridge University Press, 2010.

[4] G. Lindblad. On the generators of quantum dynamical semigroups. *Communications in Mathematical Physics*, 48:119–130, 1976.

[5] V. Gorini, A. Kossakowski, and E. C. G. Sudarshan. Completely positive dynamical semigroups of n-level systems. *Journal of Mathematical Physics*, 17:821, 1976.

[6] Gregory Bulnes Cuetara, Massimiliano Esposito, and Gernot Schaller. Quantum thermodynamics with degenerate eigenstate coherences. *Entropy*, 18(12):447, 2016.

[7] Göran Lindblad. Completely positive maps and entropy inequalities. *Communications in Mathematical Physics*, 40:147, 1975.

[8] Herbert Spohn. Entropy production for quantum dynamical semigroups. *Journal of Mathematical Phyics*, 19:1227, 1978.

[9] C. Flindt, C. Fricke, F. Hohls, T. Novotny, K. Netocny, T. Brandes, and R. J. Haug. Universal oscillations in counting statistics. *PNAS*, 106:10116–10119, 2009.

[10] Tobias Brandes. Waiting times and noise in single particle transport. *Annalen der Physik (Berlin)*, 17:477, 2008.

[11] Gavin E. Crooks. Entropy production fluctuation theorem and the nonequilibrium work relation for free energy differences. *Phys. Rev. E*, 60:2721–2726, Sep 1999.

[12] Marin Bukov, Luca D'Alessio, and Anatoli Polkovnikov. Universal high-frequency behavior of periodically driven systems: From dynamical stabilization to Floquet engineering. *Advances in Physics*, 64:139, 2015.

[13] Krzysztof Szczygielski, David Gelbwaser-Klimovsky, and Robert Alicki. Markovian master equation and thermodynamics of a two-level system in a strong laser field. *Phys. Rev. E*, 87:012120, Jan 2013.

[14] T. Shirai, T. Mori, and S. Miyashita. Condition for emergence of the Floquet-Gibbs state in periodically driven open systems. *Phys. Rev. E*, 91:030101, Mar 2015.

[15] Gregory Bulnes Cuetara, Andreas Engel, and Massimiliano Esposito. Stochastic thermodynamics of rapidly driven systems. *New Journal of Physics*, 17:055002, 2015.

[16] G. Kießlich, C. Emary, G. Schaller, and T. Brandes. Reverse quantum state engineering using electronic feedback loops. *New Journal of Physics*, 14:123036, 2012.

[17] M. Esposito, K. Lindenberg, and C. Van den Broeck. Universality of efficiency at maximum power. *Physical Review Letters*, 102:130602, 2009.

[18] Massimiliano Esposito and Gernot Schaller. Stochastic thermodynamics for "Maxwell demon" feedbacks. *Europhysics Letters*, 99:30003, 2012.

[19] Gernot Schaller. Feedback-charging a metallic island. *Phys. Status Solidi B*, 1600549:1600549, 2017.

[20] Philipp Strasberg, Gernot Schaller, Tobias Brandes, and Massimiliano Esposito. Thermodynamics of a physical model implementing a Maxwell demon. *Physical Review Letters*, 110:040601, 2013.

[21] Andre C. Barato, David Hartich, and Udo Seifert. Rate of mutual information between coarse-grained non-Markovian variables. *Journal of Statistical Physics*, 153:460, 2013.

[22] Jordan M. Horowitz and Massimiliano Esposito. Thermodynamics with continuous information flow. *Phys. Rev. X*, 4:031015, Jul 2014.

[23] Tobias Brandes. Feedback control of quantum transport. *Physical Review Letters*, 105(6):060602, 2010.

[24] Lukas Fricke, Frank Hohls, Niels Ubbelohde, Bernd Kaestner, Vyacheslavs Kashcheyevs, Christoph Leicht, Philipp Mirovsky, Klaus Pierz, Hans W. Schumacher, and Rolf J. Haug. Quantized current source with mesoscopic feedback. *Physical Review B*, 83(19):193306, 2011.

[25] M. Büttiker. Four-terminal phase-coherent conductance. *Phys. Rev. Lett.*, 57:1761–1764, Oct 1986.

[26] N. Linden, S. Popescu, A. J. Short, and A. Winter. Quantum mechanical evolution towards thermal equilibrium. *Physical Review E*, 79:061103, 2009.

[27] Gabriel E. Topp, Tobias Brandes, and Gernot Schaller. Steady-state thermodynamics of non-interacting transport beyond weak coupling. *Europhysics Letters*, 110:67003, 2015.

[28] H. Haug and A.-P. Jauho. *Quantum Kinetics in Transport and Optics of Semiconductors*. Springer, 2008.

[29] G. Schaller, P. Zedler, and T. Brandes. Systematic perturbation theory for dynamical coarse-graining. *Physical Review A*, 79:032110, 2009.

[30] A. Dhar, K. Saito, and P. Hänggi. Nonequilibrium density-matrix description of steady-state quantum transport. *Physical Review E*, 85:011126, 2012.

[31] Li-Ping Yang, C. Y. Cai, D. Z. Xu, Wei-Min Zhang, and C. P. Sun. Master equation and dispersive probing of a non-markovian process. *Phys. Rev. A*, 87:012110, 2013.

[32] G. B. Arfken and H. J. Weber. *Mathematical Methods For Physicists*. Elsevier LTD, Oxford, 2005.

[33] P. Zedler, G. Schaller, G. Kießlich, C. Emary, and T. Brandes. Weak coupling approximations in non-markovian transport. *Physical Review B*, 80:045309, 2009.

[34] U. Kleinekathöfer. Non-markovian theories based on a decomposition of the spectral density. *The Journal of Chemical Physics*, 121:2505, 2004.

[35] Ya. M. Blanter and M. Büttiker. Shot noise in mesoscopic conductors. *Physics Reports*, 336:1–166, 2000.

[36] G. Schaller, T. Krause, T. Brandes, and M. Esposito. Single-electron transistor strongly coupled to vibrations: counting statistics and fluctuation theorem. *New Journal of Physics*, 15:033032, 2013.

[37] J. Koch and F. von Oppen. Franck-condon blockade and giant Fano factors in transport through single molecules. *Physical Review Letters*, 94:206804, 2005.

[38] G. D. Mahan. *Many-Particle Physics*. Springer Netherlands, 2000.

[39] T. Brandes. Coherent and collective quantum optical effects in mesoscopic systems. *Physics Reports*, 408:315–474, 2005.

[40] Milton Abramowitz and Irene A. Stegun, editors. *Handbook of Mathematical Functions*. National Bureau of Standards, 1970.

[41] G.-L. Ingold and Yu. V. Nazarov. *Single Charge Tunneling*, volume 294 of *NATO ASI Series B*, chapter Charge Tunneling Rates in Ultrasmall Junctions, pages 21–107. Plenum Press, 1992.

[42] M. Esposito, K. Lindenberg, and C. Van den Broeck. Entropy production as correlation between system and reservoir. *New Journal of Physics*, 12:013013, 2010.

[43] R. Martinazzo, B. Vacchini, K. H. Hughes, and I. Burghardt. Universal Markovian reduction of Brownian particle dynamics. *The Journal of Chemical Physics*, 134:011101, 2011.

[44] S. Sachdev. *Quantum Phase Transitions*. Cambridge University Press, 2000.

[45] Jacek Dziarmaga. Dynamics of a quantum phase transition: Exact solution of the quantum ising model. *Physical Review Letters*, 95:245701, 2005.